**US Army Corps
of Engineers**

Cold Regions Research &
Engineering Laboratory
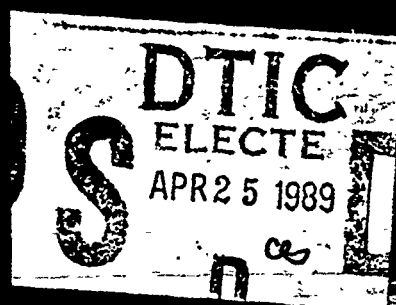
Special Report 89-6

FIRST INTERNATIONAL CONFERENCE
ON
SNOW ENGINEERING

Santa Barbara, California, July 1988

DTIC
ELECTE
APR 2 5 1989
S

89 4 25 142

AN ENGINEERING FOUNDATION CONFERENCE

Cover: Like the snow on the roof of this building, snow engineering is both an art and a science.(Photograph provided by Karl Gabl.)

First International Conference on Snow Engineering

Santa Barbara, California, July 1988

CRREL Special Report 89-6

February 1989

Best Available Copy

FOREWORD

The conference, *A Multidisciplinary Approach to Snow Engineering*, was held in Santa Barbara, California, July 10–15, 1988. Scientists, engineers, and architects discussed the nature, distribution, and behavior of snow as it affects constructed facilities. Participants came from Austria, Canada, China, Hungary, Japan, Norway, Poland, Sweden, United States, and West Germany.

The Engineering Foundation served as conference coordinator, while the National Science Foundation and National Research Council of Canada provided financial support. The International Standards Organization, American Society of Civil Engineers Technical Council on Cold Regions Engineering, and American Society of Civil Engineers Subcommittee on Modeling Drifting Snow and Sand contributed technical backing for the conference. The Cold Regions Research and Engineering Laboratory of Hanover, New Hampshire, edited and produced the conference proceedings. The Engineering and Housing Support Center of the Corps of Engineers helped fund publication of the proceedings.

The technical sessions focused on:
1) Ground snow;
2) Structural case histories;
3) Analytical modeling techniques;
4) Experimental modeling techniques;
5) Snow control;
6) Mechanical properties and behavior;
7) Codes and standards;
8) Design considerations.

The final session entitled, "Perspectives: Past, Present, Future," was a wide-ranging discussion that summarized, stimulated, and challenged participants.

At the end of the Conference the Steering Committee agreed that a second "snow engineering" conference should be held in three to four years. In light of this, they decided to change the name of this conference to the *First International Conference on Snow Engineering*.

RONALD SACK
Chairman

FIRST INTERNATIONAL CONFERENCE
ON SNOW ENGINEERING

Chairman
Dr. Ronald Sack
School of Civil Engineering and Environmental Science
University of Oklahoma
Norman, Oklahoma, USA

Co-Chairman
Dr. Michael O'Rourke
Department of Civil Engineering
Rensselaer Polytechnic Institute
Troy, New York, USA

Steering Committee

Dr. Jack Cermak
Cermak/Peterka and Assoc.
1415 Blue Spruce Drive
Fort Collins, Colorado, USA

Dr. Peter Irwin
Rowan, Williams, Davies
and Irwin Inc.
Guelph, Ontario, Canada

Dr. Donald Taylor
Institute for Research in Construction
National Research Council of Canada
Ottawa, Ontario, Canada

Wayne Tobiasson
Cold Regions Research and
Engineering Laboratory
Hanover, New Hampshire, USA

Engineering Foundation
Harold Comerer, Director
Dr. Gordon Fisher, Secretary, Conference Committee
Donna McArdle, Conference Coordinator

National Science Foundation
Dr. Eleanora Sabadell, Director, Natural and Man-Made Hazard Mitigation Program.

Proceedings Editors
Edmund Wright, CRREL
Wayne Tobiasson, CRREL

ATTENDEES

Edward E. Adams, Research Scientist
Keweenaw Research Center
Michigan Technological University
Houghton, Michigan, 49931 USA

Sture Åkerlund, Associate Professor
Structural Engineering Department
Lund Institute of Technology
Box 118, S-22100
Lund, Sweden

Robert Albrecht, Professor
Department of Architecture
University of Washington
Seattle, Washington, 98195 USA

Russell Alger, Research Engineer
Keweenaw Research Center
Michigan Technological University
Houghton, Michigan, 49931 USA

Yutaka Anno
Department of Civil Engineering
Hokkaido University
Kita 8, Nishi 13
Sapporo, Japan

Kristoffer Apeland, Professor
Oslo School of Architecture
Fredensborgveien 24G
0177 Oslo, 1, Norway

Randal Baker, Graduate Student
Department of Civil Engineering
University of Idaho
Moscow, Idaho, 83843 USA

Alfred Bedard, Jr., Supervisory Research Scientist
NOAA/ERL/Wave Propagation Laboratory
325 Broadway
Boulder, Colorado 80303-3328 USA

Robert Brown, Professor
Civil Engineering Department, Cobleigh Hall
Montana State University
Bozeman, Montana 59717-0007 USA

Jack Cermak, President
Cermak, Peterka and Assoc.
1415 Blue Spruce Drive
Ft. Collins, Colorado 80524 USA

Qigao Chen, Professor
Chongqing Institute of Architecture and
Engineering
Chongqing, Sichuan, China

Charles De Angelis, Senior Engineer
Factory Mutual Research
P.O. Box 9102 1151 Boston-Providence TP
Norwood, Massachusetts, 02062 USA

Gordon Fisher
Engineering Foundation
345 East 47th Street
New York, New York 10017 USA

Karl Gabl
Regional Forecast Center for Zentralganstalt
fur Meteorologie
Kranebitter Alle 97, A-6020
Innsbruck, Tyrol, Austria

Manfred Granzer
Landesstelle F. Baustatik
Baden-Wurttemberg Nauklerstr. 41
Tubingen, D-7400 West Germany

Douglas Hamilton, Associate Engineer
Snow Country Consultants
Whistler Box 103
Brackendale V0N 1H0 British Columbia, Canada

James Harris, Principal
J.R. Harris & Co.
1580 Lincoln Street, Room 770
Denver, Colorado, 80203-1509 USA

Dana Hart
Raychem Corp.
300 Constitution Drive
Menlo Park, California, 94025-1509 USA

Halvor Høibø, Professor
Department of Building Technology
Agricultural University of Norway
Ås, NLH 1432 N, Norway

Peter Irwin, Principal
Rowan, Williams, Davies and Irwin Inc.
650 Woodlawn Road, W.
Guelph, Ontario, N1K 1B8, Canada

Nicholas Isyumov, Manager and Director
Boundary Layer Wind Tunnel Laboratory
University of Western Ontario
London, Ontario, N6A 5B9, Canada

James Iversen, Professor
Department of Aerospace Engineering
Iowa State University
304 Town Engineering Bldg
Ames, Iowa, 50011 USA

Tamás Kármán
Institute of Building Science
David Ferenc U. 6
1113 Budapest, Hungary

Shun'ichi Kobayashi, Professor
Research Institute of Hazards in Snowy Areas
Niigata University
Ikarashi, Niigata 950-21 Japan

Sung Lee, Director
Keweenaw Research Center
Michigan Technological University
Houghton, Michigan 49931 USA

Michael Lepage, Microclimate Specialist
Rowan, Williams, Davies and Irwin, Inc.
650 Woodlawn Road West
Guelph, Ontario, N1K 1B8 Canada

Shii Lu, Associate Professor
Chongqing Institute for Architecture and
 Engineering
Chongqing, Sichuan, China

Ian Mackinlay, Architect
MacKinlay, Winnacker, McNeil and Assoc.
2333 Harrison Street
Oakland, California 94612 USA

Donna McArdle
Engineering Foundation
345 East 47th St.
New York, New York, 10017 USA

Robert Meroney, Professor and Director
Civil Engineering Department
Engineering Research Center, Room B 217
Colorado State University
Fort Collins, Colorado, 80523 USA

Hirozo Mihashi, Associate Professor
Department of Architecture
Tohoku University
Aramaki Aoba
Sendai, 980, Japan

Michael Mikitiuk, Research Associate
Boundary Layer Wind Tunnel Laboratory
University of Western Ontario
London, Ontario, N6A 5B9, Canada

Michael Newark, Head
Building Climatology
Atmospheric Environment Service
4905 Dufferin Street
Downsview, Ontario, M3H 5T4, Canada

Michael O'Rourke, Associate Professor
Civil Engineering Department
Rensselaer Polytechnic Institute
Troy, New York, 12181 USA

Jonathan Paine, President
Snow Country Consultants Ltd.
Box 562
Whistler, British Columbia, V0N 1B0, Canada

Douglas Powell
Department of Geography
University of California-Berkeley
Berkeley, California, USA

Ronald Sack, Director
Department of Civil Engineering
202 West Boyd Street, Room 334
University of Oklahoma
Norman, Oklahoma 73019 USA

Shuji Sakurai
Hokkaigakuen University
W-11, S-26 Chuouku
Sapporo, Hokkaido 064 Japan

Rune Sandvik
Norwegian Council for Building Standardization
Kobenhavngt 10
0566 Oslo, 5, Norway

Katuhiro Shibayama
(Associate of Y. Anno)

Narendra Srivastava, Professor
School of Engineering
Université de Moncton
Moncton, New Brunswick, E1A 3E9, Canada

Fred Storey
Raychem Corp.
300 Constitution Drive
Menlo Park, California, 94025-1164 USA

Jiro Suzuya, Professor
Department of Architecture
Tohoku Institute of Technology
Yagiyama Kasumi-Cho 35-1
Sendai, Japan

Ronald Tabler, Engineering Consultant
Tabler and Associates
P.O. Box 576
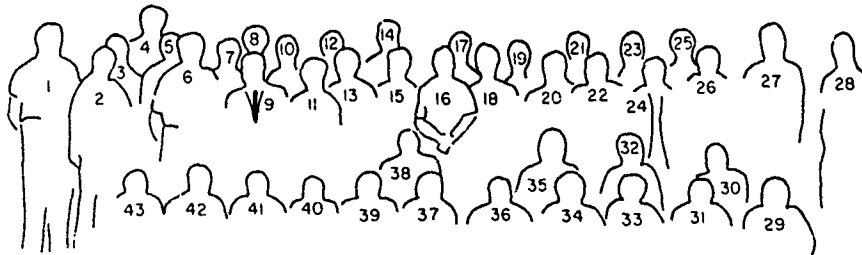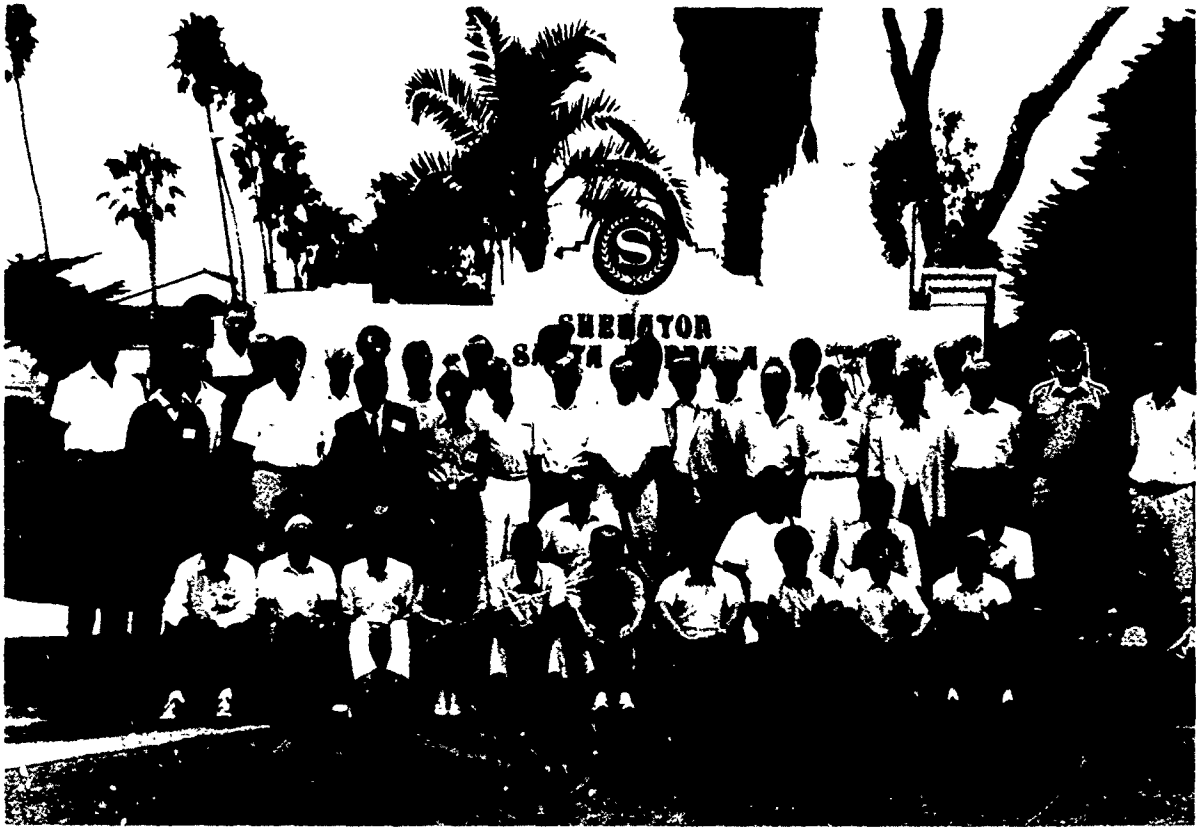Laramie, Wyoming, 82070, USA

Toru Takahashi, Graduate Student
Department of Architecture
Tohoku University
Aramaki Aza Aoba
Sendai, 980, Japan

Donald Taylor, Research Officer
Institute for Research in Construction
National Research Council of Canada
M-20 Montreal Road
Ottawa, Ontario, K1A 0R6, Canada

Wayne Tobiasson, Research Civil Engineer
Cold Regions Research &Engineering Laboratory
72 Lyme Road
Hanover, New Hampshire 03755-1290 USA

Edmund Wright, Technical Writer–Editor
Cold Regions Research & Engineering Laboratory
72 Lyme Road
Hanover, New Hampshire 03755-1290 USA

Jerzy Zuranski
Institute for Building Technology
Filtrowa 1
00950 Warsaw, Poland

1 Mikitiuk, Michael	15 Tabler, Ronald	29 Shibayama, Katuhiro
2 Lu, Shii	16 Isyumov, Nicholas	30 Suzuya, Jiro
3 Høibø, Halvor	17 Baker, Randal	31 Gabl, Karl
4 Tobiasson, Wayne	18 Apeland, Kristoffer	32 Takahashi, Toru
5 DeAngelis, Charles	19 Bedard, Jr., Alfred	33 Sakurai, Shuji
6 Lee, Sung	20 Hamilton, Douglas	34 Taylor, Donald
7 Iversen, James	21 Newark, Michael	35 Anno, Yutaka
8 Harris, James	22 Åkerlund, Sture	36 Meroney, Robert
9 Chen, Qigao	23 O'Rourke, Michael	37 Mihashi, Hirozo
10 Adams, Edward	24 Granzer, Manfred	38 Fisher, Gordon
11 Kobayashi, Shunichi	25 Irwin, Peter	39 Paine, Jonathan
12 Hart, Dana	26 Zuranski, Jerzy	40 McArdle, Donna
13 Kármán, Tamás	27 Mackinlay, Ian	41 Sack, Ronald
14 Storey, Fred	28 Sandvik, Rune	42 Cermak, Jack
		43 Albrecht, Robert

Missing from photo:
Alger, Russell
Brown, Robert
Lepage, Michael
Powell, Douglas

vi

CONTENTS

Page

1. GROUND SNOW

2. STRUCTURAL CASE HISTORIES

3. ANALYTICAL MODELING TECHNIQUES

4. EXPERIMENTAL MODELING TECHNIQUES

GROUND SNOW
Sture Åkerlund, Chairman

The long walk to get a representative sample. (Photograph by Ben Whistler.)

Snow Depth and Snow Load in Umeå

Sture Åkerlund[1]

ABSTRACT

Snow depth data are avalible for Umeå, a small town in the north–east part of Sweden, since the winter 1904/05 and snow density data from the period 1909–1925.

Maximum snow depth ever recorded was observed on the 16th of March this year (1988). The 50 year MRI (mean recurrence interval) snow depth is calculated based in the 30, 35, 40,...80, 83 and 84 first observations of maximum snow depth per year.

When the Swedish snow load code was written (1973) it was assumed that depth and density are independent – not in general but at the time when the snow load on the ground has its maximum. Based in the assumption the 50 year MRI snow load is calculated and compared with the corresponding value from 1973.

CURRENT SNOW LOAD CODE IN SWEDEN

The current snow load code in Sweden was written in 1973 and was based on

1/ snow depth observations from 154 stations during the period 1930–60

2/ snow density and snow depth observations from 52 stations during the period 1909–25.

Snow depth observations have been recorded long before 1930 for the main part of the stations but those data are not yet on magnetic tape. All the data, 1/ and 2/, was treated by Nord/Taessler (1) who came to the conclusion that depth and density according to 2/ are mutually independent, see FIG 1, not in general but at the time when the snow load on the ground was at its maximum. It was shown by Nord/Taessler (1) that the distribution of density fairly well fitted the normal distribution for the northern part of Sweden with a mean value of $\bar{\gamma} = 2.24$ kN/m^3 and standard deviation $s_\gamma = 0.44$ kN/m^3; line a/in Fig 2. On the same figure a lognormal approach is drawn, curve b/, though does not fit very well. (The lognormal distribution seemed to be a better fit for the density in the southern part of Sweden).

Then the independent stochastical variables depth (d) and density (γ) were multiplied and the 50 year MRI was estimated from the distribution for $s = \gamma d$. As for Umeå, a small town in the north east part of Sweden, see FIG 3, the 50 year MRI for snow load was estimated by Nord/Taessler (1) to $s = 2.8$ kN/m^2.

---

[1]Assc. prof, Dept of Civ. Engineering
Lund Inst. of Technology, Box 118, S–221 00 LUND, Sweden

FIG 2. Snow density versus $(1-F(\gamma))$ at the time of maximum ground snow load in the northern part of Sweden during the period 1909–25 on normal probability paper. The straight line a) and the dots are from (1).

In the figure:

$1-F(\gamma)$

a) $1-\phi\left(\dfrac{\gamma-2.24}{0.44}\right)$

b) $1-\phi\left(\dfrac{\ln(\gamma/2.20)}{0.1942}\right)$

Density, kN/m^3

FIG 1 Snow depth versus density at the time of maximum ground snow load in the northern part of Sweden. From (1).

Density kN/m^3 γ

Depth d, cm

4
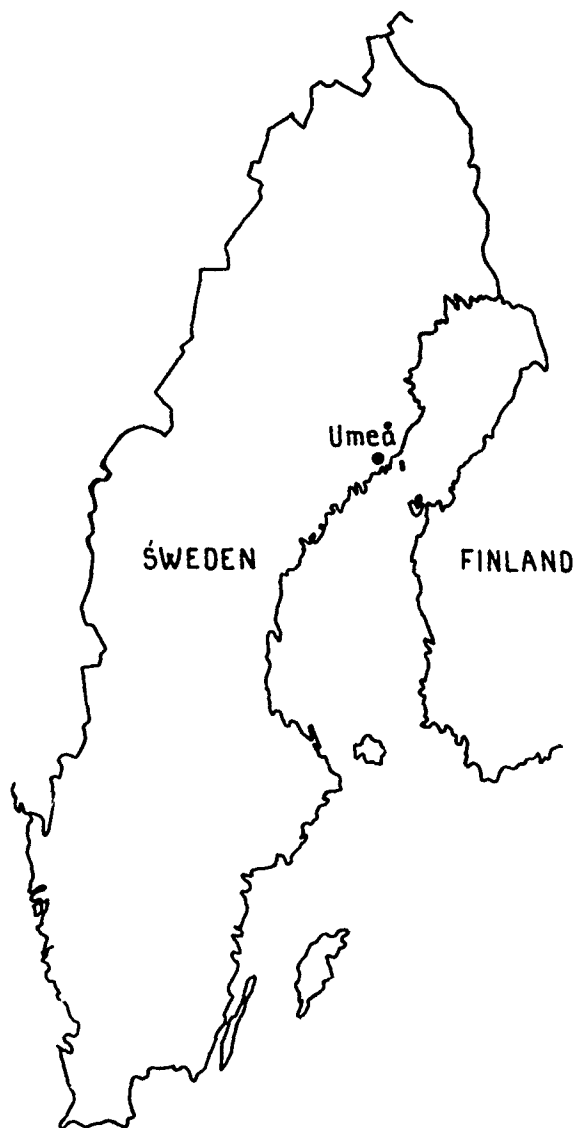
FIG 3. Location of Umeå.

WHAT HAS HAPPEND SINCE 1973?

On the 16th of March this year (1988) the maximum snow depth (127 cm) ever recorded in Umeå was observed. Snow depth has been recorded in Umeå since 1904/05. From 1930/31 onwards all data are on magnetic tape. Density or water equivalents were not measured. Therefore the ground snow load is unknown. The heavy snowfall in the middle of March this year caused 12 major failures in Umeå and it was claimed by the local building authority that the 50 year MRI snow depth and snow load might be affected substantially if last winter's snow depth were taken into account — which was the matter to be analysed.

FIG 4 shows the maximum snow depth since 1904/05 on extreme value probability paper. The dashed line, that corresponds a lognormal approach, will somewhat

5
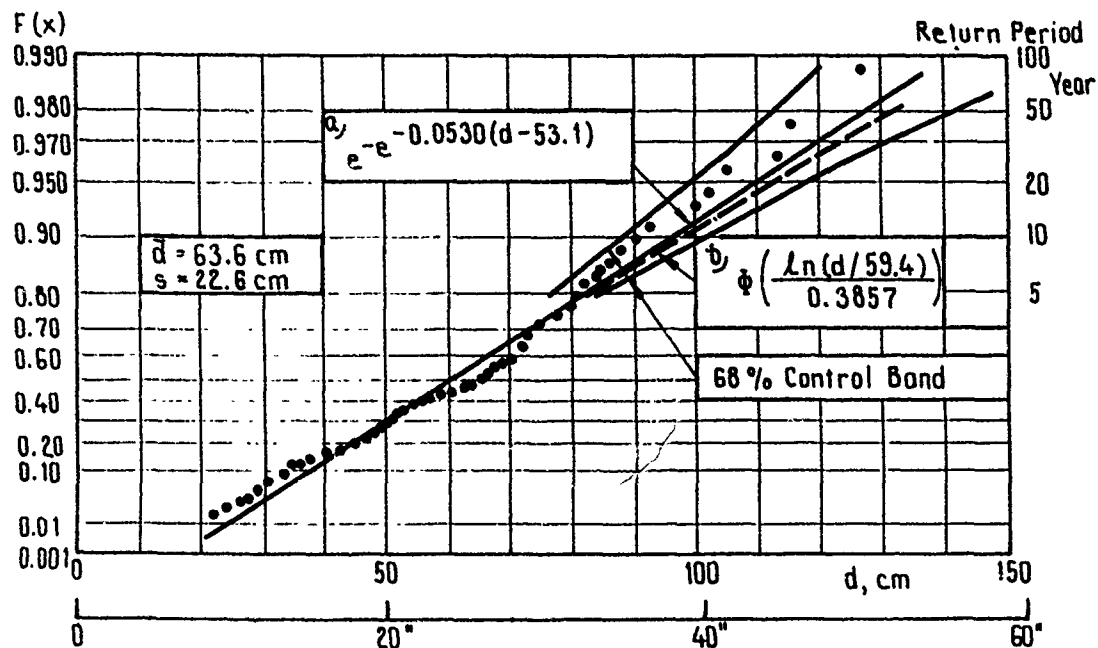
FIG 4. Maximum snow depth per year in Umeå from 1904/05 to 1987/88 (84 observations) on extreme value probability paper.
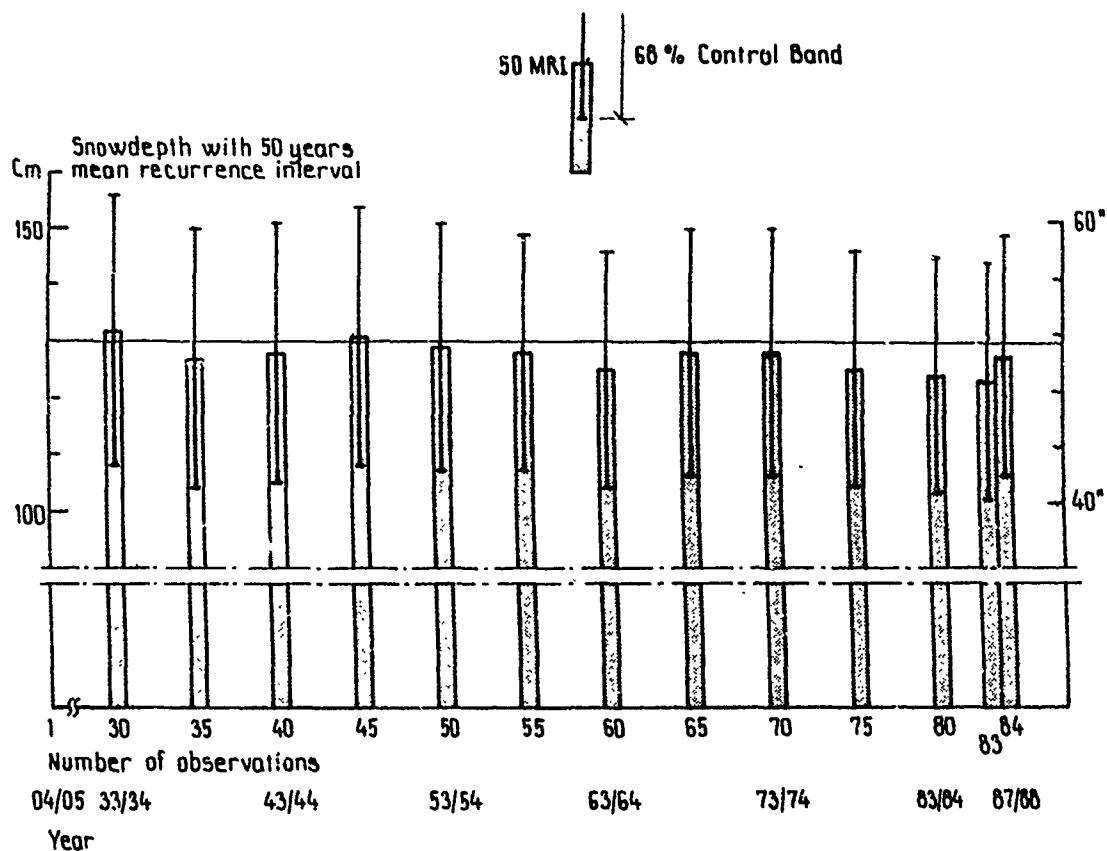
FIG 5. The 50 year MRI snow depth in Umeå – if extreme value distributed– based on the 30, 35, 40, ... 83 and 84 first observations.

6

overestimate the snow depth. The solid line shows that last winter's snow depth in fact corresponded to the 50 year MRI snow depth.

FIG 5 shows the 50 year MRI snow depth in Umeå – if extreme value distributed – based on the 30, 35, 40, ... 83 and 84 first observations and it can be deduced that the

. * 30 first years correspond to 132 cm (maximum)
* 83 first years correspond to 123 cm (minimum)
* 84 first years correpsond to 127 cm

This paper was not intended to be part of the proceedings and it was written only after the conference. However, it gives us an opportunity to compare with Harris' paper, "Snow Data Analysis for Structural Safety ", and to conclude that the winter s in the north east part of Sweden seem to be very stable.

With the convenient assumption that depth and density are mutually independent the 50 year MRI was estimated with the Pearson distribution to

$s = 2.8$ kN/m^2

if depth is extreme and density normally distributed, curve a/ in FIG 2 and 4, i.e., the very same value that Nord/Taessler (1) arrived at 1973.

The lognormal approach, which is very easy to handle since $s = \gamma d$ also will be lognormallly distributed though it will overestimate high values for both depth and density, curve b/ in FIG 2 and 4, gives $s = 3.2$ kN/m^2.

REFERENCES

(1) Nord/Taessler   Snötäckets densitet och massa i Sverige,
                                     Statens Inst. för byggnadsforskning, R21/1973

Snow Loads in Mountainous Terrain

Karl Gabl[1]

ABSTRACT

Measurements of snow loads on the ground were the principal data
for the revision of the Austrian standard (OENORM B 4013).
Austria lies in the transition zone between oceanic and contin-
ental climatic zones, but the Alps additionally influence the
regime of precipitation and snow cover by orographic effects.
Thus, the country had to be divided into six different areas of
snow loads on the ground. The measurements of the water equi-
valent of snow cover from a 30-year period were collected. From
these data the maximum load for a 50-year return period was calcu-
lated with the probability distribution by Gumbel. Over 10,000
measurements from nearly 500 locations did not give a satisfactory
accuracy for loads of the standard. Therefore, other climatologi-
cal records such as snow depth and density at various sea levels
and regimes of precipitation were used. Also values of the pre-
vious standard and our own field measurements in a winter of ex-
treme snow depths were taken into account. The result of these
investigations was that the Austrian standard still causes us
problems with the reducing factor between the load on the ground
and on roofs. Especially the meteorological influences, e.g. wind
speed, radiation, etc., are creating difficulties in mountainous
terrain.

INTRODUCTION

A few years ago the Austrian Standards Organization asked for a revision
of the up-to-then valid OENORM B 4000 Part 4, Snow- and Ice-Loads, edition
October 1960. Several factors influenced this decision:

1. Every snow load zone had a range between 40 and 100 $kg\ m^{-2}$ and, in urban
    areas with a high difference in elevation, it was not possible to deter-
    mine the exact snow load for a certain elevation. In higher altitudes
    there existed only loads up to a value of 650 $kg\ m^{-2}$, but in snowy
    winters these values did not prove to be sufficient.

2. The revision should take into consideration the concept of the IOS pro-
    posal no. 4355, edition 1981.

3. A comparison with the neighboring states of Switzerland and West Germany
    should be carried out in an area along the borders covered by the Alps.

I. Director, Regional Forecast Center of Zentralanstalt für Meteorologie,
A-6020 Innsbruck, Tyrol, Austria

Former standards for the determination of snow loads were normally set up in an indirect way. The snow loads on the ground were often calculated indirectly with the help of the depth of snow and the measured distribution of density. Experiments by Martinec (1975, 1977) to determine the water equivalent of the snow cover from the depth of snow were based on theoretical settling curves of snow, from which the water content of snow could be derived. With this method, a satisfying result was obtained between the measured and the calculated water equivalent of the snow cover. At that time there was no regional differentiation in the SIA-Standard in Switzerland, where two-thirds of the area are covered by the Alps.

Further research was carried out in Western Germany by Caspar and Krebs (1971) to derive the snow loads on the ground from maximum depths of snow together with measurements of the density of snow and water equivalent. Altogether four different zones were used, including one with high snow loads in the alpine area near the Austrian border.

USE OF DATA

The basic data consisted of about 11,000 measurements from nearly 500 sites covering a period of 30 years, ranging from 150 m up to 2700 m above sea level. However, the data were not homogeneous, because there was neither an areal nor a chronological continuity. Statistical methods commonly used in climatology could therefore not be used. The examination of the measurements of the water equivalent of the snow cover was absolutely necessary, because the published data were partly incorrect due to misprints and erroneous measurements; e.g., a density value of snow of more than 700 kg m^{-3} was hardly acceptable.

Austria was divided into 22 regimes of precipitation (Steinhauser 1974). They were combined into six snow load zones because of a lack of data in some regimes. For the design of snow load zones, additional material from already existing maps of the mean zones, additional material from already existing maps of the mean maximum depth of snow and the total sum of new snow were used. Furthermore, use was made of my own measurements in winters with heavy precipitation, when damage to buildings occurred. Information was also given by the building authorities about regional snow loads. A differentiation according to the exposure of the site was not possible. The evaluation of the measurements of water equivalent was basically carried out as recommended in the ISO Standard 4355 (1981) with the help of the extreme value distribution by Gumbel. A return period of 50 years was chosen. For this period, usually actual measurements of the water equivalent from 30 years show acceptable results (Martinec 1975).

DETERMINATION OF EXTREME SNOW LOADS

Because of the already mentioned temporary and local inhomogeneity of the measurements it was not possible to evaluate the expected 50-year maximum of the water equivalent of snow for every site of measurement, but the data were combined in zones. For all sites of a zone, the maximum water equivalent of one year was chosen and plotted into a diagram in relation to the altitude. From this an exponential curve fit was made by the method of least squares.

9

As examples, two calculations from the snowy winter of 1974/1975 (Fig. 1) and the dry winter of 1963-1964 (Fig. 2) are shown with the corresponding values. The slope of the curves characterizes the conditions of precipitation of a winter. A dry, short winter, for example, the winter of 1963/1964 in Austria when the Olympic Games were held in Innsbruck, demonstrates smaller loads at higher altitudes than in the winter of 1974/1975 with heavy snowfall.

For all winters of the 30-year period, curve fitting was done as for the winters shown above. Afterward, the water equivalent for a certain altitude was derived by steps of 200-m difference in height. The method for the calculation of the values for the different zones was used as was recommended by ISO Standard 4355.

From the abovementioned method, relations between the maximum yearly snow water equivalent and the altitude for various return periods were determined.

Figure 3 shows the evaluated loads for all altitudes of zone I. The small difference between the loads with a return period of 30 and 50 years is remarkable. The curve fit displayed a satisfactory correlation coefficient. After the snow loads were determined for all zones it turned out that a reduction could be made from 6 to 5 zones.

Because of the irregular distribution of the sites of measurements, an exact boundary of the zones in a mountainous region could not be given; therefore, additional methods had to be taken into consideration.
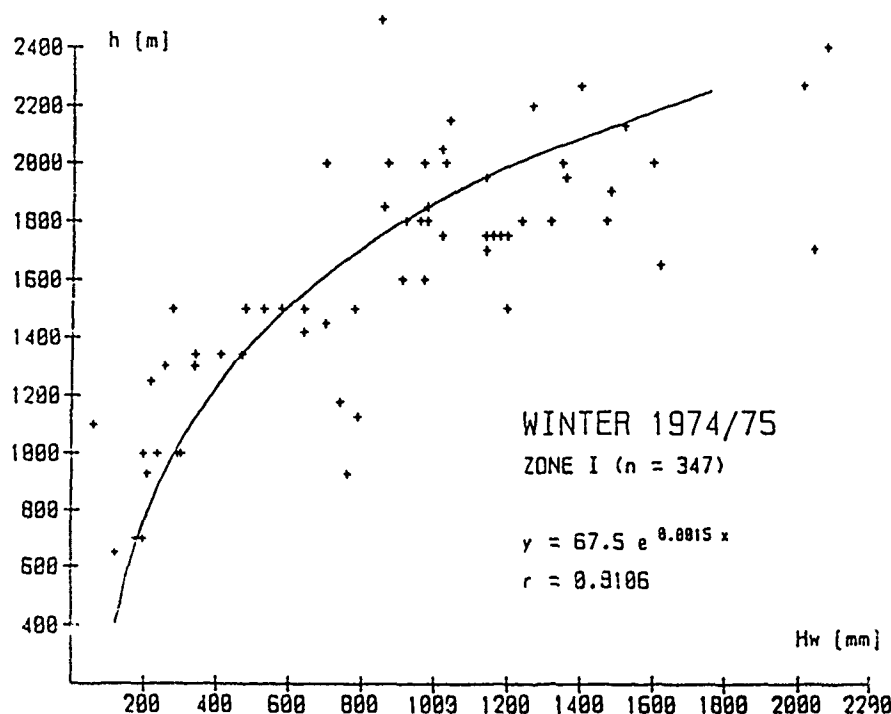
Figure 1. The maximum water equivalent of snow (Hw in mm) of every site in zone I during winter of 1974/75 (n = number of measurements, r = correlation coefficient, h = altitude in meters).

10
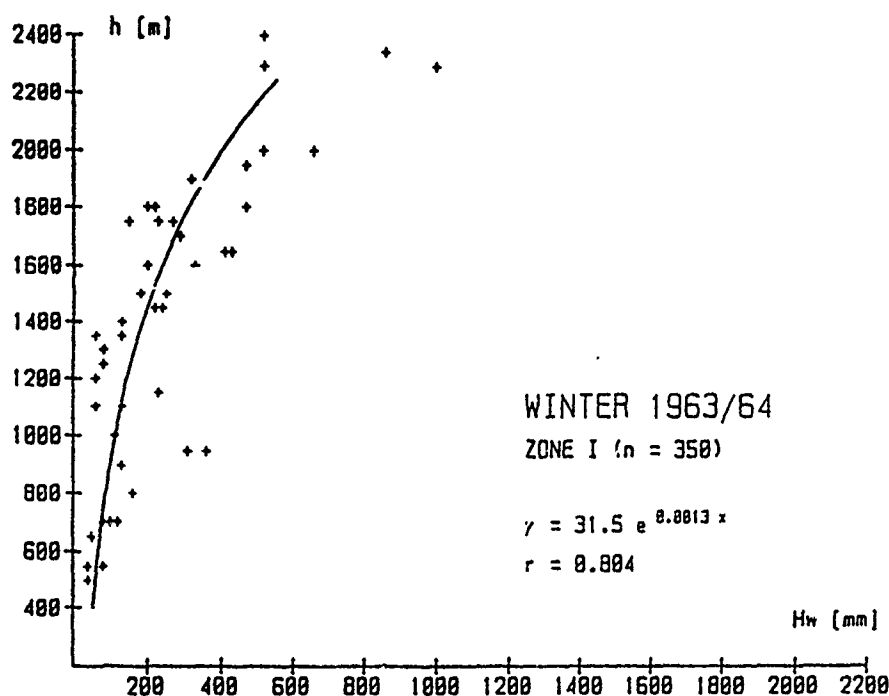
Figure 2. The maximum water equivalent of snow in zone I during winter of 1963/64 (explanation see Fig. 1).
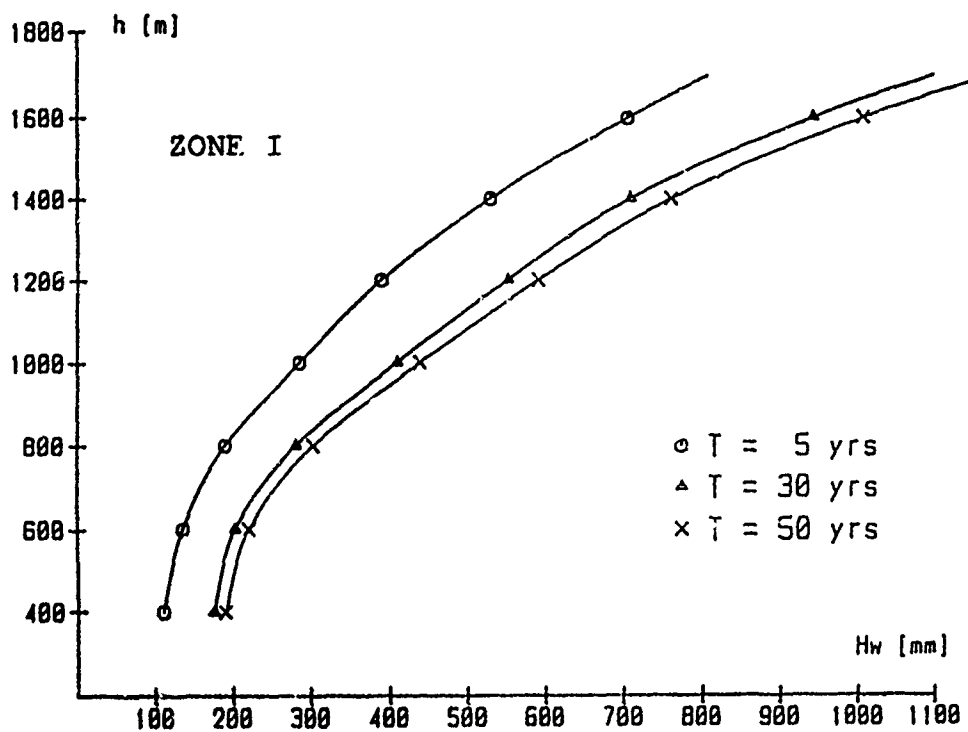
Figure 3. Relation between the maximum water equivalent and the altitude for return periods of 5, 30 and 50 years.

CHECKING METHODS

- A map of the distribution of precipitation in the Alps (Fliri, 1974) turned out to be a valuable help.
- The method used in Switzerland (Martinec, 1977) which is based on the calculation of the water equivalent from settling curves of snow could not be used, because the daily measurements of the depth of snow were not available.
- A further possibility of determining the snow loads on the ground was the correlation of the water equivalent, the mean value of the density of snow and the depth of snow depending on the specific altitude. With the help of the existing data a correlation was made.

As shown in Figure 4, the mean values of snow density in Austria are between 0.25 and 0.30 g cm^{-3} at altitudes under 1000 m, around 0.30 g cm^{-3} between 1000 and 1500 m, and between 0.35 and 0.40 g cm^{-3} between 1500 and 2000 m. With the help of these densities, together with long series of measurements of the depth of snow, which are available in most countries, the snowloads on the ground can be determined for a certain location.

In Austria, a connection between snow density and duration of snow cover like that in Sweden was not made. Meteorological experience shows, that in our climatic conditions, e.g. when rain falls into a snow cover that is only a few days old, a dramatic increase of the density of snow can occur. At lower altitudes such rainfalls frequently happen.
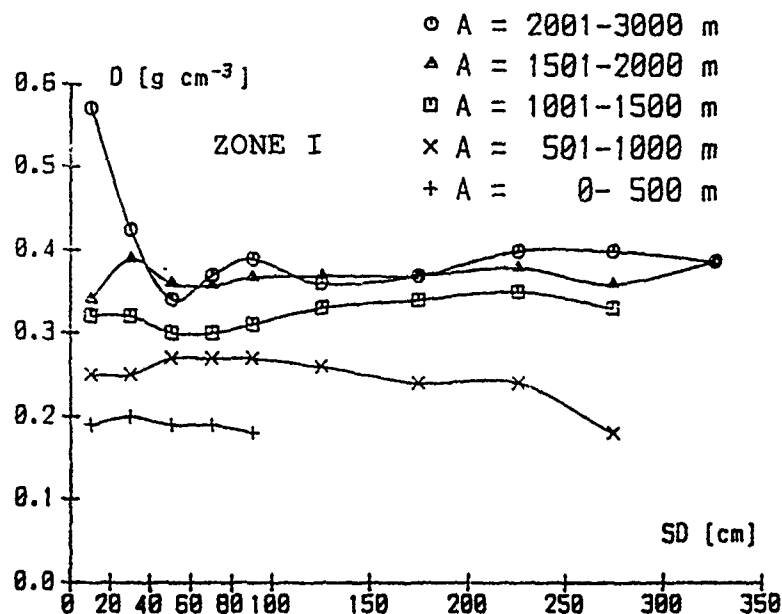
Figure 4. The density of snow (D) in relation to depth of snow (SD) for different altitudes (A) in the Austrian Alps.

12

The relation between snow densities, average air temperature and wind force, used in the USSR, was not applied in our country, because of orographic and meteorological reasons. First of all, the wind conditions may change in the terrain within a short range. Besides, the average wind speed during the period of snow accumulation in mountainous terrain and the wind speed during and after the snowfall, especially in weather situations like föhn (when warm, dry winds come down a mountain), play a more important role. Secondly, temperature inversions in winter can be found in the Alps during roughly 50 to 60% of all hours. Thirdly, air temperature alone does not give enough information about melting or freezing processes in the snow cover, but the whole energy budget must be considered.

These circumstances require an extensive knowledge of alpine climatology. Therefore all determinations of snow loads in a mountainous region can only be done with an additional meteorological expertise.

CONCLUSION

The determination of the ground loads in Austria was carried out with the measurements of water equivalent, but for the zoning other investigations, e.g. maps of the distribution of precipitation and the snow cover, were necessary.

Especially in the mountainous terrain great differences exist between the ground loads and the roof loads in wind-exposed regions, where a decrease in roof loads at higher altitudes was observed. Further investigations of loads on flat and inclined roofs are necessary, because at high altitudes in the Alps flat roofs seem to have smaller loads.

ACKNOWLEDGEMENTS

REFERENCES

Caspar, W. and M. Krebs, 1971, "Ergebnisbericht ueber die Auswertung langjaehriger Beobachtungen ueber Schneehoehen und Schneelasten (DIN 1055, Bl.5)," Deutscher Wetterdienst-Zentralamt Offenbach, Juli 1971.

Chow, V T., 1964, Handbook of Applied Hydrology, MacGraw Hill, New York, 27-34, 1964.

Flir, '., 1974, "Niederschlag und Lufttemperatur in Alpenraum," Wissenschaftliche Alpenvereinshefte Nr.24, Oesterreichischer Alpenverein, Innsbruck, 1974.

Gabl, K., 1976, "Extremwertbetrachtungen der taeglichen Neuschneehoehen und der maximalen Schneedeckemhoehen," Das Klima von Hochserfaus, Diss. Universitaet Innsbruck, 213-231, 1976.

OENORM B 4000, Teil B, 1960, "Schnee-und Eislasten," Oesterreichisches Normungsinstitut, Wien, Ausgabe Oktober 1960.

OENORM B 4013, 1983, Schnee- und Eislasten, Oesterreichisches Normungsinstitut, Wien, Ausgabe 1. Dezember 1983.

Hydrographischer Dienst, "Karte der Neuschneesummen (1901-1950)." Vienna.

ISO Standard 4355, 1981, International Standards Organisation, Snow loads on roofs, edition 1981.

Martinec, J., 1975, "Periodizitaet der Schneelasten in der Schweiz," Eidgenoessisches Institut fuer Schnee- und Lawinenforschung Weissfluhjoch, Davos, Int. Bericht Nr. 545, Sept. 1975.

Martinec, J., 1977, "Expected snow loads on structures from incomplete hydrological data," Journal of Glaciology, Vol. 19, No. 81, 185-195, Cambridge, 1977.

Steinhauser F., 1974, Die Schneeverhaeltnisse Oesterreichs und ihre oekonomische Bedeutung," 70. - 71. Jahresbericht des Sonnblickvereines, 3 - 42, 1974, Vienna.

Snow Data Analysis for Structural Safety

James Robert Harris[1]

ABSTRACT

Current standards for design of structures specify snow loads by starting from the predicted 50 or 100 year mean recurrence interval value of ground snow load. A study of weather data for Denver, Colorado, illustrates that data analysis to reach this starting point must be conducted with considerable care. Data for Denver indicate infrequent unusual occurrences of snowfall that are of real significance for the safety of structures, which must focus on rare events. Thus the upper tail of probability models controls the results of the analysis. The weight of snowpack is the property of interest, yet the U.S. Weather Service has recorded such data at only selected stations since the late 1940's. These two facts combine to create a need to add older data for depth alone to the analysis. A technique for inclusion of such data is described, including secondary checks on the validity of such extrapolated data. Finally, techniques for comparing the predictions from the analysis to the record of history are demonstrated and advocated.

INTRODUCTION

The design of a structure to resist the weight of snow must include the step of determining what magnitude of snow weight can reasonably be expected to occur during the life of the structure. Current structural engineering practice for this step in the United States is generally based on the provisions of American National Standard A58.1, "Minimum Design Loads for Buildings and Other Structures." In this standard the design load for the structure is directly related to the expected value for the weight of snow on the ground at the location of the structure in question. For nearly all types of loads to which a structure is exposed, the standard specifies a statistical approach for determining the load. For common buildings, the specified probability is that the chance of exceeding the standard load during any one year is 1/50 or 0.02. This load is usually referred to as the "50 year mean recurrence interval load." For structures of high importance or sensitivity the 100 year mri load (probability of being exceeded in one year = 0.01) is specified.

Standard A58.1 contains maps and tables to permit the user to determine the weight of the 50 year mri snow load on the ground for most locations in the U.S. (Mountainous regions are not mapped due to extreme local variations.) The mapped values are based on several statistical analyses of snow data at over 9000 locations. Most of the analysis was performed at the U.S. Army Cold Regions Research and Engineering Laboratory (ANSI A58.1). 184 of the locations were first order weather stations at which data existed for both depth and

---

[1]President of J.R. Harris & Company, Structural Engineers, Denver, Colorado.

weight of snow on the ground. Examination of the data led to the decision to use a lognormal distribution to represent the statistics of the annual extremes and to calculate the 50 year mri values (Ellingwood and Redfield 1983, 1984). Essentially all of the analysis was performed on data from the years 1950 through 1980.

Selection of a single statistical model greatly simplifies the enormous computation and interpretation required to produce the maps and tables in the standard. However, it appears to err very significantly for some locations. The bulk of this paper is a case study of one such location, Denver, Colorado, at which the error is on the unsafe side. From both the map and the table in A58.1, the 50 year mri value for weight of snow on the ground is 15 psf (720 N/m^2). The procedure for determining a 100 year mri value yields 18 psf (860 N/m^2). The analysis that follows will show that more reasonable values are 25 psf (1200 N/m^2) and 35 psf (1680 N/m) for the 50 and 100 year mri values, respectively. The difference in values is certainly very significant for the purposes of structural safety checking, being of the same order as conventional factors of safety.

HISTORICAL RECORD FOR DENVER

Figure 1 is a chart of the annual maximum ground snow expressed as inches of water for the years 1893-1984. (Inches of water is the standard record of the National Weather Service; to obtain pounds per square foot, multiply by 5.2; to obtain Newtons per square meter, multiply by 249.) The data for years prior to 1951 are inferred as will be explained subsequently. Note the degree to which maximum values exceed 15 or 18 psf (2.9 inches or 3.5 inches). The statistical analyses reported in this paper do not include the data from years 1893 to 1904, because the data had not been discovered at the time the analyses were performed.

Beginning in 1951 the NWS station at Denver recorded for each day the depth and weight of the snowpack on the ground. Table 1 presents this data. Note that the maximum depth and weight are not simultaneous in many of the years.

In order to make use of the prior years NWS data in which only the depth of the snow pack was recorded, a relation between depth and weight was developed from the data in Table 1. For each year a relative density was obtained by dividing the maximum weight (inches of water) by the maximum depth (inches of snow). For many occasions this meant combining data from different snowfalls. In over half the occasions this results in a lower density than occurred at the time of maximum weight and a higher density than occurred at the time of maximum depth. This procedure appears to be the most accurate method of predicting the maximum annual weight of snowpack from data on maximum depth. Figure 2 is a plot of this density for each year versus the maximum depth from that year.

A linear regression of depth-density data was performed to obtain the following best fit equation:

$$\gamma = 0.0729 + 0.0042d \tag{1}$$

where γ is the relative density and d is the depth of snow in inches. The
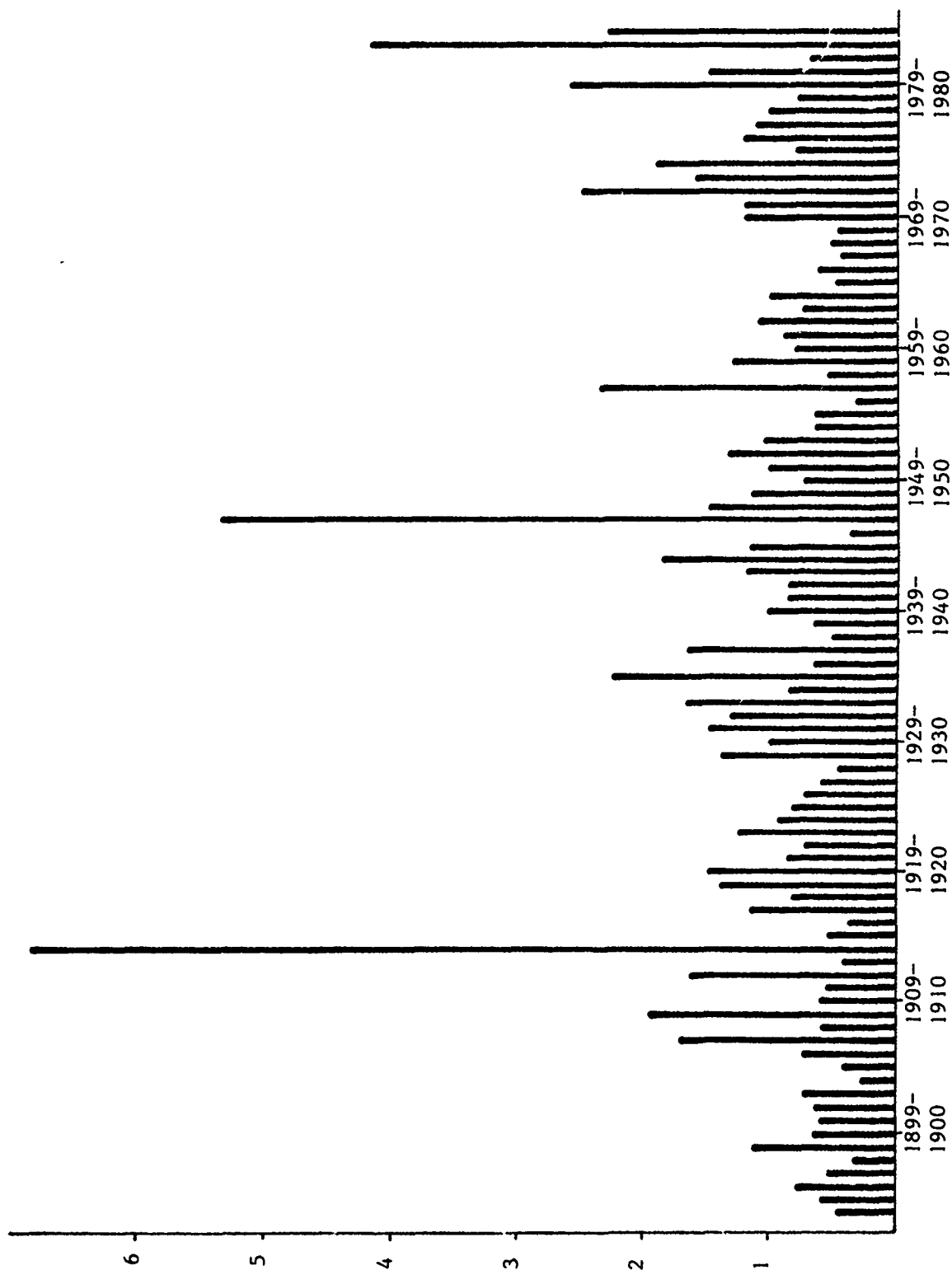
Figure 1 Annual Maximum Snowpack, Inches of Water, Denver, Colorado

TABLE 1

33 YEARS DATA WITH WATER CONTENT MEASUREMENTS AT DENVER, COLORADO

Year	Maximum Snow Depth				Maximum	Weight	
	Date	Snow Depth inches	Water Content inches	Date	Snow Depth inches	Water Content inches	Weight psf
(1)	(2)	(3)	(4)	(5)	(6)	(7)	(8)
1951-52	3/21	13	0.85	3/22	11	1.32	6.7
53	2/20	10	1.05	2/20	10	1.05	5.5
54	4/30	5	0.65	4/30	5	0.65	3.4
55	12/27	8	0.49	12/28	8	0.65	3.4
56	3/15	5	0.25	1/30	3	0.32	1.7
57	4/2	16	2.2	4/3	14	2.35	12.2
58	1/20	7	0.55	1/20	7	0.55	2.9
59	3/26	12	1.30	3/26	12	1.30	6.8
60	9/29	7	0.50	9/30	4	0.80	4.2
61	12/26	9	0.69	12/10	5	0.88	4.6
62	1/8	12	1.04	1/22	9	1.09	5.7
63	3/4	9	0.79	3/5	5	0.73	3.8
64	4/4	10	0.99	4/4	10	0.99	5.1
65	2/16	7	0.49	2/16	7	0.49	2.5
66	2/13	7	0.60	2/13	7	0.60	3.1
67	10/14	7	0.43	10/14	7	0.43	2.2
68	11/2	6	0.50	11/3	4	0.51	2.7
69	3/2	6	0.47	3/2	6	0.47	2.4
70	10/12	11	1.20	10/13	11	1.20	6.2
71	1/۵	8	0.8	1/4	8	1.2	6.2
72	۵/ ،	13	1.17	4/27	12	2.5	13.0
73	۵ 1	13	1.6	11/11	13	1.6	8.3
74	1ᴢ/26	13	1.9	12/26	13	1.9	9.9
75	4/1	8	0.8	4/1	8	0.8	4.2
76	11/9	7	0.9	2/21	5	1.2	6.2
77	3/10	8	1.1	3/11	8	1.1	5.7
78	5/6	8	0.9	5/7	6	1.0	5.2
79	12/6	6	0.6	4/11	4	0.8	4.2
80	11/21	17	1.9	11/22	14	2.6	13.5
81	3/4	10	1.5	3/4	10	1.5	7.8
82	12/22	7	0.7	12/22	7	0.7	3.6
83	1ᴢ/24	24	3.6	12/26	24	4.2	21.8
1983-84	11/27	18	2.4	11/27	16	2.3	12.0

to obtain mm, multiply inches by 25.4
to obtain N/m^2, multiply psf by 47.9

correlation coefficient is not particularly high, being 0.53. Analysis of the same data in logarithmic form yielded a logarithmic equation which had a slightly lower correlation coefficient. Analysis of subsets of the data yielded essentially the same equations. (Using only points for depths exceeding 10 inches gives 0.0726 + 0.0042d; depths exceeding 15 inches gives 0.0774 + 0.0039d). Figure 3 is an arithmetic plot of weight versus depth for Equation 1 along with the data points. Table 2 shows the maximum recorded depth from years prior to 1951 and the calculated density and weight (inches of water). Figure 1 was plotted from this data and the data in Table 1.

STATISTICAL ANALYSIS FOR DENVER

Figure 4 is a frequency diagram for the 80 years of data from 1904 to 1984. Ideally, the probability distribution selected should fit this diagram. The diagram clearly indicates the importance of the three extreme values above 4 inches of water - this region is referred to as the upper tail of the frequency diagram, or probability distribution. Because those values are so important they were scrutinized by examining all the available NWS data about their occurrence. For example, the largest snow occurred in December, 1913, and the daily records show:

| Date | Precipitation, inches | | Maximum | | |
	Snow	Water	Temperature	Wind	Snow Depth
12/1	4.2	0.54	30 °F		
2	1.5	0.18	30		
3	2.4	0.02	31		
4	20.9	2.12	32		
5	16.5	1.32	34	44 mph	32.6"
6	0.2	0	39		

The summation of daily precipitation yields 4.18 inches of water, yet the estimate from 32.6 inches of snow yields 6.84 inches of water. This discrepancy is more apparent than real, due to the effect of wind on the NWS precipitation records. For example, consider the December, 1982, storm:

| Date | Precipitation, inches | | Maximum | | | |
	Snow	Water	Temp	Wind	Snow Depth	Water Content
12/24	23.6	2.00	33 °F	51 mph	24 inches	3.6 inches
25	0.2	0.02	31	31	24	3.3
26	0	0	31	10	24	4.2

Here the discrepancy is between **estimated** precipitation and **measured** water content of snowpack. Precipitation is estimated when winds are high, due to the nature of the equipment used to capture precipitation. During snowfall accompanied by wind, the precipitation is estimated at Denver by the station personnel using the relation one foot of snow = one inch of water (personal communication with NWS staff). The measured quantity is certainly the more reliable. The variation in the measured quantity on successive days without further accumulation or melting is simply an indication of the very real errors in sampling. (4.2 inches has been used in this analysis.)
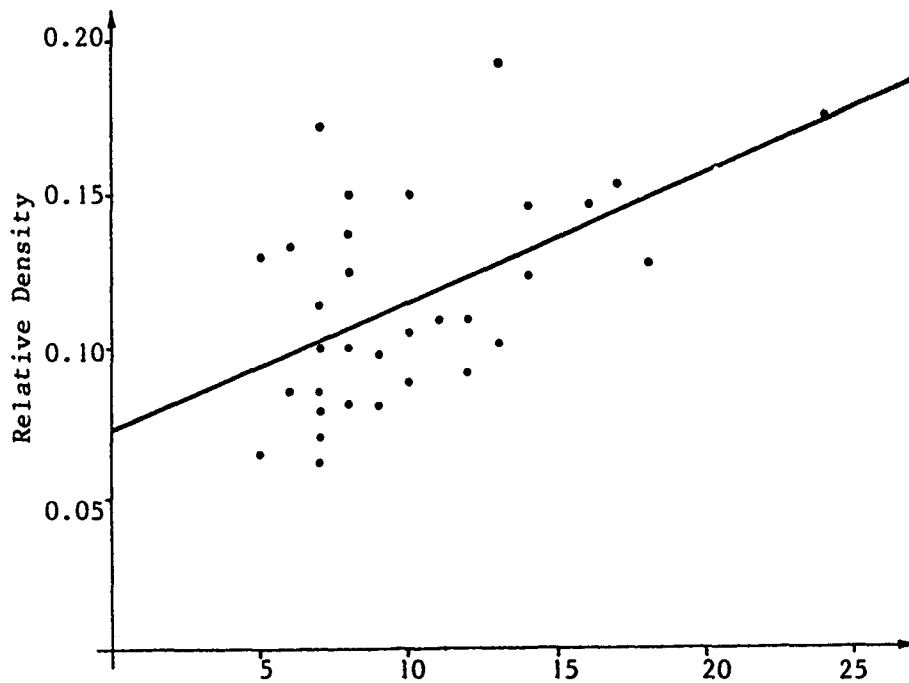
Figure 2   Snow Depth, inches, versus Relative Density
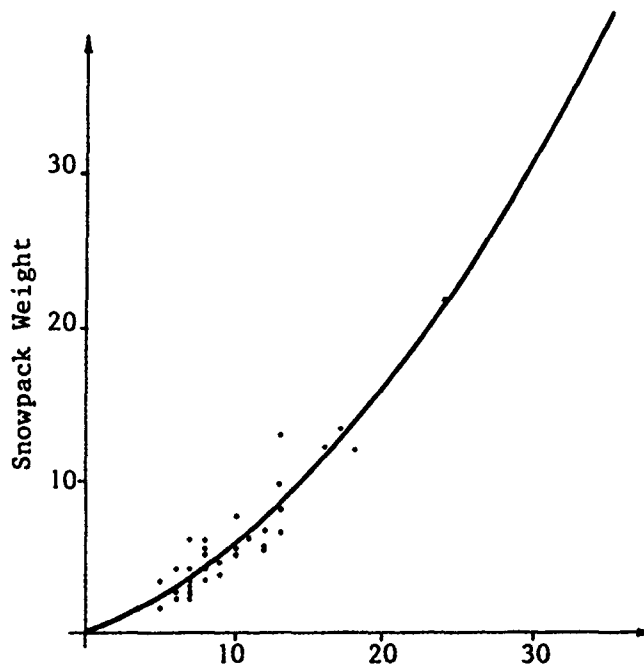
Figure 3   Snow Depth, inches, versus
Snow Weight, pounds per square foot

TABLE 2

58 YEARS OF WATER CONTENT DERIVED FROM DEPTH
AT DENVER, COLORADO

Year (1)	Snow Depth (2)	Relative Density (3)	Water Content inches (4)	Year (1)	Snow Depth (2)	Relative Density (3)	Water Content inches (4)
1893-94	4.8	0.0931	0.45	1922-23	10.5	0.1170	1.23
95	6.0	0.0981	0.59	24	8.5	0.1086	0.92
96	7.5	0.1044	0.78	25	7.8	0.1057	0.82
97	5.5	0.0960	0.53	26	7.0	0.1023	0.72
98	3.7	0.0884	0.33	27	6.0	0.0981	0.59
99	9.8	0.1141	1.12	28	4.8	0.0931	0.45
1899-1900	6.5	0.1002	0.65	29	11.4	0.1208	1.38
01	6.0	0.0981	0.59	30	9.1	0.1111	1.01
02	6.4	0.0998	0.64	31	12.0	0.1233	1.48
03	7.0	0.1023	0.72	32	11.0	0.1191	1.31
04	3.1	0.0859	0.27	33	13.0	0.1275	1.66
05	4.5	0.0918	0.41	34	8.0	0.1065	0.85
06	7.0	0.1023	0.72	35	16.0	0.1401	2.24
07	13.3	0.1288	1.71	36	6.5	0.1002	0.65
08	6.0	0.0981	0.59	37	13.0	0.1275	1.66
09	14.5	0.1338	1.94	38	5.5	0.0960	0.53
10	6.0	0.0981	0.59	39	6.5	0.1002	0.65
11	5.6	0.0964	0.54	40	9.1	0.1111	1.01
12	12.8	0.1267	1.62	41	8.0	0.1065	0.85
13	4.6	0.0922	0.42	42	8.0	0.1065	0.85
14	32.6	0.2098	6.84	43	10.2	0.1157	1.18
15	5.5	0.0960	0.53	44	14.0	0.1317	1.84
16	4.0	0.0897	0.36	45	10.0	0.1149	1.15
17	10.0	0.1149	1.15	46	4.2	0.0905	0.38
18	7.8	0.1057	0.82	47	28.0	0.1905	5.33
19	11.5	0.1212	1.39	48	12.0	0.1233	1.48
20	12.0	0.1233	1.48	49	10.0	0.1149	1.15
21	8.0	0.1065	0.85	50	7.0	0.1023	0.72
22	7.0	0.1023	0.72	51	9.0	0.1107	1.00

Following the review of large storms, it was decided that none of the weight values estimated in Table 2 would be changed. Second order statistics (mean and variance) were calculated for the 80 years of data as well as for overlapping 33 year periods. The values for all groups were quite similar, giving some indication that use of the extended data set is not biasing the analysis. Using the lognormal distribution (as recommended in ANSI A58.1), the following values are obtained:

$$50 \text{ year mri value: } 18 \text{ psf}$$
$$80 \text{ year mri value: } 20 \text{ psf}$$
$$100 \text{ year mri value: } 21 \text{ psf}$$

These values are slightly higher than given in the standard, primarily because the years included in the analysis to develop the standard do not include any of the three largest values. A modern measure of the appropriateness of the probability distribution, the "Probability Plot Correlation Coefficient (PPCC) is 0.983 for the lognormal distribution, indicating a good fit. (See Ellingwood, 1984, or Filliben.) Of more significance, however, is that the recorded values are significantly higher than the values predicted by the lognormal distribution. Such an occurrence is quite unlikely if the lognormal distribution were truly representative of the sample. If we assume the extreme value in any one year is statistically independent from those in other years, we can express the probability that the N year mri value will be exceeded a times by the following expression:

$$P(x > X_N \text{ a times}) = (1/N)^a (1-1/N)^{N-a} \binom{N}{a} \tag{2}$$

where P( ) is the probability and $\binom{N}{a}$ is the binomial coefficient (Benjamin and Cornell). For the 80 year period, this yields probabilities of 0.366, 0.370, and 0.185 for no occurrences, one, and two, respectively. Thus the probability that the 80 year mri value will be exceeded three or more times in an 80 year period is 0.079. In fact, given N years of record, the maximum observed value is a good estimate of the N year mri value (Ellingwood and Redfield, 1983). By both these measures, the lognormal distribution is a very poor model for the Denver data, even though the PPCC indicated a good fit.

Another candidate probability distribution is a Type II distribution of largest values (Ellingwood and Redfield, 1983, 1984). Such a distribution is a three-parameter expression. Selecting successive values of one parameter allows one to calculate the other two by second order statistics. The best set of values can be selected by use of the PPCC. For this data, the result is

$$50 \text{ year mri value} = 25 \text{ psf}$$
$$80 \text{ year mri value} = 31 \text{ psf}$$
$$100 \text{ year mri value} = 35 \text{ psf}$$

The PPCC is 0.990, only slightly better than the PPCC for the lognormal. Other, less sophisticated tests are more meaningful. The 80 year prediction is exceeded one time in the data. Equation 2 would predict a probability of 0.634 that the value would be exceeded one or more times. The maximum value of record is 14 percent more than the predicted value, which is certainly better than the 74 percent difference with the lognormal distribution.

Ellingwood and Redfield (1983, 1984) report a study of 76 first order weather stations in which 38 stations each having 28 years of data were examined to determine the most appropriate probability distribution. They found the lognormal to be the best fit for 34 percent, the log-Pearson Type III for 26 percent, the Type I for 19 percent, and the Type II for 21 percent. They point out that sampling errors inherent in a sample of 28 will lead to misdiagnosis of the best fit distribution; for example they found that 25 percent of lognormal distributions would be identified as Type I. Such errors appear to be very understandable if the real population has a very long upper tail but the sample misses all the points in the upper tail. Consider Figure 4: the distribution used in ANSI A58.1 is a good representation if the three high values are omitted. The most apparent means to avoid such a sampling error is to obtain data samples that cover longer periods of time.

Ellingwood and Redfield also discuss a trend towards shorter tails (such as a Type I distribution) for northern sites where most years show large amounts of snow versus a trend towards longer tails for more southerly sites. They do not reach a conclusion that such a trend should be applied in practice. The effect of using a distribution that shortens the upper tail appears to be quite significant for locations with relatively light amounts of snow, such as Denver.

SUMMARY AND CONCLUSION

Analysis of the record of snow accumulation at the NWS station in Denver, Colorado, has yielded surprisingly large discrepancies from standard practice for estimating ground snow loads for use in design of structures:

Source	50 year mri	100 year mri
Standard A58.1	15 psf	18 psf
Lognormal on extended data	18 psf	21 psf
Type II E.V. on extended data	25 psf	35 psf

This example demonstrates that use of a single probability distribution for predicting ground snow load at all locations can lead to very inadequate estimates for some locations. This is in spite of relatively good estimates of fit by the Maximum Probability Plot Correlation Coefficient which only changed from 0.983 to 0.990 (1.0 being perfect correlation) as the estimate for the 100 year mri value changed by 67 percent.

The example further demonstrates that there is no substitute for a critical examination of the raw data, to compare recorded maxima with predicted values, to examine the validity of the data, and to incorporate as much data as possible.

ACKNOWLEDGEMENT

REFERENCES

ANSI A58.1, Minimum Design Loads for Buildings and Other Structures, American National Standards Institute, Inc., New York, 1982.

Benjamin, Jack R., and Cornell, C. Allin, Probability, Statistics, and Decision for Civil Engineers, McGraw-Hill, Inc., 1970

Ellingwood, Bruce, "Statistical Tests of Environmental Load Data", Journal of Structural Engineering, American Society of Civil Engineers, Vol. 110, No. 6. June 1984.

Ellingwood, Bruce, and Redfield, Robert, "Ground Snow Loads for Structural Design", Journal of Structural Engineering, American Society of Civil Engineers, Vol. 109, No. 4, April 1983.

Ellingwood, Bruce, and Redfield, Robert, "Probability Models for Annual Extreme Water-Equivalent Ground Snow", Monthly Weather Review, American Meteorological Society, July, 1984.

Filliben, J.J., "The Probability Plot Correlation Coefficient Test for Normality", Technometrics, Vol. 17, No. 1, Feb. 1975.
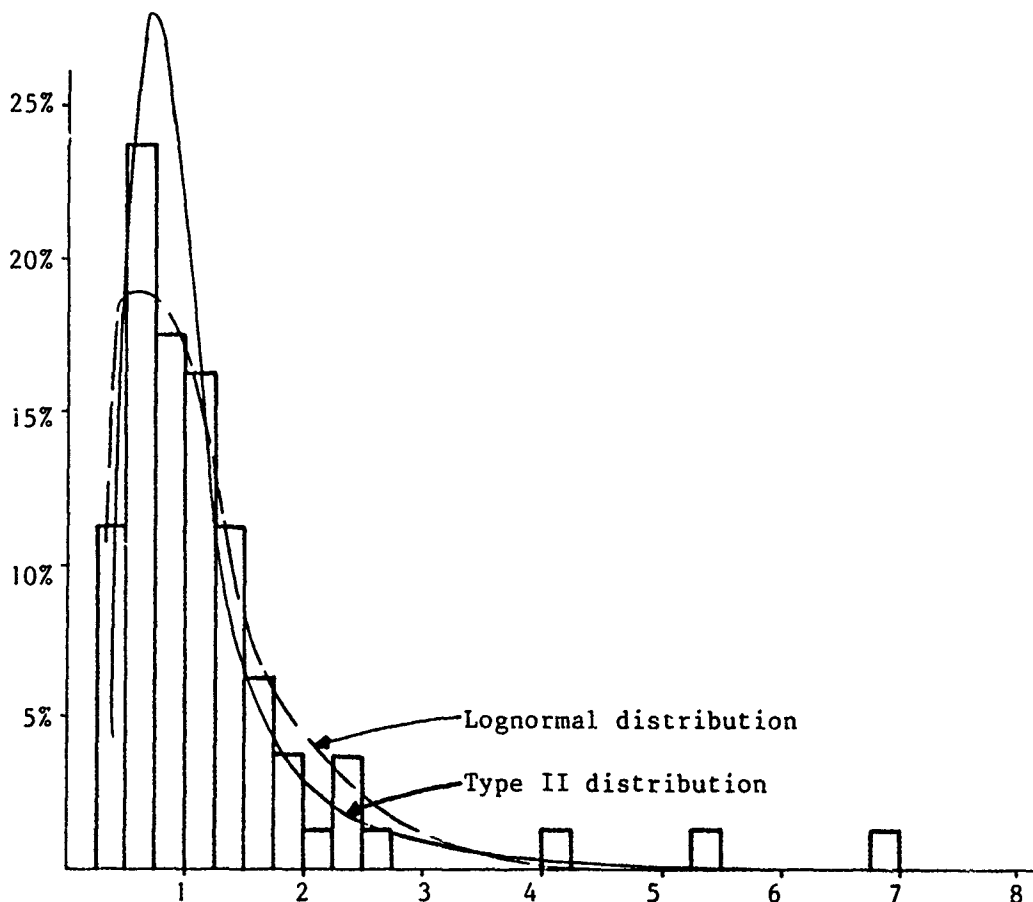
Figure 4   Frequency Diagram for Annual Maxima

24

Statistical Properties of the Annual Maximum Series and a New Approach to Estimate the Extreme Values for Long Return Periods

Masanori Izumi[I], Hirozo Mihashi,[II] and Toru Takahashi[III]

ABSTRACT

Statistical properties of two kinds of annual maximum series are estimated by using five types of probability distribution functions with two plotting techniques. These maximum series are annual maximum snow depth (AMD) and annual maximum increasing intensity of snow depth (AMI), which are observed at 423 weather stations in Japan. The behavior of AMD or AMI at these stations cannot be explained by any sole distribution or sole plotting technique. The proposed method, however, is applicable to almost all stations. In this method, the linear regression analysis is applied only to the maximum 1/3 of the whole data of AMD or AMI on Gumbel probability paper. This method is more reasonable than conventional techniques due to consideration of the snowfall mechanism for the calculation of the values of AMD and AMI for a long return period.

INTRODUCTION

Up to the present, in Japan, the design snow load for buildings has been based on the snow depth because of the lack of data of the snow load itself. For snow depth, the annual maximum snow depth (AMD) has been considered as one of the most important factors. In the U.S., Thom (1966) and Ellingwood et al.(1983) have estimated the statistical properties of annual maximum water equivalent series, and have shown that a log-normal distribution was preferable. On the other hand, in Japan, Maeda (1980) has investigated types I and II extreme value distributions and log-normal distribution for AMD at several points in Hokuriku district, and concluded that the log-normal distribution was available for AMD. Sakurai et al. (1986) analyzed types I, II and III extreme value distributions, normal distribution and log-normal distribution by means of Filliben method, and pointed out that statistical properties of AMD were not explained by any sole distribution. These research works, however, discussed which probability distribution function is appropriate but scarcely considered their behavior on probability paper.

In this paper, not only the behavior of AMD on Gumbel probability paper but also the properties of the population of AMD are studied in order to propose a reasonable method of calculating more appropriate return period values of AMD. Furthermore, in order to take account of the heavy short-term snowfall, the annual maximum increasing intensity of snow depth (AMI) is also investigated. Five types of probability distribution functions are applied with two plotting techniques to AMD and AMI at 423 observation points in Japan.

I.   Professor, Dept. of Architecture, Tohoku Univ., Sendai, Japan
II. Associate Professor, Dept. of Architecture, Tohoku Univ., Sendai, Japan
III. Graduate Student, Dept. of Architecture, Tohoku Univ., Sendai, Japan

METHODS OF ANALYSIS

Daily snow data used in this paper were obtained at the 423 weather stations which belong to the Japan Meteorological Agency (JMA). Five types of probability distribution functions were applied with two plotting techniques, whose distributions are types I, II and III extreme value distributions, normal distribution and log-normal distribution. The plotting techniques are the Thomas plot and the Hazen plot. Then fitness of these distributions is checked by the normalized error given by Eq.1. For a description of the extreme value distribution and plotting method, see Gumbel (1958) or Schuëller (1981).

Normalized Error

For the purpose of verification of fitness for these probability distribution functions, normalized error (NER) is defined as follows:

$$NER = \sqrt{\frac{1}{n} \sum_{i=1}^{n} (x_i - \hat{x}_i)^2} \Big/ \mu_X \tag{1}$$

where x_i is the ith largest observed value, $\hat{x}_i$ is the estimated value of x_i and μ_X is a mean value of the observed series.

Proposed Method

The authors have proposed a method which is available to calculate the values for a long return period in Tohoku district (Izumi et al., 1985). In this method, linear regression analysis is applied to only the maximum 1/3 of the whole data on Gumbel probability paper. In this paper, we study the applicability of the method to all districts in Japan. Though the average number of the observed series is 34 years, the estimated values are almost similar to the values estimated in 1985 by using about 67 years' data.

Type Classification

The authors have proposed the type classification of statistical properties on Gumbel probability paper as shown in Figure 1 (Izumi et al., 1985). The criteria for type classification are as follows:

$$DIF = \frac{(RPV-T100) - (RPV-T100-2)}{RPV-T02}$$

Type A: $-0.2 < DIF < 0.2$
Type B: $DIF \leq -0.2$
Type C: $DIF \geq 0.2$ \qquad (2)

where RPV-T100 is a value for a return period of 100 years, estimated by the type I extreme value distribution. RPV-T100-2 is a value for a return period of 100 years, estimated by the proposed method. RPV-T02 is a value for a return period of 2 years, estimated by the type I extreme value distribution.

STATISTICAL PROPERTIES OF AMD

Figure 2 shows various data exhibited on Gumbel probability paper. Table 1 shows results of judgment by Eq.1. For example, the frame "39＼58" means that there are 97 points whose best fitted distribution is a type III extreme value distribution in a Hazen plot and type I distribution in a Thomas plot. In that frame, 39 points are best fitted in a type III distribution with a Hazen plot, and 58 points are best fitted in a type I distribution with a

Figure 1. Type Classification on Gumbel Probability Paper.

Kagoshima Pref. Miyanojo
Lognormal, Type B

Figure 3. Best Fitted Distribution
Cannot Always Estimate
Reasonable Values
(Gumbel Probability Paper, Hazen Plot).

Yamagata Pref. Shinjo
Normal, type A

Ishikawa Pref. Kanazawa
Lognormal, type A

———— : Extreme Type I
—·—·— : Extreme Type II
———— : Extreme Type III
—··—··— : Normal
·········· : Lognormal
———— : Linear Regression only to
the Maximum 1/3 Data on
Gumbel Probability Paper

Figure 2. Fitting of Probability
Distribution Functions
on Gumbel Probability
Paper (Hazen Plot).

Hokkaido Shizunai
Extreme I, type A

Gifu Pref. Tochio
Extreme II, type B

Aomori Pref. Wakinosawa
Extreme III, type C

Table 1. Appropriate Plotting Methods for the Five Distribution Types.

		Thomas plot				
		Extreme I (225)	Extreme II (44)	Extreme III (94)	Normal (9)	Lognormal (51)
Hazen plot	Extreme I (83)	58\ 21	1\ 3	0\ 0	0\ 0	0\ 0
	Extreme II (21)	1\ 0	19\ 0	0\ 0	0\ 0	1\ 0
	Extreme III (189)	39\ 58	0\ 0	62\ 30	0\ 0	0\ 0
	Normal (11)	0\ 0	0\ 0	2\ 0	9\ 0	0\ 0
	Lognormal (119)	47\ 1	20\ 1	0\ 0	0\ 0	49\ 1

Number of observation points of minimum error [in Hazen plot\in Thomas Plot]
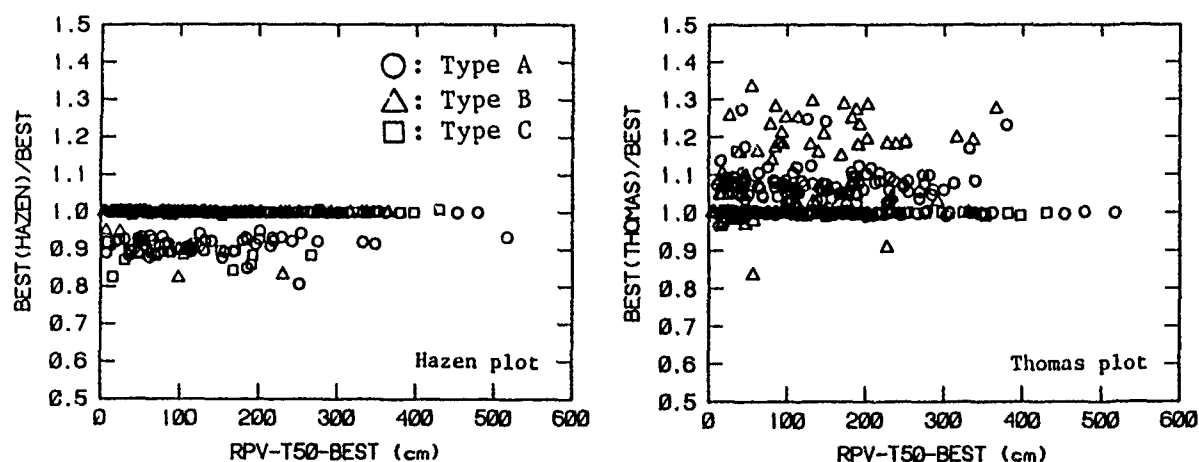
Figure 4. Comparison of Estimated Values of Two Plotting Methods
(Expected Values for Return Period of 50 Years).

Thomas plot. Considering Table 1, one can see that the statistical properties of AMD are not explained by a sole distribution or a sole plotting method.

Values of the best fitted distribution on the basis of assessment by Eq.1 are shown in Figure 4. Estimated values of AMD in a Thomas plot are more scattered compared with those in Hazen plot. Therefore, from now on, we will use a Hazen plot to estimate the extreme values. Figures 5 and 6 show a comparison of the estimated value of each distribution to that of best fitted distribution (including the Thomas plot). The type III distribution, log-normal distribution and/or the proposed method estimate relatively steady values for a return period of 50 years. Considering a return period of 100 years, however, the type III distribution leads the points of type B to be underestimated, while the log-normal distribution leads the points of type B to be underestimated and the points of type C to be overestimated. With the proposed method, the estimated values are sometimes scattered when the values of AMD are small but otherwise quite reasonable. In such a case, as show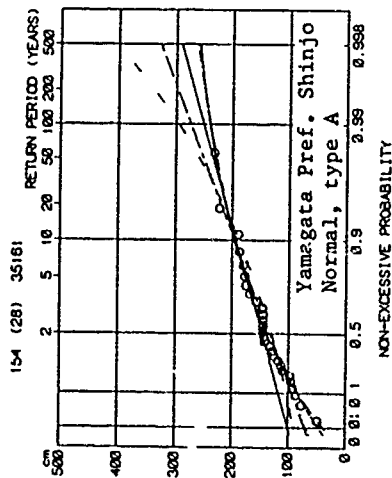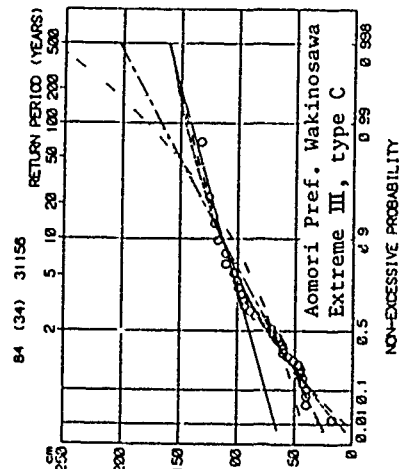n in Figure 3, however, the best fitted distribution does not produce reasonable values at all the cases. Accordingly, the proposed method is best applicable for estimating the extreme values.

STATISTICAL PROPERTIES OF AMI COMPARED WITH AMD

In recent years, buildings have been studied and planned that leave the
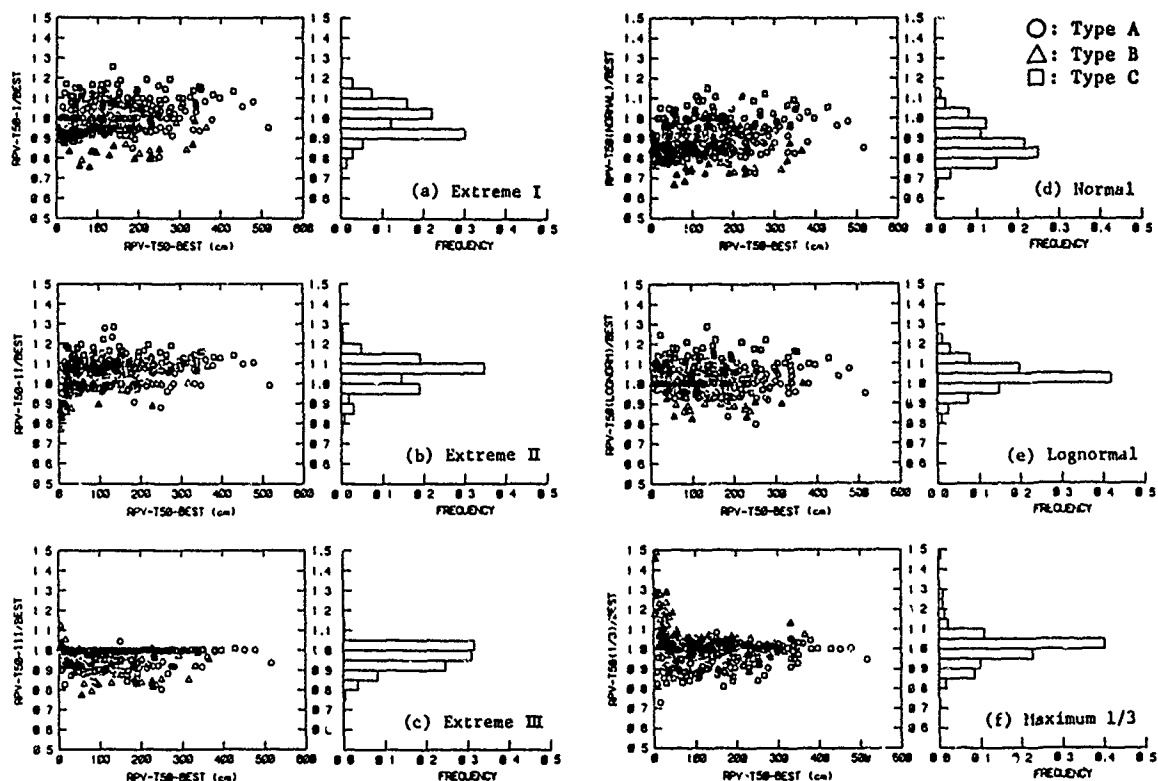
Figure 5. Ratio of Estimated Value to the Best Fitted Distribution
(Expected Values for Return Period of 50 Years, Hazen Plot).
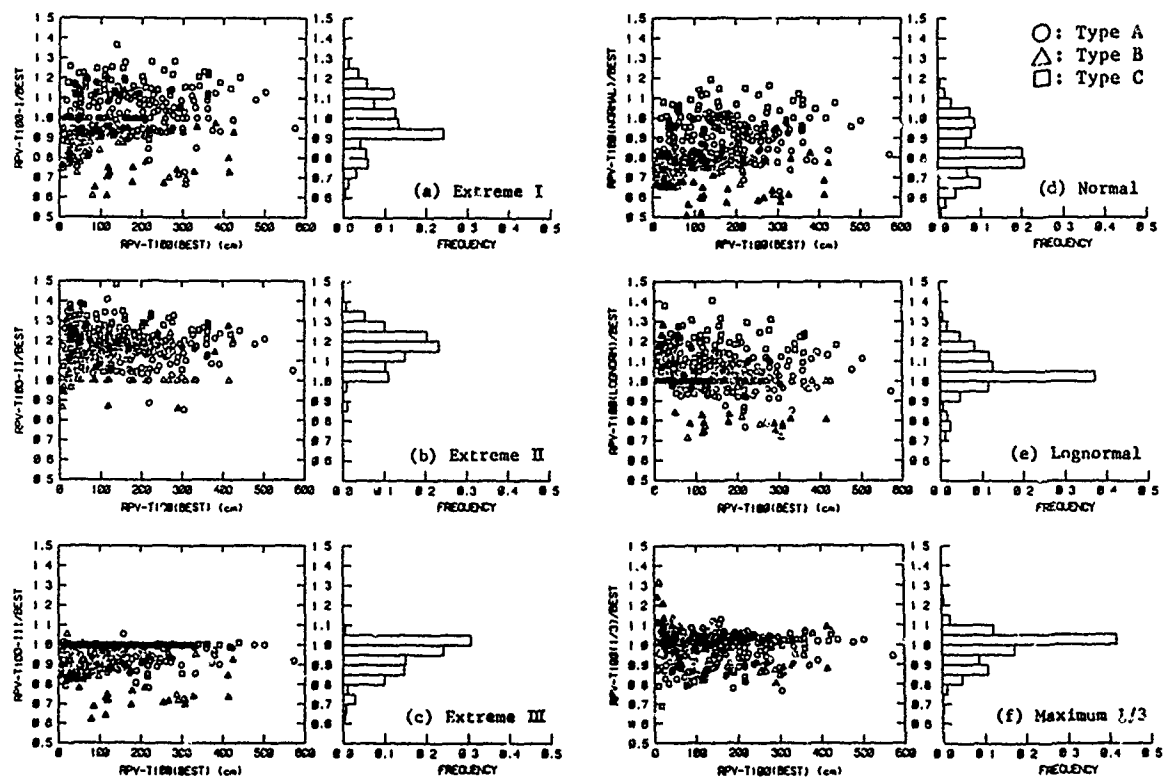
Figure 6. Ratio of Estimated Value to the Best Fitted Distribution
(Expected Values for Return Period of 100 Years, Hazen Plot).

29

snow loads remaining on the roofs or have snow-melting apparatus. In these cases, there is a problem of how to consider heavy short-term snowfall. Murota (1981) defined the annual maximum increasing intensity of snow depth (AMI) in a short term (3 or 7 days). Nevertheless, the behavior of AMI has not been clarified yet. In this paper, the statistical properties and the regional characteristics of the AMI-3 and AMI-7 have been studied by making a comparison with those of the AMD.

Figure 7. Definition of Annual Maximum Increasing Intensity of Snow Depth (AMI).

Definition of AMI

As shown in Figure 7, the increasing depth of snow in a short time period was calculated and the maximum value among snow depth values in the season was taken as AMI.

Cross-Sum of Type Classification in Nine Districts

Ten districts in Japan are shown in Figure 8. Since Tokai does not have any observation point, a cross-sum of the type classification of AMD and AMI-3 of all Japan and a division of nine districts are shown in Table 2. In Hokkaido, ratio of the points of type C or A in AMD and type A or B in AMI-3 are higher than average of all Japan. On the other hand, in Hokuriku, the ratio of the points of type B in AMD and type A or C in AMI-3 are higher than the average of all Japan. These results show the difference of snowfall mechanisms among the districts in Japan.

Relation Between AMD and AMI

Figure 9 shows relations between AMD and AMI-3 in mean values. In Hokkaido, a value of AMI-3 corresponding to a given value of AMD is smaller than in Hokuriku. In Figure 10, on the other hand, the difference of expected values for a return period of 50 years of Hokkaido and Hokuriku is not clear. In Hokkaido, many points are classified to type B in AMI-3. Therefore the values of return period of 50 years are large in comparison to their mean values. The reason may be that small-scale low pressure sometimes appears on the west coast of Hokkaido and brings heavy snow in a short term (Muramatsu,1975).

Spearman's Correlation Coefficient

At an observation point, the year of large AMI does not necessarily accompany with large AMD. Then Spearman's correlation coefficient between AMD and AMI-3 was calculated as shown in Figure 11. The coefficient is small in points whose coefficient of the variation of AMI-3 is small. In Hokkaido the coefficient is smaller than in Hokuriku. This result means that a low pressure shown above is not always to cause the increase of AMD.

Comparison of AMD, AMI-3 and AMI-7

Two antithetical examples on Gumbel probability paper are shown in Figure 12. In Hokkaido, because of low temperature, AMD becomes large at the end of

30
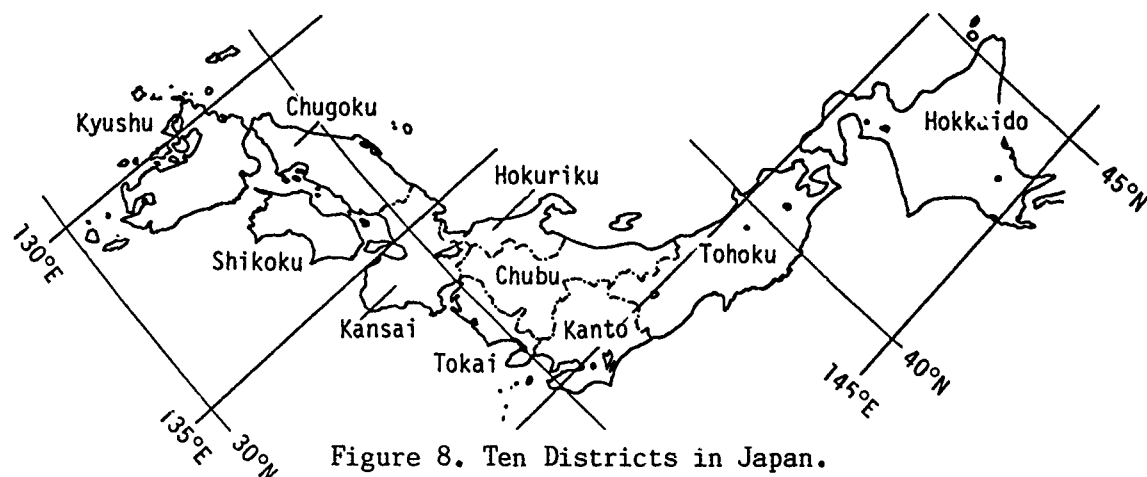
Figure 8. Ten Districts in Japan.

Table 2. Cross-Sum of Type Classification (Hazen Plot).

Table 2-1. Cross Sum of Type Classification

All Japan		AMI−3*2			Total
		Type A	Type B	Type C	
AMD*1	A	150 (35.5)	27 (6.4)	25 (5.9)	202 (47.9)
	B	25 (5.9)	91 (21.5)	8 (1.9)	124 (29.3)
	C	47 (11.1)	7 (1.7)	43 (10.2)	97 (22.9)
Total		222 (52.5)	125 (29.6)	76 (18.0)	423 (100.0)

Table 2-2. Cross Sum of Type Classification

Hokkaido		AMI−3			Total
		Type A	Type B	Type C	
AMD	A	41 (50.6)	10 (12.3)	6 (7.4)	57 (70.4)
	B	1 (1.2)	4 (4.9)	0 (−)	5 (6.2)
	C	8 (9.9)	5 (6.2)	6 (7.4)	19 (23.5)
Total		50 (61.7)	19 (23.5)	12 (14.8)	81 (100.0)

Table 2-3. Cross Sum of Type Classification

Tohoku		AMI−3			Total
		Type A	Type B	Type C	
AMD	A	34 (34.0)	11 (11.0)	5 (5.0)	50 (50.0)
	B	4 (4.0)	11 (11.0)	0 (−)	15 (15.0)
	C	20 (20.0)	2 (2.0)	13 (13.0)	35 (35.0)
Total		58 (58.0)	24 (24.0)	18 (18.0)	100 (100.0)

Table 2-4. Cross Sum of Type Classification

| Kanto		AMI−3			Total
		Type A	Type B	Type C	
AMD	A	13 (56.5)	1 (4.3)	0 (−)	14 (60.9)
	B	0 (−)	6 (26.1)	1 (4.3)	7 (30.4)
	C	1 (4.3)	0 (−)	1 (4.3)	2 (8.7)
Total		14 (60.9)	7 (30.4)	2 (8.7)	23 (100.0)

Table 2-5. Cross Sum of Type Classification

Chubu		AMI−3			Total
		Type A	Type B	Type C	
AMD	A	23 (36.5)	3 (4.8)	4 (6.3)	30 (47.6)
	B	3 (4.8)	7 (11.1)	0 (−)	10 (15.9)
	C	16 (25.4)	0 (−)	7 (11.1)	23 (36.5)
Total		42 (66.7)	10 (15.9)	11 (17.4)	63 (100.0)

Table 2-6. Cross Sum of Type Classification

Hokuriku		AMI−3			Total
		Type A	Type B	Type C	
AMD	A	12 (50.0)	0 (−)	1 (4.2)	13 (54.2)
	B	2 (8.3)	5 (20.8)	3 (12.5)	10 (41.7)
	C	1 (4.2)	0 (−)	0 (−)	1 (4.2)
Total		15 (62.5)	5 (20.8)	4 (16.7)	24 (100.0)

Table 2-7. Cross Sum of Type Classification

Kansai		AMI−3			Total
		Type A	Type B	Type C	
AMD	A	10 (47.6)	1 (4.8)	3 (14.3)	14 (66.7)
	B	1 (4.8)	2 (9.5)	0 (−)	3 (14.3)
	C	0 (−)	0 (−)	4 (19.0)	4 (19.0)
Total		11 (52.4)	3 (14.3)	7 (33.3)	21 (100.0)

Table 2-8. Cross Sum of Type Classification

Chugoku		AMI−3			Total
		Type A	Type B	Type C	
AMD	A	11 (22.0)	1 (2.0)	5 (10.0)	17 (34.0)
	B	12 (24.0)	9 (18.0)	4 (8.0)	25 (50.0)
	C	1 (2.0)	0 (−)	7 (14.0)	8 (16.0)
Total		24 (48.0)	10 (20.0)	16 (32.0)	50 (100.0)

Table 2-9. Cross Sum of Type Classification

Shikoku		AMI−3			Total
		Type A	Type B	Type C	
AMD	A	4 (13.8)	0 (−)	1 (3.4)	5 (17.2)
	B	0 (−)	21 (72.4)	0 (−)	21 (72.4)
	C	0 (−)	0 (−)	3 (10.3)	3 (10.3)
Total		4 (13.8)	21 (72.4)	4 (13.8)	29 (100.0)

Table 2-10. Cross Sum of Type Classification

Kyushu		AMI−3			Total
		Type A	Type B	Type C	
AMD	A	2 (6.3)	0 (−)	0 (−)	2 (6.3)
	B	2 (6.3)	26 (81.3)	0 (−)	28 (87.5)
	C	0 (−)	0 (−)	2 (6.3)	2 (6.3)
Total		4 (12.5)	26 (81.3)	2 (6.3)	32 (100.0)

※ Number of Observation Points (Percentage)

*1 AMD : Annual Maximum Snow Depth
*2 AMI−3 : Annual Maximum Snow Depth Increase Intensity

31
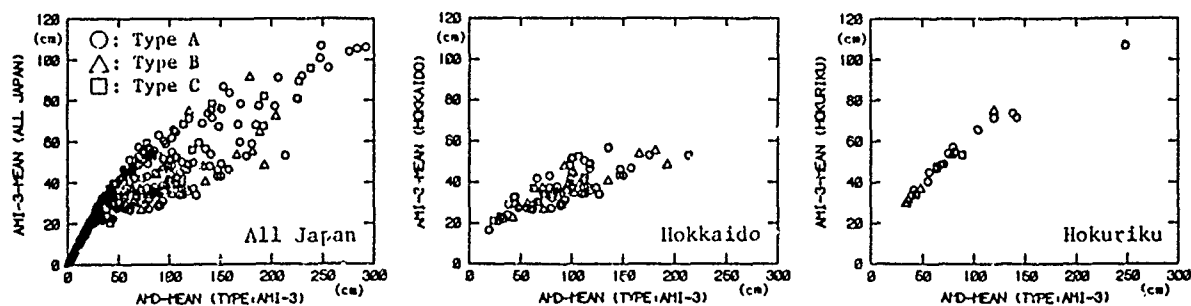
Figure 9. Relation Between AMD and AMI-3 (Mean Values).
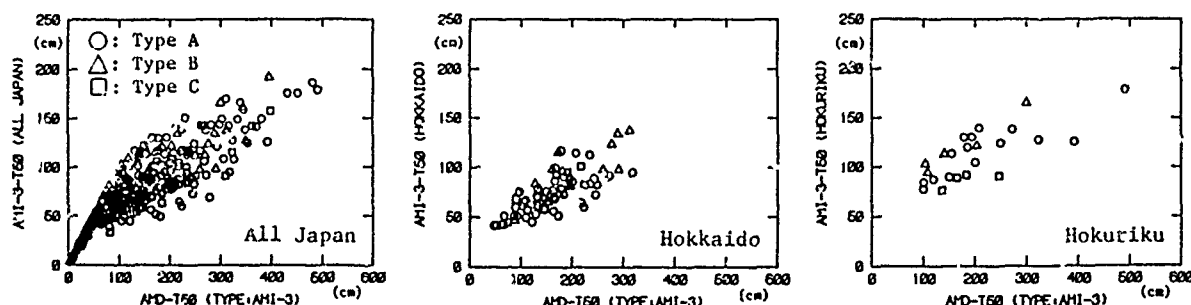
Figure 10. Relation Between AMD and AMI-3
(Expected Values for Return Period of 50 Years).
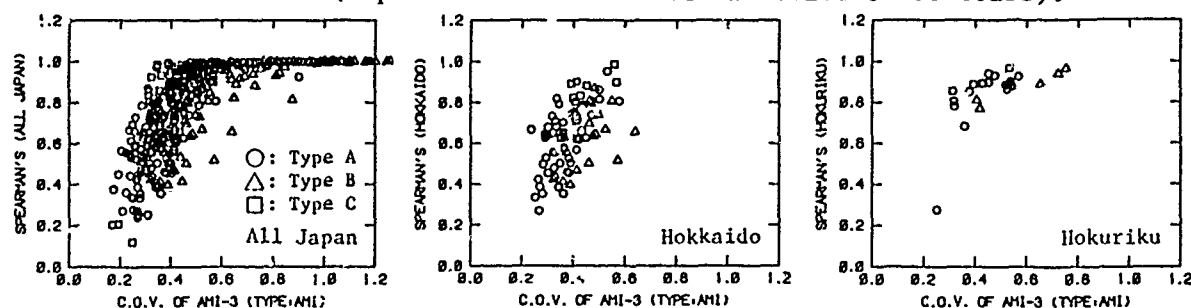
Figure 11. Spearman's Correlation Coefficient.

winter in spite of small AMI. This is one of the reasons that the Spearman's correlation coefficient is small in Hokkaido. In such a comparatively warmer and heavier snow area as Hokuriku, though it seems that the value of AMI-3 has a upper limit, continuous snowfall almost directly leads to the value of AMD.

SNOWFALL MECHANISMS IN JAPANESE REGION

Under the condition of Figure 13(a) and Figure 14, the Japan Sea side has heavy snow in winter. On the other hand, as shown in Figure 13(b), the Pacific Ocean side sometimes has heavy snow at the end of winter. Observation points on the Pacific Ocean side tend to have type B data, because these low pressures come near capriciously. Therefore, snowfall mechanisms get complicated, especially at the points of type B. In other words, the snowfall mechanism for long return periods is different from that of average year. This is one more reason for the applicability of the proposed method.

CONCLUSIONS

Although the behavior of AMD cannot be explained by any sole distribution or sole plotting technique, the proposed method is applicable to almost all

Figure 12. Comparison of AMD, AMI-3 and AMI-7
(Gumbel Probability Paper, Hazen Plot).
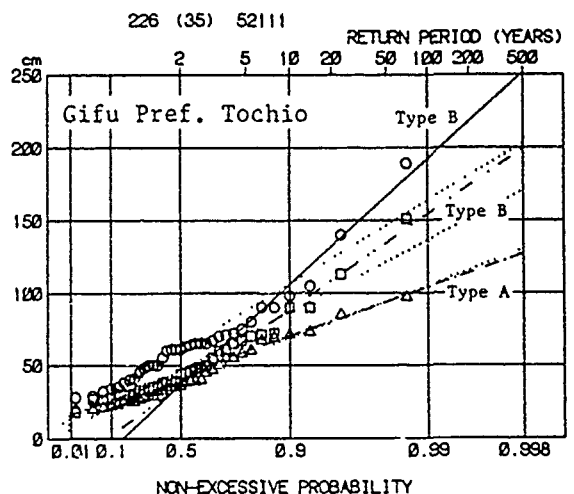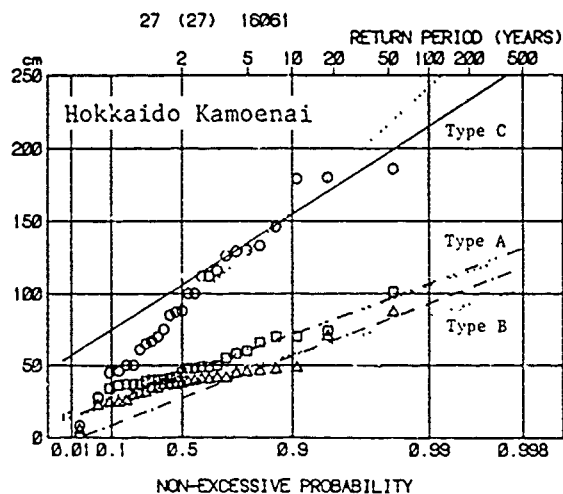
(○: AMD, △:AMI-3, □:AMI-7)

Extreme Type I (AMD,AMI-3,AMI-7)
AMD ⎫ Linear Regression only to
AMI-3 ⎬ the Maximum 1/3 Data on
AMI-7 ⎭ Gumbel Probability Paper
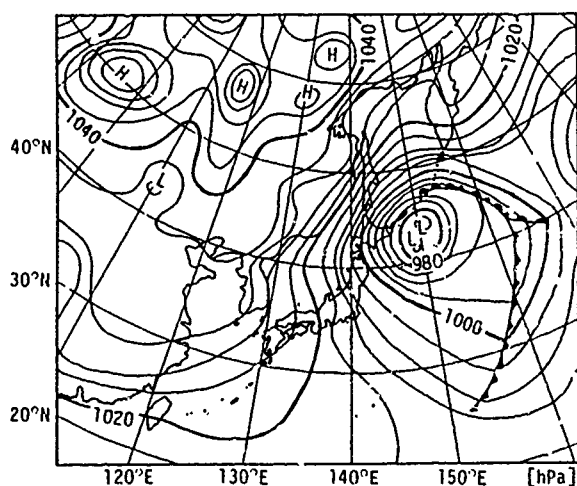
(a) Typical Winter Pressure Pattern
January 25, 1974 (JMA, 1974)
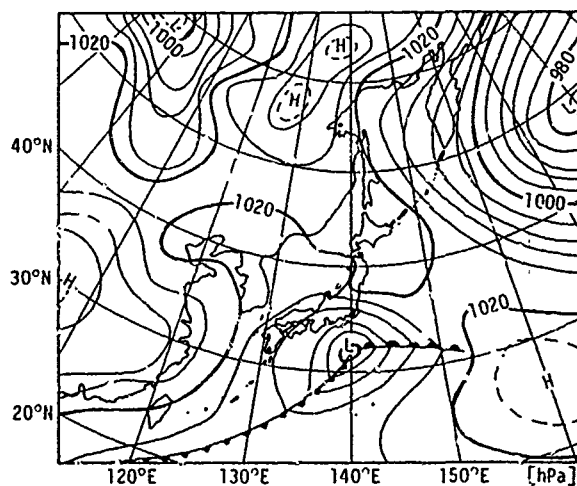
(b) Low Pressure at Southern Coast
March 27, 1974 (JMA, 1974)

Figure 13. Weather Maps Causing Heavy Snow.
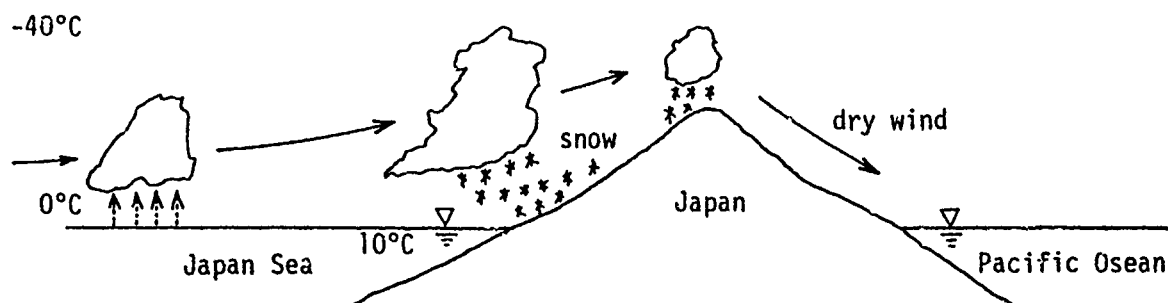
Figure 14. One of the Typical Snowfall Mechanisms in Japan
Coresponding to Figure 13 (a).

33

points. In the method, the linear regression analysis is applied only to the maximum 1/3 of whole data set of AMD or AMI on Gumbel probability paper. Moreover, this method can be said to be more reasonable than the others for calculating the values of AMD and AMI for a long return period when the snowfall mechanism is considered.

The behavior of snow depth increasing intensity in a short term (3 or 7 days) was studied by using the daily snow depth data. By means of the classification of types of the statistical property on Gumbel probability paper, it was interpreted logically that regional differences of statistical characteristics of AMI-3, AMI-7 and AMD are caused by regional differences of snowfall mechanisms.

ACKNOWLEDGMENTS

REFERENCES

Ellingwood, B. and R. Redfield, 1983, "Ground Snow Loads for Structural Design", Journal of Structural Engineering, Vol.109, No.4, 950-964, April 1983

Gumbel, E.J., 1958, Statistics of Extremes, Columbia Univ. Press, New York.

Izumi, M., H. Mihashi, T. Takahashi, K. Konno, 1985, "Statistical Properties of the Annual Maximum Snow Cover Depth in Tohoku District", Journal of Structural Engineering, Vol.31B, 73-80, March 1985 (in Japanese with English abstract).

Japan Meteorological Agency, 1974, "Geophysical Review, No.893, January 1974" and "Geophysical Review, No.895, March 1974", Japan Meteorological Agency, Tokyo (in Japanese).

Maeda, H., 1980, "Extreme Value Distribution of Snowcover Depth", Bulletin of Fukui Institute of Technology, Vol.10, 23-31, 1981 (in Japanese with English Abstract).

Muramatsu, T, S. Ogura and N. Kobayashi, 1975, "The Heavy Snowfall Arisen from Small Scale Cyclone on the West Coast of Hokkaido Island", TENKI, Vol.22, No.7, July 1975 (in Japanese).

Murota, T., 1981, "Reduction of Roof Snow Load due to Snow-Removal Works", Report of the Building Research Institute, No.96, 1981, Building Research Institute, Ministry of Construction (in Japanese with English Abstract).

Sakurai, S., H. Fujita, O. Jo, T. Shibata, 1986, "Statistical Analysis of Annual Extreme Ground Snow Loads after Filliben (part 2)", Summaries of Technical papers of Annual Meeting B, 41-42, Architectural Institute of Japan, August 1986 (in Japanese).

Schuëller, G.I., 1981, Einführung in die Sicherheit und Zuverlassigkeit von Tragwerken, Wilhelm Ernst & Sohn, Berlin/München (in German, Translated into Japanese: Maruzen, Tokyo).

Thom, H.C.S., "Distribution of Maximum Annual Water Equivalent of Snow on the Ground", Monthly Weather Review, Vol.94, No.4, 265-271, April 1966.

Snow Load and Snow Load Design in Hungary

Kármán Tamás[1]

ABSTRACT

This paper presents the results of a survey based on a long-term observation of snow parameters in Hungary. It has been found that highest snow loads usually develop as a result of a single enormous snowfall and not as the outcome of a long-term snow accumulation. The empirical distribution of snow depth winter maximum can be well followed by the type I Gumbel extreme value distribution. The paper also presents special safety considerations of the Hungarian Standard concerning snow load on light-weight structures and the unified algorithm given in the Standard in order to take into account the rearrangement of snow-mass on any kind of roof.

INTRODUCTION

Hungary has a special geographical location between continental and Mediterranean climates in the temperate zone of Europe. Therefore it is interesting to study characteristics of snow, the formation process of maximum snow load and the theorem of its statistical distribution. These characteristics may not necessarily be similar to the characteristics of snow in big-snow northern countries.

The importance of snow load research in Hungary is also stressed by unfavourable experiences obtained in connection with snow on light-weight structures. This type of structure, coming in the seventies into general use, showed at first a relatively high rate of failure under snow.

In Hungary there is fortunately a network of meteorological stations having sufficiently reliable snow depth measuring data convenient for a statistical analysis. This paper is based first of all on these meteorological observations.

DISTRIBUTION OF WINTER MAXIMUM

Figure 1 shows the geographical sites of the meteorological stations, the snow measurements of which were taken into account in this study. They are 172 stations having snow observations all together 5030 station-winters.

The average distribution deduced from winter maximum snow depth distributions of each station can be seen in Figure 2, where the straight line shows the type I Gumbel extreme value distributi-

I. Prof.Dr.tech.C.E.,S.E., M.E., Institute of Building Science, Budapest, Hungary

on (Eq.2),

$$F(x) = \exp\left[-\exp\left(-\frac{\widetilde{\pi}}{\sqrt{6}} \frac{x-m}{s} - c\right)\right] \tag{1}$$

and the other curve represents the Gaussian normal distribution (Eq.2),

$$F(x) = \frac{1}{s\sqrt{2\pi}} \int_{-\infty}^{x} \exp\left[-\frac{1}{2}\left(\frac{x-m}{s}\right)^2\right] dx \tag{2}$$

From this figure it is obvious that the empirical distribution can be well followed by the Gumbel distribution, which is very easy to manage in engineering practice because the maximum of a longer period T years has the same type of distribution as the yearly maximum with the same standard deviation but with a higher mean value as follows (eq.3):

$$m_T = m + \frac{\sqrt{6}}{\pi} s \ln T \tag{3}$$

Any quantil belonging to the non-exceeding probability F can also be defined by the simple formula (Eq.4):

$$x_F = m - \frac{\sqrt{6}}{\pi} s \left[\ln(-\ln F) + c\right] \tag{4}$$

SNOW DENSITY

The study of meteorological data concerning days and processes preceding the occurence of maximum snow shows that snow load in Hungary must not be taken into account as if it were a reduced snow load of big-snow countries. The so-called "old snow" having a density at about 220 kg/m^3 amounts to not more than 60% of the maximum snow depth on the ground, and at least 40% comes from uncommonly large snowfalls as "fresh snow" having a lower density at about 100 kg/m^3. Moreover, old snow usually has a considerable loss from the roof. Therefore, the ratio of old snow depth to the new one is about 50-50% and so the average density of a large snow accumulation takes the value of about 160 kg/m^3 (10 pcf).

SAFETY

According to the Hungarian standard, design values of permanent loads and live loads are their 95% fractile. This means that the non-exceeding probability of a load combination including dead load and live load together is expected to be generally at about 99%.

Generally, but there are special cases. For instance, for light-weight structures where dead load isn't significant and the probability of load combination will be determined by probability level of snow load alone, which therefore must have a non-exceeding probability of 99% in order to obtain the same safety level. It

needs a complementary safety factor (γ_c) for snow on light-weight structures according to the Hungarian estimation $\gamma_c = 1.25$.

REARRANGEMENT OF SNOW ON ROOF

It is well-known that the regulations of most countries specify the use of many factors for every kind of roof profile in order to take into account the effect of snow accumulation on roof valleys and this creates considerable diffuculties, especially in computer-aided design.

According to the Hungarian Standard increasing snow load in any kind of roof valley can be determined automatically with a unified algorithm as Figure 3 shows.

The first step of the algorithm is to draw the basic snow profile on the roof where basic snow depth is 80% of observed ground-snow, usually $h_0 = 0.5$ m, but it increases with altitude above sea level and decreases with the rise of the roof. Then the second step is to assume that the whole snow profile valley will be filled by snow carried by wind. As a third step, the first two steps must be checked and corrected so that

- Snow-depth at the bottom must not be higher than 3 h_0,
- Snow profile should not be steeper than 60^0,
- Inclination of the carried snow profile to the roof must be at least 30^0.

The snow profile constructed on this way will be multiplied by a density of 160 kg/m^3 and this gives the snow load that must be taken into account in design.

REFERENCES

Year-books of the Central Institute of Meteorology of the Meteorological Service of the Hungarian People's Republic. Pt.3., Climatological data. Budapest 1962, 1963, ... 1984.

Silva Lame, R.A., 1954, "Os extremos de amostras ocasionaise suas aplicacoes a engenheria," Sao Paulo, Brazil.

Gumbel, E.J., 1960, "statistics of Extremes," Columbia University Press, New York.

Schriever, W.R., and Otstavnov, V.A., 1967, "Snow Loads," CIB Report no.9. 1967.

Kármán, T.G., 1974, "Snow Loads in Hungary," CIB 6th Congress, Congress Book Volume II. 112-120. 1974. Budapest, Hungary.
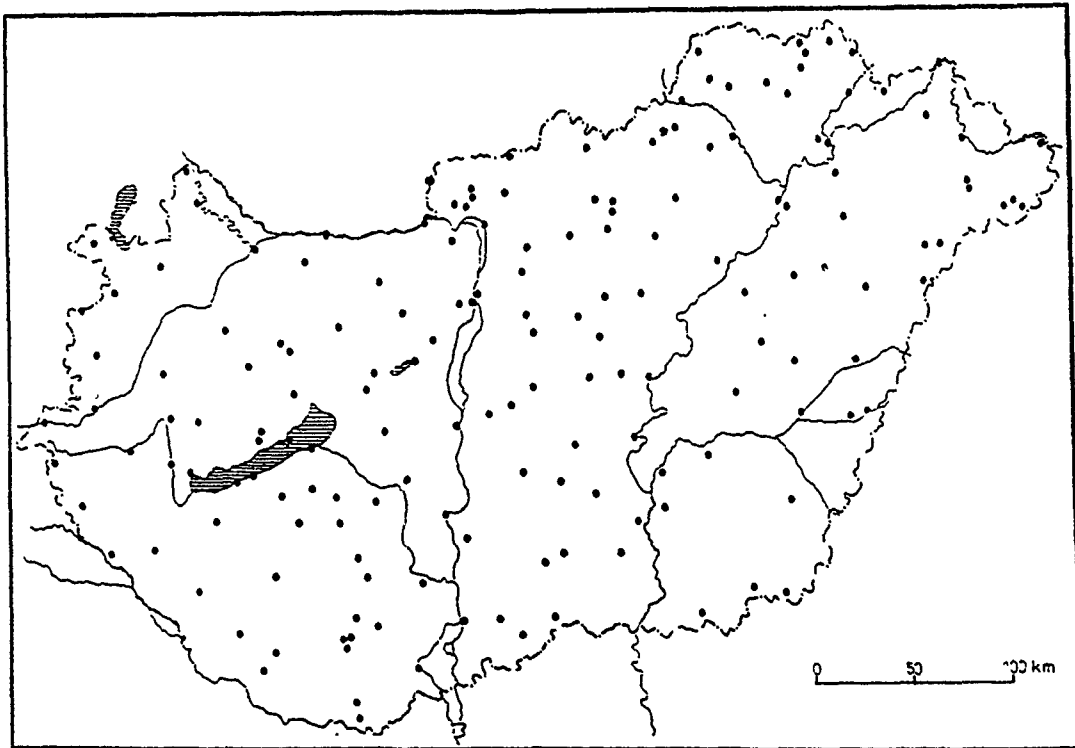
Figure 1 The meteorological stations
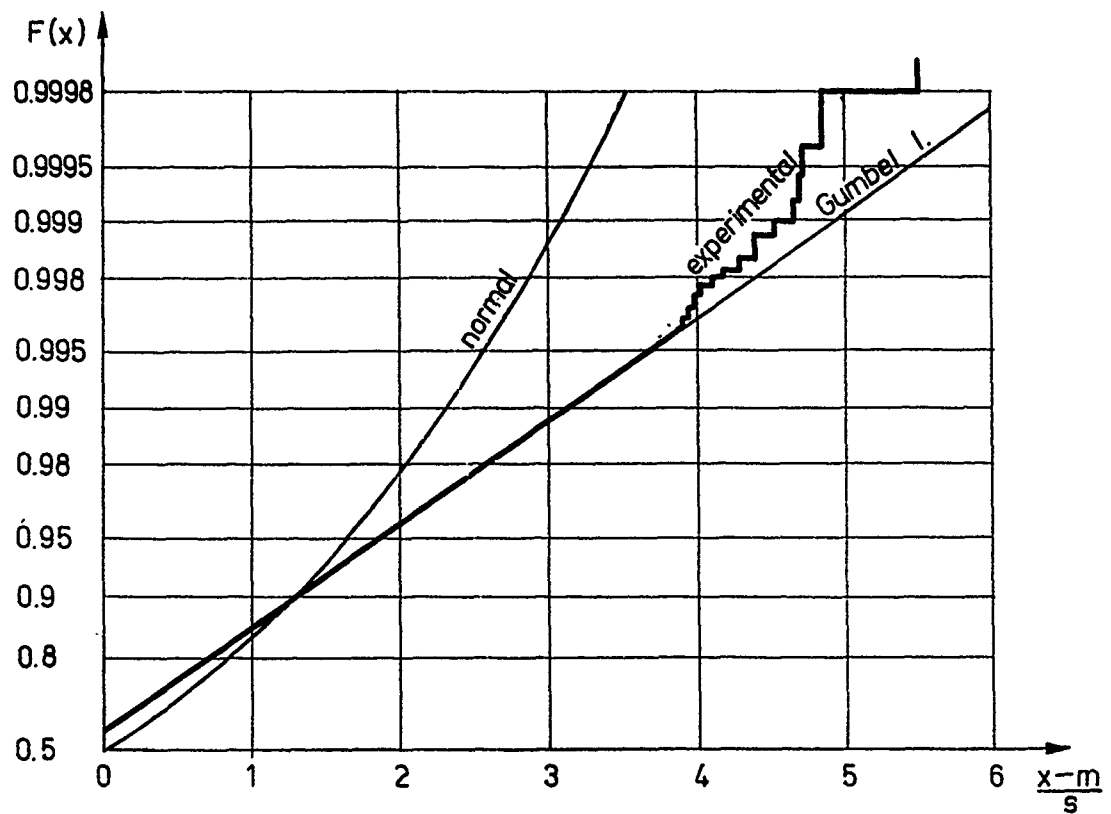
Figure 2 Distribution of extreme values
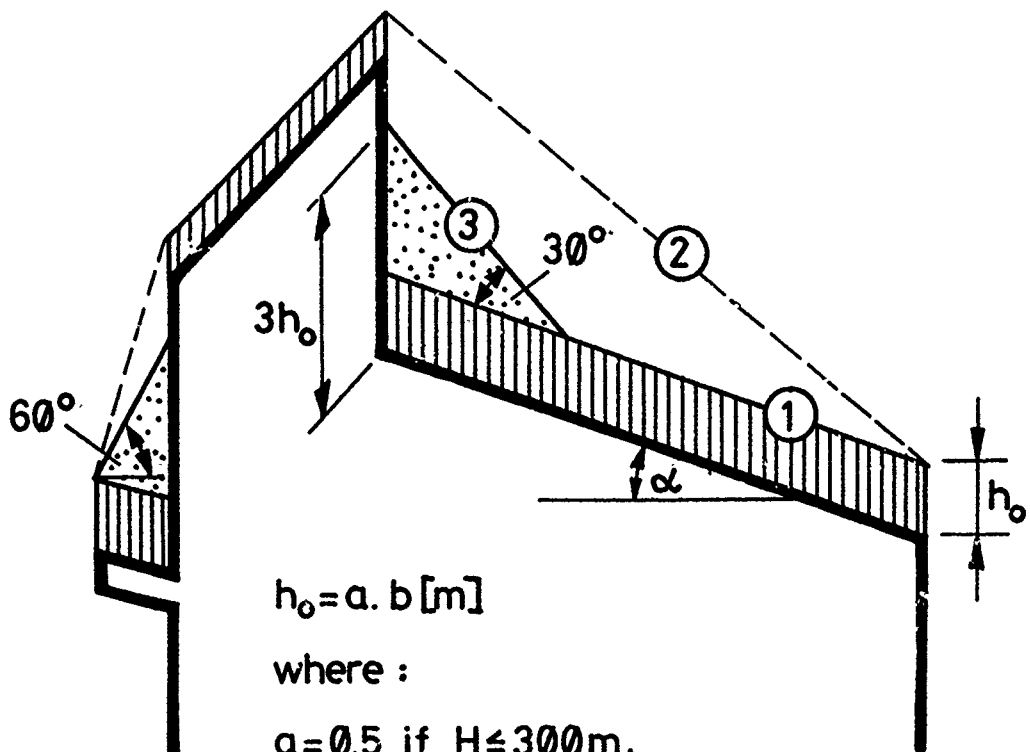
$$h_o = a \cdot b \ [m]$$

where :

$a = 0.5$ if $H \leq 300m$,

$a = \dfrac{100 + H}{800}$ otherwise,

$b = 1$ if $\alpha \leq 30°$

$b = \dfrac{60 - \alpha}{30}$ if $30° < \alpha < 60°$

$b = 0$ otherwise

Figure 3 Snow accumulation

Ground Snow Loads for the 1990 National Building Code of Canada

M.J. Newark[1], L.E. Welsh,[1] R.J. Morris,[1] and W.V. Dnes[1]

ABSTRACT

The last systematic recalculation of ground snow loads in the Supplement to the National Building Code of Canada was made in 1977 and used data up to 1975. Data from three times as many stations are now available and there is also an extra 10 years of record. Using this expanded data base, ground snow loads have been recalculated for the 1990 Supplement.

Several changes in methodology have been utilized, the most significant of which is the use of an objective technique to estimate ground snow loads at Code (or other)locations. It explicitly incorporates an assumed dependence of the snow load on topographical elevation, and accounts for the magnitude of errors at snow depth observation sites.

Results show an average national decrease of 6.6% in the 1990 loads compared to those in the 1985 Supplement. A regional exception is in the Northwest Territories where the use of a greater snow density has led to an average increase of about 16% in the loads. A reduction in the standard deviation about the mean load suggests a more spatially consistent set of values for the 1990 Supplement.

INTRODUCTION

In Canada, ground snow loads are used as a basis for the determination of the roof snow loads. Therefore, they form part of the basic climatic information needed for building design and are given in Chapter 1 of the Supplement to the National Building Code of Canada (National Research Council, 1985). The total ground snow load can be divided into two components, namely: (a) the snow component S_s which is based on a return period of 30 years; and (b) the rain component S_r which accounts for wetting of the snow by rain. In order to revise the 1990 issue of the Code, these values have been calculated as described in this paper.

A number of specific changes in data and procedures have occurred since they were last recalculated in 1977. Firstly, more data is now available, thus providing a number of new stations as well as a longer period of record at many of the stations used previously. Secondly, variables such as snow density and the melting index have been re-examined. Thirdly, a different method of fitting the time series of

---

1. Atmospheric Environment Service
   4905 Dufferin Street, Downsview, Ontario, Canada. L6W 1W5

annual maximum snowdepths at a station to the extreme value distribution has been used. Fourthly, the method of obtaining the rain component has been changed.

Locations listed in the Supplement are not coincident with climatological stations and therefore a procedure is required to estimate the load and its errors at a given point from nearby data. It should be noted that even if a Code location and a climatological site were co-located, such a procedure would still be necessary for reasons concerning errors in the data. The process by which the required design values, S_s and S_r, for Code locations are determined from data at surrounding climate sites is called the codification procedure. The mainly objective technique used in the current analysis constitutes a significant change from methodologies employed previously.

LOAD CALCULATIONS

For the 1990 Code, the load at a location with observations of snow depth is calculated by the same general means as in the 1977 Code (the last time ground snow loads were recalculated). This involves;

(a) the estimation of a 30-year return period maximum snow depth from a mathematical model, namely the Type 1 (Gumbel) extreme value distribution. A modified method of least squares was previously used to fit the distribution to the observed annual maxima, however a number of investigators (Watt and Nozdryn-Plotnicki,1980; Cunnane, 1978; Lowery and Nash, 1970) have shown that this introduces a bias, while the method of moments is not only practically unbiased but is also a more efficient fitting technique. Hence the method of moments was used to fit the data in the present work.

(b) the conversion of the 30-year depth to a load (SL) by means of an assumed snow density, and a correction factor as indicated in the following equation;

[1] $SL = 0.01 \times \gamma \times Y(T) \times d$ kPa

where the unit weight of snow γ (kPa/m) $= g\rho$
        g is the acceleration due to gravity (km/sec^2)
        ρ is the average density of the annual snowpack (kg/m^3)
        Y(T) is the T-year return period maximum snow depth
        d is the melting index (dimensionless)

The use of a varying density value appears to be more realistic than the previous practice of using a fixed value of 200kg/m^3. Therefore average values of the seasonal snowpack density were derived from snow course data and mapped for different regions across the country as described by Newark (1934), and an appropriate value was assigned to each climatological station. The density values range approximately from 200 to 500 kg/m^3. Typically the values average 205 kg/m^3 east of the continental divide (except 300 kg/m^3 north of the treeline), and range from 260 to 430 kg/m^3 to the west of the divide.

The difference in the frequency of snowdepth measurement between stations which make daily observations, and stations which make observations only at the end of the month cause the values of (SL) calculated from the two types of data to be incompatible. This is because thawing episodes can radically change the snowdepth during the course of a month in regions with mild winter climates. The maximum annual snowdepth as determined from month-end data is usually an underestimate compared to that obtained from daily data. The factor d (or melting index described by Newark,1984) is used to adjust the magnitude of the annual maxima derived from month-end data in order to compensate for this difference. In the case of maximum annual snowdepth values derived from data measured daily, $d = 1.0$ in the calculation of SL.

SNOW COMPONENT S_s

It is important to note that S_s is not the load SL at an observation point. It is instead the code value for a specified location which is very unlikely to be at the observation location. The way in which S_s is calculated for the 1990 Code represents a significant change from previous procedures. A mainly objective technique was used as follows;

(a) By means of the following equation, the loads calculated at observation locations were normalized to mean sea level to reduce the effects of elevation on load variability;

[2] $normalSL = SL - bZ$

where normalSL = SL normalized to mean sea level (kPa)
           Z = location elevation above mean sea level (m)
           b = change of SL with elevation (kPa/m)

Schaerer (1971) and others have shown that a quadratic relationship exists between snow load and elevation in regions with wet climates, but the change with height is nearly linear in dry, cool regions. It is considered that a linear relationship in the form of Eq. [2] is a reasonable approximation in dry interior climates, or at a low elevation range in moist climates.

The value of b (the rate of change of snow load with elevation) was derived from a map based on the following assumptions: (i) the parameter varies in a continuous fashion except along the edges of extreme elevation gradients (for example the Rocky Mountain foothills); (ii) a range of 0.001 to 0.008 kPa/m is appropriate (Claus, 1981; Dingman et al, 1978; and Martinec, 1977); (iii) values are lowest in regions where there is little snowmelt and little winter rain; (iv) values are highest in regions where relatively more of the total precipitation falls as rain at lower elevations.

To aid in the construction of the map, the country was divided into regions and the factors which influence b were assessed for each one. The three most important factors are seasonal snowmelt; the proportion of

42

precipitation that falls as snow; and the elevation range. These were evaluated by examining such indicators as the number of degree-days above 0°C for the winter season (December to March), the seasonal proportion of snowfall relative to total precipitation, and the elevation range.

(b) From the normalized values, a new weighted set was calculated at grid points taking into account distance, sampling error, site error, and climatological representativeness as follows;

$$[3] \quad gridSL = \sum_{i=1}^{i=N} \{normalSL/(D_i^2+E_i^2+F_i^2)\}/ \sum_{i=1}^{i=N} \{G_i/(D_i^2+E_i^2+F_i^2)\}$$

where the weighting factors are as follows:
    distance weighting $(D_i) = 0.002$ (km^{-1}) x L (km)
        and L = distance of station from grid point
    sampling error weighting $(E_i) = S(SL_i)/SL_i$
    site representativeness weighting $(F_i) = 0.4$
    climatological representativeness weighting (G_i) ranges from 0 to 1

The merits of each contributing climatological station value of normalSL are accounted for in this way because stations closest to the grid point, and/or with the smallest errors are weighted the most.

At each grid point it is necessary to determine either the size of the area to be incorporated (containing a variable number of stations), as was done by Tallin and Ellingwood (1987), or the minimum number of stations to be used in the averaging procedure over a variable area. The second option was chosen because it allows the reduction of the standard error at a grid point to an acceptable level. Since the grid point standard error is proportional to $1/(N-1)$, and a coefficient of variation of 15% is probably as good as can be realistically achieved at a grid point, then for stations with worst case coefficients of variation of 0.53, this implies that $N = (0.53/0.15)^2 \approx 13$. In regions of sparse data, the size of the area searched in order to find 13 stations must be limited to avoid smoothing across different climatological zones and a maximum radius of inclusion of 300 km was chosen.

(c) From a contour map of the grid-point values, an interpolated value (S) for any particular Code location was converted to S_s simply by substituting its elevation (Z) in the following equation (given b);

$$[4] \quad S_s = S + bZ$$

RAIN COMPONENT S_r

The calculation of the rain component of the load S_r is also significantly different from previous procedure. In the 1985 Code it was the maximum one-day winter rain during the period of record at an observing station, and not a return period value. In the 1990 Code, S_r is the 30-year return period one-day winter rain amount.

Snow pack water equivalent amounts were modeled on a day-to-day basis for the period of record for about 2500 climate stations across Canada (since observed daily snow depths are available for only a few hundred locations). An annual maximum series of one-day rainfall amounts for each of these locations was compiled from one-day rainfall observations, where the rainfall amount was limited to the modeled snow pack water equivalent amount on each day. This limit is similar to that used by Boyd (1961) in assuming that the snow pack has a limited capacity to retain liq-id water.

The U.S. Army Corps of Engineers snow pack melt model based on a day-to-day accumulation of melting degree-days (Bruce and Clark, 1966; page 257) was used to calculate the day-to-day evolution of the snow pack. In the model runs, the snow pack was accumulated based on a 10:1 ratio of snow fall to water equivalent.

A 30-year return period one-day winter rain amount was calculated using the method of moments for each locations's annual maximum series. A 30-year return period is considered appropriate because the annual maximum series represents those one-day rainfall amounts occurring concurrently with near maximum snow pack water equivalent amounts. Therefore, large one-day rain amounts falling onto small or non-existent snow packs are not reflected in the calculation of S_r.

For the purposes of the Code, a representative value of S_r was then assigned to specific map regions.

THE MAPS

A series of 74 maps were constructed, covering Canada at a scale of 1 in 1 million (for example see Figure 1). These depict the variation of the smoothed normalized value (S) of the snow component of the load, and give either the value of the rain component (S_r) of the load, or in the case of mountainous regions, an equation to calculate it. The value of S_s at a location is obtained by means of Eq. [4]. To make such a calculation it is necessary to know the location precisely (in order to obtain the correct interpolated value of S), and its elevation (in metres).

INCREASED DATA AND OTHER CHANGES

The annual maximum depth of snow on the ground (Y_i) is available for a total of 1,618 principal and climatological stations which satisfied the criteria established to screen out stations with missing data (3.37 times the number used in the 1985 and earlier codes). The period of record (varying from 7 to 38 years) is generally longer than in 1985. Table 1 summarizes the changes in the methodology used to calculate the load components at a meteorological observing site.

Table 1. *Changes in determining the variables used to calculate the load*

Variable	1985 NBC	1990 NBC
ρ	200 kg/m^3	205 kg/m^3 (east of Rocky Mountains) 300 kg/m^3 (Tundra regions) 260 to 430 kg/m^3 (B.C.)
Y(30)	Estimated from a Gumbel extreme value distribution (using adjusted least squares method of fit)	The same, but using the method of moments fit
d	For month-end snowdepths, a constant = 1.235	Varies geographically from 1.07 to 1.91
One-day Rain	Maximum observed in one day at the time of maximum cover	1 in 30-year maximum one-day rain falling into snow where the weight of rain is less than the water equivalent of the snow
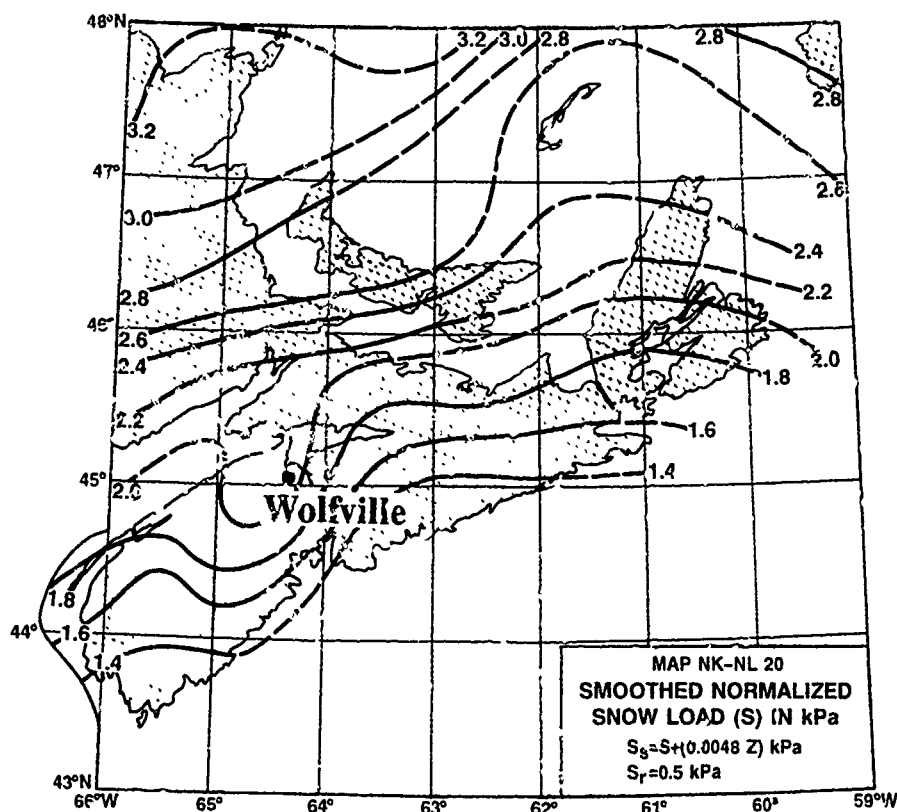
Figure 1. *An example of one of 74 maps of ground snow load (reduced from original scale 1:1 million). The snow component of the load (S_s) for Wolfville, Nova Scotia (45° 05'N 64° 22'W, elevation 34 metres) is;*
$S_s = 2.0 + (0.0048 \times 34) = 2.2$ kPa. The rain component (S_r) = 0.5 kPa.

45

THE EFFECT OF CHANGES

The net effect of these changes, plus those introduced by the new codification procedure, varies by region and is summarized in Table 2 which compares various statistics of the total load due to snow and rain at NBCC locations. The net change from 1985 to 1990 is a decrease of 6.6% in the total load values. Given that increases due to increased snowpack density tend to be counterbalanced by decreases due to the reduction in the rain component, this net change is an amount consistent with the decrease in the 30-year maximum snowdepth due to using the method of moments.

Table 2. *A statistical comparison of 1985*
and 1990 loads at 650 NBCC locations

Region	1985 Av. Load (kPa)	1990 Av. Load (kPa)	% Change 1985-90
CANADA	2.55	2.73	- 6.6
B.C.	2.75	2.76	0.3
ALTA	1.38	1.77	- 5.5
SASK	1.77	1.68	- 4.8
MAN	2.24	2.12	- 5.3
ONT	2.65	2.36	-10.6
QUE	3.40	3.10	- 8.8
NB	3.43	3.26	- 4.9
NS	2.64	2.41	- 8.7
PEI	3.48	3.14	- 9.7
NFLD	4.18	3.92	- 6.3
YUK	2.21	2.01	- 9.1
NWT	2.28	2.66	16.6

A comparison of load changes at individual code locations shows that 73.4% have changed by less than 1 standard deviation, 94.8% by less than 2 standard deviations, and 98.4% by less than 3 standard deviations:- a set of statistics close to what would be expected if the changes were normally distributed.

CONCLUSION

Although the 1990 work provides information on a much more detailed scale than previously available, it has not altered the basic geographical distribution of ground snow load values across Canada, (ie., large loads in the east and also in mountainous parts of the west, with a broad zone of small loads stretching northwards from the prairies into the arctic). Nor has it significantly changed the frequency distribution of individual values.

Compared to 1985, the 1990 values are; (i) 6.6% lower on average, (ii) more spatially consistent, (iii) less variable, and (iv) easier to obtain for any particular location. The 1990 work ensures that values

derived for locations not published in the Supplement to the National Building Code of Canada will be consistent with those that are, and furthermore, that consistent results will be obtained no matter who interpolates values from the maps.

ACKNOWLEDGMENTS

REFERENCES

Boyd, D. W., 1961: Maximum Snow Depths and Snow Loads on Roofs in Canada. DBR Research Paper No. 142, National Research Council, Ottawa. (Reprinted from the Western Snow Conference, pp 6-16. April, 1961).

Bruce, J. P. and Clark, R. H., 1966: Introduction to Hydrometeorology. Pergammon Press, London.

Claus, B. R., 1981: The Variation of Ground Snow Load with Elevation in Southern British Columbia. Master's Thesis, University of British Columbia, Dept., of Civil Engineering.

Cunnane, C., 1978: Unbiased Plotting Positions - A Review. Journal of Hydrology, Vol. 37, pp 205-222.

Dingman, S. L., Henry C. E., and R. L. Hendrick, 1978: Variation of Snow Properties with Elevation in New Hampshire and Vermont. Proceedings, Modeling of Snow Cover Runoff, CRREL, Hanover, New Hampshire.

Lowery, M. D., and J. E. Nash, 1970: A Comparison of Methods of Fitting the Double Exponential Distribution. Journal of Hydrology, Vol. 10, pp 259-275.

Martinec, J., 1977: Expected Snow Loads on Structures from Incomplete Hydrological Data. Journal of Glaciology, Vol. 19, No. 81, pp 185-195.

National Research Council, 1985: Supplement to The National Building Code of Canada. NRCC No. 23178, Ottawa.

Newark, M. J., 1984: A New Look at Ground Snow Loads in Canada. Proceedings, Eastern Snow Conference, Vol. 29, 41st. Annual Meeting, Washington, D.C., pp 37-48.

Schaerer, P. A., 1971: Variation of Ground Snow Loads in British Columbia. DBR Research Paper No. 479, National Research Council, Ottawa.

Tallin, A., and B. Ellingwood, 1987: Structural Load Estimates from Geographically Sparse Data. Journal of Structural Engineering, Vol. 113, No. 3, pp 628-632.

Watt, W. E., and M. J. Nozdryn-Plotnicki, 1980: Rainfall Frequency Analysis for Urban Design. Proceedings, Canadian Hydrology Symposium, NRC, Ottawa, Ontario, pp 42-52.

2
STRUCTURAL CASE HISTORIES
Kristoffer Apeland, Chairman
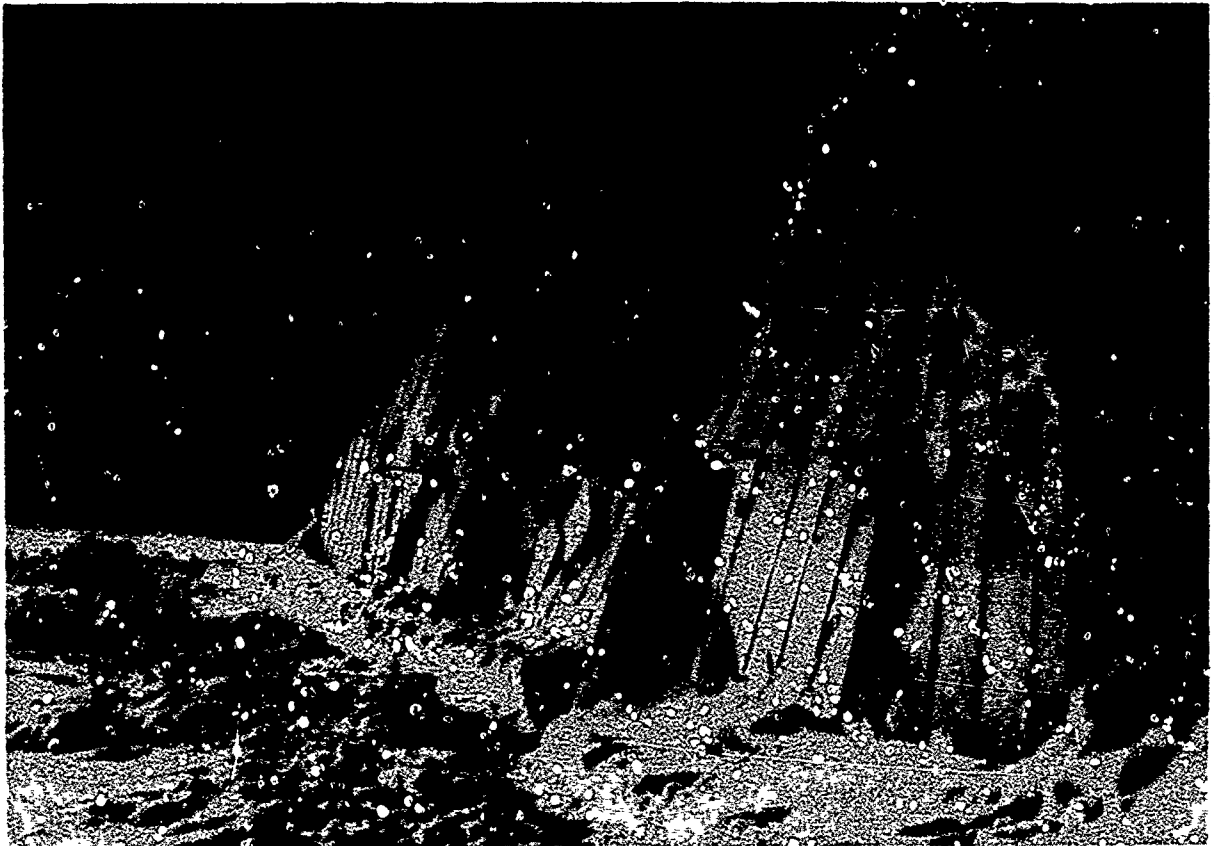
An Austrian greenhouse destroyed by snow. (Photograph provided by Karl Gabl.)

Wind Effect on the Distribution of Snow Depth on a Large Dome

Shuji Sakurai,[1] Osamu Joh,[2] and Takuji Shibata[3]

ABSTRACT

Snow depth on a large dome of 103-m diameter and about 32-m height was measured in Sapporo, where we have heavy snow accumulation and varying winds. It was found that the mean snow depth on the entire roof area measured at 36 points was about 70 % of the ground snow depth. The maximum snow depth measured on the roof was 120 cm, which was about 1.4 times the ground snow depth. The ratio of the mean snow depth on the scoured half surface of the roof to the mean snow depth on the drifted half surface was about 1:2. The most frequent wind direction, measured with a propeller-type anemometer on the roof, did not correspond to the direction inferred from the snow drift distribution. It was observed that a wind with a velocity greater than about 5-6 m/s was effective in causing the snow drift on the roof, when the mean air temperature during the referring period was about -4 °C. This measurement suggests that it is not adequate to predict the probable snow drift distribution on a roof immediately from the most frequent wind direction in the snowfall period.

INTRODUCTION

To determine design snow load on a large dome in cold and heavy snow regions, it is particularly important to estimate the snow drift distribution. There are, however, not enough necessary basic data.

Snow cover on a large dome in Sapporo was surveyed on February 5, 1985. The direction and the velocity of wind on the roof were measured as well as the air temperature from early winter. The natural ground snow depth was also measured at a neighboring point for the purpose of comparison. The purposes of the present paper are 1) to determine the ratio of mean snow depth and drift snow depth on the roof to the ground snow depth; 2) the comparison between the average density of snow cover on the roof and the density of the ground snow; 3) the relation between the drift distribution and the most frequent wind direction.

OUTLINE OF THE DOME

The dome, Makomanai Indoor Skating Rink, was constructed as one of the permanent facilities for The Sapporo Winter Olympic Games in 1972. It is located at longitude $141° 20'E$, latitude $43° 00'N$ and situated on open flat terrain. As shown in Figures 1 and 2, it is 103 m in diameter, and the height of the eaves and the top of the roof are 13 m and 32.63 m, respectively, from

---

the ground level. The shape of the roof is a polyhedron with 24 triangular
plates and its roof structure consists of steel trusses. The surface of the
roof is covered with oil-painted steel plates of 4.5-mm thickness. The
pitches of the plane surfaces are 1.9/10, 4.3/10 and 5.4/10 in terms of
the tangent of slope angles, respectively, downwards from the top, and the
pitches of the arris. (descending ridges) are 1.8/10 and 5.2/10 in the same
manner. The space under the dome is not warmed and is used exclusively for
skating in the winter.
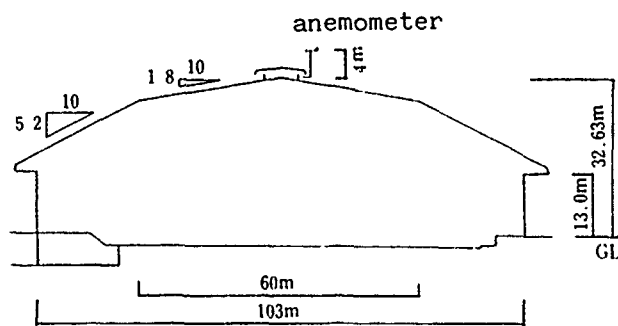
Figure 1. Cross section of the dome.
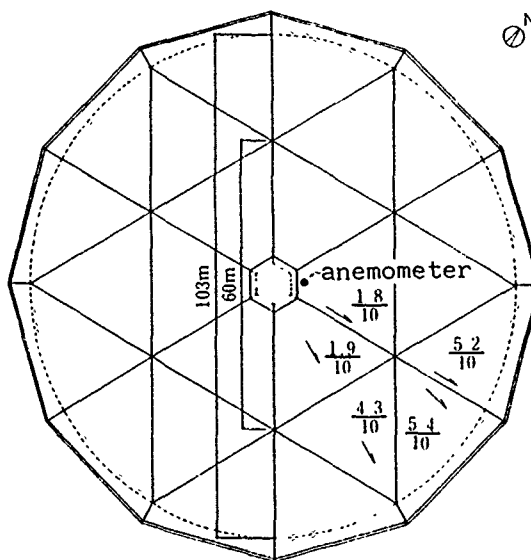
Figure 2. Roof plan of the dome.

GENERAL CONDITIONS OF SNOWFALL AND SNOW DEPTH
IN SAPPORO DURING THE WINTER OF 1984-85

Figure 3 shows the daily snowfalls and snow depths on the ground meas-
ured at Sapporo District Meteorological Observatory, which is about 7 km from
the dome, during the winter of 1984-85. Continuous snow accumulation started
on December 14. In January, we had heavy snowfalls. The monthly total snow-
fall was 265 cm, which was the second highest snow depth in January since
1953. The maximum snow depth reached 111 cm on February 2. On February 5,
the day when the snow cover on the roof was measured, the ground snow depth

near the dome was 87 cm and the snow depth measured at the Observatory was 94 cm.
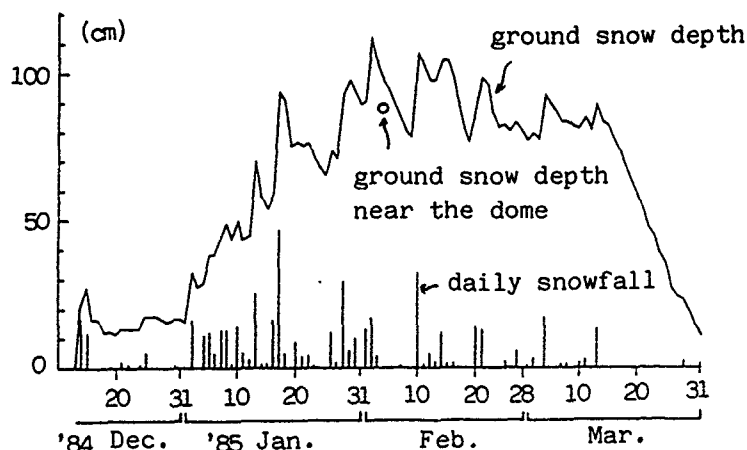
Figure 3. Daily snowfall and snow depth at Sapporo District Meteorological Observatory during the winter of 1984-85.

SNOW LOAD ON THE ROOF

Snow depth

The snow depths at 36 points of the entire roof area and the ground snow depth near the dome were measured on February 5, 1985. As shown in Figure 4, the snow cover on the roof was significantly affected by drifting action so as to be distributed nonuniformly. The maximum snow depth was 120 cm (see Line ⑤ in Figure 4), about 1.4 times that of the ground snow depth of 87 cm (Table 1). The minimum snow depth on the roof was 20 cm (see Line ② in Figure 4), 23 % of the ground snow depth. The mean snow depth on the roof was 63 cm, 73% of the ground snow depth.

In Figure 4, the ratios between the measured values at 36 points on the roof and their mean values are shown in parentheses. Most of these ratios at the points on Lines ①, ② and ③ were less than 1.0. The mean snow depth at 18 measured points on these three lines was 43 cm, which is 69 % of the mean snow depth of the entire roof area and about 50 % of the ground snow depth. On the other hand, on Line ④, ⑤ and ⑥ most of the parenthesized values at 18 points were 1.0 or more. The mean value of them was 1.32. The mean snow depth at these 18 points was 83 cm, which is nearly equal to the the ground snow depth. These results of the measurement show that the entire roof surface area was divided into a scoured half and a drifted half with al -most equal areas. The ratio between the mean values of snow depth within the respective areas was about 1:2.

Snow density

The snow cores were obtained by boring vertically through the entire snow depth at four points on the roof, marked with double circles in Figure 4, with a brass cylinder of about 0.5-mm thickness and 75-mm outer diameter.

53
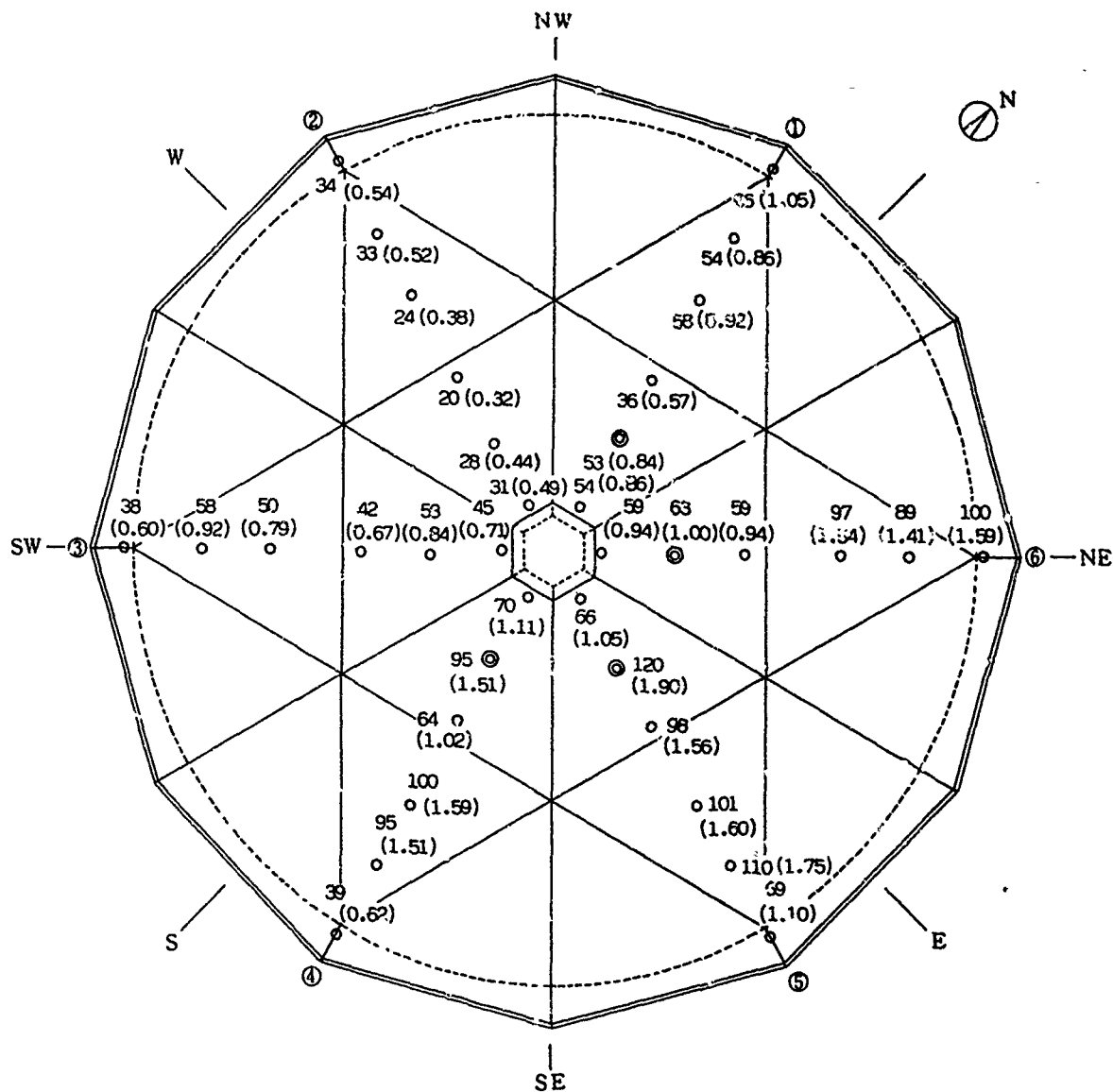
Figure 4. Snow depth on the roof on Feb. 5, 1985. The numbers in the parentheses are the ratio of each depth to the mean depth. The double circles show the coring points for determining snow density.

Table 1. The mean values of snow depth and snow density.

ground			roof(mean value)			$\dfrac{h_r}{h_s}$	$\dfrac{W_r}{W_s}$	$\dfrac{\rho_r}{\rho_s}$
h_s (cm)	W_s (kg/m²)	ρ_s (g/cm³)	h_r (cm)	W_r (kg/m²)	ρ_r (g/cm³)			
87	226	0.26	63	164	0.26	0.73	0.73	1.00

h:depth, w:weight, ρ:density, $\rho_s = W_s / h_s$, $W_r = h_r \cdot \rho_r$

The average density converted from the total weight of each snow core obtained from the roof snow was within a small range between 0.24 g/cm³ to 0.28 g/cm³. The mean value of the variation was 0.26 g/cm³. As shown in Table 1, the average density of the ground snow was 0.26 g/cm³, which agreed with the mean density of the roof snow.

Snow load

The ground snow load converted from the weight of the snow core was 226 kg/m². The mean snow load on the roof obtained from the product of the mean depth and the mean density was 164 kg/m².

WIND EFFECT ON THE SNOW DISTRIBUTION ON THE ROOF

Wind velocities and directions were measured with a propeller-type anemometer installed at about 4 m in height on the top of the roof and recorded on IC memories automatically. Wind velocity in the meteorological observation is usually indicated with the averaged value for ten minutes before the observation time. In the measurement of wind velocity at this dome, a standard method was adopted. The wind direction was recorded at every minute and the most frequent direction for ten minutes before the observation time was adopted as the representative wind direction at the time. In the paper, the relation between the snow distribution and the wind direction is discussed on the data obtained during 35 days from January 1 to February 4, the day before the day of roof snow measurement, because the snow cover on the roof had not been observed until the end of December.

Figure 5 shows the daily mean wind velocities, which are the average value of 144 measurements per day, and the daily maximum wind velocities. The former varied from 0.7 m/s to 9.2 m/s. The latter varied from 2.4 m/s to 29.4 m/s. Figure 6 shows a wind rose describing the variation of wind direction, without winds of a velocity of less than 0.3 m/s, during the above-mentioned period. The principal part of the snow-drifted area on the roof is shown in the same figure. As is obvious from Figure 6, the most frequent wind direction was SW and not corresponding with the direction inferred from the snow drift distribution, which had the main axis in WNW near Line ②. Figure 10 (a)-(g) show the wind roses within the respective bands classified with the velocity ranges of 0.3-1.0 m/s and every 1.0 m/s from 1.0 m/s to 7.0 m/s. Figure 10 (h) shows the wind rose of the range of wind velocity higher than 7.0 m/s. As the wind velocity increased, the frequent wind direction intended to change from SW to NW. Although the most frequent wind directions in the wind roses from the band of 3.0-4.0 m/s to the band of 6.0-7.0 m/s are SW, the axis of integrated wind direction rotates gradually toward WNW as wind velocity become higher. It can be observed from the figures that the directions of wind axes and drift axes almost correspond with each other in the respective bands of velocity range higher than 5-6 m/s. The frequency of the wind velocities 5 m/s or more was 16.5 % of the entire observations for the 35 days as shown in Figure 7. Figure 8 shows the daily hours of recorded wind velocity of 5 m/s or more; the total time was 138 hours during the 35 days.

As shown in Figure 9, there were 28 ice days in the reference period of 35 days, and the mean value of the daily mean air temperature was about -4 °C. The critical wind velocity for giving rise to snow drifting on the roof
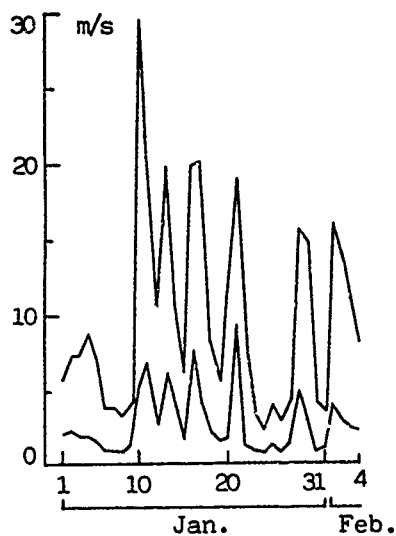
Figure 5. Daily mean and
max. wind velocity.

Figure 6.   Wind rose and the
principal part of the snow
drifted area.
(wind velocity ≥ 0.3 m/s)

A: v < 0.3
B: 0.3 ≤ v < 1.0
C: 1.0 ≤ v < 2.0
D: 2.0 ≤ v < 3.0
E: 3.0 ≤ v < 4.0
F: 4.0 ≤ v < 5.0
G: 5.0 ≤ v < 6.0
H: 6.0 ≤ v < 7.0
I: 7.0 ≤ v

v: wind velocity (m/s)

Figure 7. Frequency in each band of
classified with wind velocity for
35 days, Jan. 1 to Feb. 4.
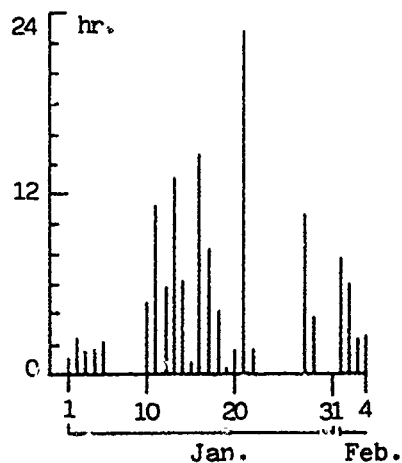
Figure 8. Daily hour record-
ing wind velocity of 5 m/s
or more.
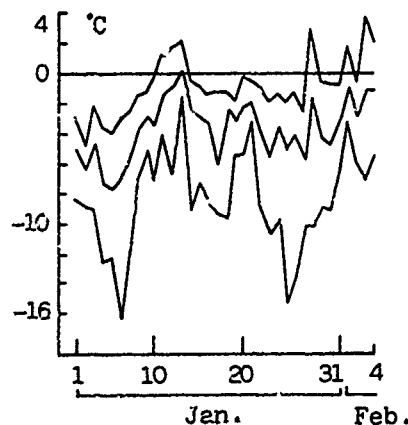
Figure 9. Daily mean, max.
and min. air temperature
near the roof.

(a)$0.3 \leq v < 1.0$

(b)$1.0 \leq v < 2.0$

(c)$2.0 \leq v < 3.0$

(d)$3.0 \leq v < 4.0$

(e)$4.0 \leq v < 5.0$

(f)$5.0 \leq v < 6.0$

(g)$6.0 \leq v < 7.0$

(h)$7.0 \leq v$
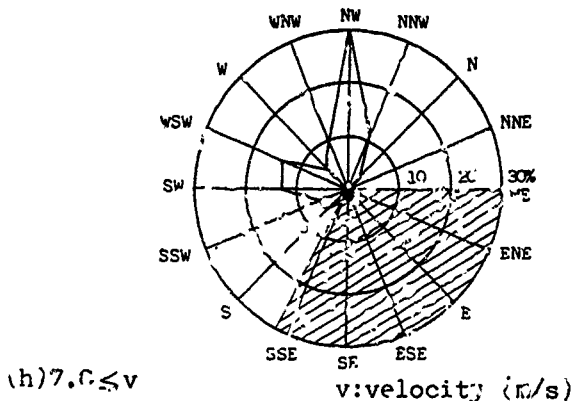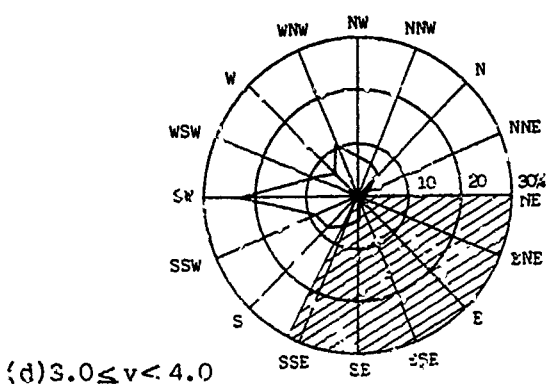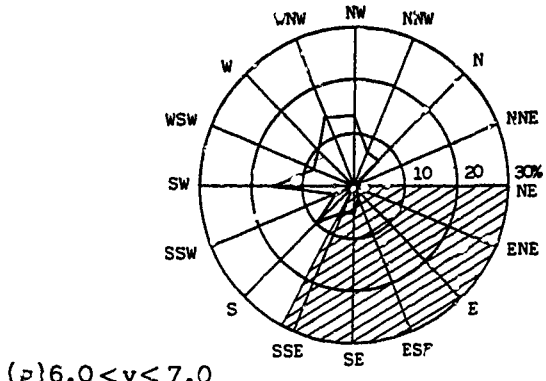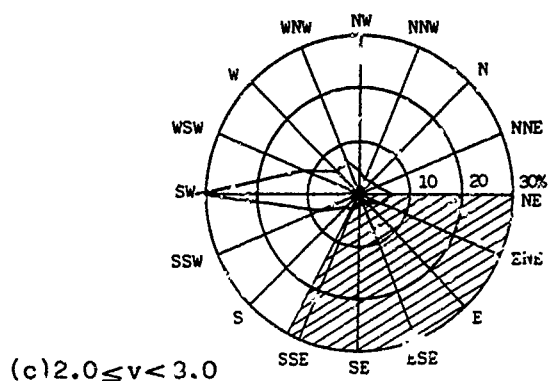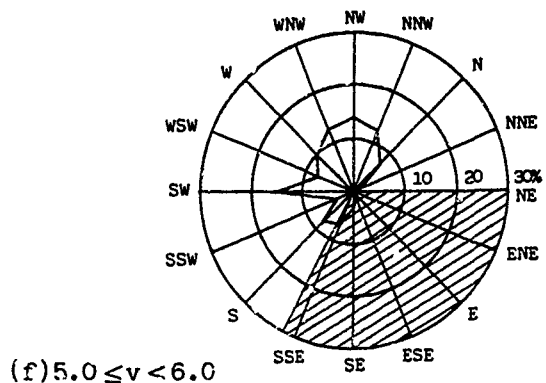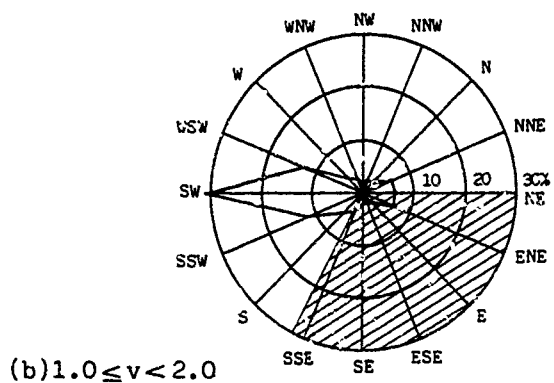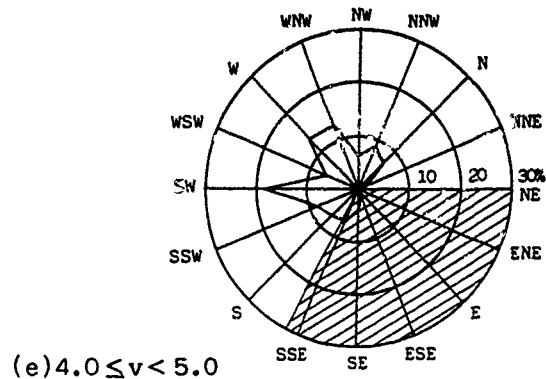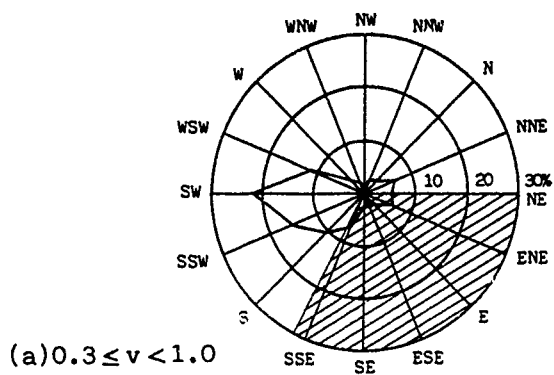
v:velocity (m/s)

Figure 10. Wind roses classified with wind velocity.
The principal part of the snow drifted area.

57

probably depend on the air temperature. Although substantial data that establish this relation have not been obtained in this case, the critical wind velocity of 5-6 m/s and the average air temperature of -4°C are well corresponding with the relation between the critical wind velocity and air temperature in open fields observed by S.Satoh(1962), as shown in Figure 11 (Maeno, 1982).
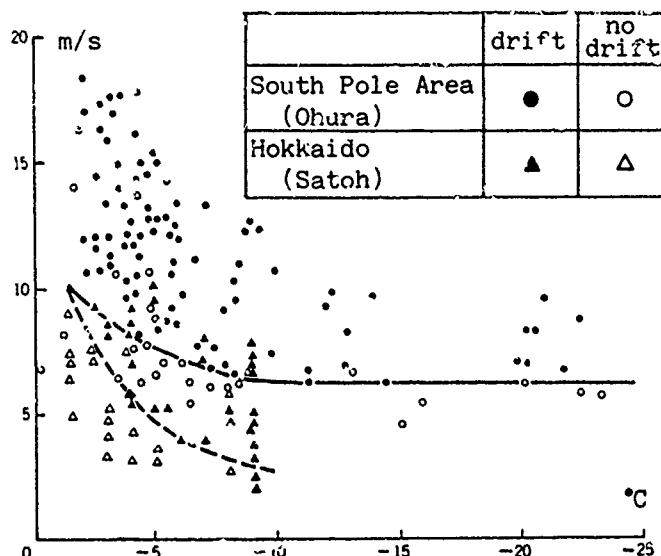
Figure 11. Relation between the critical wind velocity and air temperature to cause snow drifting.

CONCLUSION

Snow cover on a large dome, 103 m in diameter, about 32 m in height and located in an open flat terrain, was investigated in Sapporo. The mean snow depth on the entire roof area measured at 36 points was 63 cm, 73 % of the ground snow depth. The maximum snow depth on the roof was 120 cm, which was about 1.4 times the ground snow depth. The mean snow depth on the scoured half surface of the roof was about 50 % of the ground snow depth. The mean snow depth on the drifted half surface was about equal to the ground snow depth. The mean snow density measured at 4 points on the roof was 0.26 g/cm³, which agreed with the density of the ground snow. Observations of the relation between the snow drift distribution on the roof and the wind directions classified with wind velocities have shown that the snow drift distribution on a roof is brought about by the wind with a velocity of about 5-5 r/s or rore at mean air temperature of -4°C. This result suggests that it is not adequate to predict the probable snow drift distribution on a roof immediately from the most frequent wind direction in the snowfall period.

REFERENCES

1 Satoh, S, 1962, "On the criterion of the railway guard-patrol during a snow storm in Hokkaido" Journal of the Japanese Society of Snow and Ice, Vol. 24, No. 2, 1962. (in Japanese)

2 Maeno, N, 1982, "Generating mechanism of snow drifting and fluidization of snow" The Science(monthly journal), Vol. 52, No. 1 Jan. 1982.(in Japanese)

Characteristics of Snow and Snow-Induced Building Damage in Japan

Jiro Suzuya[1] and Yasushi Uematsu[2]

ABSTRACT

The heavy snow experienced during the 1962-63 and 1980-81 winters caused considerable damage to many buildings and structures in Japan. In this paper, the causes for the building failures are analyzed based both on the on-site failure investigations and on the response analysis of the damaged buildings; particular attention is paid to the estimation of the design snow load and the load carrying capability of the structures. The results of a three-dimensional frame analysis of a steel-framed structure with a simple-pitched roof indicate that the actual stress induced in some members, such as tie beams in the longitudinal direction, will exceed the design stress estimated from a planar frame analysis. Furthermore, as for some structures with simple-pitched roof trusses, it is found from an elasto-plastic planar frame analysis that a total building collapse could be triggered by the yielding of some members, followed by the buckling of compressive members or by the fracture of the joints.

INTRODUCTION

In winter. about 60% of Japan is covered with a lot of snow owing to snowfall of the monsoon type, and many buildings and structures are damaged. Since the north latitudes of the heavy snow areas range from 30 to 45°, the characteristics of the snow and snow-induced structural damage change considerably from place to place. The heavy snow experienced during the 1962-63 and 1980-81 winters resulted in a lot of building failures on the Main Island of Japan. In particular, a number of wooden frame and steel-framed buildings with relatively large clear spans, such as sports gymnasiums, sustained severe damage. Figure 1 shows the locations of the collapsed buildings in the 1962-63 and 1980-81 winters together with a map of the maximum ground snow depth; snow depth is expressed in units of cm. We have analyzed the causes for the building failures, and some important aspects to be considered in the structural design of these buildings are pointed out in this paper.

The ratio r of the actual roof load W to the design roof load W_d is plotted against W_d for the fully- (closed symbols) and partially-collapsed buildings (open symbols) in the 1962-63 and 1980-81 winters; in practice, W was estimated from the ground snow load and the roof geometry etc.. Generally, the value of r is large for the buildings in the areas subjected to infrequent snowfalls and snow accumulations. On the other hand, many buildings in the areas frequently receiving heavy snowfall, i.e., in the

1 Professor, Department of Architecture, Tohoku Institute of Technology, Yagiyama Kasumicho 35-1, Sendai 982, Japan.
2 Research Associate, Department of Architecture, Tohoku University, Aoba aza Aramaki, Sendai 980, Japan.

areas expressed by $W_d > 3kPa$, have values of r lower than unity; i.e., they collapsed under snow loads smaller than the design loads. The data points for the collapsed buildings are scattered across a wide range, which suggests that the causes for the building failures should be analyzed from the viewpoint of the estimation of the design snow load as well as of the load carrying capability of the structures; a discussion of these two aspects will be given in the succeeding sections.

(a)1962-1963
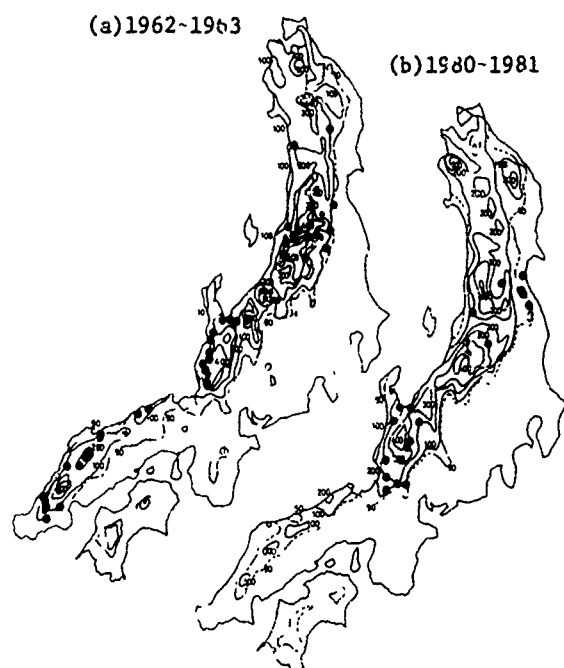
(b)1980-1981

Figure 1   Locations of Collapsed Buildings and Maps of the Maximum Ground Snow Depth in 1962-1963(a) and 1980-1981 Winter(b)
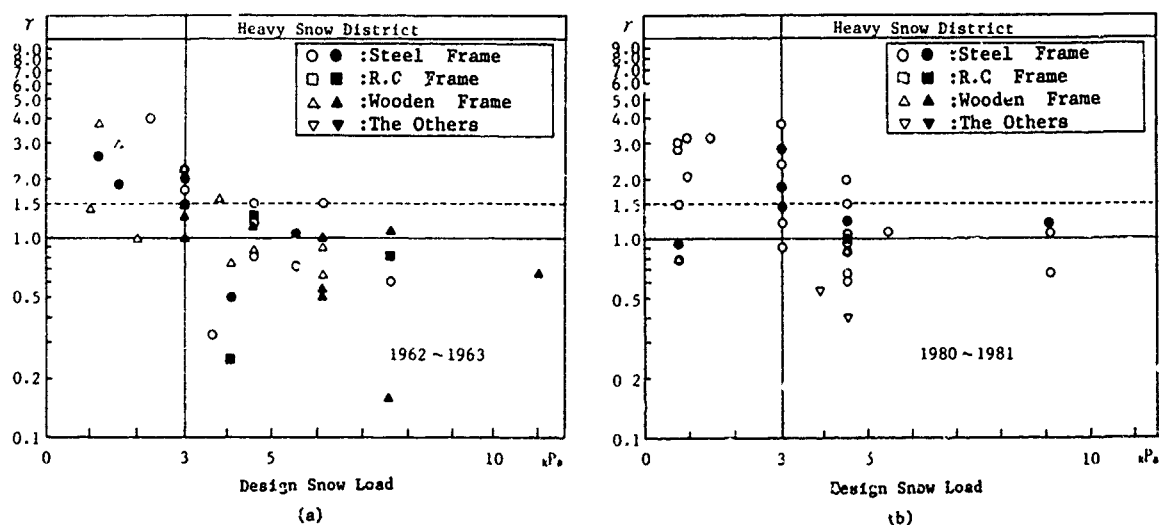
Figure 2   Ratio of Actual Roof Load to Design Roof Load for Collapsed Buildings: (a) 1962-63 Winter, (b) 1980-82 Winter

Table 1 Maximum and 50-yr Mean Recurrence Interval
Ground Snow Depth for Some Locations in Japan

Location	d_g50 (cm)	d_{gmax} (cm)	Year of d_{gmax}	Year of Record
Aomori	175	209	1945	91
Akita	90	117	1974	95
Sendai	39	41	1936	58
Yamagata	103	120	1981	92
Fukushima	48	80	1936	84
Niigata	104	120	1961	95
Takada	330	337	1945	62
Toyama	193	208	1940	46
Kanazawa	161	181	1963	92
Fukui	210	213	1963	88
Tsuruga	165	196	1981	87
Gifu	50	58	1936	96
Hikone	91	93	1918	91

DESIGN SNOW LOAD

Design roof snow loads are usually calculated from the depth d_g and the averaged density ρ_g of the ground snow at the building site. Thus, these two values should be estimated accurately to determine the design roof snow load. In Japan, the maximum ground snow depth d_{gmax} recorded in the past has often been used as a design snow depth. Recently, however, there has been some progress made in developing a more rational, or statistical approach for specifying the snow loads. That is, the ground snow depth d_g50 for a 50-year mean recurrent interval estimated from a series of annual maxima of the ground snow depth tends to be used in the structural design. Table 1 lists the values of d_g50 and d_{gmax}, together with the year when d_{gmax} was recorded, for some locations shown in Figure 1; d_g50 is estimated by assuming that the probability distribution of the maximum annual snow depth is described by the Weibull distribution. From this table, it is found that d_{gmax} was recorded in the 1962-63 winter at two locations and in the 1980-81 winter at another two locations. Note that d_{gmax} exceeds d_g50 at many locations. This, in turn, indicates that the actual snow load can exceed the design snow load when d_g50 is used as a design basis.

After the heavy snowfall in the 1980-81 winter, the data on the averaged snow densities, ρ_g and ρ_r, both on the ground and on the roof, have been compiled by many investigators. Figure 3 shows ρ_g and ρ_r plotted against the snow depth measured at some locations in the 1980-1981 winter. The closed symbols represent the values measured at the maximum ground snow depth, while the open symbols are the values measured after the maximum ground snow depth. The data on ρ_g related to d_{gmax} collapse into a narrow region around the solid line given by the following equation:

$$\rho_g = 4.838 \times 10^{-4} d_g + 0.185$$

in which d_g is expressed in units of cm. From this figure, the value of ρ_g measured at $d_g = d_{gmax}$ is found to be roughly proportional to d_g. On the
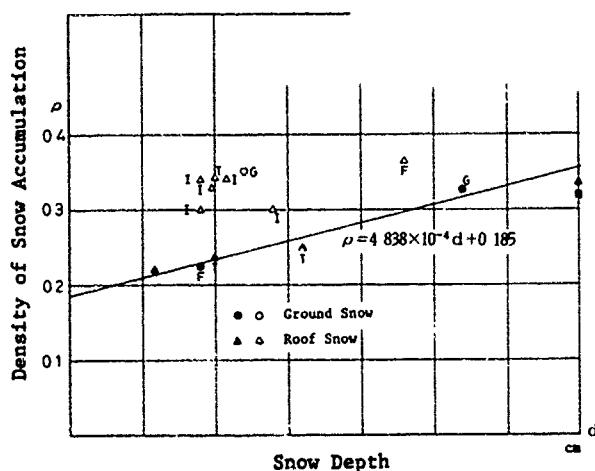
Figure 3 Averaged Density of Snow Accumulation versus Snow Depth
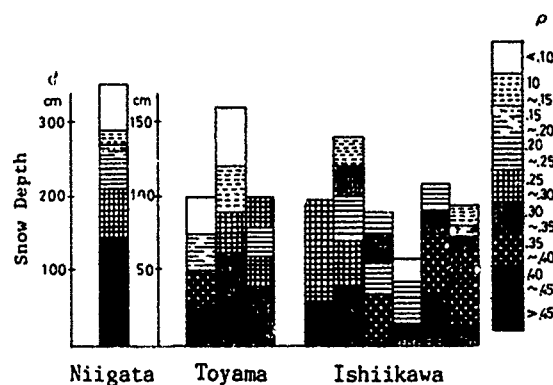
Figure 4 Vertical Distribution of Density of Snow Layers on the Ground

other hand, the data measured after the maximum ground snow depth are widely scattered and no conclusive relationship between ρ_g and d_g can be observed.

Figure 4 shows sample results on the density distribution of snow accumulation both on the ground and on the roof measured in the 1980-81 winter. At $d_g = d_{gmax}$, the value of ρ_g is relatively small, because the upper part of the snow accumulation consists of newly-fallen fresh snow with density less than 0.1. The value of ρ_g increases in accordance with the settlement of the snow accumulation, in other words, with time. Thus, the maximum ρ_g occurs fairly soon after the maximum snow depth.

The current building code of Japan prescribes ρ_g as 0.3 for buildings in the heavy snow areas. However, as has been shown in Figure 3, values of ρ_g greater than 0.3 were observed and, furthermore, d_{gmax} exceeded d_{g50} at many locations in the 1962-63 and 1980-81 winters. In addition, the actual roof snow loads will exceed the design loads:

1. when the structure was designed to take advantage of the reduced loads resulting from snow removal and, despite this, the roof snow is not removed;
2. when the drift loads resulting from the geometry and surroundings of the building are not estimated properly in the structural design; and
3. when the presence of rain increases the snow load significantly.

From the results shown in Figure 1, it is found that there are many damaged buildings with design roof snow loads about 2.94kPa, which corresponds to the lowest snow load allowed in the building code when snow removal is done in a systematic manner. For these buildings, snow removal could not be done probably due to a continuous heavy snowfall, which might have lead to total building failure.

STRUCTURAL RESISTANCE TO SNOW LOAD

General Features of Structural Failures

As mentioned above, the roof snow load can exceed the design snow load even if the design load is determined by properly considering the available snow load data. Thus, structures should be designed to have a load carrying capability even when the snow load exceeds the design load to some degree, in

particular, for structures such as barrel vaults and portal frames with large clear spans which are generally sensitive to a change of snow load in both magnitude and distribution. It is also thought that structures would sustain severe damage when they suffer unusual stress or deformation mode.

The 1962-63 winter resulted in many failures of wooden frame buildings with large clear spans. For some of these buildings, the failure was found to be initiated by a lateral movement of the main frame due to a low structural resistance to lateral forces. We made an on-site investigation of the failures of many steel-framed structures with simple-pitched roofs in the 1980-81 winter. The results suggested that, in many cases, the total building collapse was triggered either by failures of the lateral bracings and the tie beams which restrain the main frames from lateral movement, or by the fracture of the bolts jointing these members. This type of structure is usually analyzed as an assembly of a series of planar frames, and the tie beams and the lateral bracings are designed to resist relatively small lateral forces such as seismic and wind loads. However, oftentimes the appearance of the damaged structures gives rise to an observation that these structures behaved as a three-dimensional structure, not as a planar structure, in the process of collapse. This evidence suggests that it is necessary to make the tie beams and the lateral bracings stiff and strong enough to resist the additional forces resulting from such a three-dimensional frame effect.

Three-Dimensional Frame Effects

Here we briefly discuss the three-dimensional frame effects on the response of a steel-framed structure with parallel single-span frames braced with one another; the method of analysis and more detailed results are presented in Yamada et al. (1987, 1988). This type of structural system has frequently been used for sports gymnasiums and warehouses etc., and a number of buildings have been damaged in the past. The structural model used in this
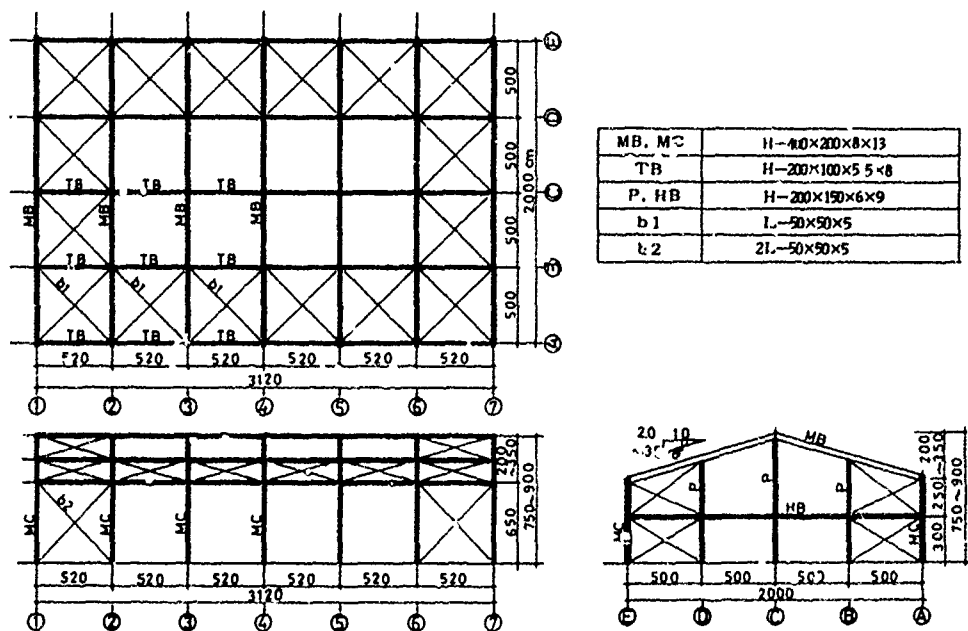
Figure 5 Analyzed Structural Model

63

study is illustrated in Figure 5. The roof slope θ was varied in a range given by $tan\ \theta = 0.20 - 0.35$. The cross section of each member is also shown in Figure 5. The axial forces N and the bending moments M induced in the members under a uniform vertical load of 0.98kPa were computed by using both a planar and a three-dimensional frame model. Figures 6 and 7 compare both results; in each figure, (a) and (b) represent the results for a planar frame model, and (c) and (d) are the results for the three-dimensional frame model. The magnitudes of N and M induced in the main frames are generally smaller for the three-dimensional frame model than for the planar frame model; i.e., the safety factor is larger for the planar frame model than for the three-dimensional frame model regarding the main frames. However, the axial forces induced in the tie beams and the lateral bracings become fairly large in the three-dimensional frame analysis. Thus, it appears that if these members are not designed properly, they will be damaged first and this will lead to a total building collapse under a snow load lower than the design load.

Elasto-Plastic Planar Frame Analysis of Some Damaged Buildings

In this section, we discuss some other possible causes for the building failures besides the above-mentioned three-dimensional frame effect, based on the results of an elasto-plastic planar frame analysis and of the on-site investigation of three steel-framed structures damaged in the 1981-82 winter. For simplicity, the following assumptions are made in the analysis:
1. The yield stress of the material is 1.2 times the allowable stress prescribed in the building code.
2. The tangent modulus of the material after yielding is $E/10$, with E being the elastic modulus.
3. Neither the buckling of compressive members nor the failures at joints are taken into account.
4. The roof load W_r including the dead load of the roof is expressed as a uniformly-distributed vertical load.

Figures 8 to 10 show the shape of the main frame and the relationship between the load and the deflection at the top of the frame for the three structures, respectively. The solid and broken lines, labeled "ERL" and "DRL" in the figures, stand for the estimated collapse roof load and the design roof load, respectively. Hereafter, we consider the cause for the failure of each building separately; a description of the building failures and the results of analysis are presented in Uchiyama et al. (1981) and Suzuya (1987).

Case 1. - Figure 11 shows the damage to the main frames. Riveted connections with gusset plates were used between the chord and lattice members, which are assumed to be pin joints in the analysis. The collapse load estimated from the on-site investigation is nearly equal to the design load of 1.67kPa. According to the analysis, the first yield occurs at a load of only $W_r = 0.51$kPa, and the upper chord member has a yield point at the center of the beam when the load reaches the estimated collapse load. It appears that the compressive members at the knee of the frame buckled first, followed by the yielding of the upper chord members near the center of the beam which led to a progressive failure of the structure as a whole.

Case 2. - The shape of this building is similar to that of the case 1 building. Examples of damage to the main frames are given in Figure 12. The main frame consisted of light gauge steel members and welding was used for the connections. The connections are again assumed to be pin joints in the analysis. The estimated collapse load was nearly equal to 3.14kPa at which yield is reached somewhere in the structure; this value is reasonably larger

than the design load of 1.67kPa. It is thought that the total building collapse was triggered by the fracture of the welded joints together with the yielding of the chord members at the knee of the frame.

Case 3. – The main frame consisted of steel-framed reinforced concrete columns and a warren truss beam. The members of the beam were circular steel pipes and were welded to each other at the joints; the connections between the chord and lattice members are assumed to be rigid in the analysis. Figure 13 shows the collapse mode of the main frame and the fracture of the joints. Yielding of the members occurs at W_r = 4.80kPa. The estimated collapse load was nearly equal to 7.84kPa, at which all lattice members in a range near the beam edge up to about one sixth of the span were found to yield from the analysis. The roof collapse is thought to have been initiated by the fracture of the joints between the chord and lattice members.

CONCLUDING REMARKS

It has been shown that actual roof snow loads will exceed the design load. In particular, the following three factors will result in a considerable increase in the actual roof snow load; that is, (a) reduction of the design snow load by taking snow removal into account, (b) snow drift, and (c) rainfall on the accumulated snow. However, building failures related to these factors could be avoided by designing the structures carefully. As mentioned above, a number of portal and gable frames with large clear spans have been damaged due to heavy snowfall. In order to design such structures to safely resist even a snow load somewhat larger than the design load, the structural designers should pay special attention to the following points:

1. Make the roof rigid so that a deflection of the main frame in a side-sway mode would not occur under snow loads.
2. Design the tie beams and the lateral bracings carefully by considering the three-dimensional frame effects when the structure is analyzed as an assembly of a series of planar frames.
3. Raise not only the buckling load of the compressive members but also the strength of the joints between the main frames, tie beams and lateral bracings.

REFERENCES

Suzuya, J., "Elasto-Plastic Behavior of the Damaged Steel-Framed Structures Due to Heavy Snowfall," _Proc. 2nd Symp. on Snow Engrg._, 71-76, Feb., 1986.

Uchiyama, K. et al., "Snow Damage to Steel Structures in Tohoku and Hokuriku District," _JSSC_, Society of Steel Construction of Japan, Vol. 17, No.185, 1-48, Dec., 1981.

Yamada, M., Suzuya, J., Uematsu, Y., and Shimada, H., "Three Dimensional Effects on the Steel Construction with Paralleled Single-Span Frames Braced with One Another Subject to Snow Load, Part 1. In the Case of Gabled-Roof Frames under Uniform Load," _Proc. 3rd Symp. on Snow Engrg._, 69-76, Jan., 1987.

Yamada, M., Suzuya, J., Uematsu, Y., and Shimada, H., "Three Dimensional Effects on the Steel Construction with Paralleled Single-Span Frames Braced with One Another Subject to Snow Load, Part 2. In the Case of Barrel Vaults under Uniform Load," _Proc. 4th Symp. on Snow Engrg._, 93-98, Jan., 1988.
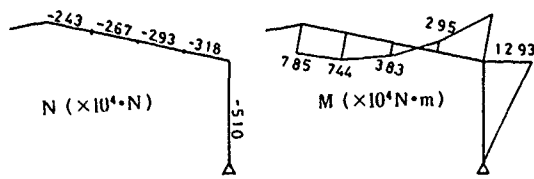
(a) Axial Force (b) Bending Moment
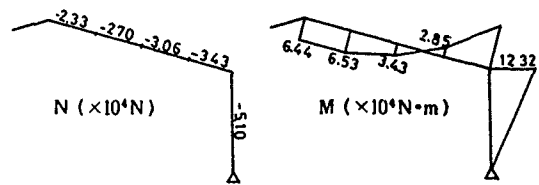
(a) Axial Force (b) Bending Moment
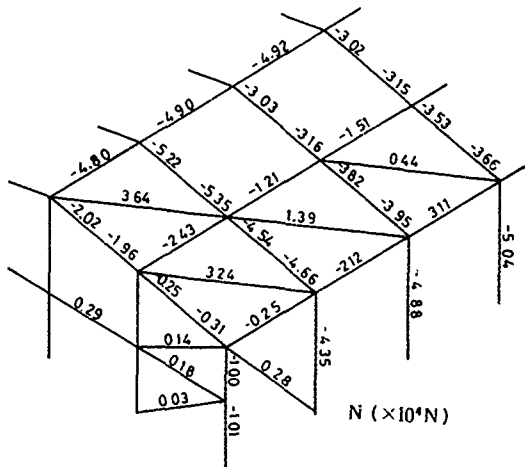
(c) Axial Force
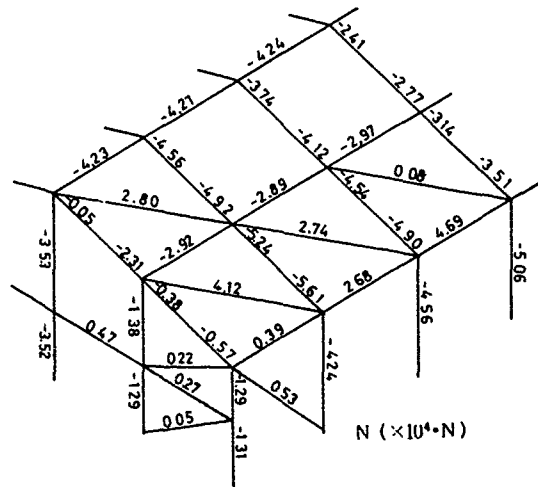
(c) Axial Fo ce
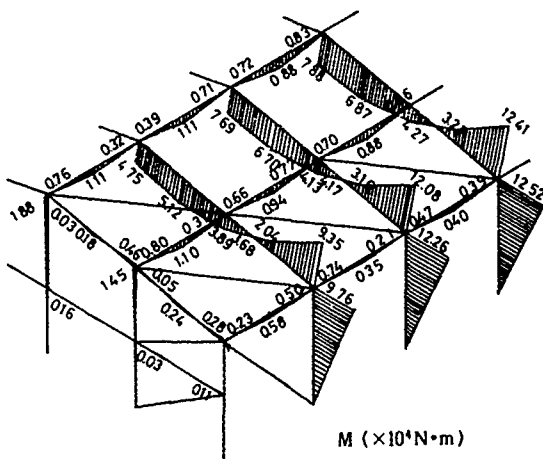
(d) Bending Moment
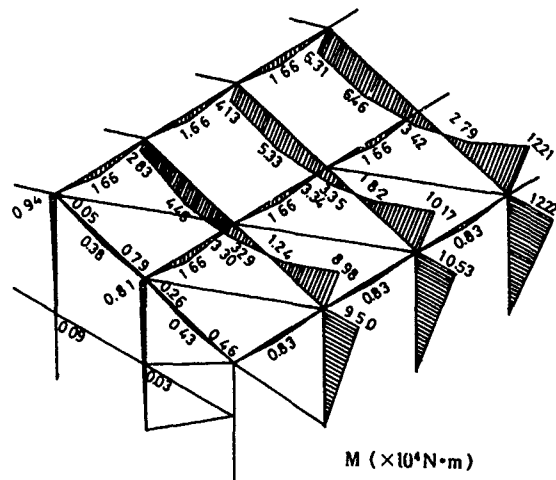
(d) Bending Moment

Figure 6   Distribution of Axial Force and Bending Moment for $\tan\theta = 0.20$: (a,b)Planar Frame Analysis, (c,d)Three-Dimensional Frame Analysis

Figure 7   Distribution of Axial Force and Bending Moment for $\tan\theta = 0.30$: (a,b)Planar Frame Analysis, (c,d)Three-Dimensional Frame Analysis
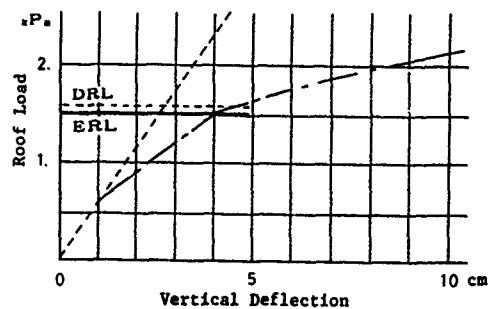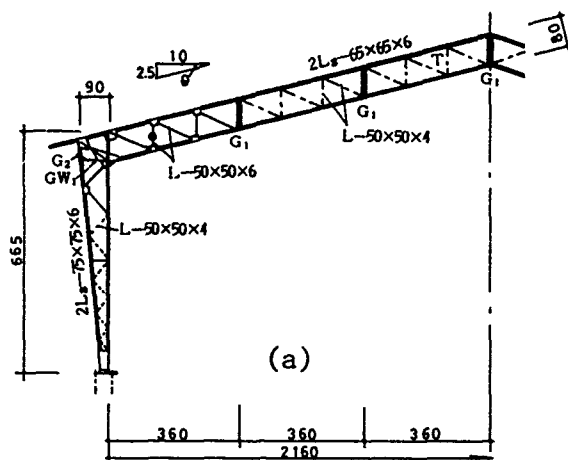
Figure 8   Main Frame(a) and Load–Displacement Relationship(b)
of Collapsed Building: Case 1
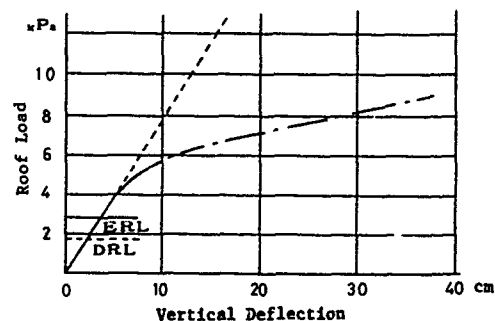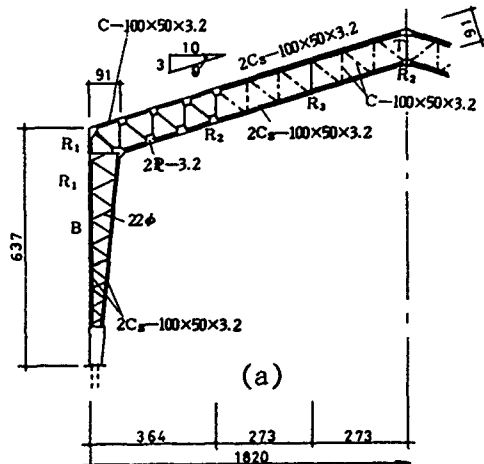
Figure 9   Main Frame(a) and Load–Displacement Relationship(b)
of Collapsed Building: Case 2
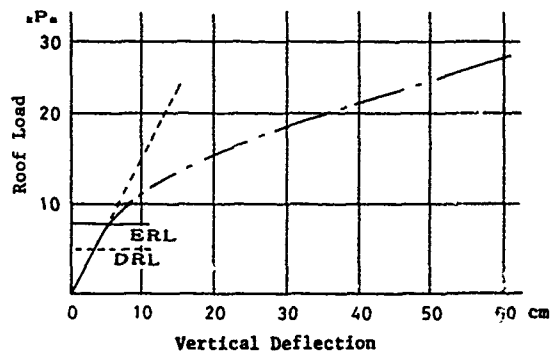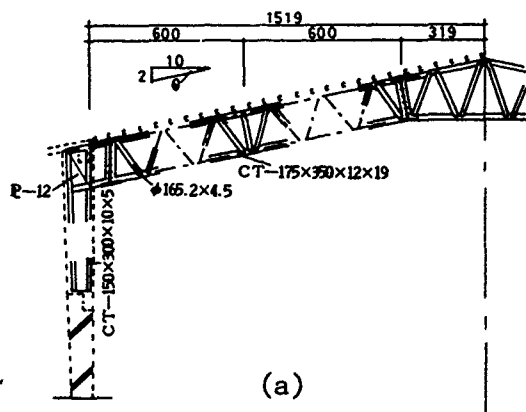
Figure 10   Main Frame(a) and Load–Displacement Relationship(b)
of Collapsed Building: Case 3

| (a) | (b) |

Figure 11   Snow-Induced Damage to the Structure: Case 1
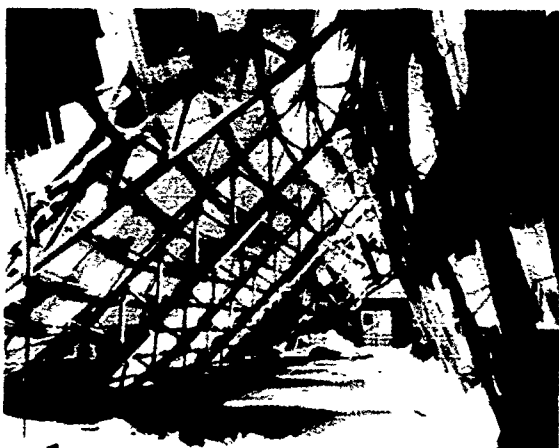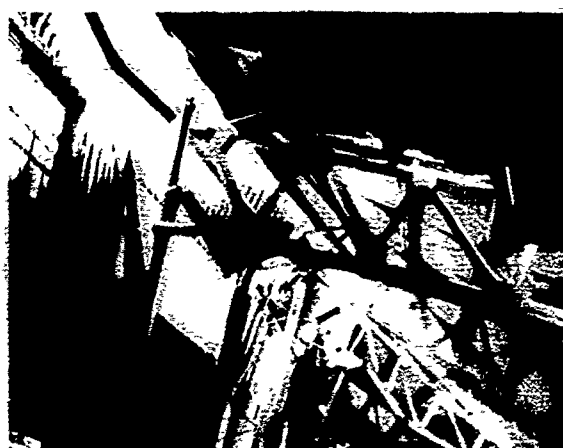
| (a) | (b) |

Figure 12   Snow-Induced Damage to the Structure: Case 2

| (a) | (b) |

Figure 13   Snow-Induced Damage to the Structure: Case 3

Snow Loads on Roofs—Three Case Histories in Warsaw

Andrzej Sobolewski[1] and Jerzy A. Zuranski[2]

ABSTRACT

The paper deals with three snow load case histories from one winter
with heavy snow-falls in Warsaw. Detailed measurements of snow
depth, density and load were made on the nearly flat 140 x 84.5 m
roof in the City center. Three profiles of snow depth and load were
taken from the large saw-tooth roof influenced by adjacent buil-
dings. Snow load profile on the single two pitch canopy roof is
also presented.
Snow depth, density and load on roofs are compared with the same
variables measured on the ground at a sheltered area.

INTRODUCTION

During January 1979 heavy snow-falls occured in central Poland.
Several snow load case histories were then investigated in the region of
Warsaw. Time histories of snow-falls, air temperature and snow loads on the
ground in Warsaw are presented in Figures 1 and 2. Ground snow load measured
in the city center on the lawn at the permises of the Institute for Building
Technology served as reference data for the results of measurements of snow
accumulation on roofs.

Two snow-storms occured during the winter: on January 6 from the East
and on January 31 from the West. They resulted in snow drifts on roofs.

ROOF OVER THE CENTRAL RAILWAY STATION

The roof of the Warsaw Central Railway Station is 140 m long and
84.5 m wide, its approximate height above the street level is 17 to 20 m,
depending on the side, entrance levels, car-parks, etc. An outline is shown
in Figure 3.

The roof consists of five flat surfaces with 5% slope each, forming
a crest in the center, two valleys and two slightly raised external wings.
Roofing is made of corrugated sheet steel, insulated with mineral wool and
waterproof plastic fail. The underroof space is closed and used for ventila-
tion plant; therefore it is slightly heated. During the measurements the
inside air temperature directly under the roof was 13°C.

The Station is located in the city center. It is surrounded by the
built-up area with buildings of the similar height and some higher ones.
An open, wide street and railway band stretches from the West side and a
large open square is located at the East side.

---

1. Research and Design Centre for Industrial Building "BISTYP", Warsaw,
   Poland

2. Institute for Building Technology, Warsaw, Poland

Snow load and density measurements were made by the snow sampler described elsewhere /Sobolewski, Żurański, 1988/; the snow depth was measured also by a rod.

Results are presented in Figures 4 and 5. Their main features are as follows:

a/ even a slope as small as 5% has the influence on snow accumulation; snow load at the crest was almost twice smaller than at the valleys /Fig.4/;

b/ the roof-to-ground conversion factor was 0.4 for the crest and 0.7 for valleys; reference load on the ground was measured approximately 1.5 km away from the Station;

c/ the mean values of snow density was ρ = 317 kg/m^3 on 22 February and ρ= 343 kg/m^3 on 23 February against 270 kg/m^3 on the ground; the tentative roof measurements on 6 February gave ρ= 275 kg/m^3 against ρ = 240 kg/m^3 on the ground, on 16 February it was 288 kg/m^3 on the roof and 250 kg/m^3 on the ground.

In this comparison some lower values of snow load at the roof rands were omitted. Recapitulation is given in Tables 1 and 2.

SAW-TOOTH ROOF

Three bays of a large saw-tooth roof over an industrial building at the western outskirts of Warsaw were investigated on 27 and 28 February 1979.

These bays were located close to the adjacent higher buildings as it is shown in Figure 6. The western building with a two pitch, 30 m wide and 10% slope roof is 14.8 m high at the crest. The eastern building has a mono pitch, 9.6 m wide and 10% slope roof. Its height is 15.5 m. The height of the saw-tooth roof is 11.7 m, each tooth being 2.1 m high. The slope is 30° at one and 70° at the other side.

Roofing is made of corrugated sheet steel, insulated with mineral wool and black roofing paper.

Buildings were at final stage of construction. They were closed but not heated. External air temperature during measurements was +1°C.

Surrounding territory may be classified as an open territory.

The results of measurements are presented in Fig.7,8 and 9, and given tables 3 and 4.

The shape of snow layer between neighbouring skylights is strongly influenced by vortices generated by wind when it is blowing perpendicularely to the skylight crests. The "waves" on snow surface caused by the vortices are seen in all three Figures.

The snow laying on the right slopes of skylights was exposed to the sun radiation. It was gradually thawn during the sunny days and water flawing down to the lowest parts of bays was frozen at nights. This resulted in the differentiation of snow density along the slopes and concentration of load at the bottom of bays.

Snow density corresponding to samples from 1 to 7 are given in Table 3. Ground snow density was 295 kg/m^3 on 27 February and 305 kg/m^3 next day. Mean snow density in bays A and C was 5 - 6% higher, in the bay B even 28% higher. Snow was here more wet.

Snow amount, defined in water-equivalent term, was 10% higher in the bay A then on the ground. In the bay C it was 62% higher. It was due to the snow drift from the adjacent buildings.

CANOPY ROOF

A simple, two pitch canopy roof is situated in the built-up area in Southern Warsaw. Its roof consists of two surfaces made of asbestos undulated tiles. An outline of the roof is given in Figure 10.

Shorter surface is 2.2 m wide while longer 4.8 m. Their slope is 19°. Total height is 4.25 and total lenght 34.8 m. Underroof space was open from one side and its temperature followed outdoor air temperature.

Only one snow profile was measured on 24 February 1979, 7.8 m from the Southern end. It is presented in Fig.10. In the roof folds there was a thin layer of ice. It was taken into account as an additional load of 0.1 kN/m^2.

Snow drift made by the wind blowing along the wider roof surface is seen on the shorter, left surface of the canopy roof. It resultered in relatively high local snow load equal to 1.4 kN/m^2.

The mean roof snow density, without ice layer, was 253 kg/m^3 with small dispersion. Ground snow load measured close by the roof varied from 0.61 kN/m^2, where large amount of newly drifted snow was present, to 0.92 kN/m^2. The mean ground load value without drifted snow was 0.86 kN/m^2, and mean density ρ = 283 kg/m^3. The drifted snow density was 224 kg/m^3 while the highest value was 288 kg/m^3.

The roof-to-ground load ratio was as follows: the mean roof load, with ice, on the right, windward surface, was 0.64 kN/m^2 and the roof-to--ground ratio was 0.74. The maximum roof load on the left, leeward surface was 1.4 kN/m^2 and the roof-to-ground ratio was 1.65. It is worth to note that the ground snow density was higher than roof snow density, certainly due to the newly drifted snow on the roof.

CONCLUSIONS

Snow loads on three different roofs were investigated.

It was stated that even as small as 3° roof slope can influence snow distribution. On the Central Railway Station roof snow load on the roof crest was approximately twice smaller than load on the roof valley.

In the case of saw-tooth roof wind plays a primary, fundamental role in snow distribution.

When the underroof space is kept unheated as under a canopy roof, roof snow density may be less than ground snow density.

REFERENCES

Sobolewski, A., Żurański, J.A.: Snow density for structural snow load in moderate climate, - A Multidisciplinary Approach to Snow Engineering, Santa Barbara, 1988.

Table 1. Roof to ground loads ratio /in sections/.
The Railway Station roof. Load in kN/m^2

Load and ratio	Roof section		
	A-A valley	B-B crest	C-C valley
mean roof load	0.81	0.47	0.83
standard deviation	0.16	0.16	0.10
mean ground load	1.18	1.18	1.22
standard deviation	0.05	0.05	0.05
roof to ground ratio	0.69	0.40	0.68

Table 2. Maximum roof load to mean ground load ratio

Load and ratio	Roof section		
	A-A	B-B	C-C
maximum local roof load	1.13	0.79	0.98
local roof to mean ground load ratio	0.96	0.67	0.80

Table 3. Snow density, in kg/m^3, in three bays
on the saw-tooth roof

Sample number	Bay		
	A	B	C
1	267	355	$\underline{208}$[1] 320[2]
2	338	447	287
3	370	430	315
4	306	343	343
5	287	350	337
6	-	388	-
7	-	430	-
mean	314	391	321[3]
standard deviation	41	43	25

1/ New, drifted and non-insolated snow

2/ Old layer

3/ Without sample 1

Table 4. Roof to ground loads ratio.
The saw-tooth roof. Load in kN/m^2

Load and ratio	Bay		
	A	B	C
mean roof load	1.38	1.1	1.98
maximum local roof load	3.13	2.55	3.25
ground load at the same time	1.25	1.22	1.22
mean roof to ground load	1.1	0.9	1.62
maximum roof to ground load	2.5	2.1	2.66
mean roof load to maximum winter ground load	1.05	0.83	1.5
maximum local roof load to maximum winter ground load	2.37	1.93	2.46
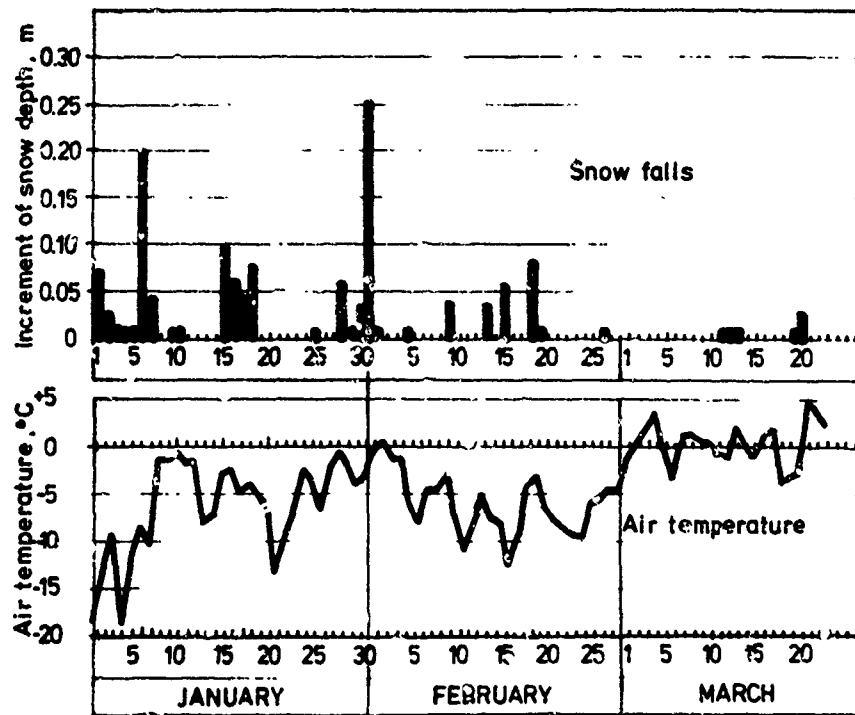
Figure 1 Snow-falls and air temperature time
histories in Warsaw, 1979
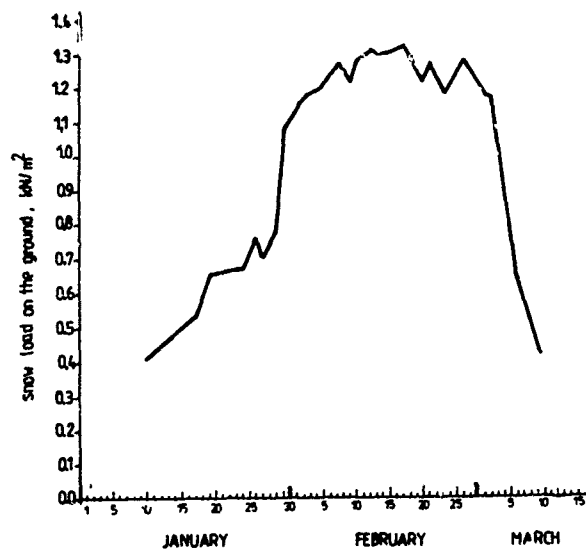
Figure 2 Snow load on the ground time history
in Warsaw City center, 1979
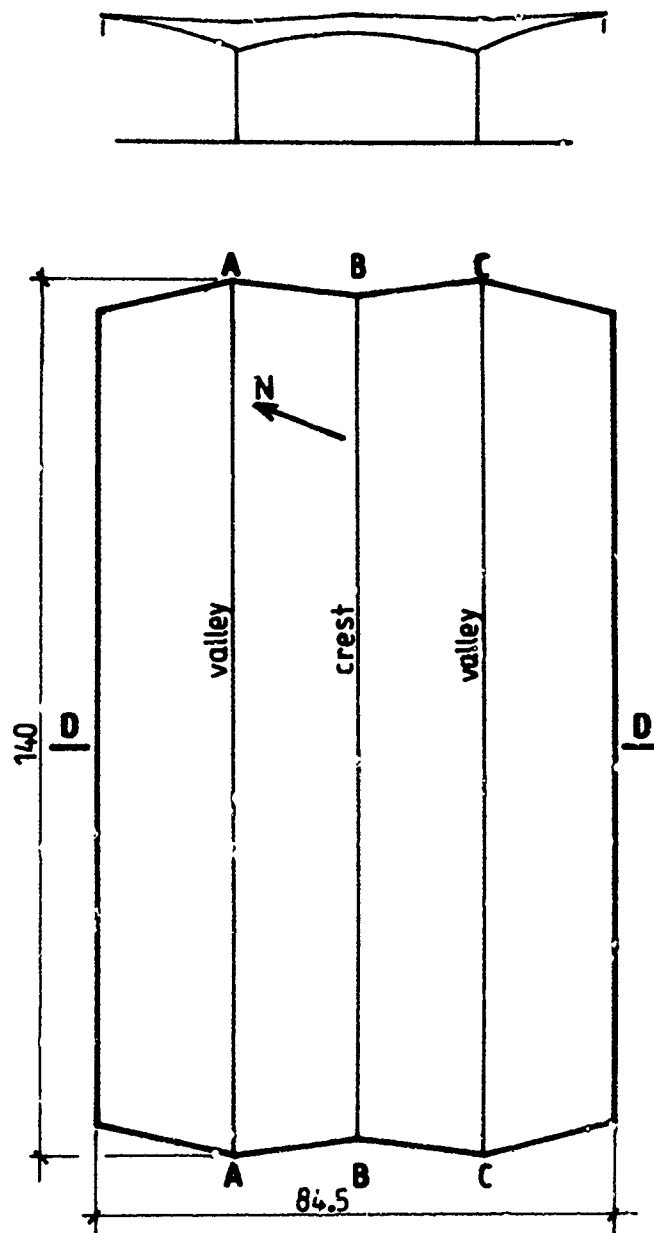
Figure 3 An outline of the roof over the Central
Railway Station in Warsaw. Four measuring
sections are marked
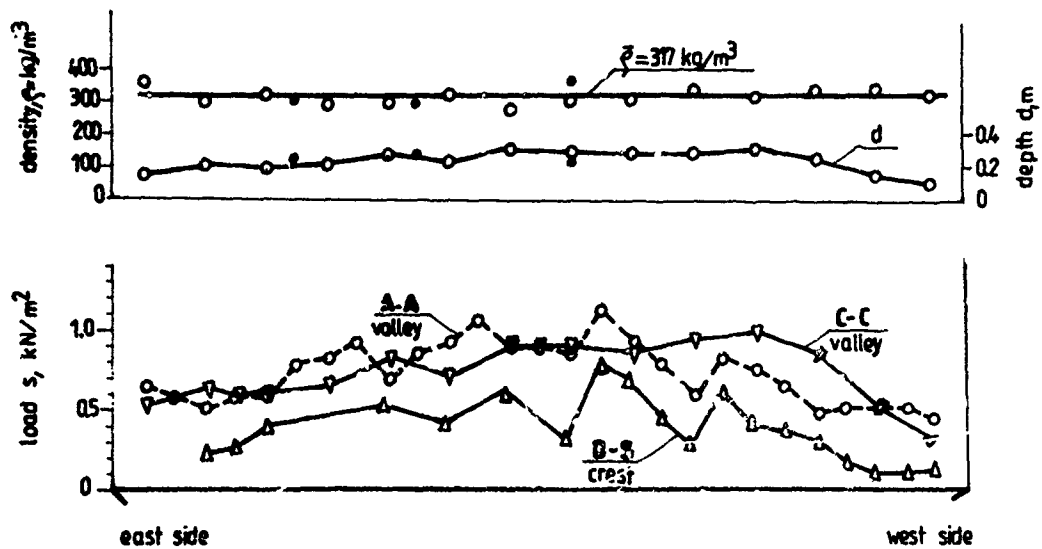
Figure 4 Snow depth, density and load distribution in three longitudinal sections
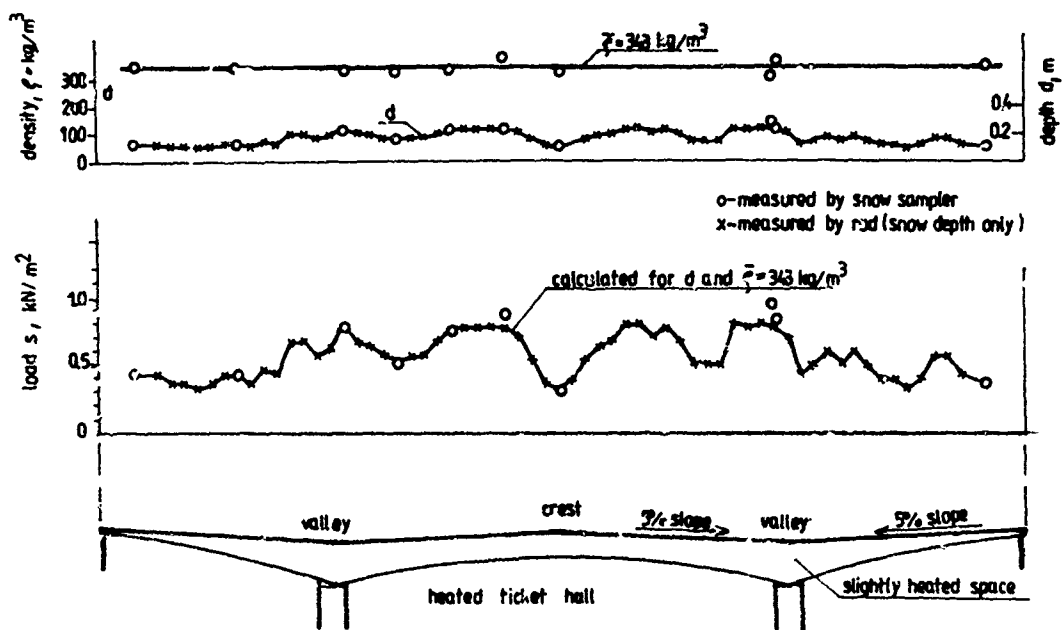
Figure 5 Snow depth, density and load in cross section
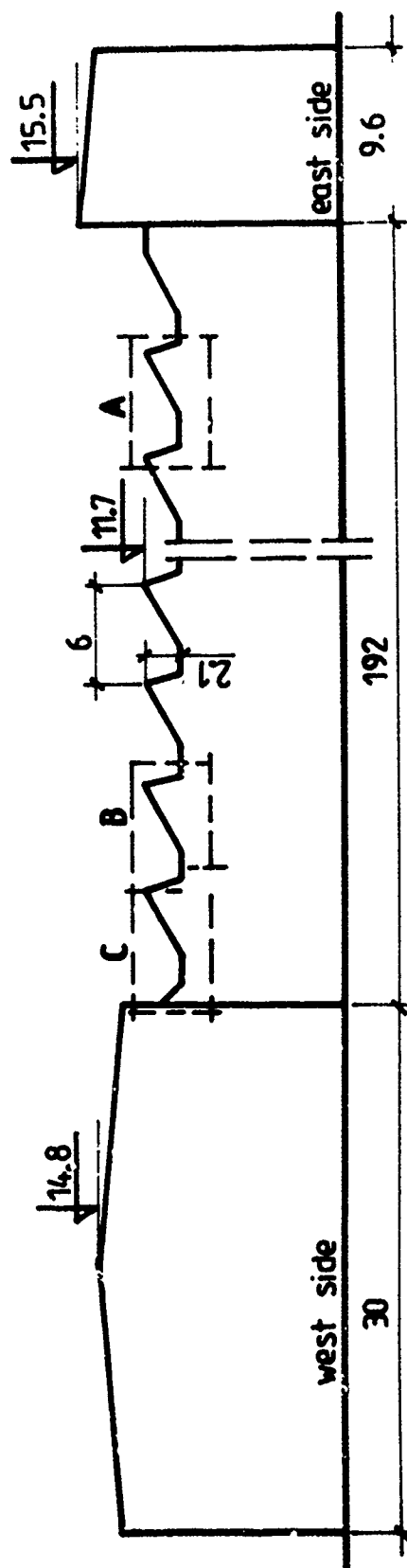
Figure 6 An outline of the saw-tooth roof

73
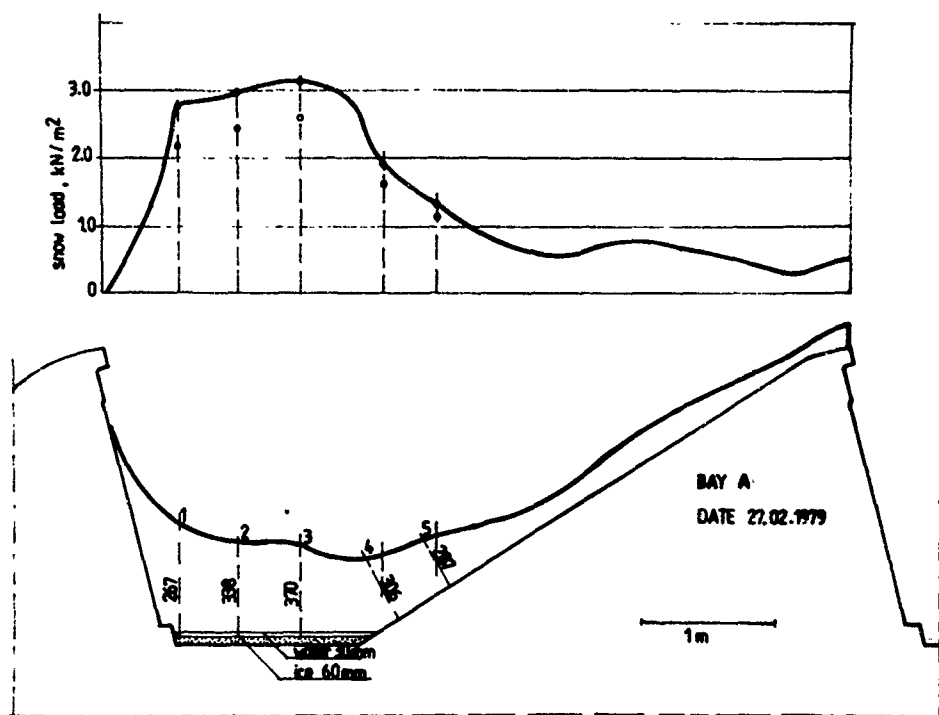
Figure 7 Snow depth, density and load distribution in the
bay A
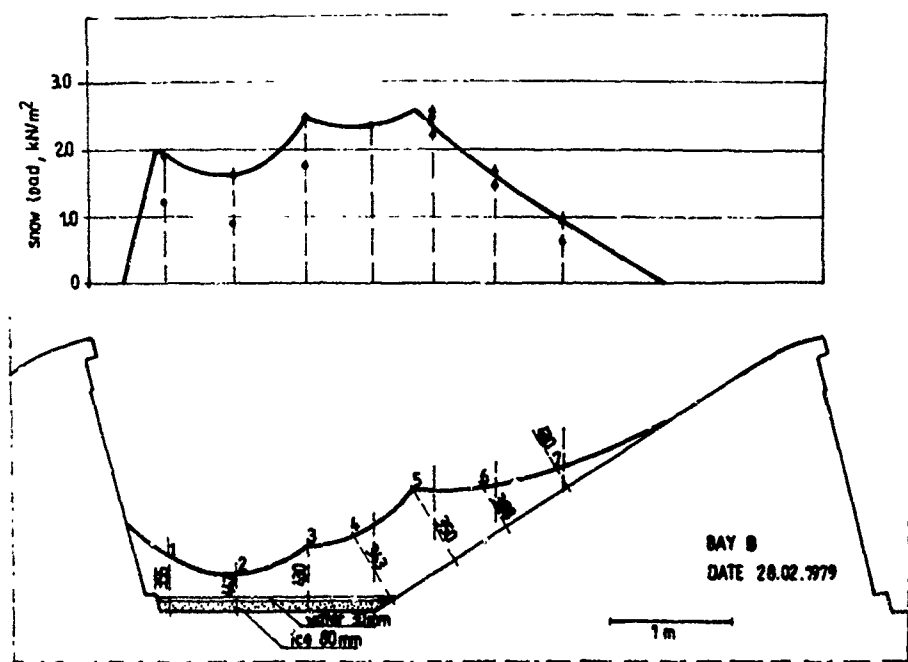
Figure 8 Snow depth, density and load distribution in the
bay B
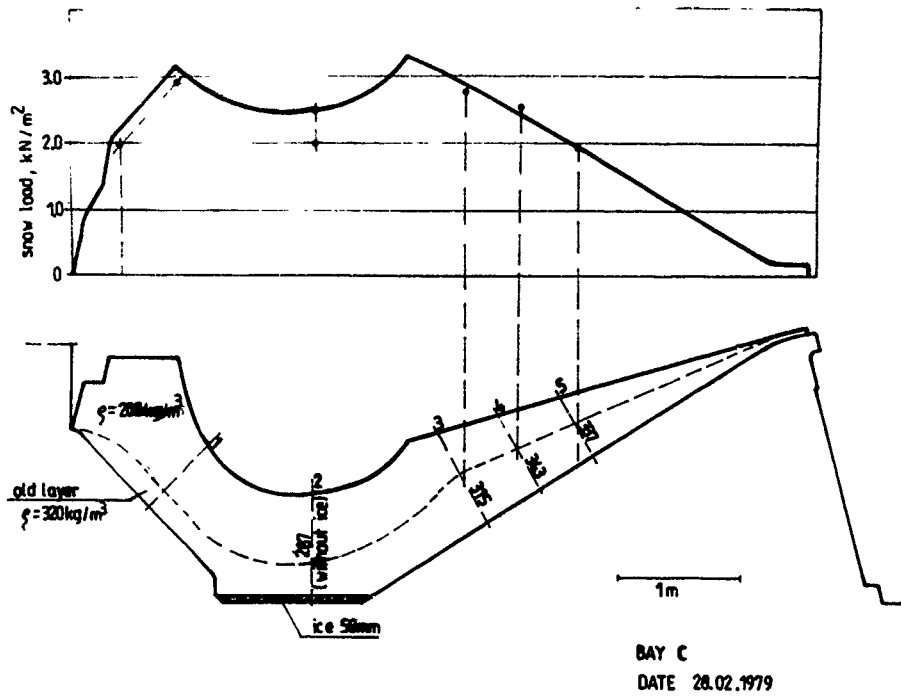
Figure 9 Snow depth, density and load distribution in the
bay C
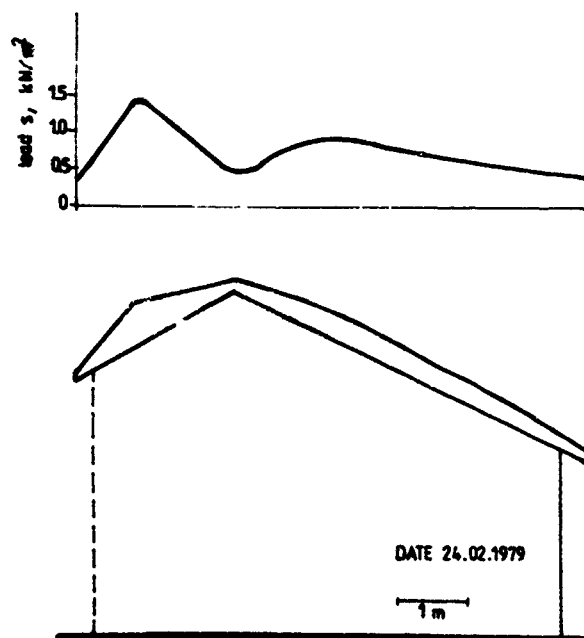
Figure 10 An outline of the canopy roof and snow depth
and load distribution

Snow Damage to Buildings in Poland, 1968–1987

Jósef Wilbik,[1] Andrzej Sobolewski,[2] and Jerzy A. Zuranski[1]

ABSTRACT

In the period of 20 years there were two winters in Poland with
very heavy snowfalls. During those winters snow loads on roofs were
twice or more higher than predicted in the standard. Many failures
to roofs were registered and some 75 cases from both winters were
analysed in detail. The paper deals with the results of this
analyse.
Failures were analysed according to the kind of structure its age
and structural solution and the relation of real snow load to the
snow load in code of practice. It has been found that most of
catastrophes were due to the errors in construction works. Conclu-
sions for the revision of the code of practice have been also
drawn out.

INTRODUCTION

When defining the snow load values for structural calculations we
must take into account three sources of data: /a/ theoretical considerations
and experiments, /b/ tradition, /c/ results of the analysis of snow damage
to buildings. A comparison of theoretical results and snow damage effects
may lead to the resonable solution. Therefore all damages caused by snow
should be analyzed.

In Poland, in the period 1968–1987 there were two winters with heavy
snow-falls: 1969/70 and 1978/79. Snow loads on the ground were then conside-
rably higher than in the Standard /Polish Standard, 1970/.

During the 1978/79 winter approximately 2/3 territory of Poland, its
Northern part, had ground snow load, on the average, 2.7 times exceeding
the characteristic value given in the Standard. If the partial safety
factor, γ_f = 1.4, is taken into account this exceedence will be of the
order of 2. This situation caused many roof failures.

DATA SOURCES

Three data sources were utilized: /1/ an inquire of design offices,
/2/ an inquire of local authorities and /3/ expertises and publications.
Unfortunately, relatively little data were collected, 33 cases from the
winter 1969/70 and 42 cases from the winter 1978/79.

It could be due to the fact that some damages were neglected by buil-
dings users. We looked also for the data at the State Insurance Company but

---

1. Institute for Building Technology, Warsaw, Poland.

2. Research and Design Centre for Industrial Building, Warsaw, Poland

snow damage to buildings are not included in its insurance service. It may confirm the assumption, that snow damage to buildings is not a great problem in our country. It should be mentioned however, that the State industrial buildings were not insured.

RESULTES OF ANALYSIS

The analysis of damages confirmed the evident findings that the mostly prone to snow overload effects are light roofs. The percentage of roof failures are given in Table 1 for different kind of structures. It is seen that steel light roofs were the 50% and recently even 67% of all cases. The timber structures are the second as snow-prone.

The next result is that most failured structures were new ones, constructed no more than 5 years before the snowy winter. It is seen in the Table 2. This is closely connected with the main causes of failures. The most important conclusion is that design or /mostly/ execution errors caused from 70% of failures in 1969/70 to appr. 90% of failures in 1978/79. If there is an error in the structure it will be revealed in early years of its exploitation, by the first, heavy snow. In fact, this is confirmed by above mentioned age of damaged or destroyed buildings.

The majority of destroyed roofs belonged to agricultural building. They were barns, ware-houses, cow-sheds etc. This is in connection with errors in construction works. More errors were found in the country than in towns, certainly due to the higher quality of works in towns.

At least, a last evident result is that the most catastrophes were in March, when snow is heaviest. The distribution is as follows: November and December 4% each, January 17%, February 25% and March 50% of roof failures.

CONCLUSIONS

The most important conclusion is that the main causes of roof damage under snow load are design and /mostly/ execution errors, even up to 90% in the winter 1978/79.

If there were hardly any damages of well designed and constructed roofs, although the design values of snow ground load were two or three times exceeded, it may mean that:

a/ actual load on roof significantly differs from the load defined by the roof shape coefficients; ground-to-roof conversion factor may be twice to high; or

b/ in the structures designed and constructed until now there are load reserves; they may result from the too conservative treatement of combinations of actions in the standards.

The return period of the ground snow load in the Polish Standard is now 5 years. The calculation showed, that the return period of the ground snow load during the winter 1978/79 was approximately 50 years on the average.

If the above conclusions are true the ground-to-roof conversion factor could be lowering twice and the return period of snow load should be 50 years.

It would result in the same design value on the roof as before. The results of the damage analysis do not entitle to the considerable increase of the design value of snow load on the roof.

REFERENCES

Polish Standard PN-70/B-02010 Loads in Static calculations. Snow loads. Actual version was revised in 1980. It has a symbol PN-80/B-02010. Polish Committee for Standardization, Measures and Quality Assurance.

Table 1. Roof damages under snow load according
to the kind of structure

Roof structure	Percentage of cases	
	1969/70	1978/79
Steel	50	67
Timber	42	30
Reinforced concrete	8	3

Table 2. Roof damages under snow load according
to building age

Building age, in years	Percentage of cases	
	1969/70	1978/79
below 5 [1/]	54	83
from 6 to 15	8	17
above 15	38	–

1/ damages during the construction works
included

Roof Snow Loads in Deep Snow Regions

Donald Taylor[1]

ABSTRACT

This paper presents interim results of the survey started in 1980-81 on snow loads on roofs in the deep snow areas of Mount Washington near Comox, Vancouver Island, British Columbia. Here the 30-year return ground snow load is greater than 24 kPa (500 psf). Recommendations are made for the design of buildings in deep snow regions and the management of heavy snow on roofs.

INTRODUCTION

In the fall of 1980 the author organized a survey of snow loads in twenty communities throughout British Columbia. The area of heaviest snow loads under survey is Mount Washington on Vancouver Island. Some existing buildings there have suffered structural damage in past years; furthermore, a large expansion of the ski village is contemplated. Continued economic development for such areas requires that the estimates of design roof loads obtained from the National Building Code of Canada be realistic and yet not overly conservative. Since last winter (1987·88), the observations have been conducted under a shared 5-year contract between the Province of British Columbia and the National Research Council of Canada.

This paper presents preliminary results from an analysis of the data collected since 1980. It makes recommendations for the design of buildings in deep snow areas and for the management of heavy snow on roofs.

DEEP SNOW AT MT WASHINGTON

Since Mt Washington is on the east side of Vancouver Island, just a few kilometres west of Comox, it is not obvious why the snowfall should be so heavy. Indeed, one would expect that the humid air blowing over the Pacific towards the Island would be forced up as it hit the mountains and would drop its moisture as rain and snow on the west side of the island. This would result in dry conditions on the east side. Mt Washington, however, gets its moisture by a different route. The winds do indeed come across the Pacific but blow through the strait of Juan de Fuca to the south of the Island (Fig. 1). They circulate counter-clockwise until they are heading north and northwest, channelled between the ridge of mountains on Vancouver Island and the coastal mountains on the mainland. Fig 1 shows why Mt Washington gets so much snow. It stands alone, cut from the ridge of mountains on the island, the highest peak directly in the path of the southeast (and northwest to northeast) winds.

I   Senior Research Officer, Institute for Research in Construction, National Research Council of Canada, Building M-20, Montreal Road, Ottawa, Ontario, K1A 0R6
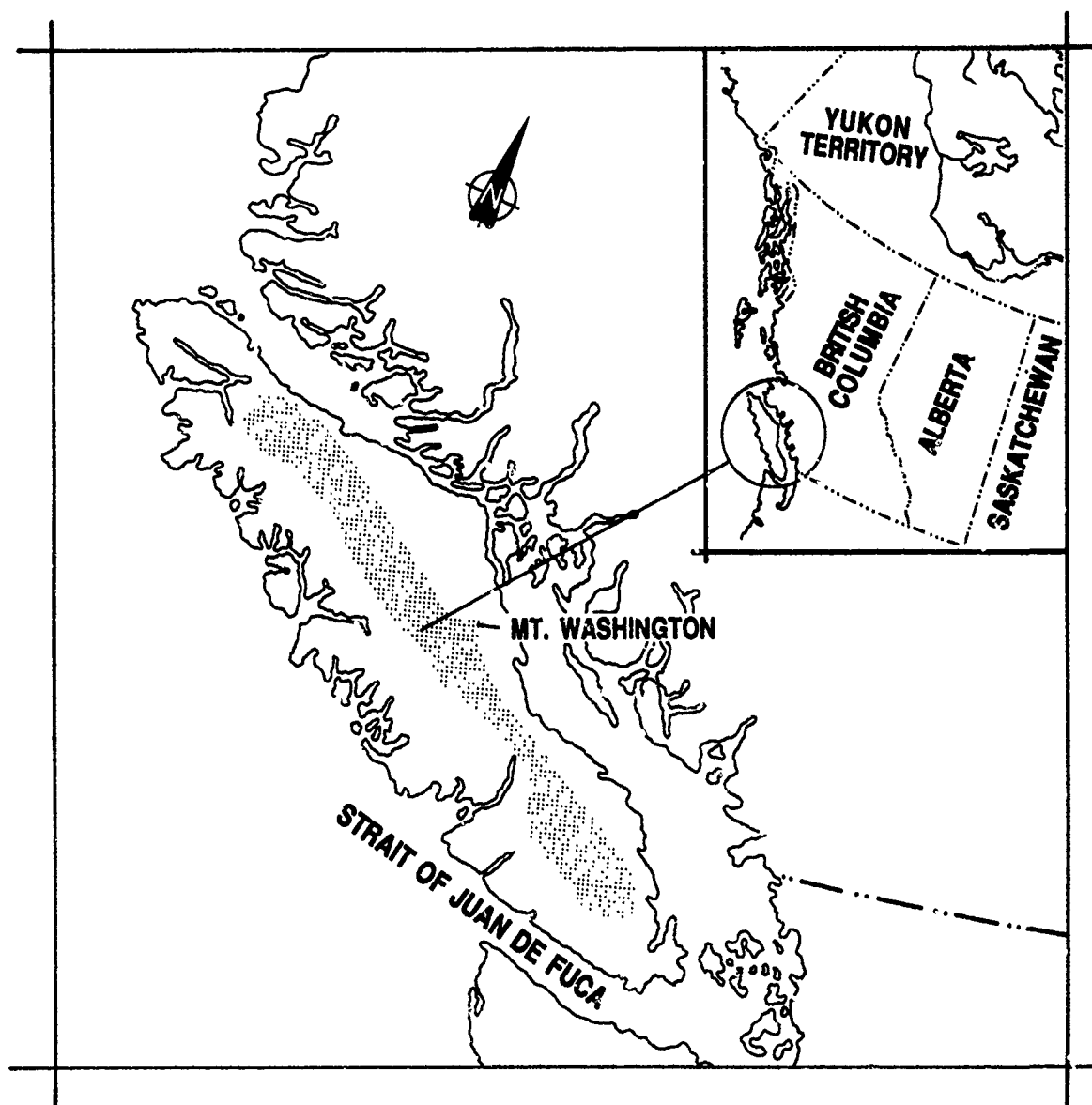
Figure 1.   Map showing location of Mt. Washington, Vancouver Island. It stands alone in the path of moisture laden winds blowing through the straits between the island and the mainland of British Columbia.

THE SKI VILLAGE

The ski runs and ski village are located on the south and southwest face of the mountain and are therefore exposed mainly to winds from the southeast and east. The building sites range from about 1100 to 1190 metres above sea level. The valley that runs westward from the east ridge of the mountain is swept by strong east winds; the low roof of a sewage treatment plant on the floor of the valley (at 1106 metres) is kept relatively clear of snow. Tall trees are plentiful around the buildings but any roofs protruding above the trees or above sheltering ridges also show evidence of snow removal by the wind. All vehicles are parked on the periphery of the village, since the village roads are not plowed because of the very deep snow. They are usable only by skiers, pedestrians, and the service vehicles--snowcats and snowmobiles.

Buildings vary from single storey chalets to three and four storey condominiums. Some roofs are flat while others are shed, gable and cruciform (intersecting) gable. The single storey buildings are almost buried during deep snow winters, and for this reason many structures incorporate storage areas at ground level in order to gain height. Thus the living areas start at the second storeys and are accessed by stairs; as the snow accumulates, fewer stairs need to be climbed! This avoids having to dig down to doorways and windows as the snow deepens.

DESIGN GROUND SNOW LOAD

When development of the ski area was begun in 1979, no formal survey of snow loads on the ground was being conducted. Observations had been taken for about 20 years at Forbidden Plateau some 11 kilometres to the southwest, but local experience indicated that the loads at Mt Washington were heavier. In any case, the basic 30-year return ground snow load had to be estimated, and it appears that some estimates used by designers of village buildings may have been too low.

Two equations are available for estimating the ground snow load. One is based on observations of snow load versus elevation on a number of mountains throughout southern British Columbia by P Schaerer and colleagues of the National Research Council of Canada. Load-elevation relationships were derived from these data for mountains in different parts of the province (Claus et al., 1984). The second was developed by the Atmospheric Environment Service (AES) using their own and Schaerer's data (M. Newark, AES - private communication). At 1170-m elevation where one of the first buildings -- the Day Lodge -- was built, predictions of the 30-year return ground load (or ground load with a 1-in-30 probability of exceedance (see Fig. 3) per annum) are as follows:

$$\text{Claus} \quad S_0 = 3.020 - 0.0193 \bullet (elev) + 0.0000481 \bullet (elev)^2 = 46 \text{ kPa}$$
$$\text{AES} \quad S_0 = 4.909 - 0.0048 \bullet (elev) + 0.000024 \bullet (elev)^2 = 32 \text{ kPa}$$

The Atmospheric Environment Service checked its equation by applying it to Forbidden Plateau, 11 km away, where by then, 29 years of observations were available. The comparison was good. Nevertheless, some people with long time local experience think the higher figure is more appropriate! Direct calculations using the 9 years of snow depths recorded at Mt Washington and a specific gravity of 0.4 give an estimate of about 20 kPa using a Gumbel Type I extreme value distribution (Newark et al., 1988). An estimate weighting the AES figure with this new one in a 1 to 2 ratio is about 24 kPa. Which of the four is most reasonable? More site observations are clearly required to rule in favour of one of these or establish an improved figure.

THE SURVEY

Even if a good estimate of the 30-year return ground snow load were available, it would still be important to make roof snow load observations. They would indicate whether the snow load factors in the National Building Code are appropriate for the design of roofs at Mt Washington. The survey, started in the autumn of 1980, was intended to do just that. In the first two years, measurements of snow depths and densities were taken on the roofs of the Day Lodge, and Condominium numbers 96, 89, 81. In the third year, the surveyor took no measurements at all. Unfortunately this was the deepest snow year. He did, however, take a number of photographs and noted that the maximum snow on the roofs was over 3.7 metres deep, the specific gravity was over 0.4 (i.e. load = 14.5 kPa), and that it was unsafe to try to get onto the roofs using a ladder.
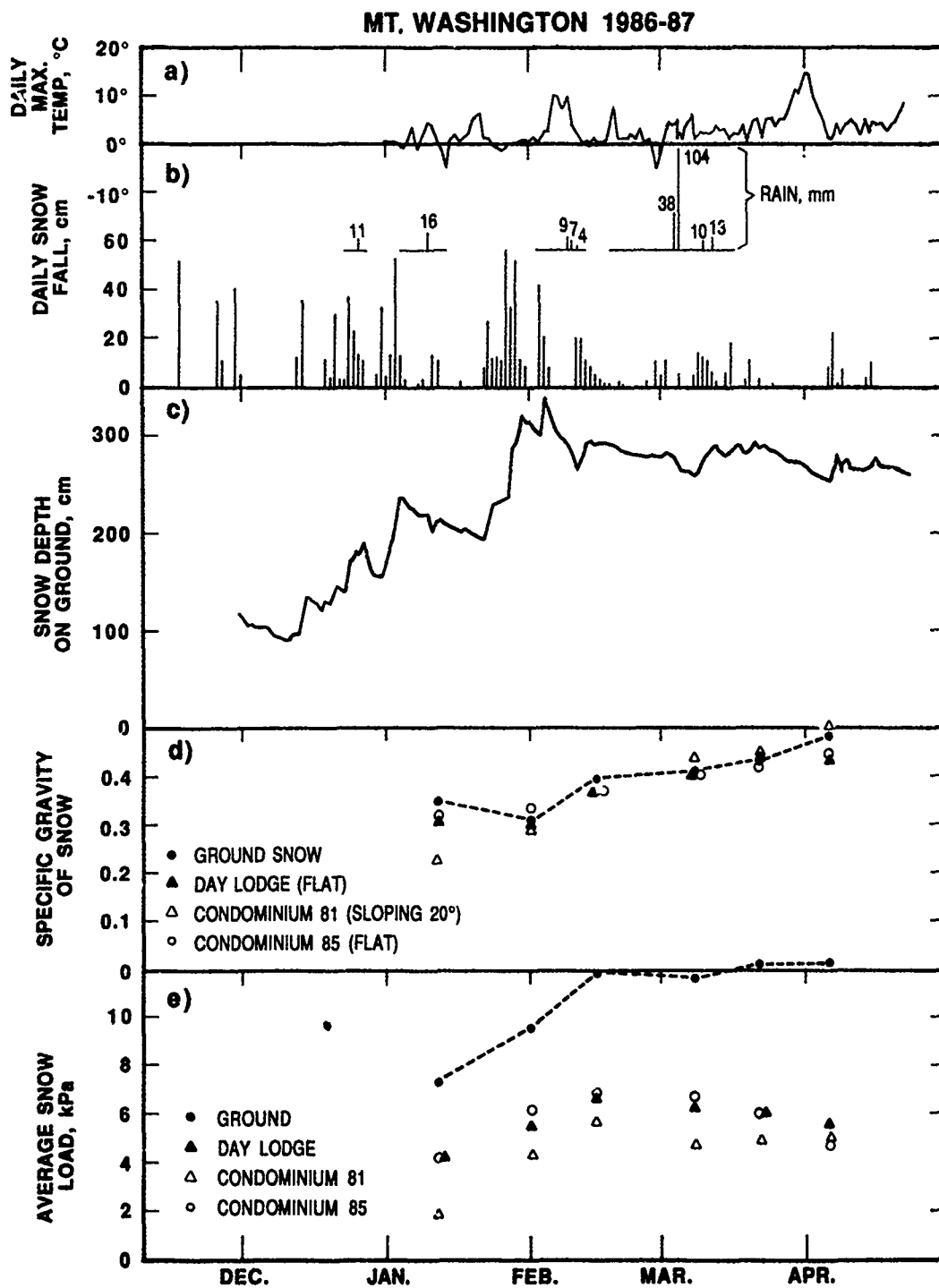
Figure 2:   Temperature and snow data at the Mt Washington ski village for winter of 1986-87

During the next year (1983-84) a new observer took measurements on the Day Lodge and Condos 95 and 81, and in 1984-85, on the Day Lodge and Condos 85 and 81. In the winter of 1985-86 he was injured skiing and was unable to find anyone to take the readings so another year of data was lost. During the last two years a new observer was hired. He recorded depths and densities on the Day Lodge and Condos 85 and 81 in 1986-87. With more resources available in the following year on account of the shared contract with the province of British Columbia, he took readings on the Day Lodge, the Maintenance Shop, the Recreational Vehicle Park Building, the Reception Building, the Sewage Treatment Plant and Condos 85 and 81. Readings were taken six times between December 27, 1987 and May 12, 1988. The same pattern of observations on the same roofs will continue for another four winters. Throughout the six winters in which observations were made, depths and densities of ground snow were also recorded.

Initially, densities were sampled vertically through the snow pack using a 1-m long tube sampler of 51-mm inside diameter. The sampler was too short to be practical in deep snow packs so the observer switched to a Federal Snow Sampler and a probe. The probe is used to get the depth to the roof surface. Then the sampler is twisted vertically downward and sections are screwed on as required until the sampler is stopped just short of the roof or the ground surface. Because the sampler has a smaller diameter (approx. 38 mm), it is not as prone to dropping the sample when it is withdrawn from the snowpack.

The only buildings surveyed each year that measurements were made were the Day Lodge and Condo 81, so the emphasis in this paper is focussed primarily on them. The Day Lodge is a two-level flat roof structure 25x35 m in plan and about 13 m high surrounded on three sides by a 1-m parapet; the upper level is 2 m high and 15m x 13m in plan and is against the northwest corner of the building. Only results for the lower roof are given. The ground elevation at the Day Lodge is about 1170 m, and the building is exposed to the wind. Condo 81 is 15 m by 15 m in plan and about 3 1/2 storeys high; it is on the mountain slope at 1162 m elevation and is sheltered by tall trees. It has an asymmetrical gable roof with the longest side facing north-west into the hill and sloping at 20 deg. The other side faces southeast and is too steep for observations.

RESULTS OF SURVEY

Temperature and Snow Data

For the winter of 1986-87, Figures 2(a) to 2(c) illustrate the daily maximum temperature, snowfall, snow depth on the ground. For the same time scale, Fig. 2(d) and (e) also present the corresponding specific gravity of snow and the average snow load on the ground and on the roofs of the Day Lodge and Condos 81 and 85. Between November 1, 1986 and April 6, 1987, 989 cm of snow fell and as Fig 2(c) indicates, it accumulated to a maximum depth of 340 cm on the ground by February 4 and stayed well into April. Although snow was denser on the ground than on the roof on January 12 when the first observations were made (Fig. 2(d)), the specific gravity of roof and ground snow differed little after February 1, increasing to an average value of about 0.47 on April 6. The ground snow load (Fig. 2(e)), on the other hand, reached a plateau of about 12 kPa on February 12 remaining more or less constant into April. Roof snow loads peaked on February 12, but decreased gradually thereafter. Maximum daily temperatures above 0°C, with diminishing snowfalls, caused the decrease. Unlike in most snow load areas of Canada (at lower elevations), the heavy snow loads on roof and ground at Mt Washington were of long duration. The ground load was at its maximum for at least two months, while the roof loads were within 16% of the maximum for about 2 1/2 months. The large rainfall of 38 mm and 104 mm on March 3 and 4, 1988 seems to have had only a small influence on the roof snow
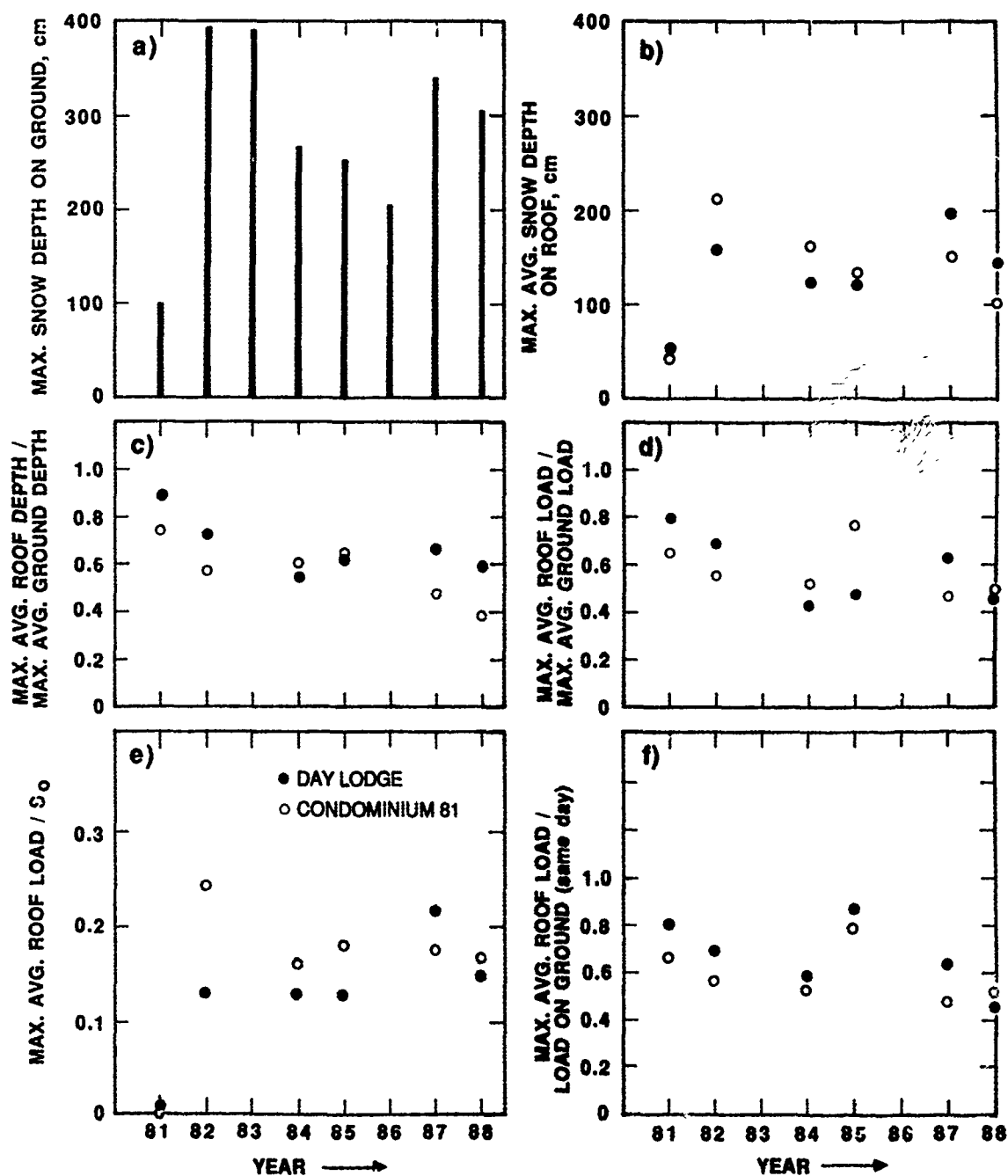
Figure 3: Snow depth and loads on roofs and ground from winters 1980-81 to 1987-88, inclusive. No observations were recorded for winters 1982-83 and 1985-86 (Year 81 on the graphs denotes the winter of 1980-81, etc.). S_0, the ground snow load with a 1-in-30 probability of exceedance per annum is calculated using the AES equation.

loads and very little effect on the ground load. This is not surprising because the rain melts some snow, reducing the load, but some is retained in the snow pack and this increases the load. The overall effect in a deep snow pack can be minimal.

Snow Loads

The following points, relating to Figure 3, should be noted:

- Measurements of snow depth and densities were taken up to six times per winter, and for each roof on each observation day a spatial average of the snow depths was calculated. Then an average load was computed from the measured snow density. The largest of these averages, for each roof, is the data point for the maximum average depth or load for that winter.

- The maximum snow load or snow depth may be as much as 50% higher than the maximum average, but it applies over a smaller (tributary) area. A more detailed study of the roof loads giving the maximum average load over local areas that are supported by purlins, beams, girders, and columns will require a substantial amount of analysis and has not yet been done.

The annual statistics of normalized snow depths and snow loads on the roofs of the Day Lodge and Condo 81 and on the ground are shown in Figure 3. Figures 3(a) and (b) show snow depths on ground and roof, respectively; their relative magnitudes are seen to correspond approximately. This gives some support to the use of ground snow loads as a basis for design roof loads at Mt Washington.

Effect of Wind

In some years, as shown in Figure 3(c) and (d), the normalized loads and depths on Condo 81 exceed those on the flat roof of the Day Lodge and vice versa. This probably indicates the influence of the different wind exposures of the two roofs and of sliding from the sloping roof of Condo 81. Certainly, in spite of the wet snow that often falls at Mt Washington, the influence of the wind is unmistakable. In the 1987-88 winter, the first of the 5-year contract with the Province of British Columbia, measurements were taken on three roofs exposed to the wind, two sheltered (including Condo 81) and two that are partially sheltered (including the Day Lodge). The average ratio of maximum average roof load to the 30 year return ground load appropriate to each site as calculated using the AES equation, was 0.25 for the sheltered, 0.18 for the partially sheltered, and 0.06 for the exposed roofs.

Code Comparisons

Figures 3(c) and (d) also show that the ratio of the maximum average roof load to the maximum average ground load (or indeed, to the ground load on the same day that the roof load is a maximum), reached 0.8. The design value from the National Building Code of Canada is also 0.8 for roofs not entirely exposed to the wind on all sides. An important point, however, is that the 0.8 value occurred in 1980-81 and 1984-85 (Figure 3(d) and (f)), but these were not the heavy snow years. Figure 3(e) shows that even the heaviest average roof loads were only about 22 to 24% of the 30 year return ground snow load, which is approximately 32 kPa at the Day Lodge and Condo 81 as obtained using the AES equation. Values of the ratio during years with ground snow loads approaching 20 kPa or more would be most interesting. That no observations

91

were taken in the heavy snow year 1982-83 is unfortunate; comparison with the previous year would have been very useful.

The collection of quality data from the same roofs as those surveyed this past winter will go a long way toward providing the basis for good economical design loads for roofs at Mt Washington. It would be unwise, however, at this time to draw conclusions about appropriate design loads derived from a discontinuous data set with only six years of readings. Instead, the following recommendations are offered to help designers avoid some of the problems already experienced at Mt Washington.

RECOMMENDATIONS FOR DESIGN AT MT WASHINGTON

Good design, especially in deep snow areas, must ensure that:

1. the design loads are safe and economical;
2. the area around the building is not made hazardous
    by falling or sliding snow;
3. the snow is managed sensibly.

Safe and Economical Design Loads

The paper, to this point, has dealt with safe loads on the main areas of the roofs. This is the conventional concern of the designer, but in deep snow areas there is much more:

a) At Mt Washington snow cornices can be enormous, equal to the roof snow in depth and may extend horizontally as much as 2.5 m beyond the edge of the roof and hang down a metre or so. The extra weight on the edge of the roof or the columns or walls beneath has been more than some structures could carry. In order to avoid problems due to cornices, the owner of one flat roof building keeps a snowblower on the roof to remove the snow within about 1.5 m of the edge of the roof--a very good idea! To get onto the four storey roof he has built a 1-m by 1-m by 2.5-m high extension with a trap door on top. A ladder inside the hatch extends to the floor below.

b) With single snowfalls as deep as one metre, cohesive wet snow may accumulate uniformly on steep gable roofs without sliding. The tensile strength of the wet snow across the ridge allows the snow on one side to anchor that on the other. The substantial loads that can be held on the roof should be considered in design, as should effects resulting from the inevitable avalanching of this snow off the roof.

c) Balconies should be designed for roof snow loads and loads due to falling cornices if they are not roofed over.

d) Railings should also be designed to take the forces from falling cornices.

e) Metal decking should not extend more than about 2 cm beyond the structural decking under it. Otherwise the heavy snow will bend the metal and damage it or make it look unsightly.

f) Windows and doors should be installed properly or vertical shortening or bending of the building components under the heavy snow loads will break the glass or jam the doors.

g)   Consideration should be given to earthquake design of the buildings accounting for the heavy and long duration snow loads. Sliding of deep snow off the roof also results in substantial dynamic loads applied to the building (Paine and Bruch, 1985).

Sliding or Falling Snow

a)   If cornices break off they could injure or kill; they have damaged building components such as balconies or stairways below, or attachments of power lines to the building. Because cornices sometimes rotate about the eave as they break, they have also broken windows and damaged siding.

b)   Sliding snow may damage chimneys, escape hatches, toilet vents, aerials, wiring stacks, skylights, ventilators, and other protrusions on the roof and may also be very dangerous to people, vehicles, stairways, balconies, wiring etc. below.

c)   Where there is a dormer or where the roof is made from intersecting gables, the snow will jam in the valleys when it tries to slide. The outstanding ribs on metal roofing will be flattened or even ripped where they impede sliding. Further, snow held in a valley will substantially increase the load on the opposing roof surface.

Management of Heavy Snow

a)   Powerlines must be very carefully considered. At Mt Washington some lines can be touched by children playing around the buildings because the wires and the attachments to the buildings are not far enough above the snow surface.

b)   Building entrances and exits should be on the gable ends, and should be reached by stairs. Where an exit (fire exit) cannot be placed above the snow level, a hatch should be built to enable escape at various levels depending on the snow depth.

c)   Parapets should be avoided to allow wind to remove snow.

d)   Positive slopes on flat roofs avoid the ponding of melt and rain water. The flat roof of the Day Lodge has a perforated plastic drainage pipe lying across it to aid drainage.

e)   Chimneys and other protrusions should be located at the ridges to avoid being sheared off by sliding snow.

f)   Balconies that are roofed over will be protected from falling cornices - so will their railings.

g)   If there is any flexibility, buildings should be located to prevent sliding snow from landing on roads or walkways.

h)   One storey buildings may have problems. Safe entry and exit may be difficult to achieve; it may be necessary to dig down to doorways. On a one storey building with a sloping roof, the snow will not be able to slide entirely off the roof. Windows may also be below ground snow level.

i)   Large overhangs of roofs are desirable to keep cornices and falling snow away from walls, doors, and windows; however, structural support of big overhangs is sometimes difficult and expensive to achieve. Columns may be required.

ACKNOWLEDGEMENTS

REFERENCES

Claus, B.R., Russell, S.O. and Schaerer, P.A., 1984. "Variation of Ground Snow Loads with Elevation in Southern British Columbia." Canadian Journal of Civil Engineering, Vol.11, No. 3, pp. 480-493.

Newark, M.J., Welsh, L.E., Morris, R.J. and Dnes, W.V., 1988. "Ground Snow Loads for the 1990 National Building Code of Canada." Proceedings, 1988 Annual Conference of the Canadian Society for Civil Engineering, Calgary, Alberta, May 23-27, 21p.

Paine, J. and Bruch, L. 1986. "Avalanches of Snow from Roofs of Buildings." International Snow Science Workshop, Lake Tahoe, California, October 22-25, 5p.

Snow Load on Gable Roofs
Results from Snow Load Measurements on Farm Buildings in Norway

Halvor Høibø[1]

ABSTRACT

The Department of Building Technology (IBT) at the Agricultural University of Norway completed a project in 1986 on snow load measurements which had been run for 20 years. The measurements were carried out on farm buildings in inland districts with lowland areas and valleys and mountainous country. About 200 of the buildings were gable roofed. The roofs were cold, ventilated roofs with no heat transfer from underneath. They had different slopes, different roofing material and were differently exposed to the wind and to the sun. <u>Metal roofing and other roofing materials</u> (asbestos cement sheeting, tile, asphalt roofing and wood shingles) were studied.

The study intended to give the form factor (μ) for the roof (μ = roof load to ground load ratio) when the snow load on the roof was at its highest during the winter.

<u>Proposal for μ_1 (for windward side of the building)</u>:

$\alpha < 20^0$: $\mu_1 = 0.85 - 0.105 \cdot Z$

$20^0 < \alpha < 45^0$: $\mu_1 = 0.85 - 0.105 \cdot Z - \begin{cases} 0.015 \cdot (\alpha - 20^0), & (1)* \\ 0.011 \cdot (\alpha - 20^0), & (2)* \end{cases}$

<u>Proposal for μ_2 (for leeward side of the building</u>:

$\alpha < 20^0$: $\mu_2 = 0.90 - 0.08 \cdot Z$

$20^0 < \alpha < 45^0$: $\mu_2 = 0.90 - 0.08 \cdot Z - \begin{cases} 0.011 \cdot (\alpha - 20^0), & (1)* \\ 0.006 \cdot (\alpha - 20^0), & (2)* \end{cases}$

α = roof slope
Z = ground snow load
(1)* metal roofing
(2)* other roofing materials

INTRODUCTION

Snow loads on roofs are an important factor that must be taken into account in building design, especially in northern countries. It is a general problem in building technology to find an appropriate design snow load and institutions that are working in general building research have the responsibility of taking care of this. The Department of Building Technology (IBT) at the Norwegian Agricultural University is working especially on farm

[1]Professor, Agricultural University of Norway, Department of Building Technology in Agriculture.

buildings. The reason why IBT, which is mainly engaged in the agricultural aspects of the buildings, has become so heavily involved in providing data on snow loads on roofs is that it has not found sufficient snow load data from other institutions to cover the need in the farm building trade.

Two factors cause the design snow load to be of special interest for farm buildings:

1. The construction costs are higher in relation to the total building costs for farm buildings than for most other types of buildings.
2. The costs when buildings collapse are more moderate in relation to the total building costs for farm buildings than for most other buildings.

These factors cause the relative economic failure risk normally to be higher for farm buildings than for buildings in other industries.

In order to design building structures with more accurate relative failure risk than usual, the need for accurately founded design loads is obvious. IBT, therefore, started preliminary snow load studies in 1958. These went on until 1965, when a main snow load study was started. This study was continued for a period of 20 years. A main aim of the studies was to improve, if possible, the Building Code treatment of snow-load reductions on sloped roofs. The studies were intended to find the form factor for gable roofs (μ-factor) when the snow load on the roof was at its highest during the winters.

PRELIMINARY STUDIES

Before the preliminary studies were started, the literature on snow loads was searched. Information from abroad mainly was gathered from the Division of Building Research, National Research Council of Canada, NRC (1,2).

The preliminary studies were made on buildings in full scale and also on small test roofs. The test roofs were placed in two groups:

1. In an opening in a forest, well sheltered from wind
2. In an open field, strongly exposed to wind.

Snow load measurements on the small test roofs were found to be inadequate for the purpose because of indeterminable wind effects on the exposed roofs.

Placing scales underneath purlins in two fullscaled test buildings was also tried - for weighing the snow load component normal to the roof area. This method was found to be sufficiently accurate as a load finding method. However, it was found to be more expensive for our conditions than observations made by depth and density measurements on regular farm building roofs.

Before the type of sampler for density measurements was selected, several samplers were appraised. It was found that with a pipe of at least 80-cm^2 crossectional area and with a sharp cutting edge density measurements could be made with a deviation of less than $\pm$ 1%.

THE MAIN STUDY

Based on the experience from the preliminary studies the following was decided:

1. Snow load on roofs should be measured on buildings in full scale.
2. Depth measurements should be taken vertically, systematically distributed over the roof area.
3. The density measurements should be taken vertically with the "IBT-type" of sampler with a fairly large cross section.
4. Ground snow load should be found as an average snow load from at least ten depth measurements around the buildings.

The study of snow loads on gable roofs was carried out on roughly 200 farm buildings in a 20-year period from 1966. The study was carried out in 3 areas, in the counties of:

Akershus (lowland district)
Buskerud (mainly valleys and mountainous country)
Hedmark (inland wide farmlands and mountainous country)

The buildings were rectangular shaped or had rectangular wings located together angularly. These buildings had no devises preventing snow from sliding off the roofs.

We intended that building shape, roofing material and climatic factors would appear as the primary factors in determining the snow load on the roofs.

The requirements of the study were:
- The roofs should be cold, ventilated roofs with no heat transfer from underneath,
- The roofs should have different slope. It worked out so that the slope varied from 0^0 to 45^0,
- The roofs should have different roofing materials, preferably 20% metal roofing, 20% asbestos cement sheeting, 20% tile, 20% asphalt shingle and 20% wood shingle,
- The roofs should be differently exposed to the wind and to the sun.

The buildings were fairly large, roughly 300 square meters in ground area and 6 m to the eaves (with large variations).

The study was intended to give the "μ-factor," given as the ratio of roof load to ground load when the snow load on the roof was at its highest during the winter. The μ-factor was intended to be used together with a characteristic ground snow load to give the design roof snow load:

$$S_{ROOF} = \mu \cdot S_{GROUND}$$

Measurements on the roofs were not taken (or load measurement data for the roofs were omitted) when the mean roof snow loads were below 0.4 kN/m^2.

The data of the snow load study on gable roofs are grouped for:
- county   (3 alternatives)
- roof number   (roughly 400)
- altitude   (4 classes)
- roofing material   (2 classes: metal roofing, 20% of the roofs, and other materials, 80%)
- slope   (9 groups of 5 degrees inclination each)
- year   (20 numbers)
- week   (14 numbers)
- roof side   (2 alt. - windward and leeward sides).

The results from the snow load measurements were calculated on this basis:

- Snow load on the roof, with mean load calculated separately for the windward and the leeward side each.
- Mean snow load on the roof, calculated for the total roof area.
- Snow load on the ground, (Z).
- μ-factor, calculated as roof load to ground load ratio, separately for the windward side (μ_1) and for the leeward side (μ_2).
- Mean μ-factor for the total roof area.
- Density for the roof snow load and ground snow load separately.
- "More-load-factor" (M-load), calculated as the ratio between the load on the most loaded 20% area of the roof and the mean load. (The most loaded 20% area of the roof was measured as a rectangle across the building.)
- "Nonsymmetry-factor" calculated as the ratio between the snow load on leeward and windward sides of the roofs (μ_2/μ_1).

It was assumed that roof shape (slope), roofing material, type of climate and wind condition affect the size of the μ-factor heavily. The amount of the snow load on the ground, orientation of the building to the sun and to the wind, and also altitude were supposed to play a certain part. However, the influence on the μ-factor from different types of climate, and from different orientations of the buildings to the sun and to the wind could not be explained from the present snow load measurements.

<u>The effect of roof slope</u>

Roof slope (α) influences the μ-factor significantly. When roof slope is below 20 degrees, however, the correlation between slope and μ-factor is questionable for the leeward side of the roof (see Figure 1.)

The influence of roof slope on the μ-factor is embodied in the final models of form factors for gable roofed buildings.

The top-left shows a graph labeled $\mu = A \cdot \alpha + B$ with axes marked 0,8; 0,6; 0,4; 0,2 and horizontal axis at (0,0), 20°, 45° α, with curves μ_1, μ_2, WIND, and a building diagram.
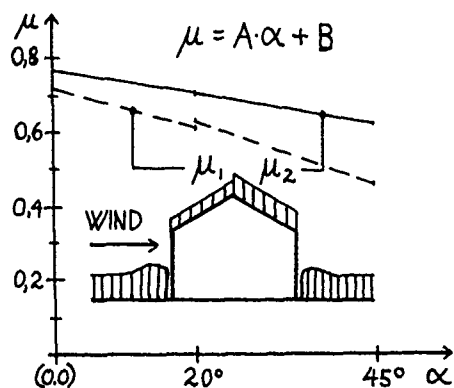
	$\alpha < 20^0$		$\alpha > 20^0$	
	μ_1	μ_2	μ_1	μ_2
A	-0.0054	-0.0026	-0.0072	-0.0038
B	0.717	0.760	0.770	0.781
n	192	192	1095	1095
r	-0.223	-0.110	-0.208	-0.114

Figure 1. The effect of roof slope on the μ-factor. As can be seen from the table, the roof slope influences the μ-factor significantly.

The effect of roofing material

For roof slopes above 25 degrees, metal roofing has given significantly lower μ-factors than the other roofing materials under consideration (see Figure 2)

Graph with μ axis (0,8; 0,6; 0,4; 0,2) and horizontal axis (0,0), 25°, 45° α, showing:

Matr. 2: $\mu_2 = 0.84 - 0.005 \cdot \alpha$

Matr. 1: $\mu_2 = 0.77 - 0.0095 \cdot \alpha$

Matr. 2: $\mu_1 = 0.82 - 0.0084 \cdot \alpha$

Matr. 1: $\mu_1 = 0.76 - 0.0084 \cdot \alpha$
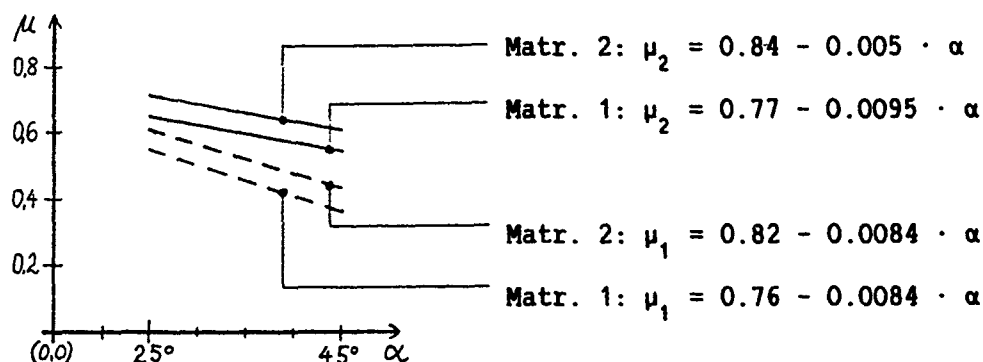
Figure 2. μ-factors for roofing material 1 (metal roofing) and material 2 (other roofing materials under consideration) for the roof slopes above 25 degrees.

For roofs with slopes below 20 degrees no difference could be found between the μ-factors for the different roofing materials. For roof slopes between 20 and 25 degrees there was a tendency of lower μ-factors for metal roofing than for the other materials of concern.

The influence on the μ-factor of different roofing materials is embodied in the final models of form factors for gable roofed buildings.

The effect of wind

The wind affects primarily the snow load on the buidings so that the mean roof load becomes less than the snow load on the ground. Further, the wind affects the snow load on the buildings so that the leeward side is getting a higher snow load than the windward side. The amount of this effect depends on the roof slope (see Figure 3).
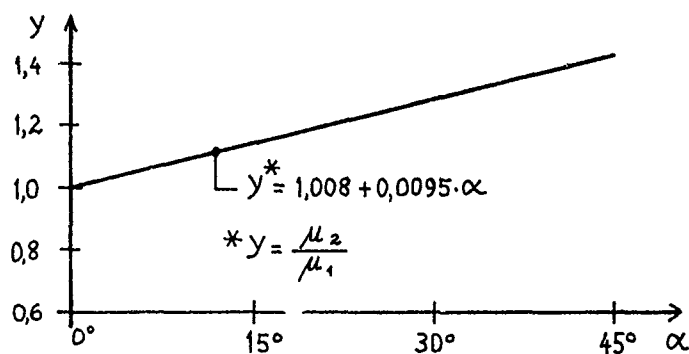
Figure 3. The nonsymmetry-factor (μ_2/μ_1) to the roof slope (α). The figures are given for the most loaded 20% part area of the roof.

The wind also affects the snow distribution along the buildings. In order to find the amount of nonuniform load along the buildings the more-load-factor, "M-load," was calculated for the most loaded 20% area of the roof.

The M-load proved to be independent of roof slope. However, it showed a slight dependency of the size of the ground snow load (see Figure 4).
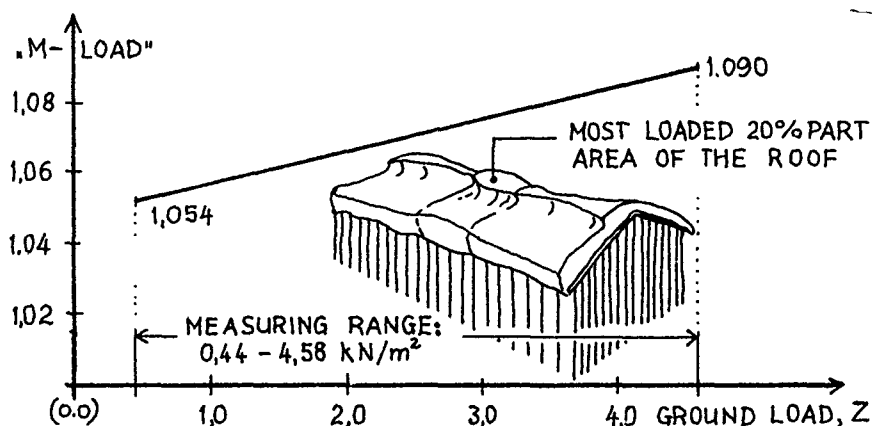
Figure 4. M-load, calculated as the ratio between the load on the most loaded 20% part area of the roof and the mean load.

The effect of the wind on snow deposition on the different roofs is embodied in the final models of form factors for the gable roofed buildings.

The snow load on the ground

An important result of the snow load measurements is that the size of the ground snow load is found to affect the μ-factor strongly. The effect is such that the μ-factor decreases for increasing size of the ground snow load. This influence is significant for gentle as well as for steep slopes (see Table 1).

100

Table 1. The influence of ground snow load on the form factors for the roof.

Windward side

$\alpha < 20^0$: μ_1 = 0.732 - 0.059 Z , n = 192 , r = -0.217

$\alpha > 20^0$: μ_1 = 0.689 - 0.105 Z , n = 1095 , r = -0.345

Joint : μ_1 = 0.699 - 0.102 Z , n = 1287 , r = -0.326

Leeward side

$\alpha < 20^0$: μ_2 = 0.816 - 0.061 Z , n = 192 , r = -0.246

$\alpha > 20^0$: μ_2 = 0.792 - 0.092 Z , n = 1095 , r = -0.311

Joint : μ_2 = 0.797 - 0.088 Z , n = 1287 , r = -0.303

As can be seen from the figures, the influence of ground snow load on the form factor is significant for the whole range of roof slopes. For roof slopes above 20 degrees, both the significance and the influence of ground snow load is higher than for roof slopes below 20 degrees.

The range of measured ground snow loads varied from 0.44 kN/m^2 to 4.58 kN/m^2, with a mean load at 1.48 kN/m^2. Fairly few measurements (28) were above 3.0 kN/m^2.

The influence of ground snow load on the μ-factor is embodied in the final models of form factors for the gable roofed buildings.

FINAL MODELS

From the previous it can be deduced that three factors might be of interest as explaining variables for the μ-factor:

1. Roof slope, α
2. Roofing materials, m (2 alternatives)
3. Ground snow load, Z.

A model worked out for the form factor, μ, based on the explaining variables is depicted in Figure 5.
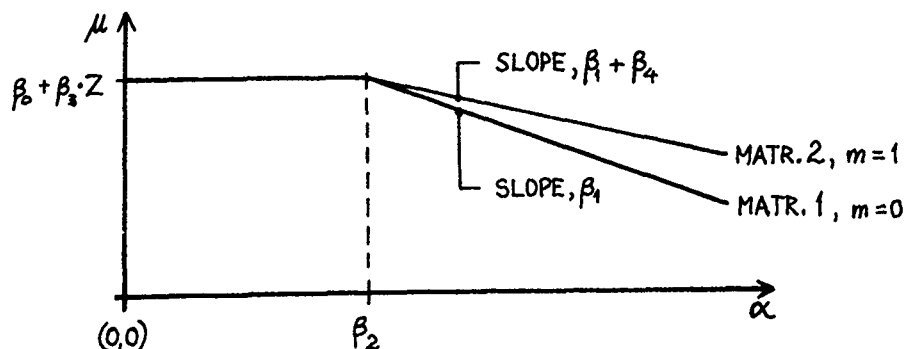
Figure 5. Form factor, μ, given in a general form.

Three alternative models explaining the form factors, μ_1 and μ_2, for gable roofs were worked out:

I The form factor as a function of the variables α, Z and m.
II The form factor as a function of the variables α and Z.
III The form factor as a function of the variable α.

Table 2 shows the actual parameters in connection with the models, see depiction in Figure 5.

Table 2. Parameter estimate for the three models of concern.

Dependent variable	Model No.	Parameter estimate					Minimum recidual of sum of squares
		$\widehat{\beta_0}$	$\widehat{\beta_1}$	$\widehat{\beta_2}$	$\widehat{\beta_3}$	$\widehat{\beta_4}$	
μ_1	I	0.8103	-0.0133	18.43	-0.110	0.0043	33.7880*
	II	0.8093	-0.0093	18.34	-0.111		34.2186
	III	0.6578	-0.0074	13.22			39.5811
μ_2	I	0.8669	-0.0096	17.47	-0.091	0.0046	31.9099*
	II	0.8637	-0.0055	18.27	-0.094		32.5016
	III	0.7280	-0.0042	13.91			36.3540

* Uncorrected total for μ_1 = 428.7102 and for μ_2 = 610.1252

As can be seen from Table 2, the best-suited model is Model I, being of this form:

$$\alpha < \beta_2 : \mu = \beta_0 + \beta_3 \cdot Z$$
$$\alpha > \beta_2 : \mu = \beta_0 + \beta_3 \cdot Z + (\beta_1 + \beta_4 \cdot m^*) \cdot (\alpha - \beta_2)$$

$m^* = 0$ for metal roofing (material 1)
$m^* = 1$ for other materials (material 2)

For more practical purposes a Model IV was worked out <u>based on Model I</u> with the parameter β_2 set at 20^0. Moreover the actual parameters are increased to take care of the more-load factor shown in Figure 4. In addition the parameters are rounded off for practical use. The resulting proposal is given below:

<u>Proposal for μ_1 (for windward side of the building)</u>:
$\alpha < 20^0$: $\mu_1 = 0.85 - 0.105 \cdot Z$

$20^0 < \alpha < 45^0$: $\mu_1 = 0.85 - 0.105 \cdot Z - \begin{cases} 0.015 \cdot (\alpha - 20^0), & (1)* \\ 0.011 \cdot (\alpha - 20^0), & (2)* \end{cases}$

<u>Proposal for μ_2 (for leeward side of the building</u>:
$\alpha < 20^0$: $\mu_2 = 0.90 - 0.08 \cdot Z$

$20^0 < \alpha < 45^0$: $\mu_2 = 0.90 - 0.08 \cdot Z - \begin{cases} 0.011 \cdot (\alpha - 20^0), & (1)* \\ 0.006 \cdot (\alpha - 20^0), & (2)* \end{cases}$

α = roof slope
Z = ground snow load
(1)* metal roofing
(2)* other roofing materials

Figures 6 a and 6 b, show a depiction of the form factors when $Z = 2.5$ kN/m^2.
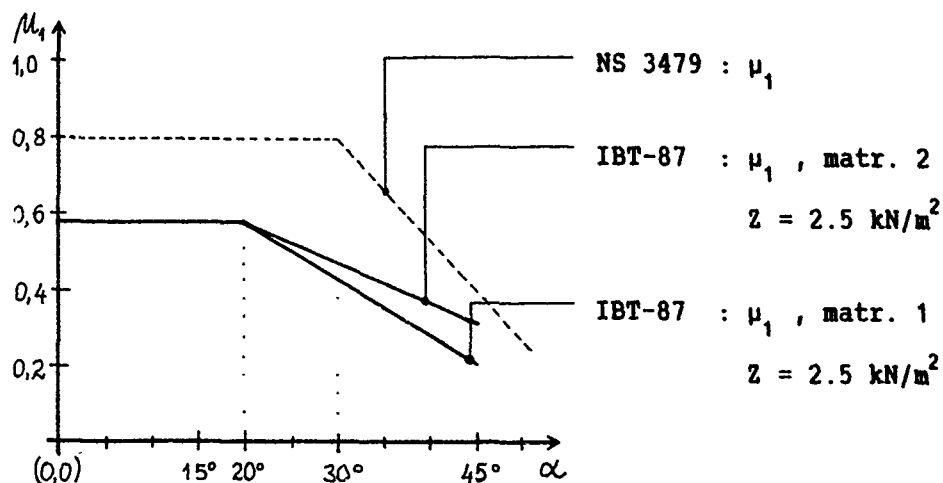
Figure 6 a. Form factor, μ, for windward side.
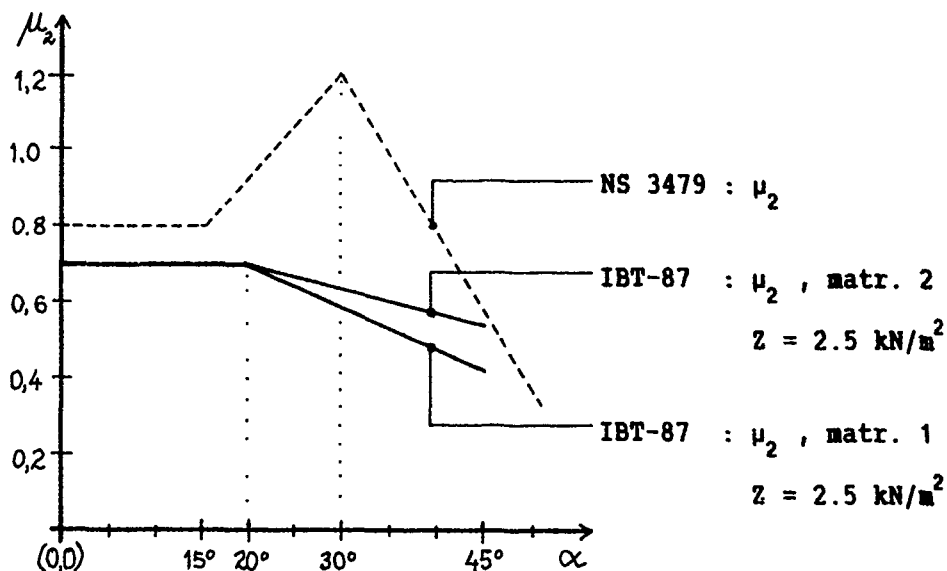
Figure 6 b. Form factor, μ, for leeward side.

The form factors for gable roofs given above are introduced in regulations for farm buildings under the Norwegian Building Code. They should be used with these restrictions:

1. The form factors shown should not be used in valleys where rectangular gable roofed wings are located angularly together.
2. The form factors shown should not be used for fully sheltered buildings.
3. The form factors should not be calculated for increasing ground snow loads above 3.5 kN/m^2.
4. The form factors should not be used uncritically in areas much unlike those where the measurements were taken.

ACKNOWLEDGEMENT

REFERENCES

[NRC 1.] Internal reports from Division of Building Research, National
Research Council of Canada:
DBR, Internal Report No. 106 (1956)
"   "   "   " 134 (1958)
"   "   "   " 163 (1958)
"   "   "   " 184 (1959)
"   "   "   " 204 (1960)
"   "   "   " 228 (1961)
"   "   "   " 260 (1963)
"   "   "   " 279 (1963)
"   "   "   " 335 (1966)

[NRC 2.] DBR, Technical Note 233 (1957).

3
ANALYTICAL MODELING TECHNIQUES
Peter Irwin, Chairman

Studying the ability of snow fences to reduce drifting against buildings. (Photograph by Darryl Calkins.)

Thermal Characteristics of a Double Roof

A.M. Baumgartner[I], R.L. Sack,[II] and J.J. Scheldorf[III]

ABSTRACT

The results of a one-dimensional steady state heat transfer model indicate that the temperature increase between eave and ridge of cavity air in a double roof is small. This has important implications for mitigating eave ice damming. Appropriate air cavity depths must be used for long roofs and various outside temperatures. Preliminary experimental results tend to substantiate the analytical approach. Future refinements include an improved analytical model and enhanced experiments to increase precision of temperature measurements and measure the velocity profile in the air cavity.

INTRODUCTION

In snow country the ubiquitous ice dam severely damages many structures. Meltwater runs down a sloping roof until encountering subfreezing temperatures. For most buildings the eave of the roof projects beyond the building and is surrounded by outside air; this is the area where ice dams usually form (Fig. 1). The eave ice load can be appreciable and may tear off roofing, gutters, and fascia materials; furthermore, the icicles are a potential hazard to pedestrians and can break building glass. Water above the ice dam will eventually penetrate the structure to rot wood, soak insulation, and damage walls. People attempt to treat the symptoms of poor design by: shortening (and lengthening) eaves; decreasing (and increasing) insulation; fastening electrical resistance cable to the eaves; attaching metal eave flashings; installing flexible roof underlayments; applying metal roofing; and removing snow and ice by shoveling, scraping, and chopping.

[I]Assoc. Env. Engr., James River Corp.; Wauna Mill, OR

[II]Professor, Dept. of Civil Engrg.; Univ. of Idaho; Moscow, ID

[III]Professor, Dept. of Chemical Engrg.; Univ. of Idaho; Moscow, ID
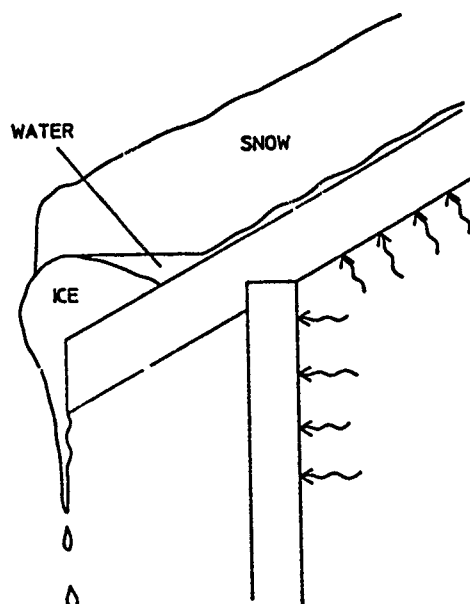
Figure 1: Typical Ice Dam Formation

Ice dams do not occur on cold surfaces such as picnic tables and roofs of unheated structures; solar gain melts the snow on these areas in much the same fashion that it melts the ground snow. This is not the case in buildings, where the ice dam can form when supplying heat to the lower surface of a roof without incorporating design features to minimize the flow of warm air to the underside of the sheathing.

The cold attic appears to be a popular design solution in some areas of the United States. Cold attic advocates assert that by combining adequate eave and ridge venting, together with sufficient ceiling insulation, heat is continuously removed from the underside of the sheathing, and snow melt at the roof-snow interface is minimized. Heat from the living area tends to collect in the peak of the typical attic; venting incorporated for vapor control is inadequate to prevent eave icing. Adequate ridge venting is difficult to incorporate into most housing designs; the foremost advocates of this approach state that "There appears to be a challenge for creative designers in the development of innovative devices for venting roofs for ice-prevention in harmony with the esthetics of acceptable appearance." (Grange and Hendricks, 1976). Sufficient ventilation to attain cold attic behavior typically allows attic winds and moisture penetration to yield shifting and soggy insulation.

The double roof has a weathering surface that is near outside ambient air temperatures (see Fig. 2). Outside air enters the cavity between the inside and outside roofs through continuous eave venting, and the air moves up and out the ridge venting. The heated room tends to increase the temperature of the cavity, but the air flow minimizes cavity heat accumulation.
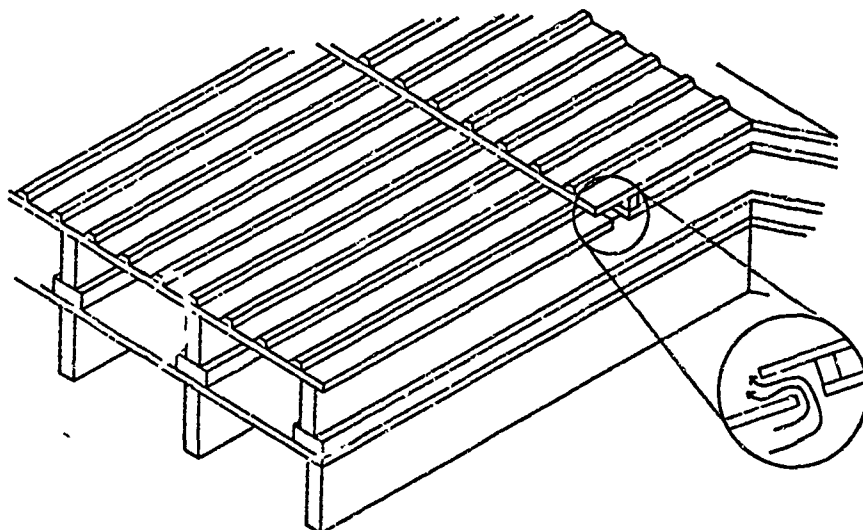
Figure 2: A Double Cold Roof

The double cold roof consists of a second roof constructed over an inside roof, which is covered by a membrane. In a typical installation, 2x4's are placed flat on the inside roof and nailed to the inside rafters to provide a nailing strip for the secondary rafters that support the outside sheathing. The continuous ridge venting is protected by the so-called "Boston Cap." Heat escaping from the cavity between roofs at the ridge maintains an open channel through the roof snow. Analytical predictions for the performance of the cold roof are nonexistent, but design rules of experience are observed. Longer roofs generally require greater airflow cavity depths.

The idea of the double cold roof was probably brought to the United States by Europeans (e.g., the miners of the upper Michigan Peninsula). One of the early double cold roofs in Western United States was constructed in 1964 on the Moritz Community Hospital in Sun Valley, Idaho. The designer was Eddie Siegel, an Austrian, trained as a railroad engineer, who worked for the Union Pacific Railroad and later for the Jans Corporation. Today, the double cold roof is the rule for new construction in Sun Valley, and many areas in snow country are realizing the advantages of this roof design. An example, is a roof on a 60-unit condominium complex in McCall, Idaho: a region with higher mean daytime temperatures than Sun Valley. The original roof design was premised on cold attic behavior, but eave icing decimated the roofing material. The first roof was removed in 1986 and replaced with an effective double cold roof; subsequently no ice dams have occurred.

A specious argument against the double cold roof is the added cost. On new projects the second roof adds less than 1% to the construction costs. The price is high to retrofit a building with a double cold roof; however, other feasible alternatives cost more.

In the absence of analytical solutions for the performance of the double cold roof, designers use rules of thumb based upon previous experience. This approach seems to yield roofs that work, but most questions of performance and cost can only be addressed when an accurate analytical description exists. Based upon existing roof behavior, designers know that the depth of the air cavity required is associated with the length of the roof. Also, some designers believe that the double cold roof should not be used in locations

where the ambient outside air temperature is high during the winter. The following presents the results obtained using a simple one-dimensional heat transfer model and minimal corroborating experimental evidence. Together these two approaches represent a beginning for rational design of the double cold roof.

ANALYTICAL MODEL

We analyze a single channel of a double roof. The airspace of the channel (i.e., the cavity) is open at the eave and peak and is formed by secondary rafters on the sides, with inside and outside roof sheathing defining the bottom and top, respectively. A layer of standard building insulation covers the bottom of the interior sheathing, and snow blankets the top of the outside sheathing (see Fig. 3). The interior of the structure is maintained at a constant temperature, and outside ambient temperature does not fluctuate. We assumed steady state heat transfer; therefore, the analysis does not predict response due to diurnal temperature cycles.
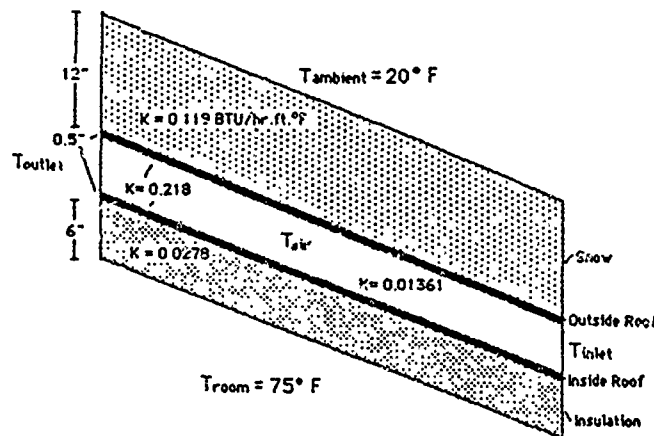
Figure 3: Physical Model

We neglected the effects of varying weather conditions and assumed that sufficient roof snow was present to insulate the roof from solar heat flux effects. The heat transfer coefficient between snow and the ambient outside air depends upon wind and snow surface conditions. Similarly, the heat transfer coefficient between room air and the insulation is influenced by the air velocity and other factors. We investigated the effects of varying the heat transfer coefficients but did not attempt to establish unique values for various conditions.

We assumed that the flow of air through the cavity from eave to ridge is straight and is driven by the difference in temperatures of the air at the inlet and outlet. We also assumed that the outside wind speed does not affect the air flow through the cavity.

The model is one dimensional so that no heat transfer takes place parallel to the eave line. That is, we assume similar air temperatures occur on either side of the secondary rafters, and we neglected the usual effects occurring at the ends of a building.

HEAT TRANSFER CALCULATIONS

We divided the channel longitudinally into small finite lengths (usually three or four), assuming that the temperature of the air in each finite volume is constant (see Fig. 4). The inlet air temperature equals the outside ambient temperature for the first finite volume. Initially, we assume an outlet air temperature for the first finite volume and calculate the corresponding average air temperature for the finite volume. Subsequently, the heat flow rate from the heated room of the building to the air cavity is calculated as follows:

$$q_1 = \frac{T_{room} - T_{air}}{\Sigma R_1} \tag{1}$$

where q_1=heat flow rate through the inside roof (W); T_{room}=temperature of heated room of the building (°C); T_{air}=average air temperature in the finite volume (°C), that is

$$T_{air} = 0.5(T_{inlet} + T_{outlet}) \tag{2}$$

ΣR_1=the sum of the thermal resistances for the inside roof [°C/W] so that

$$\Sigma R_1 = \left[\frac{x}{kA}\right]_{ins} + \left[\frac{x}{kA}\right]_{roof1} + \left[\frac{1}{hA}\right]_1 + \left[\frac{1}{hA}\right]_r \tag{3}$$

where x_{ins}=thickness of insulation (m); k_{ins}=thermal conductivity of insulation [W/(m·°C)]; x_{roof1}=thickness of inside roof sheathing (m); k_{roof1}=thermal conductivity of inside roof material [W/(m·°C)]; h_1=heat transfer coefficient between the inside roof and the air in the cavity [W/(m²·°C)]; h_r=heat transfer coefficient between the air of the heated structure and the insulation [W/(m²·°C)]; and A=area of inside roof (m²) (i.e., the product of the finite length and the distance between secondary rafters).
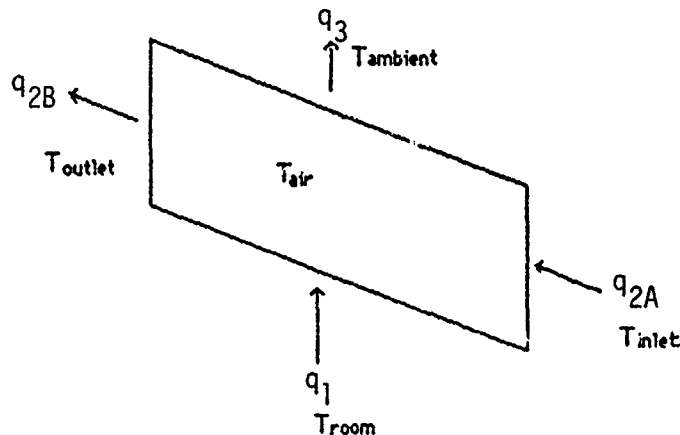
Figure 4: A Finite Volume

The heat flow rate due to airflow through the airspace normal to the roof surfaces is calculated as follows:

$$q_2 = q_{2A} - q_{2B} = \dot{m}c_p(T_{outlet} - T_{inlet}) \tag{4}$$

111

where q_2=net heat flow rate due to airflow through the finite volume (W); q_{2A}=heat flow rate due to air flowing into the finite volume (W); q_{2B}=heat flow rate due to air flowing out of the finite volume (W); $\dot{m}$=mass flow rate (kg/s); c_p=heat capacity of air [J/(kg·°C)]; T_{outlet}=temperature of air exiting the finite volume (°C); and T_{inlet}=temperature of air entering the finite volume (°C).

The heat flow rate of the air flowing normal to the roof surface from the airspace out through the outside roof is governed by the following equations:

$$q_3 = q_1 - q_2 \tag{5a}$$

and

$$\overset{*}{q_3} = \frac{T_{air} - T_{ambient}}{\Sigma R_3} \tag{5b}$$

where q_3 and $\overset{*}{q_3}$=heat flow rate through the outside roof (W) calculated by the two different procedures; T_{air}=average air temperature in the finite volume as given by Eq. 2 (°C); and ΣR_3=the sum of the thermal resistances for the outside roof [°C/W] so that

$$\Sigma R_3 = \left[\frac{x}{kA}\right]_{snow} + \left[\frac{x}{kA}\right]_{roof2} + \left[\frac{1}{hA}\right]_2 + \left[\frac{1}{hA}\right]_0 \tag{6}$$

where x_{snow}=thickness of snow (m); k_{snow}=thermal conductivity of snow [W/(m·°C)]; x_{roof2}=thickness of outside roof sheathing (m); k_{roof2}=thermal conductivity of outside roof material [W/(m·°C)]; h_2=heat transfer coefficient between the outside roof and the airspace [W/(m²·°C)]; h_0=heat transfer coefficient between the outside air and the snow [W/(m²·°C)]; A=cross-sectional area of the outside roof (m²) (i.e., the product of the finite length of channel and distance between secondary rafters).

Following the procedure outlined at the beginning of this section, we assume an outlet temperature and perform the calculations. If q_3 and $\overset{*}{q_3}$ do not agree, we assume a different outlet temperature and, returning to Eq. 1, recompute the two values of heat flow rate through the outside roof. Iteration is continued until heat flow rate values as predicted by Eqs. 5a and 5b agree within allowable limits. Subsequently, the outlet temperature becomes the inlet temperature for the next finite volume, and similar iterations are performed. We continue the process until reaching the outlet of the conduit at the ridge of the roof.

PARAMETRIC STUDY

We used the analytical model to study the effects of various significant parameters. For example, one might expect that the heat transfer coefficient between snow and air to be between 0.072 and 2.9 W/(m²·°C) (0.5 to 20 Btu/(hr·ft²·°F)), and heat transfer values between the interior room and the insulation range from 0.072 to 0.29 W/(m²·°C) (0.5 to 2.0 Btu/(hr·ft²·°F)).

112

Also, the effects of insulation thickness, cavity depth, and roof length, slope, and materials would provide the first approximate analytic..lly-based design guides for double cold roofs.

We judge that the key to the effectiveness of a double cold roof is the airflow through the cavity. That is, with a large flow rate, temperatures in the cavity will assume near-ambient temperature and reduce ice dam formation. Air flow is driven by the difference in temperature between incoming air at the eave and outflow air at the ridge; therefore, we plotted $(T_{ridge}-T_{eave})$ versus air cavity depth to judge roof effectiveness. In all plots, change in temperature decreases with increased cavity depth. Because of the larger cavity depth (i.e., cross-sectional area of the channel), more air can flow through the air space. Thus, a constant heat flow rate will raise the temperature of a larger quantity of air by a smaller amount since $q = \dot{m}c_p\Delta T$.

Parametric analysis indicated that neither the heat transfer coefficient for the snow-air interface (h_O) nor the room air-insulation interface (h_I) appreciably altered the performance of the example roof. These two heat transfer coefficients are much less than the other pertinent thermal resistances in the calculations (see Eqs. 3 and 6); therefore these trends are not surprising.
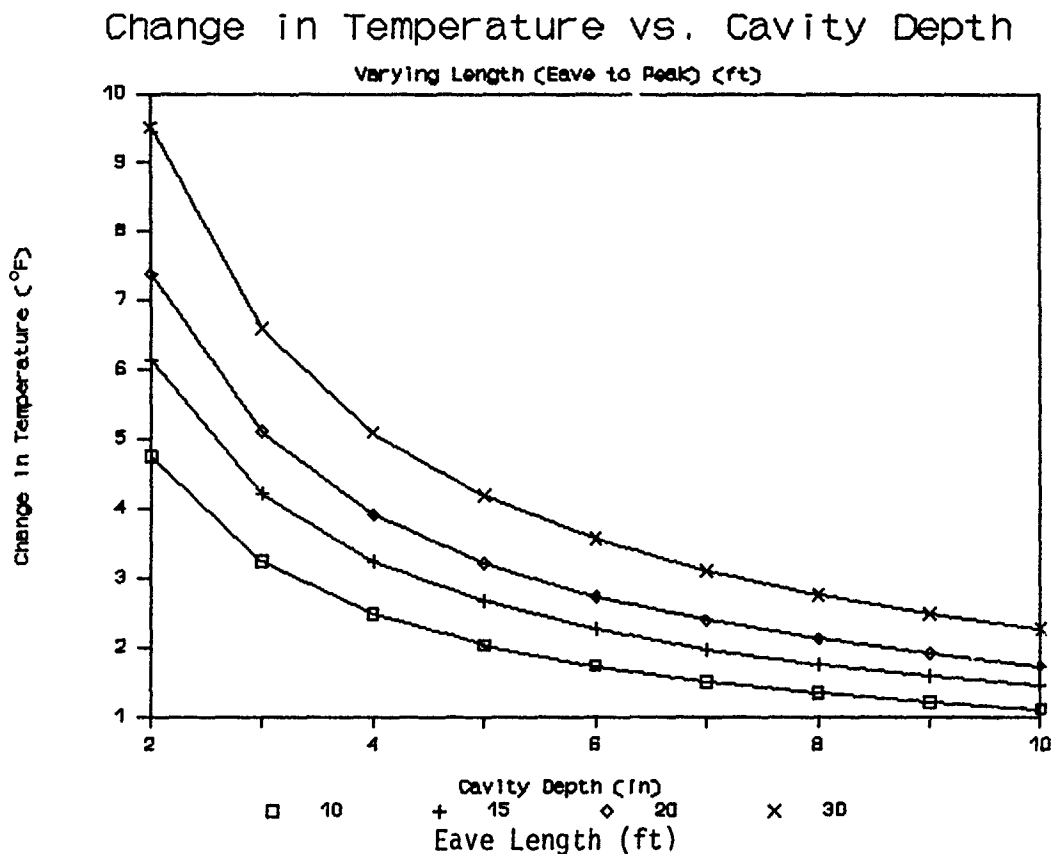
Figure 5: $(T_{ridge}-T_{eave})$ vs. Cavity Depth for Various Roof Lengths

Figure 5 shows the effects of roof length (i.e., distance from eave to peak) with outside ambient air temperature of −7°C (20°F) and room temperature of 24°C (75°F). The curves indicate that longer roofs require larger cavity depths. Thus to get the same temperature change of 2.5°F for a 10-ft and a 30-ft roof we use a 4-in. depth in the former and a 10-in. depth in the latter. It is logical that the change in temperature increases with increased roof length since the larger surface allows greater heat flow through the inside roof and heats the cavity air to a higher temperature.

Figure 6 shows the effect of outside ambient air temperature for a room temperature of 24°C (75°F) and roof length of 3 m (10 ft). We observe that higher outside ambient temperatures retard the flow of air in the roof cavity. That is, higher outside air temperatures result in smaller changes in cavity temperatures because there is a smaller driving force between the heated structure and the air space for warmer ambient air temperatures. The heat flow rate, and therefore the change in temperature, is smaller for this case.
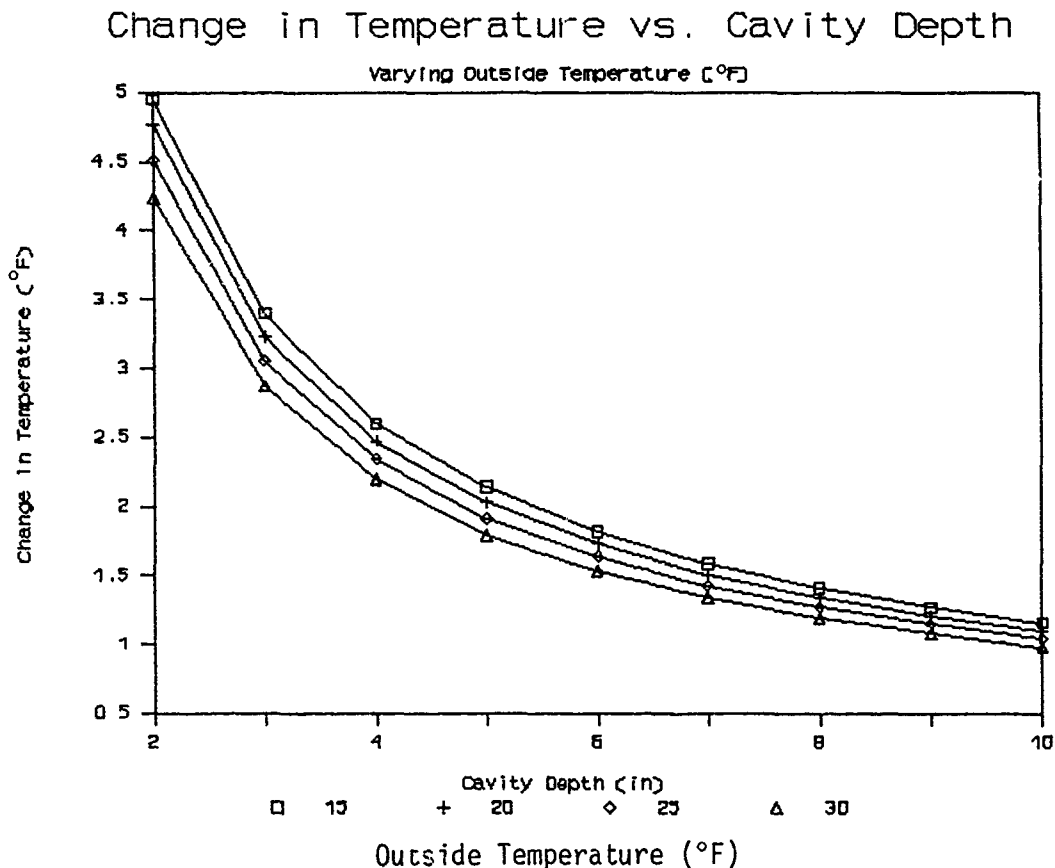
Figure 6: $(T_{ridge} - T_{eave})$ vs. Cavity Depth for Various $T_{outside}$

EXPERIMENTAL STUDY

We conducted preliminary experimental work in the cold room of the Department of Civil Engineering at the University of Idaho to check the trends obtained with the analytical model. The scale-model heated structure with a double roof shown in Fig. 7 was intended to duplicate the performance of a

typical air space between secondary rafters; it is 36.83 cm (14.5 in.) wide and 2.13 m (7 ft) long. The walls and floor are composed of 1.27 cm (1/2-in.) plywood and covered with 5.08 cm (2 in.) Styrofoam insulation. The roof sheathing is 1.91 cm (3/4-in.) plywood; there is 10.16 cm (4 in.) Styrofoam insulation below the inside roof, with 5.08 cm (2 in.) of Styrofoam above the outside roof to simulate the insulating effects of snow. The outside roof is adjustable on four steel rods so that the depth of the cavity between the two roofs could be varied from 2.54 cm (1 in.) to 25.4 cm (10 in.). The slope of the roof is 24.3°. We added extra insulation along the length of the air space to eliminate any lateral heat transfer. Therefore, our analytical assumptions that similar temperatures exist on either side of the secondary rafters and heat transfer does not occur parallel to the building eave line was imposed for this experimental study.

A 300-watt light bulb heated the interior of the model, a small fan circulated the interior air, and a thermostat controlled the temperature. We positioned the model double roof in the cold room and maintained the ambient outside air temperature at approximately 6°C (21°F). Twelve copper-constantan thermocouples monitored the temperature: four on each interior roof surface of the cavity, spaced at approximately equal intervals; three inside the heated structure; and one in the cold room (see Fig. 7).
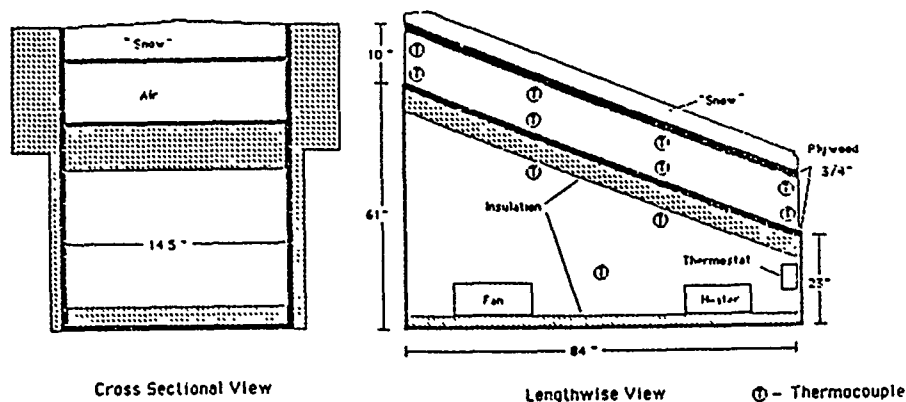
Figure 7: Experimental Roof

We investigated the change in temperature between inlet and outlet of the air channel for various cavity depths. Temperatures from all twelve thermocouples were recorded by a Hewlett-Packard Model HP3497/HP85 data acquisition system after it appeared that steady state had been reached. Figure 8 presents the data, along with the corresponding analytical predictions. While experimental and analytical results do not closely agree, we believe the data corroborate predicted magnitudes even though the experiments are preliminary.

115

Change in Temperature vs. Cavity Depth

Experimental Data
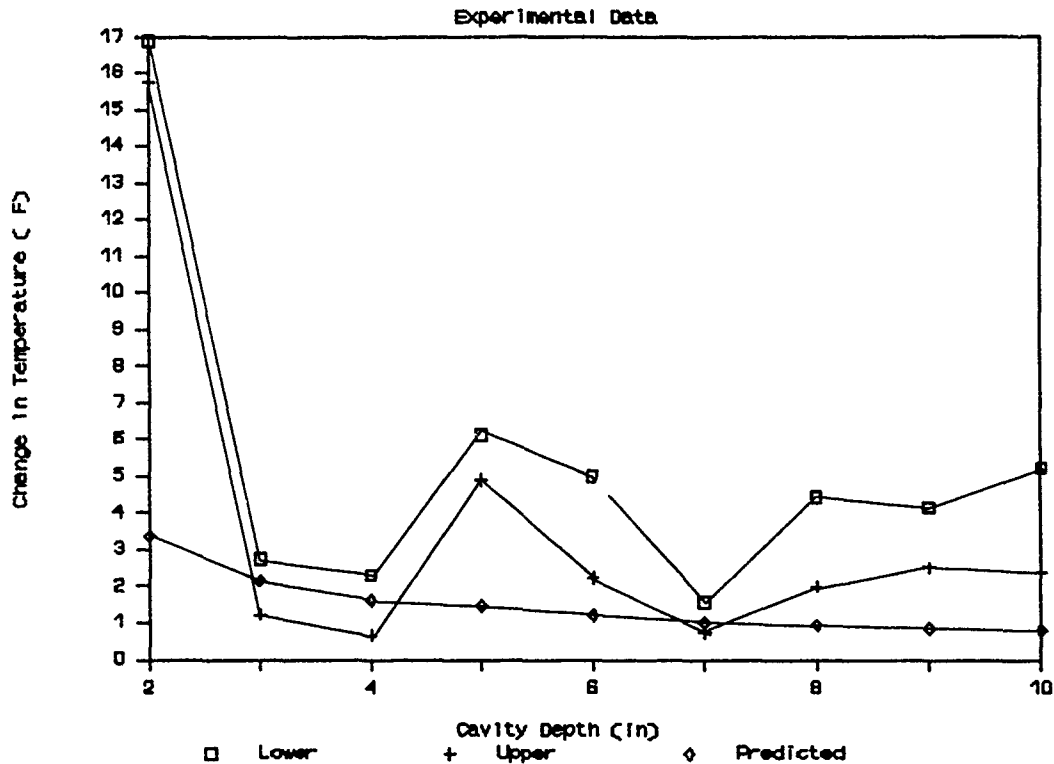
Figure 8: Change in Temperature vs. Cavity Depth

FUTURE STUDIES

Furtner carefully controlled experiments will be necessary to validate our analytical model. This work will require a precision-built scale model with no possibility for heat leakage. Tighter control on interior room temperatures must be maintained by: a) precise control on the heat source; b) a larger fan for more uniform interior temperatures; and c) additional thermocouples in the room and air cavity to record interior thermal distribution. Initially, we must run experiments to establish time required to reach steady state by recording temperatures every fifteen minutes for continuous runs of 24 to 48 hours. Subsequently, data for the experiments reported above should be recorded after reaching steady state in each case. Additionally, the effects of heated structure air temperature, cold room temperature, and roof slope should be independently varied and studied.

The velocity distribution in the air cavity influences: a) the actual heat transfer in the cavity; b) heat transfer coefficients; and c) air flow distributions in the cavity. Therefore, future studies should attempt to measure these low velocities (i.e., 0.34 m/sec (1.1 ft/sec)) in a cold environment.

SUMMARY AND CONCLUSIONS

We performed a steady state heat transfer analysis of a typical airflow channel from a double cold roof by modeling the air as a series of constant temperature finite volumes along the duct. The results indicate that change in cavity temperature between eave and ridge: a) decreases with increased cavity depth; b) increases with increased roof length; and c) is relatively insensitive to heat transfer coefficients between room and insulation and snow and air. Preliminary experimental results indicate that the analytical approach should be continued and refined. Future studies should concentrate upon refining the previous analytical and experimental results. Heat transfer coefficient correlations could be established through measurements of the velocity profile in the air cavity.

The temperature of the underside of the outside roof is the key indicator for ice dam formation. We note from Figs. 5 and 6 that the cavity air experiences modest temperature increases (i.e., -17°C (1°F) to -13°C (9°F)) as air flows through roofs of various lengths for a wide range of outside ambient temperatures. Therefore, it is reasonable to anticipate that, under the assumptions of our analytical model, eave ice will not form on the majority of the structures in our parametric study.

Our model of an idealized double cold roof indicates that temperature increases are minimal for an appropriate design. Longer roofs and increased outside temperatures require greater air cavity depths to function as a cold roof. Design rules can be established through a refined analytical model correlated with carefully run experiments.

ACKNOWLEDGEMENT

REFERENCES

Grange, H.L. and L.T. Hendricks, 1976, "Roof Snow Behavior and Ice-Dam Prevention in Residential Housing," Extension Bulletin 399-1976, Agriculture Extension Service, University of Minnesota.

Predicting Snow Loading on the Toronto Skydome

P.A. Irwin[a] and S.L. Gamble[b]

ABSTRACT

The method used for determining the design snow loading for the large, arched roof and retractable roof structure of the Toronto Skydome is described. In this method, snow drifting on the roof of the Skydome was computed from the wind velocity patterns near the roof surface using a finite area element computer model. The velocity patterns were determined as a function of wind direction and speed by detailed wind tunnel tests. Meteorological records of wind, snowfall, rainfall and temperature were used as input to the program as it computed the snow load accumulations in a time step manner. From computed time histories of snow load patterns, design load cases were selected. The calculation of these snow load cases assisted in determining overall maximum loads, non-uniform loading situations and relative deflection of adjacent, separate roof segments.

INTRODUCTION

The redistribution of snow on roofs as a result of drifting by wind causes large eccentric loadings which are important to the structural design but which have proven difficult to predict in a quantitative manner. Wind tunnel and water flume model techniques have proven useful on many building projects[1] in the role of qualitative tools for diagnosing the presence of problematic drifts and pointing the way to solutions, but new advances have been needed for making quantitative predictions. Also, computer simulation techniques have been employed as a means of taking account of the many variables affecting snow loads[2]. In this paper a method is described which makes use of the combined potential of both wind tunnel and computer simulation techniques to make quantitative predictions. The impetus for developing the method was the new domed stadium in Toronto with a 200 metre span retractable roof for which snow loading was a governing consideration in the structural design. The essentials of the method are: i) determine the detailed mean velocity distribution close (1m full scale) to the roof surface for a number of wind directions using a wind tunnel model such as that of the Toronto Dome, Figure 1; ii) supplement this with qualitative particle drifting tests, Figure 2, and tests of snowfall build-up under various wind conditions; iii) divide the roof into area elements, Figure 3, and use the velocity distribution and snow drifting flux relationships to compute the build-up or depletion of snow in each element in a time step fashion; and iv) incorporate into the computer program the change of wind speed and direction, snow fall, melting rate and rainfall at each time step and compute time histories of snow accumulations on the roof.

---

[a] Principal, Rowan Williams Davies & Irwin Inc., 650 Woodlawn Road West, Guelph, Ontario, Canada, N1K 1B8

[b] Associate, Rowan Williams Davies & Irwin Inc., 650 Woodlawn Road West, Guelph, Ontario, Canada, N1K 1B8
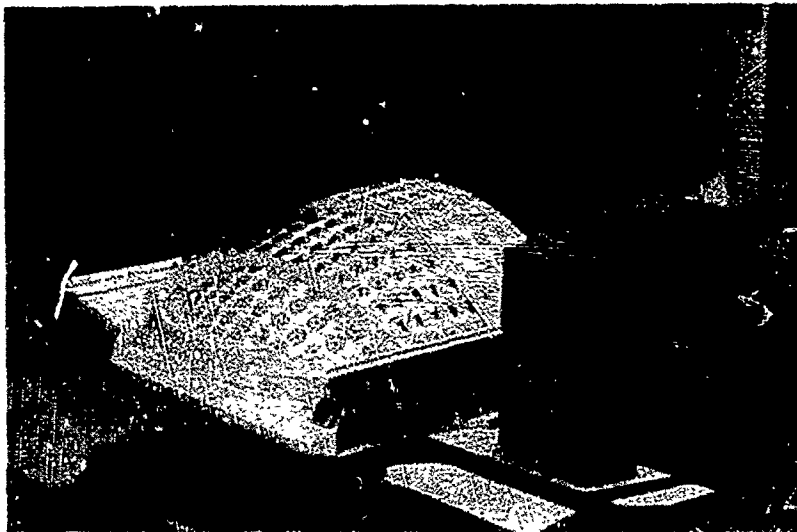
Figure 1 - Velocity Vector Measurements

Two significant assumptions involved in this approach are first that it is only the wind speed near the roof surface that effects drifting and second that the drifts do not ap-
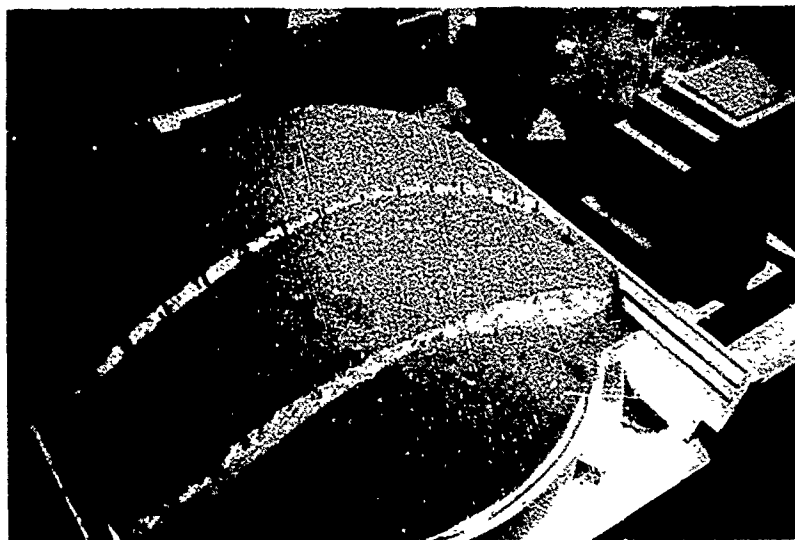
Figure 2 - Particle Drifting Tests

Figure 3 - Finite Area Element Model

SNOW LOADS kPa

N

PANEL 4

		0.00	0.03			
0.02	0.02	0.02	0.03	0.04	0.07	
0.82	0.02	0.03	0.02	0.07	0.04	0.06	0.08
1.47	1.94	1.78	1.23	0.61	0.67	2.20	1.90

PANEL 3

0.00	0.60	0.85	0.75	1.73	0.87	1.13	0.50	1.30	0.36	0.76	0.00	0.00	0.00
1.01	0.02	1.25	1.20	1.68	0.91	1.09	0.02	0.02	0.03	0.03	0.00	0.02	0.01
1.15	0.53	1.28	1.18	1.61	1.02	0.99	0.07	0.05	0.07	0.06	0.01	0.05	0.00
0.65	0.95	1.99	1.28	1.40	1.13	0.18	1.07	1.97	1.84	1.54	0.16	0.15	1.50

PANEL 2

0.63	0.84	1.00	0.97	0.99	0.02	0.02	0.03	0.02	0.02	0.00	0.01	0.01	0.00
0.81	0.68	0.97	1.08	0.99	0.55	0.01	0.08	0.08	0.04	0.01	0.00	0.01	0.02
0.88	0.70	0.87	1.01	0.75	0.77	0.03	0.10	0.07	0.07	0.04	0.00	0.00	0.08
0.93	0.75	0.84	1.01	1.05	0.02	0.03	0.07	0.07	0.06	0.07	0.05	0.08	0.05

PANEL 1

2.14	2.28	2.79	1.59	1.39	1.39	1.56	2.05	1.81	0.77
1.39	1.39	1.07	1.00	0.04	0.04	0.10	0.10	0.07	0.08
1.08	1.01	1.13	0.03	0.04	0.04	0.07	0.71		
	0.01	0.03	0.05	0.05	0.03	0.06			
	0.05			0.10					

Figure 3 - Finite Area Element Model

preciably alter the velocity distribution near the surface. There is good evidence[3] that the great bulk of snow drifting occurs very near to the surface through the saltation mechanism, which supports the first assumption. The second assumption becomes increasingly better as the dimensions of the roof become larger relative to the drift depths. This implies that the method is best applied to very large roofs and special interpretation may be required near local roof features, e.g. steps that are of similar dimensions to that of the snow depth. The advantages of the method are that it rationally incorporates the variability of the meteorological parameters (such as snow fall, wind speed, wind

120

direction, temperature, and rain fall) affecting the snow loads and that it provides a framework into which improved data on snow drift flux relations and melting characteristics can in future be fed.

DESCRIPTION OF METHOD

Finite Area Element Analysis

To perform a finite element analysis of the roof snow drifting patterns, the roof is first divided into an orthogonal grid of elements. The geometric coordinates of each node of the grid are used to calculate the length of each boundary, the surface area and the local roof slope. It is at each of these nodes that the local wind speed and direction at 1 metre above the roof surface must be known under given ambient wind directions and speeds. As an example, the Toronto Skydome roof grid is given in Figure 3. A mass balance is performed on each area element of the grid in an order which is predetermined and is based on the local velocity field. This is required since the amount of snow being drifted into and area over a period of time, Dt, depends not only on the wind velocity but also on whether or not there is driftable snow in the adjacent upwind area. Thus the order of calculation for a roof would proceed generally from the upwind edge toward the downwind edge but variations in the order may occur due to local distortions of the velocity caused by steps, obstructions, etc.

The fluxes accounted for in the program are illustrated in Figure 4 which is a diagram of a general area element (i,j). Drifting fluxes are assumed to cross grid boundaries into adjacent elements and rain, falling snow, and melt water are assumed to enter or exit through the upper and lower surfaces. In Figure 4 the velocity vectors at grid nodes as well as the fluxes are illustrated. Examples of how potential fluxes are calculated and the basic mass balance equation are also given in the figure. In the equation for the potential flux, PQ in Figure 4, C is a constant determined from field test results[4], V is the local wind speed and V_{th} is the threshold wind speed below which no drifting occurs (e.g. 4 m/s). The fluxes are termed "potential" because they are calculated assuming that there is sufficient driftable snow available. If the initial mass
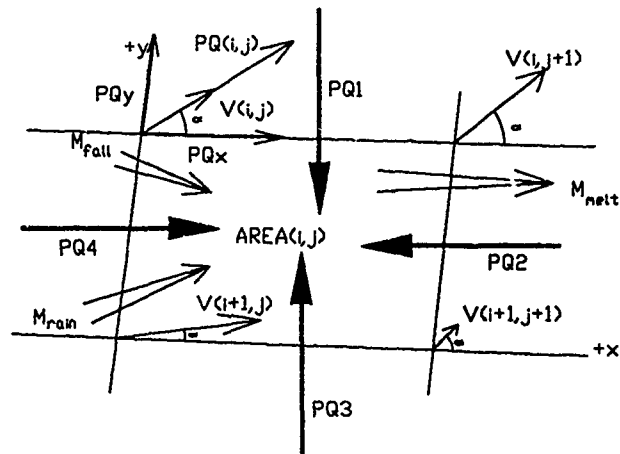
1 Potential mass flux at grid crossing point (i,j) due to V(i,j):
    PQ(i,j) = C * (V(i,j)**2) * (v(i,j) - Vth)
2 Components of potential mass flux at grid crossing point (i,j):
    PQx(i,j) = PQ(i,j) * cos(∝)
    PQy(i,j) = PQ(i,j) * sin(∝)
3 Average normal flux across area element boundaries 1 through 4:
    PQ1(i,j) = (-PQy(i,j) - PQy(i,j+1)/2
    PQ2(i,j) = (-PQx(i,j) - PQx(i+1,j+1))/2
    PQ3(i,j) = (PQy(i+1,j) + PQy(i+1,j+1))/2
    PQ4(i,j) = (PQy(i,j) + PQy(i+1,j))/2

Note: Fluxes into element are positive by convention.

4 Mass balance within area element performed:
    Dmass = (PQ1(i,j) * L1(i,j) + PQ2(i,j) * L2(i,j)
    +PQ3(i,j) * L3(i,j) + PQ4(i,j) * L4(i,j)) *Dt
    +Mfall(i,j) + Mrain(i,j) - Mmelt

Figure 4 - Mass Balance Computation

121

balance calculation finds that the element would become completely scoured of driftable snow during the time step Dt then these potential fluxes are adjusted to the values required to just remove all driftable snow at the end of Dt. The flux of material drifting into adjacent elements from the scoured element is also adjusted to reflect this condition. A refinement that was included for the Toronto Skydome studies was to make an adjustment to the potential flux at each node point for the effect of the local roof slope. Approximate theoretical expressions for this effect were derived[5] and are

$$\frac{PQ(\phi)}{PQ(0)} = 1 - \frac{\phi}{60} + \left[\frac{\phi}{75}\right]^2$$

$$\beta = -\frac{\bar{g}\theta}{46}$$

where ϕ is the angle in degrees of the roof surface to the horizontal in the direction of the local wind velocity vector, β is the rotation of the snow flux vector relative to the wind velocity vector, g is a non-dimensional constant with a value of about 0.4 and θ is the angle of the roof surface to the horizontal in a direction at right angles to the wind velocity vector.

Not all snow is driftable. When a snow pack has been exposed to surface melting, the snow is less susceptible to surface drifting since the crystals at the surface tend to form a crust. Rain or freezing rain have a similar effect. Thus, in reality the flux relationship for the snow drifting is a function of the previous history of the snow. At present, the available field data do not appear sufficient to justify a graduated form of flux relation to incorporate these effects in a detailed way, although in future this may well become feasible. In the current version of the computer model described here, the flux relation is of the simple on-off type. If the temperature exceeds 0°C, or rain or freezing rain has fallen on the snow pack then the drift patterns are fixed. No further drifting is allowed to occur regardless of subsequent temperature changes until new snow fall has landed on top of the fixed drifts. This new snow is allowed to drift but only down to the previously fixed drift pattern.

Since the computer model performs its mass balance based only on local wind velocities, it is possible for snow to accumulate in low velocity regions such as roof steps as long as there is snow available for drifting. In real world situations, an aerodynamically imposed maximum depth is noted in wind flow separations and roof steps. The simulation therefore can overestimate loads in these situations. For these regions, physical model test results and field data can be used to aid in interpreting the results.

Removal of the snow pack is by drifting and also through melting and run-off. Many factors come into play in the melting process. These are the air temperature and local wind speed, solar radiation, long wave radiation heat transfer between the snow and the sky, the position and orientation of the snow surface, heat transfer through the roof, the latent heat of evaporation at the snow/air interface and the sensible heat of rain water. To incorporate all of these factors is quite complex. The simpler approach used for the present studies, which is similar to that used by Isyumov[2], was to assume that the melting

rate is proportional to the temperature in °C above zero and the time spent above 0°C. Of the ice melted, a certain amount of liquid water is retained within the snow pack in the spaces between the ice crystals. Rain may add to this. The weight of water which the snow pack can retain is variable but it appears that the assumption that the snow can retain up to 50% of its weight in water is reasonably representative. For the Toronto Skydome studies, this assumption combined with the assumption for the melting constant of 4.1 x 10^{-5} kg/m²/s/°C, produced good correspondence with the ground snow loads specified in the Canadian National Building Code when the computer simulation was run for the ground load case.

Meteorological Information

The finite element snow accumulation program was designed to read actual meteorological conditions recorded at local weather stations to simulate the changing snow patterns on the roof for each time step, Dt. The basic flow of the program to perform the simulation is shown in a flow chart in Figure 5. For the Toronto Skydome, 21 years of meteorological data were used. The weather data required as input to the computer program is in the form of observations for each time step interval, Dt, of wind direction, wind speed, temperature, snow fall (in equivalent depth of water) and rain fall. If a more complex approach to calculating the melting rate were to be incorporated, additional information on incident solar radiation, cloud cover, relative humidity, etc. could be incorporated.

Model Tests

To establish the mean wind velocity patterns on the roof for a series of wind directions it is necessary to instrument a wind tunnel model with a large number of wind velocity sensors. For the Skydome studies 238 of the wind speed sensors described by Irwin[6] were installed in the 1:200 scale model roof at the corners of area elements. These measured the magnitude of the velocity vector , the measurement locations being visible in Figure 1. Additional tests were carried out with small wind flags and stick-on angle scales to determine the local directions at the same 238 locations. Flags are
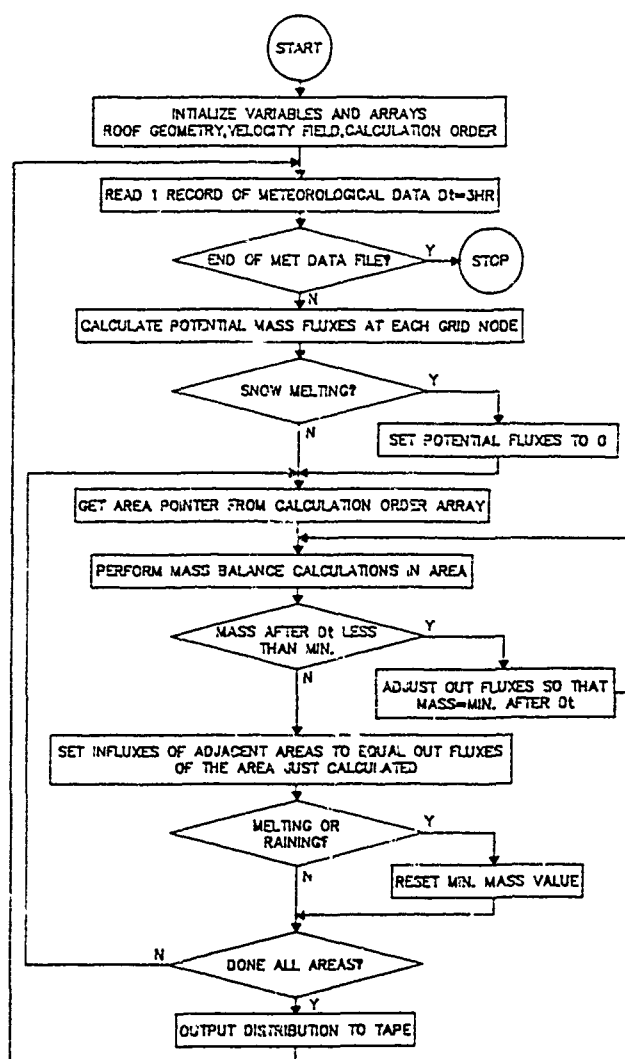
Figure 5 - Flow Diagram for Computer Program
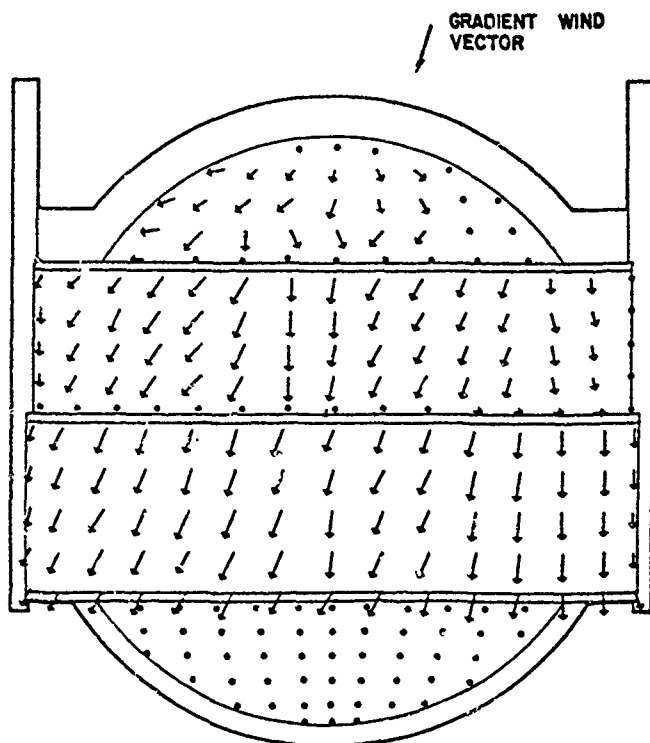
Figure 5 - Velocity Vector Measurements

also evident in Figure 1. Tests were conducted for 16 wind directions. Figure 6 illustrates test results for one wind direction. At each measurement point the local mean velocity is shown as a vector arrow to illustrate its magnitude and direction.

Supplementary tests using walnut shell particles to simulate snow were also carried out on the same model, Figure 2. A uniform distribution of particles was put on the roof and then the wind was turned on for fixed periods. The main use of these was to give the maximum drifts in roof steps and to give a qualitative picture of the drift formations. Many of the observed drift formations reappeared in the computer simulations in the same qualitative form. Additional tests were also undertaken on a 1:500 scale water flume model of the Skydome to determine the effect of wind or snowfall accumulations and to examine snow trajectories for drifting off the edge of some of the larger steps in roof elevation. Space does not permit a description of the details here.

RESULTS

For the Toronto Skydome, the computer simulation stepped through 21 winters. As an example of the type of results obtained, the numbers in the area elements in Figure 3 give the predicted area-average snow load in kPa within each area element at a particular instant in 1979. it can be seen in this example that the loads tend to be concentrated in sheltered areas at roof steps and also winds from the east side have tended to blow the snow over to the west side. In the course of the simulation a great variety of load patterns occurred. Figure 7 illustrates the predicted build up and then melting of total snow on the roof over one winter, 1978. In addition to total loads on the roof, various other quantities such as eccentric load (difference between load on the east and west halves) on particular roof sections and differential loading on adjacent independent roof segments for deflection calculations for weather seal design were monitored during the computer simulation and maximum values output for each year. Figure 8 illustrates an extreme value plot of maximum eccentric loads from which the 100 year return period eccentric load could be determined. Figure 9 shows examples of spanwise load distributions generated by the computer simulation for the Panel 2 arch (see Figure 3 for Panel notation). The load distributions shown were the maximum eccentric loads on the south half of Panel 2 computed for the winters of 1959, 1972 and 1978. For the structural design of the roof, several representative shapes of eccentric load distribution were derived by inspection of computed results such as that shown in Figure 9 and by scaling the distribution so that the

124

Figure 7 - Time History of Total Snow on
the Roof

Figure 8 - Extreme Value Analysis of
Unbalanced Load

total eccentric load on that section of the roof matched the 100 year value predicted by the computer simulation. It is interesting to note that the resulting eccentric loads were significantly less than the corresponding National Building Code of Canada loads for
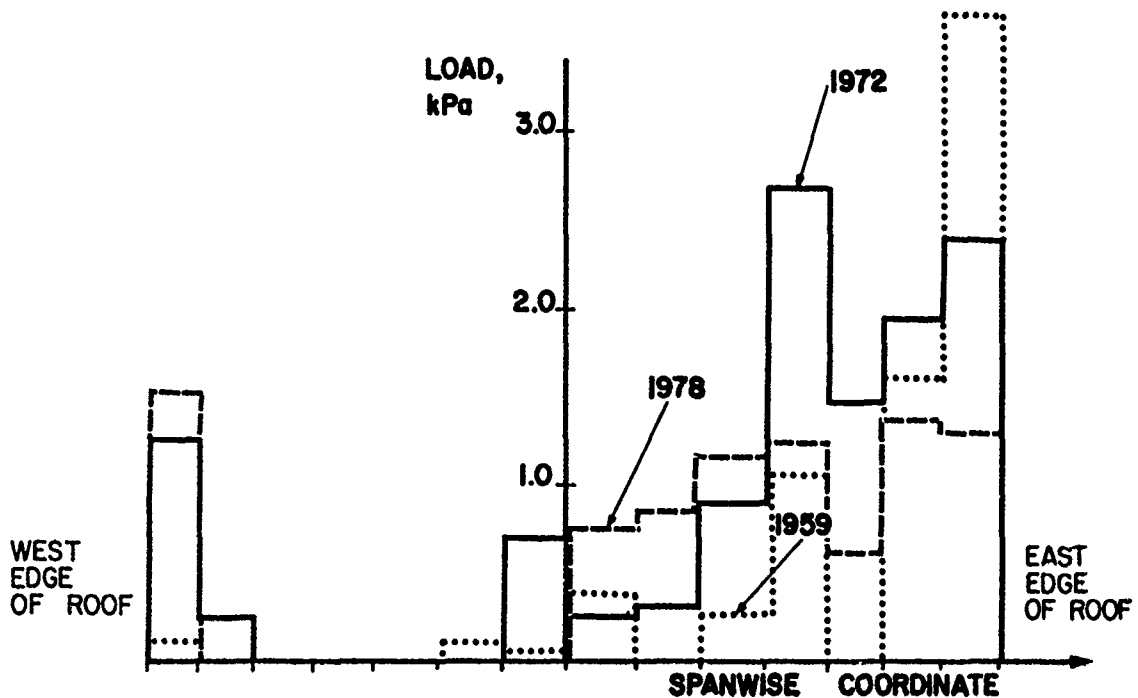
Figure 9 - Unbalanced Loading of Arch Roof, Panel 2

125

arched roofs. The physical reason for this is that the span of the Panel 2 arch in the east-west direction is over four times its length in the north-south direction. Therefore the wind does not have to deviate much from parallel to the span before it starts to blow snow off the north and south edges. This reduces the ability of Panel 2 to build up the large eccentric loads that typically occur on arches with longer relative dimensions normal to the span. The same drifting process did however lead to exceptionally heavy eccentric loads in the step at the junction of Panels 2 and 3.

The results of the snow drifting simulation for the Skydome were used to provide guidance in the design of the sealing devices for the interfaces between the movable panels. In this case the 21 years of data were re-examined to extract annual extremes of differential loading on adjacent roofs. These differentials were scaled to the 100 year values and then compared to the assumption of full 100 year unbalanced loading of each panel on opposite sides. The results for each roof step, Figure 10, are expressed as a percentage of the full 100 year loading assumption. It can be seen that the loads are somewhat lower for all steps since high loading of one panel was not generally noted concurrently with high loading on the opposite side of the adjacent panel. This information allowed some refinement of the design of the seals.

Figure 10 - Comparison of Observed Differential Loading with Full 100 Year Load Assumption

Code Comparisons

Two low-rise flat roofs of dimensions 30m x 30m and 100m x 100m, in open country and suburban exposures were also simulated using the finite area element approach. The results for Toronto, presented in Table 1 as fractions of ground snow load, show a distinct effect of roof size on snow load. Also included in Table 1 are the values specified by two major building codes of North America.

TABLE 1
Fraction of Ground Snow Load on Flat Roofs of Different Area

Exposure	100m x 100m	30m x 30m	NBC	ANSI
Open Country	.65	.27	.60	.60
Suburban	.96	.62	.80	.80

The flat roof results are in the same range but the comparison suggests that perhaps more account should be taken in codes of the roof size effect. Detailed comparisons

would be desirable with full scale data on various shape roofs. Approximate comparisons with arch roof data[7] to date have shown encouraging results.

CONCLUSIONS

The combined wind tunnel and computer simulation technique described in this paper is a powerful tool for assessing snow loads on large span roofs. It has also been applied to some ground drifting problems. In developing the method it became clear that further research on snow drift flux rates and melting behaviour is desirable. Future advances in knowledge in these areas can be readily incorporated into the method.

ACKNOWLEDGEMENTS

REFERENCES

1. Irwin, P. A. and Williams, C. J., "Applications of Snow Simulation Model Tests to Planning and Design", Proceedings Eastern Snow Conference, Vol. 28, 40th Annual Meeting, Toronto, 1983.

2. Isyumov, N., "An Approach to the Prediction of Snow Loads", Ph.D. Thesis, Faculty of Graduate Studies, University of Western Ontario, London, Ontario, Canada, September 1971.

3. Kobayashi, D., "Studies of Snow Transport in Low-Level Drifting Snow", Institute of Low Temperature Science, Sapporo, Japan, Series A, January 1973.

4. Dyunin, A. K., "Solid Flux of Snow Bearing Air Flow", NRC Technical Translation, TT-1102, 1963, from Trudy Transportno-Energich-Eskogo Institute.

5. Irwin, P. A. and Gamble, S. L., "Snow Loading Studies of the Ontario Stadium Project", RWDI Reports 48612092 and 48712041, July 1986 and February 1987.

6. Irwin, P. A., "A Simple Omnidirectional Sensor for Wind Tunnel Studies of Pedestrian Level Winds", Journal of Wind Engineering and Industrial Aerodynamics, 7, 1981, pp. 219-239.

7. Schriever, W. R., Faucher, Y., Lutes, D. A., "Snow Accumulations in Canada Case Histories: I", National Research Council of Canada Division of Building Research, Technical Paper No. 237, January 1967.

A Simulation to Predict Snow Sliding and Lift-Off on Buildings

Michael F. Lepage[1] and Glenn D. Schuyler[2]

ABSTRACT

A technique is presented that combines scale model studies with a computer simulation in order to predict the quantity of snow or ice that can accumulate and later slide or blow off sloped surfaces of buildings. The computer simulation uses several years worth of historical observations of wind, temperature, precipitation and solar radiation. In calculating snow and ice accumulations, it accounts for melting due to heat transfer through the building envelope and absorption of solar radiation. Scale model tests conducted in a water flume account for the effect of building geometry on local precipitation rates. Scale model wind load studies conducted in a wind tunnel determine whether local wind forces can cause lift-off of snow or ice. The results of the simulation consist of predicted maximum accumulations, as well as the frequency of lift-off events. For example, a simulation run for sloped surfaces on a highrise in New York City predicted that the largest snow accumulation in twenty-years would be 5.0psf. As many as nine lift-off events were predicted to occur.

INTRODUCTION

Sloping roofs are enjoying wide popularity in North American architectural design. They are turning up on schools, malls, high-rises and many other structures. In northern cities, this trend has caused an increased risk of damage or injury due to falling snow and ice.

Consider a scenario in which a severe storm produces a large accumulation of snow or ice on a sloping roof. The sub-freezing temperatures during the storm cause the precipitation to adhere to the roof, allowing it to accumulate without sliding off (Figure 1). Suppose that the storm is then followed by a warming trend, so that the roof temperature beneath the built-up layer of snow or ice hovers around freezing. The forces of adhesion that bind the snow or ice layer to the roof are reduced, so that it slides off the roof and damages a parked car or injures a pedestrian.

Consider another scenario in which a railing installed at the bottom of a sloping roof prevents snow from sliding off. The retained snow acts as a layer of insulation that

---

1. Air Quality and Climatology Specialist, Rowan Williams Davies and Irwin Inc., Guelph, Ontario.

2. Principal, Rowan Williams Davies and Irwin Inc., Guelph, Ontario.

traps heat escaping from inside the building and causes melting to occur. The melt water runs down the slope and freezes onto the unheated railing. Large icicles form (Figure 2) and eventually fall to the ground.
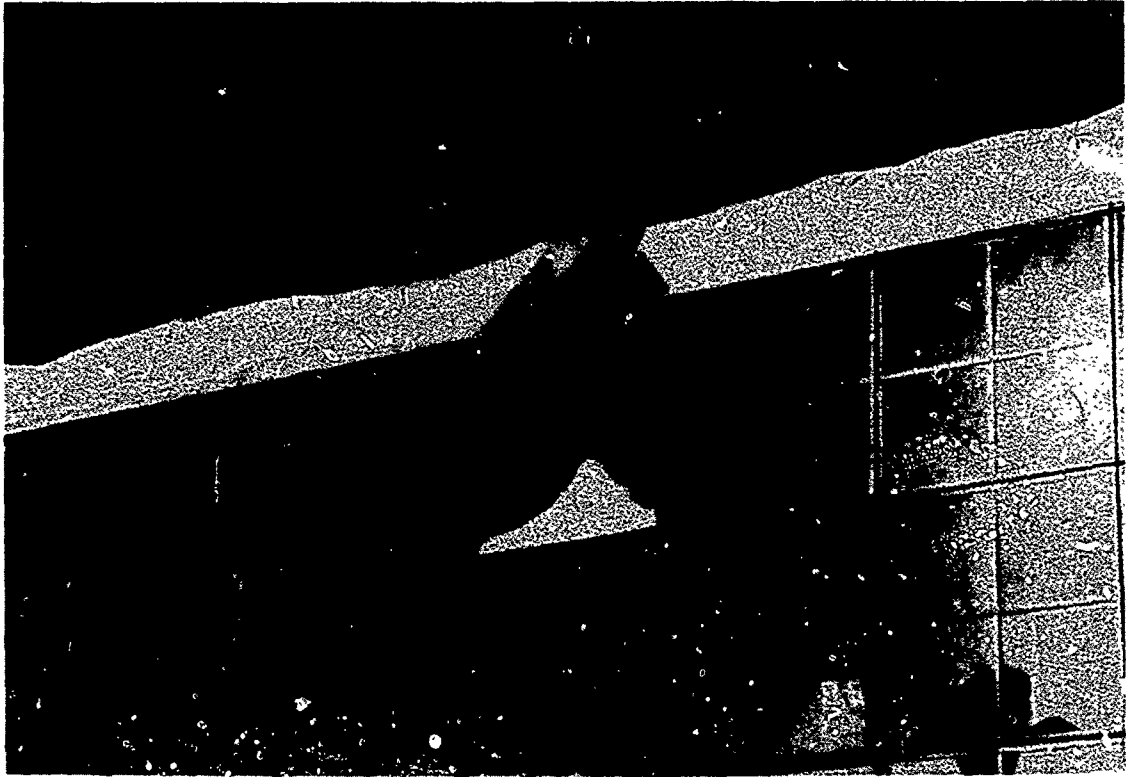
Figure 1   Snow accumulation on a sloped roof

Absorption of solar radiation during the day and cold temperatures at night cause the snow layer to go through a freeze-thaw cycle. As a result, the snow hardens into a solid mass. A high wind then comes up and lifts a hardened piece of snow into the air, transforming it into a dangerous projectile.

Scenarios like these have occurred on numerous occasions in cities like New York, Philadelphia, Denver and even Dallas. Consequently, building designers have become increasingly concerned with avoiding snow and ice problems.

A computer simulation, enhanced by scale model simulations, has been developed to assist designers in assessing the need for ice and snow control measures on proposed structures. The simulation takes building design information, scale model test data and meteorological data and predicts the formation, melt-down and lift-off of snow and ice layers in critical areas of the building. The results consist of predicted snow and ice accumulations and the frequency of wind lift-off events.

Figure 2 Icicle formation

THE SIMULATION

During the computer simulation, the study building is exposed to several years worth of meteorological conditions that have actually occurred at the site. As each snow or icing event occurs, the accumulations on sloping roofs and other critical areas are calculated. Account is taken of melting and local wind effects.

The local wind flow patterns around and over a building can have a significant impact on rain and snowfall accumulations in some areas of the building. For example, a lower roof step located downwind of a large expanse of flat roof will often experience increased snow accumulation due to particles drifting off the flat roof. For buildings of complicated design, the local wind flows can be extremely complex and difficult to simulate by computer. These wind effects are therefore accounted for by a scale model simulation in a water flume.

For every snow or ice event, the simulation records two values for each critical area of the building: the maximum depth that would be achieved and the time until it would melt away, if left undisturbed by slide-off or wind lift-off. The simulation also calculates local wind forces in order to determine if they can cause lift-off. When it encounters a sufficient wind force, it records the amount of snow or ice present at the

time (assuming that slide-off hasn't already occurred).

The local wind forces that cause lift-off are highly dependent on the geometry of the situation. In order to account for the impact of building shape and orientation, the simulation uses wind load data from scale model studies conducted in a wind tunnel.

HEAT TRANSFER AND MELTING

The physical processes modelled by the computer simulation are shown in Figure 3. Snow or freezing rain falls onto a sloping roof or other building surface and
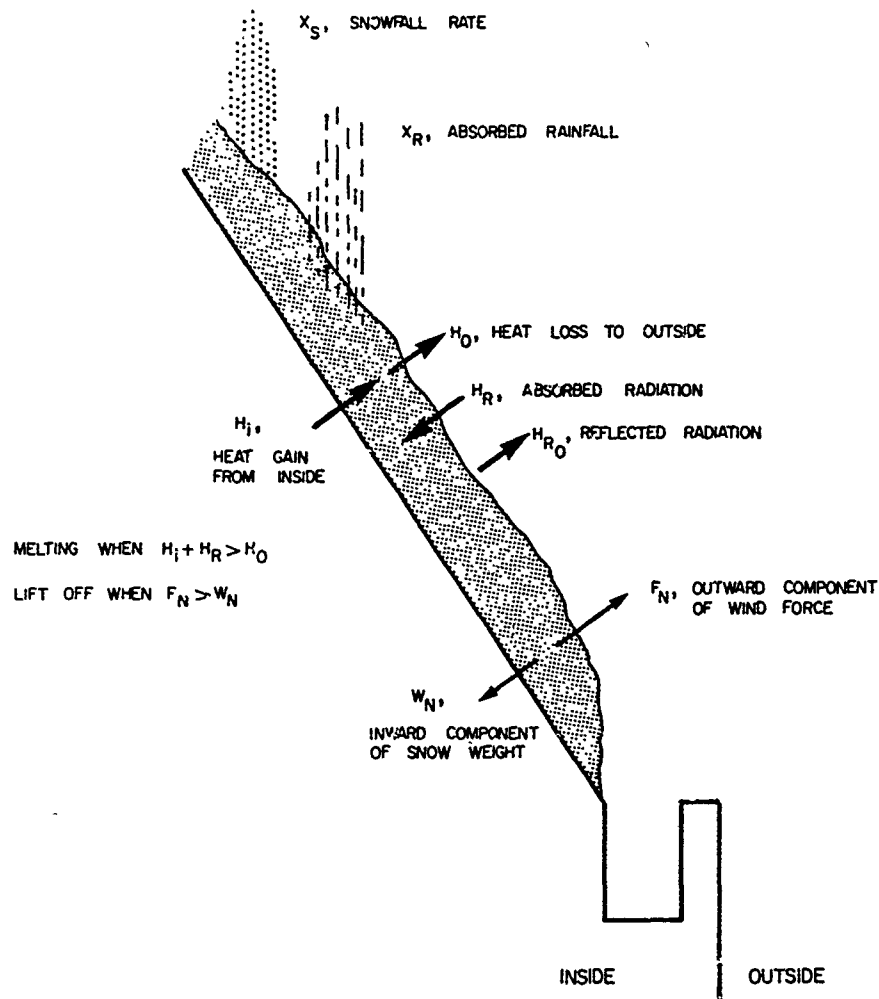
Figure 3 Physical processes modelled by the simulation

accumulates. If rain falls onto an existing snow layer, the snow absorbs a portion of the rainfall.

Eventual melting of the snow or ice occurs through a series of heat transfer processes. Depending on the thermal insulation of the building envelope, a certain amount of heat will escape from inside the building. A portion of this heat will warm up the snow or ice layer, and the rest (depending on the hardness and thickness of the layer) will escape into the outside air. If the sun comes out, the snow or ice will absorb solar radiation, causing further warming. When the warming raises any of the snow or ice layer to the melting point, melting will occur.

The equilibrium heat balance achieved by a snow or ice layer on a building is summarized as follows:

$$H_m = H_i + H_r - H_o$$

where:

H_m = flux of heat available to melt snow
H_i = rate of heat gain from inside the building
H_r = rate of heat gain due to solar radiation
H_o = rate of heat loss to the outside air.

The heat gain due to solar radiation, H_r is determined from meteorological data, taking into account the geometry of the building and local shading effects. The heat gain from inside the building and the loss to the outside air are determined from the following equations:

$$H_i = (T_i - T_o)/R_i$$
$$H_o = (T_o - T_e)/R_e$$

where:

T_i = the inside air temperature
T_e = the outside air temperature
T_o = the temperature of the roof beneath the snow/ice layer
R_i = the thermal resistance of the building envelope
R_e = the thermal resistance of the snow/ice layer including the exterior film resistance

The inside air temperature of a building, T_i, and the resistance of the building envelope, R_i are building design parameters. The temperature of the outside air, T_e is a meteorological variable, and the thermal resistance of the snow or ice layer, R_e depends on the thickness, density and age of the layer (Langham, 1981). Melting occurs when the temperature beneath the snow or ice layer, T_o has been raised to the melting point (T_m) and a surplus of heat, H_m remains. The heat available for melting is therefore determined by setting $T_o = T_m$ and calculating H_m from the equations given above. A positive value indicates that melting will occur. The corresponding rate of melting is then determined from the latent heat of fusion for snow and ice.

The resulting rate of melting will change continually as the outside temperature and the depth of the snow or ice layer changes. It is therefore continually recalculated by the simulation.

METEOROLOGICAL DATA

The meteorological parameters required for the simulation are wind speed, wind direction, dry bulb temperature, snowfall, rainfall and solar radiation. A typical data set consists of hourly values for a period of at least ten years as recorded at the nearest weather observing station that records them.

In some cases, the precipitation data are not available on an hourly basis. Six-hour or 24-hour totals are available instead. In these situations, the precipitation totals are correlated with hourly visual observations of precipitation intensity (light, moderate and heavy) in order to appropriately divide them into hourly increments.

In most cases, solar radiation data are not readily available and are therefore estimated from cloud cover data (ASHRAE, 1979). The estimated radiation is divided into two components: indirect radiation and direct radiation. Indirect radiation is the portion of the solar radiation that is scattered by atmospheric constituents before reaching the earth's surface. Direct radiation is the unscattered portion. The values of these components depend on time of day, time of year, humidity, cloud cover and atmospheric particulate content. The direct radiation impinging on a surface depends on the slope angle and orientation of the surface.

WIND TUNNEL TESTS

The wind tunnel tests are used to determine, for a given approaching wind speed, what local wind forces will exist in various areas of the building being studied. The test data needed for the snow simulation are the same as those used for design of the building's cladding elements.

The tests are conducted on a scale model of the study building and its surroundings (Figure 4). A brief description of the resulting test data is presented here. A detailed description of the theory and testing techniques can be found elsewhere (Irwin, 1987).

The test data are in the form of pressure coefficients, $c = p/p_o$, where p is the local peak wind pressure or suction measured at a particular location on the exterior of the model building for a particular wind angle, and p_o is the dynamic pressure of the wind approaching the building, as measured at a given reference height. The reference pressure, p_o can be mathematically related to the wind speed recorded in the meteorological data. Thus, for any recorded wind speed and direction, one can use the pressure coefficients to predict the local peak wind pressures and suctions that the building would experience. If V is the recorded wind speed corrected to reference height and, for a given location on the building, c is the peak suction coefficient corresponding to the recorded wind direction, then the predicted local wind suction at the given location would be $p = 0.5c\varrho V^2$, where ϱ is the air density.
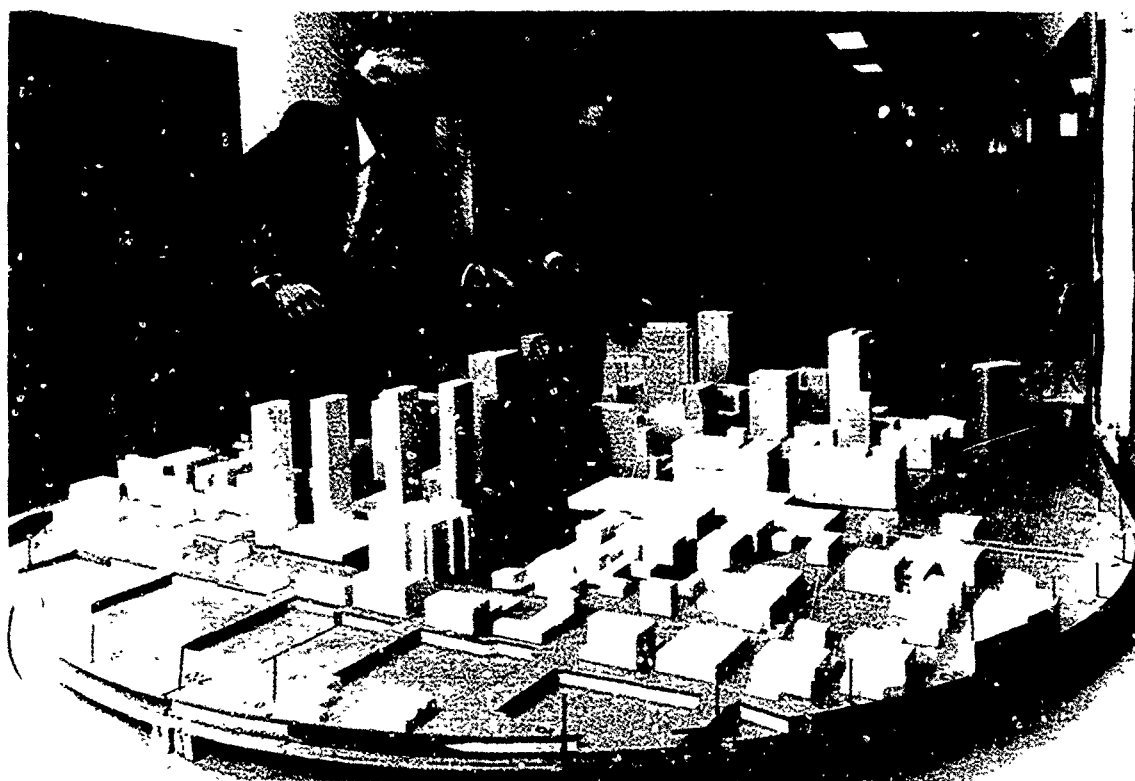
Figure 4   RWDI wind tunnel testing facility

SIMULATION OF LIFT-OFF

The snow simulation calculates local peak wind forces on all snow or ice-covered surfaces of the study building to determine whether or not lift-off of the snow or ice can occur. Lift-off will occur if the wind produces a suction force that overcomes the forces of surface adhesion and gravity. The existence of a suction force on a snow or ice layer implies there is greater static pressure beneath the layer than above it, with the size of the force being equal to the difference in pressure. This requires an air space beneath the layer. Much of the underside of the layer must be detached from the surface. This can occur if the layer creeps over an edge to form and overhang or accordions against an obstruction, forming an air pocket underneath. Since there is little surface contact in these cases, the surface adhesion is minimal and the wind suction force need only overcome gravity to produce a lift-off.

Wind force as calculated from the wind tunnel data represents the maximum static pressure difference a layer of snow or ice with an air space underneath can experience from one side to the other. The actual pressure difference may be somewhat lower, depending on the shape and location of the layer. An overhanging layer is most likely to experience the maximum value. An accordioned layer, on the other hand, will have openings in the air pocket underneath that result in partial equalization of the static pressures on either side of the layer. The degree of equalization will depend on the size

134

and location of the openings and on the local variation in exterior wind forces.

The simulation treats accordioned layers as analogous to loose-laid roof paving stones. Data from studies of wind loads on paving stones (Kind and Wardlaw, 1979) suggest the net suction force on an accordioned layer is about 25% of the full wind suction.

Typical snow layers that can experience lift-off are shown in Figure 5. Type I lift-off refers to cases in which the snow or ice experiences the maximum wind force (e.g.

(a) TYPE I UPLIFT

(b) TYPE II UPLIFT
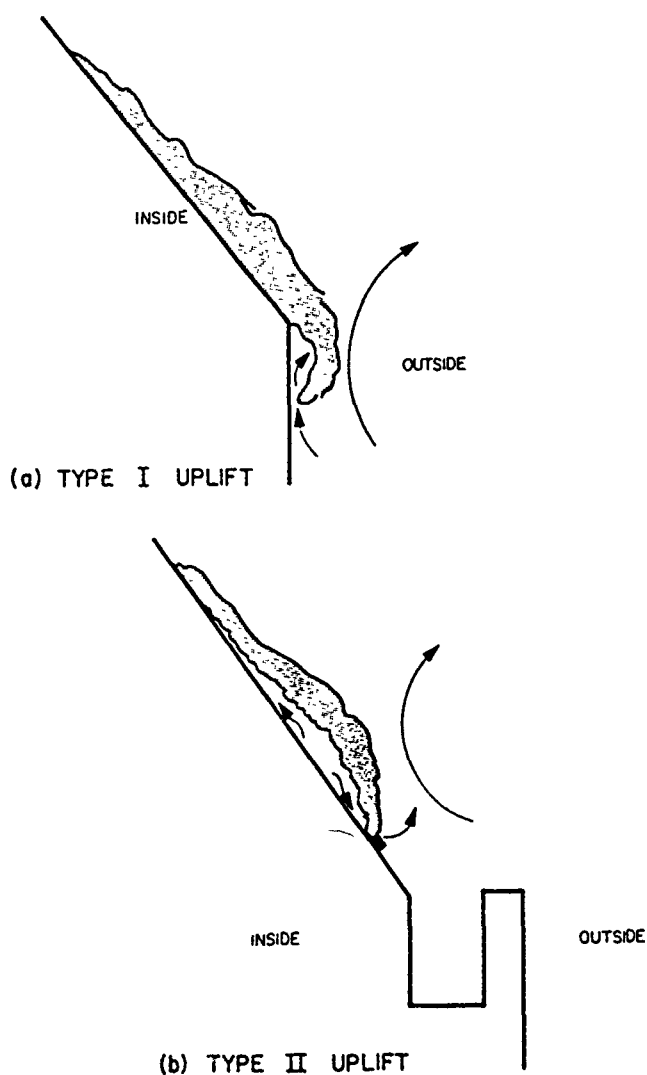
Figure 5 Type I and Type II lift-off situations

overhangs). Type II lift-off refers to cases in which the snow or ice experiences only 25% of the maximum force (accordioned layers). The formation of an overhang or accordioned layer on a sloped surface requires the adhesion of the layer to the building surface to be sufficiently weak to allow creep. This generally requires the temperature beneath the layer to be at the melting point. It follows that a lift-off is unlikely to occur unless the underside of the layer, at some time, reaches the melting point.

In the case of snow, the layer will not lift off in one piece unless it has also been hardened by wind and freeze-thaw effects. This will usually require several hours or even days. Consequently, a layer of snow is not expected to lift-off in the early stages of its formation. The wind suctions are therefore not applicable until the layer has reached a specified age. In general, this age depends on the temperature and wind conditions. For snow, the simulation assumes that a period of at least 24 hours, during which a freeze-thaw cycle occured, is needed before a lift-off is possible. For ice, it assumes lift-off can occur as soon as the underside of the layer reaches the melting point.

WATER FLUME TESTS

Snow and rainfall amounts used by the simulation are corrected to account for the effect of local wind patterns in the vicinity of the building being studied. The appropriate correction factors are determined by testing a scale model of the building and its
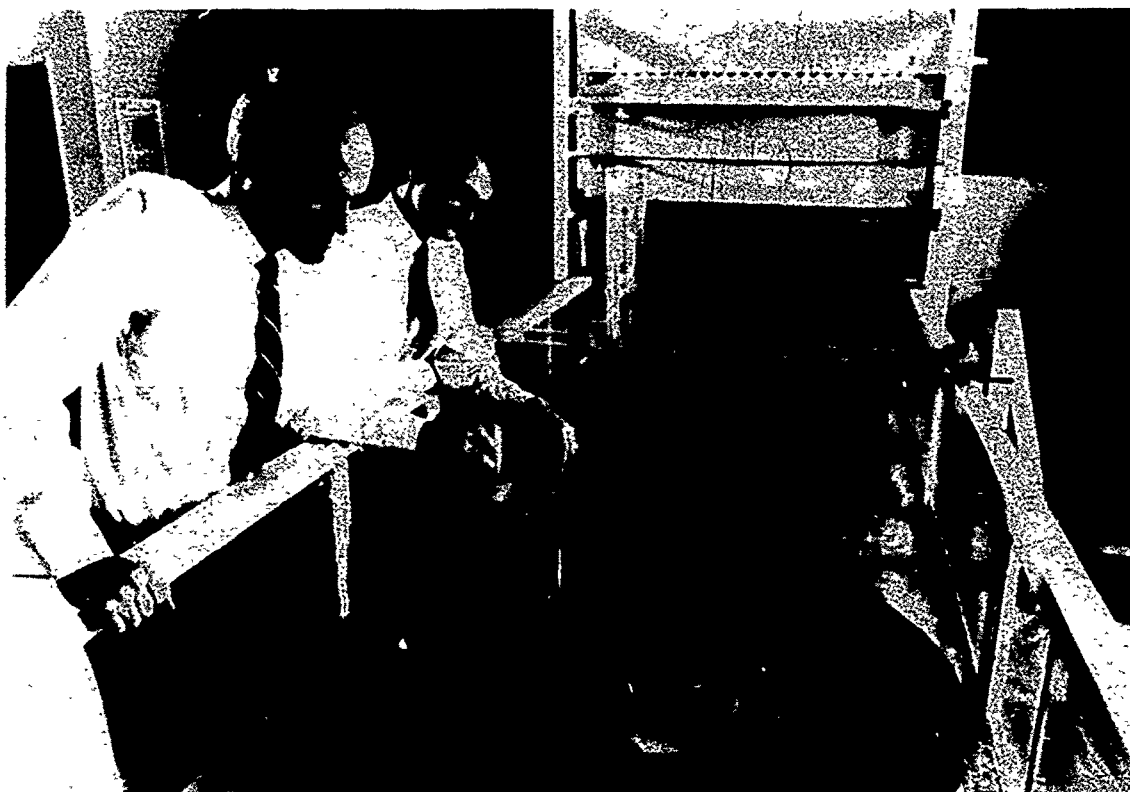
Figure 6 RWDI water flume testing facility

surroundings in an open channel water flume (Figure 6).

Water flowing over the model simulates the atmospheric wind, and silica sand simulates precipitation. Flow speeds and sand grain sizes are selected to obtain particle trajectories similar to those of snow particles or rain drops in a typical storm at the site (the scaling principals are summarized by Irwin and Williams, 1983). The techniques used to reproduce the vertical stratification and turbulence characteristics of the wind at the site are similar to those used in the wind tunnel (Irwin, 1979).

Sloping roofs and other critical areas of the model building are fitted with small slots to trap sand particles falling onto the surface of the building (Figure 7). The depth of trapped sand in each slot is compared with the depth found in a reference trap, which represents the depth of precipitation recorded in the meteorological data. The ratio of the two depths gives the desired correction factor for each slot location.
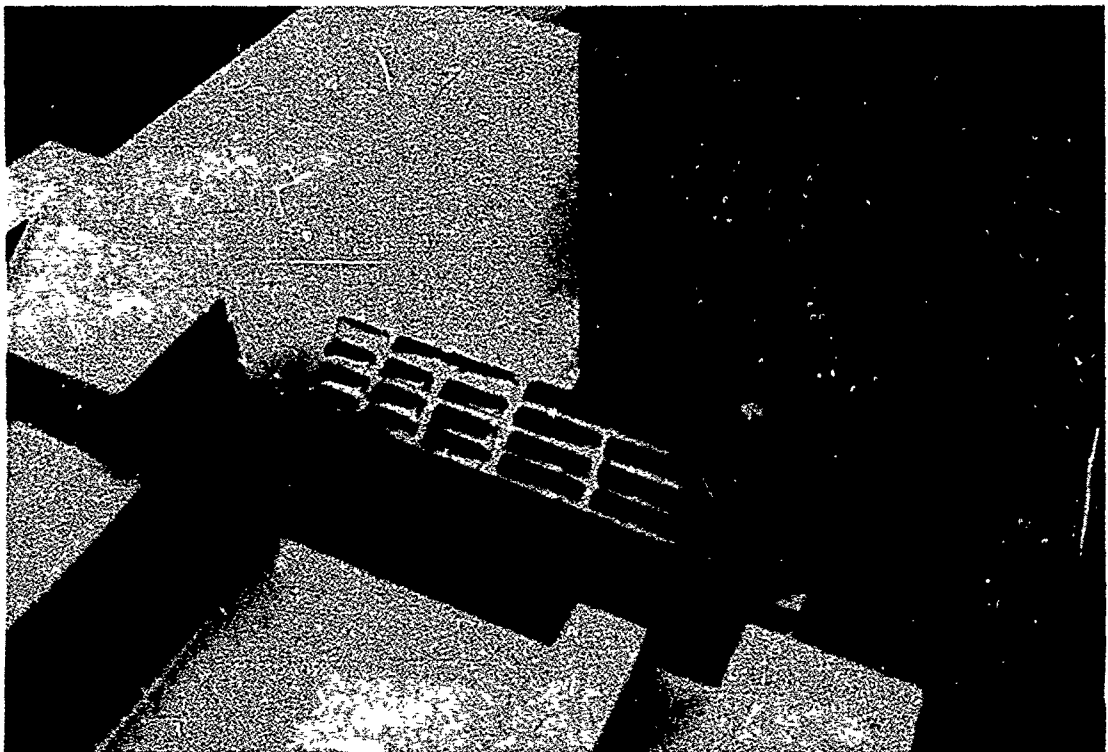
Figure 7 Sand traps

Figure 8 shows the roof plan of a high-rise office tower, with snowfall depth correction factors for various wind angles. The factors range from 0.25 to 2.5. A factor of 2.5 in a given zone of the building means that the average snowfall in that zone, during a storm with winds in the direction shown by the arrow would be 2.5 times that recorded in the meteorological data.
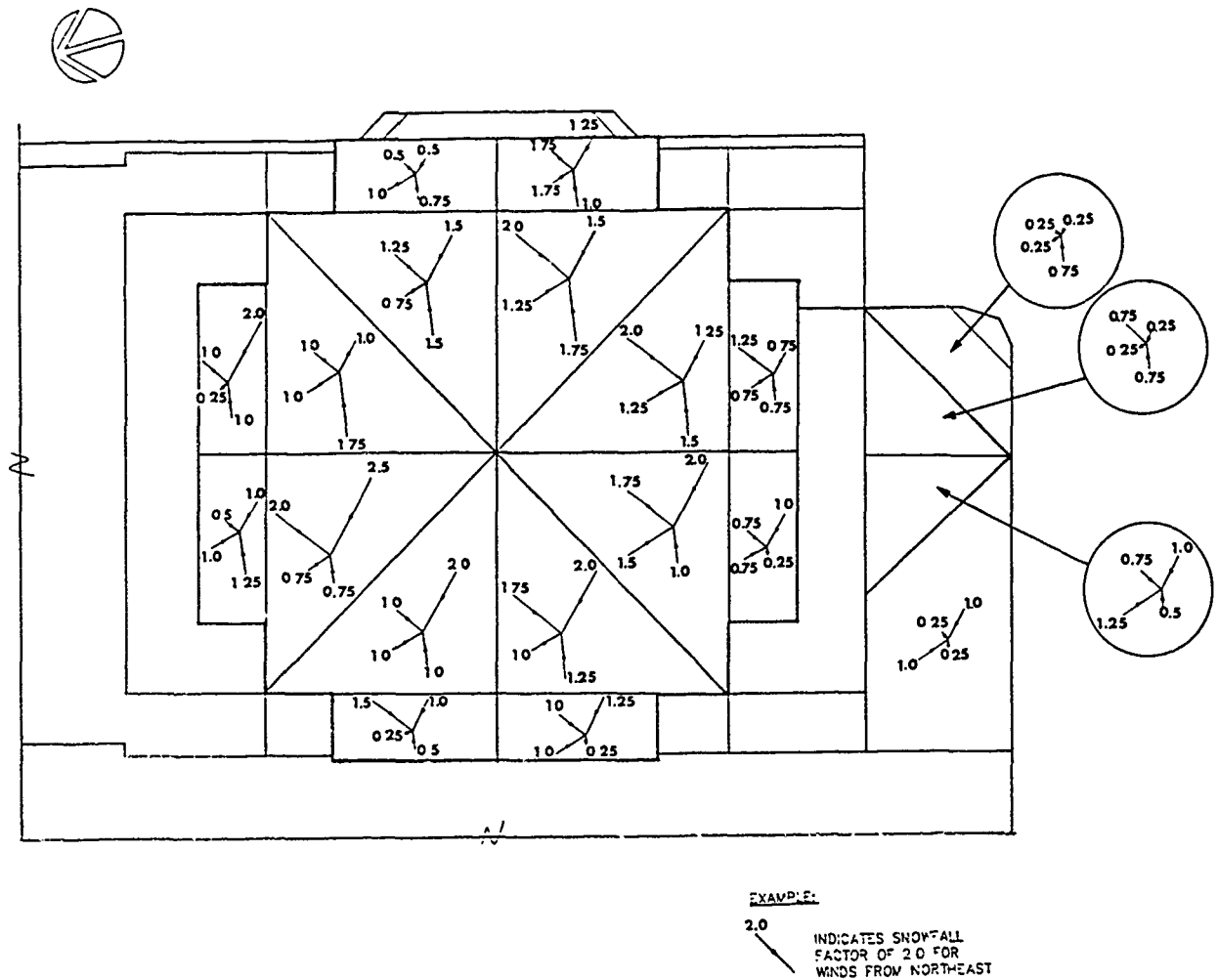
Figure 8   Water flume test results

SIMULATION RESULTS

Figure 9 shows an example of the simulation results for an area of sloped glass on a building proposed for Manhattan, New York. The figure shows predicted snowfall accumulations on the sloped glass as well as the reported ground snowfall for major events spanning the twenty-year period from 1945 to 1965. The units for the snowfall amounts are pounds per square foot (psf). Figure 9 shows only events that would have produced accumulations greater than 2.0psf (roughly 2.0 inches) on the glass.
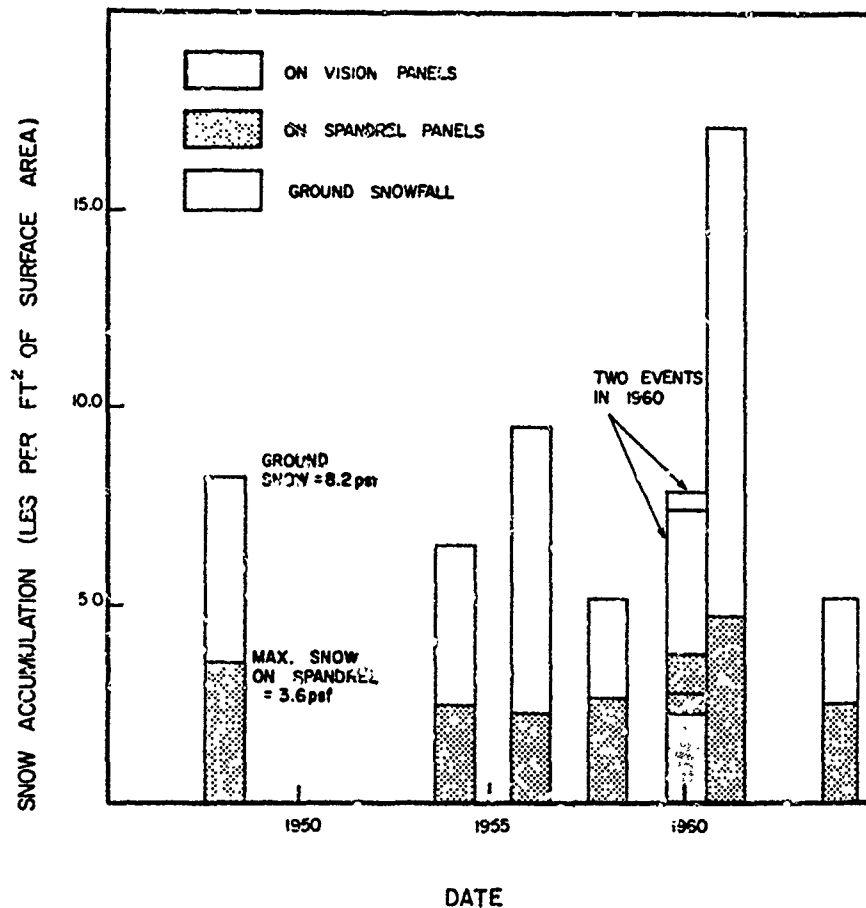
Figure 9 Example of simulation results

139

The areas identified as vision panels consisted of double panes of glass. The spandrel panels were single panes backed with 3.0 inches of glass fibre insulation. Because of the low insulation value of the vision panels, much of the snowfall melted as it fell on the glass. Consequently, the accumulations there were substantially less than on the spandrels. In fact, only one storm (1960) in the twenty years would have produced more than 2.0psf of snow on the vision panels. There were a total of nine events for the spandrels. In both cases, the accumulations on the glass were considerably lower than the reported ground snowfalls. This was primarily due to the steep slope angle of the glass (about 60 degrees) and melting caused by heat escaping from inside the building.

Wind lift-off of snow on the sloped glass was found to be a rare event except for spandrel panels on which the snow had crept over the edge of the slope to form an overhang (Type I Lift-off). Winds were sufficient to cause lift-off of overhanging snow in all nine of the events shown for spandrels. Lift-off of non-overhanging snow layers (Type II lift-off) was feasible in only two of the events. On the vision panels, there was only one event in which an uplift of any kind could have occurred.

The largest snow accumulation in the twenty years was 5.0psf, on the spandrels. This quantity, on a 30ft^2 pane of glass, represents 150lbs of snow. If this mass of snow were to slide off the glass, it could cause considerable damage below. This area was therefore designated as requiring snow control. The recommended control measures in this case were to install a snow-retainer railing at the base of the slope, to reduce the insulation of the spandrels in order to increase snow melting, and to provide adequate drainage for melt water. A snow load for use in the design of the railing was calculated by fitting the accumulations for the nine events shown in Figure 9 with an extreme value distribution and obtaining the 50 year value.

CONCLUSION

A simulation has been developed for predicting the quantities of snow or ice that can accumulate and later slide or blow off of sloped roofs and other building surfaces. The predictions are based on historical meteorological observations, with account being taken of any melting caused by local heat transfer effects. Scale model studies in a water flume account for the impact of local wind patterns on accumulation rates. Scale model studies in a boundary layer wind tunnel account for local wind effects leading to lift-off of snow or ice. These scale model studies provide the best possible simulation of the local wind effects, which can have a significant impact on snow or ice accumulation and lift-off.

This simulation is considered to be a significant improvement over the simplistic snow load calculations that were previously used to assess snow slide-off and lift-off problems. Thus far, the simulation has been applied to a proposed high-rise office tower in Manhattan, and an office tower in Philadelphia. In both cases, it was used to develop effective, designed-in snow and ice control measures while avoiding costly overdesign.

REFERENCES

ASHRAE (American Society of Heating, Refrigerating and Air-Conditioning Engineers), 1976, Procedure for Determining Heating and Cooling Loads for Computerizing Energy

Calculations, ASHRAE Inc., Atlanta, Georgia.

Irwin, P. A. I., 1979, "Design and Use of Spires for Natural Wind Simulation," N. A. E. Report, LTR-LA-233, National Research Council Canada, Ottawa, Ontario.

Irwin, P. A. I., 1987, "Pressure Model Techniques for Cladding Loads," Proceedings of the Seventh International Conference on Wind Engineering, Vol. 3, 121-130, Achen, West Germany, July, 1987.

Irwin, P. A. I., and C. J. Williams, 1983, "Applications of Snow-Simulation Model Tests to Planning and Design," Proceedings, Eastern Snow Conference, Vol. 28, 118-130, 40th Annual Meeting, Toronto, Ontario, June, 1983.

Kind, R. J., and R. L. Wardlaw, 1979, "Model Studies of the Wind Resistance of Two Loose-Laid Roof-Insulation Systems," Laboratory Technical Report, LTR-LA-234, National Research Council Canada, Ottawa, Ontario.

Langham, E. J., 1981, "Physics and Properties of Snow Cover," Handbook of Snow, Permagon Press Canada Ltd., Toronto, Ontario.

Variability of Snow Loads on Large-Area Flat Roofs

M. Mikitiuk[I] and N. Isyumov[II]

ABSTRACT

Snow loads on roofs depend on their size and shape, their surroundings and on local climatic conditions. In relatively cold climates, the maximum snow load is formed by the accumulation of snow over a period of weeks to months. In milder winter climates, on the other hand, the maximum load may be the result of an extreme single snowfall or a rain-on-snow event. Consequently, the magnitude of the maximum snow load on a roof depends on the time history of individual snowfalls and the influence of various meteorological variables which act to modify and/or reduce the snow deposit on the roof.

This paper examines the variability of snow loads on roofs which tends to be higher than that of the ground snow load. Factors which add to the variability are identified and discussed. The paper presents some techniques available to designers to improve estimates of snow loads on large flat roofs.

INTRODUCTION

Snow loads, like other environmental loads, exhibit marked variability over large geographic regions due to climatic differences. Within each region considerable variations occur from roof to roof and from winter to winter. In addition to weather and climatic variations, differences in roof snow loads result from differences in the aerodynamic, thermal and structural characteristics of roofs, the overall exposure to wind action and the aerodynamic influence of specific nearby buildings. Current code procedures allow for some of these uncertainties by specifying snow loads which tend to be adequate for the majority of construction. Such loads are not necessarily upper bounds and designers, faced with unusual situations, are prudent to consider the possibility of experiencing snow loads which differ from code values either in magnitude and/or distribution. The need for such special attention is underscored by recurring failures, sometimes of major roofs.

The objective of this paper is to examine snow loads on large-area flat roofs commonly used for commercial, manufacturing, retail and warehouse buildings. The emphasis is on single-level roofs or the upper roofs of multiple-level buildings. The special problem of drift loads formed on lower roofs adjacent or near higher ones is not specifically addressed in this paper. The main emphasis is to examine aspects of

---

[I]Research Associate, Boundary Layer Wind Tunnel Laboratory, The University of Western Ontario, London, Ontario, Canada

[II]Manager and Research Director, Boundary Layer Wind Tunnel Laboratory, The University of Western Ontario, London, Ontario, Canada

the snow climate which influence roof snow loads, including basic relationships between snow loads on roofs and on the ground; the dependence of roof snow loads on building height and surrounding terrain; the complicating aerodynamic influence of surrounding buildings; and additional loads which can be experienced due to rain and/or melt water retention. All of these collectively and individually increase the variability of the roof snow loads and hence raise the uncertainty of the estimated snow loads. Clearly there are other sources of variability not examined in this paper. These include the effects of heat loss which, in some cases, can lead to increased local melting, ponding and ice formation, which can result in larger local loads. Also, the effects of local roof details such as penthouses, ducts, billboards, mechanical and ventilating units, parapets and other aerodynamic "clutter" are not examined at this time.

CURRENT CODE PRACTICE

Roof snow loads specified for flat roofs in North American and most other building codes are based on estimates of extreme snow loads on the ground. For example, the approach taken by the National Building Code of Canada (NBCC, 1985) defines the design snow load on the roof as:

$$S = S_0 \, C_b \, C_w \, C_s \, C_a \qquad (1)$$

where S_0 is the design ground snow load; C_b is a basic roof snow load factor which allows for the existing experience that snow loads on roofs are on average lower than those on the ground; C_w is the wind exposure factor which reduces snow loads for exposed wind-swept roofs; C_s is the roof slope factor which allows for slide-off; and C_a is the accumulation factor which allows for the influence of roof shape.

In Canada, S_0 is taken as the 30-year return period annual maximum ground snow depth estimated for a particular location and converted to a load using a specific gravity of 0.245. The rain load, corresponding to the maximum recorded 1-day rainfall during the month when the ground snow depth tends to reach a maximum, is added to this value. The basic roof snow load factor, C_b is taken as 0.8. For flat roofs, $C_s = 1.0$, $C_a = 1.0$ and the wind exposure factor C_w is taken either as its basic value of 1.0 in normal situations or can be reduced to .75 in situations where the roof is fully exposed with no higher buildings within a distance of 10 times the height difference.

For simplicity and in order to avoid confusion with Code nomenclature, Eq. 1 for flat roofs in this paper is rewritten as:

$$S = \eta \, S_0 \qquad (2)$$

where η is a roof snow load coefficient. Using NBCC, 1985 η becomes 0.8 for typical flat roofs and 0.6 for fully-exposed, wind-swept roofs.

The resulting snow load is a uniformly distributed one except near local projections and changes in elevation. Some codes, like (ANSI, 1982) and (NBCC, 1985) have the additional requirement that the designer unload any portion of the roof to 50% of the uniformly distributed load in order to examine the effects of non-uniform loading. No guidance is given to help the designer to assess the possibility of exceeding this uniformly distributed load due to drifts formed by wind action on the roof or due to greater deposition in the "aerodynamic shadow" of an adjacent taller building. Some aspects of the variability of the roof snow load S are examined below using the simple expression given in Eq. 2.

SNOW CLIMATE

Although snow deposits on roofs and on the ground are influenced by the same weather and climatic effects, there are important differences in the details of the snow load formation process (Isyumov, 1971), (Isyumov and Davenport, 1974), (Isyumov, 1982). Generally, while the ground snow depth does represent a good measure of the snowfall and its persistance over the course of winter, it does not necessarily provide a reliable measure of snow loads formed on roofs. Nevertheless, the simplicity of approaches based on equations like Eq. 1 and 2 is attractive. First, a significant statistical base of S_0 has evolved. Second, roof snow load coefficients like those given in Eq. 1 and 2 have been calibrated through full-scale observations (Lutes and Schriever, 1971), (Schriever and Otstavnov, 1967), (Taylor, 1981, 1984, 1987), (Tobiasson and Redfield, 1973), (O'Rourke et al, 1983, 1984), to provide acceptable roof snow load coefficients for most construction.

Nevertheless, a number of significant uncertainties remain. For example, is the specific gravity of 0.245 appropriate for snow accumulations on roofs. There is evidence (Taylor, 1997) that a somewhat higher value may be justified. In addition, inadequate drainage can result in slush and ice formation. This is particularly important for large-area flat roofs.

Other important parameters of the snow climate are its time variation and persistence. Design ground snow loads are based on the annual extreme ground snow depth and do not distinguish whether this amount is the result of an extreme single event or the accumulation of many smaller snowfalls over the course of the winter. The former would be expected to produce larger snow loads on roofs. In contrast, lower snow loads result in climates where there are many smaller snowfalls over the course of winter and there are more opportunities to remove snow from roofs by wind action and thermal ablation.

An indication of the composition of extreme ground snow loads is provided in Figure 1 which shows the contribution of extreme 30-year, 24-hour snowfalls to the 30-year maximum ground snow load for a number of Canadian locations. In this case, the ratio of the 24-hour snowfall event to the ground snow load is plotted against the average air temperature during the winter. Contributions to the design ground snow load in colder climates with an average winter temperature of less than $-5^{\circ}C$ is around 25%. In climates with the average temperature around $0^{\circ}C$, the single extreme event may represent about 50% of the design ground snow load. As expected, for warmer climates with mean winter air temperatures above $0^{\circ}C$, ground snow loads are dominated by the single snowfall event.

An indication of the composition of the design snow load is helpful in anticipating likely loading scenarios. For example, large-area flat roofs are more likely to experience drift snow loads in excess of the code-prescribed uniformly distributed value in situations where much of the snowfall occurs in one or several extreme events. Other situations where Figure 1 is helpful are temporary structures or roofs provided with a snow melting system to keep the roof "bare" on average.

RELATIONSHIP BETWEEN ROOF AND GROUND SNOW LOADS

Unlike extreme wind effects which are caused by single events or storms, extreme snow loads, with the exception of relatively mild winter climates, tend to be formed by an accumulation of snow over a period of time. As a result, the magnitude of the maximum roof snow load depends on the time history of individual snowfalls

144

and the interaction of meteorological factors which reduce, modify and, in some cases, increase snow deposits. Wind is the dominant factor which influences both the magnitude and distribution of snow deposits on roofs. Physical model tests, using wind tunnels or water flumes, can provide information on the deposition of snow during particular weather events and the depletion of the roof snow deposit by drifting. Such models, however, are not suitable for determining the cumulative effects of many snowfalls occurring over a period of time. A mass balance approach has been developed to describe the snow accumulation process in terms of its basic meteorological and climatic parameters (Isyumov, 1971), (Isyumov and Davenport, 1974), (Isyumov and Mikitiuk, 1977). In this approach, the roof snow load is taken as the running sum of the incremental loads due to individual snowfalls and the depletion of the roof snow load by wind action and thermal ablation. This procedure has been used in Monte Carlo computer simulations to examine a relationship between maximum roof and ground snow loads. Similar methods, extended to estimate non-uniformities in deposition, are used elsewhere (Irwin and Gamble, 1987).

The results of computer simulations carried out at the Laboratory, (Isyumov, 1982), (Isyumov et al, 1984b), indicate that snow loads on roofs tend to be on average lower than those on the ground. Nevertheless, in certain circumstances, larger-than-ground snow loads can be experienced. Figure 2 provides a summary of the daily roof snow load S expressed as a ratio of the corresponding ground snow load S_0 obtained from computer simulations for an exposed flat roof. The average value of the daily roof snow load coefficient η is seen to be of the order of .3 and less. The daily variability of η for Ottawa is illustrated by histograms, which correspond to conditions where the ground snow load is equal to .5 and .9 of the 30-year extreme value. The distributions are highly skewed and the daily roof snow load coefficient occasionally exceeds 1.0. On the other hand, there are many days when the roof snow load is essentially 0.

Trends which have emerged from these computer simulations include the following:

i)   Annual maximum roof and ground snow loads do not necessarily occur on the same day. The correlation between the annual maximum roof and ground snow loads tend to be relatively small. Typically, correlation coefficients, using a linear regression analysis, are of the order of .5 and less. This confirms that while the processes are driven by common events, the snow load formation processes on the ground and on the roof have subtle differences.

ii)   Snow loads on flat roofs tend to be on average below those on the ground. The variability of roof snow loads, however, is considerably greater.

iii) The relationship between extreme roof and ground snow loads is influenced by the statistical properties of the local snowfall, air temperature, wind speed and wind direction and other meteorological variables. Extreme roof snow loads tend to be least in comparison with those on the ground for locations with well-below-freezing temperatures and where the ground snow load represents the accumulation of a large number of relatively small snowfalls. The ratio of roof to ground snow loads tends to be largest for warm winter climates where the loading process is dominated by a single extreme snowfall.

145

The variability of extreme snow loads on the ground and on flat roofs is illustrated in Figure 3. Here a Type I extreme-value distribution has been found effective in fitting the annual extremes generated over a 1000-year period. The ratio of the dispersion to the mode value is given for the distributions of the extreme ground and roof snow loads. The coefficients of variation of the annual maximum ground and roof snow loads are respectively about .26 and .56. Coefficients of variation of the annual and lifetime extremes are presented in Table 1 for four Canadian locations. The simulation results for Ottawa shown here are obtained with parameters somewhat different from those used in connection with Figure 3. The lifetime is taken as $M = 30$ years. Coefficients of variations are significantly larger for the extreme roof loads. Halifax is an exception as changes in temperature over the course of a year cause large fluctuations in the ground snow accumulations. Treating the roof snow load coefficient η as an independent variable allows an estimate of its coefficient of variation.

$$V_\eta \simeq (V_{S_0}^2 - V_S^2)^{\frac{1}{2}} \qquad (3)$$

The coefficient of variation of the roof snow load coefficient for flat roofs, obtained in this way is typically .15 and less. The corresponding load factor for lifetime extreme roof snow loads on flat roofs has been shown to be around 1.5 for a lifetime of 30 years (Isyumov et al, 1984b).

Recently-published data on full-scale snow loads on flat roofs (Taylor, 1987) provides an opportunity for comparing statistical properties of the roof snow load coefficient η with results from the Monte Carlo computer simulations. Figure 4a shows histograms of the roof snow load coefficient η which, in this case, is the ratio of the annual maximum snow load on flat roofs to the annual maximum ground snow load. The results shown from the Monte Carlo simulations are for flat roofs situated in open-country terrain in Ottawa and combined results for similar roofs in Ottawa, Quebec City and Winnipeg. The full-scale observations are for flat upper roofs and combinations of flat upper roofs and lower roofs away from drifts. The data are from roofs in Arvida P.Q., Halifax, Ottawa, Saskatoon and Edmonton. The full-scale information is for "maximum loads" typical of areas corresponding to tributary areas of roof decking, purlins and other secondary members (Taylor, 1987). The Monte Carlo loads correspond to the maximum section along the roof. The agreement is generally quite good. Figure 4b shows the probability of exceeding the annual maximum roof snow load coefficient $\hat{\eta}$. The data from the computer simulations are represented by fitted Type I extreme-value distributions.

Table 2 summarizes some of the statistical properties of these data sets. Indicated is the average value of $\hat{\eta}$, the coefficient of variation, and the probability of $\hat{\eta} > 0.6$ and $\hat{\eta} > 0.8$. These are values recommended for fully-exposed and typical flat roofs in the National Building Code of Canada (NBCC, 1985). The agreement is remarkably good. Average values of the snow load coefficient obtained from Monte Carlo simulations are comparable to the full-scale data. The computer simulation indicates somewhat greater variability and hence somewhat more skewed distributions. This is not surprising as the simulations were carried out for a period of 1000 years while the longest period of observation for the full-scale roof was 15 years for Ottawa. The probability of exceeding roof snow loads in excess of about 60% of the design ground snow load is only 0.13 based on full-scale observations. A somewhat higher probability is indicated from the Monte Carlo simulations at Ottawa. The corresponding probability for the joint Ottawa, Winnipeg and Quebec data is about 0.11.

DEPENDENCE ON BUILDING HEIGHT

Current code provisions do not include the influence of building height in the determination of the roof snow load. This shortcoming significantly adds to the variability of the snow loading estimate and obscures the influence of other parameters. Dry snow will drift at a wind speed of 2-3 metres per second near the surface and both the magnitude and the distribution of the roof snow load are therefore quite sensitive to the wind speed at roof level (Isyumov, 1971). As a result, higher roofs, due to their exposure to potentially higher wind speeds, are expected to experience snow loads which are on average smaller in magnitude but more non-uniform in distribution. Physical model studies of roof snow load formation and Monte Carlo computer model simulations (Isyumov, 1971) demonstrated that snow loads on flat roofs have a dependence on the mean wind speed at roof level and therefore vary both with the roughness of the surrounding terrain and with roof height. Expressions for the roof snow load coefficient relating the 30-year return period snow load on the roof to that on the ground, which were suggested from that work, are given in Eq. 4 and 5 for typical suburban and open-country terrains respectively.

Suburban Terrain ($\alpha = 0.25$, $Z_g = 365$m)

$$\hat{\eta} = 1.67 \, H^{-0.50} \tag{4}$$

Open-Country Terrain ($\alpha = 0.14$, $Z_g = 275$m)

$$\hat{\eta} = 0.51 \, H^{-0.19} \tag{5}$$

where H is the height above ground to the level of a flat roof, and α and Z_g are the exponent and gradient height used in power law expressions for the vertical variation of the mean wind speed.

The variation of the roof snow load coefficient with height above ground, given by these equations, is shown in Figure 5. Also shown are recently reported full-scale observations for a number of flat roofs (Taylor, 1987). The exposure of particular roofs included in the full-scale data was not indicated, however it is likely to be in the general range of open-country to suburban terrain. The variation of the roof snow load coefficient with building height suggested for these two terrains in Eq. 4 and 5, is consistent with the full-scale data. As expected, the dependence on the roof height is most pronounced for lower roofs in relatively more built-up terrain. The sensitivity reduces for taller buildings as the variation of wind speed with height above ground becomes less pronounced.

The relationship for a suburban terrain would indicate that the roof snow load is approximately inversely proportional to the square of the wind speed at roof level. The relationship on wind speed in open-country terrain appears to be more complex. A detailed explanation of the physics of the process requires further study. The dependence of the roof snow load on wind speed at roof level is confirmed by recent Japanese data (Abe and Nakamura, 1984). These results suggest that snow accumulations on roofs reduce markedly for roof-level wind speeds greater than 2.5 m/s. In view of this demonstrated dependence on wind speed, it would be highly helpful to include the influence of building height and terrain roughness in parametric models used to analyse field data. This would help to improve code models in the future.

LOAD NON-UNIFORMITIES DUE TO WIND ACTION

Wind action is dominant in determining the magnitude and the distribution of the roof snow load. During calm conditions the accumulation of snow on roofs tends to be uniformly distributed with modifications due to slide-off from inclined surfaces. In the presence of wind however, the deposition of new snow becomes non-uniform. Non-uniformities in accumulation result from drifting, which depends on the roof shape and on the speed and direction of the wind, local shielding effects of protrusions above the roof surface, and the influence of nearby buildings. These largely aerodynamic effects can be studied with wind tunnel and/or water flume models. Such studies are complicated by the additional requirement to simulate the characteristics of snow particles at a reduced scale and consistent with the modelling of the turbulent properties of atmospheric wind. The latter do become important to correctly simulate the deposition and depletion patterns of snow on roofs. Consistent modelling of the characteristics of the wind and the snow phase is difficult at a reduced scale. In view of these complications, two different modelling approaches have been taken:

i)   Direct-model studies which include the snow phase at a somewhat "relaxed" or distorted scale. The results of such approximate studies are highly useful to indicate relative if not absolute measures of snow deposition during particular snow storms. Such studies are also valuable for parametric studies of the various factors affecting the process (Isyumov, 1971), (Peterson, 1986), (Iverson, 1982).

ii) Indirect-model studies in which details of the flow field over the roof are determined in properly-scaled flow conditions and subsequent accumulations of snow are inferred using empirical data which relate snow drifting rates to wind speed (Melbourne and Styles, 1968), (Irwin and Gamble, 1987).

Photographs of snow patterns on a large flat roof are illustrated in Figure 6. This model study was carried out to visualize drift patterns on this roof located in a complex urban terrain (Isyumov et al, 1984a). The approach taken in this study was to carry out a numerical simulation to provide predictions of the overall magnitude of extreme roof snow loads and to infer likely non-uniformities in loading from wind tunnel observations of deposition patterns. The study used a 1:500 scale model of the roof tested in the presence of surrounding buildings and in boundary layer flow conditions developed over appropriately modelled upstream terrain. The velocity scale in these tests was determined by scaling of the terminal velocities of model and full-scale snow particles. This provided an overall similarity of particle trajectories approaching and over the roof. The corresponding threshold velocity to initiate surface drifting was somewhat higher in the model relative to typical full-scale values for new dry snow. The resulting somewhat greater persistence of the model snow deposit was considered helpful in at least nominally allowing for adhesion effects in full scale.

Figure 6 shows deposition patterns on the roof for various wind directions due to a single extreme 24-hour snowfall of about 50 cm in full scale. This approximately corresponds to the 100-year return period snow storm for the Chicago area (Isyumov et al, 1984a). For each of the wind directions, the mean wind speed at roof level corresponded to about 2.5 m/s in full scale. The height above ground of the larger area upper roof is about 30 m in full scale. The lower roof is to the north and is about 23 m above grade. A number of interesting observations emerge:

i) The accumulations of snow on the roof at this wind speed are generally light. Much larger deposits were observed at lower wind speeds. This is consistent with expected behaviour and results of Japanese observations (Abe and Nakamura, 1984).

ii) Deposition on the roof is highly dependent on wind direction. Deposition is least for wind parallel to the short direction of the roof and the step change in elevation between the lower and upper roofs. Somewhat larger deposits occur with the wind parallel to the long direction. This confirms that the load depletion action of wind is more effective for smaller-area roofs.

iii) A distinct local drift is formed on the lower roof at the change in elevation. It is noteworthy that this drift occurs for wind directions with the upper roof downstream, see photo for 343° and with the upper roof upstream, see photo for 163°. This clearly demonstrates that local drifts at changes in elevation are largely due to the local aerodynamic influence of the step change in height. The somewhat larger drift magnitudes observed in full scale in situations with upper roofs upstream, are attributable to continued drifting from the upper roof after snowfall stops.

iv) There is clear evidence of increased deposition on the roof due to the influence of local features. This is a cable-supported roof and there are two lines of pylons. Their effects can be clearly seen from the photographs.

v) Local buildings appear to have a significant effect for some directions. Note the distinct "aerodynamic" shadow of a building to the south of the roof as seen in the photo for 163°. Similarly there are additional local deposits on the roof due to the influence of tall buildings to the west, see 253°. Such effects are not provided for in codes and can only be identified by physical model studies.

EFFECTS OF RAIN AND MELTING

A review of the literature shows that several snow accumulation and melt algorithms have been developed for use in watershed modelling. Relatively simple approaches, using the air temperature as an index, (Linsley et al, 1975), can be used as a first approximation to estimate the ablation of snow due to melting and the inhibiting effects of surface melting and refreezing on the drifting action of wind. More detailed models based on the energy balance within a snowpack have been developed (Anderson, 1976), (Price et al, 1976). These require more detailed input data such as wind speed, vapour pressure, snowpack temperature, ground temperature and incoming solar radiation. While it is desirable to include these significant variables, which influence the growth/decay of the snowpack, such detailed data are not always available. Models of snow accumulation and melt (Anderson, 1973, 1978), (Logan, 1976) offer the advantage of a modular structure which permits the user to change program modules as better representations of the unit processes and/or improved data become available. Some of the existing expertise with snowpack melt and water retention can be directed towards improving estimates of water retention and rain-on-snow roof loads. This becomes particularly important for large-area flat roofs.

CONCLUDING REMARKS

The material presented in this paper indicates that the variability of snow loads on roofs is generally higher than that of ground snow loads. This is important to recognize in any limit-states formulation of snow loads. The variability of snow loads on large-area flat roofs is potentially higher if such roofs are exposed to wind action and are located in climatic regions where rain-on-snow loads can be significant and where air temperatures can fluctuate about the freezing point and can result in ice formation and ice dams which pond melt and rain water. In such situations, the coefficient of variation of the ground-to-roof snow load conversion factor may be much more than 0.15, as suggested for well-drained roofs. A number of specific points on these two main areas of additional concern are as follows:

Wind Effects

i) There are clear indications that snow accumulations and hence snow-imposed loads, reduce on average as the wind speed at roof level increases. Hence, snow loads should be expected to vary both with the roughness of the surrounding terrain and with roof height.

ii) While roofs more exposed to wind action are expected to see on average lower snow loads, there should be an expectation of greater variability, particularly on large-area roofs. Wind is more effective in clearing smaller-area roofs. As the dimension of the roof in the direction of the wind increases, the clearing action becomes less effective and local wind-induced drifts should be expected. As a result, there are potential dangers in using wind exposure reduction factors allowed by building codes. While a 75% reduction may be appropriate when designing the primary structural members of an exposed large-area flat roof, it may be inappropriate for the design of secondary members with smaller tributary areas.

iii) There are clear indications that snow loads depend on the orientation of the roof with the prevailing wind direction. There are advantages, to orient the roof so as to minimize drift accumulations.

iv) Current codes allow designers to take into account non-uniform snow deposition resulting from local protrusions above roof level. On the other hand, codes do not provide any assistance when dealing with the possible "aerodynamic shadow" effects of nearby structures. These can be significant in urban settings.

Rain-On-Snow and Melt Water Loads

i) Some codes (NBCC, 1985) include an allowance for rain in the design ground snow load, others (ANSI, 1982) contain special requirements to include the effects of rain. These may not be sufficient for very large area flat roofs located in climates where there are significant rainfalls during the winter and where the air temperature fluctuates about freezing.

ii) Large-area flat roofs have a greater potential for local ice build-up. This can lead to larger local load concentrations and can inhibit the drainage of rain and melt water. With inadequate drainage, the snow layer acts

like a "sponge" and the runoff or drainage times can be quite long. This increases the possibility of ice formation in areas with fluctuating temperatures.

iii)   Numerical methods are now becoming available to examine and at least "bound" the likely effects of rain and melt water.

ACKNOWLEDGEMENTS

REFERENCES

Abe and Nakamura, 1984, "Wind Effects on the Daily New Snow Depth on Flat Roofs," Japanese National Research Center for Disaster Prevention, Report No. 32. 1984.

American National Standards Institute, 1982, "American National Standard for Minimum Design Loads for Buildings and Other Structures," ANSI A58.1-1982.

Anderson, E.A., 1973, "National Weather Service River Forecast System - Snow Accumulation and Ablation Model," NOAA Technical Memorandum NWS HYDRO-17, U.S. Dept. of Commerce, Silver Spring, Md.

Anderson, E.A., 1976, "A Point Energy and Mass Balance Model of a Snow Cover," NOAA Technical Report NWS 19, U.S. Dept. Commerce, Silver Spring, Md.

Anderson, E.A., 1978, "Streamflow Simulation Models for Use on Snow Covered Watersheds," Proceedings Modelling of snow cover runoff, S.C. Colbeck and M. Ray (Editors), U.S. Army Cold Regions and Engineering Laboratory, Hanover, NH., September 26-28, 1978.

Irwin, P.A. and S.L. Gamble, 1987, "Prediction of Snow Loading on Large Roofs," 7th International Conference on Wind Engineering, Aachen, FRG, July 6-10, 1987, 171-180, 1987.

Isyumov, N., 1971, An Approach to the Prediction of Snow Loads, Ph.D. Thesis, The University of Western Ontario, London, Ontario, Canada.

Isyumov, N. and A.G. Davenport, 1974, "A Probabilistic Approach to the Prediction of Snow Loads," Canadian Journal of Civil Engineering, Vol. 1(1), 28-49, 1974.

Isyumov, N. and M. Mikitiuk, 1977, "Climatology of Snowfall and Related Meteorological Variables with Application to Roof Snow Load Specifications," Canadian Journal of Civil Engineering, Vol. 4(2), 240-256, 1977.

Isyumov, N., 1982, "Roof Snow Loads: Their Variability and Dependence on Climatic Conditions," Symposium on the Uses of Wood in Adverse Environments, Vancouver, B.C., May 15-18, 1978, Van Nostrand Reinhold Company, New York.

151

Isyumov, N., S. Helliwell and M. Mikitiuk, 1984a, "Estimates of Snow Loads for the Proposed McCormick Place Extension, Chicago, Illinois," Faculty of Engineering Science Research Report BLWT-SS34-1984, The University of Western Ontario, London, Ontario, Canada.

Isyumov, N., M. Mikitiuk and A.G. Davenport, 1984b, "Snow Loads on Roofs," 12th IABSE Congress, Vancouver, B.C., September 3-7, 1984, 859-866, 1984.

Iversen, J.D., 1982, "Small-Scale Modeling of Snow-Drift Phenomena," Int. Workshop on Wind Tunnel Modeling Criteria and Techniques for Civil Engineering Application, National Science Foundation and National Bureau of Standards, April, 1982.

Linsley, R.K., M.A. Kohler and J.L.H. Paulhus, 1975, Hydrology for Engineers, McGraw-Hill Book Co., New York.

Logan, L.A., 1976, "A Computer-Aided Snowmelt Model for Augmenting Winter Streamflow Simulation in a Southern Ontario Drainage Basin," Canadian Journal of Civil Engineering, Vol. 3, 531-554, 1976.

Lutes, D.A. and W.R. Schriever, 1971, "Snow Accumulations in Canada: Case Histories: II," N.R.C.C., Div. Building Research Tech. Paper No. 339, Ottawa, Ontario, Canada.

Melbourne, W.H. and D.F. Styles, 1968, "Wind Tunnel Tests on a Theory to Control Antarctic Drift Accumulations Around Buildings," Int. Res. Seminar Wind Effects on Buildings and Structures", Vol. 2, University of Toronto Press, 1968.

National Building Code of Canada, 1985, "Commentary H Snow Loads," NRCC No. 17724, Ottawa, Ontario, Canada, 1985.

O'Rourke, M., P. Koch and R. Redfield, 1983, "Analysis of Roof Snow Load Case Studies," CRREL Report 83-1, 1983, U.S. Army Cold Regions and Engineering Laboratory, Hanover, NH.

O'Rourke, M., R. Speck and U. Stiefel, 1984, "Drift Snow Loads on Multi-Level Roofs," Dept. Civil Eng. Rep., Rensselaer Polytechnic Inst., Troy, New York.

Petersen, R.L., 1986, "Simulating Snow Loads on Fabric Roofs," ASCE Advancement in Aerodynamics, Fluid Mechanics and Hydraulics, Minneapolis, Minnesota, 1986.

Price, A.G., T.Dunne and S.C. Colbeck, 1976, "Energy Balance and Runoff from a Subarctic Snowpack," CRREL Report 76-27, 1976, U.S. Army Cold Regions and Engineering Laboratory, Hanover, NH.

Schriever, W.R. and V.A. Otstavnov, 1967, "Snow Loads: Preparation of Standards for Snow Loads on Roofs in Various Countries with Particular Reference to the U.S.S.R. and Canada," C.I.B., Research Report No. 9, Ottawa, Ontario, Canada.

Taylor, D.A., 1981, "Snow Loads for the Design of Cylindrical Curved Roofs in Canada," Canadian Journal of Civil Engineering, Vol. 8(1), 63-70, 1981.

Taylor, D.A., 1984, "Snow Loads on Two-Level Flat Roofs," Proc. of the 41st Annual Meeting of the Eastern Snow Conference, June 7-8, 1984, Washington, D.C., 1984.

Taylor, D.A., 1987, "Snow Loads on Flat Roofs in Canada," Proc. of the Western Snow Conference, April 1987, Vancouver, B.C.

Tobiasson, W. and R. Redfield, 1973, "Alaskan Snow Loads," 24th Alaskan Science Conference, University of Alaska, August 1973, U.S. Army Cold Regions and Engineering Laboratory, Hanover, N.H.

Table 1

Coefficients of Variation of Simulated Annual and Lifetime Extreme Snow Loads on Exposed Flat Roofs

Station	Annual Extremes		Lifetime Extremes (M=30)	
	V_s	V_{s_0}	$(V_s)_M$	$(V_{s_0})_M$
Halifax	0.65	0.55	0.24	0.21
Ottawa, Ontario	0.54	0.34	0.22	0.18
Quebec City, Que.	0.51	0.30	0.21	0.16
Winnipeg, Man.	0.58	0.31	0.23	0.17

Table 2

Statistical Properties of $\hat{\eta}$ The Ratio of Annual Maximum Roof-To-Ground Snow Loads For Flat Roofs

DATA SET	Average of $\hat{\eta}$	Coefficient of Variation of $\hat{\eta}$	$P(\hat{\eta} > 0.6)$	$P(\hat{\eta} > 0.8)$
1) Monte Carlo Simulation for Ottawa, Ontario (Isyumov, 1982)	0.47	0.48	0.23	0.08
2) Monte Carlo Simulation Combined Data for Ottawa, Winnipeg and Quebec City (Isyumov, 1982)	0.35	0.61	0.11	0.03
3) Full-Scale Data For Upper Roofs* (Taylor, 1987)	0.40	0.39	0.13	--
4) Full-Scale Data For Upper Roofs and Lower Roofs away from drifts* (Taylor, 1987)	0.39	0.43	0.13	0.02

*Combined Data from Roofs at Arvida, P.Q., Halifax, Ottawa, Saskatoon and Edmonton
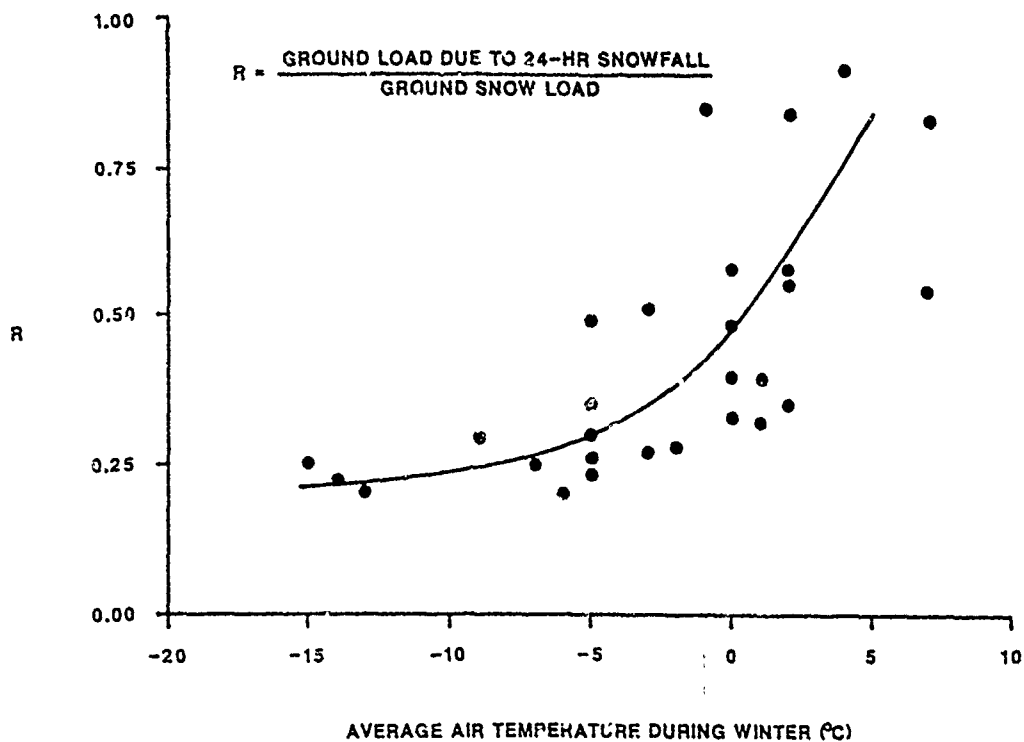
Figure 1 Contribution of extreme 30-year 24-hr snowfalls to the 30-year maximum ground snow load (28 Canadian stations)
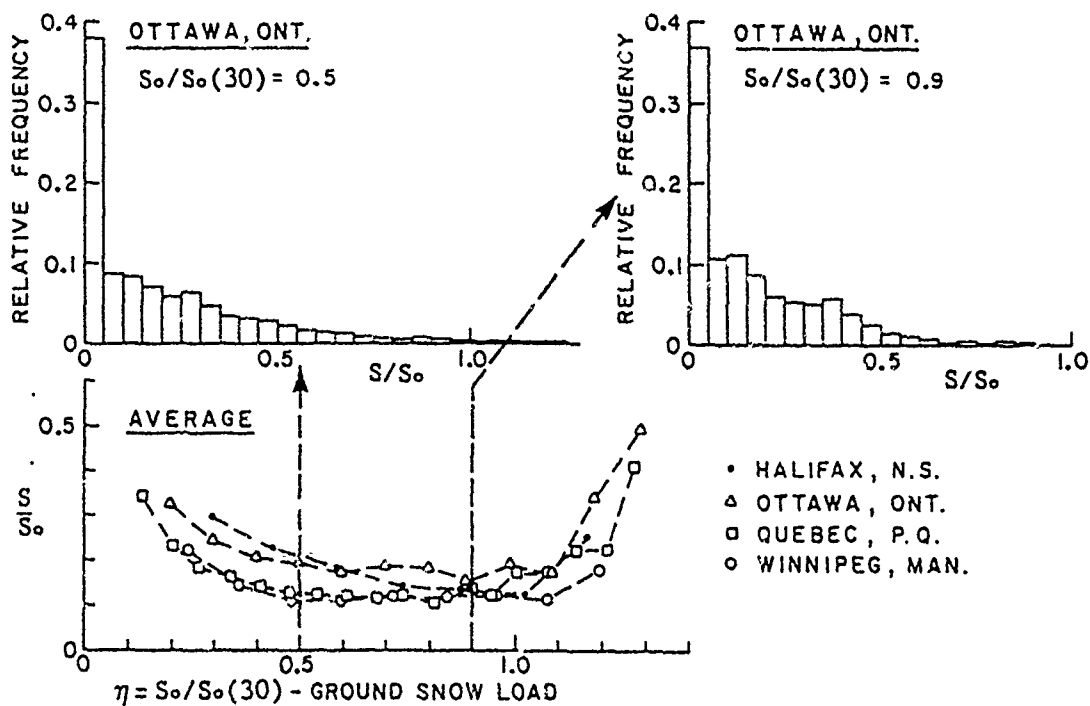
Figure 2 Ratio of daily roof snow load to the ground load; from Monte Carlo simulation for exposed flat roofs
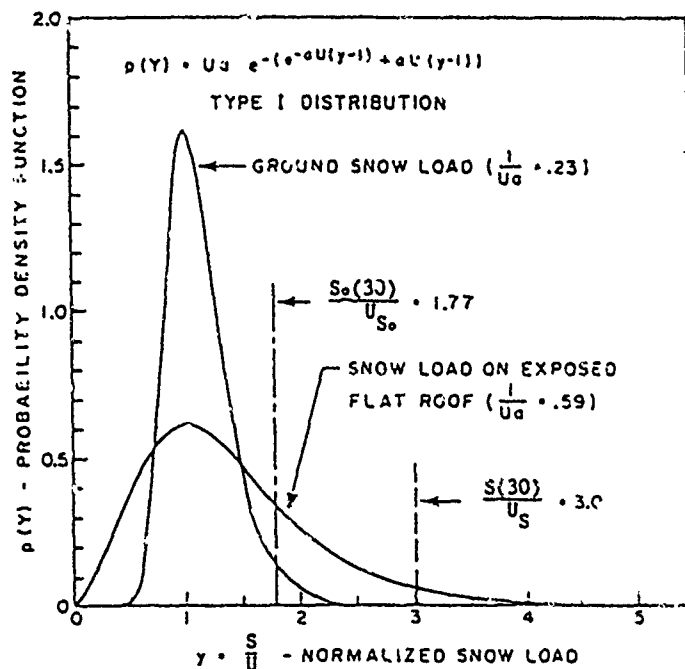
Figure 3　Typical variability of annual maximum ground and roof
snow loads (from Monte Carlo simulation)
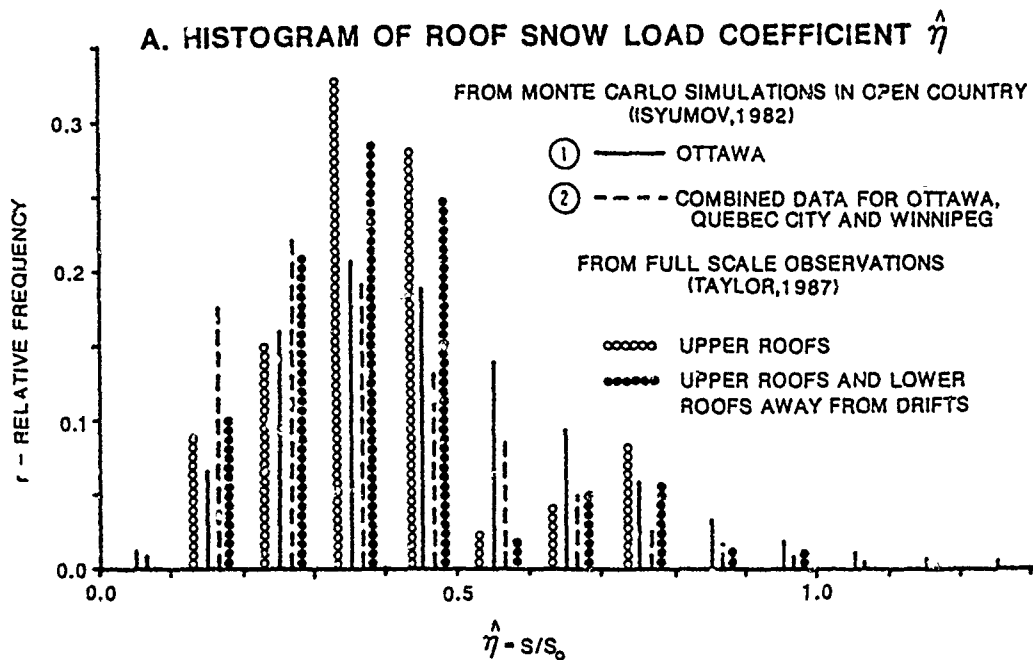
Figure 4a　Statistical properties of the ratio of annual maximum snow loads
on flat roofs to the annual maximum ground snow load from Monte
Carlo computer simulations and full-scale observations

B. PROBABILITY OF EXCEEDING $\hat{\eta}$

$$P(>\hat{\eta}) = 1 - e^{-e^{-\alpha(\hat{\eta}-u)}}$$

$u = 0.365$; $1/\alpha = 0.175$
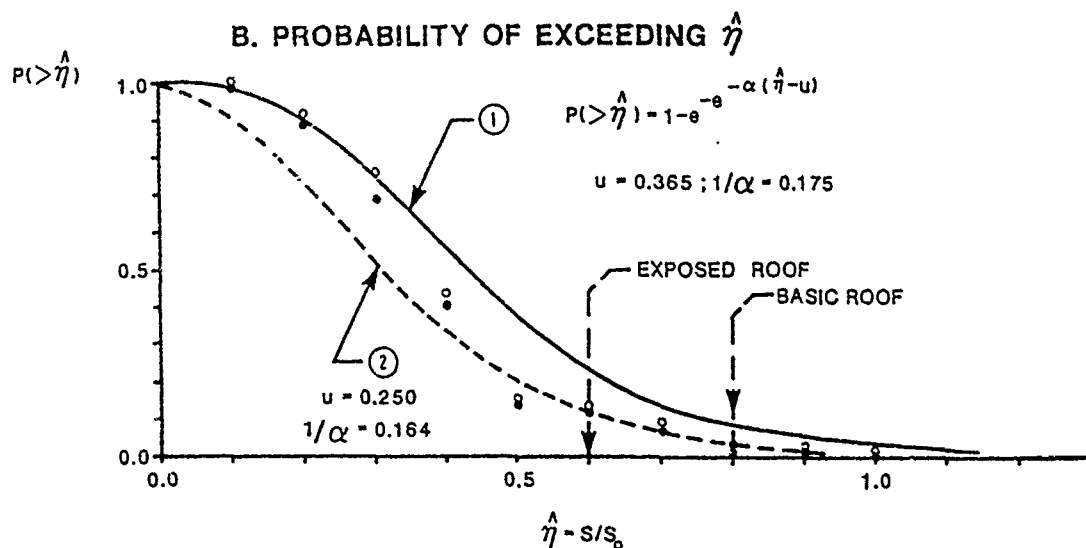
Figure 4b   Statistical properties of the ratio of annual maximum snow loads on flat roofs to the annual maximum ground snow load from Monte Carlo computer simulations and full-scale observations
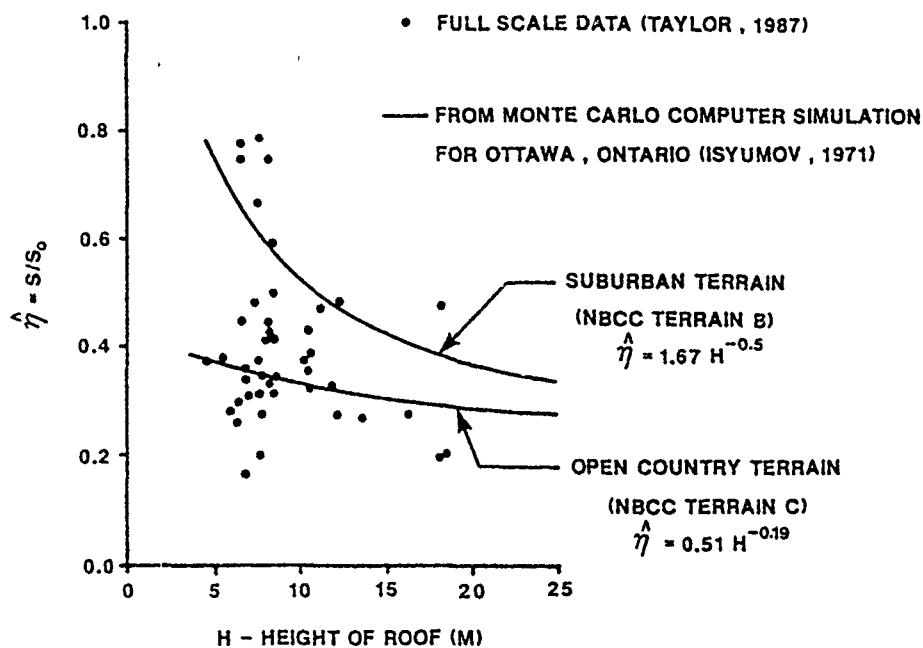
Figure 5   Dependence of the ratio of annual maximum roof-to-ground snow loads on building height for flat roofs

156
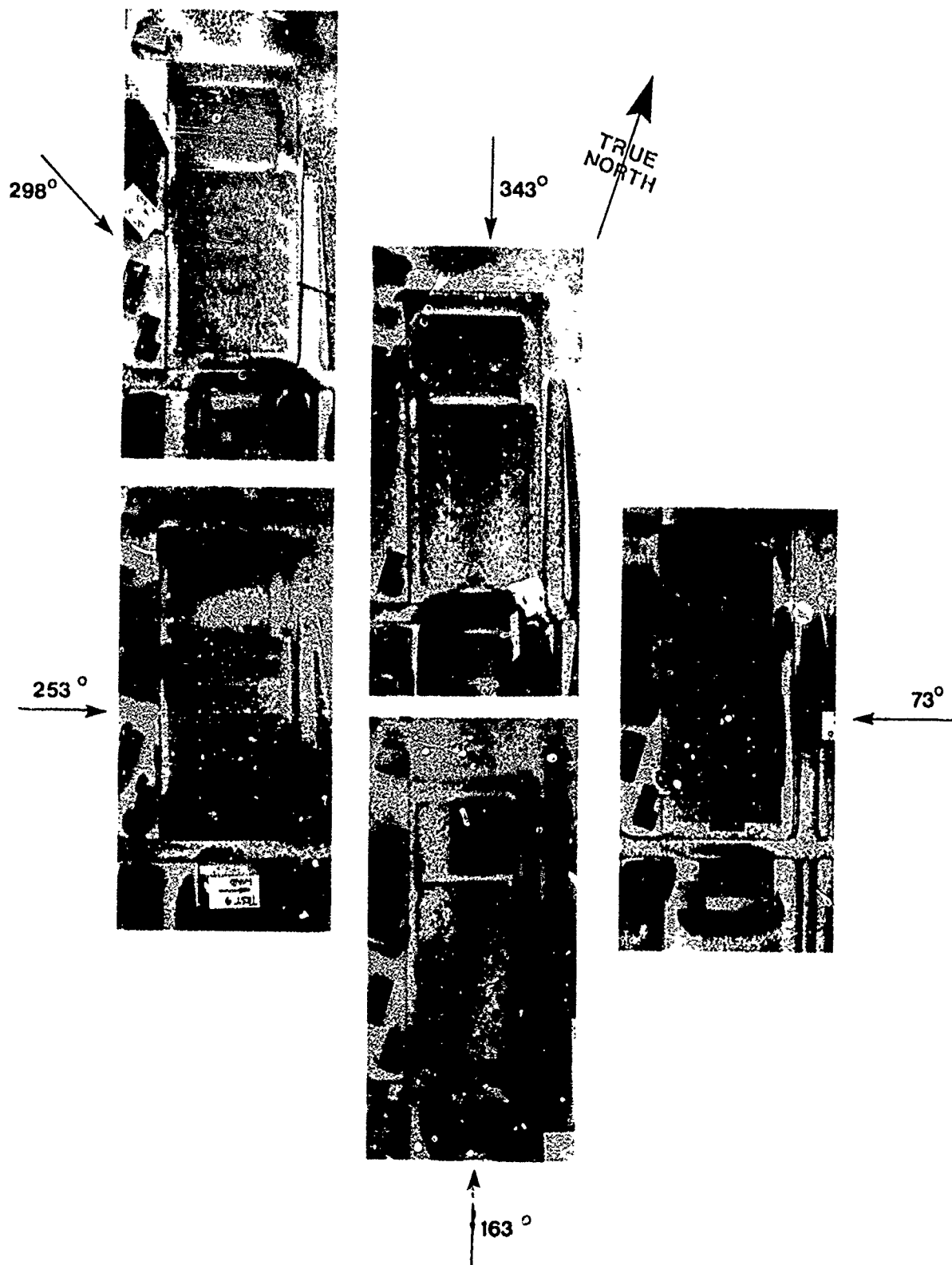
Figure 6   Snow accumulation during a particular snow storm as indicated by falling snow tests, $V_H \approx 2.4$ m/s

Wind Effects on Snow Loads

H. Mihashi[I], T. Takahashi[II] and M. Izumi[III]

ABSTRACT

Field observations of snow depth in several regions of Japan were carried
out. The relationship between ground and roof snow depth for flat
roofs is discussed from the viewpoint of the influence of wind speed.
The snow depth ratio, however, was remarkably influenced by the regional
meteorological conditions of the area. The wind effect becomes more
significant as the temperature becomes lower and/or as the snow density
decreases. Moreover, the wind effect is very sensitive to the local aero-
dynamic condition. After proposing an empirical formula to describe the
ground-to-roof snow depth ratio for flat roofs as a function of wind
speed, mechanisms of the wind effects are discussed.

INTRODUCTION

Since there are few data of snow loads on structural roofs, design snow
loads are calculated by multiplying the ground snow loads by ground-to-roof
conversion factor which reflects the influence of the shape of roof, exposure
condition and thermal characteristics. Of all the parameters which influence
snow loads on roofs, the effect of wind is probably most significant. The
mechanism of the wind effect, however, is still rather ambiguous and further
studies need to be done on quantitative values of the ground-to-roof conversion
factor.

Schriever (1978) reported that, as the wind speed increases, increasing
numbers of falling snowflakes are carried horizontally past exposed roof areas to
those of lower wind speed where the snowflakes can accumulate in drifts. At wind
speeds greater than about 20 km/h, particles are also picked up from the existing
snow cover and carried along the flow.

Taylor (1979) described qualitatively the influence of wind on snow
accumulation on roofs by classifying the range of wind speed into four levels.
While snowfalling during very light winds will tend to be distributed uniformly
on roofs, slightly higher winds will affect the deposition of falling snow and
lead moderately to low drifts. Winds above the saltation threshold may result
in considerable redistribution of snow on the roof and in the accumulation of
falling snow, forming large drifts. Very high winds often blow snow off roofs,
leaving them almost bare. The importance of the wind duration was also
indicated.

O'Rourke (1982) analyzed field observation data on ground and roof snow
loads for 199 structures. He found that the conversion factor was most strongly
influenced by the exposure of the structure. He also pointed out that the
pattern of seasonal snowfall had an effect on the conversion factor for uniform
loads. In a location of a few snowfalls where both the maximum ground load and

I. Associate Professor, Dept. of Architecture, Tohoku Univ., Sendai, Japan.
II. Graduate Student, Dept. of Architecture, Tohoku Univ., Sendai, Japan.
III. Professor, Dept. of Architecture, Tohoku Univ., Sendai, Japan.

the maximum roof load tend to occur immediately after the largest snowfall, the conversion factor would be relatively close to one. On the other hand, the conversion factor would be less than one in a location where the maximum roof load is due to the accumulation throughout the winter and modified by wind, thermal effects acting over time. Concerning the snow loads on multilevel roofs, O'Rourke (1986) obtained an empirical formula where drift surcharge height was described as a function of the length of an upper-level roof. It indicated that the major portion of wind effects was caused by saltation.

Abe and Nakamura (1984) observed the daily new snow cover on roofs comparing the ground everyday during 1980 to 1983. They also measured the wind speed and the temperature and the following conclusions were obtained. The snow depth on the roof is almost the same as that on the ground when the wind speed is less than 1.0 m/s. On the other hand, the snow depth ratio decreases as the wind speed increases, especially when the temperature is lower than zero. Even though the temperature is higher than zero, the ratio also decreases when the wind speed is very high.

Tomabechi (1985) carried out wind tunnel tests using activated clay particles and various shapes of model roofs to study the wind effects on the conversion factor. He found that stronger winds reduced snow loads on flat roofs but they had an inverse influence on drift snow loads accumulated on sloped roofs.

Otstavnov (1987) showed an empirical formula of the basic conversion factor on the basis of field observation data for 30 years in USSR.

Building codes have also recognized the wind effects on roof snow loads. In American National Standard (1982), the wind effects are handled on two scales as the exposure factor. The snow loads are first reduced by basic exposure factors (0.7 or 0.6) regionally and the conditions of local exposure are handled by the exposure factor C_e. Drifts on lower roofs are also considered by a formula. In the National Building Code of Canada (1985), the basic roof snow load factor (0.8) and the wind exposure factor are multiplied by the ground snow load. In Architectural Institute of Japan Recommendations for Building Design/ Snow Load, the wind effect on the shape factor is divided into three categories dependent on the regional climate. The conditions of local exposure are handled by the environmental factor.

The purpose of the present paper is to analyze some field observation data on flat roofs and to discuss the wind effects on snow loads.

MEASURING SNOW COVER ON FLAT ROOFS

During the winter of 1983-84, a field investigation to measure snow loads and the conversion factor on flat roofs was carried out in Japan. The location of measured sites and the meteorological data are shown in Fig. 1 and Table 1, respectively. Four different regions were investigated to study especially the influence of the meteorological conditions on the ground-to-roof conversion factor. Buildings in Aomori and Sawauchi were under construction without any heating. Measured data in Fukui are a part of those reported by Yamada, Maeda and their co-workers (1987) who measured the snow loads in Fukui during 1982 to 1987. The temperature in Fukui was above zero degrees, although the maximum snow depth on the ground was 0.95 m. Fig. 2 shows plans of measured buildings, heights of the roofs and the accumulation process where the ratio of the snow depth on the roof to that on the ground is plotted once a week.

Table 1. Meteorological Data for Measured Field.

Site	Maximum Snow Depth on the Ground (m)	Mean Temperature (°C)			Mean Wind Speed (m/s)*		
		Jan.	Feb.	Mar.	Jan.	Feb.	Mar.
Aomori	1.65 (March 8)	-2.8	-3.5	-0.6	3.0	3.0	3.0
Sawauchi	2.91 (March 1)	-5.4	-6.0	-3.3	1.3	1.4	1.3
Nagai	1.46 (February 28)	-3.3	-3.6	-1.4	1.6	2.0	1.9
Nanyo	-	-4.5	-6.0	-2.4	1.6	2.0	1.9
Fukui	0.95 (February 10)	0.9	0.3	(2.3)	2.1	2.3	(2.1)

* Normalized to 10 meters above the ground

The maximum snow loads on the roof were mostly recorded during the 10th to 12th week.

The relation between the snow depth on the roof and that on the ground is shown in Fig. 3 for each point with the ratio. The ratio in Aomori was almost constant and about 0.8. The ratio in Sawauchi was changed but it was about 0.7 to 0.8 at the stage of the maximum snow load. In Shirataka and Nagai, the values were rather scattered because they are multilevel roofs. For the lower parts, about 0.8 in Nagai and about 0.9 in Shirataka were obtained. For the upper parts, however, those values were reduced to about 0.5 and 0.6, respectively. The values in Nanyo were scattered because of the local swirl due to the penthouse. The representative value on the roof was about 0.55 to 0.6. Values of the ratio in Fukui were higher than others and slightly larger than 1.0.

DISCUSSION

The difference of the roof-to-ground snow depth ratio site by site can be explained by the influence of wind and temperature as well as heat transmission from the inside of the buildings. In Fig. 4, the relation between the wind speed and the roof-to-ground snow depth ratio observed by Abe and Nakamura (1984) is shown. The roofs are almost flat and their heights are 9.7 m and 3.8 m, respectively. The mean value of the temperature during the observation periods was - 1.9°C. The wind speed was converted from the value of wind speed meter (5.5 m high above the ground) onto those on the roof levels by means of the 1/7 power law proposed by Williams (1975). Open circles in Fig. 4 are data obtained by means of a wind tunnel test by Tomabechi (1986) where activated clay particles were used as the model snow.

The following equation may be available as an empirical formula to represent the relation between the roof-to-ground snow depth ratio and the wind speed (Mihashi, 1986).
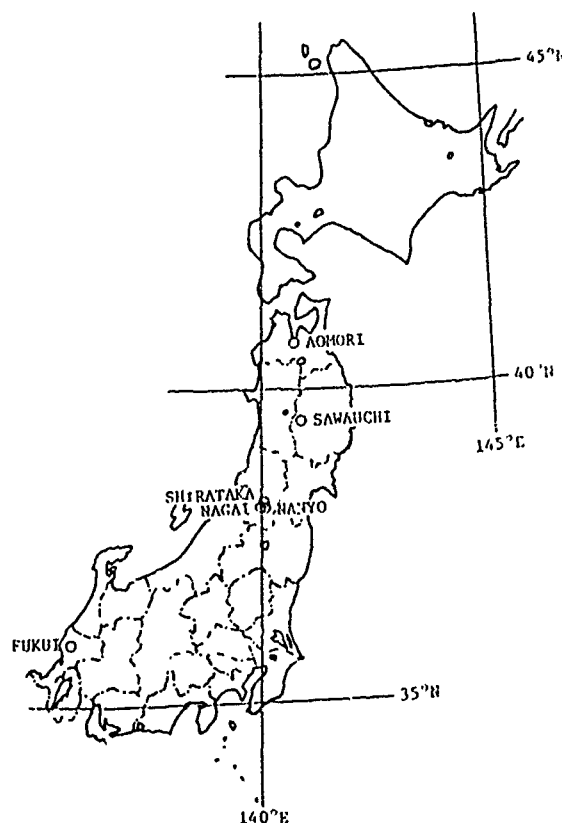
Fig. 1. Location of Measured Sites.
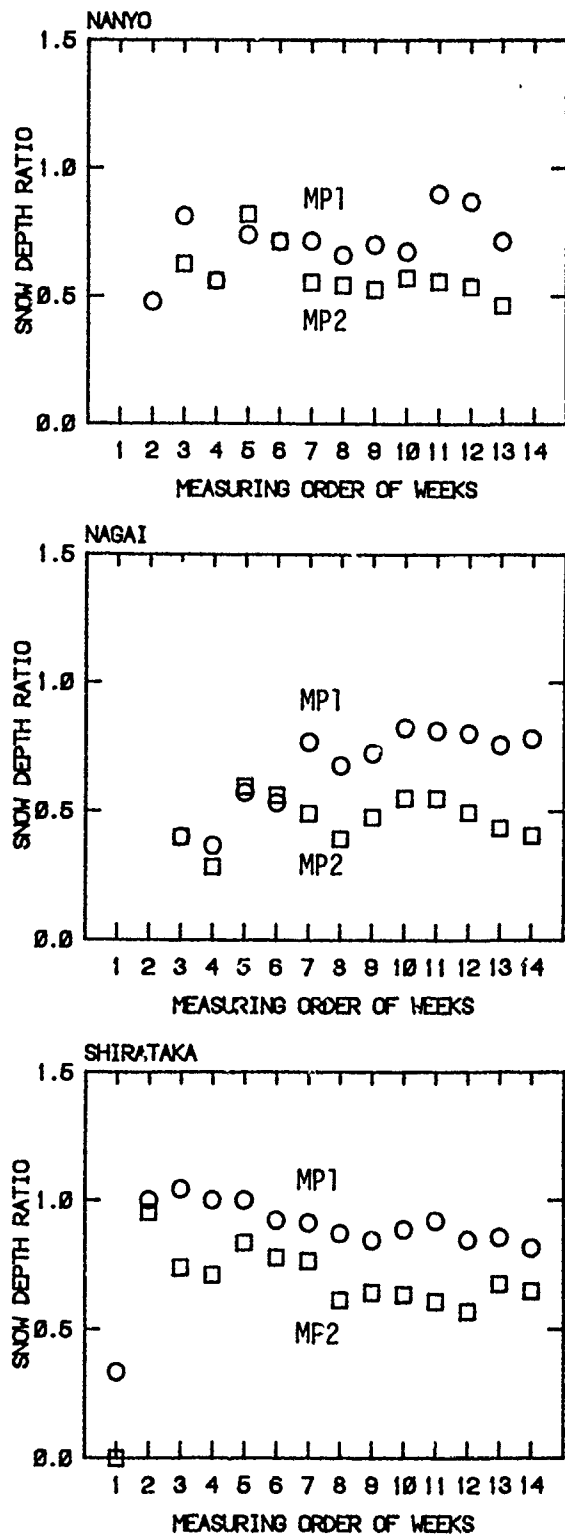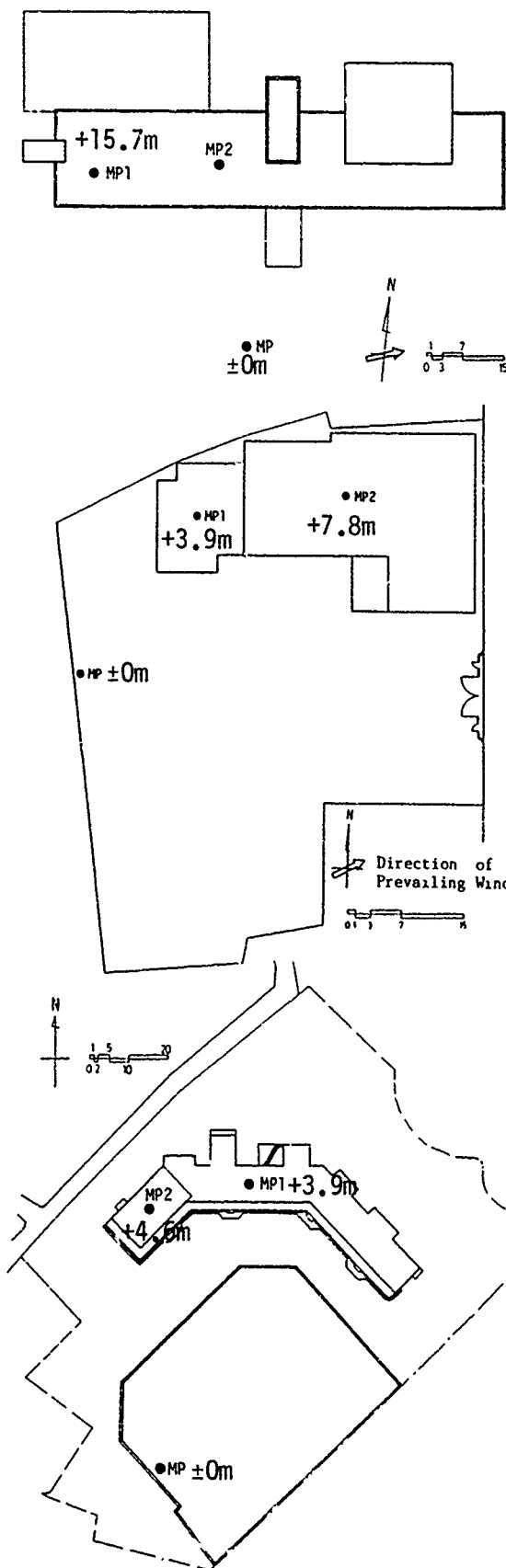
Fig. 2a. Field Observation of Snow Accumulation Process (I).

161
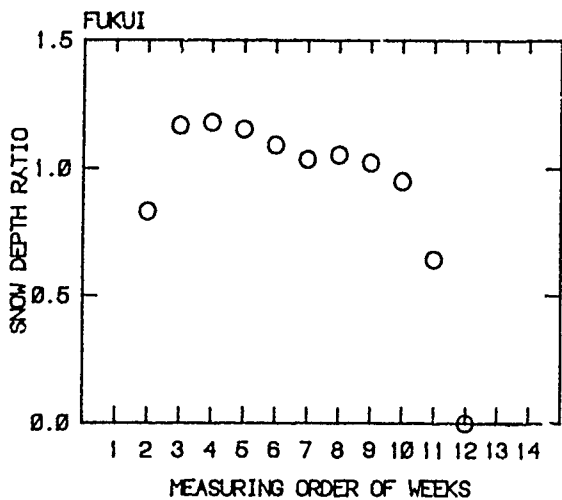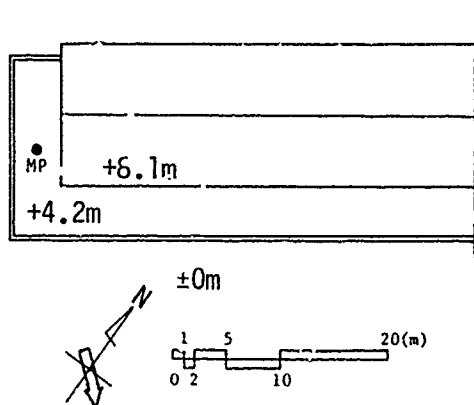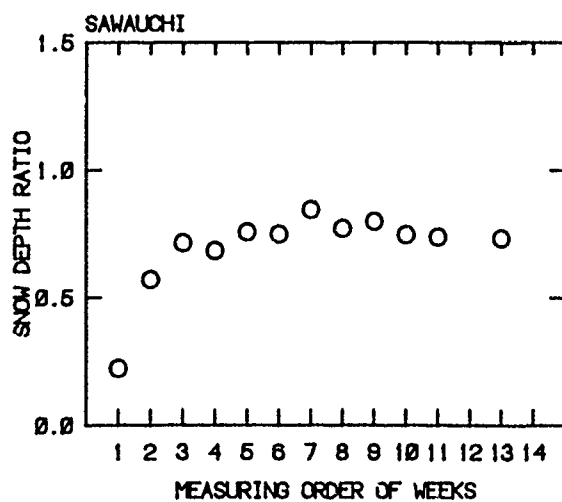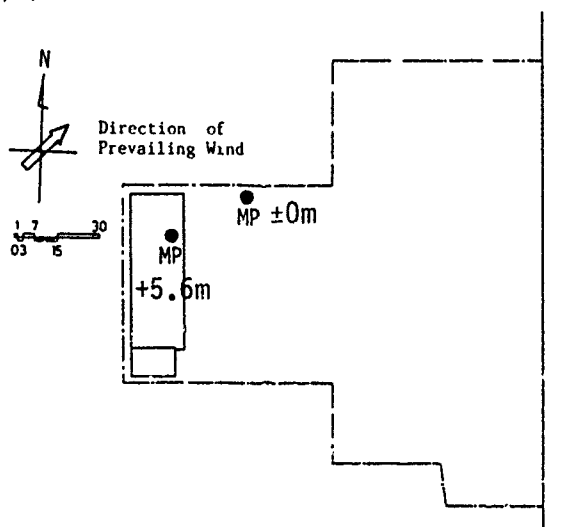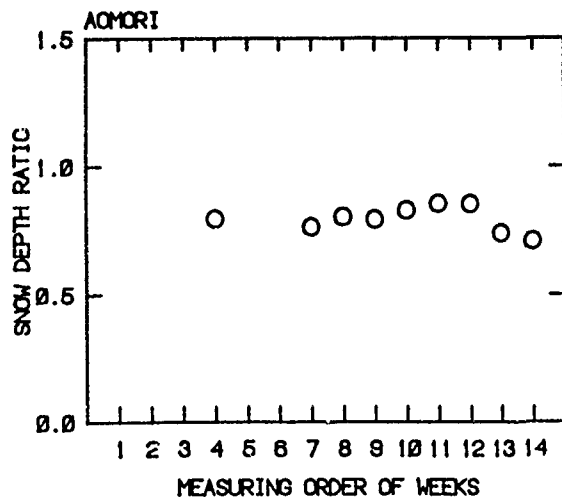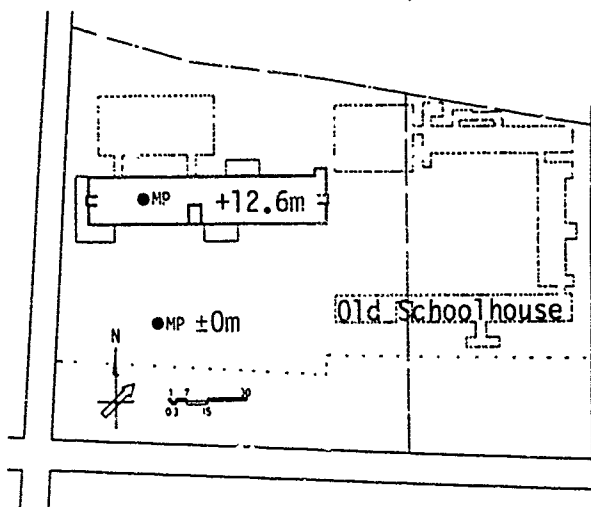
Fig. 2b. Field Observation of Snow Accumulation Process (II).
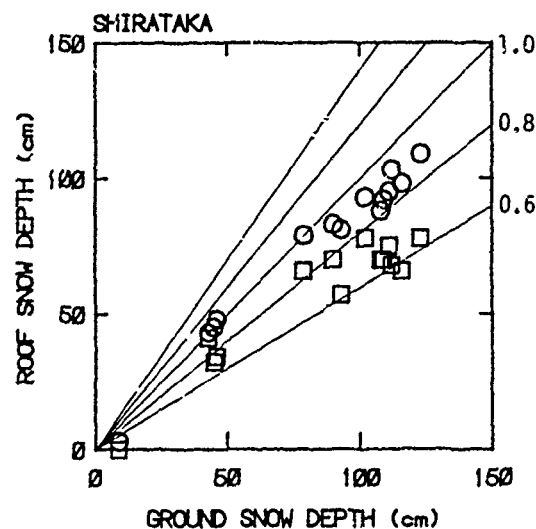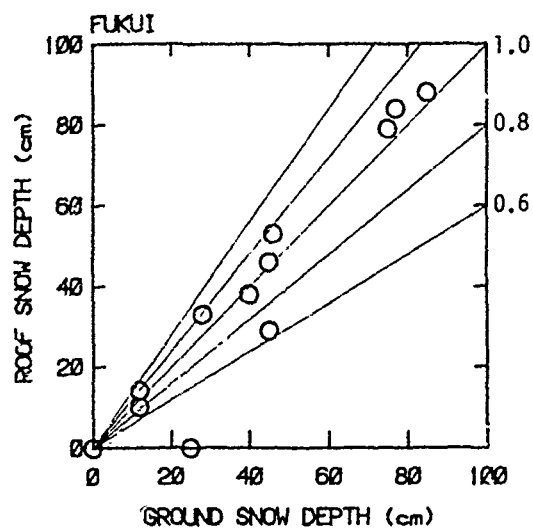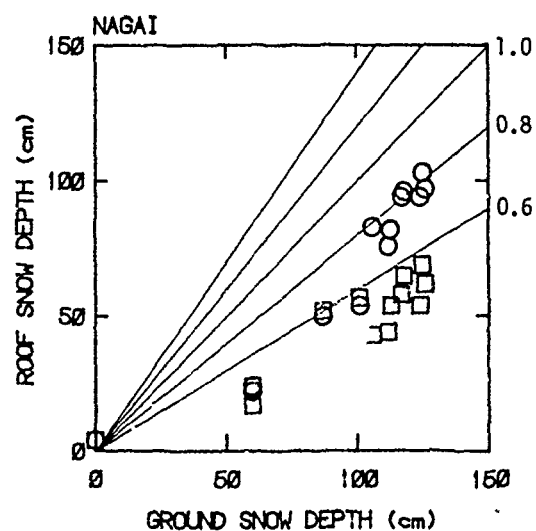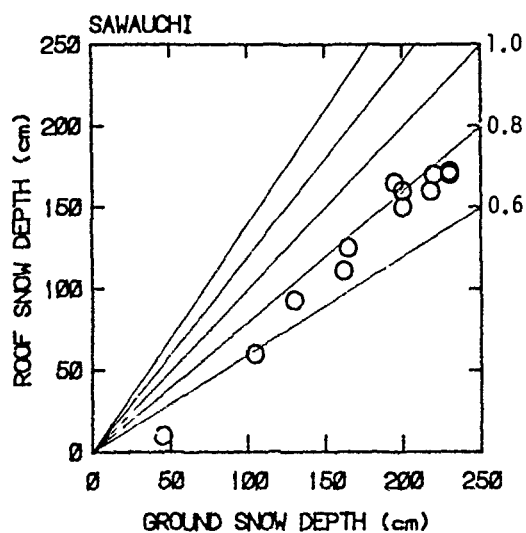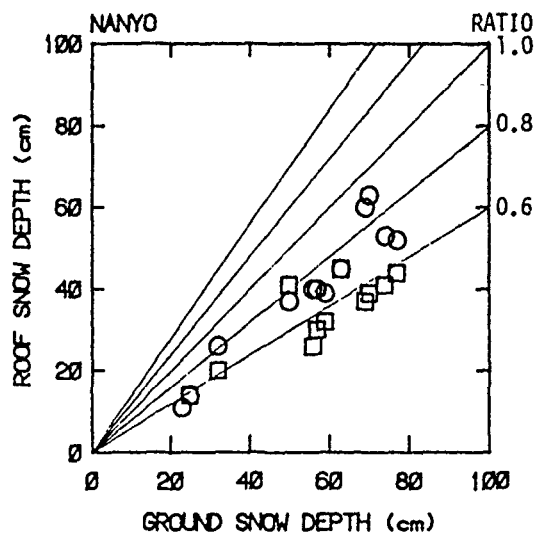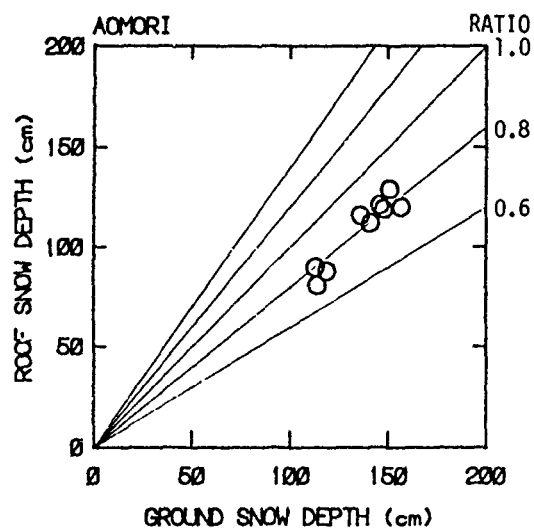
Fig. 3. Relationship between Roof Snow Depth and Ground Snow Depth.
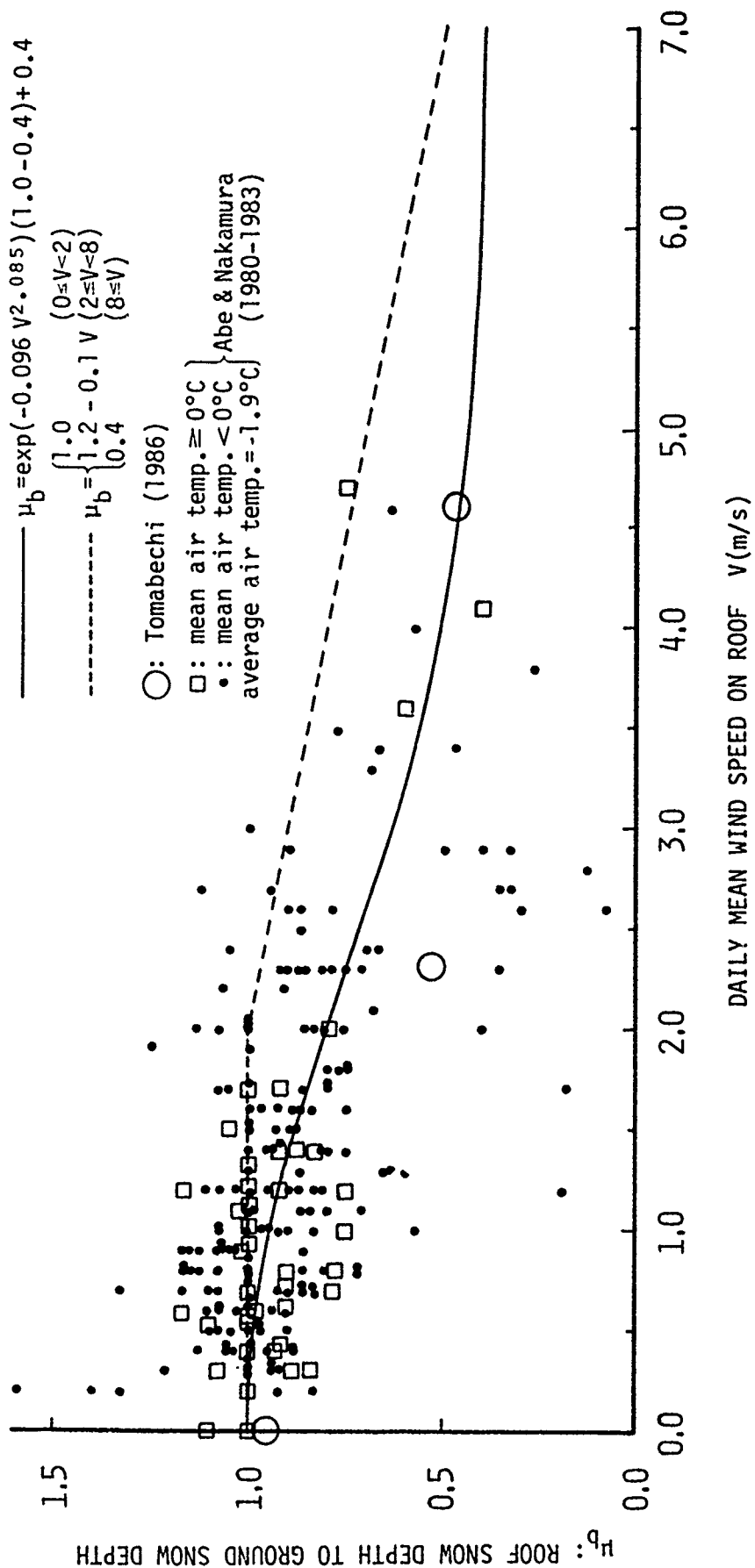
Fig. 4. Influence of Wind Speed on Roof-to-Ground Snow Depth Ratio.

$$\mu_b = \exp(- a1 \cdot V^{a2})(1 - a3) + a3 \tag{1}$$

where a1 = 0.096, a2 = 2.085 and a3 = 0.4 were obtained in this case.

Otstavnov (1987) obtained an empirical formula on the basis of observed data during 30 years in USSR as follows:

$$\mu_b = \begin{cases} 1.0 & (0 \leq V < 2) \\ 1.2 - 0.1\ V & (2 \leq V < 8) \\ 0.4 & (8 \leq V) \end{cases} \tag{2}$$

This formula is shown in Fig. 4 by the broken line. The wind speed in this case is the mean value during the winter.

Eq. 1 and Eq. 2 are situated at the mean value and the upper boundary, respectively. Field observation data shown in Fig. 2 are mostly located in the part between these two equations. Observed data in Nagai, Nanyo and Shirataka are about 75 % of predicted values by Eq. 1. This might be caused by the influence of heat transmission from the inside. The large value of Fukui should be explained by the temperature and the regenerative function of the ground.

The wind effects on snow loads are often called 'drift effects' and/or 'exposure effects' but the real mechanism has not been clarified yet. The following mechanisms are possible: 1) blowing of falling snow particles: The wind speed is increased nearby the surface of a roof on the basis of aerodynamics and the amount of snow accumulation on the roof is in inverse proportion to the wind speed if the density of snow is light enough. In the part where wind swirls, more snow is accumulated; 2) saltation and transportation of the accumulated snow particles: Drifting snow near the snow surface is sometimes observed even without any snow falling in a very cold and windy season.

The critical condition of snowdrifting may be described as a function of the temperature and the wind speed. An example of such a function is shown in Fig. 5 comparing with observed data in the field (Sato, 1962; Shiotani et al., 1966; Kobayashi et al., 1972), where symbols are showing that the snow-drift was observed on those points. The wind speed was measured 1 m high above the ground. It is quite obvious that the snowdrift occurs with the lower wind speed as the temperature is lower. If the temperature is higher than zero, the snow-drift doesn't occur even with a quite high wind speed.

Tomabechi (1986) studied the difference between the blowing effect on falling snow particles and the saltation and transportation effect on the accumulated snow particles by means of the wind tunnel test mentioned above. As shown in Fig. 6, the blowing effect on falling snow particles is much more significant than the saltation and transportation effect in his case.

Those mechanisms may mixedly work in the real situation and which is dominant may be dependent on the meteorological condition. Accordingly the explanation of the wind effects on snow loads by only one mechanism will lead to a certain error. Moreover, the regional wind effect should be separated from the local wind effect often described by "exposure effect."

CONCLUSIONS

The wind effects become more significant when the temperature is lower and the snow density is lighter. The relation between the wind speed and the ratio of roof snow depth to ground snow depth may be described by Eq. 1 if the roof is completely exposed and the shape is simply flat. Such reduction, however, should not be expected when the roof is surrounded by barriers such as parapets and trees. When the temperature is high during the snowing season, the wind effect should not be expected because the density of snow particle is much larger. Accordingly the local meteorological conditions should be considered when the wind effects are introduced into a design code.

ACKNOWLEDGMENT

Authors would like to thank Mr. S. Yamakawa of Aomori Municipal Office and Mr. T. Takahashi of Waga Agricultural Cooperative Association who could kindly collaborate to measure the snow depth in Aomori and Sawauchi, respectively.

REFERENCES

Abe, O. and T. Nakamura, "Wind Effect on the Daily New Snow Depth on Flat Roofs", Review of Research for Disaster Prevention, No. 32, The National Research Center for Disaster Prevention Science and Technology Agency, 73-87, 1984, (in Japanese with English Abstract).

American National Standards Institute, 1982, "American National Standard Minimum
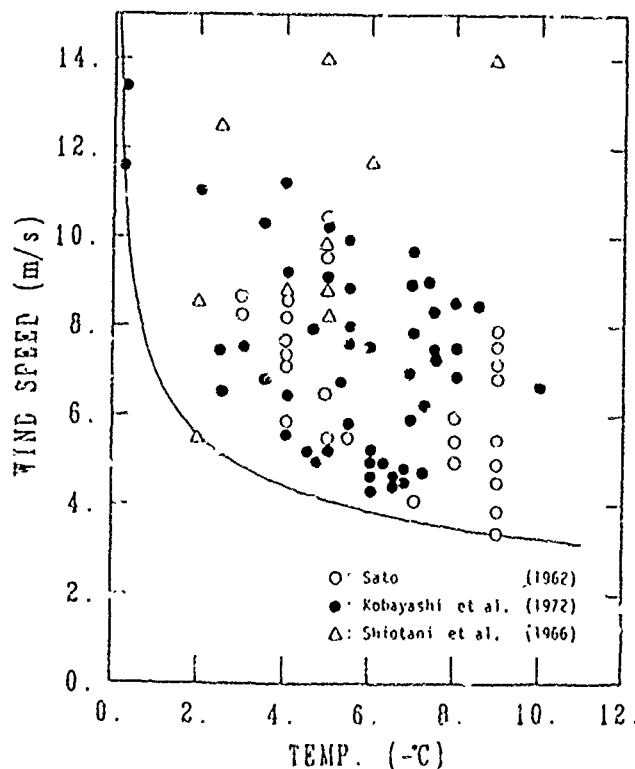
Fig. 5. Critical Condition of Snow Drift Occurrence.
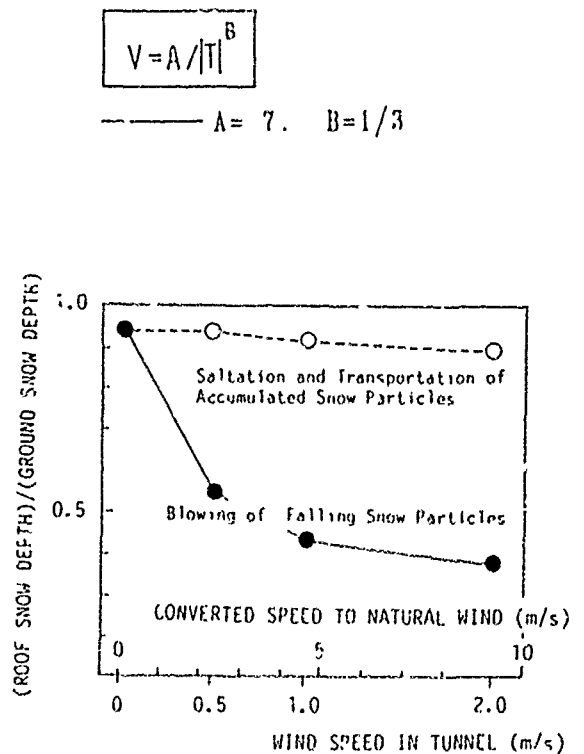
Fig. 6. Wind Tunnel Test Results on the Relation between Snow Depth Ratio and Wind Speed (Tomabechi, 1986).

Design Loads for Buildings and Other Structures", ANSI A58.1-1982, New York, N.Y.

Architectural Institute of Japan, 1986, "AIJ Recommendations for Building Design, Snow Load", Tokyo (in Japanese).

Izumi, M., H. Mihashi, T. Sasaki, and T. Takahashi, "Fundamental Study on Roof Snow Loads Estimation", Journal of Structural Engineering, Vol. 31B, Architectural Institute of Japan, 59-72, 1985 (in Japanese with English Abstract).

Kobayashi, D., "Studies of Snow Transport in Low-Level Drifting Snow", Contributions from the Institute of Low Temperature Science, Series A, No. 24, 1-58, 1972.

Mihashi, H. and Mihashi, K., "Remarks on Design Snow Load", Trans. of Tohoku Branch of Architectural Institute of Japan, No. 48, 195-198, 1986 (in Japanese).

National Research Council of Canada, 1985, "National Building Code of Canada", NRCC No. 23174, Ottawa.

O'Rourke, M.J., R. Redfield and P. von Bradsky, "Uniform Snow Loads on Structures", Journal of Structural Engineering, ASCE, Vol. 108, No. 12, 2781-2798, Dec. 1982.

O'Rourke, M., W. Tobiasson and E. Wood, "Proposed Code Provisions for Drifted Snow Loads", Journal of Structural Engineering, ASCE, Vol. 112, No. 9, 2080-2092, Sept. 1986.

Otstavnov, V.A., ISO/TC 98 Meeting in Sotchi (SC3/WG1: Snow Load), 1987.

Sato, S., "On the Criterion of the Railway Guard-patrol during a Snow Storm in Hokkaido", Journal of Japan Soc. Snow and Ice, Vol. 24, No. 2, 21-26, 1962 (in Japanese with English Abstract).

Schriever, W.R., "Estimating Snow Loads on Roofs", Canadian Building Digest, Div. of Building Research, National Research Council Canada, ISSN 0008-3097, CBD 193-1-4, Feb. 1978.

Shiotani, M. et al., Handbook of Snowproof Engineering, Morikita Shuppan, 1977 (in Japanese).

Taylor, D.A., "A Survey of Snow Loads on the Roofs of Arena-Type Buildings in Canada", Canadian Journal of Civil Engineering, Vol. 6, 85-96, 1979.

Tomabechi, T., "Geometry of Snow Accumulation on Roofs in Cold Winter Regions", Doctoral Thesis of Tohoku University, 1985 (in Japanese).

Williams, G.P., "Surface Heat Losses from Heated Pavements during Snow Melting Tests", Technical Paper, No. 427, Division of Building Research, NRC, Canada, 1-35, 1975.

Yamada, K. et al., "Snow Depth Observation on Flat Roofs in Hokuriku District", Trans. of Hokuriku Branch of Architectural Institute of Japan, No. 30, 25-28, June 1987 (in Japanese).

Snow-Melting and Snow Loads on Glass Roofs

Anker Nielsen[1]

ABSTRACT

The use of glazed roofs at high latitudes creates special problems. One of these is the snow load on the roofs. The snow load will be reduced because the snow will begin to melt if the accumulation is above a certain thickness. This thickness can be calculated dependent on the indoor temperature, outdoor temperature, thermal conductivity of the snow and the U-value of the glazing. In the figures are found calculations of different cases. The thickness of the snow and melting are given in a table. The theoretical results have been confirmed with pictures of a glass roof in Trondheim. A recommendation for dimensioning of a roof above a heated glazed space is given.

INTRODUCTION

Glass roofs in the Nordic countries require insight into a variety of problems. An important problem is winter conditions with snow. Normal roofs must be calculated from the expected snow loads given in the building regulations. Glass roofs above heated areas will have less snow load as the snow will melt or slide from the roof. In Trondheim, using half the snow load of a normal roof is allowed. Even with this reduction the snow load is an important factor in dimensioning the glass and bearing system. Because of this the Norwegian Building Research Institute (NBI) has made some calculations of the expected thickness of snow on glass roofs.

IMPORTANT PARAMETERS

In the following paragraphs is a short description of the parameters that influence the thickness of the snow-layer on a glass roof. The decisive factor is surface temperature on the outer glass pane. If the temperature is above 0°C then the snow will begin to melt from the underside and the snow will easily slide from the roof. In the following description it is assumed that the air temperature below the roof is above the freezing point.

Outdoor temperature

If the outdoor temperature is above the freezing point, then the snow will melt and disappear. Below the freezing point the snow-layer must reach a certain minimum thickness before the snow-layer begins to melt from below. This thickness will increase when the outdoor temperature goes down. Places with low winter temperatures can give the maximum snow load.

I. Senior Research Officer, Norwegian Building Research Institute, Trondheim, Norway

Indoor temperature

High indoor temperatures below the glass roof will ensure that the snow layer will be small when it starts to melt. Low indoor temperatures will give deeper snow layers. If the indoor temperature is below the freezing point then the melting will only start from above, dependent of the solar radiation and the outdoor temperature.

Snow-density and heat conductivity

The density of snow can change from 100 kg/m³ to 300 kg/m³. Newly fallen snow will typically have a density of 100 kg/m³. The density is important for the heat conductivity. At 100 kg/m³ the heat conductivity will be 0.05 W/m-K or about the same as mineral wool. Higher density of the snow can appear with temperatures around the freezing point with a mixture of snow and water. The higher density is also found in snow which has been laying a long time and therefore has been compressed. At 300 kg/m³ the heat conductivity is 0.23 W/m-K. Light snow demands a lower thickness to raise the temperature at the underside of the snow above the freezing point. In reality snowfall at temperatures below -5°C will always give low density snow.

Glass U-value

Glass with a high U-value is preferable, as the extra heat loss will melt the snow faster. But this is in contradiction with the wish to make the building energy efficient. Information on snow thickness in dependence of the U-value of the glass is important for the constructor.

Friction coefficient snow-glass

The friction coefficient between snow and glazing depends on the temperature. The lowest friction values are found at the freezing point and rise for lower temperatures. If the surface between snow and glass rises to the freezing point, then the friction will be reduced and the snow will slide.

Slope of roof

On a horizontal glass roof the snow can melt, but the water cannot disappear. Water leakage is most likely to occur, and an extra long-term load from the water can be expected. If the roof has a slope of more than 30° then the snow can slide from the roof if the friction is reduced and melted water can be drained away. For slopes less than 30° there is no information available to point out if the snow can slide.

Metal profiles

It is important to notice that the metal profiles mostly don't act as snow fences. It must be possible for the snow to glide above the horizontal profiles. The profiles must have a lower U-value than the glazing, or else the melting water can freeze at the profiles and, in the worst case, create water dams.

CALCULATION OF SURFACE TEMPERATURE

Theory

The parameters for calculation of the glass temperature are:

	Symbol	and unit	Example
Outdoor temperature	T_o	C	-10
Indoor temperature	T_i	C	20
Glass U-value	U	W/m²°C	3.0
External surface resistance	R_o	m²°C/W	0.04
Snow thickness	t	m	0.02
Snow heat conductivity	H	W/m-K	0.05
Melting heat	M	J/kg	3.3×10^5

Heat resistance from external surface of glass to indoor air

$$R_1 = 1/U - R_o \qquad\qquad 0.293 \text{ m}^2°C/W \quad \text{(for example)}$$

Heat resistance from outdoor air to external surface of glass:

$$R_2 = t/H + R_o \qquad\qquad 0.440 \text{ m}^2°C/W$$

Temperature of external surface of glass:

$$T_x = T_i(T_i - T_o) \cdot R_1/(R_1 + R_2) \qquad 8.0°C$$

The maximum rate of snow melting can be calculated from the expectation that all the heat loss can be used for snow melting:

$$S = (T_i - T_o)/(M \cdot R_1) \qquad 3.1 \times 10^{-4} \text{ kg/m}^2\text{s}$$

The surface temperature of the glazing in the example is so high that the snow will begin to melt. The friction between glass and snow will be decreased and the snow will slide.

Calculation method

The calculation is done by the computer-program SYMPHONY, which includes a spreadsheet, word processing, graphics, database and communications. It is easy to change parameters and make new calculations and drawings. In the following calculations the heat conductivity is taken to be 0.05 W/m-K.

Results for double glazing

Calculations have been done on double glazing with a U-value of 3.0 W/m² °C as this is expected to be the most used type. Calculations on single glazing have not been done as the snow loads will be less than for double glazing. Figure 1 gives the glass surface temperature with an indoor temperature of 15°C, as in all heated glazed spaces. There are 5 curves for different outdoor temperatures. In the worst case (-25°C) outdoor snow melting
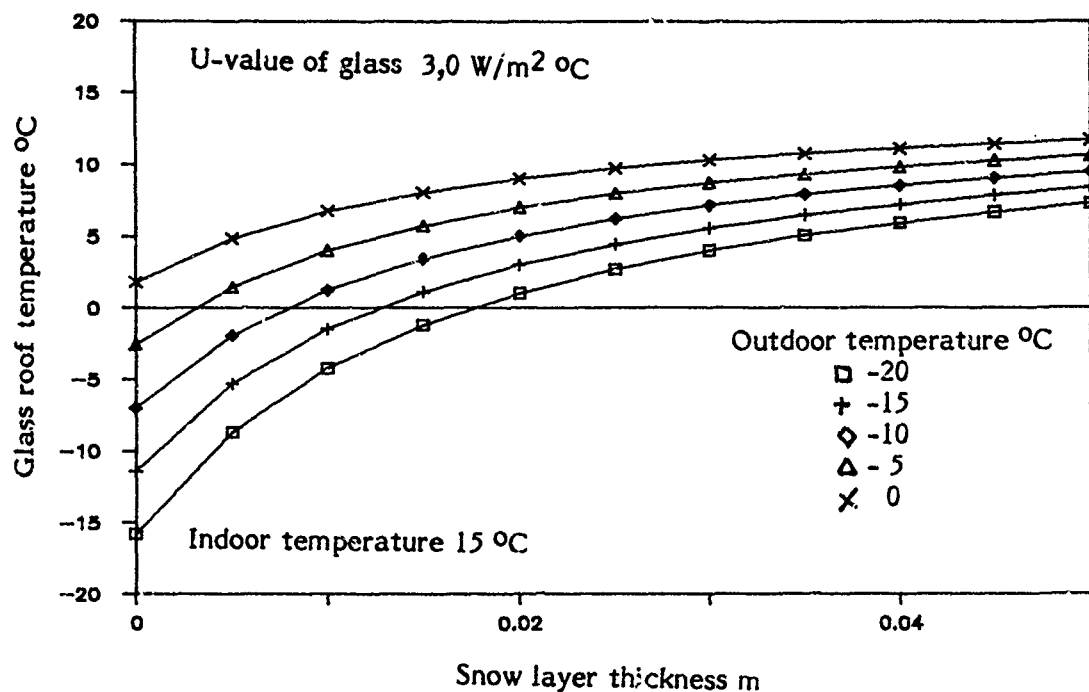
Figure 1. Effect of snow layer thickness and outdoor temperature on the temperature of the external surface of clear, double glazing with a 15°C indoor temperature.
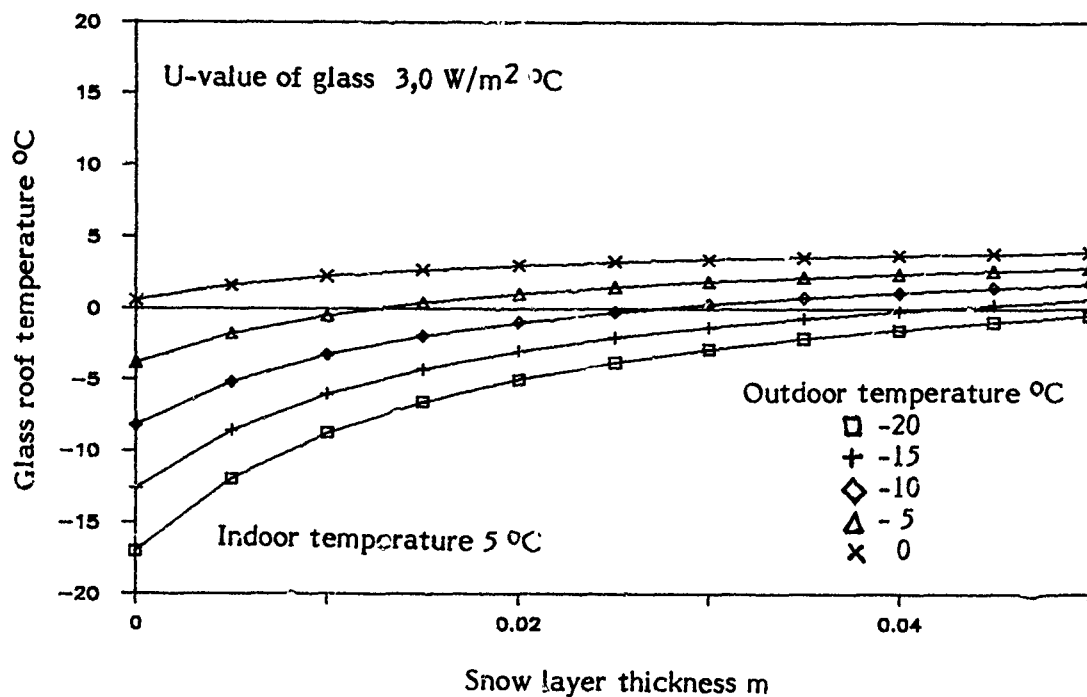
Figure 2. Effect of snow layer thickness and outdoor temperature on the temperature of the external surface of clear, double glazing with a 5°C indoor temperature.

171
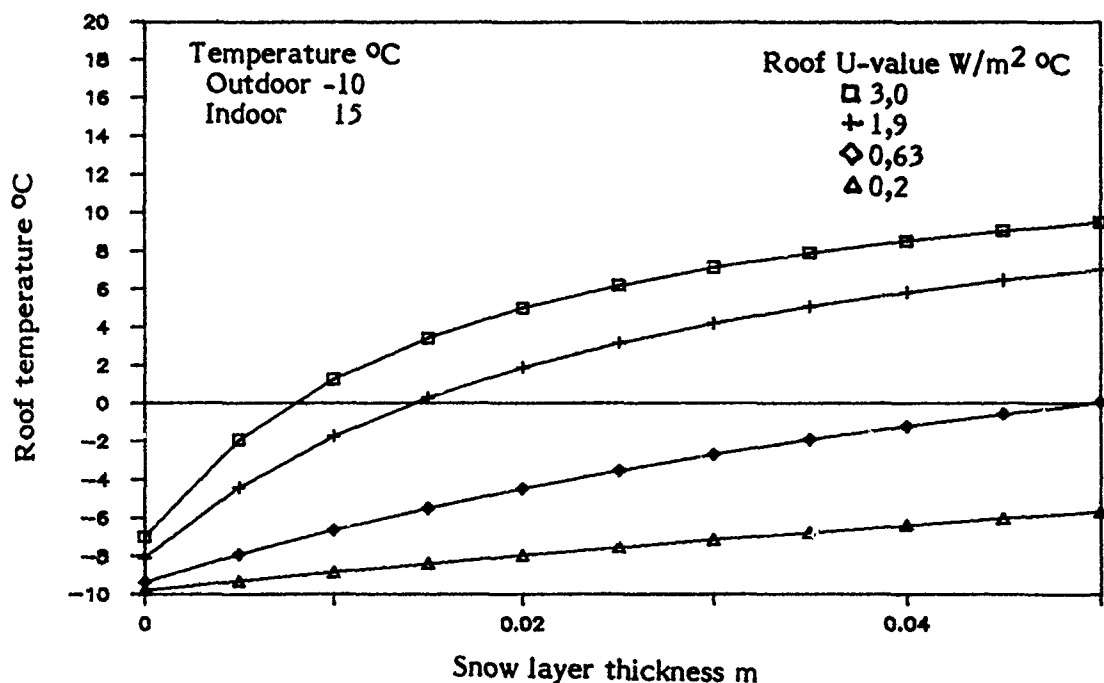
Figure 3. Effect of snow layer thickness and roof U-value on the temperature of the external surface of glass with a 15°C indoor temperature.

will begin with a thickness of more than 2 cm. The snow can either melt or slide from the roof. Figure 2 gives the glass surface temperature with an indoor temperature of 5°C, as in partial heated glazed spaces. It is seen that a low indoor temperature will increase the snow load.

Variation U-value of the roof

Figure 3 gives the surface temperature of the roof at an outdoor temperature of -10°C and indoor temperature of 15°C. The 4 curves are for different U-values of the roof:

3.0	clear double glazing
1.9	triple glazing or double with coating
0.63	roof with 6 cm of mineral wool
0.20	roof with 20 cm of mineral wool

A reduction of the U-value will result in a larger snow thickness and more load on the roof. These curves explain why it is not advisable to extend a glass roof using a well-insulated roof. The snow will melt on the glass part and the water will drain down on the well-insulated roof. Here the surface temperature will decrease and the water will freeze. An ice dam can result, which will produce water accumulation on the lower part of the glazing. Then leakage is highly probable.

Figure 4 shows the decrease in temperature when the indoor temperature is 5°C instead of 15°C.
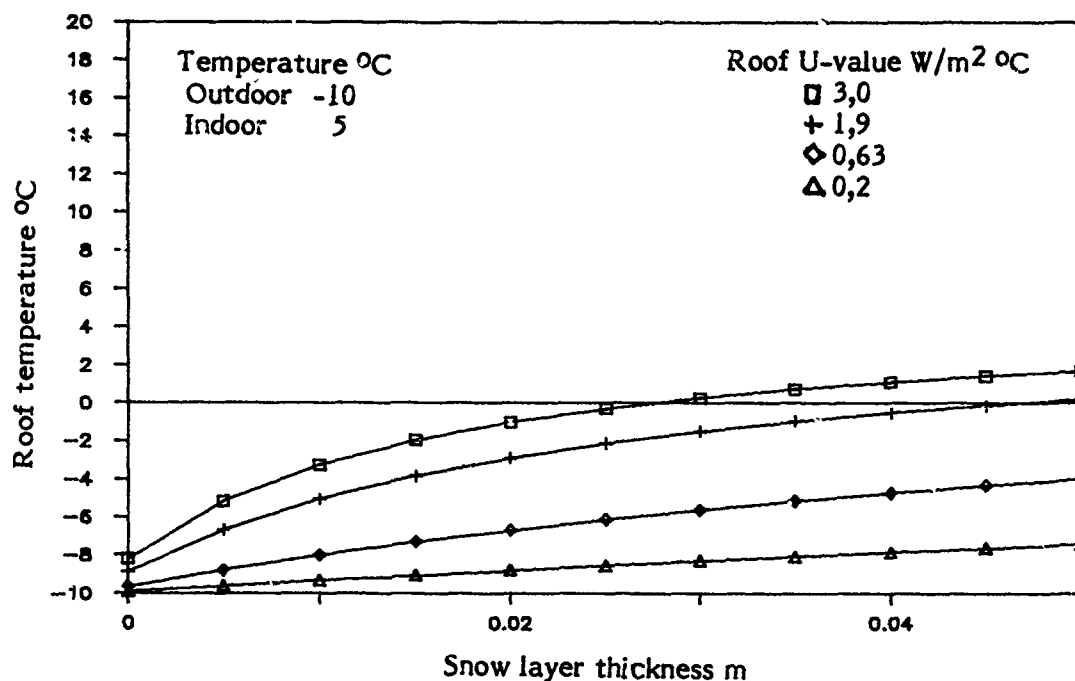
Figure 4. Effect of snow layer thickness and roof U-value on the
temperature of the external surface of glass with a 5°C indoor
temperature.

Snow loads

Table 1 is an example of the calculated snow layers and the weight of the
snow, when the snow starts to melt. It has been calculated for a glass U-
value of 1.9 $W/m^2°C$ and an outdoor temperature of -25°C. Values for snow
melting are also calculated.

Table 1. Conditions for a triple glazed roof at -25°C.

Indoor temperature (°C)	Snow thickness (m)	Snow load (kg/m^2)	Snow melting (kg/m^2-day)
20	0.03	2.8	10.7
15	0.04	3.9	8.0
10	0.06	5.9	5.3
5	0.12	12.0	2.7
2	0.30	30.2	1.1

The indoor temperature greatly influences snow loads and melting. The worst
case is a glazed space with low temperatures. To minimize such loads it is a
good idea to ensure that the indoor temperature in the winter doesn't fall
below 5°C.

PHOTOGRAPHY OF A GLASS ROOF

In the winter 1987/88 NBI selected five glass roofs for investigation of snow accumulations. At each roof was placed a camera that automatically took a photograph once every day at noon. For the period in March with most snow, the photographs show that the snow will slide from the roof and, if the weather is sunny, the glass will be clear of snow in a few days. In some cases the framing prevented the snow from sliding. After a week-long period with snow, the snow typically accumulates just below the glass roof. This will result in an extra snow load. If there is no room for the snow to slide, it will accumulate on the lower part of the glass roof.

The pictures are from a building complex at the Norwegian Technical University in Trondheim. The four glass roofs are between new and old buildings. The three gable roofs have a slope of 30°. The shed roof at the rear has a slope of 25°. Double glazing with coating is used. The U-value is 2.1 W/m²°C. The glazed areas are heated mostly from free heat from the surrounding buildings. The minimum indoor temperature in winter is 15°C. The width of the glazed areas is about 10 m. In the pictures are also seen buildings with normal roofs. A flat roof is seen in the foreground. Along the right is seen a gabled roof with a 45° slope. The photos were taken from a high building at the University, every day at noon from January 26 to April 27, 1988. Extra photos were taken if there was any special change in the snow pattern. Figures 5 through 9 are from March 9 to March 12. The outdoor temperature was about -3°C.

Most of the snow disappears fast from the glass roofs. In some cases snow accumulation is seen at the horizontal frame profiles, but only for a few hours. On the flat roof in the foreground, snow accumulates from the glass roof - compare Figures 5 and 9. The snow height below the glass roof is about

Figure 5. March 9 at 10:29. Snow on all roofs, but it is starting to slide at the upper part of many glass sections.

Figure 6. March 9 at 12:07. One and a half hours after the prior
photo, the snow has disappeared from most of the glass roofs. Snow is
only found on the lower part of each glass, because the horizontal
framing profiles offer resistance against sliding.

Figure 7. March 10 at 12:07. No snow on the gabled roofs but a little
is present on the shed roof.

1 m in Figure 9. On the shed roof there is accumulation of snow on the lower
third of the roof. This is caused by the low vertical height between the flat
roof and the glass roof. There is no place for the snow to slide to. Heat
cables must be used. The pictures show that reduction can be made in snow
loads on glass roofs but extra loads must be expected on areas where the
sliding snow accumulates, in this case on the flat roof. Visual observations
indicated that the greatest depth of snow was 50 cm on the shed roof, but it
was only 2-3 m² in area
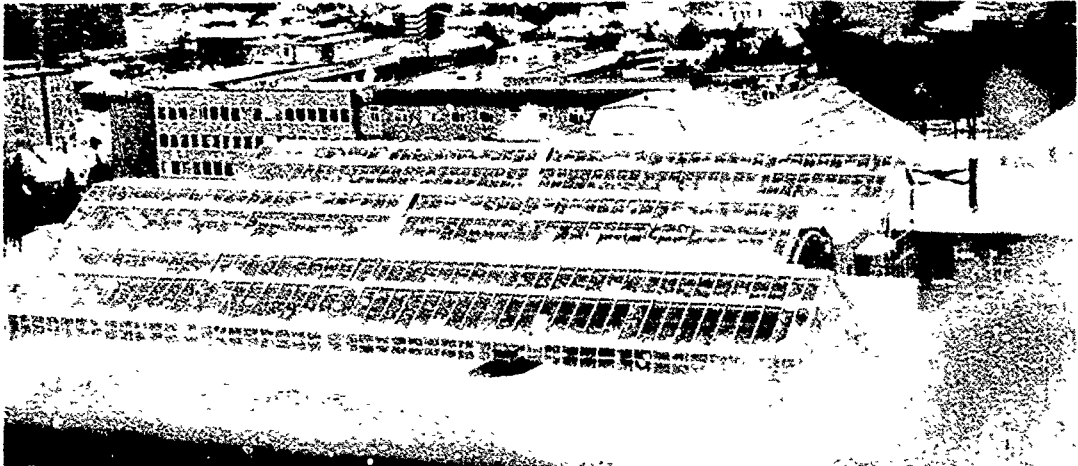
Figure 8. March 11 at 12:07. Some snow on the roofs but many areas are snow free. On the shed roof there is an accumulation on the lower part.

Figure 9. March 12 at 12:07. Less snow than the day before.

RECOMMENDATIONS

Snow load can be reduced on glass roofs above heated glazed spaces. The following recommendation is probably a very conservative estimate. If the minimum temperature in the glazed space is always above 15°C, then the load can be reduced by 50% when:

1. The slope of the roof is above 30°.
2. The U-value of the glazing is above 1.6 $W/m^2°C$.
3. The metal profiles and details are not better insulated than the glazing and they do not act as snow fences.

Experience from Trondheim shows that snow on glass roofs disappears rather fast and there is no tendency for snow to accumulate above heated

176

glazed spaces. In Norway we have not had direct failures from snow loads on glass roofs; most problems with glass roofs come from water leakage.

REFERENCES

C.Dreier, T.Gjelsvik, J.R.Herje, T.Isaksen, A.F.Nielsen:
Glassroofs (in Norwegian). Norwegian Building Research Institute Handbook 36,
1985.

Modeling Wind Effects on Drifting

Michael O'Rourke[I] and Ioannis Galanakis[II]

ABSTRACT

The evaluation of structural loads due to drifted snow on a multi-level roof is considered in this paper. Thirty five case histories of large drifts on multilevel roofs are used in developing an empirical relation to predicting drift size. The empirical relationship is the result of multiple regression analysis involving pertinent roof geometry parameters as well as environmental factors. The environmental factors considered are snow fall, wind speed and wind direction. The combination of wind and snow fall is an attempt to characterize blizzard intensity. The authors feel that the empirical relationship presented herein is an improvement over previous relationships in that wind in general and blizzard intensity in particular are included in the model.

INTRODUCTION

The American National Standard Institute A58.1 standard (ANSI, 1982) considers wind effects in establishing the surcharge load due to drifts at a change in roof elevation. A site is considered as being in one of five possible exposure categories ranging from a windy area with the roof exposed on all sides, to a densely forested area that experiences little wind. The corresponding exposure factors, C_e, range from 0.8 to 1.2. The drift surcharge load for a structure of normal importance is taken as twice the 50 year MRI ground load P_g divided by the exposure factor. Hence the drift surcharge is 2.5 P_g (2.0 $P_g/0.8$) for the most exposed sites and 1.67 P_g (2.0$P_g/1.2$) for the most sheltered sites.

Hence code provisions as well as intuition suggest that wind effects are important in determining roof snow loads. This is particularly true for drifted snow loads. In point of fact, wind is one of the three elements needed for drift formation. The others are a source of snow and a geometric irregularity where snow drifts can form.

Consider the multilevel roof shown in Figure 1, in which L_u is the length of the upper level roof, L_ℓ is the length of the lower level roof and H is the elevation difference between the upper and lower level roofs. For this structure, the change in roof elevation is the geometric irregularity which allows drift formation. For wind blowing from left to right, the roof elevation difference H corresponds to a backward facing step, while the elevation difference corresponds to a forward facing step for winds from right to left. As observed by Tabler (1975), triangular drifts tend to form at

---

backward facing steps as shown in Figure 1a. Quadrilateral drifts as shown in Figure 1b tend to form at forward facing steps. The quadrilateral shape is due in part to the vortex which, as observed by Templin and Schriever (1982), forms when wind encounters a forward facing step.

The source of snow for drifts at a backward facing is primarily snow on the upper level roof. Conversely, snow on the lower level roof is the primary source for drifts at forward facing steps.
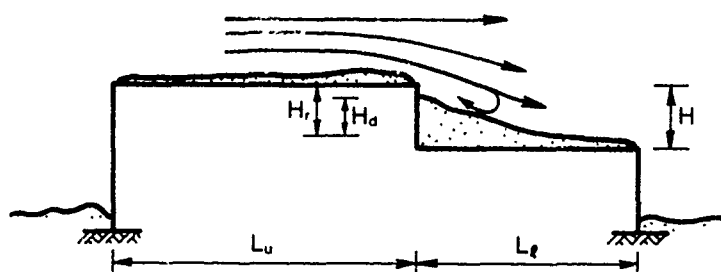
a) Triangular Drift at Backward Facing Step
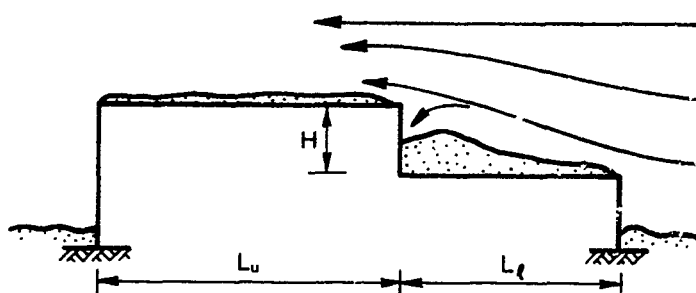
b) Quadrilateral Drift at Forward Facing Step

Figure 1   Drifts at Roof Elevation Changes

O'Rourke and El Hmadi (1987) analyzed a data base containing over 300 case histories obtained from field surveys, failure investigation and insurance company files. The data base contained both triangular drifts and quadrilateral drifts. For this data base, the triangular drifts were larger and about four times more common than quadrilateral drifts. As a first approximation, the triangular drifts were about twice as large as the quadrilateral drifts for similar snow source areas (that is, the length and width of the upper level roof at a backward facing step being about equal to the length and width of the lower level roof at a forward facing step). Hence a backward facing step (triangular drifts) appears to be a more effective drift formation geometry than a forward facing step (quadrilateral drifts).

As outlined above, snow already on the roof is a primary snow source for drifts. However not all the roof snow is susceptible to drifts. Informal observations indicate that a crust typically forms on the top of the snow a few days to a week after deposition. Hence "old snow" which fell during calm

179

conditions would not be susceptible to drifting if a sufficiently long period of time elapsed between deposition and the onset of strong winds.

Drifting requires the wind-induced movement of snow. This wind-induced movement takes two forms. One consists of snow flakes suspended in the wind stream, the other is saltation (Radok 1977). Saltation refers to individual snow particles bouncing along the snow surface, dislodging other particles in the process. In order for saltation to begin, the wind velocity must be larger than a threshold velocity (Radok 1977, Schmidt 1981) which is mainly a function of the cohesion of the snow surface.

In this paper, an empirical relationship for drifts at backward facing steps will be developed from a statistical analysis of drifts. In the next section a case history of drifts on a structure located near Boston Massachusetts will be presented to illustrate the drift formation process. In subsequent sections, multiple regression analysis of 35 drift load case histories is used to establish an empirical relationship for drift size. The influenced geometric and environmental factors are identified and discussed. The empirical relationship differs from previous efforts in that a parameter characterizing blizzard intensity is specifically induced. Finally, the accuracy of the empirical relationship is investigated by comparing actual drift size with values predicted by the empirical relations.

DRIFT FORMATION; A CASE HISTORY

In this section, a description of four drifts which formed on the roof of a Jordan Marsh facility in Squantum Massachusetts is presented. A more detailed description is available in a report by Maurice A. Reidy Engineers (1978). These drifts at Squantum, which is located about five miles south of Boston's Logan International Airport, were primarily due to a blizzard which struck the Boston area in early February 1978.
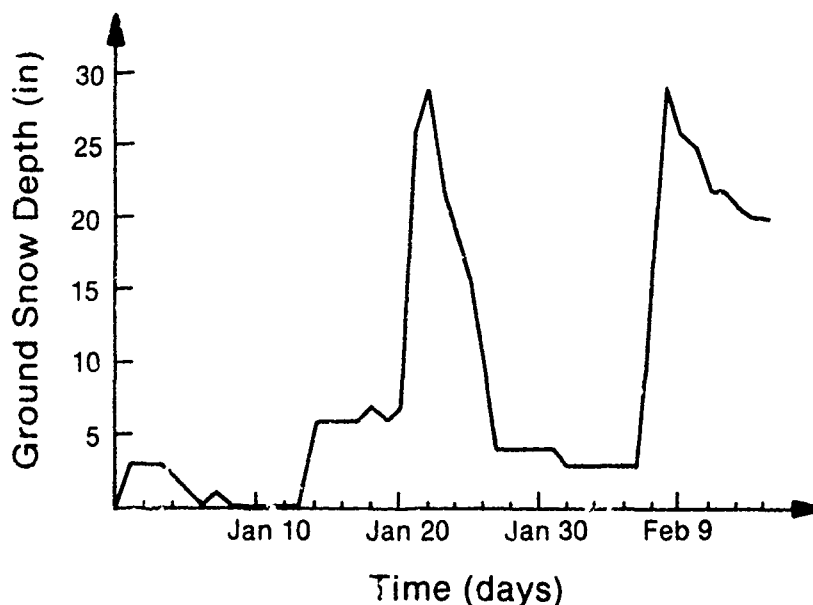
Figure 2 Ground Snow Depth at Boston, 1978

Pertinent weather information about the 1977-78 winter in Boston is presented in Figures 2 and 3. Figure 2 shows the depth of the ground snow at Logan Airport for January and the first two weeks of February. Notice that about 19 inches of snow fell on January 20th. The accompanying winds were out of the Northeast and North and ranged between 23 and 34 knots for the approximate 18 hour duration of this storm. The ground snow was reduced by above-freezing temperatures which lasted from the 24th thru the 26th, as well as rain which fell on the 25th and 26th.

A second blizzard started on the afternoon of the 6th of February and lasted until the early morning hours of the 8th. As shown in Figure 2, the total snowfall during this early February storm was about 27 inches. This storm was accompanied by high winds which originally blew out of the Northeast and then from the North. This is shown in Figure 3 which presents the fastest mile wind speed (in m.p.h.) and direction at Logan Airport for the first two weeks of February 1978. The wind speed at the height of the February storm was 44 knots and that the wind speed was above 20 knots for the full 1 1/2 day duration of the storm. In summary, the Boston area experienced two blizzards during the first two months of 1978. The stronger of the two in terms of total snowfall, wind speed and duration of strong winds, was the February blizzard.
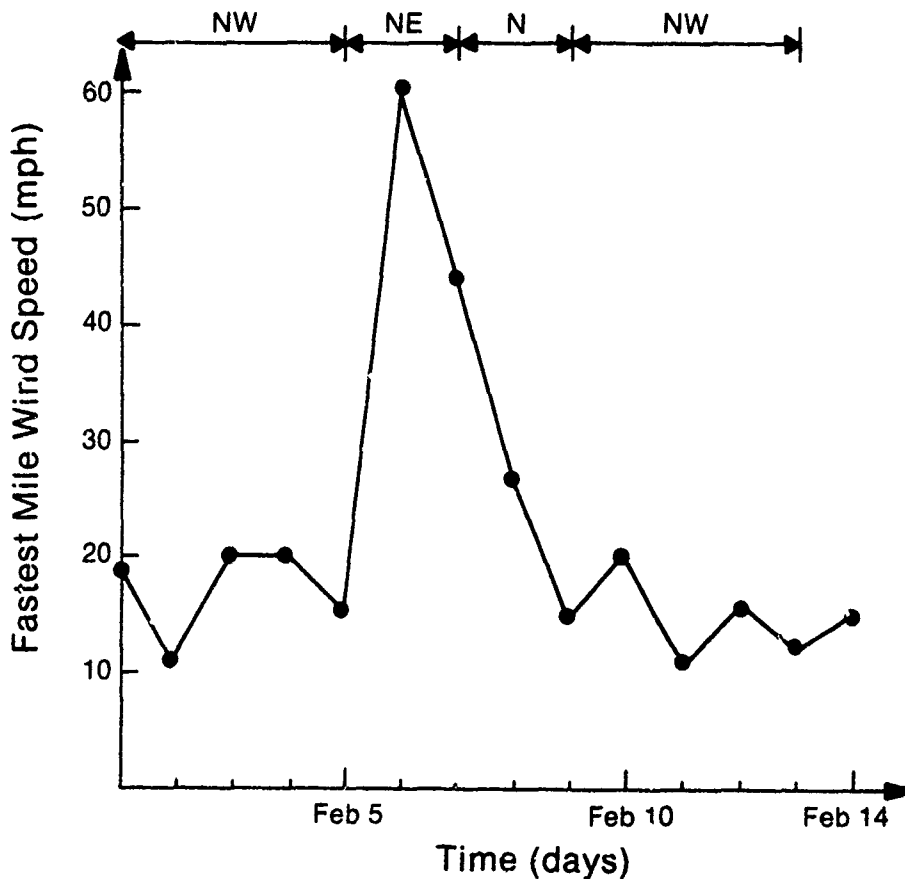
Figure 3 Fastest Mile Wind Speed and Direction at Boston, 1978

These storms generated substantial drifts on the roof of the Jordan Marsh facility in Squantum. Figure 4 is a plan view of the roof which shows the location of four drifts A, B, C and D as well as the elevation of various portions of the roof. Table 1 lists pertinent information about each drift. Included is the total drift height, the approximate depth of the old snow most likely due to the January 20th storm, the roof elevation differences H, the type of the drift (triangular or quadrilateral) and the elevation change geometry (forward or backward facing step) for winds from the North or Northeast.
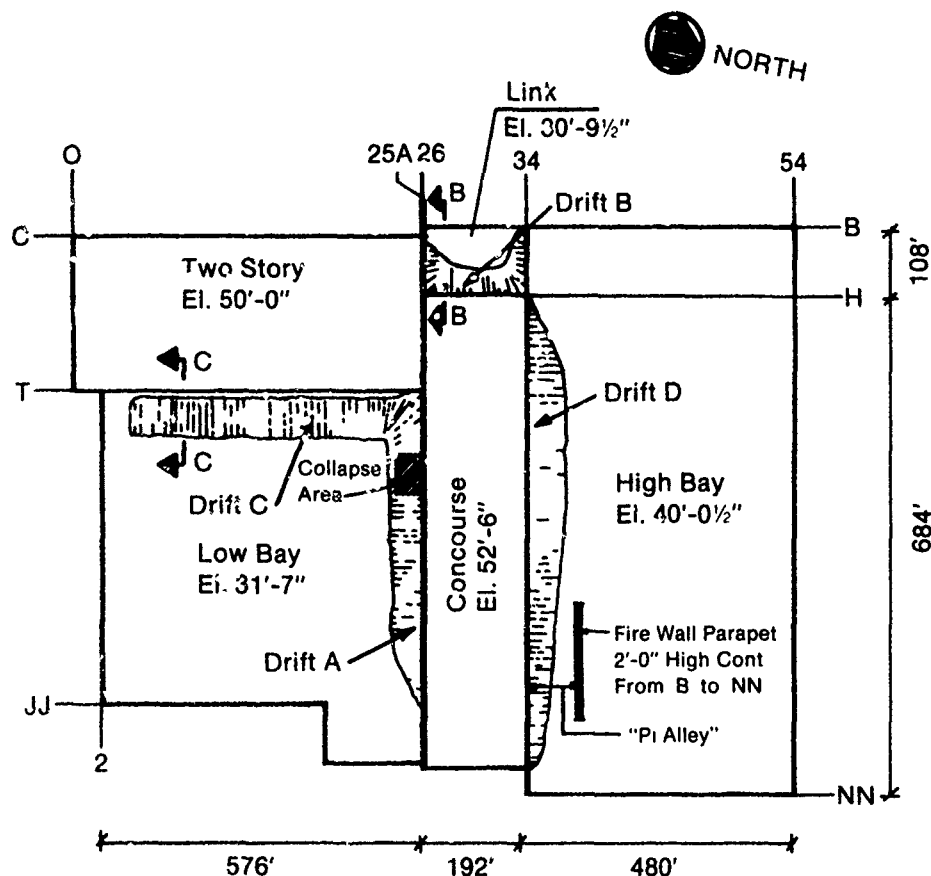
Figure 4   Plan View of Jordan Marsh Roof

The shape for Drift A, B and C are consistent with the pattern identified previously. That is for winds from the North or Northeast, the triangular Drifts A and B were observed at backward facing steps. Also a forward facing step resulted in quadrilateral Drift C. Drift D doesn't follow the pattern in that a triangular drift was observed at this forward facing step. There are two possible explanations for the shape of Drift D. It is possible that the two foot high fire wall parapet which, as shown in Figure 4, runs parallel to the drift, reduced the strength of the vortex which tends to form at forward facing steps. Another possibility is that Drift D began as a quadrilateral drift. However, as the quadrilateral drift became higher, the wind streamline no longer hit the verticle wall and the vortex was eliminated. The area between the wall and the quadrilateral drift then filled with snow resulting in a triangular shape.

182

Identification	Total Height	Old Snow Depth	Elevation Diff.	Type *	Geometry **
A	13'-7"	3'-6"	21'-0"	tri.	bfs
B	15'-9"	~2'-6"	21'-6"	tri.	bfs
C	6'-8"	~2'-3"	18'-0"	quad.	ffs
D	8'-8"	1'-4"	12'-6"	tri.	ffs

```
* tri  = triangular        ** bfs = backward facing step
  quad = quadrilateral        ffs = forward facing step
```

Table 1   Jordan Marsh Facility Drifts

As shown in Table 1, the depth of new snow at Drift B is about three times that for Drift C. However, the snow source (as measured by roof lengths) for Drift B is only about 50% larger than that for Drift C. This is further verification that backward facing steps appear to be a more effective drift formation geometry than forward facing steps.

EMPIRICAL RELATIONSHIP

In this section, an empirical relationship for the height of a triangular drift, typically generated of a backward facing step, will be presented. The empirical relationship was developed using multiple linear regression techniques on a data base consisting of 35 actual drift case histories. The 35 case histories were culled from a data base of over 200 case histories using the following criteria. Only triangular drifts at a verticle wall separating two nominally flat roofs with drift heights greater than 2 feet were considered. In addition if a number of drifts formed at a particular roof elevation change over the course of the same winter, only the largest drift was considered. Possible contributions from sliding or valley effects were eliminated by considering only nominally flat upper and lower level roofs.

As described in detail by Galanakis (1988), a number of sets of potential input parameters were considered. The empirical relation for the drift surcharge height in feet, H_d, which best fit the observed data was

$$H_d = 0.119(H_r)^{.411}(L_{diag})^{.298}(BI)^{.235} < H_r \qquad (1)$$

where H_r is the elevation difference between the upper level roof and the uniform snow in the lower level roof in feet, L_{diag} in the diagonal length of the upper level roof in feet and BI is a parameter having units of inch-knots-days which characterizes blizzard intensity.

Geometric Parameters

As shown in Eq. 1, the predicted drift surcharge height H_d is a function of the effective elevation difference H_r. This elevation difference influences drift height in a number of ways. Consider wind flow over a bluff body as shown in Figure 1a . As with an airplane wing, the velocity is higher

over the upper level roof than in the unperturbed flow well upstream of the structure. This higher velocity facilitates the scouring of snow off the upper level roof. When the flow encounters the backward facing step, the flow velocity decreases and recirculation zone forms as shown in Figure 1a. This allows some of the larger suspended snow particles to settle. At the same time, the saltating particles are bouncing over the edge of the upper roof. The percentage of saltating particles that contribute to drift formation is likely an increasing function of the effective elevation difference, For example, if H_r is small, many saltating particles would overshoot the potential drift area.

Hence all other things being equal, a larger elevation difference results in a larger recirculation zone which in turn leads to larger drifts. Similarly a large elevation difference results in a higher percentage of saltating particles falling in the potential drift area. These arguments apply to changes in roof elevation in the range of 5 to 25 ft. They would not be applicable to very larger changes in roof elevation. One rarely finds substantial snow drifts on a one-story lower roof adjacent to, say, a five-story upper roof.

Finally, the maximum drift size is the effective elevation difference. The potential drift area at the change in roof elevation will eventually fill if sufficient wind and a source of snow are avialable. These full drifts present a smooth streamlined transition from upper to lower level roof and the drift ceases growth.

As shown in Eq. 1, the predicted drift surcharge height is a function of the diagonal length, L_{diag}, of the upper level roof. As mentioned by O'Rourke and Wood (1986), L_{diag} characterize the source of snow for <u>variable</u> direction winds. Consider a multilevel roof with the upper level roof directly west of the lower level roof. If winds were only out of the West, the source of drift snow would be characterized by the length of the upper level roof L_u. However for winds out of the Northwest (drifts at southwest corner of the lower level roof) or Southwest (drift at Northwest corner of lower level roof), the upwind fetch is better characterized by the diagonal length L_{diag}.

Environmental Parameter

After a number of trials, the parameter chosen to characterize blizzard intensity was the maximum value over a three day period of the product of snow deposition and wind speed above a threshold. That is

$$BI = (h_i \cdot w_i)max \tag{2}$$

where h_i and w_i are described below. Figure 5a shows the depth of the ground snow in inches, d_i, for four winter days. The daily accumulation a_i is defined as the difference in daily ground snow depths, $d_i - d_{i-1}$, which is considered to always be positive or zero.

The amount of snow which <u>fell</u> during a three day period, h_i, then becomes

$$h_i = a_{i-2} + a_{i-1} + a_i \tag{3}$$

Figure 5b is the wind speed in knots <u>perpendicular</u> to the roof elevation change for a three day period. The cross-hatched area with units of knot-days is w_i the wind above a threshold for the three day period.

a) Snow Deposition

b) Wind
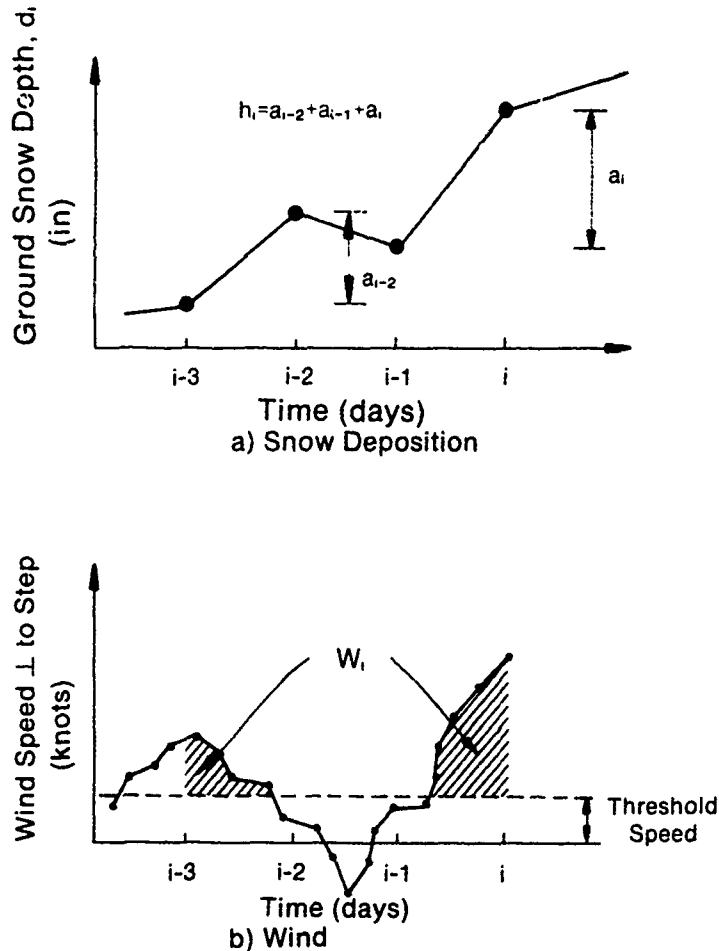
Figure 5   Parameter Characterizing Blizzard Intensity

Wind speeds at the case history structures were not available. We assumed that the wind speed and direction of the closest first order weather station (typically an airport) was identical to that at the structure. Knowing wind speed and direction at the closest airport, and the orientation of the upper level roof with respect to the lower level roof, the wind speed perpendicular to the roof elevation change was calculated from trigonometry.

As defined above, the blizzard intensity, BI, is a function of a threshold speed. This recognizes the fact that winds of a certain velocity are needed for saltation to occur. A threshold speed of 3.98 knots (2.0 m/sec) was found to yield the best match between predicted and observed drift heights. In addition blizzard intensity is evaluated for a three day period. As mentioned previously, old snow tends to form a crust which inhibits drifting. Also the duration of most blizzards is less than three days. As mentioned previously the February 1978 blizzard lasted about 36 hours in Boston. Even the Great Blizzard of '88 (March 1888) lasted no more than three days in New York City and Albany.

185

ACCURACY OF EMPIRICAL RELATION

The accuracy of the empirical relationship developed herein for the surcharge drift height at backward facing steps will be investigated in this section. This will be done by comparing the surcharge drift heights predicted by Eq. 1 with actual values from the 35 case histories discussed previously.
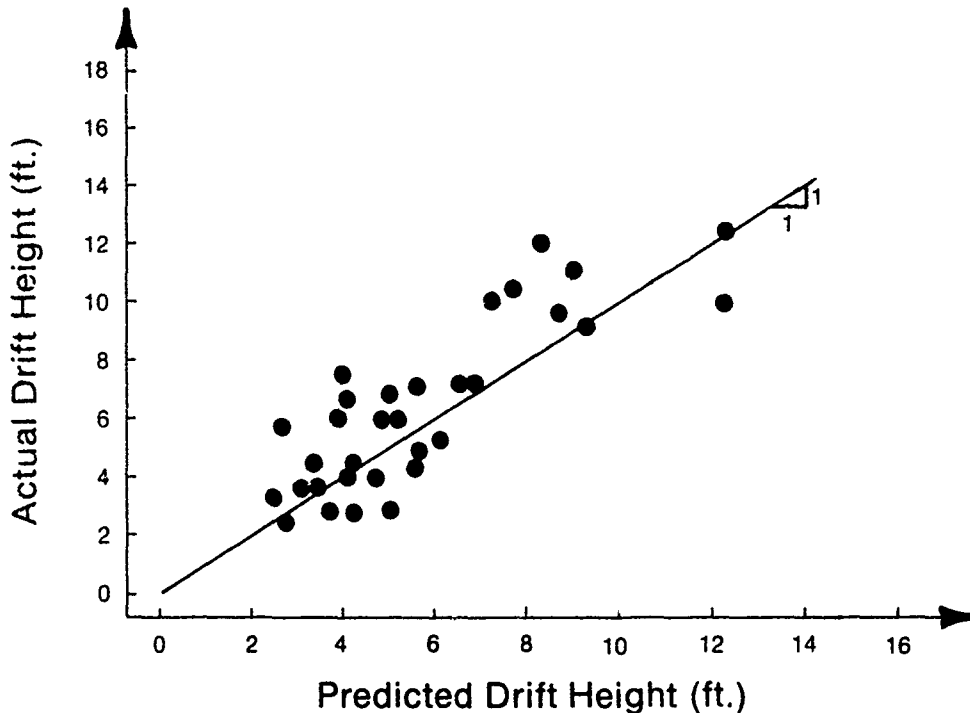
Figure 6   Scattergram of Actual vs. Predicted Drift Surcharge Heights

Figure 6 is a scattergram of actual surcharge drift heights from the 35 case histories plotted against the corresponding value predicted by Eq. 1. Notice that there are only 34 points in this Figure. Drift D at the Jordan Marsh facility was eliminated since the empirical relationship does not apply to the somewhat unusual case of a triangular drift at a forward facing step. In addition, the blizzard intensity parameter defined above characterizes wind and snowfall over a three day period. With this in mind, the depth of "new snow" was used as the surcharge drift depth for the Jordan Marsh facilities drifts. Note that the predicted values approximate the actual values in the sense that the data points are scattered about the "one to one" match line.

SUMMARY AND CONCLUSIONS

Snow drifts at multilevel roofs are investigated in this paper. A review of previous research suggests that triangular drifts which typically form at backward facing steps (ie windward upper level roof) tend to be larger than quadrilateral drifts which typically form at forward facing steps.

A data base consisting of 35 case histories was used to develop an

186

empirical relationship for triangular drifts at backward facing steps. The upper and lower level roofs in the case history data base were nominally flat. Hence sliding and valley effects are not considered. It was found through multiple linear regression that the surcharge height was a function of the effective elevation difference H_r between the upper and lower level roofs, the diagonal length of the upper level roof and a blizzard intensity parameter BI. As defined herein BI is the product of snow accumulation and wind speed above a threshold value evaluated over a three day period. It is felt that the empirical relationship presented herein is an improvement over prior work in that wind in general and blizzard intensity in particular are specifically included in the relationship.

Although it is felt that the relations for predicted drift height is a step forward, it cannot be used directly in building codes or load standards. This awaits research on the mean recurrence interval for BI at various locations throughout the country.

ACKNOWLEDGEMENTS

REFERENCES

American National Standards Institute, 1982 "Minimum Design Loads for Building and other Structures". ANSI A58.1-1982, New York, NY.

Galanakis, I, 1988, "Effects of Wind on Roof Snow Drifts", Masters Thesis, Rensselaer Polytechnic Institute, Troy, NY.

O'Rourke, M. and E. Wood, 1986, "Improved Relationship for Drift Loads on Buildings", Canadian J. Civil Engineering, Vol. 13, pp. 647-652.

O'kourke, M. and K. Elhmadi, 1987 "Roof Snow Loads; Drifting Against a Higher Wall", Proc. 55th Western Snow Conference, Vancouver B.C., pp. 124-132.

Radok, U., 1977, "Snow Drift", Journal of Glaciology, Vol. 18, No. 81 pp. 123-139.

Reidy Engineers, 1978 "The Blizzard, February 6-7, 1978", Boston, Massachusetts.

Schmidt, R. 1981, "Estimates of Threshold Windspeed from Particle Sizes in Blowing Snow". Cold Regions Science Technology, Vol. 4, pp. 187-193.

Tabler, R. 1975. "Predicting Profiles of Snowdrifts in Topographic Catchments". Paper presented at Western Snow Conference, Coronado, CA.

Templin, J., and Schriever, W. 1982, "Loads Due to Drifted Snow. Journal of the Structural Division, ASCE, Vol. 108, No. ST8, pp. 1916-1925.

4
EXPERIMENTAL MODELING TECHNIQUES
Ronald Sack, Chairman
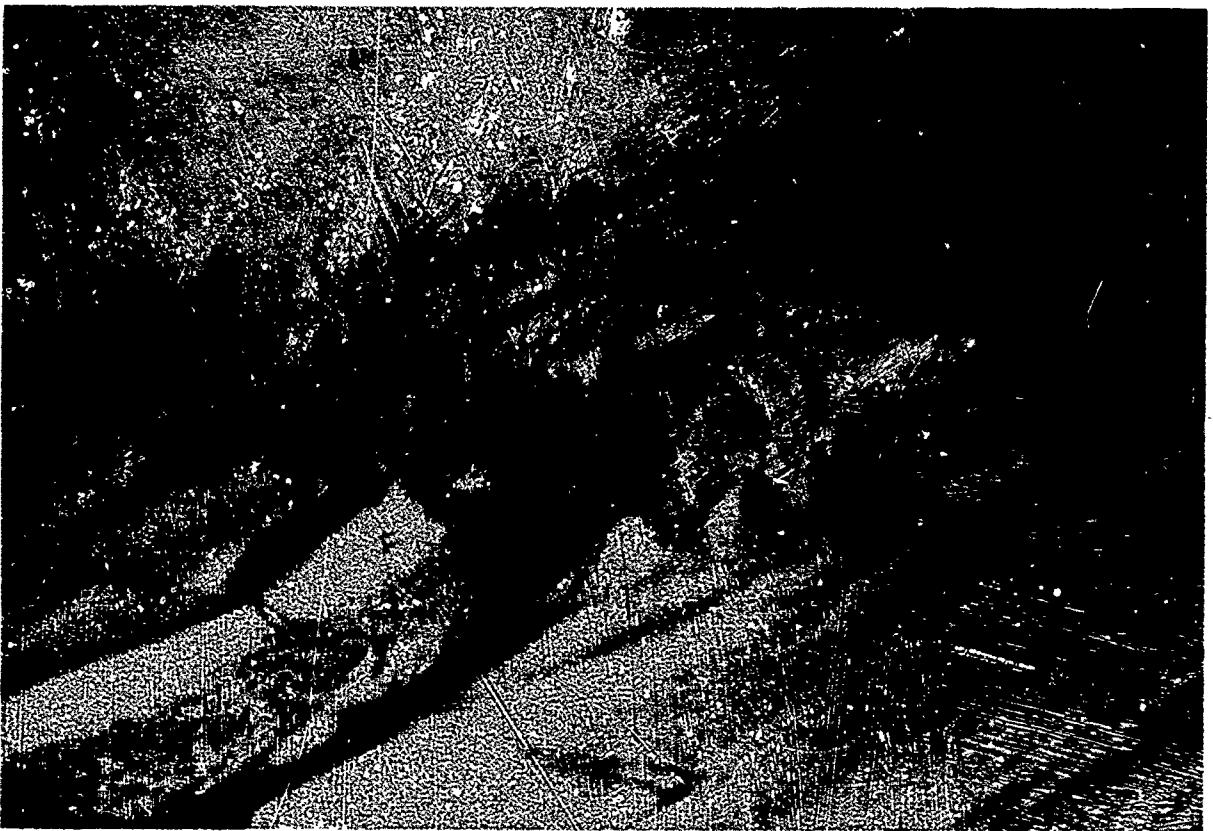
Snow drift modeling with activated clay in a wind tunnel. (Photograph provided by James Wuebben.)

Snowdrift Wind Tunnels in Japan

Yutaka Anno[I]

ABSTRACT

This paper describes snowdrift wind tunnels using activated clay particles in Japan.

INTRODUCTION

Wind tunnel experiments using model snow have been conducted by various investigators in Japan. Kuroda and Kinoshita(1940) reported that magnesium carbonate powder provided good similitude of snowdrifts between the model and prototype. As a result, magnesium carbonate powder was often used as a substitute for snow particles in the simulation of snowdrift formation around structures in wind tunnels. However, this material had a disadvantage that its particles easily cohered to each other and turned to coarse granules, with a broad size distribution. Therefore, this material could not provide good similitude of snowdrifting between model and prototype in small scale. Since the size of a model structure is restricted by the dimensions of the wind tunnel used, it is desirable to use fine particles to represent the drifting natural snow particles. Anno(1977) reported that activated clay particles provided good similitude of snowdrifting between model and prototype in a scale of 1/1000. His modeling result was apparently very realistic. After his report the use of actvated clay particles became the most practical and precise method for snow simulation in Japan. This paper describes snowdrift wind tunnels built in Japan which use activated clay particles as model snow.
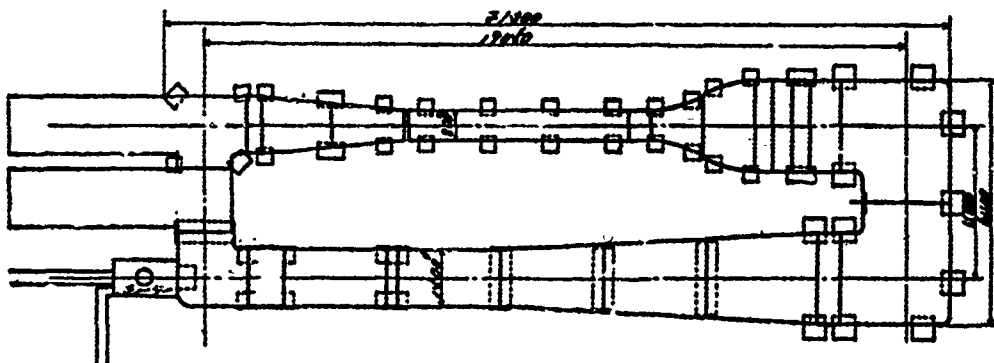
Figure 1. Snowdrift Wind Tunnel of Hokkaido Development Bureau.

I. Research Associate, Dept of Civil Eng, Hokkaido University, Sapporo, Japan.

Structure of Wind Tunnel

The first snowdrift wind tunnel using activated clay particles as model snow was that of the Hokkaido Development Bureau. This wind tunnel was originally built for the research on the aerodynamics of snow fences; however, in order to predict the shapes of snowdrift formation around the snow fences this wind tunnel was remodeled to simulate drift pattern using model snow particles. Figure 1 shows the plan view of the wind tunnel. This wind tunnel is of the open-circuit type with a testing section of 0.8m × 0.8 m in square.
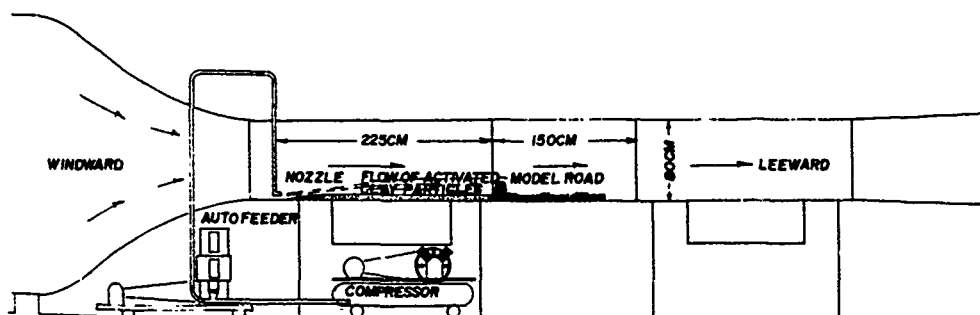
Figure 2. Testing Section and Ejector of Model Snow Particles.

Figure 2 shows the testing section and the ejector of model snow particles. Particles were ejected by compressed air. The rate of ejection of model snow particles was controlled to simulate the prototype snowdrifting rate. The maximum ejecting rate of model snow is 450 g/s when activated clay particles are used as model snow. The nozzle of the ejector was placed 3.5 m on the upwind side from the model structure.
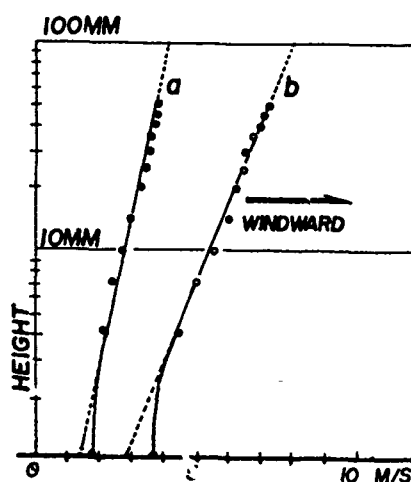
Figure 3. Wind Profile at Testing Section.

Wind Profile

The wind velocity was measured by a hot-wire anemometer placed at the center of the wind tunnel. In Figure 3, curves a and b show wind profiles measured at the testing section. As shown in this figure, wind profiles a and b indicate well-defined logarithmic distributions, except for the values of wind velocity just above the surface. The ejection of model snow particles increases the turbulence level to 5% at the height of 10 mm on the model snow surface. Therefore, it is believed that the air flow of the wind tunnel would be turbulent like natural wind. Wind velocity at the center of the wind tunnel reaches up to 30 m/s generated by 37 kW motor.

Model Experiment

Figure 4 shows a change in model snowdrift profile as a funtion of time. The model snow fence consists of 10 horizontal slats. The porosities are about 18%. Bottom clearance between the lowest slat and ground is 1.5 mm, and the height is 11.5 mm. The scale is 1/300. The wind velocity at the center of the testing section is 6 m/s. As seen in this figure, 10 minutes after the initiation of the experiment a small mound of clay particles is formed on the downwind side of the model fence, with the crest located at a distance of about 3.2 times the height of the fence. The crest shifted toward the fence with time, to a distance of approximately twice the height of the fence 40 minutes after the initiation of the experiment. The location of the crest is approximately similar to the prototype which is shown in Figure 5.

Recently, this wind tunnel was remodeled because it became necessary to simulate the snowdrift formed on the road in large mountanous terrain. The testing section was enlarged to be 1.2 m × 1.2 m in size and being changed to be a closed circuit.
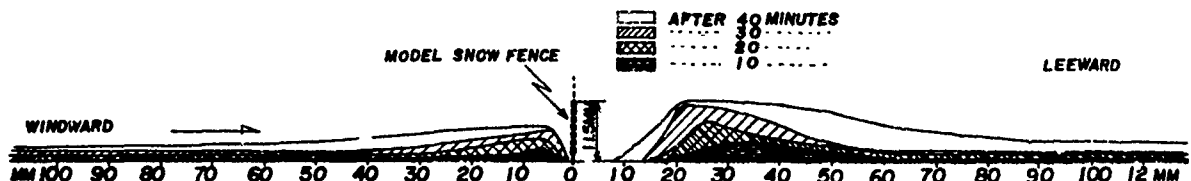
Figure 4. Change in Model Snowdrift Profile.
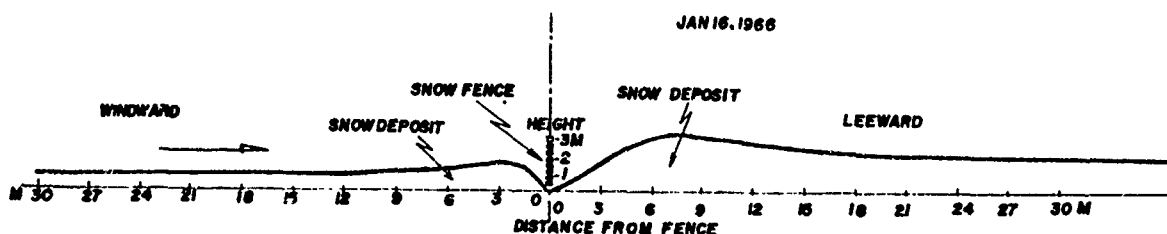
Figure 5. Prototype Snowdrift Profile.
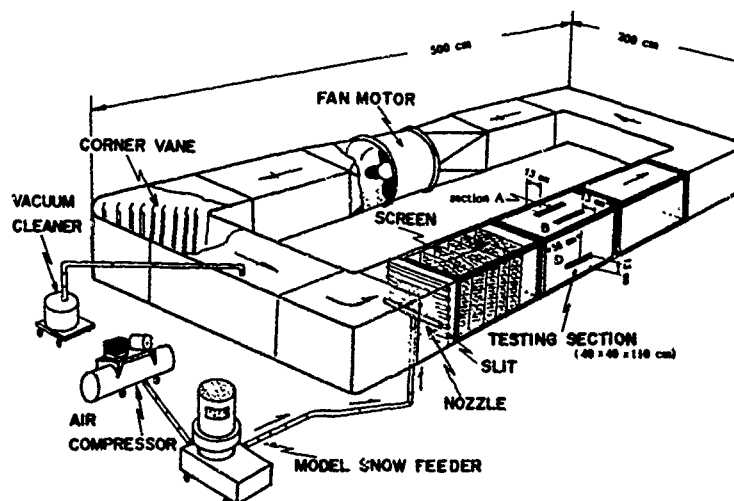
Figure 6. Snowdrift Wind Tunnel of Hokkaido Institute of Technology.

SNOWDRIFT WIND TUNNEL OF HOKKAIDO INSTITUTE OF TECHNOLOGY

Advantages of Closed-Circuit Wind Tunnel

The snowdrift wind tunnel of Hokkaido Institute of Technology is the Japan's first closed-circuit type snowdrift wind tunnel. A closed-type snowdrift wind tunnel has the following advantages;

(1) It is possible to control the water content of inner air flow since the air is isolated from the outside air.

(2) The fetch distance which is necessary to generate snowdrifting, becomes endless.

(3) The model snow particles will not leak out of the tunnel, so the operator is protected from the dust of model snow.

Basic Structure of the Snowdrift Wind Tunnel

Figure 6 shows the wind tunnel of Hokkaido Insitute of

194

Technology. It does not have any diffuser, effuser and fine-mesh screen, since model snow particles are deposited or adhere on the surface of them, causing the wind profile and turbulence level of the testing section to change during a model experiment. The testing section is square, with a 40 cm × 40 cm cross section, which is sufficient to model a snowdrift formed around a small-scale structures. In order to make the model snow start drifting in the testing section, the wind tunnel has an axial fan motor of 1.5 kW. As a result, the maximum wind velocity reaches up to 16 m/s at the center of the testing section.
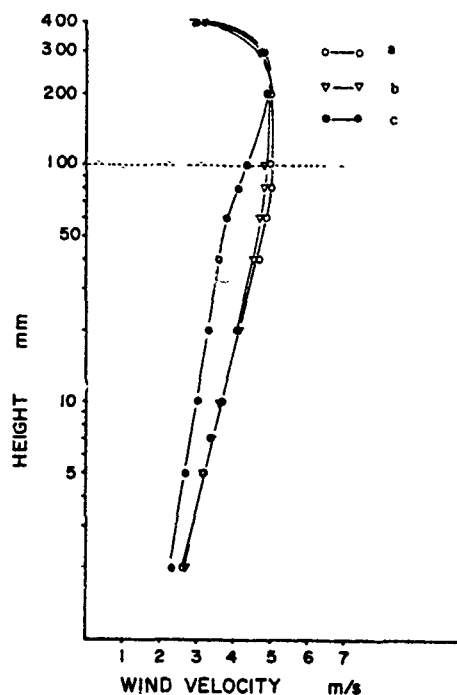
Figure 7. Wind Profile at
Testing Section.
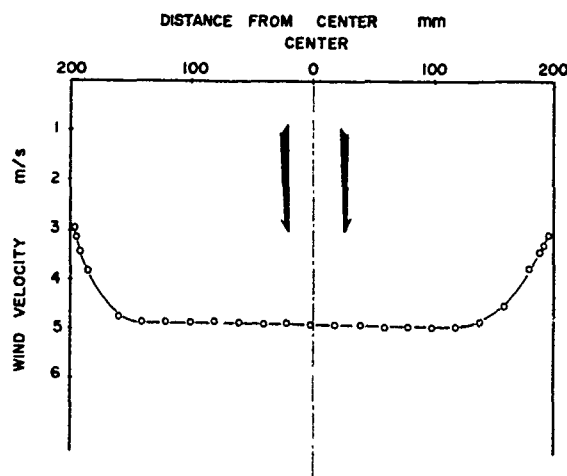
Figure 8. Horizontal Wind
Profile.

In Figure 7, curves a and b show the wind profiles measured respectively at testing section. Figure 8 shows a horizontal wind velocity distribution measured at a testing section. It is desirable that a model obstruction or building should be placed in the center area of the testing section, leaving a gap of 10 cm from the side walls, since the velocity distribution is even in this area.

Modeling Results

Snowdrift formed around a building was modeled in this wind tunnel. The prototype building was built at Showa station, Antarctica. The rate of ejection of activated clay particles was 70 g/s.

Figure 9 shows a comparison between drift profiles of the model and its prototype. The model drift profile shows a fairly good coincidence with the prototype result.
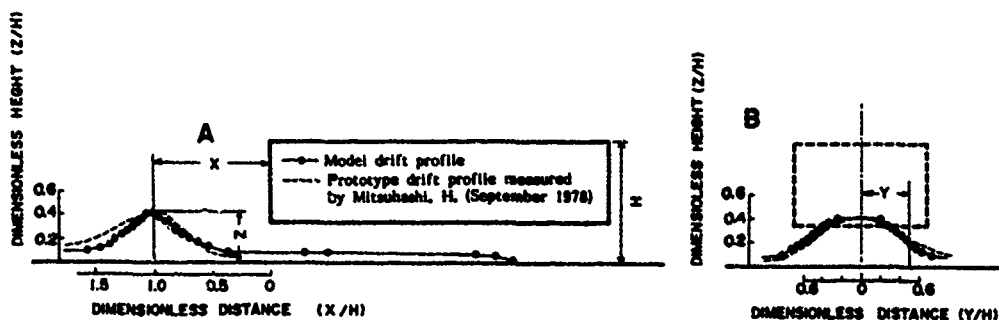
Figure 9. Comparison between Model and Prototype Snowdrift.
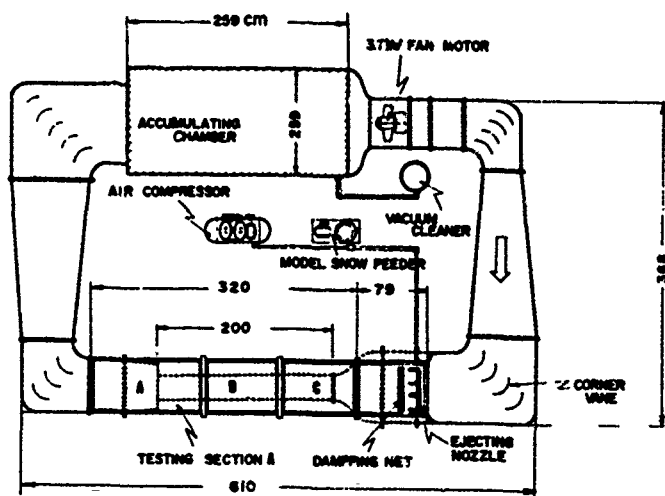
Figure 10. Snowdrift Wind Tunnel of Hokkaido University.

SNOWDRIFT WIND TUNNEL OF HOKKAIDO UNIVERSITY

Figure 10 shows the snowdrift wind tunnel of Hokkaido University.

This wind tunnel was built for research on snow disasters in agriculture. The testing section is 0.6 m × 0.5 m × 3.2 m in width, height and length respectively. These dimensions of the testing section seem sufficient to simulate the snowdrift formation around agricultural buildings and facilities. The maximum wind velocity is 13 m/s, which seems sufficient to model the snowdrift formed in Hokkaido, Japan, where snowdrifts are formed at comparatively low wind velocities.

Wind Profile

Figure 11 shows a vertical wind profile at the testing section. Figure 12 shows the horizontal wind profile measured at a height of 11 cm in the testing section. The horizontal profile is almost evened-out and the vertical profile shows a logarithmic distribution.

Modeling Result

Figure 13(A) and (B) show in plan the eroded area around the model boxes and the drift profile of crosssection A-A' in Figure 13(A), respectively, comparing its prototype result. Figure 13 shows approximate coincidence between the model and the prototype, considering maximum amplitude of wind direction 25 and gustiness 1.1 to 1.3 of natural conditions.
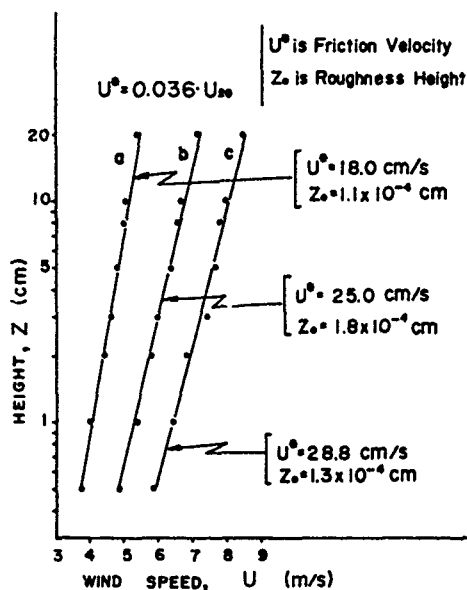
Figure 11. Wind Profile at Testing Section.
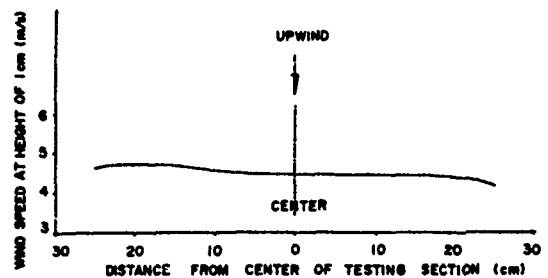
Figure 12. Horizontal Wind Profile.
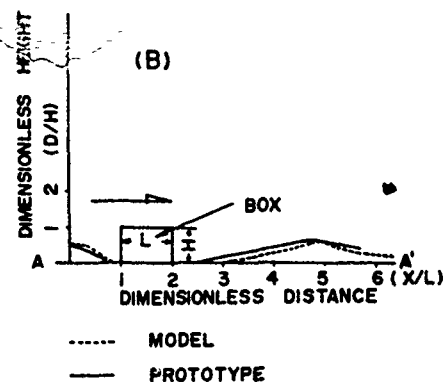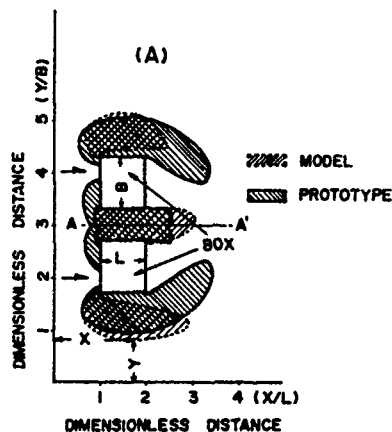
Figure 13. Comparison between Model and Prototype Snowdrift.

CONCLUSION

There is a lot of snow in winter in Japan, therefore, snow simulation is very important in snow engineering. The author reported that activated clay aprticles was the most suitable materials as model snow ten years ago. Today the means of activated clay particles is major method for the snow simulaation in Japan.

Table 1 sumarizes snowdrift wind tunnels which use activated clay particles as model snow.

Table 1. List of snowdrift wind tunnels.

Wind Tunnel	Hokkaido University	Hokkaido Development Bureau	Hokkaido Institute of Technology
Location	Sapporo, Japan	Sapporo, Japan	Sapporo, Japan
Type	Closed-cirauit	Open-cirauit	Closed-cirauit
Maximum wind velocity	13 m/s	20 m/s	16 m/s
Turbulence intensity	not measured	10%	10%
Fan motor output power	3.7 KW	3.7 KW	1.5 KW
Testing section widthxheightxlength	0.6 x 0.5 x 3.2 m	0.8 x 0.8 x 6.0 m	0.4 x 0.4 x 2.2 m
Model snow	Activated clay	Activated clay	Activated clay
Ejection system of model snow	Compressed air	Compressed air	Compressed air
Contraction ratio	2.1:1.0	9.0:1.0	No contraction
Flow conditioner	Wire screen	Wire screen	Wire screen

REFERENCES

Anno, Y., 1977, "Snow fences built at Kitami mountain pass and Bihoro mountain pass," Proc,Techn. Meeting of Hokkaido Development Bureau, 20, 859-864,(in Japanese).
Kuroda, K., and Kinoshita, M., 1940, "Report on experiments on a snowstorm in a wind tunnel," Japan Snow and Ice Soc., Paper I, 144-158(in Japanese).

Cold Room Studies for Slidir 9 Snow

R.L. Sack[I] and R.L. Baker[II]

ABSTRACT

The results of field measurements reveal that snow sliding from slippery roofs can be predicted using probabilistic methods. We measure the conditional probability of sliding using either temperature, temperature-time, or precipitation as the random variable. Combining the principles of similitude, with observations of laboratory models and roofs under field conditions, we conclude that these conditional probabilities can be reliably measured using artificial snow. Operating conditions and characteristics of the artificial snow laboratory at the University of Idaho are described.

INTRODUCTION

The design of structures in many areas of the world is governed by regional snow loads. Understanding these regional variations is difficult because of the paucity of reliable data on snow loads. Some of the phenomena affecting snow loads include micro-meteorological and large-scale meteorological factors, geographic location, and elevation. Exposure to wind and sun, roof slope, thermal losses from the building, and roofing material all play an important role in determining the roof snow load.

Since 1983 the Department of Civil Engineering at the University of Idaho has been conducting field experiments to determine the behavior of snow loads on slippery roofs. During the snow seasons from 1983 through 1985 data from six small variable-pitch shed roofs (2.4 m by 2.4 m) were collected and investigated. These shed roofs were unheated and had slopes of 10°, 30°, and 45° (two roofs per slope). During snow seasons 1986–87 and 1987–88 we studied gabled roofs made by connecting the two shed roofs of each slope at their ridges with metal ridge caps on top. We continuously monitored load cells, thermocouples, and heat flux gages using on-site computers and automatically transmitted the data to campus daily [Sack et al. 1985]. In addition, we made manual measurements of the ground and roof snow loads with a Federal snow sampler for the test roofs and ten full-size unheated roofs in the field study area. A probabilistic roof load model was developed from these data [Sack, et al. 1986; Sack et al. 1987].

[I]Professor, Dept. of Civil Engrg.; University of Idaho; Moscow, ID 83843

[II]Graduate Research Assistant, Dept. of Civil Engrg.; University of Idaho; Moscow, ID 83843

In 1986, we augmented our field study by creating a controlled laboratory environment where the effects of single parameters on the roof snow pack could be observed. We hoped to recreate a cold environment that would closely parallel our findings at our field site by generating data using artificial snow in the laboratory.

PROBABILITY MODELING AND SIMULATION

Sliding snow

To understand the mechanics of snow sliding from a roof we must consider the various forces involved in retaining the snow on the roof and those driving the snow off the roof. Retentive forces include surface friction, adhesion to the roof, tensile forces at the ridge, and compressive forces at the eave. The weight component of the snowpack acting downward tangent to the roof slope tends to cause sliding. Surface friction forces vary with temperature, snowpack characteristics, and surface properties. Adhesive forces between the snowpack and the roof surface however, are much greater than the frictional forces. Tensile forces develop at the ridge and are considerably greater on gabled roofs than on shed roofs [Taylor, 1983]. Snowmelt on a warm roof collects and refreezes on a cold eave to create an ice dam and notable compressive forces. Ice dams typically do not occur on cold roofs.

Snow slides because resisting forces at the roof–snow interface (most common) or between snow layers are reduced. Another form of snow sliding can occur when the shear strength of the snow is exceeded. A slide caused by a reduction in resisting forces is initiated by a lubricating layer of snowmelt and/or rain at the roof–snow interface; whereas, a shear failure slide occurs from the addition of weight to the snowpack in the form of precipitation.

Conditional Probability Laws for Sliding Snow

Experimental studies have shown that snow slides from roofs primarily due to a reduction in resisting forces at the roof–snow interface or shear failures between snow layers in the snowpack [Taylor, 1985; Schaerer, 1981]. From data gathered at our field site, we developed a probabilistic model [Sack, et al. 1986] using both shear failure and reduction of resisting forces to describe snow sliding from cold, slippery roofs.

An equation of joint probability of sliding based on reduction of resisting forces and shear failures can be written as:

$$P(S) = P(S_r) + P(S_s) - P(S_r)P(S_s) \tag{1}$$

where $P(S)$ = probability of sliding on any given day, $P(S_r)$ = probability of sliding on any given day due to reduction in resistance forces, and $P(S_s)$ = probability of sliding on any given day due to shear failure. Note that independence is assumed between the two types of slides in Eq. 1. Although a reduction in resisting forces could possibly cause shear failure in the snowpack, observations of slides at the field site indicate that shear failures occur mainly from increased loads while slides due to a reduction of resisting forces occur because of snowmelt.

One of two parameters, can be used as an indicator of snowmelt on the roofs: temperature and degree-hours. Predicting snowmelt allows us to predict sliding on the roofs. By applying the law of total probability with each parameter we have:

$$P(S_r) = \int_0^\infty P(S_r|X=x)P(X=x)dx \qquad (2)$$

where X,x represent either T,t (temperature) or H,h (degree-hours) depending on the parameter used. Here, $P(S_r|X=x)$ — conditional probability of sliding on any day due to a reduction in resisting forces given the high temperature T or degree-hour H equals t or h respectively. $P(X=x)$ — probability that the temperature T or degree-hour H on any day equals t or h respectively.

For temperature or degree-hours, maximums are used to determine probabilities of the sliding event. Since thawing of the snowpack occurs at temperatures above freezing, it is important to note that a probability must exist for sliding due to a reduction in resisting forces for any temperature above freezing. Positive degree-hours are a better measure of sliding because the amount of time a given temperature remains above freezing becomes implicit in the calculations of probabilities of sliding. A slide is more likely to occur at a sustained high temperature than at a peak temperature that falls rapidly.

Shear slides occur when the shear resistance of the snowpack is reduced by either snowmelt, or an increase of load on the roof, or both. The 30° and 45° roofs at the field site exhibited shear failures during periods of precipitation. Studies of avalanches [Schaerer, 1981] show shear failures do not normally occur on slopes less than 25° and are usually confined to slopes between 30° and 45°. Using precipitation as the principle sliding parameter for shear failures and the law of total probability yields

$$P(S_s) = \int_0^\infty P(S_s|R=r)P(R=r)dr \qquad (3)$$

where $P(S_s|R=r)$ — conditional probability of sliding due to a shear failure on any day the precipitation R equals r, and $P(R=r)$ — probability that precipitation on any day equals r.

Equations 2 and 3, when substituted into Eq. 1, give the total probability of sliding. A slide that occurs at or below freezing is assumed to be a shear failure and a slide occurring when no precipitation is observed is assumed to be caused by a reduction in resisting forces.

Simulation

After obtaining the conditional probabilities of sliding, a computer simulation program [Pinkard, 1985] was developed to predict roof snow loads. Thus, the loads generated with the conditional probabilities can be compared with the measured values. Initially, 25 years of meteorological data from the Hydrologic Storage and Retrieval System (HISARS) for the National Weather

Service station number 10 5708-4 were used to simulate roof snow loads; we have subsequently used 35 years of record. For each of the 25 years, six simulations were run and maximum roof snow loads were predicted. A log–Pearson type III [Kite, 1977] extreme value analysis yielded roof design loads with a fifty–year mean recurrence interval.

COLD ROOM EXPERIMENTS

A cold room, with snow–making capabilities, offers a convenient alternative to measuring the conditional probabilities of sliding (see Eq. 1) in the field. Calculations suggested that we should be able to model sloped roof behavior in the laboratory by observing the scaling laws of similitude [Giever, 1988].

Formation of natural snow occurs when the ambient temperature of the clouds is less than 0°C and supercooled water is present. Particles in the air (usually wind–blown dust) act as ice nuclei for the creation of ice crystals (i.e., the initial growth stage of snow). These ice nuclei serve as catalysts by providing a surface upon which the ice can deposit or by touching the surface of a supercooled droplet causing freezing. Ice crystals grow in size through sublimation and form snow crystals. Aggregation of snow crystals create snowflakes and riming of snow crystals create graupel. Therefore, snow may consist of snow crystals, rimed snow crystals (graupel), and snowflakes [Schemenauer, et al. 1981]. In the cold room, the same basic process occurs. Ice nuclei are introduced as either dust particles, which invariably are always in existence, or as supercooled droplets that suddenly freeze. Snow crystals form and deposit as snow on the test structure.

The snow creation process in a cold room environment must closely approximate natural conditions. The difficulties involved with creating artificial snow include trying to duplicate natural effects. A few specialized considerations also occur (e.g., it is necessary to have a controlled environment).

In 1986, Haldeman initiated a series of laboratory experiments at the University of Idaho [Haldeman, 1986]. Artificial snow was created in a walk–in freezer 3.0-m by 3.4-m by-2.7 m high. Haldeman deposited artificial snow on a small, variable–pitch shed structure similar to the full scale test structures used for our field studies of 1983–85. Six tests for each pitch of 10°, 30°, and 45° were conducted. During these tests, shear failures were not examined because no precipitation was added to the existing snowpack once the room was put into a diurnal cycle. Appropriately, Eq. 1 reduces to a single term and only slides involving a reduction of resisting forces are observed. Computer simulations were run using both the temperature index and degree–hour index as measures of sliding (see Eq. 2). Extreme value analysis with these data showed that design loads predicted by ANSI A58.1–1982 [ANSI, 1982] and Sack [Sack, 1986] overpredicted roof snow loads on sloped shed roofs.

Problems with maintaining temperatures inside the original cold room using an inefficient cooling unit mandated remodeling. Currently, the artificial snow room is 3.0 m by 5.2 m by 2.4 m high and is cooled by a 3 hp (2,240 W) Copeland refrigerating system with a two–fan condensing unit. This cooling unit is capable of delivering and maintaining low room temperatures of

-23°C to -27°C. Equipment specifications show a low temperature of -29°C is possible. As part of the snowmaking equipment, an air-baffle comprised of two, spring-loaded struts braced between the cold room ceiling and floor support a 3.0 m by 2.4 m piece of one-inch thick dense furnace filter material (i.e., Duralast) in a wire mesh. The baffle dampens out air-turbulence caused by the cooling fans and helps to reduce ice/snow build-up on the fan condensers.

A shut-off valve on the city water line is located close to the snowmaking equipment. Air originates from a 3.7 kW air compressor. Both the air and the water enter a series of copper coils (approximately 18.3 m in length) submerged in a low temperature bath (conventional chest-type freezer with a 3 to 1 mixture of ethylene glycol and water). This low temperature bath precools the water and air before they enter the cold room. From the low temperature bath, the air and water lines exit to the pressure regulators and pressure indicators. An in-line water trap is installed on the air line upstream of the regulators to drain off condensed water coming from the compressor in the air line. Without a water trap, ice forms in the air line inside the cold room before reaching the spray nozzle. This ice collects in the tubing and eventually freezes the air line shut. Thus, cold room temperature must be greatly elevated to melt the ice plug and the experiment in progress is destroyed. The water and air lines are split upstream of the pressure gages/regulators to offer a choice of lines for snowmaking. This built-in redundancy obviates the need for reheating the room in the event of line freezing.

Pressure regulators and pressure indicators are made by Spraying Systems Co. (Model Numbers: 11438-36 and 11438-46). The air line regulators can turn the flow of air off in one line when the other is being used. Although leaks can occur in the closed air line, they do not cause freezing. In contrast, it is imperative to turn off one or the other of the water lines completely. This is accomplished with two shut-off valves located upstream of the water regulators. Bleed lines are installed immediately outside the cold room to remove water in case the nozzle freezes and/or we shut the system down. If freezing occurs only at the nozzle, we install a dry nozzle. The water lines should be blown dry through the bleed lines before changing the nozzles to prevent the water lines from freezing. We blow the water lines dry by disconnecting the air compressor from the air line and reconnecting to the bleed lines.

Inside the cold room, the water and air travel through flexible, clear PVC tubing on opposite sides of the room. Metal tracking, installed on the ceiling, in combination with the flexible tubing, allows the spraying nozzle (when hooked up to the air and water line) to be slid back and forth giving a uniform spray of snow to all areas of the roof. We use a 1/4-inch, Spraying Systems Co. Model JN26-303 stainless steel air atomizing nozzle with liquid shut off needle, a wide-angle round spray air cap (No. 140-6-52-70°), and a fluid cap (No. 60100). We attach the nozzle to the PVC lines with two, 1/4-inch quick-couplers for convenient installation and removal of the nozzle. If the nozzle freezes, it can quickly be removed and replaced with no delay in snowmaking.

Temperatures must be constantly monitored during snowing and room temperatures maintained within specific operating ranges to get consistent

quality snow. Snowmaking should be suspended when room temperatures exceed allowable operating temperatures (see Table 1) during a snowing session. This is to insure against wet snow and unusually high snow densities. Cold room temperatures, quality of snow, and length of snowing time are dependent on the incoming (mixing) temperatures and pressures of both water and air (see Table 1). Precooling the incoming air and water can lengthen the snowing time as much as eight times that of a system with no precooling because the cold room cannot compensate for the sudden influx of heat from the water. Higher incoming air temperatures also add heat to the cold room, but the water temperature is primarily responsible for cold room heat build up. Air temperatures seem to be more closely related to the quality of the snow and water/air atomizing conditions at the spray nozzle. A change of 1°C to 3°C lower water temperature will not improve the quality of the snow (i.e., less dense) as much as the same change in air temperature. Often, when the air temperature is lowered a few degrees, significant improvement in the snow quality occurs. A lighter, dryer, less dense snow forms. However, coupled with this increase in snow quality is a greater chance of freezing the nozzle shut and lowering the efficiency of the snowmaking system.

Optimum air-to-water pressure ratios are 2 to 1 but this varies with temperature. Colder incoming temperatures require higher pressures and warmer incoming temperatures require lower pressures. The variability in pressures (high to low) generally do not exceed 35 to 48 kPa. Usually, we start a snowmaking session with pressures of 290 kPa and 580 kPa for the water and air, respectively. As the temperatures begin to rise inside the cold room, combinations of more precooling and different water/air pressures are used to increase snowing time.

Table 1: Operating Temperatures and Pressures

| | Water | | Air | | Cold Room |
	+Temp. (°C)	*Pressure (kPa)	+Temp. (°C)	*Pressure (kPa)	‡Temp. (°C)
Max.	14	331	17	648	-4
Min.	8	207	7	427	-16
Ideal	10	303	11	607	-16 to -4

+Measured upstream from the cold room entrance point.
*Measured at the pressure regulators.
‡Avg. of room thermocouples. Values shown are a range of snowing temperatures.

After the snow is deposited on the test structures, the cold room is put
into a simulated diurnal cycle. A conventional 1500 W baseboard heater and
the cold room cooling unit are controlled by the data acquisition equipment
and computer program. Subroutines in the controlling program close and open
electrical relays wired to the heater and cooler to recreate a diurnal cycle
based on the average temperature in the cold room. Cold room temperature is
monitored at five different locations. A characteristic sinusoidal curve
models the changing temperature. Lengths of the temperature cycles, high
temperatures, and low temperatures are varied to show a randomness in the
simulated cycle. Limitations imposed by the operating equipment make the
curve particularly hard to achieve. During the first part of the warming
cycle, the program duplicates the desired curve. However, during the warming

Diurnal Cycle

Typical Laboratory Cycle w/ Ideal Cycle
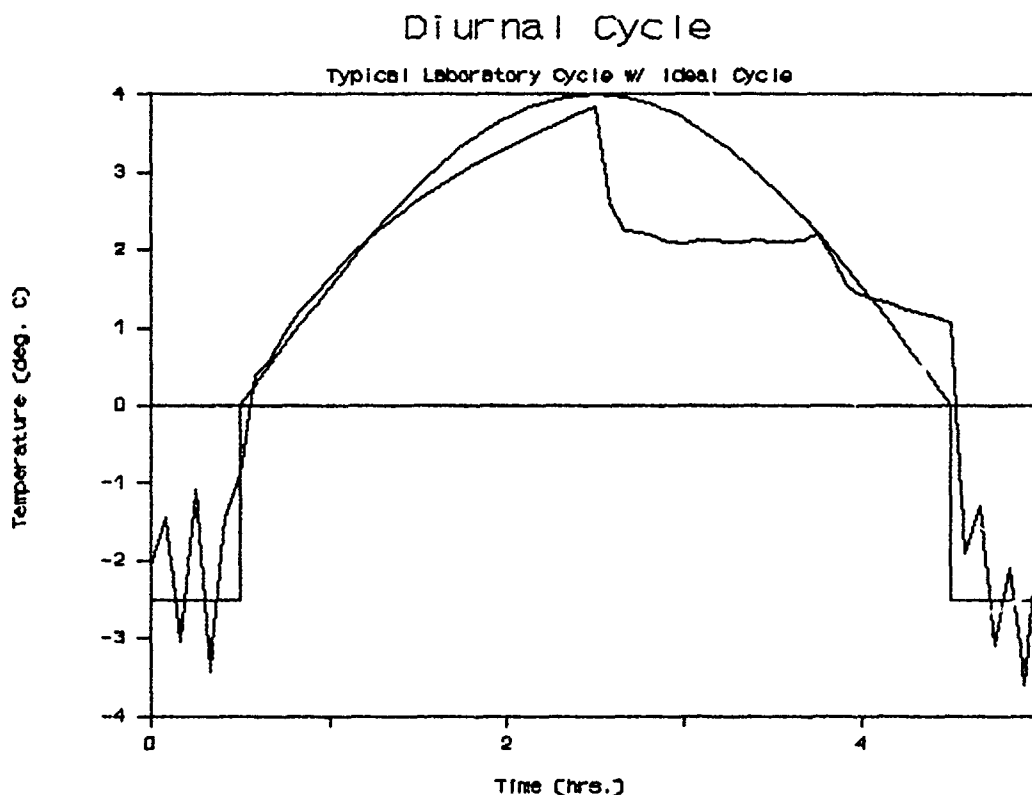
Figure 1: Typical Simulated Temperature Cycle

cycle the cooler overpowers the heater, and a jagged decline in temperature is
observed. A sudden drop in temperature ends the warming cycle. Figure 1
shows an experimental temperature curve with the desired curve superimposed.
This particular cycle comes from a curve with 0.5 hours in a cooling period
and 4 hours in the warming period, with high temperature of 4 °C and low
temperature of −2.5 °C.

With an improved cold room and enhanced snow-making equipment, we are
able to make artificial snow more reliably. The quality of the snow has
improved; snow core densities range from 0.124 to 0.179 g/cc, which is
indicative of new fallen snow [Linsley, et al. 1982]. In addition to sampling

densities, we collect and encapsulate artificial snow crystals in a Formvar [Falconer, 1967] solution. The maximum diameter of the artificial snow crystals we have observed is roughly 0.1 mm, which compares well with natural snow crystals with a range from 50 μm to 5 mm [Schemenauer, et al. 1981]. We have identified three types of crystals: hexagonal graupel (R4a), lump graupel (R4b), and conelike graupel (R4c) [Magono and Lee, 1966].

The simulated diurnal cycle improved with the baseboard heater and electrical relays to computer control the temperature cycle. We performed a number of tests in the cold room on gabled roofs. By modifying our simulation program to incorporate partial slides, we were able to obtain similar conditional probabilities from laboratory and field measurements for gabled roofs [Giever, 1988]. Table 2 shows a comparison of simulated 50 year roof design loads between slippery shed and gabled roofs using degree-hours [Sack, et al. 1987; Giever, 1988] and ANSI A58.1-1982 [ANSI, 1982] and ASCE/ANSI A58.1-1988 [ASCE/ANSI, 1988].

Table 2: Comparison of Design Loads (mm of water)

| Roof Slope | Shed Roof[#] | | Gable Roof[‡] | | Standards | |
	Field Model	Cold Room Model	Field Model	Cold Room Model	ANSI82[+]	ASCE/ ANSI88[*]
10°	191	238	477	431	616	616
30°	72	166	206	-	616	448
45°	53	137	54	66	385	280

[+]ANSI82 -- ANSI A58.1-1982
[*]ASCE/ANSI87 -- ASCE/ANSI A58.1-1988
[#]Sack87
[‡]Giever88
-Load not simulated for 30° gabled roof

CURRENT RESEARCH

We are presently studying the sliding characteristics of glass gabled roofs with a slope of 6 on 12 by using a test structure with dimensions of 1 m long by 0.91 m wide (along the slope). The base of the structure is made of wood and elevates the ridge to an approximate height of 1 m. To simulate a glass/aluminum glazing system, standard one-inch aluminum bar and angle was used. Aluminum stock was bolted to the top surface of the roofs' wood supporting members. Double-strength greenhouse grade, glass was placed on this aluminum surface and clamped to the sides with aluminum angle and a ridge cap, fashioned from aluminum bar, was placed on the ridge. All points where glass meets aluminum are sealed with silicone caulking. The sides of the structure are made of a common structural plastic (Lexan) and attached with magnetic clamps to guarantee that the walls are not load bearing since this would interfere with the load cells located in each of the six posts on the base of

the structure. Foam insulation and tape cover holes along the sides where they meet the roof structure. The entire roof assembly (including walls) rests on Teflon-coated pads just above the load cells; thus vertical loads can be monitored and load sharing on the roof eliminated.

We heat the interior of the structure with three conventional 300 watt lightbulbs evenly spaced on the floor of the structure. Two small fans point down toward the lightbulbs from the underside of the roof and circulate the heat inside the structure to achieve a desired uniform temperature. The fans run continuously, but the light bulbs are on a thermostat. Also inside the roof are seven thermocouples and two heat flux gages (Thermonetics Corp. Model No# H11-18-1-SHF, Serial No# S418, with a thermal constant of 8.23 Btu/hr·ft^2·°F or 46.73 W/m^2·°C). The heat flux gages are attached to the underside of the glass roof. We also perform tests for this structure in an unheated condition.

In studying the effects of a heated structure, we have identified two different schemes for heating the roof: a structure is continuously heated before snowing occurs; and the structure is cold when snowed upon and then heated later. If the structure is initially heated to a uniform temperature before snowing, the cold room's ability to compensate for the heat lost through the roof becomes a limiting factor. Because we are only able to deposit between 2.5 and 3.8 cm of snow on the roof during a given snow run,

Load on Heated Roof
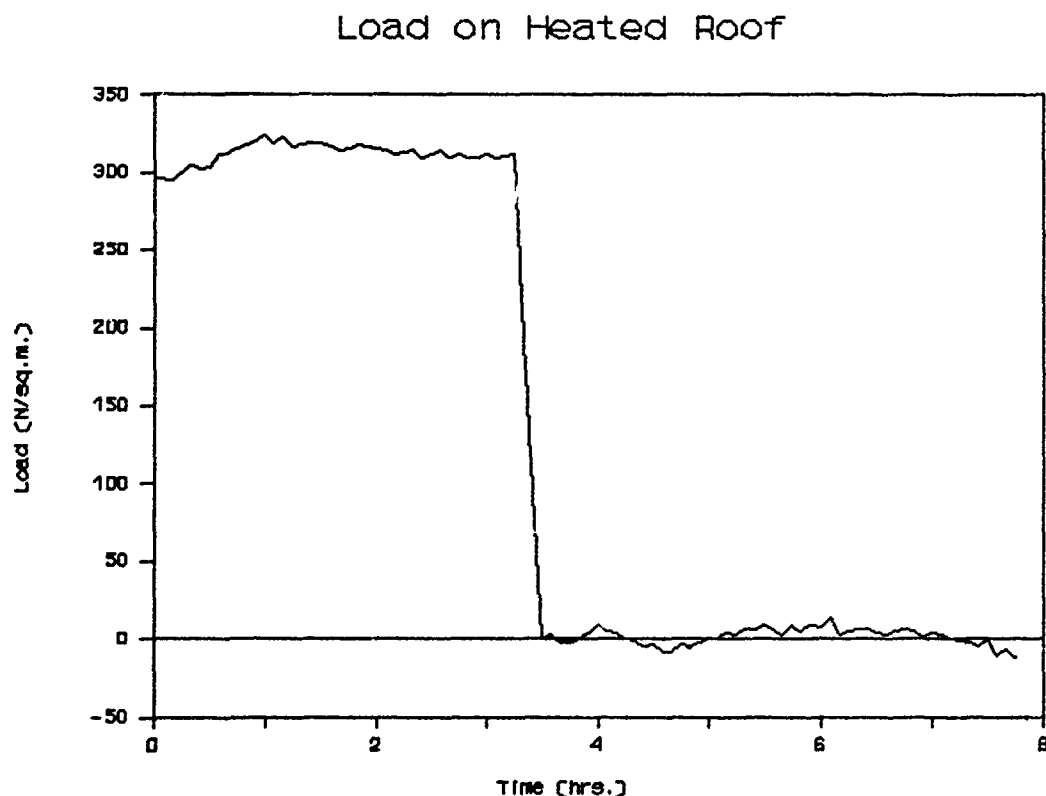
Figure 2: Load-time history of snow on a heated structure

this type of test yields little useful information. Before the cold room has time to cool down to an operating snowing environment (approximately 30 to 45 minutes), the snow that was deposited on the roof has melted and slid off within 10 to 15 minutes. If we deposit snow on a cold structure and then heat it, snow depths of 14 to 16.5 cm can be realized. Slides occur much faster than those on a cold roof with no structure heating. Comparisons between heated and unheated slides with similar room diurnal temperature cycles indicate a heated slide occurring as much as 10 times faster than an unheated slide. In fact, externally induced temperature effects (i.e., the diurnal cycle) appear to be dominated by the heat loss through the roof from the structural heating. Figure 2 shows a slide (i.e., sudden drop in load) during a test with the structure being heated.

The National Greenhouse Manufacturing Association standard [NGMA, 1985] classifies greenhouses as either continuously heated or intermittently heated (or unheated) greenhouses. Of these two types, continuously heated is subdivided as either single-glaze greenhouse and double-glaze greenhouse. Differences between the two heated types depends on the roofing material's resistance to transmitting heat (i.e., its R value). A single-glaze greenhouse has an R-value of 1.0 or less while a double-glaze greenhouse has an R-value greater than 1.0 but less than 2.0. Our roof qualifies as single-glaze. The greenhouse standard also states that the interior temperature of the greenhouse must be maintained at a temperature of 10°C or greater during the winter months.

CONCLUSIONS

Artificial snow can be produced reliably and economically in a laboratory setting to investigate the effects of snow on structures. Quality control of the artificial snow is possible by: a) monitoring specific gravities of the snow being produced; and b) encapsulating and identifying snow crystals and comparing them to known natural forms. Conditional probabilities for sliding snow can be efficiently obtained from model studies using artificial snow.

ACKNOWLEDGEMENT

REFERENCES

American National Standards Institute, Inc., American National Standard Minimum Design Loads for Buildings and Other Structures, A58.1-1982, New York, NY. (1982).

American Society of Civil Engineers, American Society of Civil Engineers Minimum Design Loads for Buildings and Other Structures, A58.1-1988, New York, NY. (1988).

Falconer, R., "Snowflakes: Identification and Preservation," Atm. Sci. Res. Ctr., State University of New York at Albany, Pub. No. 41 (1967).

Giever, P.M., "Predicting Roof Snow Loads on Gabled Structures," M.S. Thesis, Dept. of Civil Engineering, University of Idaho, Moscow, ID (1988).

Haldeman, J.S., "Predicting Sloped Roof Snow Loads Using Artificial Snow," M.S. Thesis, Dept. of Civil Engineering, University of Idaho, Moscow, ID (1986).

Kite, G.W., Frequency and Risk Analysis in Hydrology, Water Resources Publications, Fort Collins, CO. pp. 123-155. (1977).

Linsley, R.K., M.A. Kohler, and J.L.H. Paulhus, Hydrology for Engineers, McGraw-Hill, New York, NY. (1982).

Magono, C. and C. Lee, "Meteorological Classification of Natural Snow Crystals," Journal of Faculty Science, Ser. VII, Vol. 2, pp. 321-335. (1966).

National Greenhouse Manufacturers Association, STANDARDS: Design Loads in Greenhouse Structures, Ventilating and Cooling Greenhouses, Greenhouse Heat Loss, (1985).

Pinkard, J.J., "Prediction of Snow Loads on Sloped Roofs," M.S. Thesis, Dept. of Civil Engineering, University of Idaho, Moscow, ID (1985).

Sack, R.L., et al., "Data Acquisition and Communications Using Unattended Computers," Proceedings CIVIL-COMP 85, Paper No. 54. pp. 309-315. (1985).

Sack, R.L., D. Arnholtz, and J.S. Haldeman, "Sloped Roof Snow Loads Using Simulation," Journal of Structural Engineering, American Society of Civil Engineers, Vol. 113, No. 8 pp. 1820-1833 (1987).

Sack, R.L. and J.J. Pinkard, "Probabilistic Prediction of Snow Loads on Sloped Roofs," Proceedings 54th Western Snow Conference, Phoenix, AZ, pp. 41-50 (1986).

Sack, R.L. and A. Sheikh-Taheri, "Ground and Roof Snow Loads for Idaho," Department of Civil Engineering, University of Idaho, Moscow, ID, ISBN No. 0-89301-114-2. (1986).

Schaerer, P.A., "Avalanches," Handbook of Snow: Principles, Processes, Management and Use, ed. Gray, D.M. and D.H. Male, Pergamon Press, New York, NY, pp. 475-518. (1981).

Schemenauer, R.S., M.O. Berry, and J.B. Maxwell, "Snowfall Formation," Handbook of Snow: Principles, Processes, Management and Use, ed. Gray, D.M. and D.H. Male, Pergamon Press, New York, NY, pp. 129-152. (1981).

Taylor, D.A., "Sliding Snow on Sloped Roofs," Canadian Building Digest, Division of Building Research, Ottawa, Canada. (1983).

Taylor, D.A., "Snow Loads on Sloping Roofs: Two Pilot Studies in the Ottawa Area," Canadian Journal of Civil Engineering, Vol. 12, No. 2. pp. 334-343. (1985).

Wind Tunnel Modeling of Snow Drifting
Applications to Snow Fences

N. Isyumov[I], M. Mikitiuk,[II] and P. Cookson[III]

ABSTRACT

The similarity requirements for the modelling of snow drifting are much more difficult to satisfy than those needed to obtain a representative modelling of various wind effects on buildings and structures. It is impossible to achieve full dynamic similitude of the snow phase at a reduced geometric scale. As a result, scaled-model studies of snow drifting phenomena invariably only provide approximate similarity with full scale.

This paper examines some of the current modelling approaches to snow drifting using the accumulation of snow around snow fences as an example. A significant body of full-scale observations of drift accumulation at snow fences is emerging and this provides opportunities for comparing model and full-scale data. The results of such studies indicate that model simulations can provide good indications of the equilibrium shapes of drift accumulations around snow fences. The quantitative similarities of time scaling as it affects the drift flux and the rate of snow retention by a snow fence, however, are difficult. This is illustrated by results of model tests carried out in a wind tunnel at different length scales and using different particles.

INTRODUCTION

The experimental work described in this paper has been prompted by the activities of an ASCE Task Committee established to examine the physical modelling of snow drifting and the aeolian transport of sand, soil and dust. To achieve this objective it is essential to examine a number of basic snow drifting situations and to calibrate the effectiveness of various modelling techniques through full-scale comparisons. Two somewhat different but related areas are of interest. The first of these is the question of snow drifting on the ground which affects transportation and is the primary cause of the urban snow hazard. The second is the formation of snow accumulations on roofs. The resulting loads can be significant and tend to govern the cost of low-rise construction in northern parts of the U.S.A. and Canada. The first deals with the movement of snow particles close to the snow surface, largely by saltation and typically only within a few centimetres above the surface. The second involves airborne snow and how it is deposited on roofs during appreciable winds, as well as drifting on more windy portions of roofs. Again saltation is a major effect, however, transport by turbulent diffusion becomes a contributor, as winds at roof level are more turbulent, particularly in urban settings.

I   Manager and Research Director, Boundary Layer Wind Tunnel Laboratory, The University of Western Ontario, London, Ontario, Canada

II   Research Associate, Boundary Layer Wind Tunnel Laboratory, The University of Western Ontario, London, Ontario, Canada

III Former Student, Faculty of Engineering Science, The University of Western Ontario, London, Ontario, Canada

Full-scale data required to evaluate particular physical modelling procedures are not easy to obtain, even for such relatively simple objects as snow fences. Wind and/or water flume models can simulate the effects of individual snowfalls and/or drifting episodes. Such models, however, cannot reproduce accumulation over time, where other processes such as melting, refreezing, compaction, recrystallization, sublimation, etc. come into play and the wind changes both in severity and direction.

Also of interest are inter-laboratory comparisons of experimental techniques which result in different degrees of simulation of both the airflow and the snow phase. Combined with full-scale comparisons, this is expected to lead to an improved understanding of the "minimum" requirements to achieve meaningful model studies of various wind-related engineering and hydrological questions. A motivation here is the emerging trend for codes of practice to accept the results of physical model studies in lieu of code prescriptions. An ASCE manual of practice on wind tunnel model studies of buildings and structures has recently been published (ASCE, 1987). A similar manual dealing with snow-related questions is now envisaged.

OVERVIEW OF MODELLING CRITERIA

A number of detailed reviews of requirements necessary to achieve acceptable similitude of the motion, scour and accumulation of snow particles can be found in the literature (Isyumov, 1971), (Iverson, 1982), (Kind/Murray, 1982), (Irwin/Williams, 1983), (Anno, 1984), (Anno, 1985), (Iverson, 1986), (Kind, 1986). The last of these references is a thorough treatment of the similitude of both falling and drifting snow using both lightweight and heavy model particles in air and in water. A brief summary of the more important requirements for achieving similarity of the flow regime, similarity of airborne particles and similarity of surface particles is briefly summarized below.

Similarity of Flow

Similitude of the model (m) and full-scale flows (p), namely similarity of flow patterns, requires:

i) Geometric similarity of all relevant overall dimensions of objects and their surroundings.

$$\frac{L_m}{L_p} = \lambda_L \tag{1}$$

ii) Similarity of the mean velocity profile of the approach wind.

$$\left(\frac{z_o}{L}\right)_m = \left(\frac{z_o}{L}\right)_p \tag{2}$$

iii) Similarity of the salient characteristics of atmospheric turbulence. In its simplest form this means similarity of turbulence intensity. In the strict sense this means the similarity of the scales of turbulence.

$$I_m = I_p \tag{3}$$

$$\left(\frac{L_{turb}}{L}\right)_m = \left(\frac{L_{turb}}{L}\right)_p \tag{4}$$

iv) Similarity of the influence of the saltation layer on the surface shear stress is achieved by

$$\left(\frac{z_0'}{L}\right)_m = \left(\frac{z_0'}{L}\right)_p \tag{5}$$

Similarity of Airborne Particles

Similitude of model and full-scale particle motions requires similarity of the forces acting on particles and their trajectories. The more important requirements are:

v) Similarity of the gravity forces to fluid or aerodynamic forces. This is achieved by maintaining the similarity of the particle terminal velocity to a characteristic velocity of the flow; namely

$$\left(\frac{W_f}{U}\right)_m = \left(\frac{W_f}{U}\right)_p \tag{6}$$

vi) Similarity of inertia forces of the particle to its gravity forces. This is achieved by maintaining the equality of

$$\left\{\frac{U^2 \rho_s}{L g (\rho_s - \rho)}\right\}_m = \left\{\frac{U^2 \rho_s}{L g (\rho_s - \rho)}\right\}_p \tag{7}$$

For heavy particles, $\rho_s \gg \rho$ and this equality becomes the conventional Froude number, namely

$$\left(\frac{U^2}{L g}\right)_m = \left(\frac{U^2}{L g}\right)_p \tag{8}$$

It has been shown (Isyumov, 1971) that in most situations it is not necessary to model the corresponding Froude number based on particle diameter d. Exaggerating d in relation to L, however, results in a reduction of particle ability to follow rapid fluid velocity variations.

vii) Similarity of particle inertia to fluid inertia forces. This is achieved by maintaining

$$\left(\frac{\rho_s}{\rho}\right)_m = \left(\frac{\rho_s}{\rho}\right)_p \tag{9}$$

This requirement is usually relaxed as most snow particles follow flow fluctuations well.

Similarity of Particles Near the Surface

This most complex aspect of the modelling process requires similarity of particle behaviour near the surface and their entrainment by the airstream. This includes the interaction of fluid, interparticle (cohesive and mechanical) and gravity forces. The scaling of particle bed properties and the entrainment of particles into the airstream remain active, and to some degree, still controversial questions. There is much common ground between snow drift mechanics and other aeolian transport. Basically, it is necessary to ensure satisfactory kinematic similarity of particle paths in relation to the overall model dimensions. In addition to the similarity of the angle of repose and the Reynolds number regime of the aerodynamic particle forces, it is important to maintain the equality of the following:

viii) Similarity between fluid forces, most conveniently expressed by a critical surface shear stress $\rho u_{*_t}^2$, acting on particles of diameter d and the restoring forces, which relate to the action of gravity and are proportional to $(\rho_s - \rho)g\,d^3$. This leads to the requirement,

$$\left(\frac{\rho\,u_{*_t}^2}{(\rho_s - \rho)g\,d}\right)_m = \left(\frac{\rho\,u_{*_t}^2}{(\rho_s - \rho)g\,d}\right)_p \tag{10}$$

This is a densimetric Froude number based on particle diameter. It is difficult to satisfy when the overall geometric scale L_m/L_p is small. Alternative requirements are to satisfy the densimetric Froude number based on overall dimensions, namely

$$\left(\frac{\rho\,u_{*_t}^2}{(\rho_s - \rho)g\,L}\right)_m = \left(\frac{\rho\,u_{*_t}^2}{(\rho_s - \rho)g\,L}\right)_p \tag{11}$$

and to maintain the separate requirement of the threshold velocity ratio

$$\left(\frac{u_{*_t}}{U}\right)_m = \left(\frac{u_{*_t}}{U}\right)_p \tag{12}$$

Of these two parameters, the similarity of the overall Froude number, is usually regarded as the single most important parameter (Iversen, 1982, 1986, 1987). The similarity of the threshold velocity by itself may not be sufficient if Froude number scaling is excessively violated.

ix) Kind's Parameters:

From his work (Kind, 1976, 1986), (Kind and Murray, 1982), Kind suggests that similarity of surface particle forces and their ejection mechanism requires that,

$$\left(\frac{u_{*_t}^3}{2\,g\,v}\right)_m > 30 \tag{13}$$

and

$$\left(\frac{\rho_s}{\rho}\right)_m \geq 600 \tag{14}$$

213

The parameter in Eq. 13 is a roughness-height Reynolds number, as the roughness height of the saltating layer is of the order of $u_*^2/2g$ (Owen, 1964). The requirement of Eq. 14 advocates the use of heavier particles, to achieve a better similarity of particle entrainment.

In the above expressions, symbols L, d, z_0, z_0', L_{turb}, I, W_f, U, u_*, u_{*t}, g, ρ, ρ_s and v respectively represent a characteristic overall dimension, a typical particle size, the roughness length of the surface, the roughness length of the surface during saltation, a characteristic scale of turbulence, the turbulence intensity, the terminal particle velocity, a characteristic velocity of the flow, the friction velocity, the friction velocity at the threshold of particle motion, the acceleration of gravity, the density of the fluid, the density of the particles, and the kinematic viscosity of the fluid.

It is not possible to satisfy all of the above similarity criteria at a reduced geometric scale. Some relaxation and hence "distortion" of the model to full-scale process is therefore unavoidable. The approaches taken by various experimenters differ and are often chosen to provide best fit in an area of interest. Comparisons with full-scale data for such partial or approximate models are essential.

EXPERIMENT

Objectives

Wind tunnel experiments were carried out to examine the snow deposition at a snow fence in tests where the velocity scaling is based on u_{*t}/U similarity while the Froude number scaling is relaxed. In his review (Kind, 1986), Kind suggests that in the simulation of the saltation of snow particles there are distinct advantages in maintaining the roughness-height Reynolds number requirement, Eq. 13, and the minimum density ratio, suggested in Eq. 14. If necessary, Froude number scaling can be relaxed and the velocity scaling be determined by the similarity of the surface threshold velocity, Eq. 12. All of these requirements, namely Eqs. 12, 13 and 14, relate to the characteristics of the model snow material and do not relate the dimensions of the particle trajectories to other overall lengths. Saltation trajectory paths are related to the Froude number. Arbitrary choices of length and time scaling can result in non-similarities between particle motions and the dimensions of the overall process. Therefore there may be significant differences in the shapes and the growth rates of drifts.

Details of Experiment

Tests were carried out to determine the deposition of particles at a Norwegian horizontal-slat snow fence, with a porosity of 0.66. Details of the fence geometry are given in Fig. 1. Tests were made for 3 geometrically-identical fences constructed at length scales of 1:20, 1:40 and 1:70. Experiments for this snow fence, carried out at a length scale of 1:20, have been reported by Kind (Kind and Murray, 1984). Kind used 0.2 mm silica sand, as well as expanded polystyrene particles. Comparisons in this paper are made only with results reported for the 0.2 mm sand. Comparisons are also made with full-scale data for this fence (Croce, 1951).

Experiments were carried out in an open-return boundary layer wind tunnel, set-up as shown in Figure 2. A uniform layer of model particles, 5 mm thick, was spread over the central half of the wind tunnel over a total distance of about 4.9 metres upstream of the model snow fence. For the scale of 1:20, this upstream fetch corresponds to approximately 49 fence heights. The material was continued downstream of the fence. Porous fabric particle traps were located well downstream of the fence. In the

214

experiments, the wind speed was measured at a reference pitot static tube, as shown in Figure 2. Pitot static tubes, mounted at heights of 50, 200 and 400 mm above the particle surface upstream of the fence and away from the centreline, were used to monitor the wind speed during the experiments. Measurements of the vertical profile of the approach flow were made at wind speeds below and above the onset of continuous particle motion.

Three different types of particles were used. These were 0.2 mm silica sand and two commercially available, find-grained cereal particles. These are "wheatlets" which are granular in shape, and small "bran" particles which are flake-like. Properties of these materials are summarized in Table 1. All experiments were carried out at a wind speed corresponding to 1.5 times the critical speed. The critical speed of each material was predetermined by separate observations without the snow fence. Experiments continued for up to 1 hour in some cases. The deposition of material both upstream and downstream of the fence was measured visually using graduated depth markers.

Further details of the experiment, which was carried out as part of Mr. Cookson's thesis, are described in detail elsewhere (Cookson, 1987).

Results

It became clear during the experiment that the 1:20 tests did not have sufficient upstream particle material for obtaining an appreciable deposition around the snow fence. In all tests the particle layer was 5 mm thick. As a result, the 1:20 scale results are not comparable with either the full-scale nor Kind's data. The upstream particle fetch was judged to be sufficient for both the 1:40 and 1:70 tests.

Summaries of the drift profiles, taken along the wind tunnel centreline, are presented in Figures 3 and 4. In Figure 3, data are presented to show results for each material for all 3 tested length scales. Also shown in each case are the full-scale data and Kind's results (Kind and Murray, 1982) obtained with a 0.2 mm sand. In the case of the bran, the 1:70 tests were spoiled and are not reported. Figure 4 shows drift profiles obtained at the same geometric scale for each material tested.

The results for the 3 different length scales, see Fig. 4, indicate that the 1:70 data overestimate the full-scale observations, while the 1:20 tests, as mentioned above, were constrained by the insufficient upstream supply of material. The observed drift profiles for the 1:40 scale fit the full-scale data best. Of the 3 materials, the "bran" and the "wheatlets" provide the better agreement at this scale. This is also evident from Fig. 3, where the data are grouped by different materials. For sand, a better scale may be somewhat between 1:40 and 1:70. Wheatlets appear to provide the better fit of both shape and drift magnitude. The data for bran are inconclusive as results are available only for the 1:40 scale.

In all cases the drift shapes are somewhat different from equilibrium full-scale drifts where the maximum depth of the leeward drift is typically at $x/H \simeq 5$ to 8. This study shows a downstream distance of x/H of approximately 2 to 3 to the maximum drift height. Some of the data from this study are plotted to examine the dependence of the location of the maximum drift on Froude number. The data, shown in Figure 5, follow Iversen's format (Iversen, 1986). The sand data are different from those reported by Kind (Kind and Murray, 1982). The data shown for bran appear to be in better agreement with data from Iversen and Tabler suggesting that drift shapes are more like commonly reported ones.

While the measured values of W_f and u_{*t} appear to be consistent with those for the other two materials, see Table 1, they are significantly higher than $W_f = 0.81$ m/s and $u_{*t} = 0.15$ m/s, reported for the same 0.2 mm sand by Kind (Kind and Murray, 1982). Both W_f and u_{*t} measurements are difficult to make and it is planned to repeat these experiments.

Effect of Different Scaling

(1) Drift Geometr_i_

A summary of the maximum depth of the leeward drift $(y/H)_{max}$ and its location (x/H) is given in Table 2, along with similar data for the full-scale drift profile and Kind's data. Also shown are values of u_{*t}. This experiment was carried out with $u_* = 1.5u_{*t}$. Values of u_{*t} are of the same order but there are large variations in the Froude number. Nevertheless, the variation of the position of the maximum drift depth is not large. Comparisons of $(y/H)_{max}$ in this case are less justified as the time scaling of the drift formation is not necessarily similar. Apart from the data for bran, the location of $(y/H)_{max}$ is similar in all cases. This general similarity of drift shape over a wide range of Froude number is encouraging. It suggests that particle accumulations in the influence zone of bluff bodies or flow discontinuities are primarily shaped by the local aerodynamics. The particle saltation path length "ℓ", which depends on Froude number plays a lesser role as long as "ℓ" is small in comparison with characteristic dimensions of the drift and the properties of the approach flow are determined by the roughness of the terrain rather than the shear stress due to the saltation layer. For example in the case of a snow fence, the downstream extent of the aerodynamic shelter zone L_s is typically $15\,H < L_s < 30\,H$, depending on the fence solidity and the roughness of the approach terrain. Even for the 1:70 scale simulation $L_s \gg \ell$. However, proper modelling of the mean and turbulent characteristics of the approach flow is important in order to representatively simulate the shelter effects of the snow fence.

The significant differences between the data for bran and the wheatlets, which have the same u_{*t} and u_*^2/gH, and similar particle Froude numbers, raise questions about the relative importance of other parameters, including ρ_s/ρ and particle shape.

(2) Deposition Rates

Information on time scaling and hence the overall dynamic similitude can be obtained from comparisons of deposition rates of the drifts formed behind the snow fence. The rate of change of particular drift profiles was determined by evaluating the change in cross-sectional area between observation times. Figure 6 shows plots of the deposition rate q, normalized to examine the importance of different scaling assumptions. The normalized deposition rates are plotted against non-dimensional time Tu_*/H, where T is the time from the start of the experiment.

Top Graph

Here the volumetric deposition rate q is normalized by Hu_* which is proportional to the volumetric flow rate per unit "lane" or unit width perpendicular to the direction of the approach flow. While there is considerable scatter, the data for the different materials, except for bran, and for the two length scales tend to follow a similar trend. A collapse of the various curves would suggest that the rate of change of the drift volume is identical and that the scaling of the drift geometry is not sensitive to differences in saltation characteristics but is determined by scaling H and the approach flow field. The largest differences occur early in the drift development and are in part

216

attributed to differences in deposition in the immediate vicinity of the fence. With bran a scoured zone developed immediately upstream and downstream of the fence and was not filled in until later in the test.

Middle Graph

This graph shows the mass deposition rate of the drift $\rho_s\,q$, normalized by $\rho\,Hu_*$ which is proportional to the mass flow rate per unit lane of the approach flow. Note ρ_s is taken as the bulk density of the drift. The agreement between the various data is not as good as for the strictly "kinematic" scaling implied by similar volumetric deposition rates.

Lower Graph

Here the time rate of change of the mass of the drift is normalized by the potential particle mass transport rate within the salation layer whose depth is proportional to u_*^2/g. While the data for each of the length scales appear to be in better agreeement, there is a noticeable difference in the trends from the 1:40 and 1:70 scale tests. The potential mass transport rate within the saltation layer remains the same for a particular material while the drift magnitude and its rate of change depend on H.

CONCLUDING REMARKS

The drift formation at a snow fence was studied with three (3) different materials and at three (3) geometric scales. The scaling of the wind speed was based on maintaining equality of the threshold drift speed u_*t/U and allowing the Froude number u_*^2/gH to vary. Notwithstanding the experimental difficulties with the largest scale (1:20), the overall similarity of the drift deposits is encouraging. The findings of this study suggest that drift formation in the influence zone of an obstacle, such as a snow fence, is primarily determined by the local aerodynamics. These are sensitive to the characteristics of the approach flow field, which therefore must be representatively modelled. Similarity of the saltation path length however is expected to become important in situations where the saltation length is no longer small in comparison with characteristic drift dimensions.

Simple kinematic scaling of deposition rates of the drift appears to give best agreement for the scales and materials examined in this study. Nevertheless, some of the differences warrant further attention. The results of tests for "bran" particles, carried out at the same u_*t/U_H and u_*^2/gH as those for "wheatlets", are sufficiently different to suggest that other parameters such as ρ_s/ρ and particle shape and initial conditions at the snow fence may play a part. Clearly more detailed and matched comparisons with full-scale data are needed to lend greater confidence to the modelling process.

REFERENCES

American Society of Civil Engineers, 1987, "Wind Tunnel Model Studies of Buildings and Structures," ASCE Manual and Reports on Engineering Practice No. 67., 1987.

Anno, Y., 1984, "Requirements for Modeling of a Snowdrift," Cold Regions Sci. Technology, Vol. 8, 1984.

Anno, Y., 1985, "Froude Number Paradoxes in the Modelling of a Snowdrift," Cold Regions Sci. Technology, Vol. 10, 1985.

Cookson, P., 1987, Model Study of Drift Accumulation of a Snow Fence, University of Western Ontario B.E.Sc. Thesis, London, Ontario, Canada, 1987.

Croce, K., 1951, in Snow Studies in Germany, National Research Council of Canada Tech. Memo. 20 (DBR), Ottawa, Ontario, Canada.

Irwin, P.A. and C.J. Williams, 1983, "Application of Snow-Simulation Model Tests to Planning and Design," Proc. Eastern Snow Conference, Vol. 28, Toronto, Ontario, June 1983.

Isyumov, N., 1971, An Approach to the Prediction of Snow Loads, University of Western Ontario Ph.D. Thesis, London, Ontario, Canada, 1971.

Iversen, J. D., 1980 a, "Drifting Snow Similitude - - Transport Rate and Roughness Modelling," Journal of Glaciology, 26, 393-403, 1980.

Iversen, J. D., 1981, "Comparison of Wind-Tunnel Model and Full-Scale Fence Drifts," Journal Wind Engineering and Industrial Aerodynamics, 8, 231-249, 1981, Elsevier Scientific Publishing Company, Amsterdam.

Iversen, J.D., 1982, "Small-Scale Modeling of Snowdrift Phenomena," Proc. Int. Workshop on Wind Tunnel Modeling Criteria in Civ. Eng. Applications, Gaithersburg, Marlyland, April 1982, Cambridge Univ. Press.

Iversen, J.D., 1986, "Small Scale Wind Tunnel Modeling of Particle Transfer - Froude Number Effects," Proc. 17th Annual Geomorphology Symposium, Guelph, Ontario, 1986.

Iversen, J.D., 1987, "Froude Number Effects in Sediment Transport," 7th Int. Conf. on Wind Engineering, Vol. 3, Aachen, West Germany, 1987.

Kind, R.J., 1976, "A Critical Examination of the Requirements for Model Simulation of Wind-Induced Erosion/Deposition Phenomena Such as Snow Drifting," Atmos. Environment, Vol. 10, 1976.

Kind, R.J. and S.B. Murray, 1982, "Saltation Flow Measurements Relating to Modelling of Snow Drifting," J. Wind Engineering and Ind. Aerodynamics, 10, 89-102, 1982, Elsevier Scientific Publishing Company, Amsterdam.

Kind, R.J., 1986, "Snowdrifting : A Review of Modeling Methods," Cold Regions Science and Technology, 12 (1986), Elsevier Scientific Publishing Co., Amsterdam.

Tabler, R. D., 1980 a, "Geometry and Density of Drifts Formed by Snow Fences," Journal of Glaciology, 26, 405-419, 1980.

Tabler R. D., 1980 b, "Self Similarity of Wind Profiles in Blowing Snow Allows Outdoor Modelling," Journal of Glaciology, 26, 421-434, 1980.

Tabler, R. D., 1985, Personal communication.

Wuebben, J.L., 1978, "A Hydraulic Model Investigation of Drifting Snow", CRREL Report 78-16, U.S. Army Cold Regions and Engineering Laboratory, Hanover, N.H.

TABLE 1 MODEL SNOW PROPERTIES

Parameter	Silica Sand	Wheatlets	Bran
● Typical particle diameter d (mm)	0.2	0.3	0.4
● Density ρ_S (Kg/m^3)	1600 *	670 *	340 *
● Density Ratio ρ_S/ρ**	2100	520	265
● Angle of Repose(^{O})	33	35	39
● Drift threshold u_{*t} (m/s)	0.36	0.28	0.28
● Falling Velocity W_f (m/s)	2.1	1.03	1.32
● W_f/u_{*t}	5.8	3.7	5.1
● Roughness Height Reynolds number (Kind's parameter) $u_{*t}^3/2g\nu$	160	75	75

*   Bulk density
** These are significantly higher if based on the actual rather than bulk density of the material.

TABLE 2

OBSERVED DRIFT DIMENSIONS FOR DIFFERENT SCALING

MATERIAL	u_{*t} m/s	Geometric Scale 1:20			Geometric Scale 1:40			Geometric Scale 1:70		
		u_*^2/gH	$(y/H)_{max}$	x/H to $(y/H)_{max}$	u_*^2/gH	$(y/H)_{max}$	x/H to $(y/H)_{max}$	u_*^2/gH	$(y/H)_{max}$	x/H to $(y/H)_{max}$
Prototype snow	0.15	0.003	0.75	2.9	–	–	–	–	–	–
Kind (Kind and Murray, 1982) (using 0.2mm sand at λ_L = 1:20)	0.15	0.051	0.75	2.9	–	–	–	–	–	–
Sand (this study)	0.36	0.30	0.20	3.0	0.60	0.50	2.8	1.03	1.00	2.0
Wheatlets (this study)	0.28	0.18	0.25	2.5	0.36	0.78	2.8	0.62	1.00	2.5
Bran (this study)	0.28	0.18	0.45	4.9	0.36	0.74	4.0	0.62	–	–
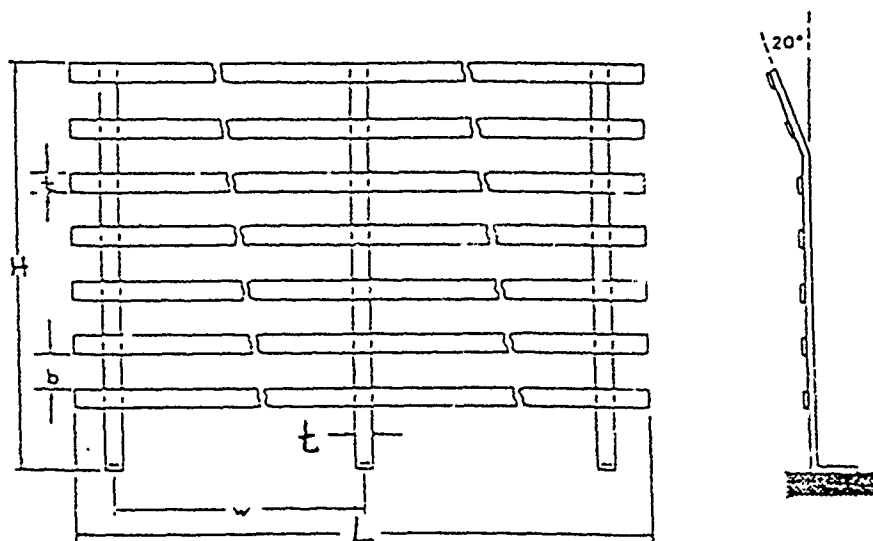
- ALL DIMENSIONS IN mm
- SOLIDITY· 0.34

(o) NORWEGIAN-TYPE FENCE

Length Scale	Overall Length L (mm)	Height H (mm)	Slot Spacing b (mm)	Slot Width t (mm)	Distance Between Posts w (mm)
1:20	1110	101	8.75	4.75	222.0
1:40	1110	50	4.4	2.4	111.0
1:70	1110	29	2.5	1.4	63.5

FIG. 1   DETAILS OF MODELS OF NORWEGIAN – TYPE SLAT SNOWFENCE
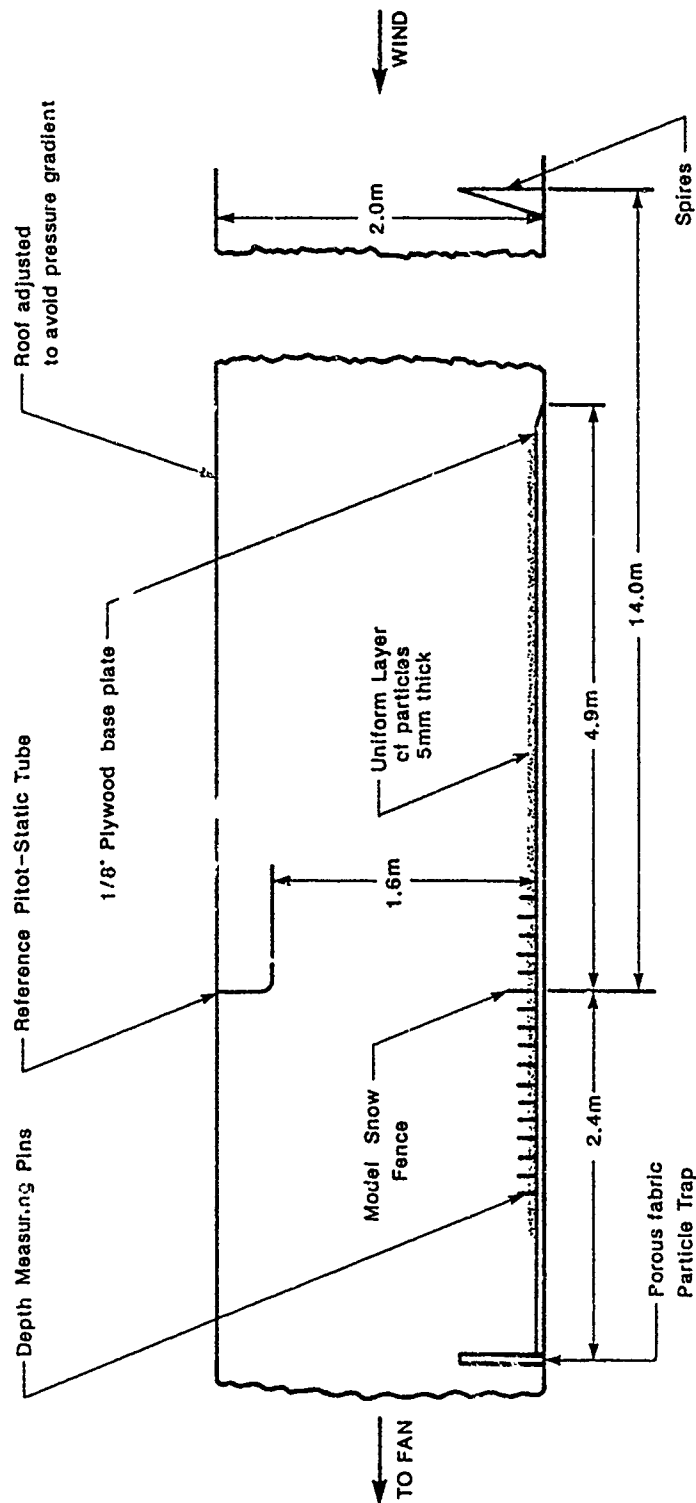
FIG. 2   **SCHEMATIC OF EXPERIMENTAL SETUP IN BLWTL'S OPEN RETURN BOUNDARY-LAYER WIND TUNNEL.**

KEY

▭——▭		FULL SCALE
▭- - - -▭		KIND
▭— — —▭		1:20
▭—·—▭		1:40
▭······▭		1:70
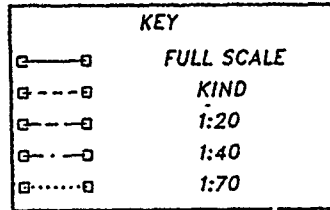
COMPARISON OF SCALES FOR SILICA SAND
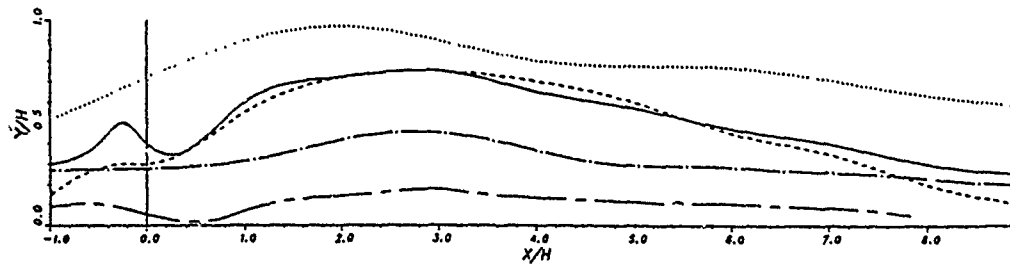
COMPARISON OF SCALES FOR WHEATLETS
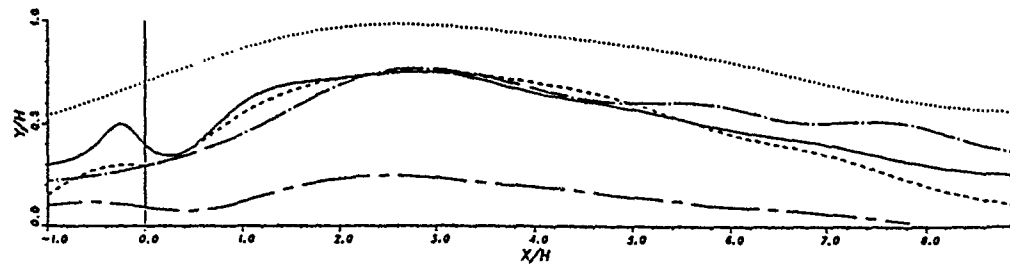
COMPARISON OF SCALES FOR BRAN
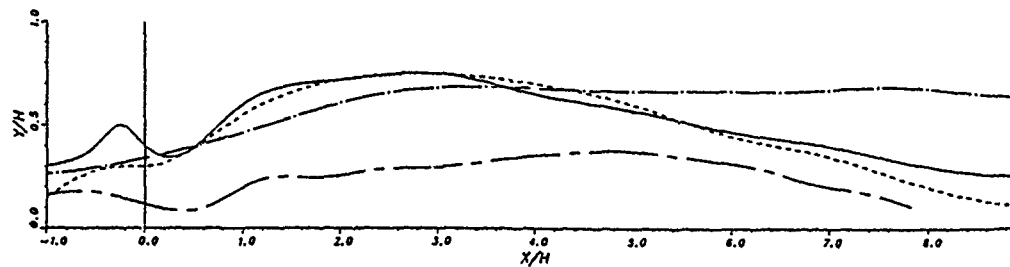
FIG. 3   DRIFT PROFILES OBTAINED WITH DIFFERENT MODEL SNOW PARTICLES FOR DIFFERENT LENGTH SCALES

223

KEY

▭——▭	FULL SCALE
▭– – –▭	KIND
▭— — —▭	WHEATLETS
▭— · —▭	SAND
▭······▭	BRAN

DRIFT PROFILE PRODUCED BY MODEL FOR 1:20 SCALE

DRIFT PROFILE PRODUCED BY MODEL FOR 1:40 SCALE

DRIFT PROFILE PRODUCED BY MODEL FOR 1:70 SCALE
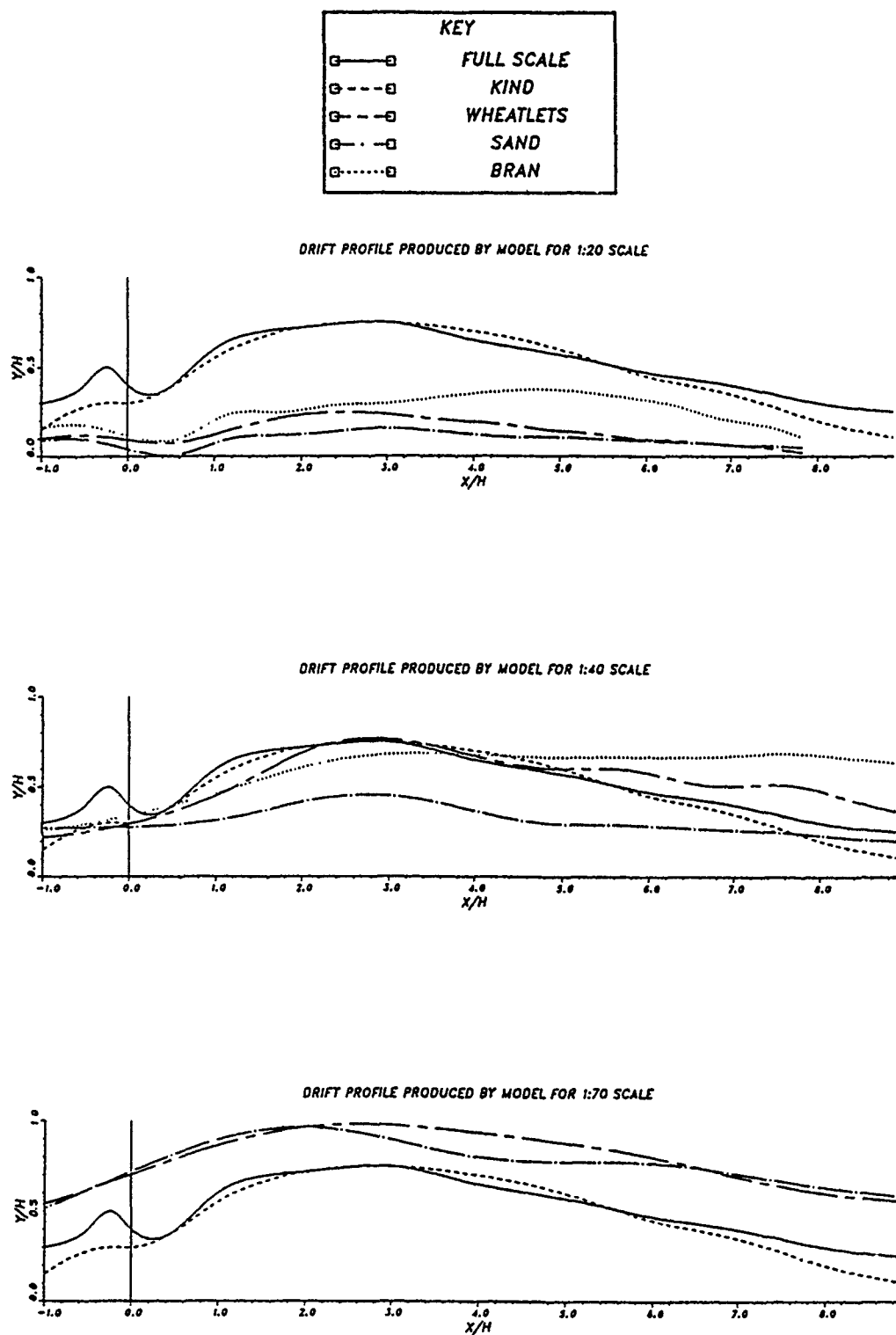
FIG. 4   DRIFT PROFILES OBTAINED AT DIFFERENT LENGTH SCALES WITH DIFFERENT MODEL SNOW PARTICLES

224
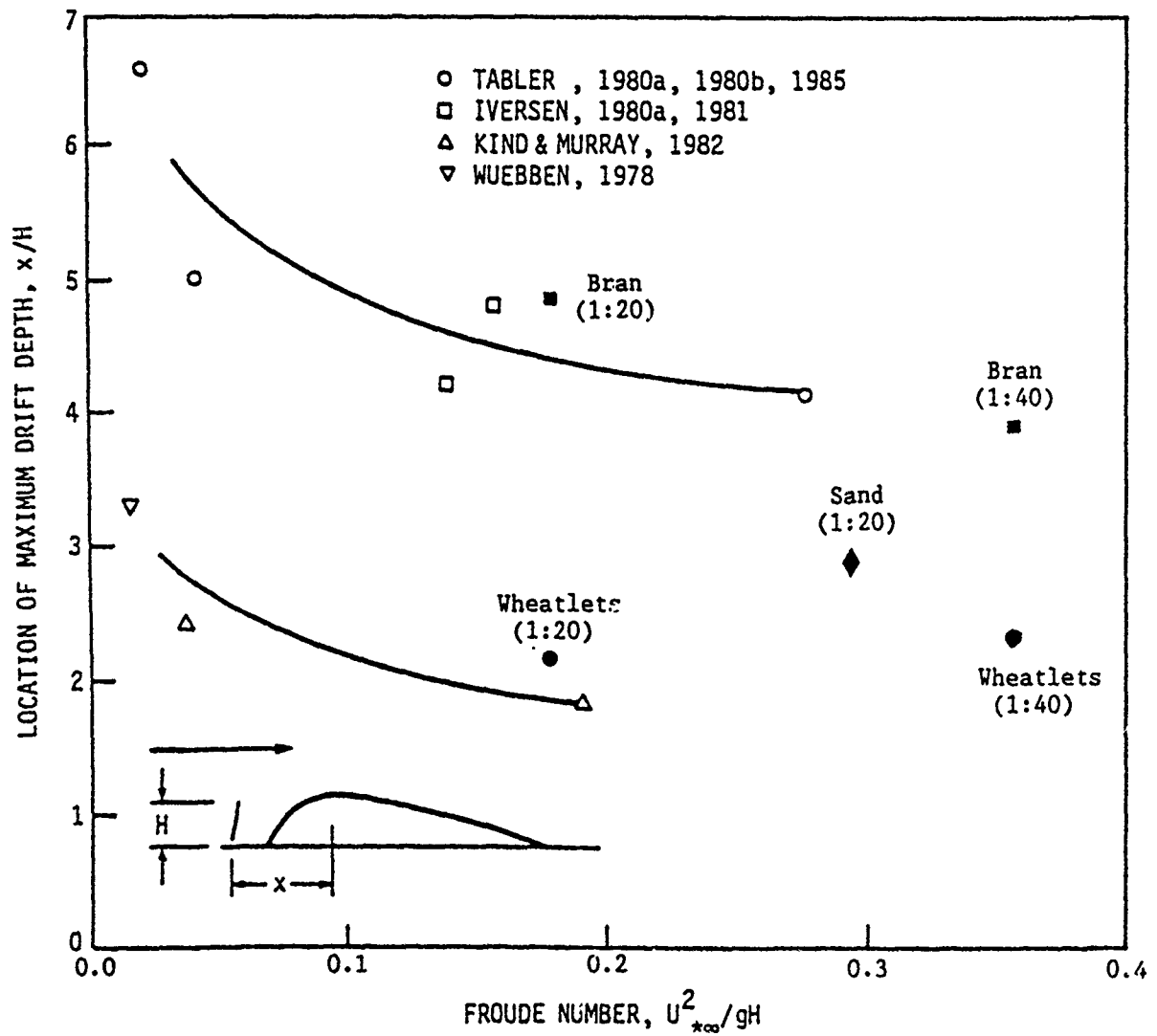
FIG. 5   COMPARISON OF THE LOCATION OF MAXIMUM DRIFT DEPTH WITH OTHER DATA (AFTER IVERSEN, 1986)

Mass Flow Rate Scaling :

₵ of Drift Profile
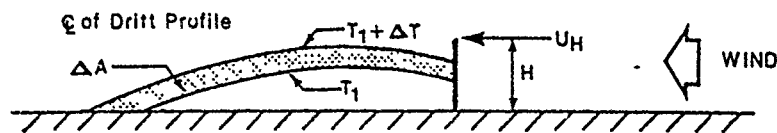
Volume Deposition Rate Per Unit

Time Per Unit Width : $q = \dfrac{\Delta A}{\Delta T}$ $[m^2/s]$

Scale / Material	1:40	1:70
Wheatlets	——	·······
Sand	– – –	– · – ·
Bran	–·–·–	

VOLUMETRIC DEPOSITION

MASS DEPOSITION
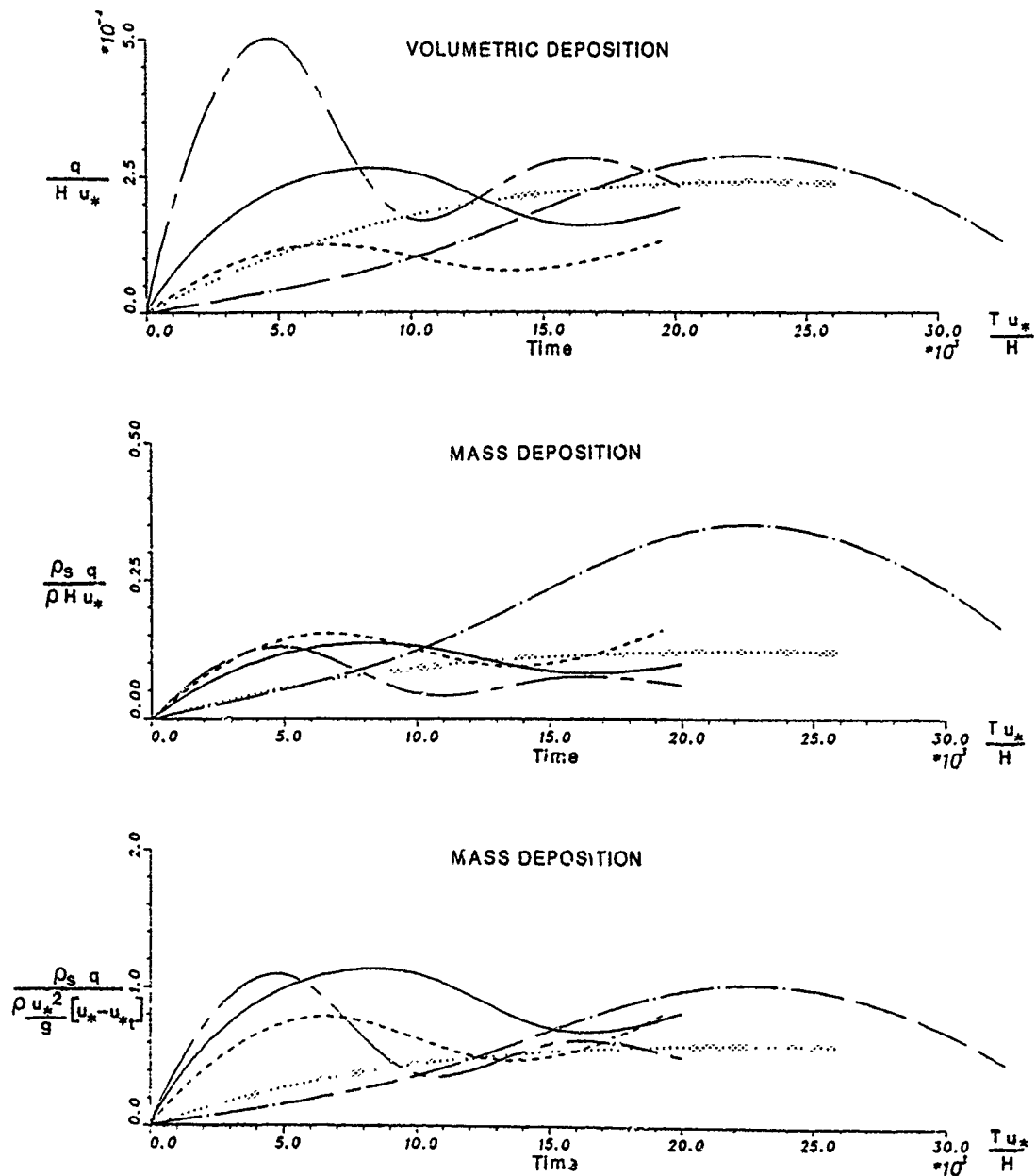
MASS DEPOSITION

FIG. 6   COMPARISON OF DEPOSITION RATES BEHIND SNOW FENCE

Modeling Drift Geometry in Wind Tunnels

James D. Iversen[1]

ABSTRACT

The aeolian wind tunnel is a useful instrument for studying salta-
tion physics as well as for modeling drift geometry at small scale.
For small-scale modeling, it is shown that, although the dimen-
sionless deposition or deflation rate may be a function of several
other dimensionless parameters, the Froude number is one of the
more important ones. Examples are presented illustrating the
dependence of dimensionless deposition or deflation rate or drift
geometry on the Froude number, density ratio, and the ratio of
wind speed to threshold wind speed.

INTRODUCTION

The small-scale modeling of sand-transport phenomena is indeed a complex
area of study. Wind-tunnel modeling of control structures has sufficient
advantages over field testing to warrant some discussion of the realism
of such experiments. Control of experimental factors, such as wind direction
and duration, is a primary advantage. It also is advantageous to be able
to perform many experiments over a short period of time and even to alter
particle properties by using different grain materials.

Maintaining similitude for modeling at small scale the effects of
blowing particles of dust, sand, or snow is a problem because of the large
number of variables. It is important to arrange the variables in dimen-
sionless groups (Iversen 1982). In a true model, these parameters must
all have the same value in the model as in full scale, but because this
is impossible, it is necessary to abandon the attempt at a true model.
The only way it is possible to obtain realistic quantitative (and perhaps
also qualitative) results for a distorted model is to vary the degree of
distortion in order to facilitate extrapolation to full scale. The degree
of distortion is varied by changing the experimental values of the dimen-
sionless parameters as much as possible by changing particle density and
diameter, wind speed, and model scale. In addition, interpretation of
results is aided by grouping the dimensionless parameters by theoretical
means in order to reduce the number of variables.

Effects of Froude Number and Density Ratio

An example experiment has been described previously (Iversen 1980)
which has been used to determine the snowdrift deposition rate associated
with an interstate highway grade separation structure. The data for mass
deposition rate from ten experiments are illustrated in Figure 1. It has

_____

I. Professor and Interim Chairman, Dept. of Aerospace Engineering, Iowa
    State University, Ames, IA 50011.

been shown previously (Iversen 1987) that the functional curve fit shown is a closer fit to the data than by using either the Froude number u_*^2/gH or the densimetric Froude number $\rho u^2/\rho_p\, gH$ alone as a correlating parameter. This kind of functional relationship enables one to estimate full-scale deposition rates from model scale time-dependent measurements. The specific function is model dependent.
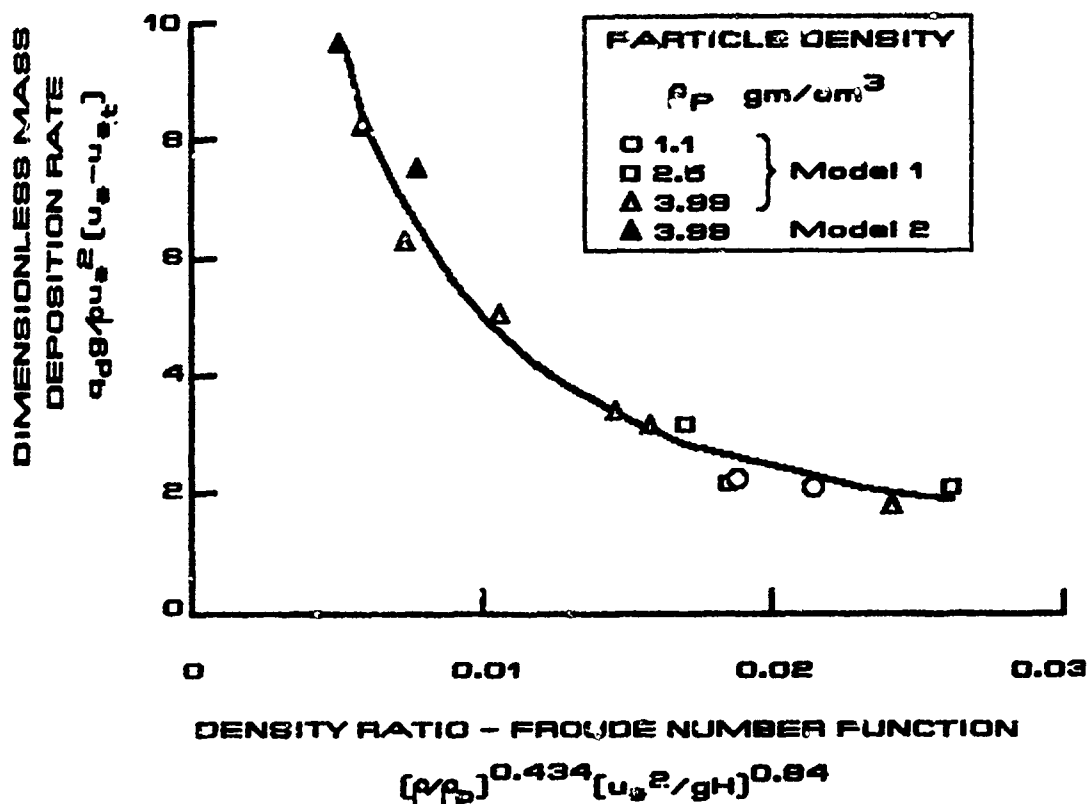
Figure 1. Rate of deposition of simulated snow on a model roadway, as a function of density ration Froude number parameter (Iversen 1982)

Figure 1 illustrates that the drift evolution rate is a function of more than one parameter. More generally,

$$\frac{D(A_d/L_r^2)}{D(u_*t/L_r)} = \frac{\rho u_*^2}{\rho_p gH} = f\left\{\frac{u_*}{u_{*_t}}\, ,\ \frac{u_*^2}{gH}\, ,\ \frac{z_o}{H}\, ,\ \frac{z_o'}{H}\, ,\ \frac{U_F}{u_{*_t}}\, ,\ \frac{u_*L}{v}\, ,\ \frac{\rho}{\rho_p}\, ,\ \text{geometry}\right\} \quad \text{Eq. 1}$$

This equations allows for the possibility of vertical geometric distortion and uses Jensen's (1958) criterion for normal roughness modeling. Usually not all of the full-scale values of these parameters can be matched in the model. The saltation wind tunnel model is thus distorted. By varying particle size and density, model speed, scale, and possibly vertical distortion, a range in degree of distortion can result so that full-scale predictions can be made. The effects of distortion become particularly serious, however, if small-scale features such as surface ripples become

large enough to obscure or interfere with gross drift geometry associated
with important topographic features of the model. Since it is easier to
measure wind speed than surface friction speed, it may be convenient to
replace the u_* and u_{*_t} in most of the factors in the equation with the
reference wind speeds at reference height H, i.e., U and U_t. For obstructions
having height only a fraction of the saltation layer depth, the density
ratio ρ/ρ_p seems to be one of the important separate functional parameters.

Effect of Froude Number and Model Geometry

Two of the important parameters in the equation are the speed ratio
u_*/u_{*_t} (Anno 1984) and the Froude number u_*^2/gH (Tabler 1980). For modeling
snow, particularly falling snow, the particle parameter U_F/u_{*_t} (or U_F/u_*)
is of significance, since the portion of the material carried in suspension
relative to the total mass transport is a function of this ratio.

The effects of speed ratio appear to be most important when the wind
speed is very near the threshold of motion (Iversen 1987). The effect
of Froude number has been approximately calculated for drift deposition
windward of forward facing steps and leeward of porous control barriers.
The effect of Froude number for the forward facing step is shown in Figure
2.
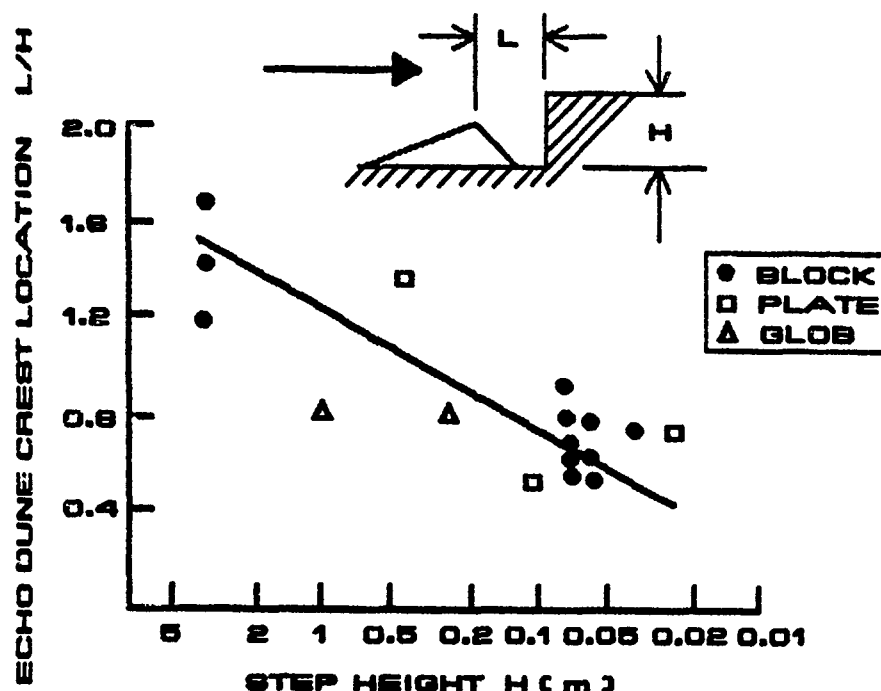
Figure 2. Experimental data for the echo dune crest relative
stand-off distance as a function of step height.
The corresponding Froude numbers would increase to
the right as the step height decreases.

A separated flow region is formed upwind of the step, which causes
an upwind flow near the surface just windward of the step base (Tsoar 1983).
Particles are thus blown upwind near the base, and an echo dune is formed
some distance upwind of the base. The location of the dune crest is due
not only to the step geometry but also to the value of Froude number.
For the larger Froude numbers (higher wind speed or smaller step height),
the trajectories of the particles blown from upwind penetrate relatively
farther into the low-speed area near the separation point (Owen 1980) and
the dune crest forms relatively closer to the step. This is clearly illus-
trated in Figure 2, where the trend is toward smaller relative stand-off
distance L/H for smaller steps. The data scatter is due partly to lack
of knowledge of the wind speeds (Iversen 1987) and partly due to variations
in step geometry (step geometry representing data in the figure is for
various shapes, some of which approach a two-dimensional shape).

A series of wind tunnel experiments has been initiated for the purpose
of testing a variety of prismatic and cylindrical model shapes. Preliminary
results for the cylinders indicate that the windward stand-off erosion
depth increases with an increase in cylinder height-diameter ratio. On
the other hand, leeward erosion far downstream is more pronounced for smaller
values of the height-diameter ratio.

There exists a leeward vortex system, probably shed from the top of
the obstruction which persists for a long distance downwind. For a tall
cylinder, this vortex system might never come close enough to the surface
to much affect particle transport. For the broad, short cylinder, however,
this vortex system is relatively closer to the surface and causes alternate
rows of deposition and erosion which has been observed for many diameters
downwind of the obstruction. The erosion capability downwind of the cylinder
increases with decrease in aspect ratio, an opposite trend to the windward
erosion. A center-line cross-section of the drift associated with a 6
cm cube is shown in Figure 3.
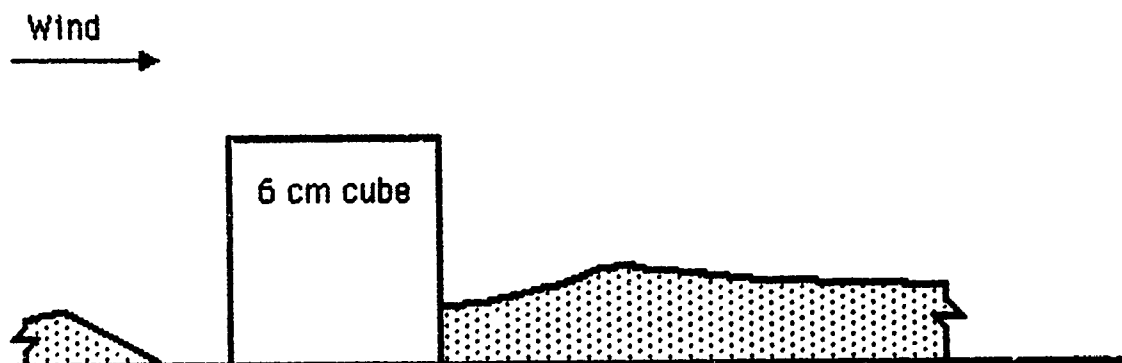
Figure 3.   The windward vortex creates the echo dune
            and the windward moat as shown. Net deposition
            occurs immediately downwind of the cube.

CONCLUSIONS

The aeolian wind tunnel has proven to be a useful instrument not only for investigating the physics of the saltation phenomenon, but also for modeling at small scale topographic control of drift conformation. For quantitative extrapolation to full scale, however, it is necessary to run a series of experiments through various degrees of model distortion in order to determine the effect of that distortion.

ACKNOWLEDGMENTS

REFERENCES

Anno, Y., 1984, "Applications of Anno's modeling conditions to outdoor modeling of snowdrifts," Cold Regions Science & Technology, 9(2), 179-181.

Iversen, J. D., 1980, "Drifting snow similitude--transport rate and roughness modeling," Journal of Glaciology, 26, 393-403.

Iversen, J. D., 1982, "Small-scale modeling of snow drift phenomena," Wind Tunnel Modeling for Civil Engineering Applications, Cambridge University Press 522-545.

Iversen, J.D., 1987, "Wind tunnel modeling requirements for shelterbelt and topographic drift geometry," Preprint, Inernational Seminar on the Integrated Control of Land Desertification, Lanzhou, People's Republic of China.

Jensen, M., 1958, "The model-law for phenomena in natural wind," Ingeniøren, 2, 121-128.

Owen, P. R., 1980, "The physics of sand movement," Workshop on Physics of Desertification, International Centre for Theoretical Physics, Trieste, Italy.

Tabler, R. D., 1980, "Self-similarity of wind profiles in blowing snow allows outdoor modeling," Journal Glaciology, 26, 421-434.

Tsoar, H, 1983, "Wind tunnel modeling of echo and climbing dunes (Fig. 3,5)," M. E. Brookfield and T. S. Ahlbrandt, eds., Eolian Sediments and Processes, Elsevier, Amsterdam, 247-259.

Cold Room Studies for Snow and Ice Control on Buildings

Michael F. Lepage[1] and Colin J. Williams[2]

ABSTRACT

The paper describes a technique of testing snow and ice control devices for sloped surfaces before they are implemented in the field. A full scale mock-up of a section of the sloped surface is tested in a refrigerated room. The room is 6.0m by 3.6m by 2.4m and is equipped to simulate the temperature and snowfall conditions of actual snow storms. A spray nozzle, air compressor, air cooler and water pump produce simulated snow at a rate of up to 0.035m³/min. As an example, the paper presents a case study of a rail designed to retain snow on a 45° slope. The initial design did not effectively retain the snow. The rail had too much contact with the building surface and was warmed to the melting point by heat escaping from inside. Melt water then lubricated the surface and allowed snow to creep over the rail. Snow also extruded through slots in the rail and formed icicles. These problems were solved by mounting the rail on insulated spacers to detach it from the building surface and keep it cold. This and other case studies have led to general recommendations for snow rails and other snow control devices.

INTRODUCTION

The trend toward sloping roofs on high-rises, malls, schools and other structures has increased the risk of sliding snow or ice in many North American cities. The following are examples of the problems that can occur.

(1)   On a sunny day, the underside of a snowdrift on the sloped roof of a New York building reaches the melting point. The snow loses its adhesion to the roof because of melting, slides off and crushes a van parked on the street below.

(2)   Water from snow melting on the sloped roof of a Philadelphia high-rise freezes onto a window washing rail, forming icicles. The icicles fall, damaging parked cars.

(3)   Snow on the sloped window sills of a Toronto building hardens because of alternating freeze-thaw effects. Melting on a sunny day causes dozens of the hardened chunks of snow to slip off the sills, threatening pedestrians below.

---

1. Air Quality and Climatology Specialist, Rowan Williams Davies & Irwin Inc., Guelph, Ontario.

2. Principal, Rowan Williams Davies & Irwin Inc., Guelph, Ontario.

(4)   An ice storm in Dallas forms a sheet of ice on the sloped surface of a high-rise, the ice falls off the slope, killing a pedestrian.

Fortunately, a number of devices are available for preventing such events. If these devices are not carefully designed, however, failure or undesirable side effects will result.

This paper describes a technique for testing snow and ice control devices before they are implemented. The technique involves testing a detailed, full scale mock-up of a sloped roof. The tests are conducted in a refrigerated room, equipped to simulate the temperature conditions and snowfall of a heavy storm. The object is to recreate the problem and evaluate various control devices (e.g. retaining fences, heat tracing, etc.). A case study of a rail designed to prevent snow slide-off on a specific section of sloped roof provides the backdrop for the discussion.

GENERAL CONCEPTS

The two mechanisms causing snow or ice to fall from a sloped building surface are slide-off and wind lift-off. In the case of slide-off, the forces involved are gravity and surface adhesion. Sliding occurs when the former overcomes the latter. In the case of lift-off, gravity and surface adhesion are both overcome by wind suction forces.

A flat, dry layer of snow or ice has so much adhesion to the surface that it will rarely experience either slide-off or lift-off. If the underside of the layer starts to melt, however, the lubricating effect of the liquid film causes the layer to move down the slope. Depending on the angle and roughness of the slope, the movement may vary from a slow creep to a rapid slide. On a very rough surface (i.e. a fluted metal roof or a glass slope with exposed mullions), the layer may take hours or even days to fall over the edge.

For lift-off to occur, the layer must be free of adhesion and must also be able to experience a wind suction force. The existence of a wind suction implies there is greater static pressure beneath the layer than above it. This can occur only if there is an air space beneath the layer. The two most common circumstances under which a lift-off can occur are when the layer creeps over an edge to form an overhang, and when it accordions against an obstruction (e.g. a mullion), forming an air pocket underneath. In both cases, the snow or ice layer experiences both melting and creep before lifting off.

Thus, slide-off and lift-off generally do not take place until the layer has undergone melting. This invariably happens when the outside air temperature reaches 0C (32F). It can also happen at lower temperatures because of heat escaping from the building interior or absorption of solar radiation. The minimum temperature for melting depends on the thermal insulation of the building envelope, the thickness of the snow or ice layer, the density of the layer and the amount of incoming solar radiation. Lepage and Schuyler (1988) give a further description of the processes of heat transfer responsible for melting.

Control of slide-off and lift-off is generally achieved by one of two approaches:

(a)   the building surface is designed to encourage sliding; slide-off of a single, large layer of snow or ice is then replaced by repeated slide-off of small, insignificant layers;

(b)   The bottom of the slope is fenced off to prevent slide-off, and the layer of snow or ice is melted away before experiencing lift-off.

The first approach consists of making the building surface very smooth and letting plenty of heat escape from inside. On a smooth surface, the relatively low insulation value of double glazing usually allows enough heat flow to make this approach effective. Even small obstacles on the surface, however, such as 3mm high mullions can impede the sliding process.

In the second approach, the heat escaping from the inside is often sufficient to melt away the snow or ice in a reasonable amount of time. In some cases, however, additional heat must be applied. Whenever melting at outside temperatures below 0C occurs, the potential exists for water to freeze onto cold surfaces (e.g. eaves, window-washing rails, mullions, etc.). Icicles will then form. In this case, either heat must be applied to the cold surfaces or drainage must be provided to prevent the melt water from reaching the cold surfaces.

CASE STUDY

The tests were designed and conducted by Rowan Williams Davies & Irwin, Inc. of Guelph, Ontario. The object was to evaluate a snow rail designed to control an existing problem with sliding snow on sloped glass surfaces of a large commercial building.

The refrigerated room, shown in Figure 1, was located at the Canada Centre for Inland Waters at Burlington, Ontario. The room was 6.0m long, 3.6m wide, 2.4m high, and had an adjustable temperature ranging from -30C to +15C. Snow was produced by a nozzle attached to a moveable frame, adjustable from 0.9m to 1.9m above the floor. Air, on its way to the nozzle, passed through a 10HP compressor, a 1.0m³/min dryer, a 1.0m³/min cooler and was mixed with water from a 0.75HP water pump (Environment Canada, 1982). The fine water droplet mist, produced when this mixture was ejected at the nozzle, converted to snow crystals as it approached the mock-up. The rate of snow production was adjustable from 0.007m³/min to 0.035m³/min.

Figure 2 shows the mocked-up section of sloping roof. The mock-up was approximately 2.4m wide and 2.4m high, and resembled the actual roof down to the smallest details of the glass, mullions, other structural members between the panes, caulking, weather stripping, spandrel insulation, et cetera. Figure 3, showing a cross-section of a mock-up mullion, gives an indication of the level of detail involved. Space heaters inside the mock-up simulated the interior temperature of the building.

Four test configurations were examined:

(1)   a sloped surface of sealed double glass and no rail;

(2)   same as (1) but with an initial design of snow rail at the base of the slope (Figure 2);

(3)   a sloped surface of insulated spandrel glass, with the initial design of rail;

(4)   same as (2) but with a modified rail.
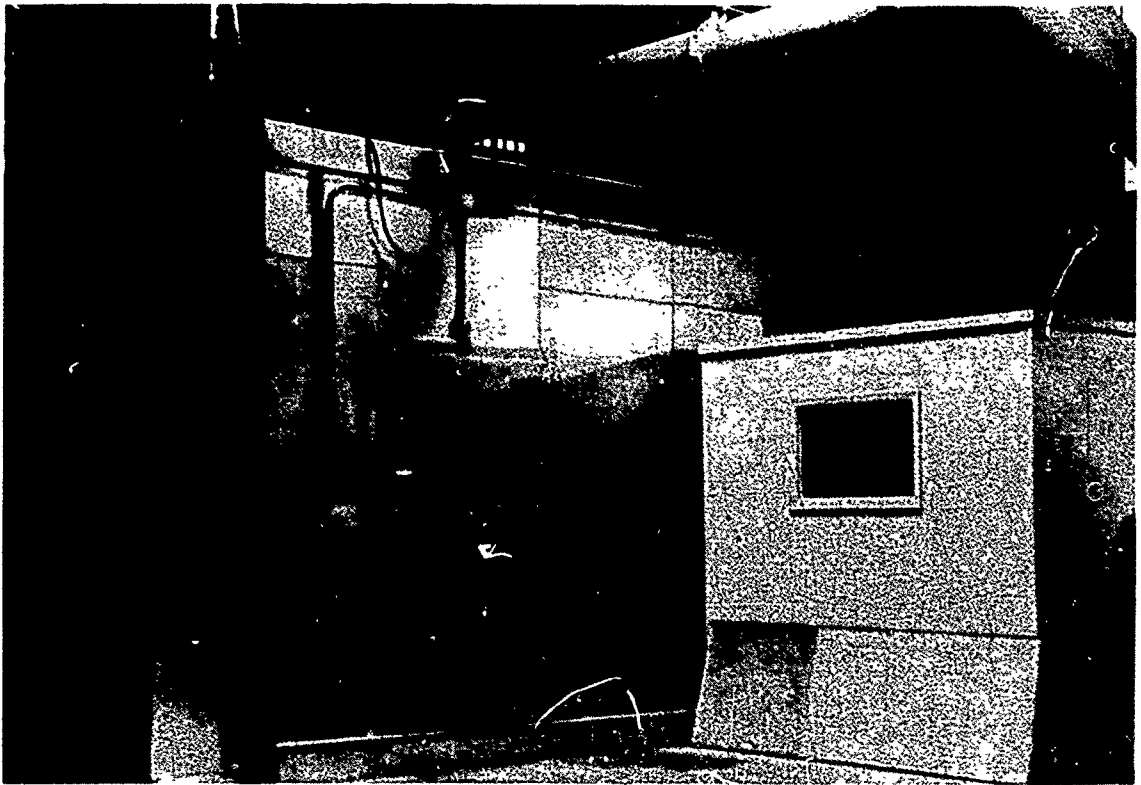
Figure 1   Refrigerated room
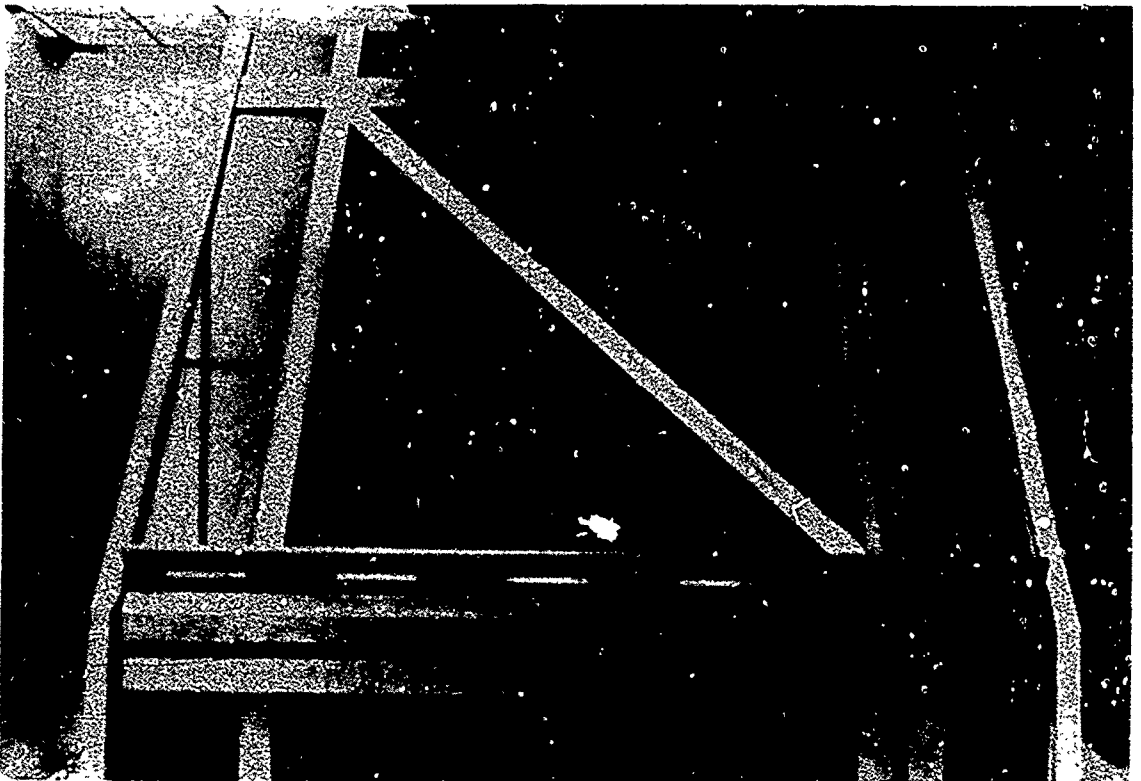
Figure 2   Test mock-up of sloped surface

235

The failure of the initial design of rail prompted the study of the modified design. During the tests, the temperature inside the mock-up was 21C (room temperature), while the exterior temperature ranged from -9C to +4C. A 24-hr run time produced approximately 10cm to 15cm of snow on the surface of the mock-up. The precise depth depended on whether the sealed double panes or the insulated spandrel panels were in place. Once a snow layer was produced, video equipment monitored its behaviour for as long as 72hrs.

The temperature of the refrigerated room and the quantities of snow produced were
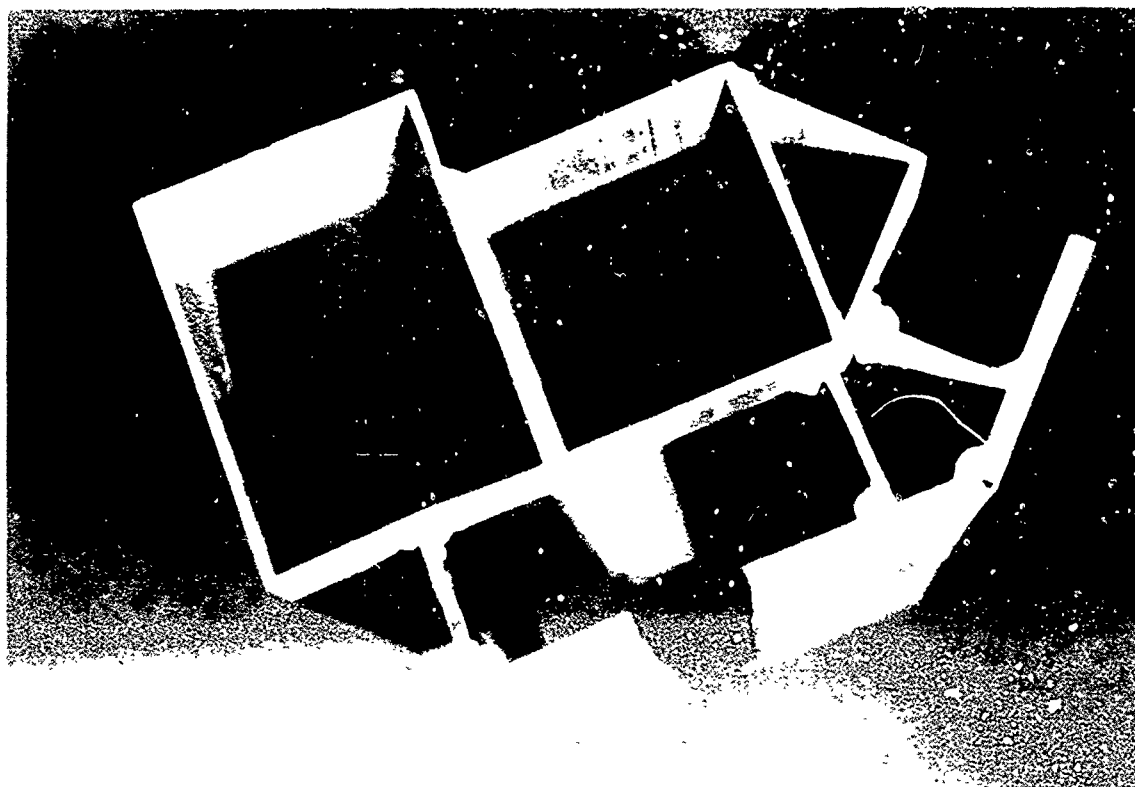
Figure 3   Cross-section of mullion showing level of detail of mock-up

chosen to represent real-life conditions at the site of the building being studied.   To establish these conditions, several years worth of hourly temperature observations and 24-hour snowfall measurements from the nearest weather observing station were analyzed to obtain statistics on snowfall and on temperatures during and after heavy snowfalls.

RESULTS

Figure 4 shows the behaviour of a snow layer on a sloped surface of sealed double glass with no rail.   Melting of the underside of the layer began when the layer's thickness reached 3cm to 5cm.   The layer then crept over the edge of the slope and eventually fell
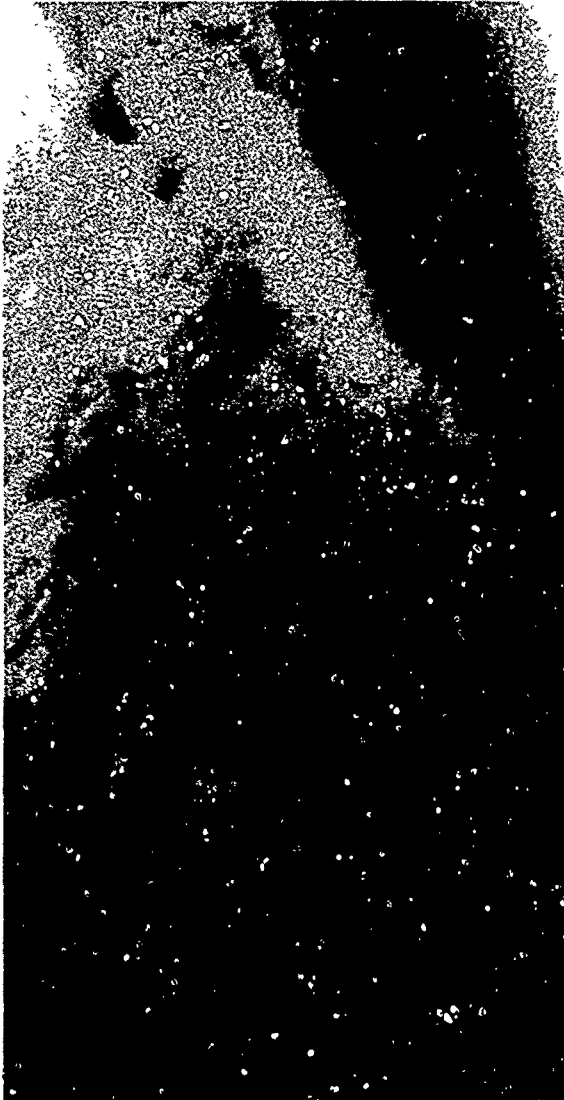
Figure 4 Before slide-off

Figure 5 After slide-off

off (Figure 5).

Figure 6 shows the same surface, with a snow rail in place. The snow continued to creep over the edge, demonstrating the inadequacy of the rail design. The problem was related to the continuous contact between the rail and the building surface. Heat escaping from inside warmed the railing, permitting the snow layer to creep over. This effect was more dramatic for the insulated spandrel case. The higher insulation value of the building envelope reduced the melting rate of the snow layer, allowing a greater accumulation to occur. Figure 7 shows a 20cm to 25cm thick layer hanging over the rail.
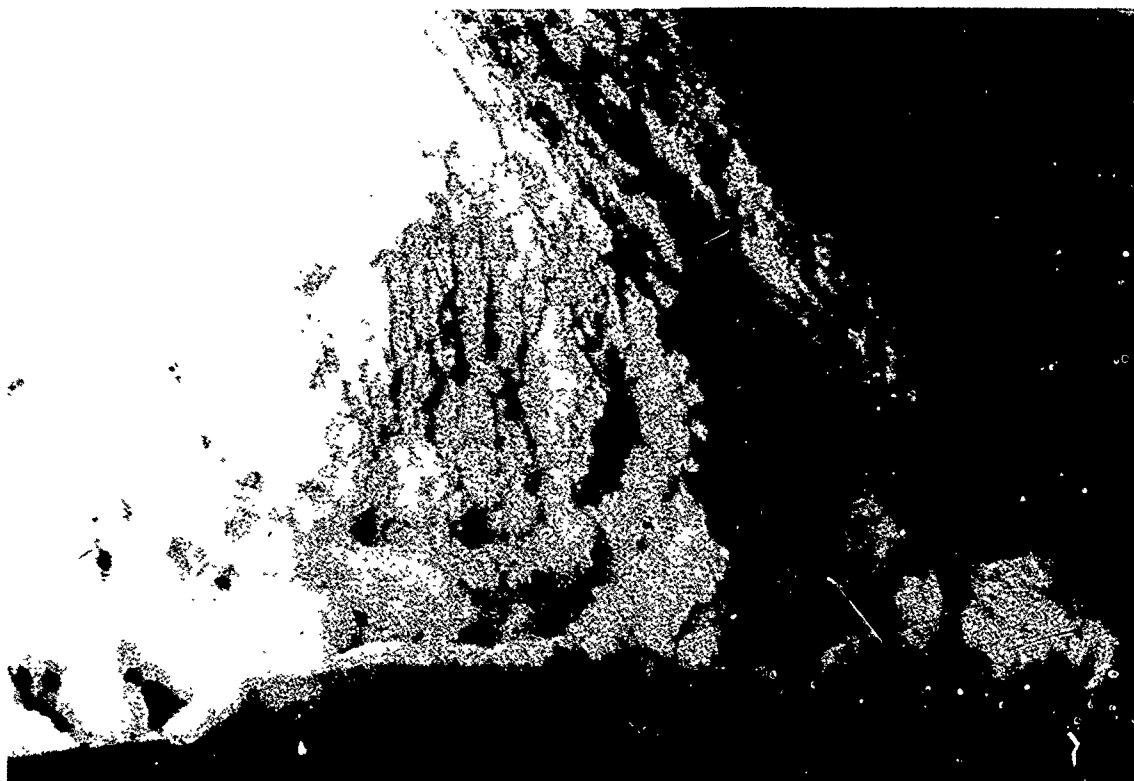
Figure 6   Snow creeping over warm rail on vision glass

Figure 7   Snow creep and icicles on spandrel glass

Figure 7 also shows an unforseen secondary problem with icicle formation. The icicles formed in the slots of the rail (Figure 8), which were intended for drainage. As the snow layer crept over the rail, snow extruded through the slots, losing contact with the building surface. Since it no longer received heat from inside the building, the extruded snow froze. Melt water running down the slope then froze onto the extrusions, forming icicles.

As shown in Figure 9, replacement of the slots with rows of 6mm diameter holes solved the icicle problem. A set of 6mm high spacers separating the rail from the building surface solved both the icicle and the creep problem. The rail then remained

Figure 8 Snow cut away to show icicles at slots

cold, provided no lubrication and prevented the snow layer from creeping or extruding through the slots. A C-bar attached to the upslope side of the rail provided additional friction. The result is shown in Figure 10.

CONCLUSION

Snow simulation tests conducted in a refrigerated room provide a valuable means of refining the design of snow and ice controls for buildings. In the case study, these tests identified unforseen problems with a snow rail. The design was modified to ensure that snow would be retained by the rail and to avoid icicle formation.
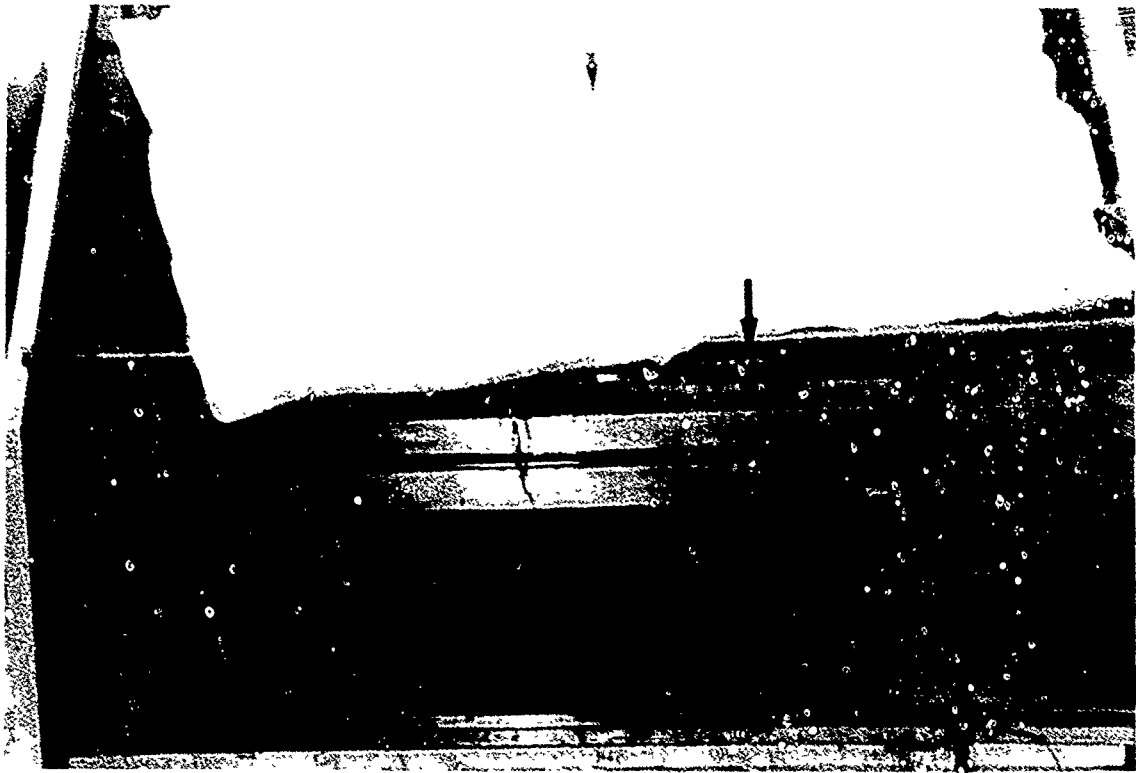
Figure 9 Icicles controlled by replacing slots with 6mm holes
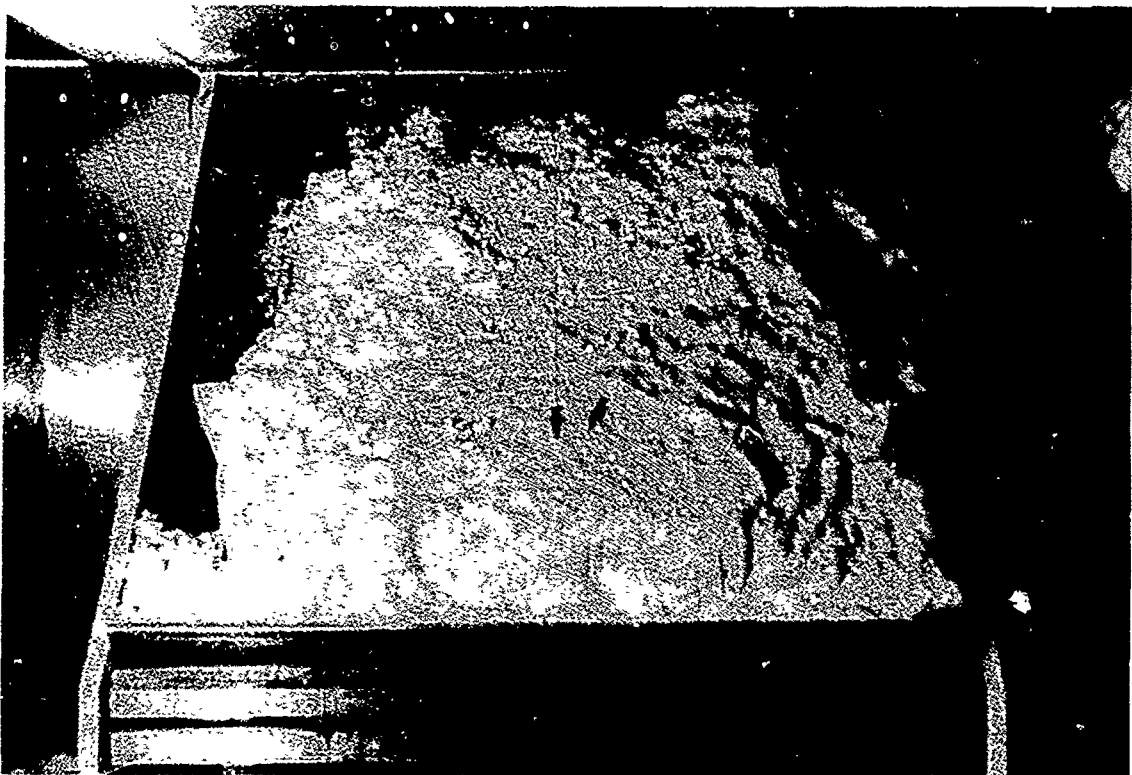
Figure 10 Snow creep and icicles controlled by cold rail

Other snow control devices studied by snow simulations on mock-ups include heat-tracing to promote repeated slide-off on sloped glass and snow-retaining devices for sills. The studies conducted to date have led to a number of general recommendations for snow rails and other devices. These include:

(1)   put snow rails on spacers to keep them away from the surface and as cold as possible;

(2)   design the rails with rough edges (preferably an L-shape, facing upslope) to provide friction for a snow layer attempting to creep over;

(3)   if the rail is near the bottom edge of the slope, make sure it has no openings through which snow can extrude;

(4)   design snow rails to withstand the potential downslope weight of retained snow (for traditional rails, consisting of horizontal bars, design for an uplift force caused by snow wedging under the bars -- a phenomenon that has led to many failures in the past);

(5)   control of sliding snow on recessed granite sills is achieved using a pan with a 2.5cm lip, and 2.5cm of rigid insulation between sill and pan to
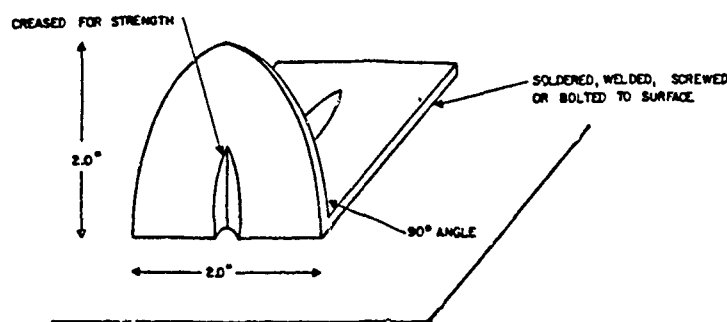
(A) DETAILS OF SNOW CLIP
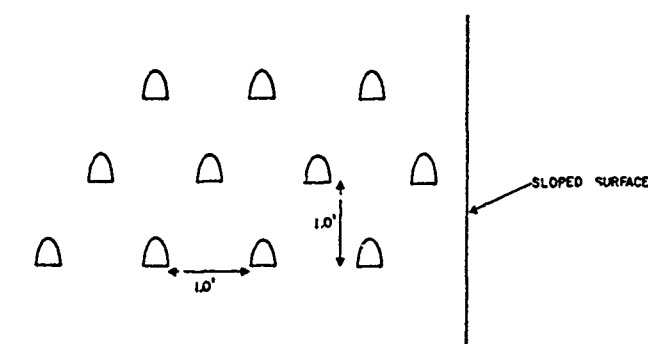
(B) DISTRIBUTION OF SNOW CLIPS

Figure 11   Example of snow clips

Minimizing Snow Accumulation Around the Entrance of a Building
An Experimental Case Study

Regent Dickey* and N.K. Srivastava**

ABSTRACT

The paper contains the methodology and results of a wind tunnel study on a model of a building by simulating snowstorm with a view to obtain simple and economical solutions for minimizing accumulation of snow around its entrance.

INTRODUCTION

Accumulation of snow around an entrance, especially of a public building in a heavy snow region, can result in costly winter maintenance and security risks. However, the effect can often be minimized by proper orientation of the building during construction. When the orientation is dictated by other factors or in the case of an existing building with problems of excessive accumulation, a detailed study of each particular situation is needed. The solution of the problem could be very simple, such as planting trees at a certain distance and in a certain pattern, adding a few projections here and there in the building, or erecting a commemorative sculpture or a sign at a particular distance and of particular size. However, to determine the most economical and effective solution in such cases, an experimental study for each particular case is often needed. The advantages and eventual savings to the maintenance of the buildings offset many times the cost of this type of study.

The paper contains the methodology and results of an experimental study with a view to obtain alternative solutions for minimizing accumulation of snow during a snowstorm around an entrance. The building under study is the sports complex at the campus of the Université de Moncton due to problems encountered only after the construction of the building. The snowstorms at this site have been simulated in a boundary layer wind tunnel and different solutions are being experimentally studied on models of the building and its surroundings.

MODELLING

The sports complex building of the campus was chosen for the study because the problem was acute and the conventional method of snow removal was getting expensive. Another reason to choose this building was because it was relatively a new construction and hence no trees or vegetation affected its surroundings. This gave us a chance to better simulate the surroundings during the lab experiment, with a hope that the eventual solution recommended would be economically put into practice as a part of the new landscaping.

---

*TRANSPORT CANADA
**UNIVERSITE DE MONCTON

It was decided to study the problem on a model subjected to simulated snowstorms in the Low Speed Boundary Layer Wind Tunnel of the University. The past meteorological data were collected and verified by measurements on site to recreate the dominant profile and orientation of wind during snowstorms between the months of September and April. The dominant direction was found to be from the west-southwest (WSW). To study different directions of wind the model was placed on a rotating table flush with the floor of the wind tunnel. However, the authors chose only 30° of rotating flexibility in favour of a larger model.

A model was constructed at a scale 1:192 taking account of the basic criteria of modelling and the restrictions imposed by the size of the test section 6 m x 2 m x 2 m of the wind tunnel. We could accommodate four buildings and three parking lots in the model [Fig. 1].

SNOW STORM SIMULATION SYSTEM

Several types of powders were considered for simulating snowstorms. Fine powders like chalk and flour made a mess of the inside and outside of the tunnel and were difficult to catch at the end of the tunnel. For these reasons we opted for a rough powder of borax salt.

To disperse the powder during the test, two different systems were tested. One was a vibration box with holes at the bottom, which did not give a uniform dispersion in the simulated flow. The other system, which worked better, was a snow box, approx. 32 cm.L x 3.5 cm.W x 3.1 cm.H, attached to the roof of the wind tunnel across its width (Fig. 2). There were 32 slots (3.2 mm x 50 mm) across the bottom of the box, which opened and closed in a uniform rythm through a system driven by a small motor. Caution was taken to place this snow box filled with borax salt sufficiently away from the model so that it did not create undue turbulence and at the same effectively simulated a snowstorm on the scale model of the building by uniformly distributing the powder across the section.

A flexible curtain was attached at the end of the tunnel to catch and prevent most of the powder from getting out.

TESTS

Wind Velocity Profile

It was important to simulate the actual wind profile in the test section. A hot wire anemometer was used to control this profile. Tests were done without and with the snow box to find its ideal position. The ideal position is as described previously.

Verification of Final Placing of the Model

To conform the snow accumulation on the model as closely to the reality as possible, photos were taken to make the comparison easier. Quantitative

measurements of the accumulation were done with a graduated needle positioned by an dolly over designated points of the grid. Figure 3 shows qualitative conformability of the simulation with reality.

Other Test Details and Observations

■ Because of the scale used, the 3-directional hot-wire anemometer could not be used to determine the wind direction and local vortices on the surface of the model. For this purpose, light, colored threads were attached to each point of the grid drawn on the surface of the model. The rectangle in front of the main entrance of the model, 7.5 cm x 21 cm (3 in. x 8 in.), was divided into a 2.54 cm x 2.54 cm (1 in. x 1 in.) square grid. This helped us to observe the general wind direction and formation of local wind vortices (Fig. 4).

■ For the major orientation of the building, tests were conducted for three different wind directions, the principal direction of the snowstorm (WSW), and the directions WSW ± 15°. This was to determine the degree of variation and sensitivity due to error in simulation of exact wind direction. The results obtained were pratically similar for all the three directions, thereby giving an assurance for good practical results.

■ A constant wind velocity was maintained for each test.

■ Wind profile tests were conducted for four wind velocities: 3 m/s (9.8 ft/s), 5 m/s (16.40 ft/s), 7 m/s (23 ft/s) and 10 m/s (32.80 ft/s).

■ Study of the movements of the threads on the grid was done for four wind velocities, 4 m/s (13.12 ft/s), 5.25 m/s (17.23 ft/s), 6.75 m/s (22.15 ft/s) and 8 m/s (26.24 ft/s), to visually observe the variation of the local vortices for different wind velocities.

■ Snowstorm simulation tests were conducted at an average wind velocity of 5.3 m/s (17.3 ft/s). This velocity was arrived by tests which permitted the best uniform accumulation on the model during the final experiments.

■ The Reynolds number of the model was approximately 1/200 of that of the prototype.

■ An equal quantity of borax salt was used for each test to be able to compare one test from the other. Total comsumption of borax was 22.5 litres (5 gallons).

■ Several schemes were tested to minimize the snow accumulation at the entrance. Four simple and promising ones were chosen for detailed testings. These solutions and the results of these tests are presented in the next section.

PROPOSED SOLUTICNS TO MINIMIZE SNOW
ACCUMULATIONS AND CORRESPONDING TEST RESULTS

Proposal 1

Proposal 1 consists of erecting a 40mm (1.6 in.) wide and 13mm (0.5 in.) high simple rigid wall barrier at a certain distance from the entrance of the scale model. Several pretests were done to find the best location of this wall barrier in relation to the entrance of the model. The best location is shown in Figure 5a. Graphic representations of the results for this location are shown in Figures 5b, 5c and 5d.

Proposal 2

This proposal consists of erecting an L-shaped rigid wall barrier at a pretested critical location. The dimensions and the best location are shown in Figure 6a. The graphic representations of the results are shown in Figures 6b to 6d.

Proposal 3

This proposal consists of erecting an L-shaped barrier, with trees planted along one arm of the barrier and a rigid wall on the other arm (Fig. 7), again at a pretested best location. The graphic representations of the results for this proposal at this location are shown in Figures 7b to 7d.

Proposal 4

This proposal consists of building a triangular wedge-shaped earth mound at a pretested best location. The dimensions and the location are shown in Figure 8. The graphic representations of the results are shown in Figures 8 b to 8 d.

OBSERVATIONS AND CONCLUSIONS

■ All the four abovementioned proposals have the potential to greatly minimize the snow accumulation at the entrance if placed strategically. Proposal 1, however, was the worst of the four for minimizing accumulation around the entrance.

■ Proposals 3 and 4 by far gave the best results near the entrance. However for a zone 4 cm (8 m) away along the wall from the entrance, solution 2 gave an accumulation of nearly half that for the proposals 3 and 4.

■ In the context of the building in question, proposal 4 was considered to be the best by the authors.

■ The authors strongly recommend that such tests be done before the construction of a building in order to suggest its proper orientation as well as to suggest proper landscaping with a view to minimize snow accumulation around its desired entrance. Convenient locations of entrances derived from such tests can also be suggested to architects.

ACKNOWLEDGEMENTS

WIND DIRECTION

MEASURING AREA

C.E.P.S., UNIVERSITE DE MONCTON

Major Orientation of Wind WSW
(September to April)

Figure 1 . Scale model.

SNOW BOX

		1 in = 2.54 cm	
VERT. SCALE: 1"=4"		DATE: MAY 16, 1981	
HOR. SCALE: 1"=16"			

Detail 1

DRIVING HANDLE
(TRUE SCALE)

PULLEY
(TRUE SCALE)

HOLES

HOLE 3/32" DIA.
HOLE 3/16" DIA.

Figure 2

1 1/2" HINGE

1" HOOK

1/8" SLIT

1/4" SLIT

SEE DETAIL 1

MOTOR

38 SLITS

TYPICAL 2"

1 1/2" (TYPICAL)
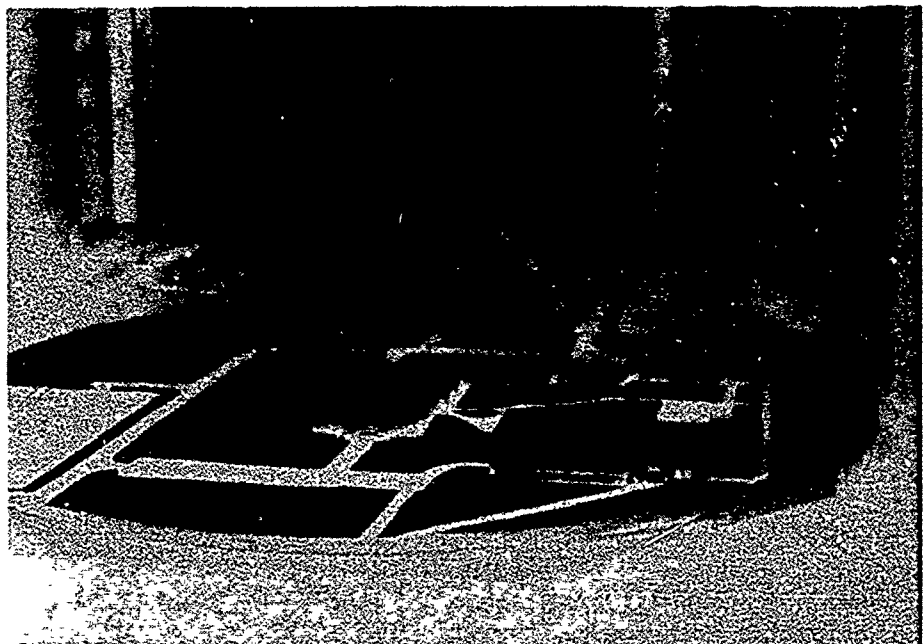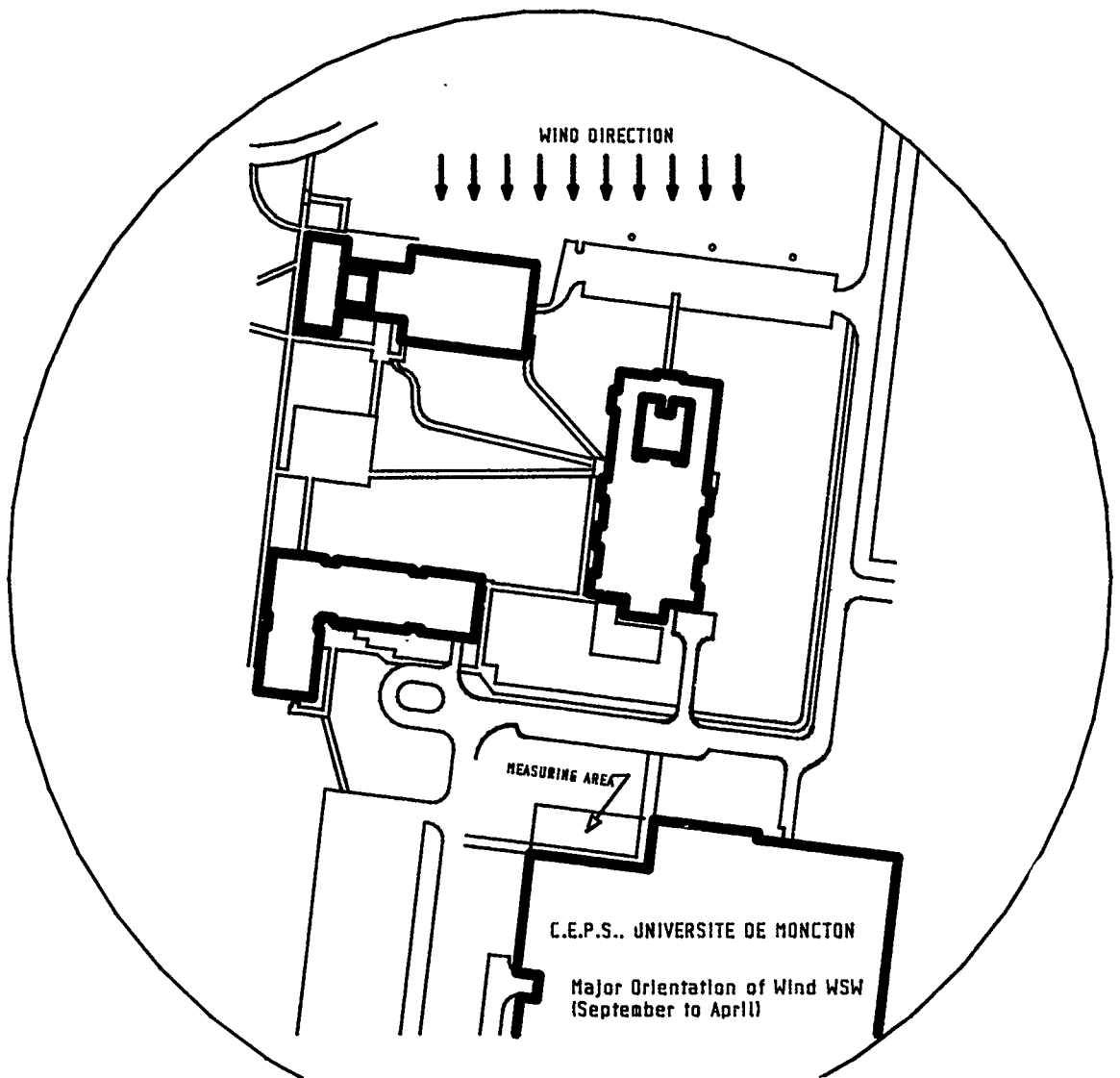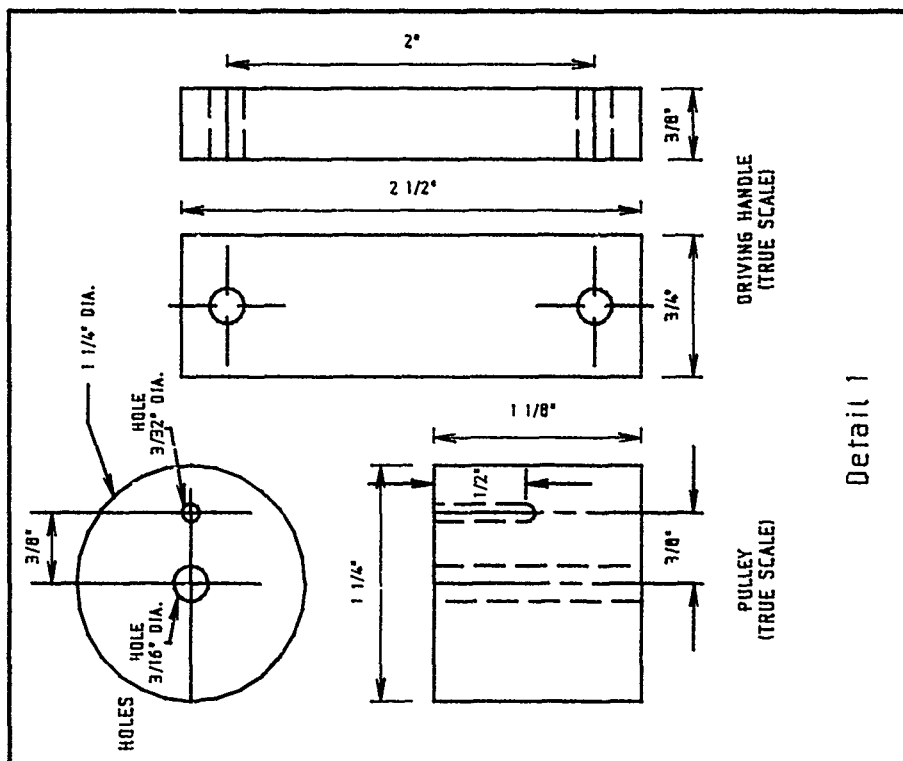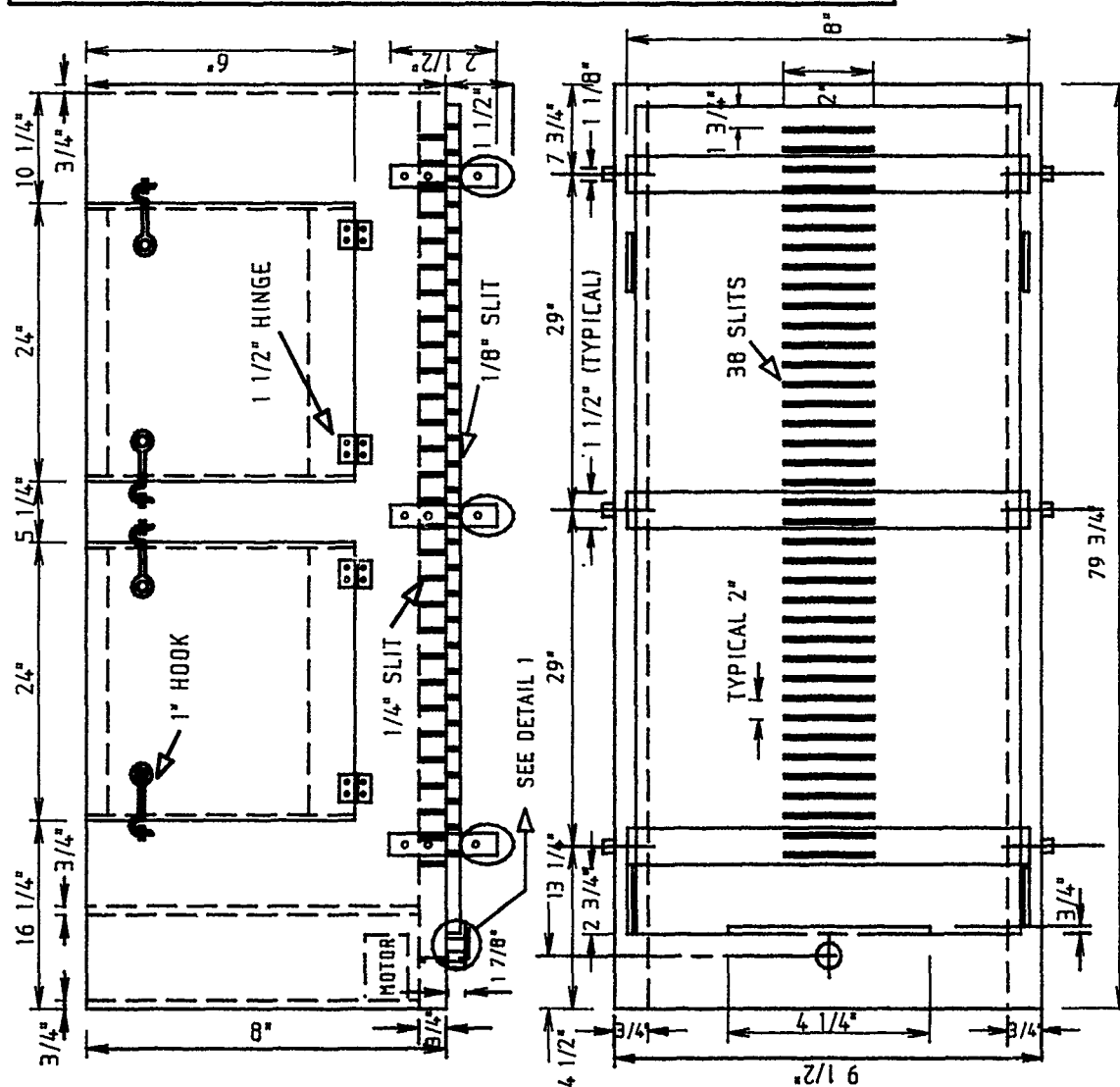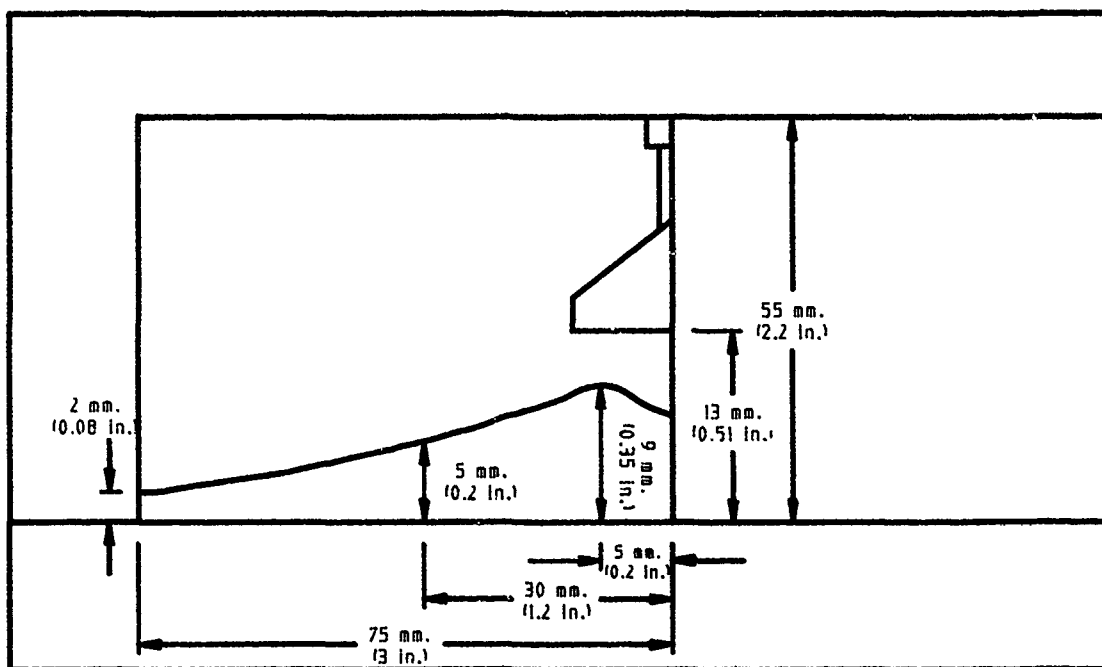
Figure 3a. Measurements on scale model.
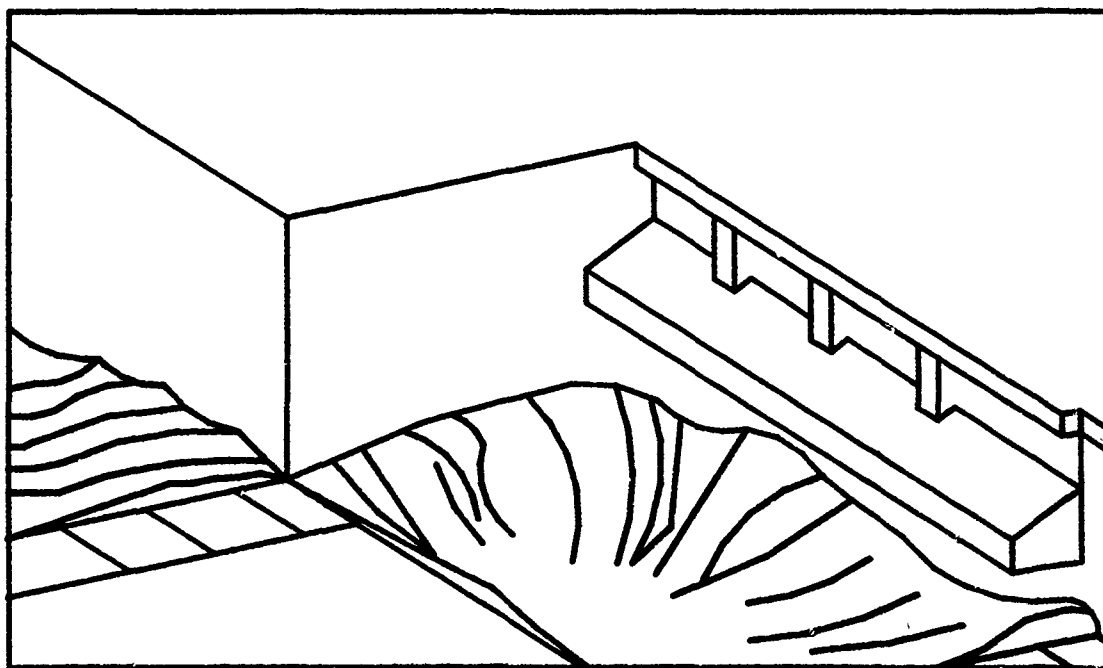
Figure 3b. Representation of the problem.

Figure 3. Snow accumulation near the entrance.
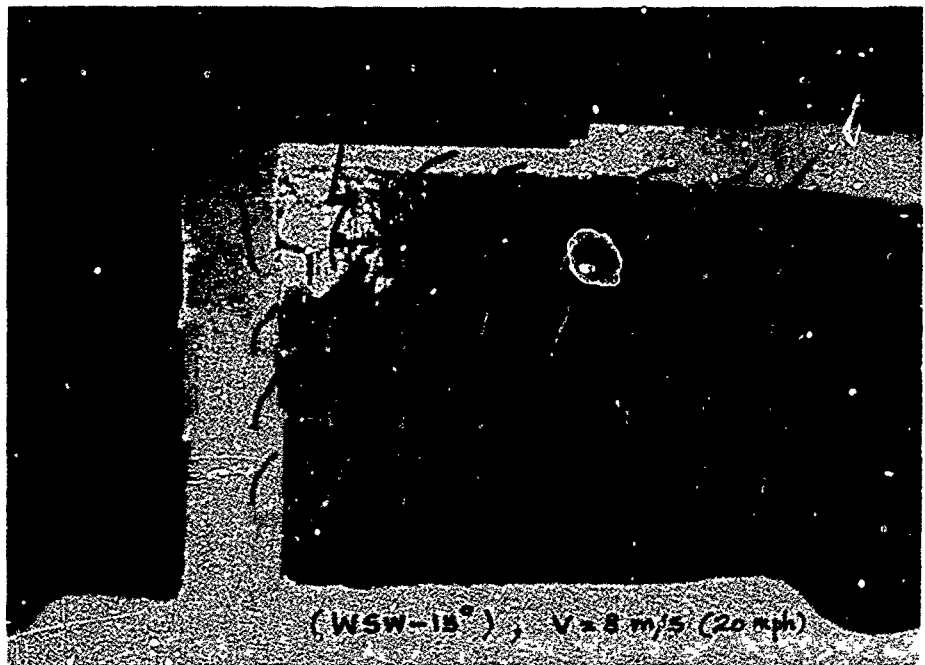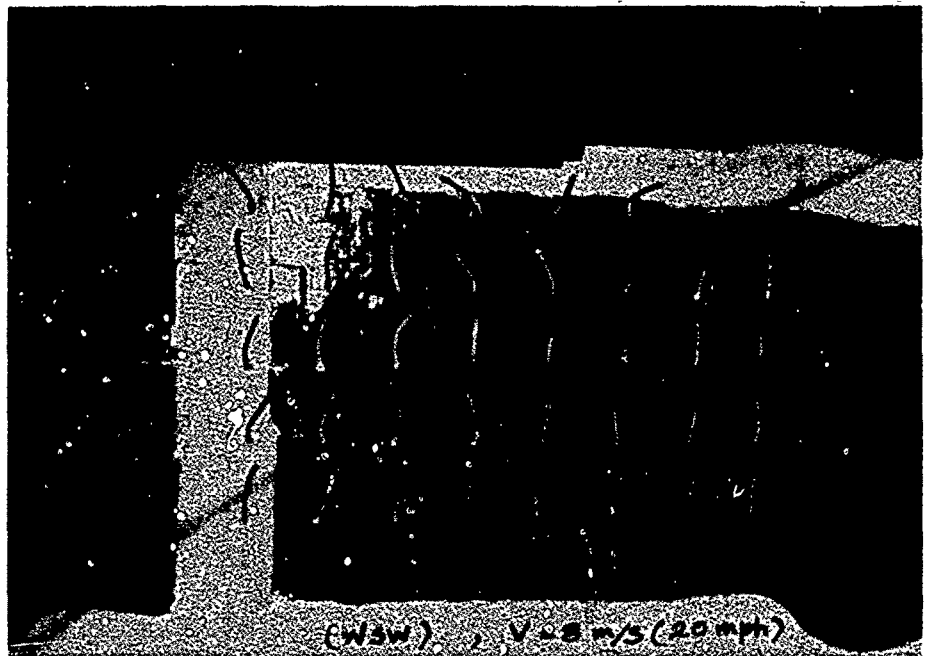
Figure 4. Threads attached to square grid
to detect wind direction and general vortices.

Figure 5b. Door area cross section X = 1.0 cm (0.4 in.).

55 mm. (2.2 in.)

13 mm. (0.51 in.)

(mm) (in)

5 0.2
10 0.4
20 0.8
30 1.2
40 1.6
60 2.4
75 3.0

13 mm. (0.51 in.)

y

Figure 5d. Cross section X = 7.0 cm (2.76 in.).

55 mm. (2.2 in.)

13 mm. (0.51 in.)

(mm) (in)

5 0.2
10 0.4
20 0.8
30 1.2
40 1.6
60 2.4
75 3.0

13 mm. (0.51 in.)

y

Figure 5a. Proposal no. 1.

35 mm. (1.38 in.)

X

y

65 mm. (2.56 in.)

40 mm. (1.5 in.)

SINGLE RIGID WALL

Figure 5c. Cross section X = 4.0 cm (1.6 in.).

55 mm. (2.2 in.)

13 mm. (0.51 in.)

(mm) (in)

5 0.2
10 0.4
20 0.8
30 1.2
40 1.6
60 2.4
75 3.0

13 mm. (0.51 in.)

y

Figure 6b. Cross section X = 1.0 cm (0.4 in.).

Figure 6d. Cross section X = 7.0 cm (2.76 in.).

Figure 6a. Proposal no. 2.

Figure 6c. Cross section X = 4.0 cm (1.6 in.).

253

Figure 7b. Cross section X = 1.0 cm (0.4 in.).

Figure 7d. Cross section X = 7.0 cm (2.76 in.).

Figure 7a. Proposal no. 3.

Figure 7c. Cross section X = 4.0 cm (1.6 in.).

Figure 8b. Cross section X = 1.0 cm (0.4 in.).
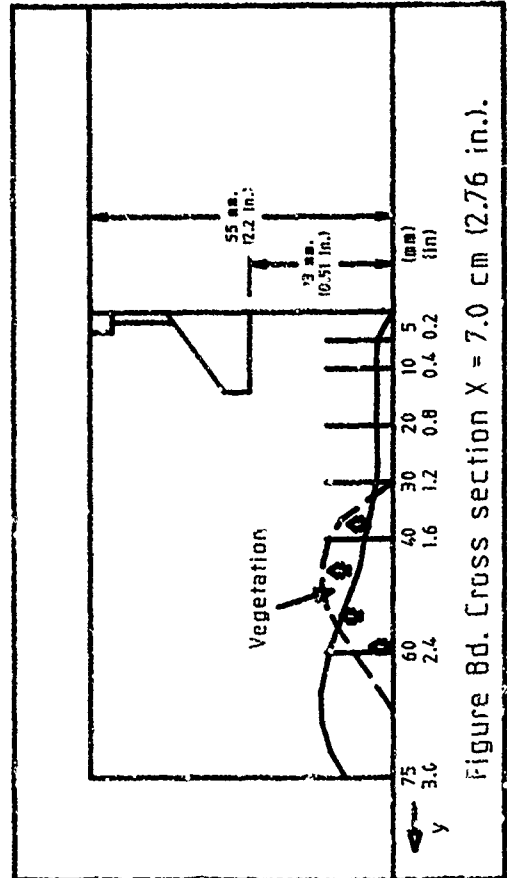
Figure 8d. Cross section X = 7.0 cm (2.76 in.).

Figure 8a. Proposal no. 4.

Figure 8c. Cross section X = 4.0 cm (1.56 in.).

255

Consideration of Wind Effect in Standardization of Snow Load

V.A. Otstavnov[1] and L.S. Rosenberg[1]

ABSTRACT

The results of observations show that average values of snow load on roofs are usually lower than the average weight of precipitation that falls in winter. This is mainly caused by drift of snow by wind and snow thaw. The maximum snow drifts occur on flat roofs. The codes of some countries, in particular, U.S.S.R. and Canada provide for a positive effect of wind in forming snow accumulations on such roofs. According to Canadian codes, the snow loads on flat roofs are 20 percent less than for those of a complex shape, and snow load is decreased by 20 percent on flat roofs for regions with an average for many years of wind velocity over 4 m/s in the U.S.S.R. codes. The investigations to obtain appropriate decreasing of snow load for mentioned roofs were carried out in the U.S.S.R. in connection with a great number of buildings constructed with flat roofs, amounting in area to some dozens of hectares. The main results of these investigations carried out by the authors are presented below.

INTRODUCTION

The snow load on a flat roof may be determined by the formula:

$$P_f = P_1 - P_2 - aP_3 + P_4 \qquad (1)$$

where P_f = actual load on roof to the winter end (kg/m²)

P_1 = weight of snow fallen in winter

P_2 = weight of snow drifted by wind

P_3 = weight of snow thawed on the roof

a = factor which takes into account removal of thawed snow from the roof

P_4 = weight of ice formed on the roof in autumn before snowfalls.

The values incorporated in this formula may differ greatly for various winter conditions. Thus, the many-year range of P_f values has a random

---

[1]CNIISK; Moscow, U.S.S.R.

[2]CNIISK; Moscow, U.S.S.R.

nature, and the value of P_f expected during the service life of a structure may be obtained by using an integral distribution based on data for several winters.

The weight of ice forming in some cases on particular parts of flat roofs in autumn before winter snowfalls may be defined by accounting for structural peculiarities of flat roof (deflections due to a dead weight of structures, etc.). This problem is not difficult. Decreasing snow load due to snow thawing on the roof is usually observed in cases of great snow accumulations as well as in conditions of frequent thaws and has not yet been sufficiently investigated. However, in most cases this effect has a positive meaning in relation to a load and should be considered before current investigations are completed.

The value of snow load, considering only some drifts, may be presented as difference for particular winter:

$$P_f = P_1 - P_2 \tag{2}$$

where P_1 is found from data of the hydrometeorological service and P_2 may be determined according to the procedure given below.

Snow redistribution and drifting mainly occur during snowfalls when falling snow particles are poorly interconnected and may be easily transferred by wind. Transferring particles of deposited "old" snow, which are more congealed, requires greater wind velocity.

Moderate wind conditions on the whole are governed by velocities sufficient for transfer of poorly connected particles of falling snow. Strong winds, which are required for transferring connected snow particles, rarely occur.

Considering two types of snow drift (type "A" in snowfalls and type "B" with no snowfalls) a total drift may be presented in the form as follows:

$$P_2 = P_2^A + P_2^B \tag{3}$$

where

P_2^A = drift in snowfalls;

P_2^B = drift with no snowfalls (kg/m²)

On the basis of a number of known investigations, as well as those obtained in carrying out the given investigation of materials, one may accept design values of wind velocity in drifting as follows:

in snowfalls   -   4 m/s, and
with no snowfalls   -   6.5 m/s

Two assumptions are made in considering a snow drift of the "A" type:

1)   Processes of snow falling and drifting on roofs (snowstorms with snowfall) occur simultaneously, with intensity varying about an average value, which may be conditionally taken as a constant value in the course of snowstorm;

2)   The ratio of the amounts of both drifted and fallen snow in a snow-storm (or drift factor n_m) is defined by wind force and depends on average wind velocity in the course of a snowstorm (subscript "m" shows that the given parameter is pertinent for a particular snowstorm).

Actual values of n_m for 24 cases of snowstorms are revealed as results of measurements of type "A" drift from a flat roof of an area of about 100,000 m² in Moscow. Figure 1 shows the dependence of n_m on wind velocity in snowstorms, which may be expressed as:

$$n_m = 0.15V_m^A - 0.39 \tag{5}$$
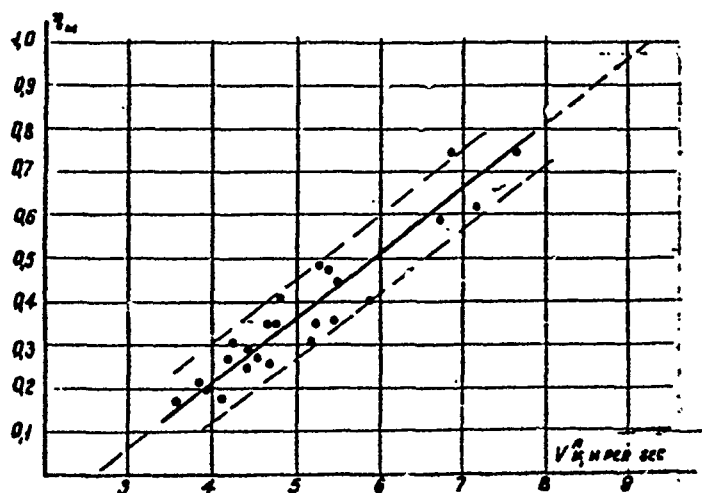
Fig. 1. Drift Factor depending on wind velocity.

In extrapolating from a particular snowstorm to the whole winter period, one may consider cumulative action of all winter snowstorms from a single conventional snowstorm governed by average values of both wind velocity and drift factor. Unification of snowstorms is illustrated by a diagram (Fig. 2) in which

$t = t_1 + t_2 + \ldots\ldots\ldots + t_n$ is the summarized duration of all snowfalls.
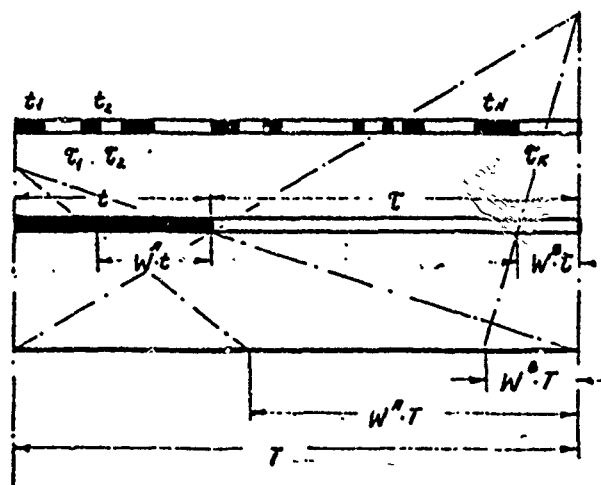
Fig. 2. Diagram to account for drift duration in winter.

In this case, the duration of drifting and of snowfalls is not the same, as this was taken for a particular snowstorm, because some snowfalls occur at a wind velocity of up to 4 m/s, and are not followed by drifting. A complete duration of drifting for winter is determined by the duration of wind action at a wind velocity 4 m/s and over. For a whole winter period, T, duration of such winds is W^AT, where $W^A<1$ = recurrence of these winds.

Introducing the concept of a "summary" snowstorm and taking into account considerations relative to its duration, an equation of drifting in snowfalls for the whole winter period may be obtained after elementary transformations:

$$\eta = \frac{P_2^A}{P_1} = (0.15V^A - 0.39)\ w^A \qquad (6)$$

where V^A = average value of all velocities recorded for winter, starting from 4 m/s and over;

W^A = wind recurrence.

In connection with the fact that snowstorms may occur in different periods of winter, the most probable wind conditions for a summary snowstorm will coincide with the wind conditions for the whole winter. This means that some period of winter may be characterized by the same recurrences of wind velocity as for the whole period of winter. In this case duration of the summary snowstorm will be W^At.

The drift of "B" type depends on force and duration of wind effect on a snow cover. For drift time without snowfall, equal to τ_i, the amount of previously deposited and drifted snow is as follows:

259

$$P^B_{2m} = q\tau_i \qquad (7)$$

where q = an average intensity of drifting during a snowstorm. This value may be determined depending on an average wind velocity for drift time equal to V^B_m according to a graph (Fig. 3) obtained by generalization of numerous measurements of snow transferring on the ground surface, carried out by a number of the U.S.S.R. investigators.
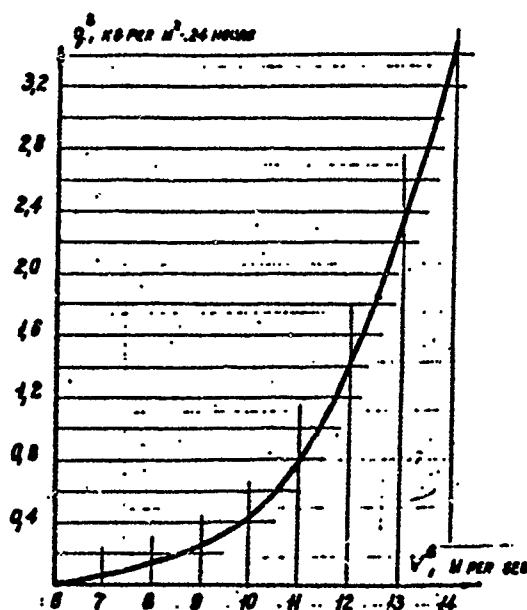
Fig. 3. Graph to determine drift intensity without snowfalls.

The method of summarizing snowstorms is also appropriate to use for estimating drifting without snowfalls during the winter period (see Fig. 2). A potential duration of drifting of deposited snow, during which snowfalls don't occur, is as follows:

$$\tau = \tau_1 + \tau_2 + \ldots\ldots\ldots + \tau_k$$

However, in fact drift will occur not for the whole period of τ but only for the time period of $W^B\tau$, where $W^B<1$ = recurrence of winds of 6.5 m/s velocity and over. In this case, by using expression (7) drifting of the "B" type for the winter period may be determined by the formula:

$$P^B_2 = q\tau W^B \qquad (8)$$

To obtain q = value according to the graph (see Fig. 3) one may use a value V^B = average of all velocities recorded for winter if the values are 6.5 m/s and over.

Computation according to equation (8) is difficult because the data on τ-time are not recorded by the hydrometeorological service. Definition of τ as difference of T-t is also practically impossible because the duration of

the precipitation is not given in Climatological Reference books. This problem may be solved by using a number of days with precipitation (n) instead of t, taking into account that a total duration of falling precipitation does not coincide with the number of days with snowfalls. The difference between t and n is smoothed over if only sediments forming snow cover are taken into account and poor sediments are neglected. An average duration of such a snowfall is about 24 hours.

In the reference books the number of items in which the number of days with snow cover is given is usually limited. Therefore, n-values may be obtained in terms of its connection to the weight of ground snow cover. The analysis of meteorological data shows that a close correlation is estimated between the number of days with snowfalls and the amount of snow fallen for winter. This correlation is given in Fig. 4 for 225 winters in relation to different points of the U.S.S.R.
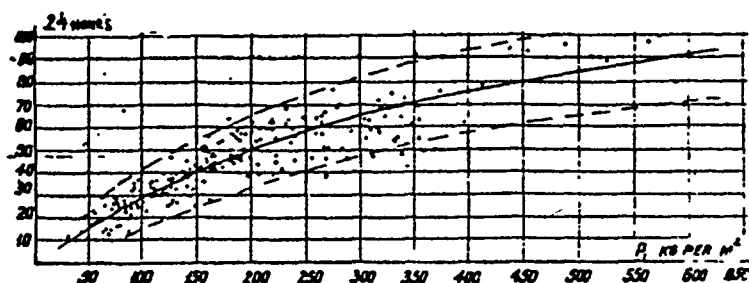
Fig. 4. A number of days with snowfalls (n)
depending on the amount of fallen snow (P_1).

Searching for winter duration for concrete years in the reference books makes the calculation more complicated. The value of T_y (40 days) may be used instead of T with sufficient precision for practical application. In this case T_y = an average many-year value of the period with a steady snow cover, 40 = a correction factor which takes into account both variability of annual T values and negative effect of transition periods with unsteady frosts early and later in winter on the results of calculation.

Accounting for given revisions for definition, expression (8) will be as follows:

$$P_2^B = qW^B(T_y - n - 40) \tag{9}$$

where q = average intensity of drifting

    n = number of days with snowfall

    T_y = average of many-year value of the period with a steady snow
          cover

    W^B = recurrence of winds of 6.5 m/s velocity and over.

In observations on 26 flat roofs the effect of roof area on the value of drifting was not revealed. Snow remaining after drifting is considered as uniformly distributed on the flat roof when this is not encumbered by superstructures.

The results of investigations were used:

1) for a graphical correlation with values of the total drift, computed for winter data relative to roofs located in regions with strong winds (average wind velocity for winter 5 to 7 m/s) (Fig. 5);

2) for a graphical comparison of theoretical and experimental values of drift in snowfalls (Fig. 6).
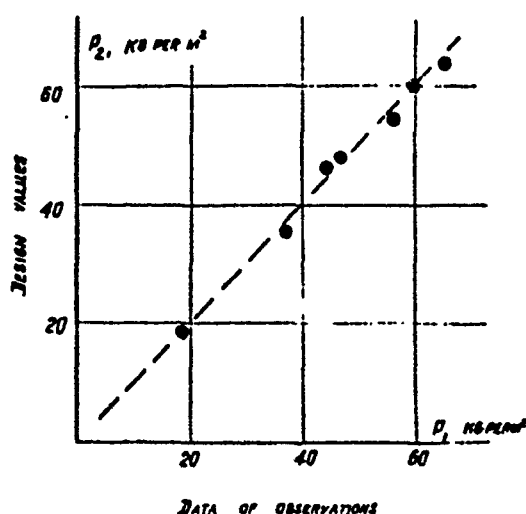
Fig. 5. Correlation of total drift values for points with high wind velocity.
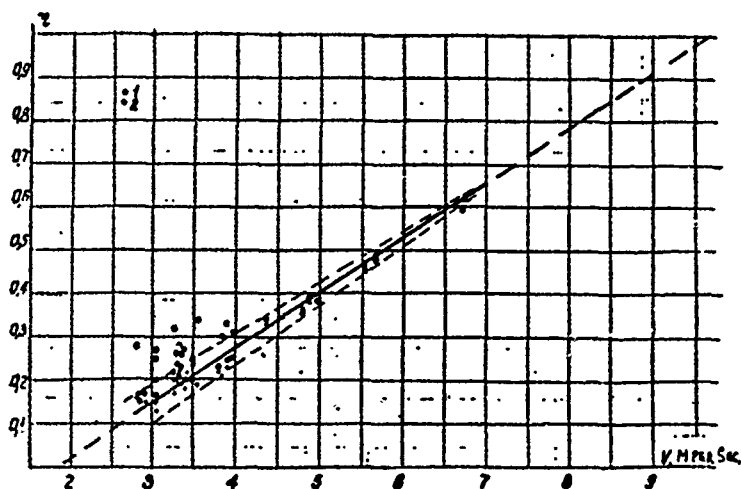
Fig. 6. Comparison of experimental and computed values of drift in snowfalls and relation of drift value to an average wind velocity (V) for winter.

In the graph a clear correlation of η and V is shown, where V = average wind velocity in meters per second for winter. This correlation may be used for practical calculations of type "A" drift instead of expression (6):

$$n = 0.13V - 0.24 \tag{10}$$

The positive results of investigation of drift regularities permit us to use formulae (2), (3), (10) and (9) to estimate a possible snow load on flat roofs for a particular winter in practical application according to the formula:

$$P_f = (1.24-0.13V)P_1 - qW^B(T_y-n-40) \tag{11}$$

The hydrometeorological data bases now available in the U.S.S.R. contain the data which are required to define snow load, taking into account snow drift for some winters in many points of the country.

From these data bases possible snow loads on flat roofs for 20 to 30 winters were obtained for definite points of the country. Also it was revealed that snow load for the whole expected service period may be close to zero in regions with strong winds, but in those with low winds snow load may be slightly different from the weight of the ground snow cover.

In relation to distributions of ground snow cover weight, the integral distributions of loads on flat roofs, based on the data for particular winters, have shown, that in some cases variability of ground snow cover weight may differ from that of snow load on flat roofs.

The technique worked out to determine snow loads on flat roofs is expected to decrease rated loads on these roofs.

5
SNOW CONTROL
Jack Cermak, Chairman

Avalanche defense structures on the hills above Hammerfest, Norway. (Photograph by Wayne Tobiasson.)

On the Feasibility and Value of Detecting and Characterizing Avalanches Remotely by Monitoring Radiated Sub-Audible Atmospheric Sound at Long Distances

A.J. Bedard, Jr.,[I] G.E. Greene,[II] J. Intrieri,[III] and R. Rodriguez[I]

ABSTRACT

Because avalanches frequently occur in remote areas, it is often difficult to establish the timing or extent of snow movement. Such information is valuable for verifying avalanche prediction models, as well as establishing regional statistics. We summarize techniques developed for measuring low-frequency, small-amplitude sound waves in the atmosphere. Infrasonic observations made along the front range near Boulder, Colorado, suggest that it may be possible to detect low-frequency sound waves related to avalanches at distances of hundreds of kilometers. Several acoustic radiation mechanisms are possible. Source region acoustic measurements should be made of controlled avalanches in an effort to understand the acoustic radiation sources, and optimize measurement techniques.

INTRODUCTION

As the population of mountainous regions increases and recreational use expands, more persons and properties are subjected to avalanche risks. Systems have been created to provide warnings (e.g., Judson, 1976), usually relying on a model or models of avalanche triggering mechanisms as well as observations of avalanche occurrences. However, observations of avalanches are often reported late with the time unknown (or may not be available at all for remote areas). Prompt reporting can provide the basis for warnings since the instabilities and external forces that trigger avalanches often occur over wide areas. Early identification of an avalanche can be a good index of the likelihood of subsequent avalanches. Thus, there is a need for improved hazard warnings. Also, it is difficult to obtain quantitative data to evaluate prediction models, since the timing of natural avalanches is rarely known and the best observations are usually of controlled avalanches. This paper presents observations of atmospheric infrasound made during periods of avalanche activity. We discuss the possibilities of using remote acoustic observations for avalanche monitoring. In the past, measurements were made near avalanches using infrasonic microphones, but the results were inconclusive. Harrison (1976) made some preliminary measurements near small avalanches recording both seismic and infrasonic data. He detected weak, high frequency seismic signals (with peaks at 4 Hz and 6.5 Hz in one case), but no infrasonic signals. The acoustic sensors he used were not effective at frequencies above about 0.3 Hz, and he noted that if the seismic and infrasonic signals have a common cause it will probably be necessary to use microphones with a frequency response between 2 and 20 Hz. Using seismometers located in avalanche starting zones St. Lawrence and Williams (1976) obtained seismic signals with characteristics that could be distinguished from other sources. They suggested that seismic monitoring of a major slide path may be valuable indication of instability for a region.

I.   NOAA/ERL/Wave Propagation Laboratory, 325 Broadway, Boulder, CO 80303.
II. Private Contractor to Wave Propagation Laboratory.
III. Cooperative Insitute for Research in Environmental Sciences (CIRES),
     University of Colorado/NOAA, Boulder, CO, 80309.

Salway (1978) presented seismic data indicating that an avalanche passed over a seismometer in a series of surges. Pressure sensors measured corresponding successive peaks. Salway observed that most of the seismic energy with an avalanche was between about 2 and 20 Hz. The instrumentation and techniques we have developed for measuring infrasound from 0.1 to 20 Hz seem better suited than instrumentation for avalanche monitoring limited to frequencies <0.5 Hz.

Infrasonic Detection Techniques

Infrasound has been observed from a variety of geophysical sources including earthquakes (Young and Greene, 1982), meteors (Bedard and Greene, 1981), volcanoes (Tahira, 1988), severe weather (Georges, 1973; Bedard et al., 1986), and air flow over mountains (Bedard, 1978). The pressure amplitudes measured from the sources are usually quite small (typically ~1 µbar), and noise reducing techniques have been developed to detect such small pressure changes in a turbulent atmosphere (Bedard, 1977). Most of our past investigations have involved measurements at frequencies below about 0.5 Hz. Recently we adapted our noise reduction techniques for use at higher frequencies and reported both on measurements related to severe weather (Bedard et al., 1986) and on improved processing techniques (Bedard et al., 1988). We use measurements from an array of six microphones located around the meteorological tower of the Boulder Atmospheric Observatory (BAO). The microphones, iced 100–800 m apart, are equipped with noise-reducing devices. The system is usually not operated continuously because of the high data rates and intensive processing applied. Using cross-correlation analysis we obtain signal azimuth, horizontal phase speed, and correlation coefficients are obtained as well as power spectral data for the summed signal at maximum correlation. During the winters of 1986/87 and 1987/88 we made a special effort to record during times of probable avalanche hazard.

OBSERVATIONS OF INFRASOUND DURING TIMES OF AVALANCHE ACTIVITY

20 February 1986

On 20 February 1986 at 1535 MST we detected a signal from the direction of an avalanche near the Eisenhower tunnel about 40 miles from the BAO. The amplitude was about 0.5 µbar peak-to-peak. The signal continued for approximately 20 seconds from an azimuth of 240°. Figure 1 presents weighted power spectrum and a time series for two channels clearly showing the signal. The direction and time corresponded to an avalanche that had been triggered with small explosives. The spectral peak of this signal is about 1.5 Hz; some signal energy is as low as 0.5 Hz. Gubler (1977) presented seismic measurements of explosives used for avalanche release, observing waves with a frequency of about 30 Hz. Methods typically used to trigger avalanches artificially would not explain the sounds we observed, since they generate much higher frequencies.

Earlier on 20 February 1986 (0729 MST) we observed a signal from the northwest. We show the power spectrum and time series in Figure 2. The waveforms we observed in this and in many other avalanche-related cases are quite different from most signals detected from other sources in that the acoustic energy is often concentrated near a dominant spectral peak. This is evident in the sinusoidal segment of the trace of Figure 2b.

18 November 1987

Sixteen avalanches were reported on this date. Times were not provided for these, and the cases were primarily southwest of the BAO. Eight were in the Breckenridge, Colorado, region; several were reported from Copper Mountain. Two good infrasonic signals corresponded to these regions with 18 detected between 1520 and 2400 MST. Most signals were small in amplitude. Between 1600 and 1700 three excellent infrasonic signals were observed, coming from the west to west-northwest. The

power spectra for the interval including these signals is shown in Figure 3a, and the time series for the signal from 278° is shown in Figure 3b.
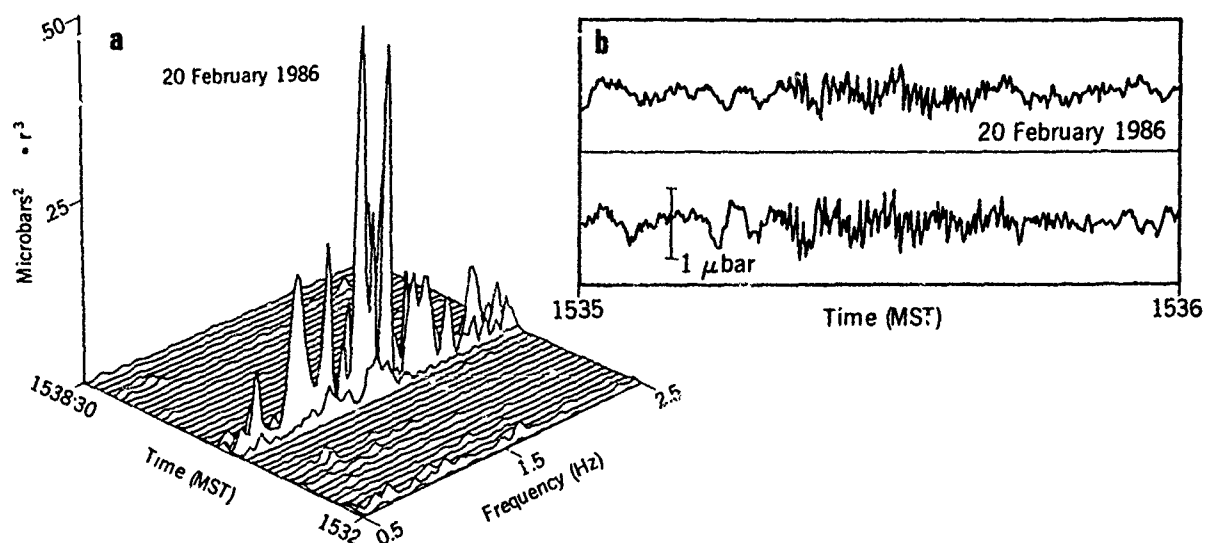
Figure 1. Infrasonic signal associated with an avalanche near the Eisenhower tunnel on 20 February 1986. (a) Power spectrum; (b) time series for two channels. The ordinate of Figure 1a and subsequent power spectral plots is weighted by multiplying by r^3 where r is the correlation coefficient. This weighting enhances regions of good signal in the display relative to periods of noise.
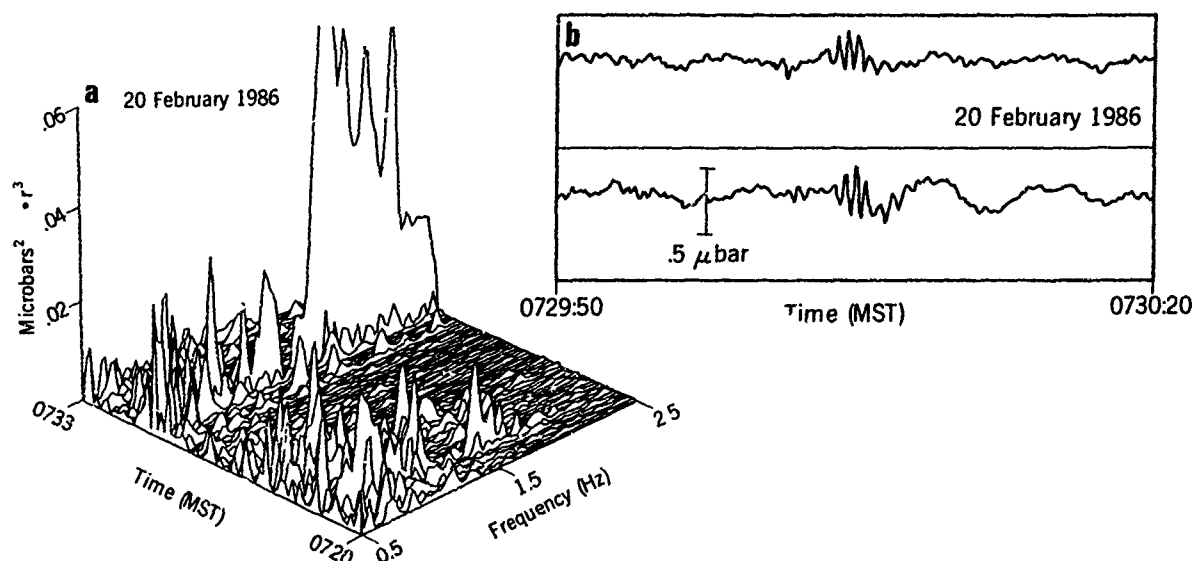
Figure 2. Infrasonic signal from the northwest on 20 February 1986. (a) Power spectrum; (b) time series for two channels.

269
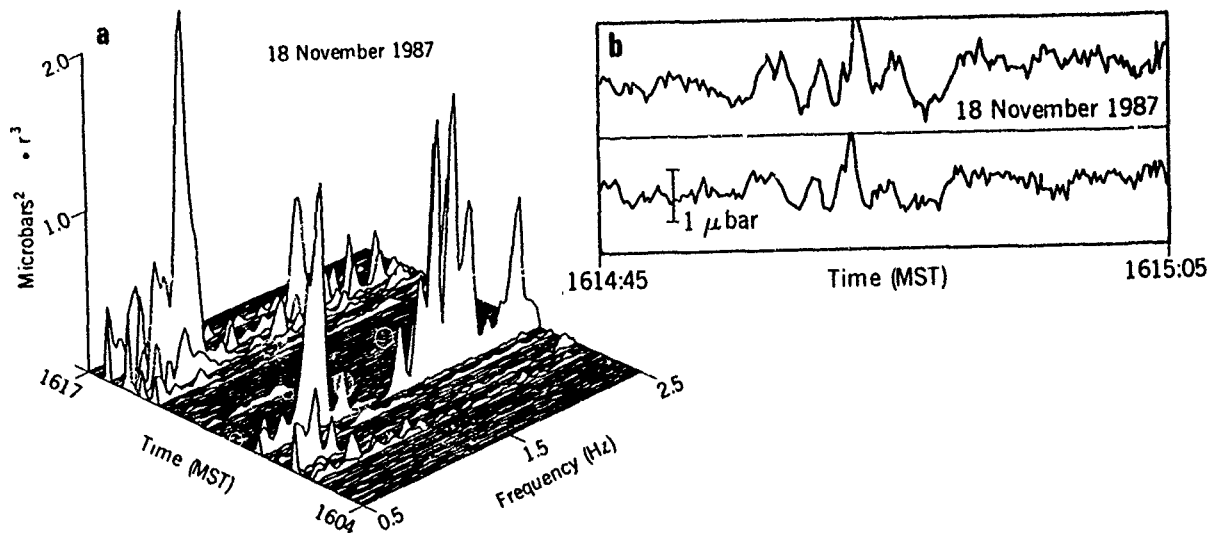
Figure 3. Several infrasonic signals from the west to west-northwest on 18 November 1987. (a) Power spectrum; (b) time series for the signal from 278°.

5/6 January 1988

During this interval 5 avalanches were reported for the northern mountains (Berthoud, Copper Mountain, Loveland, and Vail) and 31 for the central and southern mountains. There were 16 infrasonic signals between 1640 MST on 5 January and 0118 MST on 6 January. An excellent signal occurred between 1640 and 1650 MST on 5 January. The peak between 1640 and 1646 arrived from an azimuth of 214° and could have originated in the southern mountains. The peak in the energy occurred between 1 and 2 Hz, the amplitude of the signal was about 0.25 μbar peak-to-peak.

11 February 1988

On 11 February 1988 11 avalanches were reported for Loveland (east and west sides of tunnel), Vail, and Berthoud. Figure 4a shows the power spectrum from 1054 to 1100 MST, two clear peaks being present. The azimuths pass near Loveland Pass. Figure 4b is a time series for one of these signals, both of which had amplitudes of about 2 μbars peak-to-peak. For these cases there are several cycles at the same frequency.

Later in the day two more excellent signals were detected (1502 and 1503 MST). The power spectra and time series appear in Figure 5a and b. The frequency content peaks at higher frequencies (~2 to 2.5 Hz) than the earlier signals (~0.7 Hz) but the measured directions are almost identical. The amplitude for these signals is also about 5 μbars peak-to-peak.

INTERPRETATION AND POSSIBLE INFRASONIC SOURCE MECHANISMS

A number of signals detected during periods when avalanches were occurring were unique in that the acoustic power was concentrated in frequency. The time series plots showed several or many cycles of approximately constant frequency. Also, these acoustic signals should be distinguishable from other sources since the frequency was much lower than would be generated by several pounds of explosive. Furthermore, numbers of these events were recorded near or after midnight, an unlikely time for mining operations to be using larger quantities of explosive.
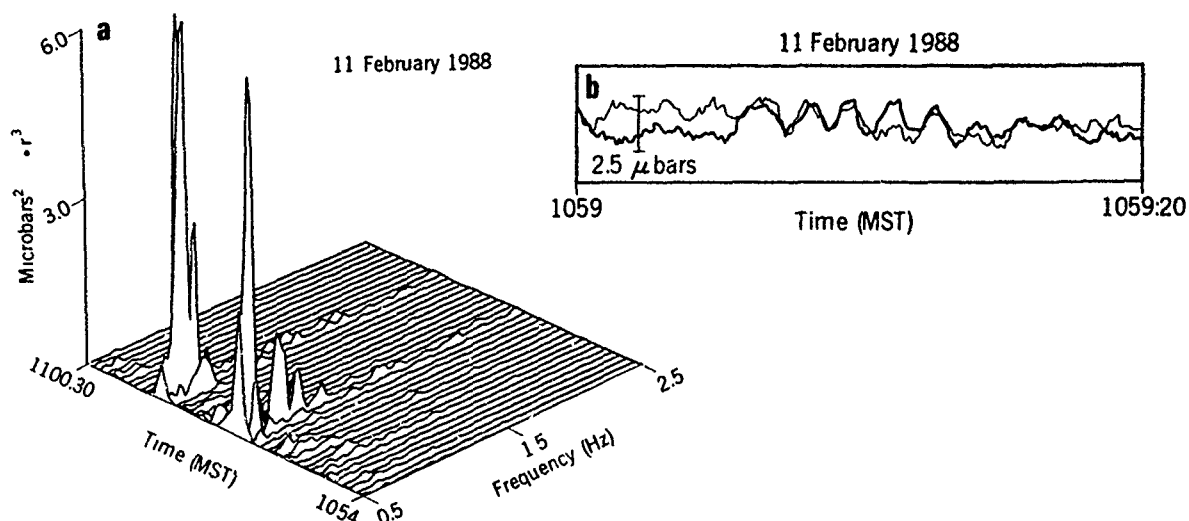
Figure 4. Infrasonic signals on 11 February 1988 from a bearing passing near Loveland Pass. (a) Power spectrum; (b) time series for two channels.
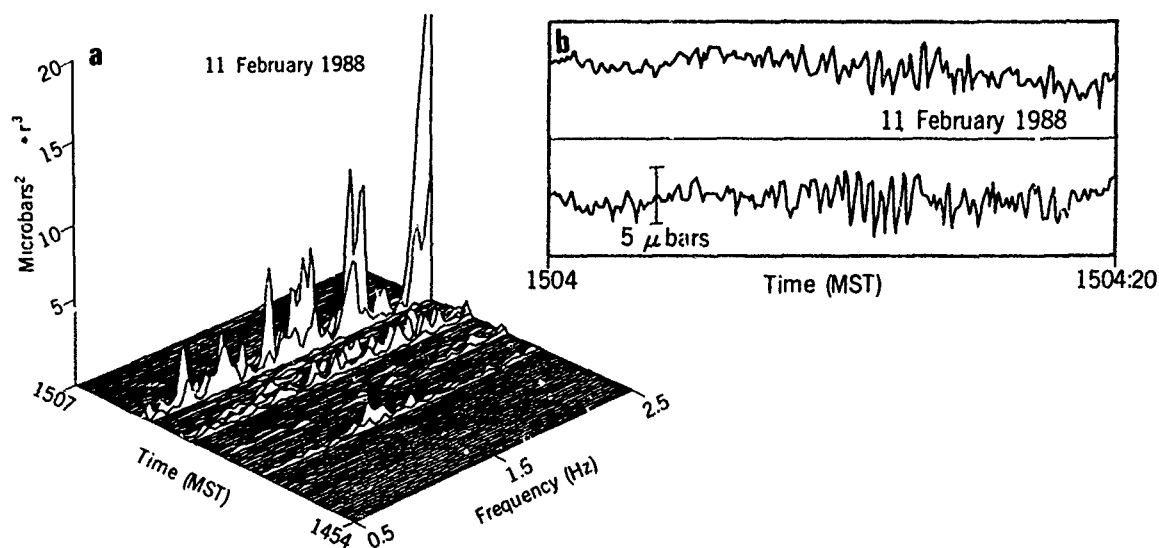
Figure 5. Infrasonic signals on 11 February 1988 also from a bearing passing near Loveland Pass. (a) Power spectrum; (b) time series for two channels.

There are several acoustic source mechanisms that could produce significant infrasound during avalanches. Figure 6 is a cross-section view indicating key regions of an avalanche. There is observational evidence for the existence of roll features near the leading edge. For example, Shimizu et al. (1980) made measurements of high-speed avalanches in Kurobe Canyon, Japan. Three load cells at different locations clearly showed the presence of a number of wavefronts. An aneroid barometer set in a nearby tunnel exit measured a pressure drop of 21 mb, and pressure gauges usually detected a pressure decrease of several millibars followed by a pressure increase often composed of several waves. Their observations documented frictional heating at the surface. Such leading edge roll features could explain the tendency for the "monochromatic" signals to be observed during periods of ava-

271

lanche activity. These roll waves have been observed in model studies (Hopfinger and Tochon–Danguy, 1977), Simpson (1988) and the roll details computed theoretically (Dressler, 1949).
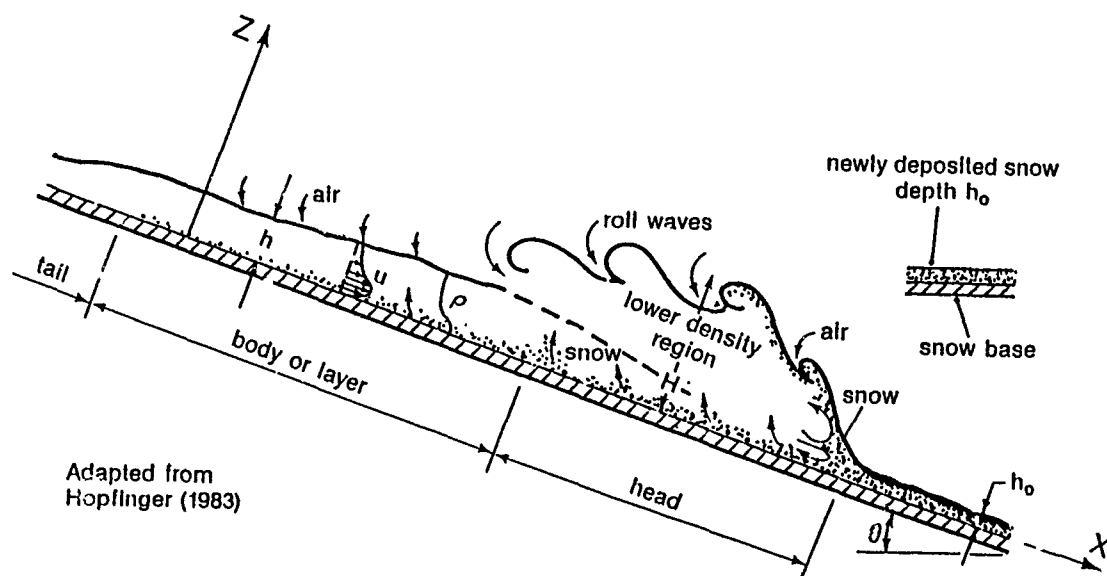
Figure 6. Cross-section view of an avalanche indicating important regions and processes (patterned after Hopfinger, 1983).

The wavelengths λ of the rolls are usually in the range between 10 h and 25 h (average 18 h) where h is the height of the avalanche as defined in Figure 6. If the acoustic frequency f, is related to the motion of the rolls past a fixed point, we can set

$$f = \frac{U}{\lambda} = \frac{U}{18h}$$

where U is the speed of motion of the avalanche. Setting $U = F_r(\Delta\varrho/\varrho \ gh)^{1/2}$ the frequency may be written

$$f = \frac{F_r(\Delta\varrho/\varrho \ g)^{1/2}}{18h^{\cdot/2}} ,$$

where F_r is the Froude number (for these calculations $F_r = 1$), $\Delta\varrho$ is the density difference between the medium density ϱ and the avalanche density (0.1 cm^{-3} is used here), and g is the gravitational acceleration. Figure 7 is a plot of the frequency as a function of height h and Figure 8 is a corresponding plot of U as a function of h. The frequency range predicted for these conditions is 3–1 Hz, with the stronger, faster moving avalanches producing lower frequencies.
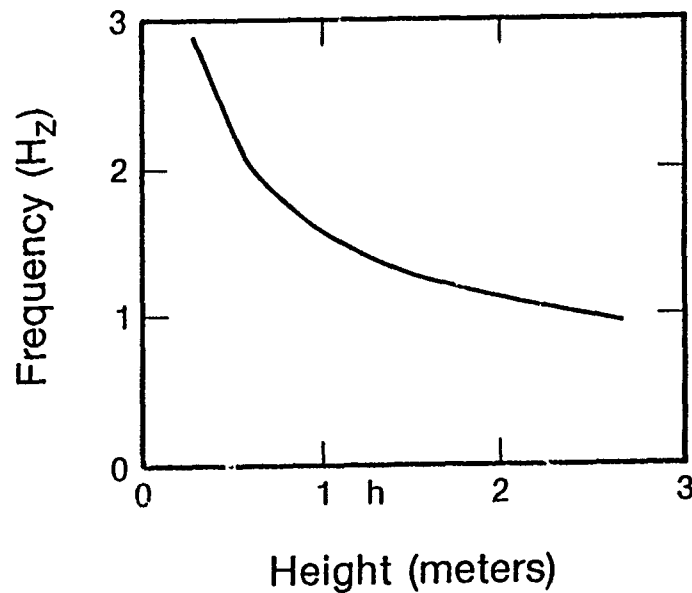
Figure 7. Computed frequency as a function of avalanche height h indicating the potential of avalanche rolls to produce the observed infrasonic spectral content.
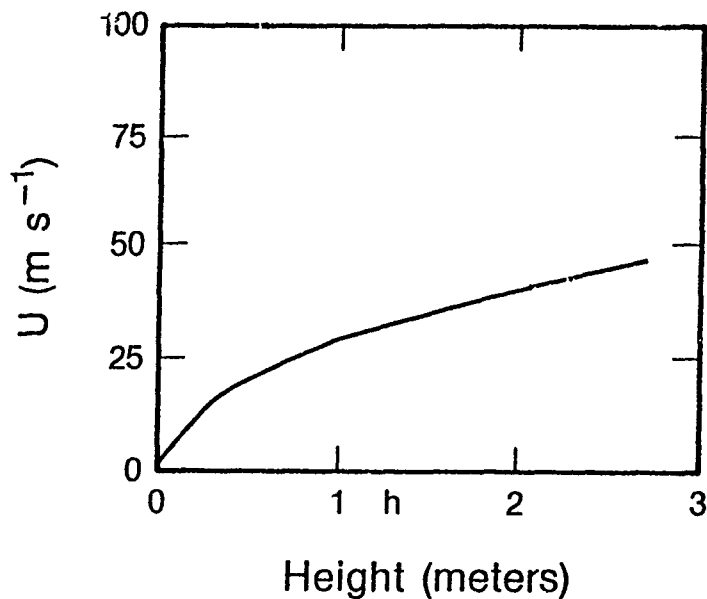
Figure 8. Avalanche speed U as a function of height h. These speeds correspond to the data presented in Figure 7.

This analysis, although indicating that the frequency content produced by roll waves corresponds to our observations, does not address the question of the acoustic generation mechanisms or the magnitudes of pressure disturbances produced. One possibility is that water vapor and water droplets rapidly cooled as the avalanche terminates produce regions of heating from the release of latent

273

heat of condensation or fusion. The surface frictional heating would be an important component of the process warming air that is entrained in the rolls. Subsequently, the warmed air in the rolls containing a mixture of water vapor and water droplets could be rapidly cooled by mixing with the ambient air after the lower region h stopped moving. The rolls could act as a series of monopole acoustic sources. There are numerous observations of "airwaves" causing damage for considerable distances beyond the point where the lower snow stops (e.g., Matveyev, 1940). Turbulent wakes could also be a source of infrasound.

CAUTIONARY REMARKS AND RECOMMENDATIONS FOR FUTURE RESEARCH

We have presented a summary of the characteristics of infrasonic signals measured during periods of avalanche activity. However, we had only one observing station and hence only bearing information and not distance from the site. A second station would be required to triangulate the source location. Many questions remain, including the following:

- What is the acoustic signature in the source region?

- What mechanisms produce the "monochromatic" infrasound observed?

- Can we relate the distant acoustic signature to detailed avalanche characteristics (e.g., depth, average density, height)?

- What is the effect of propagation on the acoustic signature?

- What is the practical potential of infrasound as an avalanche detection tool?

We recommend that infrasonic measurements be made in the vicinity of controlled avalanches. The use of combined remote sensor systems such as Doppler radar and Doppler lidar would provide data on both the internal and external avalanche flow fields. An infrared radiometer could monitor the temperature changes associated with avalanches, which may be a factor in the generation of infrasound. A final step should be the addition of a secon infrasonic observatory so that triangulation techniques can be tested.

ACKNOWLEDGMENTS

REFERENCES

Bedard, A. J., Jr., 1977, "The d-c Pressure Summator: Theoretical Operation, Experimental Tests and Possible Practical Uses," Fluidics Q, Vol. 9, 26–51.

Bedard, A. J., Jr., 1978, "Infrasound Originating Near Mountainous Regions in Colorado," J. Appl. Meteorol, Vol. 17, 1014–1022.

Bedard, A. J., Jr., 1988, "Infrasound from Natural Sources," Proc. Inter-Noise 88, Avingnon, France, 30 August 1988.

Bedard, A. J., Jr., and G. E. Greene, 1981, "Case Study Using Arrays of Infrasonic Microphones to Detect and Locate Meteors and Meteorites," J. Acoust. Soc. Amer., Vol. 65(5), 1277–1279.

Bedard, A. J., Jr., J. Intrieri, and G. E. Greene, 1986, "Infrasound Originating from Region of Severe Weather," Proc. 12th International Congress on Acoustics, Toronto, Canada, July 1986.

Dressler, R., 1949, "Mathematical Solution of the Problem of Roll-Waves in Inclined Open Channels," Communications on Pure and Applied Mathematics, Vol. 2, 149–194.

Georges, T. M., 1973, "Infrasound from Convective Storms: Examining the Evidence," Rev. Geophys. Space Phys., Vol. 11, 571–594.

Gubler, H., 1977, "Artificial Release of Avalanches by Explosives," J. Glaciology, Vol. 19, 419–429.

Harrison, J. C., 1976, "Seismic Signals from Avalanches, Ch. 7: Avalanche Release and Snow Characteristics, San Juan Mountains, Colorado," Final Report San Juan Avalanche Project Institute of Arctic and Alpine Research; U. of Colorado, Boulder, CO. Editors, R. L. Armstrong and J. D. Ives, 145–152.

Hopfinger, E. J., 1983, "Snow Avalanche Motion and Related Phenomena," Ann. Rev. Fluid Mech., Vol. 15, 47–76.

Hopfinger, E. J., and J. C. Tochon-Danguy, 1977, " A Model Study of Powder-Snow Avalanches," J. Glaciology, Vol. 19, 343–363.

Judson, A., 1976, "Colorado's Avalanche Warning System," Weatherwise, Vol. 29, 268–277.

Matveyev, S. N., 1940, " The Airwave Accompanying a Snow Avalanche," Problemy Fizicheskoi Geografoi, Vol. 9, 83–90.

Salway, A. A., 1978, "A Seismic and Pressure Transducer System for Monitoring Velocities and Impact Pressures of Snow Avalanches," Arctic and Alpine Res., Vol. 10(4), 769–774.

Shimizu, H., T. Huzioka, E. Akitaya, H. Narita, M. Nakagawa, and K. Kawada, 1980, "A Study on High-Speed Avalanches in the Kurobe Canyon, Japan," J. Glaciology, Vol. 26, 141–151.

Simpson, J. E., 1988, "Gravity Currents: In the Environment and the Laboratory," Halsted Press, New York.

St. Lawrence, W., and T. R. Williams, 1976, "Seismic Signals Associated with Avalanches," J. Glaciology, Vol. 17, 521–526.

Tahira, M., 1988, "A Study of the Long-Range Propagation of Infrasonic Waves in the Atmosphere (1) Observation of the Volcanic Infrasonic Waves Propagating Through the Thermospheric Duct," J. Meteorol. Soc., Japan, Vol. 66, 17–26.

Young, J. M., and G. E. Greene, 1982, "Anomalous Infrasound Generated by the Alaskan Earthquake of 28 March 1964," J. Acoust. Soc. Amer., Vol. 71, 334–339

Application of Physical Modeling for Assessment of Snow Loading and Drifting

Ronald L. Petersen and Jack E. Cermak[1]

INTRODUCTION

Petersen (1986) reported on the application of physical modeling for the assessment of snow loads on fabric roofs; namely the Minneapolis Metrodome and the Canada Place Project (now named the Pan Pacific Hotel and Convention Center) in Vancouver, B.C. This paper discusses additional applications of physical modeling for assessing snow loading and snow drifting and some of the uncertainties associated with the physical simulation. The applications that will be discussed relate to the following two projects: 1) a new lodge/cafeteria at Rim Village (RV), Crater Lake, Oregon, and 2) the Minneapolis Convention Center (MCC). For the Rim Village (RV) project, physical modeling was conducted to provide information on the snow drifting patterns for two different configurations of a new lodge/cafeteria/interpretive center. For the MCC project, the physical model was to provide information on the expected snow loading on the roof as well as information on the drifting patterns around entrances. For these applications, the mechanisms of particle transport would be a combination of snowfall through an ambient wind field and saltation once the particles deposit on the ground or roof.

This paper presents the criteria used to simulate falling and blowing snow (saltation), the experimental methods and typical results from both projects. Also included is a comparison of observed snow accumulations at Rim Village with those observed in the wind tunnel.

SIMILARITY REQUIREMENTS

Similarity of snow transport, deposition and erosion by wind may be considered as the aggregate of four subsimilarities. These subsimilarities, which can be approximated by independent measures in physical modeling for specific applications, are as follows: 1) similarity of natural wind; 2) similarity of local flow over objects of concern (buildings, fences, etc.); 3) similarity of snow characteristics; and 4) similarity of time sequence for snowfall and meteorological variables.

Simulation of natural wind in boundary-layer wind tunnels can be achieved, as discussed by Cermak (1975), with sufficient accuracy for wind-engineering applications. Local flow similarity is obtained by construction of model buildings, fences, etc. to preserve geometrical similarity. However, the local Reynolds number must be in excess of a minimum value if Reynolds number

---

[1]Vice President and President, respectively, CERMAK PETERKA PETERSEN, INC., 1415 Blue Spruce Drive, Fort Collins, CO 80524, (303) 221-3371.

independence is to be attained. Similarity of snow movement in wind must be addressed separately for falling snow and for drifting snow. Characteristics of snow and the resulting dimensionless parameters for these two cases are discussed in the following paragraphs. Similarity parameters for time dependence and time sequences of falling snow, drifting snow, melting and freezing have not been developed sufficiently for general physical modeling. Treatment of a special case not considering melting and freezing is presented for the Rim Village study.

Based on dimensional analysis and discussions in Iversen (1980) and Kind (1986), the following similarity criteria which are common to both the falling and drifting snow simulations were applied for this evaluation:

- undistorted scaling of geometry,
- similar velocity and turbulence profiles in the wind tunnel and atmosphere,
- sufficiently high building Reynolds number, $Re = h\, U/\nu$ (1)
- sufficiently high roughness Reynolds number, $Re_{zo} = U_* \, z_o/\nu$
- similar atmospheric stability, and
- proper scaling of the roughness elements (i.e., z_o/z_r in model and full-scale approximately equal).

For the falling snow simulation, the following additional requirements are necessary:

- Match velocity ratio, R,   (2)
- Match buoyancy Froude Number, Fr.

where

R = U_h/U_t,
Fr = $\rho_a \, U_h^2/(g\rho_p D)$,
ρ_a = ambient air density,
ρ_p = snow particle density,
D = particle diameter,
U_h = wind speed at height h (m/s),
U_t = terminal velocity of snow particle,
z_o = surface roughness length, and
z_r = reference height.

For the blowing snow simulations, the main parameters to match are the ratio of threshold transport speed to friction velocity and Froude number. Several other parameters were not matched in model and full scale (i.e., moisture content of the snow, frictional factor between roof and snow, particle size distribution, friction between particles). At present, the technology is not available to match these parameters or to accurately simulate falling and blowing snow simultaneously. A method was developed on a trial and error basis however, to reasonably reproduce field drift patterns that were a result of falling and blowing snow for the Rim Village evaluation. This method is discussed in the results section.

Regarding snow movement similarity, Iversen (1987) and Kind (1986) reported that the Froude number is important for simulating the saltation phenomena and Iversen et al. (1987) reported that the threshold friction speed for small particles is a function of the particle to fluid density ratio. For the

277

applications reported here, the density ratio in model was 2500 and in full scale 300. Iversen's results suggest that in this range, the dimensionless threshold velocity is essentially constant. When model Froude numbers are higher than full scale, Iversen suggests that slightly lower maximum drift depths will occur in the model as well as a small change in the location of the maximum depth and larger change in location where the drift begins.

Regarding the physical characteristics of snow particles, in 1951 the Commission of Snow and Ice of the International Association of Hydrology suggested a classification for solid precipitation particles in which the particles were divided into the following ten classes: plate, stellar crystal, column, needle, spatial dendrite, capped column, irregular crystal, graupel, ice pellet and hail. Since 1951, Magono and Lee (1966) developed another classification scheme with 78 categories. For most snowfall simulation applications, an aggregate particle will apply. Figure 1, taken from Hobbs (1974), shows the fall velocity of various types of snow crystals versus the maximum dimension of the crystal. The fall velocities range from 0.25 to 2.5 m/s. For solid ice columns, needle crystals, and hollow columnar ice, the bulk density was reported to vary between 0.6 and 0.9 Mg/m^3. Magono and Nakamura (as reported in Hobbs, 1974) made simultaneous measurements of terminal velocities, sizes and densities for snowflakes. For the density range 0.1 to 0.3 Mg/m^3, the following equation was found to fit the observations:

$$U_t = 88(\rho_p - \rho_a)^{\frac{1}{2}} d^{\frac{1}{2}} \tag{3}$$

where U_t is in m/s, d in meters and $(\rho_p - \rho_a)$ in Mg/m^3. Full-scale properties of falling snow are found to vary significantly and thus make it difficult, if not impossible, to accurately specify a particle density, size and terminal velocity to simulate. The physical properties of the model snow particles were reasonably well known. The physical properties of the full-scale snow were computed so that model and full-scale Froude number and velocity ratio equality were maintained.
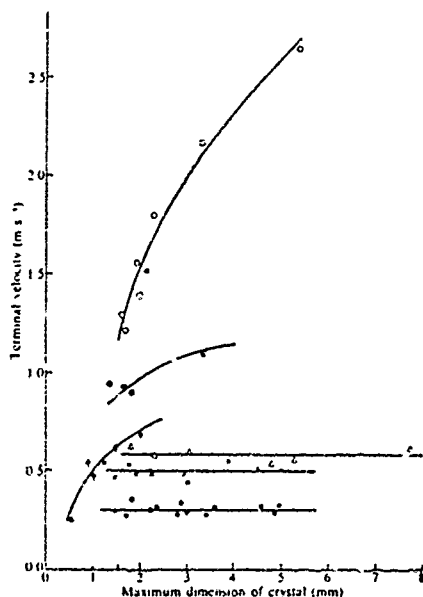
Figure 1. Terminal velocities of snow crystals as a function of their maximum dimensions. O--Graupel, ⊖--Rimed crystal, ♦--Needle, Δ--Spatial dendritic, x-- Powder snow, ¢--Dendritic. From Nakaya and Izima (1935) with changes.

278

Table 1 shows the model and full-scale parameters for the Rim Village falling-snow and blowing-snow simulations. The nominal particle size in the model was 0.010 cm, the particle density 2500 kg/m^3 and the fall velocity approximately 1 m/s based on Stokes law. For a model wind speed of 1 m/s, the Froude number is 0.42. If the full-scale particle diameter is taken to be 10 mm (a reasonable snowflake size from Hobbs), the fall velocity is approximately 2 m/s. For the falling-snow simulation, equal velocity ratio scaling requires that the full-scale wind speed be 2 m/s. To obtain equal Froude numbers in model and full scale, the snowflake density would have to be 97 kg/m^3. This is a reasonable full-scale density, and hence, the falling-snow simulation should be representative of that expected in the atmosphere for the physical properties assumed.

TABLE 1
MODEL AND FULL-SCALE PARAMETERS FOR THE SNOW SIMULATION
AT RIM VILLAGE (1:240 MODEL SCALE)

Parameters	Full-Scale	Model
Snowfall		
1. Fluid Density--ρ_a (kg/m^3)	1.29	1.02
2. Ambient Temperature--T_a ($^\circ$K)	273	293
3. Snowfall Particle Density--ρ_p (kg/m^3)	97	2500
4. Particle Diameter--D (cm)	1.00	0.010
5. Terminal Speed--U_t (m/s)	2.0	1.0
6. Wind Speed--U_r (m/s)	2.0	1.0
7. Reference Height--z_r (m)	240.0	1.0
8. Velocity Ratio--U_r/U_t	1.0	1.0
9. Froude Number--$Fr = \rho_a U_r^2/g\rho_p D$	0.42	0.42
Saltation		
10. Friction Velocity Ratio--U_*/U_r	0.05	0.05
11. Threshold Friction Speed U_{*t} (m/s)	0.24	0.24
12. Particle Density -- ρ_p(kg/m^3)	329	2500
13. Particle diameter -- D (cm)	0.1	0.010
14. Froude Number-Fr $= \rho_a U_{*t}^2/g\rho_p D$	0.023	0.023

For the blowing-snow simulation, the wind speed (U_r) was increased until particle transport along the surface of the model was observed. This speed was approximately 6 m/s. The velocity profile was then analyzed to obtain the ratio of friction velocity to wind speed which was found to be 0.05, resulting in the friction velocity given in Table 1. The full-scale threshold velocity was assumed equal to the model threshold. The model Froude number based on the friction velocity was computed to be 0.023. With a full-scale particle diameter of 0.01 cm and density of 329 kg/m^3, model and full-scale Froude numbers could be matched. The full-scale diameter is in the range observed in the atmosphere for needles, plane dendrites and powder snow and the density is typical of graupel-like snow, solid columns, and needle crystals.

EXPERIMENTAL METHODS

The Wind Tunnel and Scale Models
All model testing was carried out in an open-circuit, boundary-layer wind tunnel similar to the one described in Cermak (1975). The Rim Village (RV) and Minneapolis Convention Center Models (MCC) and vicinity were fabricated at scale reductions of 1:240 and 1:250, essentially identical. For the Rim Village

project (Petersen, 1985), a model of the existing cafeteria, proposed lodge/cafeteria/interpretive center and surrounding terrain was fabricated. Figure 2 shows a plan view of the area modeled, Figures 3 and 4 show photographs of the existing cafeteria (after a snowfall simulation) in model and full scale, respectively. Figure 5 shows a picture of the MCC model and surroundings. Upwind of the circular models, a characteristic surface roughness was installed to obtain the approaching wind and turbulence profiles characteristic of the site.

Figure 3. Model of Existing Rim Village Cafeteria and Simulated Snow Accumulations for the SE Wind Direction After Blowing Snow Conditions Simulated
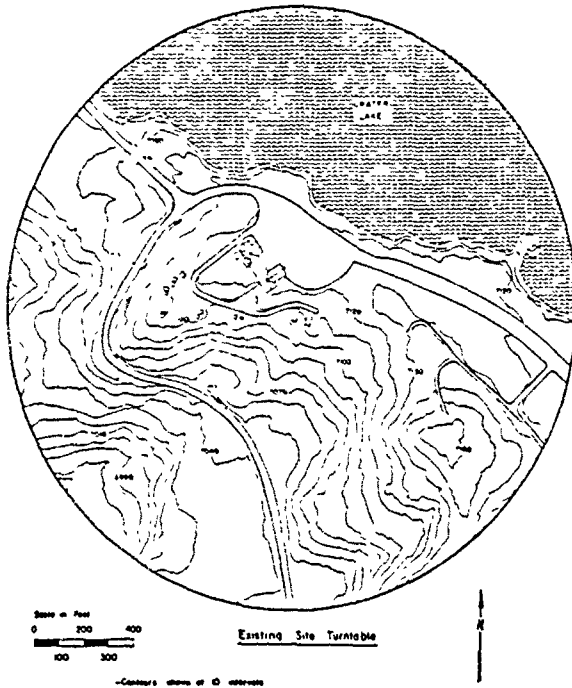
Figure 2. Terrain Area Modeled at 1:240 Scale and Existing Site Plan for Rim Village

Figure 4. Full-Scale Drift Patterns for the Rim Village Cafeteria - Rim Village
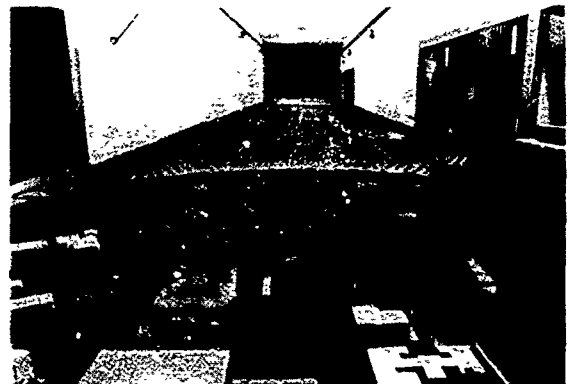
Figure 5. Photograph of Minneapolis Convention Center Model Installed in Wind Tunnel

Velocity Measurements

To document the representativeness of the wind-tunnel test setup, velocity and turbulence profiles approaching the models were measured. By fitting the measured data to the following equations:

$$U/U_* = 2.5 \ln (z/z_0) \tag{4}$$
$$U/U_r = (z/z_r)^n$$

the equivalent full-scale surface roughness factor (z_0) and power law exponent (n) were estimated to be approximately 50 cm and 0.25, respectively, for both studies. These values are representative of that expected for cities or forested areas (Snyder, 1981). Hence, the dimensionless velocity distribution approaching the models approximately matched that expected at the actual site. The friction velocity ratio (U_*/U_r) of the approaching flow was estimated to be 0.05. The friction velocity ratio around the RV site and around the MCC site will vary significantly from the approaching value due to local surface roughness inhomogeneities.

Snow-depth Measurements

For the RV and MCC assessments, falling snow was simulated by releasing 0.01 cm glass beads from an elevated seeding device upwind of the target area as discussed in Petersen (1986). Glass beads were released until a representative ground depth was observed (approximately 0.6 cm for RV and 0.25 cm for MCC). The resulting depths of simulated snow were measured at locations on the ground and roof as appropriate.

Blowing snow was simulated (only for the RV study) by increasing the tunnel speed above the threshold speed for glass bead movement. The snow that had accumulated during the falling-snow simulation was used as the base for the blowing-snow test. After the drift patterns appeared to stabilize, photographic or quantitative measurements were obtained.

All measured depths for the RV assessment were converted to full-scale concentrations by multiplying by the scaling factor of 240. For the MCC study, all measured depths on the roof were converted to depth/snow-load coefficients, C_s, by dividing by the ground-snow depth, or

$$C_s \quad = \quad D/D_0 \quad = \quad L/L_0$$

where

D,L	=	local snow depth or load
D_0, L_0	=	ground-snow depth or load

To compute full-scale loads, the C_s values must be multiplied by the appropriate full-scale ground-snow load.

LOCAL CLIMATOLOGY

To utilize the snow load or depth coefficients from the wind-tunnel tests, the appropriate ground depth or ground load is required. There are two appropriate ground depths, one based on the 24-hour snowfall and one based on the accumulated snow load that occurs once in 50 years. If snow removal strategies are to be applied as they were for the MCC, the 50-year, 24-hour snowfall is the more appropriate case.

The ground load based on the 50-year, 24-hour snowfall was determined by analyzing measured snowfall data at the Minneapolis airport over the period of 1956 through 1982. Using an extremal Type I distribution, the 50-year, 24-hour snowfall was found to be 41.66 cm. Freshly fallen snow will be less dense than snow that has had a chance to settle; hence, the lowest ANSI A58.1-1982 specific weight category was used (15 lb/ft^3 or 240 kg/m^3). This resulted in a ground-load value L_0 of 100 kg/m^2 (20.6 lb/ft^2) for a 50-year recurrence interval. Hence, to determine roof loads for 24-hour accumulations, the snow-load coefficients (C_s) must be multiplied by 3.5.

In order to establish the wind directions that were used for testing, joint frequency distributions of wind speed and wind direction for all days and days of more than 7.6 and 12.7 cm of snowfall were computed. Based on an analysis of these results, wind directions and speeds were selected for testing. The analysis is discussed in detail in Petersen (1986).

For the Rim Village site, a detailed description of the climatology was furnished by the U.S. Forest Service. The greatest snow depth ever recorded was 6.15 m measured at the Crater Rim. The average seasonal maximum depth was 3.94 m. The prevailing wind direction during wind storms was found to be from the southwest, but some significant storms were observed to occur with directions from the east through west (moving clockwise). Based on the climatological analysis, wind-tunnel testing was conducted using winds in the sector SE through SW.

DISCUSSION OF RESULTS

Rim Village

Prior to evaluating the snow-drifting characteristics for the proposed new construction, the snow-simulation method was evaluated by comparing wind-tunnel drifting patterns (Figure 3) observed about the existing cafeteria with those observed in the field (Figure 4). The first method used to obtain ground drifting consisted of releasing snow from an overhead seeding device until a representative ground depth was observed and then the wind speed was increased until particle movement was noticed. The resulting snow drift patterns did not agree well with observations. Upon consultation with the U.S. Forest Service it was discovered that the parking lots were cleared after every snowfall and much of the snow was blown into the area of large observed snow accumulation. Based on this information, the following procedures were developed: 1) after setting appropriate wind speed in the wind tunnel, release sufficient snow material (27.2 kg) to obtain a ground depth of approximately 0.6 cm; 2) clear parking lot as done in the field; 3) release additional material (13.61 kg) from overhead seeding device; 4) clear parking lot; 5) increase the wind speed above particle threshold for saltation; 6) after drifts stabilize, obtain photographs and snow depth measurement. Figure 3 shows the snow drift patterns that occurred after such a procedure was followed and Figure 4 shows the drifting patterns observed in the field. Good agreement is noted and the method appears to be qualitatively correct.

After qualitatively validating the snow simulation method, drifting patterns around several configurations of the proposed new lodge/cafeteria/interpretive center were obtained using the same method. The main goal of the testing was to determine whether the proposed designs would show large snow accumulations in entrance areas. Figure 6 shows the results of one of the snow simulations and demonstrates that entrance areas will generally be scoured and kept free of

snow. The small building, on the other hand, has a large accumulation on the entrance. Figure 7 shows a second simulation where a 5 m wedge-type snow fence was installed upwind of the entrance area. The figure shows that the area is now relatively free of snow accumulations.

Figure 6. Photographs of New Lodge/ Interpretive Center and Snow Accumulations for the SSW Wind Direction After Blowing Snow Conditions Simulated

Figure 7. Photographs of Snow Accumulations with 5 m Wedge Snow Fence and SSW Direction for New Lodge/ Interpretive Center After Blowing Snow Conditions Simulated

Minneapolis Convention Center

Snowfall simulations were conducted for varying wind speeds and wind directions. Generally, snow accumulations were found to be significant only for the low wind speed cases ($\approx$ 2 m/s full scale) and as the wind speed increased, the accumulations on the roof domes decreased. Figure 8 shows the effect of wind speed on dome snow accumulations for each wind direction.
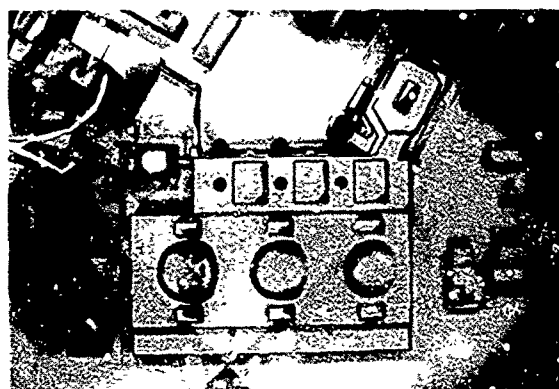
Figure 8a. Photograph of Snow Accumulations on the MCC for the E Wind Direction and Low ($\sim$ 2 m/s) Wind Velocity
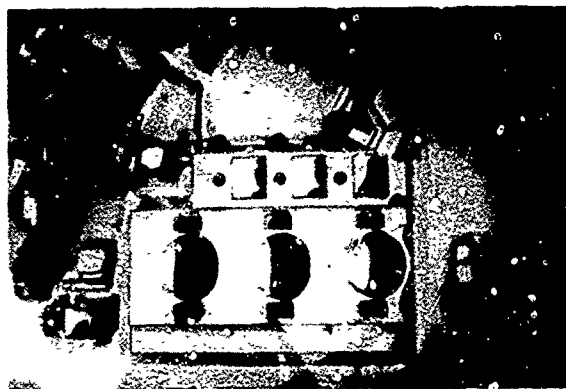
Figure 8b. Photograph of Snow Accumulations on the MCC for the E Wind Direction and Moderate ($\sim$ 4 m/s) Wind Velocity

For each case simulated, snow depths were measured at the locations showing the largest accumulations. For the low wind speed cases, measurements were obtained at approximately 100 locations and for the high wind speed cases, fewer measurements were required. Snow depth or loading coefficients were then computed at each measurement point.

. The loading coefficients for each case simulated were used to compute a worst case loading configuration for the roof. The highest loading coefficient at each measurement location was plotted on a plan view of the roof. Figure 9 was prepared for use in designing for maximum snow accumulations. This procedure is conservative but the building was designed to adequately handle the computed loads. Therefore, no further refinements in the technique were necessary.
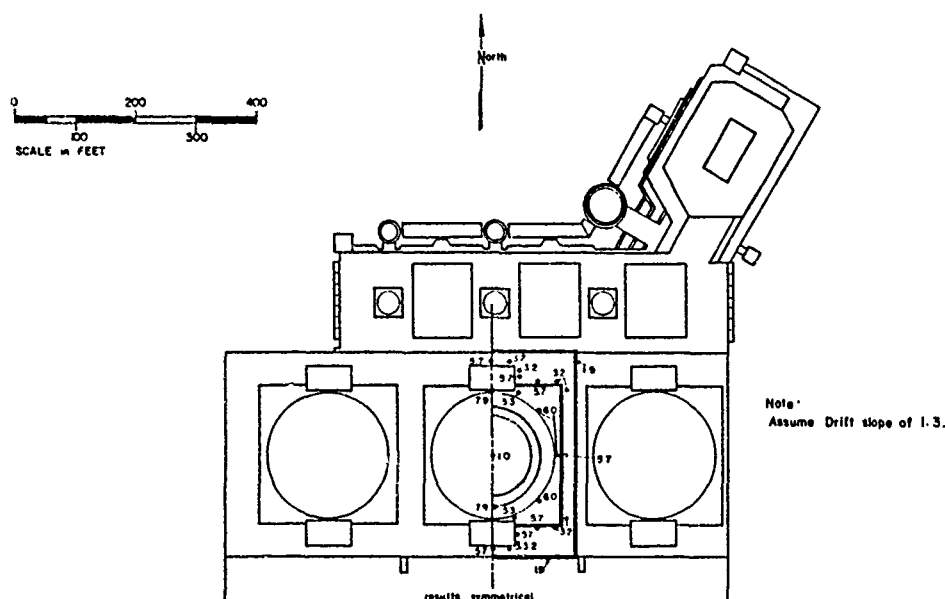
Figure 9. Composite Snow Loading Coefficients in Vicinity of Minneapolis Convention Center Large Dome

CONCLUSIONS

The results and discussions presented have shown that physical modeling is a useful method for helping designers assess the effect of falling or drifting snow. The wind tunnel can also provide conservative estimates of the maximum loads that can be expected on roofs. A comparison of a wind-tunnel simulation of snow accumulations due to falling and blowing snow was developed and compared against the drifting patterns observed in the field. The comparison was good and qualitatively validated the procedure used.

Even though the wind tunnel showed qualitative agreement for the case discussed in this paper, in general, insufficient field/wind-tunnel comparisons of snow simulations on roofs or around buildings have been conducted. A series of field tests are needed where roof, near-field and far-field snow depths are measured during isolated storms along with wind speed, wind direction, snow density, and snow type. The wind tunnel could then try to simulate the measured accumulations so that the relative accuracy of the wind tunnel for this application could be assessed.

REFERENCES

Cermak, Jack E., "Applications of Fluid Mechanics to Wind Engineering--a Freeman Scholar Lecture", ASME Journal of Fluids Engineering, 97, Ser. 1, No. 1, pp. 9-38, March, 1975.

Cermak, Jack E., "Wind-tunnel Design for Physical Modeling of Atmospheric Boundary Layers," Special Volume on Advances in Fluid Mechanics, ASCE Journal of Engineering Mechanics, 107, No. EM3, June, 1981.

Hobbs, Peter V., Ice Physics, Clarendon Press, Oxford, England, 1974.

Iversen, J.E., "Drifting Snow Similitude-Transport-Rate and Roughness Modeling," Journal of Glaciology, 6, No. 94, 1980.

Iversen, J.E., "Froude Number Effects in Sediment Transport Modeling", 7th International Conference on Wind Engineering, Aachen, West Germany, July 6-10, 1987.

Iversen, James D., Ronald Greeley, John R. Marshall, and James B. Pollack, "Aeolian Saltation Threshold: The Effect of Density Ratio", Sedimentology, 34, pp. 699-706, 1987.

Kind, R.J., "Snowdrifting: A Review of Modelling Methods," Cold Regions Science and Technology, 12, pp. 217-228, Elsevier Science Publishers, 1986.

Magono, C., and C. Lee, "Meteorological Classification of Natural Snow Crystals," Journal of Faculty of Science, Hokkaido Imperial University, Ser. VII, 2, 321-35, 1966.

Nakaya, Ukitiro, and Tuneo Izima, "Physical Investigation on Snow, Pt. I., Snow Crystals Observed in 1933 at Sapporo and Some Relations with Meteorological Conditions," Journal of Faculty of Science, Hokkaido Imperial University, Ser. II, Vol. I, No. 5, 1934.

Petersen R.L., "Wind and Snow Study for Minneapolis Convention Center," prepared for Skilling Ward Rogers Barkshire Inc., Seattle, WA, by Cermak Peterka and Associates, Report No. C/PA 86-0373, December, 1986.

Petersen, R.L. "Simulating Snow Loads on Fabric Roofs", ASCE, Advancement in Aerodynamics, Fluid Mechanics, and Hydraulics, Minneapolis, MN, June 3-6, 1986.

Petersen, R.L., "Wind Tunnel Study of Snow Conditions at Rim Village Crater Lake National Park, Oregon", prepared for Fletcher Finch Farr Ayotte by Cermak Peterka Petersen, Inc., Report No. CPP 86-0361, August, 1987.

Snyder, William H., Guideline for Fluid Modeling of Atmospheric Diffusion," Environmental Sciences Research Laboratory, Office of Research and Development, U.S. Environmental Protection Agency, Research Triangle Park, NC 27711, April, 1981.

Snow Control with Vortex and Blower Fences

Brett N. Meroney and Robert N. Meroney[1]

ABSTRACT

Blower fences (jet roofs) and vortex style blower fences were examined in a small wind tunnel to examine their ability to prevent snow deposition downwind. A series of experiments were performed to evaluate optimum fence geometries, fence orientations, and comparative performance characteristics. Forty-five combinations of blower-fence height and fence angle were tested to determine optimum blower fence proportions. A blower fence located 1.5 times its table width above the ground at an angle of attack of 15° appeared optimum. Additional runs were performed on a delta-wing vortex fence. The structure was constructed from an equilateral triangle oriented at a 15° angle into the wind. Tests over a range of fence heights from 0.25 to 0.75 triangle heights supported at the delta-wing centroid did not identify a strong dependence of fence performance on wing height above the ground. The vortex fence generally outperformed the blower fence tested. Scaled fences were also tested around a model house to eliminate snow deposition over driveway surfaces. The blower fences eliminated drifts which otherwise developed in the absence of protection.

INTRODUCTION

Most conventional snow fences are designed to produce preferential deposition of snow in the sheltered area behind the fence. Accumulation of drifting snow in these regions protects downwind areas through a process of attrition of particles from the air stream near the ground. An alternative approach is to devise a structure which protects a downwind region through an increase in surface scour. The tabletop type blower fence is designed to accelerate the wind flow locally by diverting the wind flow downward through a constriction between the blower roof and the ground. A vortex-style blower fence produces counter-rotating vortices which align axially with the wind and increase surface stresses downwind.

This paper reviews the physical principles and experience associated with such fences, discusses simulation concepts required to develop fence design criteria through physical modeling, and presents the results of an experimental program to optimize the size and shape of such devices.

Blower Fences

Blower fences made from panels mounted on vertical supports and inclined with the higher end toward the prevailing wind have been variously called "pupitre" or "Pultdächer" (desks or desk roofs), "Düsendächer," "toits," "blower roofs," "snow blowers," or "jet roofs." They are used frequently when

I Professor, Civil Engineering
   Director, Fluid Dynamics and Diffusion Laboratory

the snow-bearing wind varies little in direction, and they are especially useful when the quantity of snow is large enough to swamp the ordinary type of fence.

In the winter of 1946-47, staff at the Canadian Army base at Fort Churchill, Manitoba, noted that during a blizzard the area lying underneath the wings of aircraft parked facing the wind was blown clear of snow. Subsequently, army personnel and the Department of Highways in Ontario carried out a program during the winter of 1948-49 to evaluate the performance of blower fences at nine separate locations along Canadian highways (Fraser, 1949, 1950). Conventional vertical slat snow fences were supported on steel fence posts, inclined at various angles, and arranged with the lower edge at various heights and distances from the roadway. Some 3.3-km (10,850 lineal feet) of fence were constructed at sites ranging from 0- to 5-m (0- to 17-ft) from the roadway, 0.75- to 1.2-m (2.5- to 4-ft) above ground, 30° to 60° inclination to the horizontal, and along flat roadway or 3-m (10-ft) deep highway cuts. Although many of the fences were buried under accumulated snow from plows, three fences kept roadway centers free in cuts normally filled 2.5- to 3.5-m deep by blizzards, and others worked well until they were plowed under.

Fraser (1949, 1950) concluded that the installations were definitely beneficial at the top of slope locations and worked well at flat road locations when not plowed under. No definite relationship was determined between inclination angle, height, and effectiveness. Several other authors like Pugh (1950), Pugh and Price (1965), Mellor (1965), Schaerer (1972), and Verge and Williams (1981) mention blower fences briefly, but they conclude that such devices are often difficult to support in high winds, can produce worse drifting if the wind blows in a direction opposite to that expected, and a flatter inclination angle may allow snow to build up on the roof.

Blower roofs can provide effective modification or prevention of snow cornices along mountain ridges. Unstable snow cornices frequently trigger avalanches in recreation areas, and the avalanches present serious safety problems. Montagne et al. (1968) constructed ten jet roof fences along the Bridger Range in Southwestern Montana during thee winters of 1965-68 incorporating various designs, inclinations and materials. Hopf and Bernard (1963) reported avalanche control experience in the Austrian Tirol using baffles and jet fences. They concluded,

a. An efficient construction technique used a solid 2.4 x 3-m (8 x 10-ft) solid panel mounted on two upright posts by pivot bolts. The structures were guyed to the ground using no. 9 gauge wire and 1.2-m (4-ft) cement rebar anchor pins. It took about 4 hrs for two men to erect each fence at a materials costs of $25 (1968 US dollars),

b. Multiple jet roofs should be separated no wider than the width of the panel,

c. Jet roofs consisting of panels with open slats have proven less effective than solid panels; however, open slats avoid accumulation of snow on the panel top,

d. Jet roofs are best in areas where snow does not accumulate in windless storms, and

e. The most efficient inclination angle is parallel to the angle of the lee slope. Steeper angles dig out a sharp cup-shaped hollow in the snow to the lee of the structure, but a secondary cornice accumulated beyond the hollow.

Montagne et al. (1968) erected a full-sized jet roof on a level field which was not snow covered. They used cup anemometers to measure winds speeds upwind and downwind from the center of the jet roof. Downwind accelerations were maximized with inclination angles between 10° and 20°. A measured 12% increase in wind speed in the lee of the fence was associated with a 20% increase in frictional drag or scour along the ground. The researchers also repeated their study in a wind tunnel using a 1:48 scale model. Measurements over a range of wind speeds produced similar results, but percent changes in wind speed were less.

Dawson and Lang (1979) prepared a numerical simulation of jet roof geometry for snow cornice control. Their two-dimensional marker-and-cell program solved the laminar Navier-Stokes equations for regions of recirculation above the jet roof and stagnation zones along the ground. They concluded that an inclination angle of 9.5° produces the minimum stagnation and recirculation regions. They recommended the fence be located at the ridge line, nearly parallel to the lee slope, with the upwind fence edge directly over the hill crest.

Another design used to remove snow is the "kolktafeln" or vertical baffles with undergaps of 1 m (3 ft) (Wopfner and Hopf, 1963). Japanese scientists report such fences incorporating air-foil shaped turning vanes are effective, but they are more expensive and difficult to maintain (Japanese Construction and Mechanical Assoc., 1987). Sometimes buildings or radar stations have been elevated above the snow surface on poles or extensible columns (Strom et al. 1962; Mellor, 1965; Sherwood, 1967). The expectation was that air accelerating beneath the structures would sweep the base free of snow. Unfortunately, stagnation regions downwind of the bluff-shaped elevated obstacles produced accelerated deposition and large drifts eventually swamped the structures.

Vortex Style Blower Fence

Longitudinal vortices aligned with the wind are known to persist for great distances without dissipation. A fence designed to generate a pair of counter-rotating vortices will sweep the snow to the side away from the fence centerline. The vortices are similar to two weak tornadoes laying parallel to the ground. Tangential velocities beneath the vortices create high surface shear stresses which exceed the values required for snow movement. In the near wake the regions of highest local shear stress are directly under the vortices. Further downstream, the entrained air causes the regions of maximum shear stress to merge to the wake centerline.

Iverson et al. (1974) considered the vortices generated by a short horizontal wing suspended above a particulate surface of uniform depth. Twin eroded streaks developed downwind of the airfoil. Later the streaks merged except for a triangular particle deposit just downstream of the wing. Such vortices generated by short jet roof fences may explain their effectiveness; indeed, a series of short separated jet roof fences may be more effective than

one continuous fence.

Strong vortices are known to be generated by delta-wing-shaped triangles inclined at about 30° to the approaching wind field. Some inventors have suggested using such devices to channel high speed winds into windmills (Walters et al., 1976); whereas other designers suggest using vortex generators to mix and dilute hazardous gases at ground level (Kothari and Meroney, 1982). A rotating vortex generator snow fence should be effective for all wind orientations and may provide long range downstream protection.

SIMULATION OF DRIFTING SNOW

Simple wind tunnel experiments using fine particles such as sawdust, mica, sand, borax, glass-beads, and even ice-particles or snow have yielded useful information on the shapes and dimensions of drifts near buildings, roads, and mountain ridges. Some experiments have attempted to satisfy similitude requirements, at least partially. In other experiments, modeling laws have been ignored. The exact similitude requirements for scale modeling of drifting snow problems are not met at small scales because of the large number of modeling parameters that cannot be satisfied simultaneously (Strom et al., 1962; Odar, 1965; Mellor, 1970; Kind, 1980; Iverson, 1980a, 1980b, 1981).

Many researchers emphasize the importance of modified Froude number, $Fr = U/(g(sg-1)L)^{1/2}$, where U is a characteristic wind velocity and sg is the specific gravity of the snow relative to air. But Iverson (1980a) argues that for similarity in final drift shape and growth rate a mass-transport rate parameter and an aerodynamic roughness parameter govern drifting behavior:

$$\rho U^2/(2 \rho_p gH) (1 - (U_o/U)), \quad \text{transport rate parameter,}$$

$$A_1^2(D_p/H)(U_*/U_{*t})^2, \quad \text{equivalent roughness,}$$

where A_1 is dimensionless threshold friction speed (Froude number with friction speed as characteristic velocity), U_o is the threshold wind speed, U_* is the surface friction speed, U_{*t} is the threshold friction speed, ρ is the air density, and ρ_p is the particle density.

Since the present study primarily was concerned with particle movement in the immediate vicinity of sharp-edged fences and buildings, an effort was made to develop reasonable approach profiles of wind and turbulence. Asymptotic drift shape was evaluated rather than growth rate or drift development time.

MODEL BLOWER FENCE AND VORTEX GENERATOR EXPERIMENTS

Three sets of experiments were performed to evaluate blower and vortex fence performance. First, a 50% porous conventional snow fence was compared to full-scale snow measurements performed by Tabler (1979) and wind-tunnel glass-bead measurements made by Iverson (1980b). Second, a series of tests were performed to examine the influence of fence dimensions on snow removal performance, and, third, a study was performed to compare relative ability of various snow fences to clear areas about a model building.

Experimental Techniques and Equipment

Experiments were performed in a small open-circuit blower tunnel, with

test section dimensions of 20 x 61 x244-cm (Figure 1). The approach wind profile was produced by an upwind set of spires, barrier, and a surface layer of particles. Additional particles were added to the airstream at the front of the tunnel using a particle dispersal bin. A sand trap was placed at the end of the wind tunnel to collect particles moving beyond the test section. Velocity profiles were measured with a conventional Prandtl pitot-static tube and pressure transducer. Wind speeds were set using a calibrated drag sphere anemometer.

Validation and optimization experiments were performed with a fine sand of average diameter 0.115-mm (size range 0.08- to 0.2-mm), and model building studies were performed using fine detergent-grade borax powder (approximate diameter 0.1-mm). When the tunnel was run without obstacles or fences present, the 25-mm bed of particles remained flat with minor ripples (2.5-mm) over the 1-m test length in the wind tunnel. Adding particles at the beginning of the test section maintained bed depth within 3-mm.

Conventional Snow Fence Experiment

A 1:100 scale model of a 50% porous horizontal-slat vertical snow fence was placed above a 25-mm bed of fine sand. The 29-mm high fence was located 66-cm from the vortex spires, had a 25-mm subsand barrier and a 5-mm gap (16% open area) at the bottom of the fence. The wind speed at fence height was set at 4.5-m/sec (10-mph), and the model fence was allowed to accumulate sand for nine hours. Sand depth measurements were taken up- and downstream from the fence every hour.

Within 3 hours the drift had reached its average height, 1.2H at x = 6H, and after 6 hours the sand extended the drift downwind to about x = 27H. Figure 2 demonstrates that the modeled drift profile replicated the full scale snow drift measurements of Tabler (1979), the 1:25 scale measurements performed on a frozen lake-bed using real snow by Tabler (1981), and the 1:100 scale model studies by Iverson (1980) using glass-beads.

Blower Fence Measurements

A 1:50 scale model of a blower fence was installed above the sand surface about 66 cm downwind from the vortex spires. The roof width (W) was 45-mm by 153-mm long. It was supported by two vertical end plates which permitted pivoting the roof to various inclination angles (0° to 30°). The lee edge of the fence roof was placed at various heights (H) above the undisturbed sand bed, (H/W = 0.75 to 2.1). Sixteen combinations of inclination angle and lee height were examined in some 45 test runs. Each test lasted three hours, and sand depths were measured at the end of each hour out to distances 25W downwind of the blower fence.

All fences removed sand downwind and prevented subsequent accumulation. Angles greater than 22.5° tended to immediately scour out a hole immediately downwind of the fence, but then further downwind the surface was very uneven, and large drifts appeared relative to the new average depth (Figure 3). The 15° tabletop inclination removed great amounts of sand and left the surface much smoother and almost ripple free (Figure 4). Given a criteria based on the minimum and maximum scour which occurs over the 25W fetch examined it appears that a 15° table inclination arranged with its lee edge 1.5W above the particle surface produces maximum protection in the fence wake (Figure 5). An

optimum table inclination of 15° agrees with the full-scale wind speed experiments performed by Montagne et al. (1968). Their experiment was only performed for a H/W ratio of 0.5; thus, they may have found even greater effects by raising their table top.

Vortex Generator Measurements

A 1:50 scale model of a delta-wing vortex generator was also installed above the sand surface about 66 cm from the entrance spires. The wing was formed of an equilateral triangle 102 mm on a side, (triangle height, TH = 88 mm). One tip was inclined upwind at an angle of 15°. The lee edge of the generator was placed at various initial heights above the sand bed (H/TH = 0.28 to 0.73). Only four heights were examined in some 12 test runs. Each test lasted three hours, and the sand depths were measured at the end of each hour out to distances 12TH downwind of the vortex generator.

The maximum scour produced by the vortex generator was slightly greater then than produced by the optimum blower fence, and the minimum scour measured was very similar. Over the range of generator heights examined no optimum position appeared; thus, any moderate height is suitable, but, intuitively, heights greater than 2TH seem extreme (Figure 5).

Building Area Protection Experiments

A 1:75 scale model of a typical two-story Ft Collins home was installed downwind of the entrance spires. The model included surrounding trees, fences, and an upwind house. Snow was known to drift across the front of the house and driveway for winter storms approaching from the west. In these experiments borax was used as a snow simulant. Experiments were performed without any mitigation technique, and using inclined vertical-slat model snow fences with 50% porosity, model hedges, model blower fences (15° inclination), and model vortex generators. Comparisons were made between snow patterns around the model and full-size house. Snow drifts and scour regions formed during several storms from the 1978-1980 snow seasons compared very well. Drifts appeared across the front of the house and driveway, around two Austrian pine trees just downwind of the driveway, and over the patio at the rear of the house. Scour areas occurred at the rear of the house and immediately behind the downwind corner of the front of the house.

Model snow fences and hedge rows placed along the upwind property line accumulated snow downwind; however, the drifts produced actually increased snow deposition across the front of the model house and driveway. Two blower fences, placed just upwind of the driveway, swept the driveway and downstream area completely free of particles for westerly winds. For northwesterly winds (blower fences at a 45° angle to the approach wind) the fences only cleared one/third of the driveway and permitted drifts to form across the garage doorway.

CONCLUSIONS

Properly proportioned blower fences and vortex generators provide effective protection from excessive snow deposition out to distances of 25 times characteristic fence heights or widths. Such fences perform most effectively in regions where storms approach predominantly from one direction and snow falls under windy conditions. Nearby or upwind vegetation and

obstructions will reduce the effectiveness of these devices.

Acknowledgements

REFERENCES

Dawson, K.L. and Lang, T.E., 1979, "Numerical Simulation of Jet Roof Geometry for Snow Cornice Control," USDA For. Serv. Res. Pap. RM-206, 19p.

Fraser, C., 1949, "An attempt to control snow drifting by the use of an elevated, inclined snow fence," Research Council of Ontario REport, No. 5-2-49.

Fraser, C., 1950, "Experiments with Elevated, Inclined Snow Fence on Ontario Roads," Roads and Construction, April 1950, pp. 88-90, 115-117.

Hopf, J. and Bernard, J., 1963, "Windbeeinflussend Bauten in der Lawinen-verbauung und-vorbeugung, (Wind control structures in avalanche defence and prevention)," Mitteilunger der Forstlichen Bundes-Versuchsanstalt Mariabrunn, 60, pp. 605-681. Also see National Research Council of Canada Technical Translation 1348, Ottawa, 1968.

Iverson, J.D., 1980a, "Wind-Tunnel Modeling of Snow Fences and Natural Snow-Drift Controls," Proceedings of 37th Eastern Sonw Conference, Peterborough, Ontario, Canada, pp. 106-124.

Iverson, J.D., 1980b, "Drifting-Snow Similitude – Transport-Rate and Roughness Modeling," Journal of Glaciology, 26, pp. 393-403.

Iverson, J.D., 1981, "Comparison of Wind-Tunnel Model and Full-Scale Snow Fence Drifts," Journal of Wind Engr. and Ind. Aerody., 8, pp. 231-249.

Iverson, J.D., Greeley, R., White, B.R., and Pollack, J.B., 1974, "Eolian Erosion on the Martian Surface; Part 1: Erosion Rate Similitude," Icarus, 26, pp. 321-331.

Japanese Construction and Mechanical Engineering Association (editors), 1988, Handbook of Snow Drift Control Engineering, Morikita Publishing Co., Tokyo, 527 pp.

Kind, R.J., 1981, "Snow Drifting," Handbook of Snow: Principles, Processes, Management and Use, D.M. Gray and D.H. Male, editors, Pergamon Press, New York, pp. 338-359.

Mellor, M., 1965, "Blowing Snow," Cold Regions Science and Engineering Part III, Section A3c, AD630328, 85 pp.

Mellor, M., 1970, "A Brief Review of Snowdrifting Research," Snow Removal and Ice Control Research, U.S. Army Cold Regions Research and Engineering Laboratory, Special Report 115, pp. 196-209.

Montagne, J., McPartland, J.T., Super, A.B., and Townes, H.W., 1968, "The Nature and Control of Snow Cornices on the Bridger Range Southwesern Montana," USDA Forest Service, Wasatch National Forest, Alta Avanalanche Stud. Cent., Misc. Rep. No. 14, 23 pp.

Odar, F., 1965, "Simulation of Drifting Snow," U.S. Army Cold Regions Research and Engineering Laboratory, Research Report 174, 16 pp.

Pugh, H.Ll.D., 1950, "Snow Fences," Dept. of Scientific and Industrial Research, Road Research Laboratory, Technical Paper No. 19, 52 pp.

Pugh, H.Ll.D., and Price, W.I.J., 1954, "Snow Drifting and the Use of Snow Fences," Polar Record, 7, No. 47, pp. 4-23.

Schaerer, P.A., 1972, "Control of Snow Drifting about Buildings," Canadian Building Digest, CBD146, pp. 146-1 to 146-4.

Sherwood, G.E., 1967, "Preliminary Scale Model Snowdrift Studies Using Borax in a Wind Duct," U.S. Naval Civil Engineering Laboratory, Fort Hueneme, CA, Project No. Y-F011-11-01-025, 16 pp.

Strom, G.H., Kelly, G.R., Keitz, E.L., and Weiss, R.F., 1962, "Scale Model Studies on Snow Drifting," U.S. Army Snow Ice and Permafrost Research Establishment, Research Report 73, 50 pp.

Tabler, R.D., 1981, "Geometry and Density of Drifts Formed by Snow Fences," J. Glaciol., 26, No. 94.

Tabler, R.D., 1981, "Self-similarity of wind profiles in blowing snow allows outdoor modelling," J. Glaciol., 26, No. 94.

Verge, R.W. and Williams, G.P., 1981, "Drift Control," Handbook of Snow: Principles, Processes, Management and Use, D.M. Gray and D.H. Male, editors, Pergamon Press, New York, pp. 630-647.

Walters, R.E. and Fanucci, J.B., 1976, "Innovative Wind Machines, Executive Summary and Final Report," Department of Aerospace Engineering, U. of West Virginia, 215 pp.

Wopfner, H. and Hopf, J., 1963, " Versuche mit Kolktafeln an der Schneeforschungsstelle Wattener Lizum (Tirol) in den Jahren 1950-1955 (Tests with baffles at the Wattener Lizum Snow Research Station (Tyrol) in the years 1950-1955)," Mitteilungen der Forstlichen Bundes-Versuchanstalt Mariabrunn, 60, pp. 633-665. Also see National Research Council of Canada, Technical Translation 1348, Ottawa, 1968.
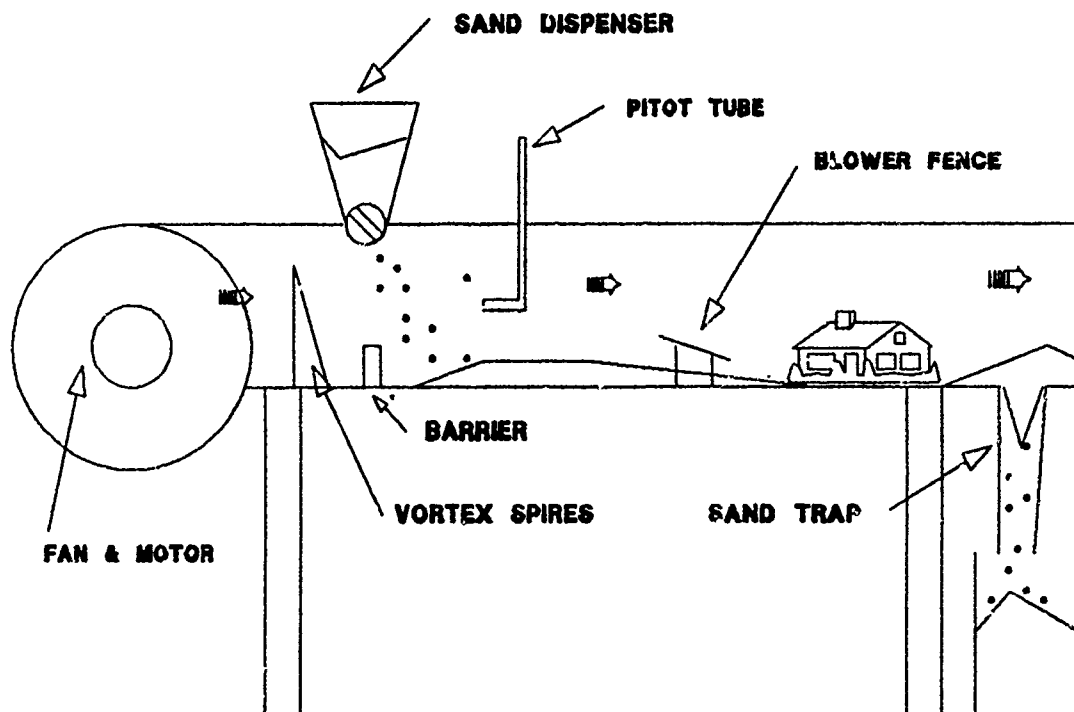
Figure 1. Schematic of open-circuit snow-drift wind tunnel.
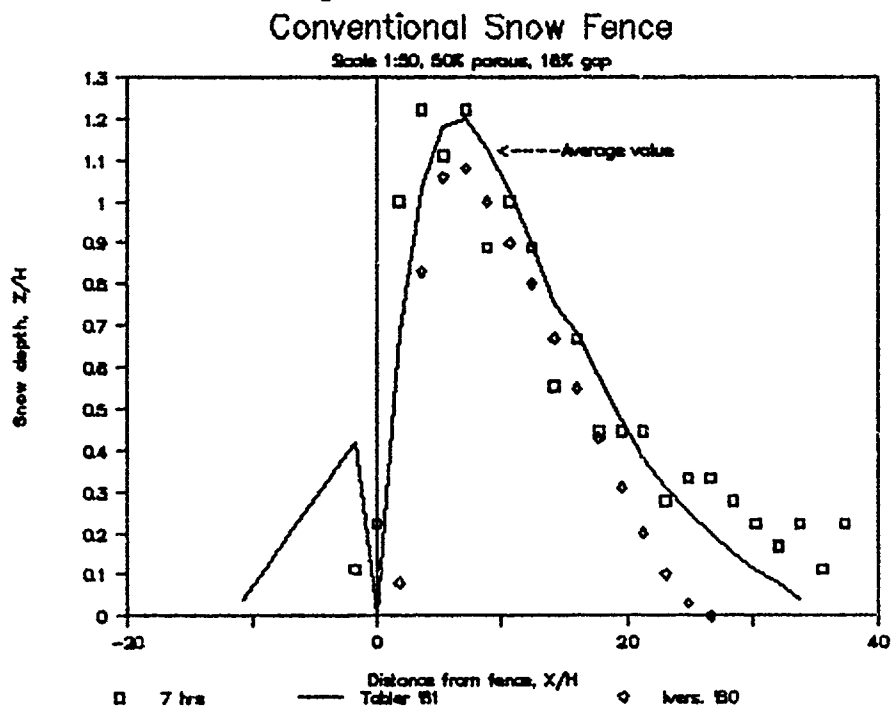
Figure 2. Particle depths deposited downwind of a 50% horizontal-slat Wyoming type snow fence with a 16% undergap.

Blower Fence Experiment
Fence height = 3.5 cm, Time = 3 hrs
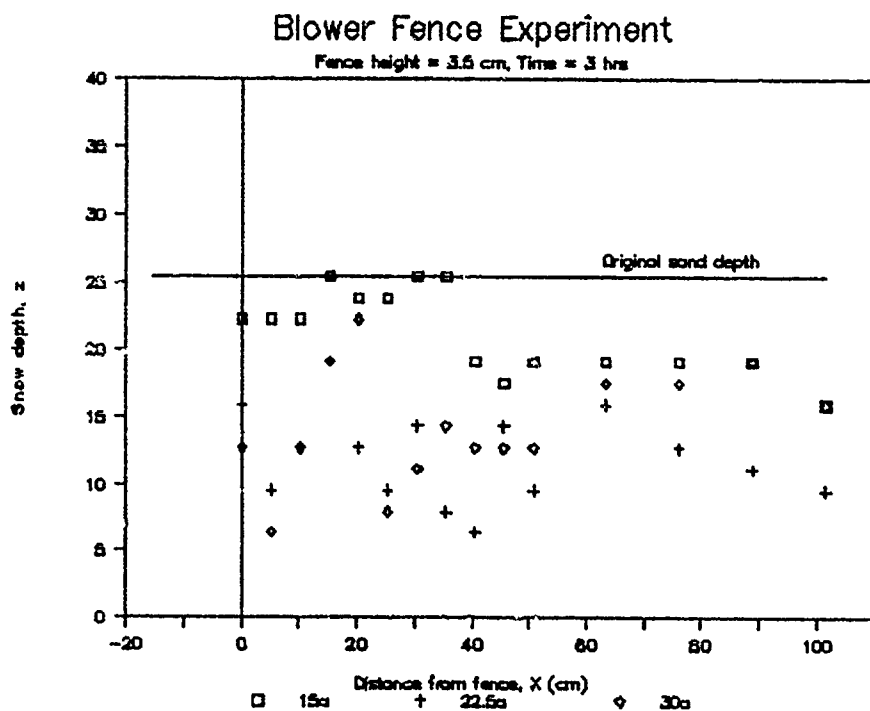
Figure 3. Blower fence performance at 3.5 cm height, with various tabletop inclination angles.

Blower Fence Experiment
Fence height = 6.5 cm, Time = 3 hrs
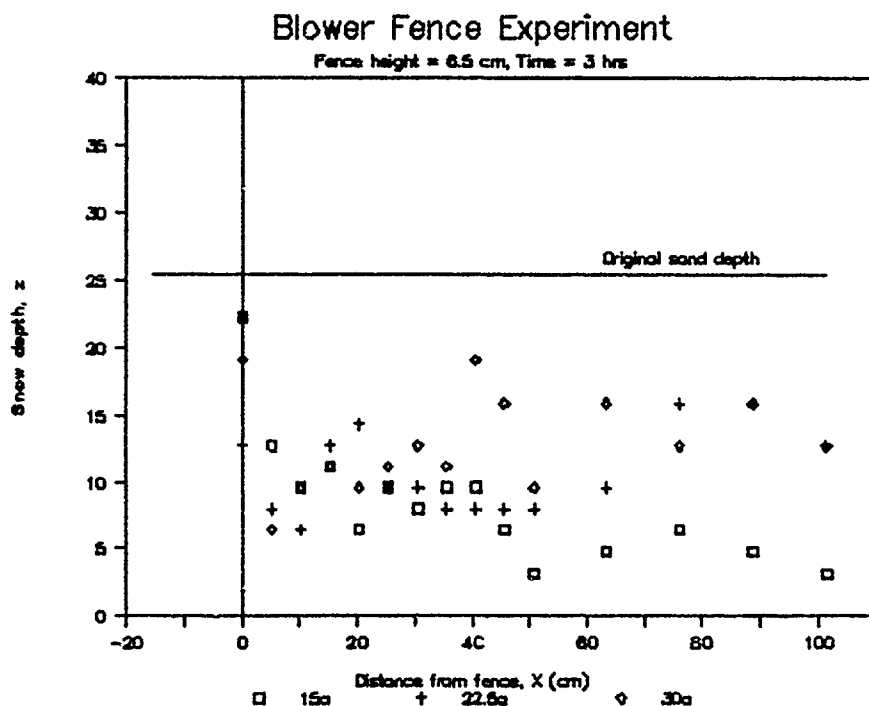
Figure 4. Blower fence performance at 6.5 cm height, with various tabletop inclination angles.
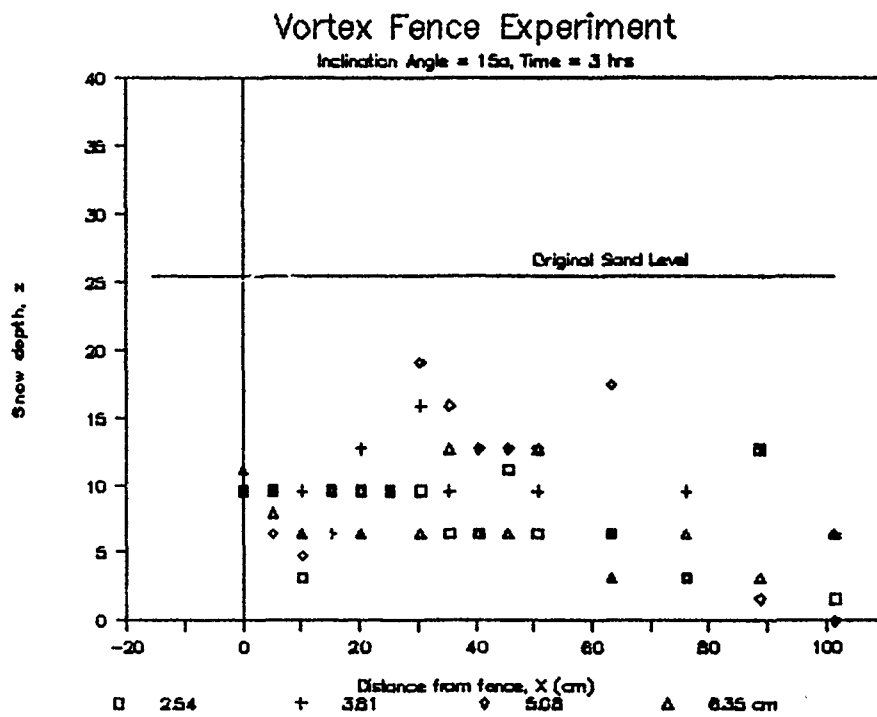
Figure 5. Vortex fence performance at various delta-wing heights.

Snow Fence Technology
State of the Art

Ronald D. Tabler[1]

ABSTRACT

Engineering criteria developed within the last 20 years have resulted in snow fence systems that are exceptionally effective in preventing drifts and improving both visibility and road surface conditions. Definitive information on the shape and density of drifts formed by snow fences, and a method to estimate snow transport, allow fence height and placement to be optimized. New materials and improved structural designs are available for tall fences, which are more effective and more economical than multiple rows of shorter fence having the same capacity. The 4.2-m-tall standard fence used by the Wyoming Highway Department has a snow storage capacity of $2 \cdot 10^5$ kg per metre of length, and in 1987 was built under contract for $30 per metre.

Although existing guidelines have proven satisfactory, their empirical derivation suggests revisions will be required as experience is gained in new environments, particularly in mountainous terrain. Guidelines could be improved through basic research on turbulent mixing as it controls snow deposition, but empirical studies will be necessary to provide useful results in the near future. Priority should be given to research on snow fence trapping efficiency, and a continuing objective should be to develop new fence designs that store more snow in less space at less cost. Practical needs include a method for anchoring surface-mounted fences on permafrost soils, and improved designs for temporary snow fences.

INTRODUCTION

There are two basic types of snow fences. *Deflector* fences deflect the wind and blowing snow in such a way as to provide a sheltered area. Lateral deflectors, such as livestock shelters, force the snow *around* the area to be protected. "Blower" fences, commonly used in Japan, deflect snow downward and accelerate the wind so as to reduce deposition and improve visibility in the immediate vicinity of the fence. Blower-type fences are also used to prevent the formation of cornices in avalanche starting zones. An opposite approach is to deflect the snow *over* the area to be protected using solid fences or embankments of snow or earth.

I. Consultant in Snow Engineering, Tabler & Associates, P.O. Box 576, Laramie, Wyoming 82070

Collector fences reduce snow transport arriving at the protected area by inducing deposition upwind, and can be used for water supply augmentation as well as drift control. This paper outlines the state of the art for collector fences in the United States.

HISTORY OF SNOW FENCES

Although snow fences have been used in the United States for at least 100 years, no significant improvements in fence design or placement guidelines were made until 1971. The standard fence used by the Wyoming State Highway Department as late as 1970, for example, was nearly identical to that used by the Union Pacific Railroad in 1885 (Tabler, 1988a). This stagnation of drift control technology, spanning nearly a century, was remarkable considering the popularity of snow fences as automobiles came into general use following World War I. By 1932, 169 km of snow fence were in place along highways in Wyoming (Wyoming Highway Commission, 1932), and Finney's report two years later marked the beginning of drift control research. In spite of this early interest in snow fencing, the two decades following World War II saw passive control measures replaced by brute force as a consequence of improved snow removal equipment and inexpensive fuel and manpower.

Table 1 Snow fence projects contributing to the evolution of guidelines described in this paper.

Year constructed	Fence heights	Fence length	Location of project and references
	-m-	-km-	
1971-72	1.8 - 3.8	18.4	Wyoming I-80, Mile 246-280 (Tabler, 1974)
1973-79	2.4 & 3.8	33.5	" " Mile 242-289 (Tabler and Furnish, 1982)
1973-88	2.4 - 4.2	>50.0	Wyoming - other highways
1976-79	3.7	3.7	Arizona State Route 260 near Greer
1979	2.4 & 3.8	1.1	Montana I-90 near Livingston
1980	2.4 & 3.8	3.9	Union Pacific Railroad, Rock River, WY
1982	4.6	0.8	Village of Wainwright, AK (L.C.M.F. Ltd., 1983)
1983	2.4	0.4	Water supply for City of Shishmaref, AK (Farnwald and Crum, 1986)
1983	3.8	0.8	Water yield from Stratton Watershed, WY (Tabler and Sturges, 1986)
1983-84	3.7 & 4.6	0.8±	Thompson Pass, Alaska Highway 4
1984	4.2	3.2	Exxon plants @ Shute Creek and LaBarge, WY
1984	3.7	0.3	ARCO Storage Pad C, Prudhoe Bay, AK
1984	2.4 & 3.8	6.3	Chevron Carter Creek Field, WY
1986	5.5	0.4	Summitville Mine near Wolf Creek Pass, CO
1988	4.1 - 4.6	0.8	Standard Alaska Gathering Center 2, Prudhoe Bay, AK
1988	4.6	0.8	ARCO Alaska Lisburne Production Center and L-2 well pad, Prudhoe Bay, AK

New guidelines for fence design, placement, and storage capacity were used in 1971 to design 18.4 km of snow fence on Interstate Highway-80 in Wyoming (Tabler, 1974; Martinelli et al., 1982). The success of that project prompted installation of 33.5 km of additional fencing on the same section of highway over the next 8 years, and marked the beginning of improved drift control technology in the United States. This $2 million project cut snow removal costs by more than one-third and reduced accidents by 70% (Tabler and Furnish, 1982), leading to a progression of applications (Table 1) from which the guidelines summarized in this paper evolved.

PRESENT ENGINEERING GUIDELINES

Snow Storage Capacity

The most important requirement for a fence system is sufficient capacity to store snow transported over the design winter. Snow storage capacity is primarily determined by the height, length/height ratio, porosity, bottom gap, and topographic placement of a fence. It has long been recognized that fences having 50% open area ("porosity") form the largest drifts (Mellor, 1965). Opening size and shape are less important, but influence the tendency for a fence to become buried in the drift (Tabler, 1988a). On flat terrain, the storage capacity of the 50%-porous horizontal-slat "Wyoming" fence, described later in this paper, is given by

$$Q_c = 8500 \ H^{2.2} \tag{1}$$

where Q_c is snow storage capacity in kilograms per metre of fence length, and H is fence height in metres (Tabler, 1988a). Equation 1 is an upward revision of a previous estimate (Tabler, 1980), incorporating additional years of data. Although the cross-sectional area of a drift is proportional to the square of fence height (Tabler, 1980), storage capacity is proportional to $H^{2.2}$ because the density of drifted snow increases with depth according to

$$D = 522 - (304/1.485Y)\{1 - \exp(-1.485Y)\} \tag{2}$$

where D is snow density (kg/m^3) before the onset of melt, and Y is snow depth (m) (Tabler, 1985).

Although some blowing snow particles are carried aloft to great heights, transport above 4 metres comprises such a small percentage of the total (Budd et al., 1966) that it can be ignored for purposes of drift control. Snow transport within this 4-m height can be determined from field measurements of drifts, or estimated from the equation (Tabler, 1975)

$$Q_t = 0.5P_rT(1 - 0.14^{F/T}) \tag{3}$$

where Q_t = snow transport in kilograms per metre of width across the wind
   P_r = Relocated precipitation (millimetres, water-equivalent)
   T = Maximum transport distance in metres, usually assumed to be 3000 m
   F = Fetch distance (metres)

The progenitor of Eq. 3 (Tabler, 1971) was inspired by A. A. Komarov's (1954) idea of estimating snow transport by accounting for evaporation of blowing snow. Subsequent refinement was made possible by R. A. Schmidt's (1972)

mathematical model for evaporation, and related field measurements (Tabler and Schmidt, 1972; Tabler, 1975). Equation 3, or earlier versions, have been used to design the projects listed in Table 1.

Equations 1 and 3 provide the basis for determining the required height or number of rows of snow fence. An additional consideration is how snow trapping efficiency of a fence changes as a drift grows. "Trapping efficiency," expressed as the percentage of snow transport retained by a fence, remains greater than 80% until a fence is about 75% full, but deteriorates rapidly as the drift assumes a streamlined shape such as shown by stages 6 and 7 in Figure 1 (Tabler, 1974; 1988a). This suggests that storage capacity should be approximately 25% more than the design snow transport to maintain efficient snow trapping. Other considerations and procedures for capacity design are described by Tabler (1982; 1987; 1988a; 1988b).
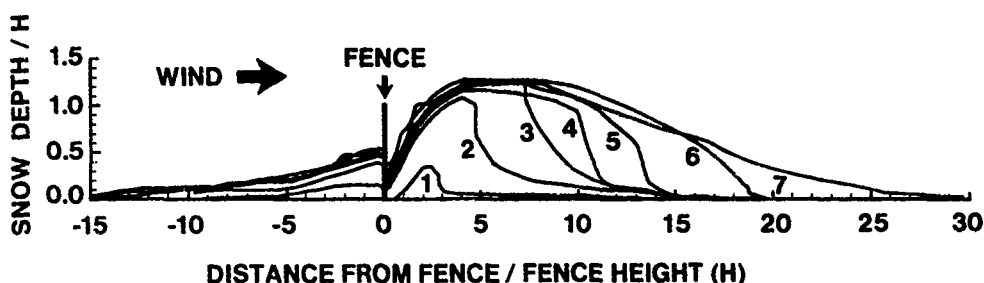
Figure 1 Stages in the growth of a snowdrift formed by a 3.8-m-tall "Wyoming" fence with 15-cm bottom gap (Wyoming I-80 Mile 254.8, 1983-84 winter). On the last date, this fence was about 89% full, containing 141 t/m.

Fence Design and Materials

Height is the most important factor in fence design. Over the range of heights commonly used, the cost of building a snow fence is approximately proportional to fence height, H. Because the capacity of a fence increases in proportion to $H^{2.2}$, it is more economical to use a single tall fence than multiple rows of shorter fences having the same capacity. This generalization is supported by data from construction contracts in Wyoming (Figure 2). Because less space is required, easement costs can be less for a tall fence than for multiple rows of shorter fence. Most important, however, the percentage of snow transport intercepted by a fence, and hence trapping efficiency, increases with fence height (Tabler, 1974).

Although maximum storage capacity is achieved with a porosity of 45-55%, the shallow, uniform drifts formed by more porous fences can be useful for agricultural applications, and the shorter drifts formed by more dense fences can be advantageous where space is limited. Snow deposition occurs primarily on the upwind side of solid barriers until the windward drift is filled, suggesting that tall solid fences could be used where deposition must be restricted to the windward side of the barrier (Tabler, 1988a).
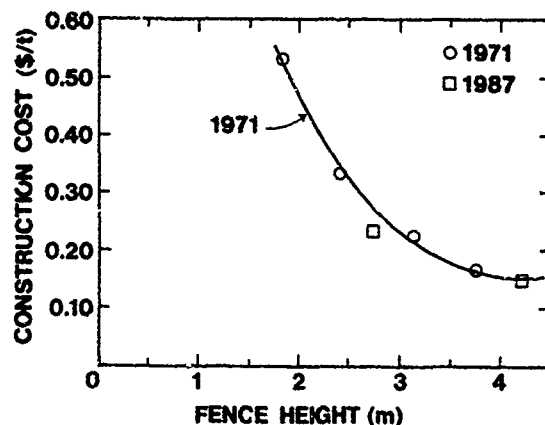
Figure 2   Fence construction cost per tonne of snow storage, as a
function of fence height, for the "Wyoming" fence in 1971 and 1987.

Leaving a space between the bottom of a fence and the ground surface
reduces the tendency for fences to become buried in the drift. Burial reduces
effective fence height, with a commensurate loss in effectiveness, and often
causes structural damage to the fence because of the large forces exerted by
snow settlement and creep. Optimum bottom gap is 10-15% of total fence
height, with wider gaps reducing storage capacity and trapping efficiency
(Tabler, 1988a). Because spaces between horizontal slats serve as bottom gaps
to retard burial, vertical-slat fences, and fences with small openings, have a
greater tendency to become buried. To provide a bottom gap for the common
vertical-slat "picket" fencing, every slat must be fastened to a horizontal
support to prevent the slats from falling through the wire loops. Plastic
fencing materials have the advantage of not requiring horizontal supports.

Most of the plastic fencing materials currently available, as summarized
by Coker (1986), are made from polyethylene. High tensile strength (up to
$39 \cdot 10^6$ kg/m^2) can be achieved through molecular orientation. Although ultra-
violet (UV) radiation can cause rapid deterioration of plastics, fencing
products are made resistant to UV degradation by adding chemicals and by
optimizing the thickness of the material. Because carbon-black is an effec-
tive additive for this purpose, black fencing materials have the greatest
resistance to UV degradation. Laboratory tests indicate life expectancies in
excess of 10-15 years, and field tests by the author show no apparent change
in the properties of some materials after 4 years of exposure at 2400 m in
Wyoming. Most plastic fencing materials are unaffected by temperatures from
-50 to +95°C (Coker, 1986). Plastics were used for the fences built in 1988
at Prudhoe Bay (Table 1), and were installed at temperatures as low as -40°C
with no significant changes in handling characteristics. Solid polyethylene
strap, 0.6 mm x 152 mm x 300 m, manufactured by High Performance Plastics
Division, ITW Enterprises, Inc., under the trade name "Sno-Strap," can be used
to build fences of any desired porosity or height.

The snow fence used by the Wyoming State Highway Department since 1971,
referred to as the "Wyoming" fence, consists of horizontal 25- x 150-cm wood
slats, fastened to wood trusses which rest on the ground surface. The fence
design has undergone numerous revisions since it was first described (Tabler,
1974). The current version (Figure 3) has a porosity of about 50%, a bottom

301

gap equal to 14% of the total height, and a 15° inclination from vertical. The structure is designed to withstand winds of 55 m/s, snow settlement pressures associated with complete burial on level terrain, and forces imposed by livestock. The two standard heights now used, 2.74 m (9 ft) and 4.2 m (14 feet), have storage capacities of 78 Mg and 200 Mg per metre of fence length, respectively. Low bids for construction in 1987 were $19.03 per lineal metre for the 2.74-m height, and $30.84 for the 4.2-m fence. Design improvements have compensated for inflation over the last 17 years, keeping construction costs from increasing (Figure 2).

Placement

Definitive studies of the shape of equilibrium drifts formed by snow fences have improved guidelines for fence placement. The latest information on drift dimensions (Tabler, 1988a) uses additional years of data to revise previous estimates (Tabler, 1980). To a close approximation, drift dimensions are scaled with fence height, at least over the range of heights for which data are available (Tabler, 1980). For the horizontal-slat Wyoming snow fence on level terrain and for a single wind direction, the drift on the windward side of the fence extends to about 12H, and the leeward drift extends to about 35 H (Figure 4). The windward drift is roughly triangular in cross-section, with a maximum depth of about H/2. Shape of the lee drift is approximated by

$$Y/H = 0.43 + 0.303(X/H) - 0.0412(X/H)^2 + 0.002193(X/H)^3 - 5.421 \cdot 10^{-5}(X/H)^4 +$$
$$+ 5.105 \cdot 10^{-7}(X/H)^5, \quad (X/H) < 34 \tag{4}$$

where Y is snow depth at distance X from the fence. Although these dimensions are strictly applicable only to the Wyoming fence, drifts are similar for other fence geometries having 50% porosity provided they are less than half buried.

Length of the equilibrium drift defines the closest permissible placement of a fence to the protected area, assuming that the fence fills to capacity. Closer spacing is possible if the fence is sufficiently tall that it does not fill to capacity, taking advantage of the lee drift being confined to within 20H of the fence up to the time a fence is 75% full (Figure 1). Drift shape is greatly affected by topography, and few quantitative relationships are available (Tabler, 1974; Tabler, 1988a). For a given topographic setting, equilibrium drift dimensions are believed to be the same everywhere, provided that fence height is adjusted for "background" snow depth.
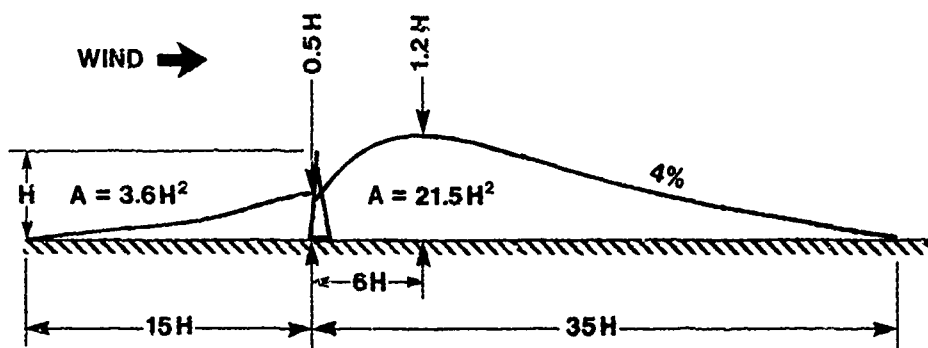
Figure 4 Dimensions of equilibrium drifts formed by "Wyoming" fences (H = fence height, A = cross-sectional area).
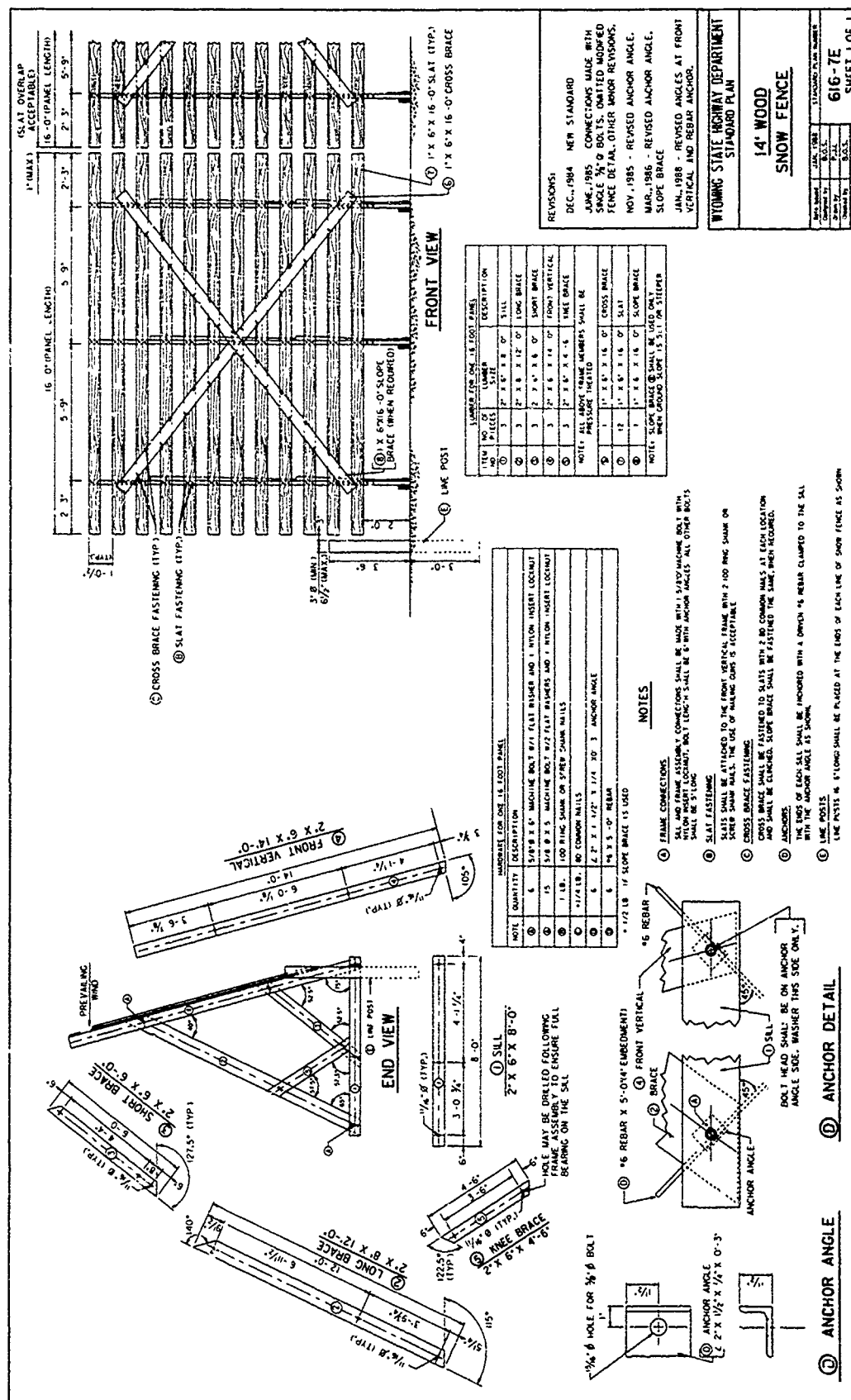
Figure 3 Standard-plan 4.3-m snow fence used by the Wyoming State Highway Department.

Although fences should generally be oriented perpendicular to the prevailing wind direction, no loss in effectiveness is noted with departures as great as 25°. For deviations of this order, drift shape, as measured parallel to the wind, is essentially unaffected by orientation (Tabler, 1980). Theoretically, the effective porosity of a thin fence increases as the wind becomes more oblique, with a proportionate loss in storage capacity. Although it is possible to compensate for this effect by reducing the porosity of fences that are not perpendicular to the wind, no such adjustment is required for the Wyoming fence because the resistance offered by the truss members, and hence the solidity ratio, increases as the attack angle becomes more oblique.

General rules for fence placement allow for a 30° variation on either side of the mean prevailing direction (Tabler, 1988a), defining the distance fences should extend on either side of the area to be protected, as well as the amount of overlap required for openings or staggered rows of fencing.

RESEARCH NEEDS

Although present engineering guidelines for snow fences are adequate for applications in flat to moderately rolling topography, design criteria for mountainous terrain are not as well quantified, and effects of background turbulence are largely unknown. The empirical nature of existing guidelines suggests future revisions may be required as experience is gained in new environments. It is particularly important that estimates for snow transport be validated in every new location where fences are built, implying that the value assumed for the maximum transport distance be verified when Eq. 3 is used.

Basic research to improve drift control technology must focus on some challenging problems. One model that has been proposed (Tabler and Schmidt, 1986) is that blowing snow is deposited wherever the surface shear stress decreases with distance along the mean flow direction, implying that the surface of a snowdrift is in equilibrium with the particle-transporting flow when the time-averaged surface shear stress is uniform. A mechanism allowing this quasi-uniform shear stress to be attained over stable drifts is the turbulent mixing that takes place in the region where layers of air having different velocities are mixing together. Although this phenomenon can be modelled mathematically (Abramovich, 1963), turbulent mixing behind a porous snow fence is complicated by the multiple jets and wakes generated by barrier elements. Research on turbulent mixing offers a promising approach, but empirical studies will be needed to provide useful results in the near future.

Research to determine how trapping efficiency of a fence varies with wind speed, residual storage capacity, and surrounding topography, could lead to improved criteria for snow storage requirement, placement, and fence design. Although existing snow fence designs are effective and economical, the search should continue for a better snow trap that stores more snow in less space at less cost. Studies are also needed to better define the effects of fence porosity on drift dimensions and trapping efficiency.

Practical needs include a method for anchoring surface-mounted fences on permafrost soils, and improved temporary snow fences.

304

REFERENCES

Abramovich, G. N., 1963, The theory of turbulent jets, The M.I.T. Press, Cambridge, Mass.

Budd, W. R., R. Dingle, and U. Radok, 1966, "The Byrd snowdrift project: outline and basic results," Studies in Antarctic Meteorology, American Geophysical Union, Antarctic Research Series, Vol. 9, 71-134.

Coker, W., 1986, "The growth of plastics in the fence industry," Fence Industry/Access Control, Vol. 29(1), 11-20.

Dyunin, A.K., 1959, "Fundamentals of the theory of snowdrifting," Izvest. Sibirsk. Otdel. Akad. Nauk SSSR (12), 11-24 (in Russian), National Research Council of Canada Technical Translation 952 (1961).

Farmwald, J.A. and J.A. Crum, 1986, "Developing a community water system for Shishmaref, Alaska," Proceedings, Fourth International Conference on Cold Regions Engineering (February 24-26, 1986; Anchorage, Alaska), 597-608.

Finney, E. A., 1934, "Snow control on the highways," Michigan Engineering Experiment Station, Michigan State College, Bulletin 57.

Komarov, A. A., 1954, "Some rules on the migration and deposition of snow in western Siberia and their application to control measures," Trudy Transportno-Energeticheskogo Instituta, Tom 4, 89-97. National Research Council of Canada Technical Translation 1094 (1963).

L.C.M.F. Ltd., 1983, "Wainwright snowdrift study," Report prepared for North Slope Borough.

Martinelli, M. Jr., R. A. Schmidt, and R. D. Tabler, 1982, "Technology transfer in snow control engineering," Journal of Technology Transfer, Vol. 6(2), 27-37.

Mellor, M., 1965, "Blowing snow," CRREL Monograph, Part III, Section A3c, U.S. Army Cold Regions Research and Engineering Laboratory, Hanover, New Hampshire.

Schmidt, R.A., 1972, "Sublimation of wind-transported snow -- a model," U.S. Forest Service, Rocky Mountain Forest and Range Experiment Station, Research Paper RM-90.

Tabler, R. D., 1971, "Design of a watershed snow fence system and first-year snow accumulation," Proceedings, Western Snow Conference (Billings, Montana; April 20-22, 1971) Vol. 39, 50-55.

Tabler, R. D., 1974, "New engineering criteria for snow fence systems," Transportation Research Record, Vol. 506, 65-78.

Tabler, R. D., 1975, "Estimating the transport and evaporation of blowing snow," Proceedings, Symposium on Snow Management on the Great Plains, (Bismarck, N. Dak.; July 1975), Great Plains Agricultural Council Publication No. 73, 85-104.

Tabler, R. D., 1980, "Geometry and density of drifts formed by snow fences," Journal of Glaciology, Vol. 26(94), 405-419.

Tabler, R. D., 1982, "Frequency distribution of annual peak water-equivalent on Wyoming snow courses," Proceedings. Western Snow Conference (Reno, Nev.; April 20-23, 1982) Vol. 50, 139-148.

Tabler, R. D., 1985, "Ablation rates of snow fence drifts at 2300-meters elevation in Wyoming," Proceedings, Western Snow Conference (Boulder, Colo.; April 16-18, 1985) Vol. 53, 1-12.

Tabler, R. D., 1987, "Slide rule for snow fence design," Proceedings, Western Snow Conference (Vancouver, B.C.; April 14-16, 1987), Vol. 55, 162-165.

Tabler, R. D., 1988a, Snow fence handbook (Release 1.1), Tabler and Associates, Laramie, Wyoming.

Tabler, R. D., 1988b, "Estimating dates of the snow accumulation season," Proceedings, Western Snow Conference (Kalispell, Montana; April 18-20, 1988), in press.

Tabler, R. D. and R. P. Furnish, 1982, "Benefits and costs of snow fences on Wyoming Interstate-80," Transportation Research Record, No. 860, 13-20.

Tabler, R. D. and R. A. Schmidt, Jr, 1972, "Weather conditions that determine snow transport distances at a site in Wyoming," Proceedings, UNESCO / WMO Symposia on the Role of Snow and Ice in Hydrology, (Banff, Alberta; September 6-13, 1972), 118-127.

Tabler, R. D. and R. A. Schmidt, 1986, "Snow erosion, transport, and deposition in relation to agriculture," Proceedings of the Symposium Snow Management for Agriculture, Great Plains Agricultural Council Publication No. 120, 11-58.

Tabler, R. D. and D. L. Sturges, 1986, "Watershed test of a snow fence to increase streamflow: preliminary results," Proceedings, Cold regions Hydrology Symposium (Fairbanks, Alaska; July 22-25, 1986), American Water Resources Association, 53-61.

Wyoming Highway Commission, 1932, Eighth biennial report of the State Highway Commission of the State of Wyoming, for the period beginning October 1, 1930, ending September 30, 1932, Cheyenne, Wyoming.

Field Observations of Wind Deflection Fins to Control Snow Accumulation on Roofs

C.J. Williams[1]

A field study has recently been conducted to demonstrate that a wind deflection fin can effectively prevent drifting snow from collecting in a roof step. The fin was designed using experience gained from previous roof mounted wind deflection fins.

A 4 ft high by 24 ft long fin was installed on a warehouse roof in Cambridge, Ontario, Canada. The snow accumulation was monitored following a blowing snow event showing that complete prevention of drifting at the base of the step is possible. Modifications to the initial fin design to improve the overall effectiveness of the fin are discussed.
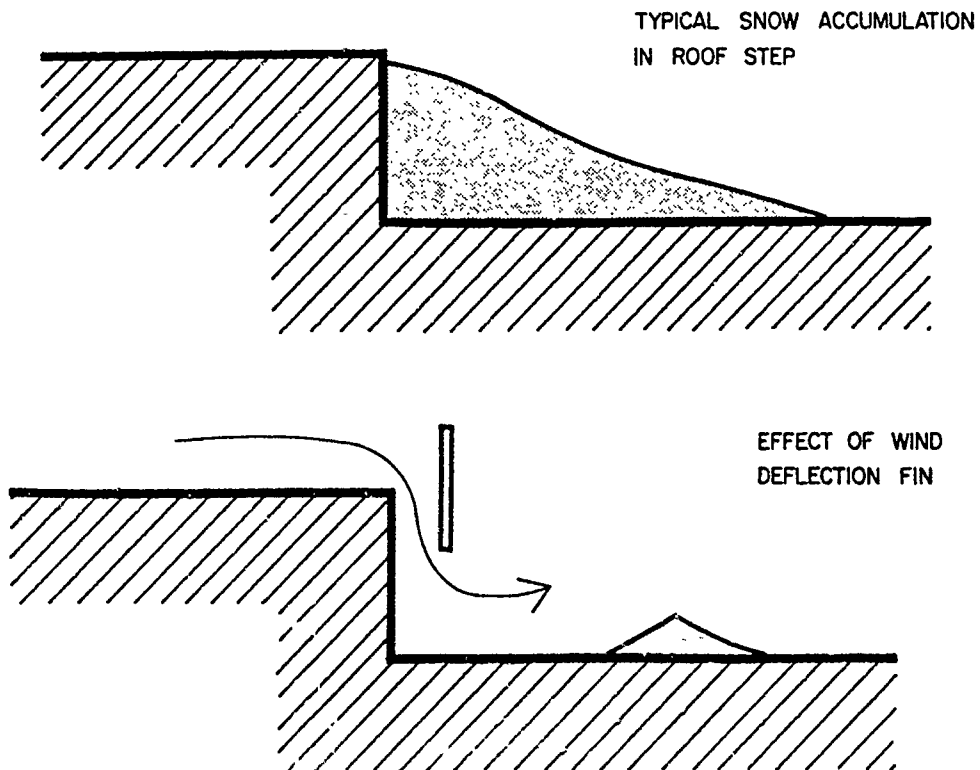
FIGURE 1

WIND DEFLECTION FIN

[1] Ph.D., P.Eng., Rowan Williams Davis & Irwin Inc., 650 Woodlawn Road West, Guelph, Ontario N1K 1B8.

Background

Wind deflection fins have been used for many years on railways and highways to prevent problematic snow accumulations. These fins deflect wind into still air regions to prevent snow particles from collecting as shown in Figure 1.

Wind deflectors have been used successfully by RWDI to prevent snow accumulation at doorways and windows in buildings. Two examples are the clerestory windows on a school in Coral Harbour in the Northwest Territories and skylights on the Coast Guard Base in Parry Sound, Ontario, Canada. Figure 2 shows a site photograph of the wind deflector fins on the school in Coral Harbour. The increased wind speed beneath each fin prevents snow accumulation, with each fin being made taller than the upwind fin to ensure that it will deflect sufficient wind down to the roof level. The spacing and size of each fin was designed by scale model tests using a water/sand analogy to simulate drifting snow.

FIGURE 2

**WIND DEFLECTION FINS TO PREVENT
ACCUMULATION AGAINST CLERESTORY WINDOWS**

The same snow simulation procedure was used to design the wind deflection fins shown in Figure 3. In this case, skylights needed to be protected from snow accumulation and again the curved deflector fins were found to perform well on the actual building.
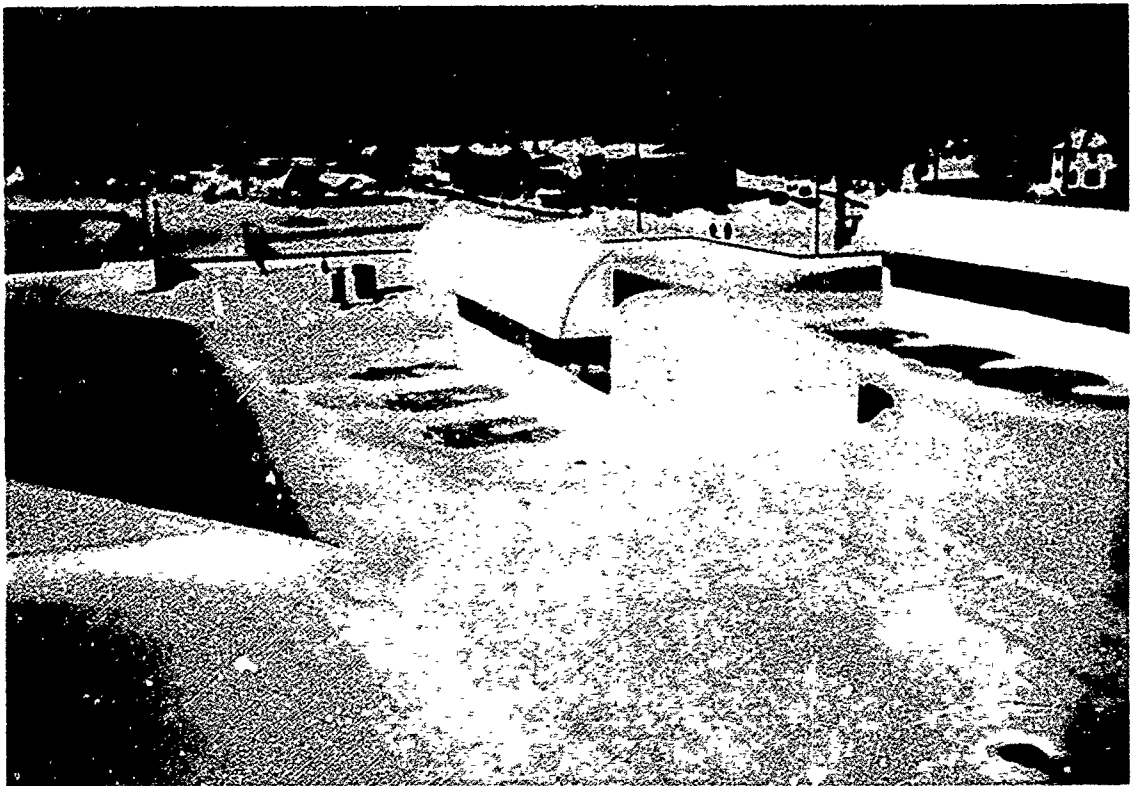
FIGURE 3

ROOF SKYLIGHTS PROTECTED BY WIND DEFLECTION FINS

Figure 4 shows an example of a doorway on the above school in Coral Harbour which was protected by a wind deflector fin. A scale model test was used to develop the dimensions required for the fin.
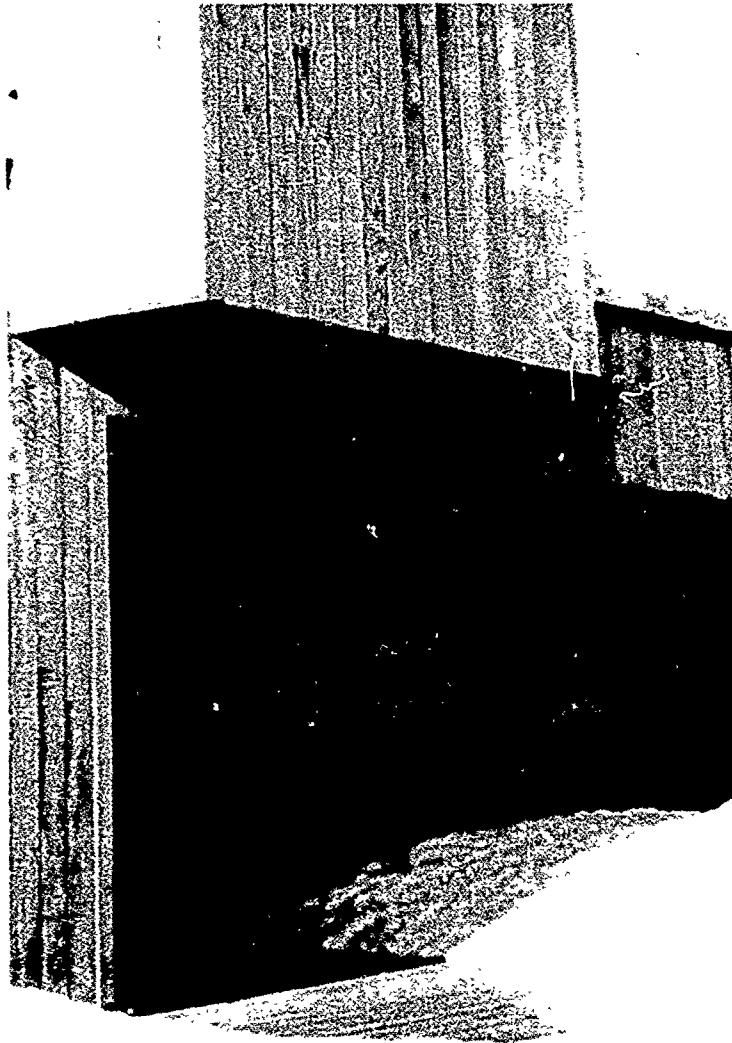
FIGURE 4

WIND DEFLECTOR TO CLEAR SNOW FROM AN ENTRY AREA

The experience gained from observing the drifts produced by these and other wind deflection fins provided the following problems which can occur with deflector fins:

1. Plugging of the gap beneath the deflector with snow.

2. Drift formation downwind of the fin.

3. Drift formation of the upper roof with wind blowing into the roof step.

If, following a heavy snowfall with little or no wind, the accumulation beneath a fin is sufficient to reach the lower edge of the fin, any future scouring beneath the fin could be prevented and a potentially dangerous situation exists. Future blowing snow events could create a drift to the top of the fin producing a load at the roof step greater than the conditions without a wind deflector fin.

Drift formation downwind of a fin is a result of the reduced wind speed caused by the fin itself. This could produce a potential roof overload situation as, although the drift is minimized at the roof step, a drift larger than that which would exist without the fin can be produced further away from the roof step.

Care must also be taken in designing a fin to ensure that no additional accumulation is created on the upper roof. This could occur as a result of the reduced wind speed created by the fin protruding above the upper roof when a blowing snow event occurs in the opposite direction for which the fin was originally designed.

With the above background information available, the case study described below was undertaken.

Case Study

RWDI was contacted by the owner of a warehouse in Cambridge, Ontario who was concerned that the snow loading on a 4 foot roof step of his 400 ft x 1000 ft building could lead to a roof collapse. Although he had not experienced a collapse his concern for the value of the materials he was warehousing had led to an annual expense over the last few years of $4,000 for snow removal from the roof step. The damage sustained to the roofing material by the snow removal process was also a cost consideration.

During the winter of 1986 - 1987, RWDI measured the roof snow load on two separate occasions and found that the load equalled the design snow load. As this was early in the winter, and melting and refreezing of the drift by heat loss from the building could result in compaction of the drift, it was considered that any future blowing snow events could result in exceedance of the design snow load. A rainfall event could also result in additional load.

The wind deflection fin shown in Figure 5 was designed to overcome plugging of the gap beneath the fin by providing a gap beneath the fin (2 ft) which was larger than the known maximum snowfall for the area. It was not known how large the drift downwind of the fin would be and therefore the drift was observed to ensure that an overload situation would not occur. Similarly any drift formation on the upwind roof was monitored.

FIGURE 5

WIND DEFLECTION FIN, CAMBRIDGE, ONTARIO

The effectiveness of the fin was tested during a blowing snow event which occurred during December 1987. Approximately 15 cm of wet snow fell followed by westerly winds. The resulting drift accumulations are shown in Figures 5 and 6. Figure 5 shows that the fin was effective in preventing any accumulation at the base of the roof step and that the drift in other parts of the roof nearly filled the step. Figure 6 clearly shows that the fin provides a higher scouring velocity than is necessary beneath and beyond the fin. At approximately 2 roof step heights downwind of the roof step, a drift had accumulated, indicating that the fin did produce a reduced wind speed in that area of the roof. If this drift were to increase in depth with subsequent blowing snow events this could cause a localized roof overloading situation. Figure 5 also shows that a drift was not formed on the upper roof.

The conclusions from the field test are:

1) The wind deflector fin, as designed, effectively prevented snow from accumulating in the roof step.

2) An improved fin should be designed to minimize the accumulation downwind of the fin. It would be acceptable to reduce the scouring velocity beneath the fin to achieve this.

312

Suggested Design Improvements

The dimensions of the fin, shown in Figures 5 and 6, used for the field test reported in this paper are shown in Figure 7A. During future field tests it is proposed to test wind deflection fins which will reduce the downwind drift on the lower roof by minimizing the velocity deficit produced by the fin. Figures 7B and 7C show suggested fin designs which should achieve this objective. The scouring velocity directly beneath the fin will be reduced but this should be acceptable because, as shown in Figure 6, the larger fin used in

FIGURE 6

WIND SCOUR BENEATH WIND DEFLECTION FIN, CAMBRIDGE, ONTARIO

the field test produced a sufficiently large scoured area at the base of the roof step. It is considered that even with a significant reduction in the scouring velocity beneath the fin, the drift at the base of the roof step will be prevented from occurring.
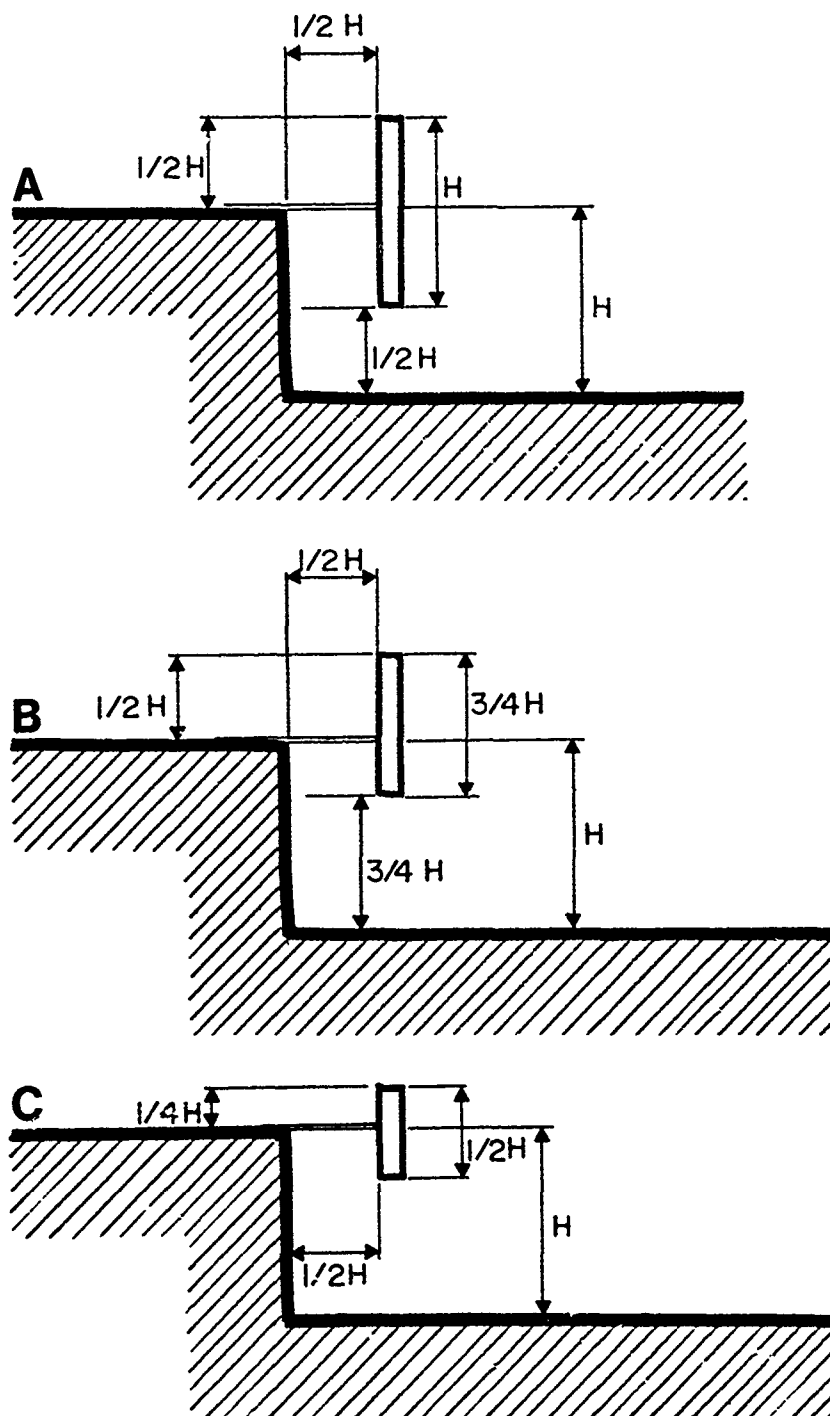
FIGURE 7

WIND DEFLECTION FIN DIMENSIONS

6
MECHANICAL PROPERTIES
AND BEHAVIOR
Rune Sandvik, Chairman
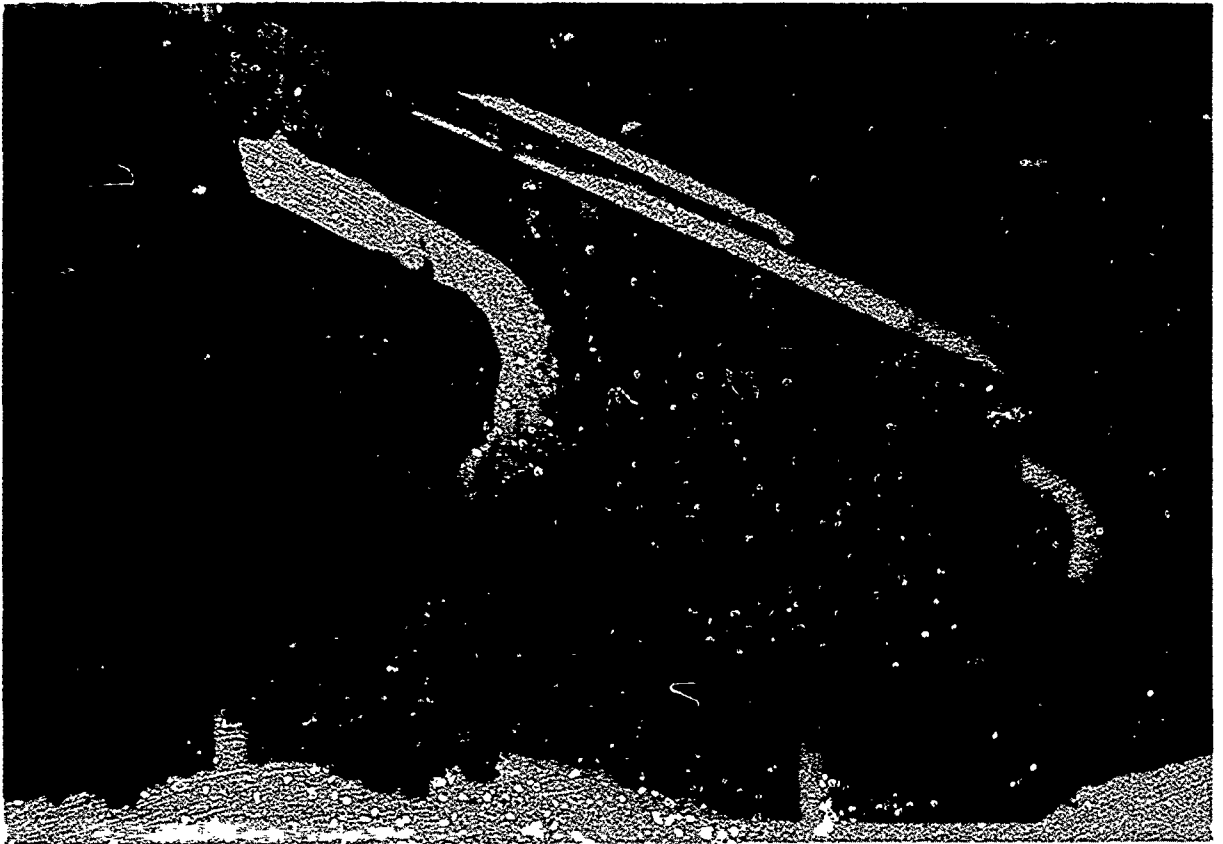
Snow curl formed by downslope creep of snow. (Photograph by Ian Mackinlay.)

Calculation of Maximum Snow Load on Roofs with High Thermal Transmittance

Rune Sandvik[1]

ABSTRACT

In this paper a simple numerical heat transfer model is applied to calculate the reduction of snow load on a roof caused by the heat loss through the roof. Thirty years of data on precipitation, temperature and wind speed for a meteorological station on the southern coast of Norway are used. A snowfall event causing maximum load throughout this period is studied for roofs with two different heat transmittance values corresponding to typical one- and two-layer glass roofs. The loads with certain return periods are calculated and compared to corresponding loads on the ground to estimate the thermal reduction factor.

INTRODUCTION

Design values of snow load on roofs with high thermal transmittance cannot be deduced from the rules in the Norwegian load standard (NBR, 1981). This has become a problem during the last few years since glass roofs are getting more common in design of new buildings.

The great variation in winter climate in Norway makes it difficult to transform limited experience on snow load on such roofs in one location to other parts of the country. The current revision of the standard (NBR, 1981) raised the problem of calculating conservative values of the thermal coefficient, C_t, on the basis of available meteorological data, as no field measurements, useful for statistical treatment, exist.

The author and the Norwegian Meteorological Institute have together selected 10 meteorological stations sited in different part of Norway, all with a minimum of 30 years of recordings. The snow loads on roofs located at these stations will be calculated as well as the C_t values. The result of these calculations is expected to give conservative values of C_t, as no sliding off and no melting caused by external temperature above zero are considered. So far, data from one station, Kjevik, on the southern coast of Norway, have been processed.

THE MODEL

The mass of melted snow per unit area, ΔM, for the period of time, Δt, caused by heat transfer through a roof, is calculated by Eq. 1:

$$\Delta M = \frac{\Delta t}{L} (k_1 U_1 (T_1 - T_b) - k_2 U_s (T_b - T_2)) \tag{1}$$

I: Meteorologist (MSc), Norwegian Council for Building Standardization (NBR), Oslo, Norway.

where:

- L is the heat of melting per unit mass for snow

- U_r is the thermal transmittance of the roof putting the outside thermal surface resistance equal to zero

- U_s is the thermal transmittance of the snow layer on the roof putting the thermal surface resistance at the bottom of the snow layer equal to zero

- T_1 is the internal temperature

- T_2 is the external temperature

- T_b is the temperature at the bottom of the snow layer

- k_1 and k_2 are coefficients taking the values 1 or 0 according to the rules given below

A certain external temperature, T_{2c}, will just be low enough to stop the melting process on a roof for a given snow layer and internal temperature. This temperature can be calculated as follows.

Assume that the density heat flow rate through the roof is given by q_r:

$$q_r = U_r (T_1 - T_b) \qquad (2)$$

and the density heat flow rate through the snow layer is given by q_s:

$$q_s = U_s (T_b - T_2) \qquad (3)$$

At the bottom of the snow layer the temperature cannot be above 0 °C. However, when the external temperature decreases and reaches T_{2c}, the total heat flow through the roof will equal the total heat flow through the snow layer as no melting occurs, i.e. $q_r = q_s$. And by means of Eq. 2 and Eq. 3:

$$T_2 = T_b - (U_r/U_s)(T_1 - T_b) \qquad (4)$$

Putting $T_b = 0$ °C and $T_2 = T_{2c}$ in Eq. 4 gives:

$$T_{2c} = -(U_r/U_s)T_1 \qquad (5)$$

The coefficients, k_1 and k_2, in Eq. 1 are now being determined as follows:

- If $T_2 \leq T_{2c}$ then $k_1 = k_2 = 0$ (corresponding to T_b lower than 0 °C)

- Or if $T_2 > T_{2c}$ then $k_1 = k_2 = 1$ if $T_2 \leq 0$ °C, or $k_1 = 1$ and $k_2 = 0$ if $T_2 > 0$ °C (possible melting is restricted to heat loss from inside the building)

Applying Eq.1 ΔM can be determined for arbitrary intervals of time when specifying internal and external temperatures and thermal transmittance of the roof. The thermal transmittance of the snow layer is determined by the effective thermal conductivity of snow as given by E.J. Langham (Gray and Male, 1981), specifying the density, and by giving the the current snow load on the roof. The density used was 250 kg/m³ giving the conductivity value of 0.18 W/(mK).

The snow load on the roof at time t, S(t), is calculated by:

$$S(t) = S(t_0) + g \, \Sigma (P_i(t) - \Delta M_i) \tag{6}$$

where:

- P_i is the mass of snow precipitation per unit area over a period of time, 12 hr

- ΔM_i is the mass of melted snow per unit area over the same time period

- g is the acceleration due to gravity

- t_0 is the starting time for summation

CALCULATION DATA

The available data, useful for this purpose at Kjevik, are the precipitation, every twelve hours, and recordings on wind speed, temperature, snow depth and snow cover.

The station is located at the southern coast, and has a mean temperature of –1.0 °C for the three coldest months of the year. Heavy snowfalls are usual, but because of the coastal climate, melting is effective, and the 5-year snow load on the ground is calculated to be 2.6 kPa (NBR ,1981). Glass roofs are regarded as sensitive to the relatively high intensity of snowfalls in this area.

It is well known that the effiency of standard rain gauges, even with various wind shields, may vary considerably for solid precipitation. In Norway the results of Hamon´s study (Hamon, 1973) are used for the Norwegian gauge with wind shield using the wind speed and the temperature as parameters in correcting solid precipitation recordings:

$$P_c = P_m \, e^{a(T) \, v} \tag{7}$$

where:

- P_c is the corrected precipitation

- P_m is the measured precipitation

- v is the wind speed at the gauge orifice

- a(T) is a constant for certain intervals of temperature and wind speed

Values of a(T) for Norwegian measurements are given in NHP (1986). Because only a few stations are observing wind speed, the formula is not being used on a routine basis by the Norwegian Meteorological Institute.

The snowfall event causing the highest calculated snow load on a roof with $U_r = 3$ W/(m²K) for the period 1957 – 86 appeared at the end of February 1970. Actually two snow falls, separated by one day with no snowfall, resulted in a total of nearly 160 mm in 6 days starting on day number 50 (Fig. 1).

Figure 1 gives the recorded (left–hand bars) and the corrected (right–hand bars) snowfall according to formula (7). The temperature is given as the solid line in Figure 4. This clearly shows the need of correcting snow fall intensities recorded by the standard Norwegian gauge with wind shield.

In Figure 2 the mean wind speed for the snowfall event is given.
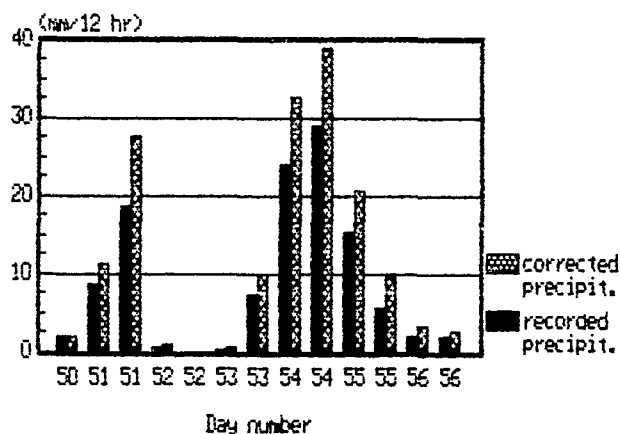
Figure 1. Recorded and corrected precipitation. Data from year 1970. (Station: Kjevik).
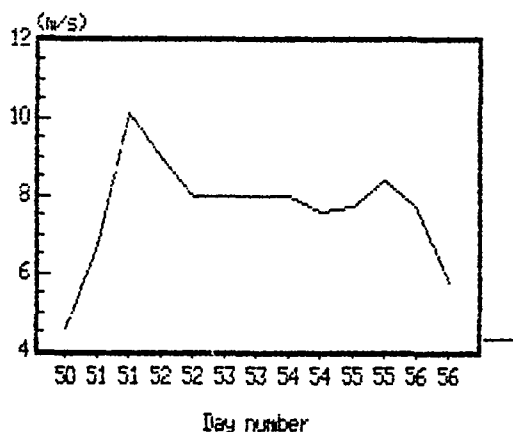
Figure 2. Mean wind speed, data from year 1970. (Station: Kjevik).

CALCULATION RESULTS

The calculations of roof loads for the snowfall event shown in Figure 1 result in maximum loads of 921 Pa and 573 Pa for U_r values of 3 W/(m²K) and 5 W/(m²K) respectively. In Figure 3 the loads on a roof for the above U_r values are shown for the whole period with snow on the roof. While this was the greatest load for the roof with the lowest U_r, the other roof had a higher load, 670 Pa, another year during the 30-year period. The cumulative snowfall for the same period is given by the solid line in Figure 3.

Figure 3 shows that the first of the two separated snowfalls in Figure 1 only influences the maximum load for the roof with the lowest thermal transmittance.
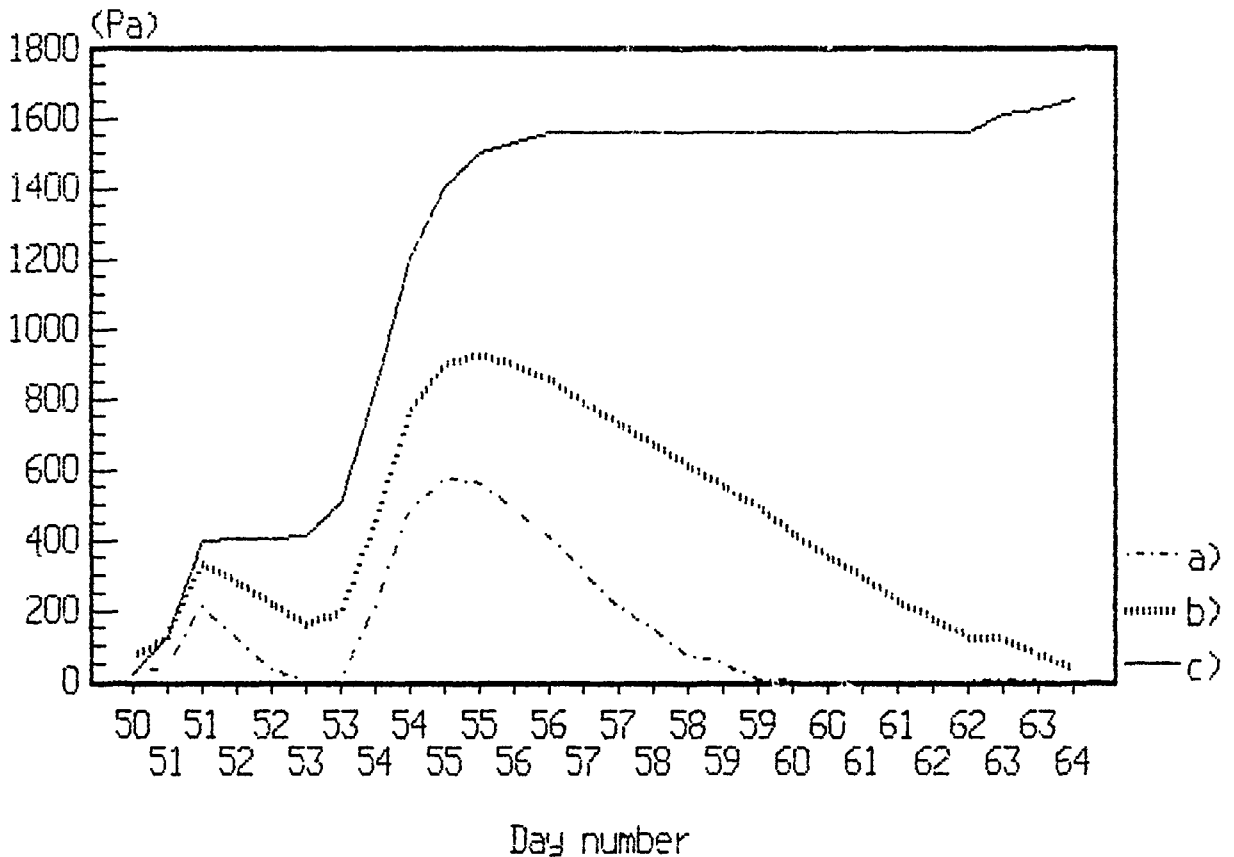
Figure 3. Calculated snow load on roof, data from 1970 (Station: Kjevik).
a) Snowload, U = 5 W/(Km²) b) Snowload, U = 3 W/(Km²) c) Cumultative snowfall.

For this snowfall event no melting caused by external heat flow is possible until the maximum load is reached, as the external temperature is below 0 °C (Fig. 4).

In Figure 4 the lowest external temperature for melting, T_{2c}, according to Eq. 5 is also shown for both values of thermal transmittance. (Only values greater than −100 °C are plotted.)
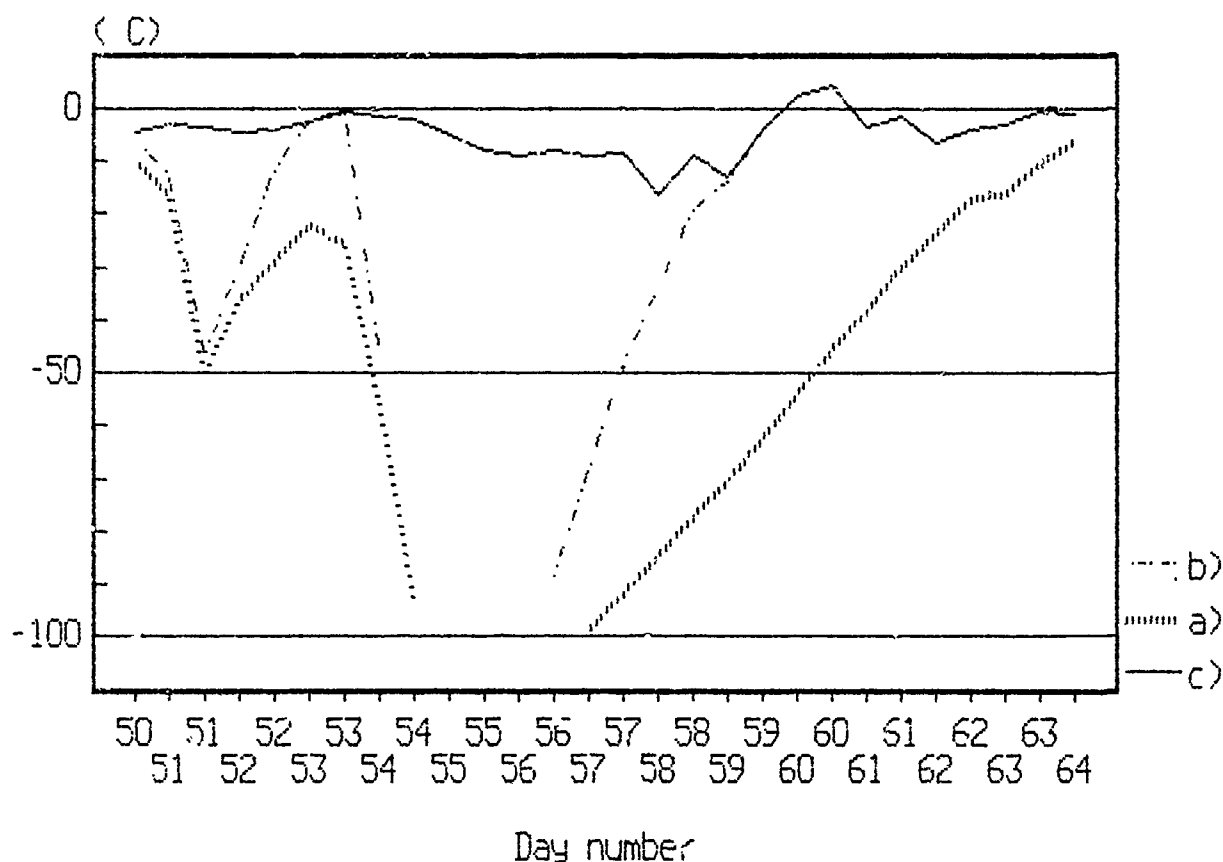
Figure 4. Temperature. a) Critial temperature, U = 3 W/(Km²). b) Critical temperature, U = 5 W/(Km²). c) External temperature, data from 1970 (Station: Kjevlk).

The roof loads with return periods of 5, 20 and 50 years for internal temperatures of 5, 10 and 18 °C are calculated by means of the Type 1 extreme value distribution. The results are given in Table 1.

Table 1: Loads (kPa) on roof for various return periods and internal temperatures.

T_i	Return period (years)			T_i	Return period (years)		
(°C)	5	20	50	(°C)	5	20	50
5	0.99	1.50	1.82	5	0.84	1.36	1.68
10	0.65	0.98	1.19	10	0.48	0.73	0.89
18	0.46	0.70	0.85	18	0.33	0.51	0.63

a) U = 3 W/(m²K)   b) U = 5 W/(m²K)

322

As the snow load on the ground is calculated for the same return periods for this station in the load standard (NBR, 1981) as in Table 1, the thermal coefficient C_t can be calculated from a general equation converting snow load on the ground to snow load on a roof:

$$S = C_t \, \mu \, S_0 \qquad\qquad (8)$$

where:

– S and S_0 are the snow loads on roof and on ground respectively

– and μ is the shape coefficient of the roof

Putting $\mu = 1$ in Eq. 8 is in coresspondence with earlier calculation of S from Eq. 6. The results of the calculation of C_t are shown in Table 2.

Table 2: Thermal coefficient for various return periods and internal temperatures.

T_1	Return period (years)			T_1	Return period (years)		
(°C)	5	20	50	(°C)	5	20	50
5	0.38	0.44	0.47	5	0.32	0.40	0.43
10	0.25	0.29	0.31	10	0.18	0.21	0.23
18	0.18	0.21	0.22	18	0.14	0.15	0.16

a) U = 3 W/(m²K)   b) U = 5 W/(m²K)

For this station it appears from Table 2 that the C_t factor is below an upper bound of 0.31 for both one- and two-layer glass roofs as long as the internal temperature is kept above 10 °C.

The calculations of snow load on roofs in this paper are based on a very simple theory of heat transfer, and this must be kept in mind when using the model. As mentioned in the introduction, rather conservative values are needed for the purpose of standardization as no useful field measurements are available.

For roofs with low thermal transmittance, rain on snow are sometimes added to the maximum load calculated from the ground load. For roofs with high thermal transmittance, however, the adding of rain is of no importance in most cases as far as the maximum snow load is considered. This because the rapid melting off after a snow fall will reduce the snow load on the roof by more than the increase from adding rain over the same time period. It can also be assumed that after a major snowfall the probability of having a rainstorm of importance to the load on the roof, without at least one preceeding day with neglectible precipitation, is small.

For rather high internal temperatures the snow layer on a roof will be melted all away or down to a thin layer, for low external temperatures, and only a small portion of the initial snow load can remain and be added to a later snowfalls separated by a week or more. The model reflects this quite well and is reliable as long as the external temperature is below 0 °C. For steady temperatures above 0 °C possibly accompanied by strong winds, in a period less than one week between two major snowfalls, the model can possibly overestimate the snow load considerably, especially for two-layer roofs and low internal temperatures.

CONCLUSION

A simple model for calculating the snow load on roofs with high thermal transmittance has been developed and run for climatological data on a meteorological station on the southern coast of Norway. Considering melting caused by heat flow through the roof as reduction of snow load, the model seems to give reliable snow loads useful for standardization purposes in Norway when no actual field measurements exist. The effect of rain added to the snow precipitation is not considered to be of inportance as far as the maximum load is considered.

The model is overly sensitive to weather situations with several major snow falls separated by short periods (less than one week) with warm and windy weather. For such situations the model will overestimate the snow load on the roof, especially for thermal transmittances comparable to that of two-layer glass roofs and low internal temperatures.

REFERENCES

NBR (Norwegian Council for Building Standardization), 1981, "Prosjektering av bygningskonstruksjoner. Dimensjonerende laster", Oslo, Norway.

Gray, D.M., and D.H. Male, 1981, "Handbook of snow", 294 – 298, Pergamon Press, New York.

Hamon, V.V, 1973, "Computing actual precipitation", WMO/OMM, No 326, Vol 1, Geneva, Switzerland.

NHP, (Nordic Hydrological programme), 1986, "The improvement of point precipitation data on an operational basis", Report No 17, Stockholm, Sweden.

Shear and Compressive Strength Measurements of Snow Using the Bevameter

Russell G. Alger[1]

ABSTRACT

The prediction of trafficability in snow depends on various strength parameters. These parameters can be measured in a number of ways, one of which is the bevameter. Measurement using a bevameter has not been wide spread in the past due to the fact that the instrument is usually cumbersome and difficult to use. The Institute of Snow Research (ISR) has developed a mobile bevameter system that is quite accurate and easily operated in the field. This system is being used to develop relationships between snow characteristics and strength and also to verify the results of the various shallow snow mobility models. This paper is a review of the advancements in strength measurements using the bevameter and how the results are being used to simplify trafficability/mobility modeling.

INTRODUCTION

Mobility models depend on the input of certain parameters that describe the terrain that the vehicle is traveling over. In cases where there is a snow cover, these parameters can be as simple as density and crystal type, or as complete as some sort of measured strength parameters. These strength parameters can be measured in a number of ways.

Strength measurements can be obtained as simply as observing the support provided by the snow pack to a man on foot or on skis. A hardness gauge such as the Canadian Hardness gauge or possibly a Rammsonde can also give an indication of strength. The vane cone incorporates the values of compressive strength and shear strength of the pack. Several other such methods also exist to arrive at a strength indication for snow.

Probably the most complicated but accurate of the techniques is the bevameter. ISR has developed a system that eliminates some of the difficulties in using the bevameter and allows for comparisons to be made to other measurement techniques, correlations between basic snow characteristics and snow strength, qualification of existing mobility models and possibly development of new ones.

THE BEVAMETER

The term "bevameter" is used to describe the combination of two strength measurement systems. These are the plate sinkage and the annular shear tests. ISR has developed a system which is mounted on a Pole Cat vehicle that con-

---

I. Research Engineer, Institute of Snow Research, Michigan Technological University, Houghton, Michigan.

tains both the sinkage and shear devices. The load cells for each are connected to a data acquisition board in an IBM PC located inside the vehicle. The PC and interior equipment are all run by a generator mounted on the vehicle. Figure 1 is a photo of the apparatus and vehicle.
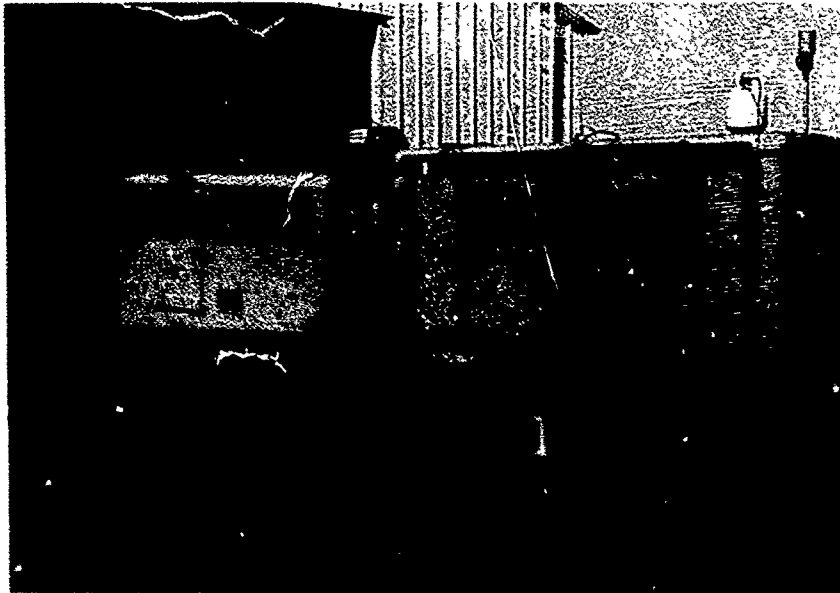
Figure 1   The Pole Cat and Bevameter System

The ISR bevameter contains 3 separate hydraulic systems. The first system is used to raise and lower the whole test apparatus. This allows the shear head and sinkage plate to be positioned just above the pack before a test. The second supplies fluid to the hydraulic motor that turns the shear annulus and the third pressurizes the cylinder that is used to push the sinkage plate into the pack. Figure 2 shows a closer view of the hydraulics and the whole system. Figure 3 shows the arms that lower the system to the pack.

The computer and the data acquisition system are controlled through the hydraulic control system switches. After the appropriate site and snow condition data has been input into the program and stored inside the vehicle the outside operator controls the operation of the system. This eliminates any signaling back and forth between two operators and allows the test to be run by one person if need be.

One of the major problems with the bevameter is that it must be heavy enough to counteract the loads applied during the plate sinkage test. This problem has been overcome by mounting the whole system on the vehicle. This allows the weight of the vehicle to be a counterbalance. The vehicle also allows the system to be easily moved. The system is mounted on a slide rail. Since several tests must be performed at each site, the bevameter is constantly being moved. The slide rail allows more tests to be run without moving the vehicle by allowing the bevameter to be moved over a new area of snow without moving the vehicle. Two or three full sets of shear tests can be run without moving the vehicle.
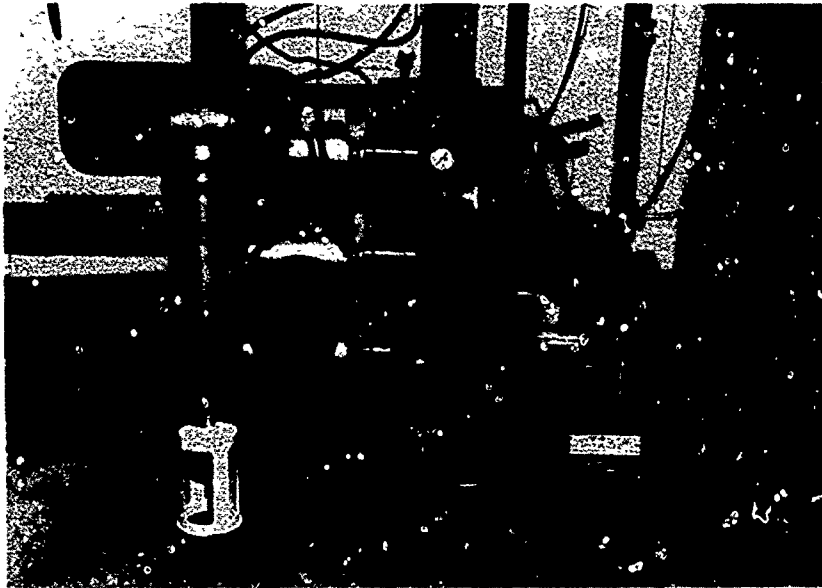
Figure 2   Close-up View of the Bevameter System
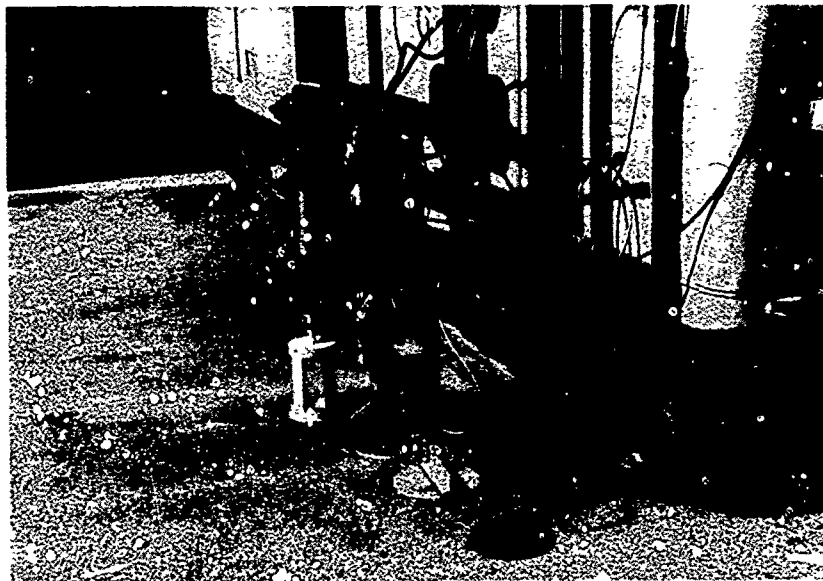
Figure 3   Side View of Bevameter System

PLATE SINKAGE TESTS

The plate sinkage test is used to determine the "Bekker" (Bekker, 1969) values $k_\emptyset$, k_c and n. The test involves forcing a circular plate into the snow pack at a constant sinkage rate. The load on the plate is measured throughout the test and recorded by the data acquisition system on a floppy disk. The

327

sinkage of the plate is also recorded with the load data. In order to obtain sinkage values, a potentiometer mounted on a stationary plate that is set on the pack is used. This system allows for any lifting of the vehicle to be eliminated from the measurement. Figure 4 is a photo of the plate sinkage device.

Several references on the plate sinkage test have been written in the past. These include Bekker (1969), Harrison (1981) and Yong, Fattah, Skiadas

Figure 4   Plate Sinkage Device

(1984). Variations of the bevameter have been built and tested and the test procedures have been documented. Most of the work done to date has been in soil systems, although some work has been done in snow. For purposes of this discussion no further explanation of the test itself will be given. The plate sinkage tests run with the new bevameter at ISR to date have all been performed with an 20.3 cm diameter plate. The larger diameter plate seems to work quite well in snow. The speed that the plate is initially traveling is approximately 5 cm/sec.

Most of the plate sinkage data collected to date at ISR has not been thoroughly analyzed since the major emphasis has been to work with the annular shear test. For each shear set run, however, a plate sinkage test has been run since the instruments are both mounted on the same platform. Once the data for a test has been stored on a disk, a computer program developed at ISR reduces it and calculates the required parameters. The program also plots the data in two different formats.

The first plot that is generated by the system is shown in Figure 5(a). This plot of the data for load and sinkage shows the snow strength characteristics. As seen in the figure, the sinkage starts out high as compared to the load until the snow compresses to the point where it has some strength and
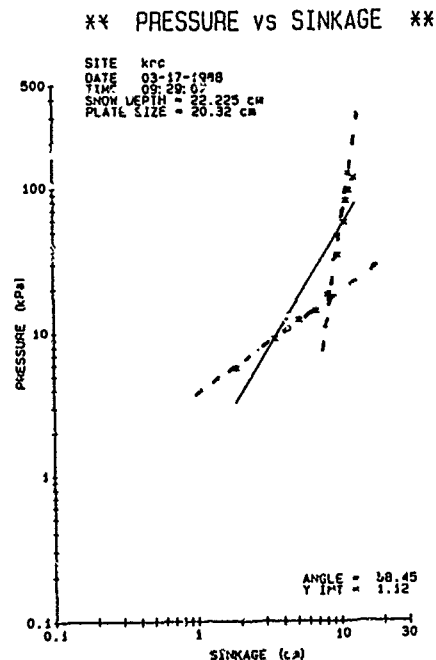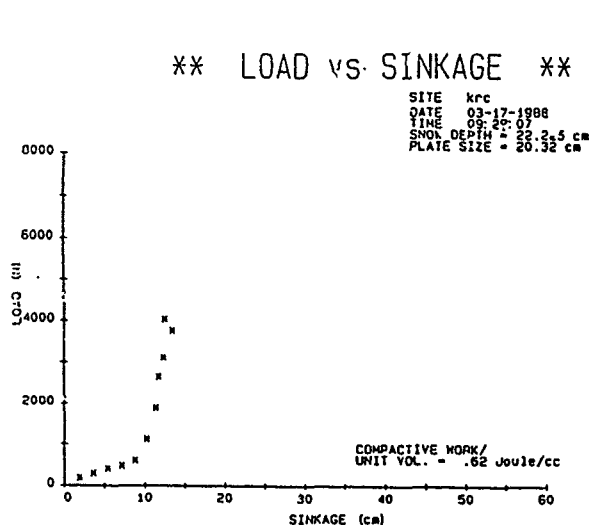
Figure 5   Plate Sinkage Results

the sinkage approaches zero. This pattern is representative of porous materials such as snow. From this plot, the work involved in compacting the snow is computed by the program as the area under the curve.

The second plot that results from the program is shown in Figure 5(b). This plot is the log-log plot of the pressure exerted on the pack over the circular area against sinkage. Normally, the natural logarithms of the data should closely approximate a straight line. For snow, however, there are usually at least two separate zones that are linear. There are two reasons for this phenomena. The first is the fact that the snow is weak in compression in its undisturbed state. This allows for a large sinkage before pressure can be built up. Once the snow layer is compacted it has considerable strength and the sinkage is much less pronounced. This accounts for the two different straight line zones shown on the graph. The second reason for discontinuities in the results is that older snow packs usually are stratified and sometimes contain ice lenses and frozen snow layers. These discontinuities result in changes in slope throughout the graph and thus show layers of varying strength. The slope of the straight line portion of this graph is n where n = the tangent of the angle the straight line makes with the horizontal axis. The values of k_ϕ and k_c are calculated from the y-intercepts of the log-log plots using two different plate sizes during a test.

As mentioned earlier, little work has been done to date with the plate sinkage data collected. The computer program calculates a best fit linear model, shown as a solid line on Figure 5(b), using all of the data although this is being modified at present to incorporate the calculation of models

through the different zones along the curve. The dashed lines shown on Figure 5(b) are drawn only to show the different zones for that particular set of data. Future work in the area of compressive strength will involve comparing vehicle sinkage to plate sinkage results for both wheeled and tracked vehicles. The effect of snow characteristics on the sinkage will also be investigated further in the future with both current field data and data that will be collected over the next several winters.

ANNULAR SHEAR TESTS

The annular shear test is performed by rotating either a grousered or rubber covered ring shaped annulus on the snow pack with varying normal load. ISR uses a rubber covered annulus for all tests to simulate the rubber on a tire or track. The inside diameter of the ring is 6.67 cm and the outside diameter is 9.21 cm. This gives the ring an area of 126.6 cm^2. Figure 6 is a close-up view of the annulus and load cell mounted on the bevameter.
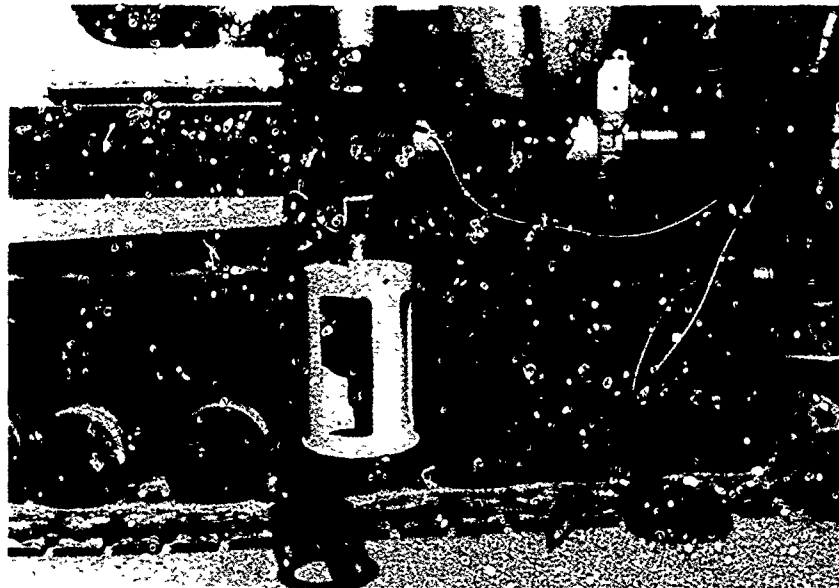
Figure 6   Shear Device

An annular shear test actually consists of five full sets of data. Five normal loads are placed on the annulus consisting of 20, 40, 60, 80 and 100 pounds. Each test is run on undisturbed snow through a rotation of 360 degrees. As the annulus is turned on the snow a torque cell records the torque implied to the rubber and the data is stored on disk. The angular displacement of the ring is recorded as time, since for snow, the rotation of the ring is constant with time.

The computer program developed at ISR takes the data directly from the disk and reduces it to perform the required calculations. Figure 7(a) is a plot of five sets of data collected at a site on March 17, 1988. All five tests were run in close proximity so the snow characteristics are the same for the set. The calculated shear strengths are also shown on the graph.

From the plot of the shear vs time, the average shear strength of the pack can be determined for each normal load. Theoretically a straight line of zero slope can be fit through the latter portion of the data because the shear strength should be constant after the initial particle bonds are broken.
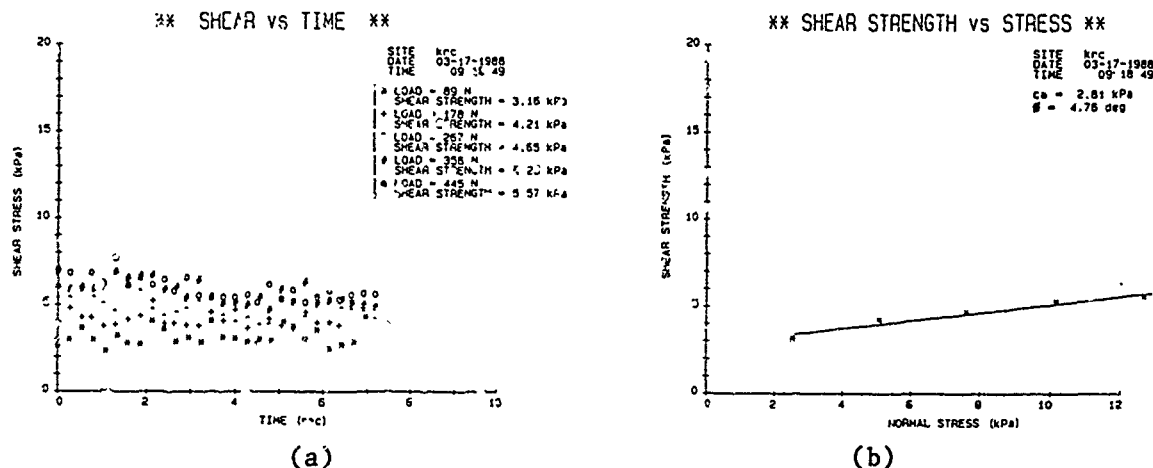
Figure 7 Shear Test Results

Figure 7(b) is the plot of the shear strength vs. normal stress. Values of ca and $\emptyset$ are obtained from this plot. The magnitude of ca is the y-intercept of the best fit straight line through the five points and $\emptyset$ is the angle that the line makes with the horizontal axis. All of these values are calculated by the computer program.

OUTCOME OF WORK AT ISR

Mobility models are generally intended to serve two purposes. The first use is as an aid to design engineers working on new concepts for vehicle drive systems. The second is to aid troops in the battlefield by predicting the best possible route to take or the best vehicle to use in a given situation. In order for these models to be useful to troops, they must be easy to use and the input parameters must be easily measured.

In order to use the models as design tools, they must be verified in the field. This verification comes from testing vehicles in conjunction with bevameter tests. ISR is in the process of making this comparison along with USACRREL and WES under the "Wheels vs Tracks Program". Further work in this area is required before any conclusions to the validity of the models can be made.

Simplification of the measurement of snow parameters used by troops has been the primary focus of past work at ISR. The intent is to develop relationships between the basic properties of the snow pack and the strength parameters. These relationships would allow the user in the field to make simple measurements and arrive at a good approximation of mobility. The work done at ISR in this area has taken two directions. The first is an attempt to relate the shear strength to snow variables such as density, temperature, crystal structure and free water content. The second is the development of a simple apparatus to directly measure the strength in the field.

331

ISR is in the process of developing a simple, small and easily operated system that would yield comparable results to those obtained using the full sized bevameter. This instrument is in the development stages and will hopefully be tested alongside the ISR bevameter later this year.

Under a contract with USACRREL through part of the 1987-88 winter an attempt was made to develop a relationship between the shear strength parameters and average pack density. Over this period, 49 shear tests and 20 plate sinkage tests were run. Along with bevameter tests, density and temperature measurements, some visual observations were made to determine which properties could be measured in the future to further refine the results. These observations included crystal size and type along with a visual estimation of free water content. The data was analyzed first by comparing density with shear strength for each normal load. This analysis resulted in a linear relationship between strength and density. Figure 8 is a plot of the shear strength vs normal stress for four different densities.
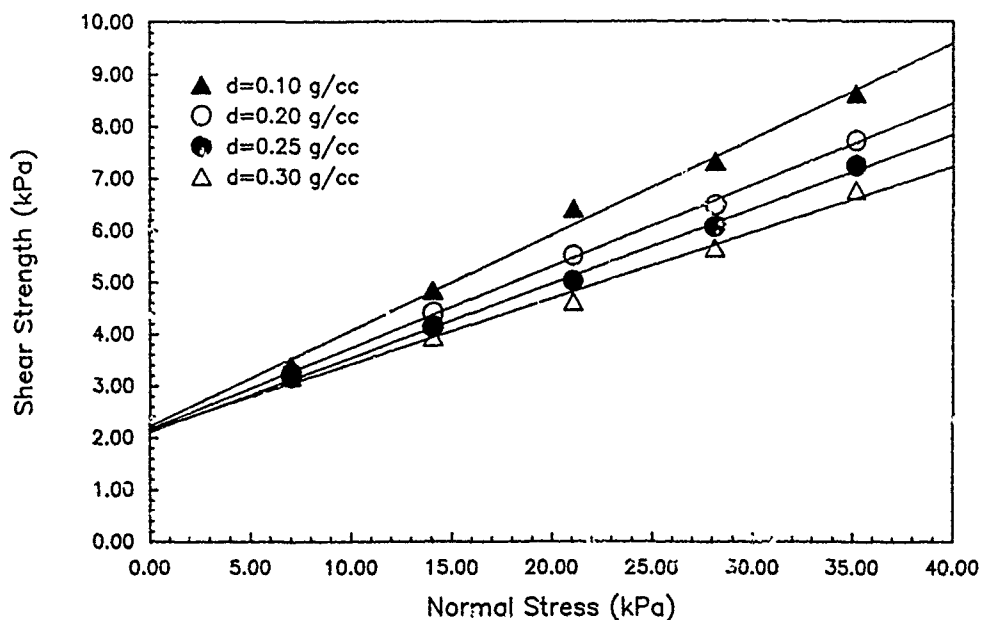
Figure 8   Shear Strength/Normal Stress Relationship

The angle $\emptyset$ was calculated for each line on the graph and the result is shown in Figure 9. The graph demonstrates the linear relationship between the angle and density. Although this relationship is quite simple, it could be used as an estimate for modeling purposes. A linear regression through the four points on the graphs results in equation 1 where d = average snow density in g/cc.

$$\emptyset = 12.071 - 15.971 * d \tag{1}$$

From this equation an estimate of the shear angle can be obtained if the average snow pack density is known. Further work will be required to refine the relationship between density and the value of ca.

Looking at the data obtained, it became obvious that the strength parameters are highly dependent on the free water content within in the pack.

332
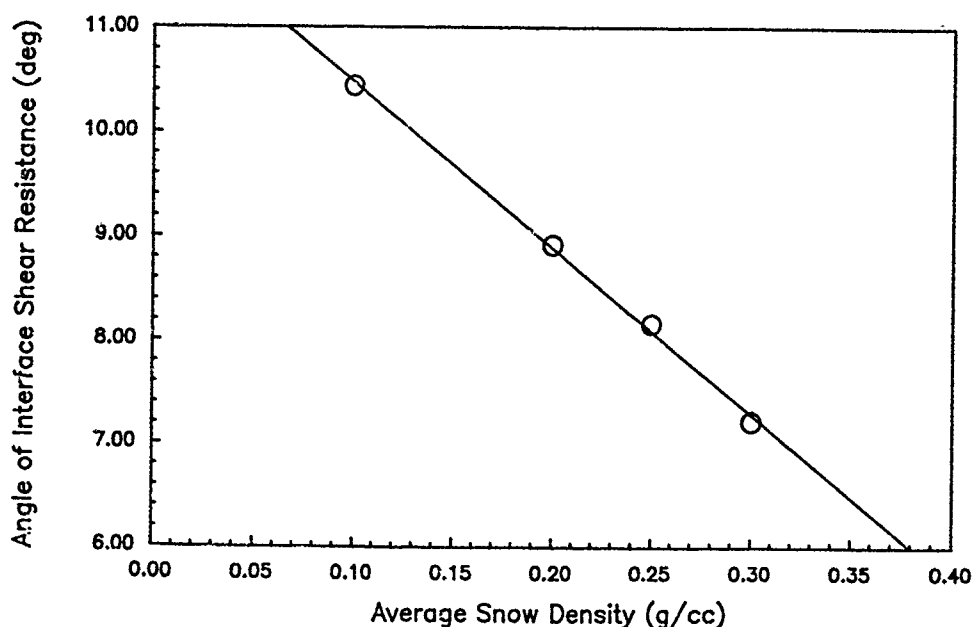
Figure 9 Angle/Density Relationship

Although no actual calorimeter measurements were taken along with the bevameter tests, the visual observations of wet and dry snows are as shown in Figure 10.
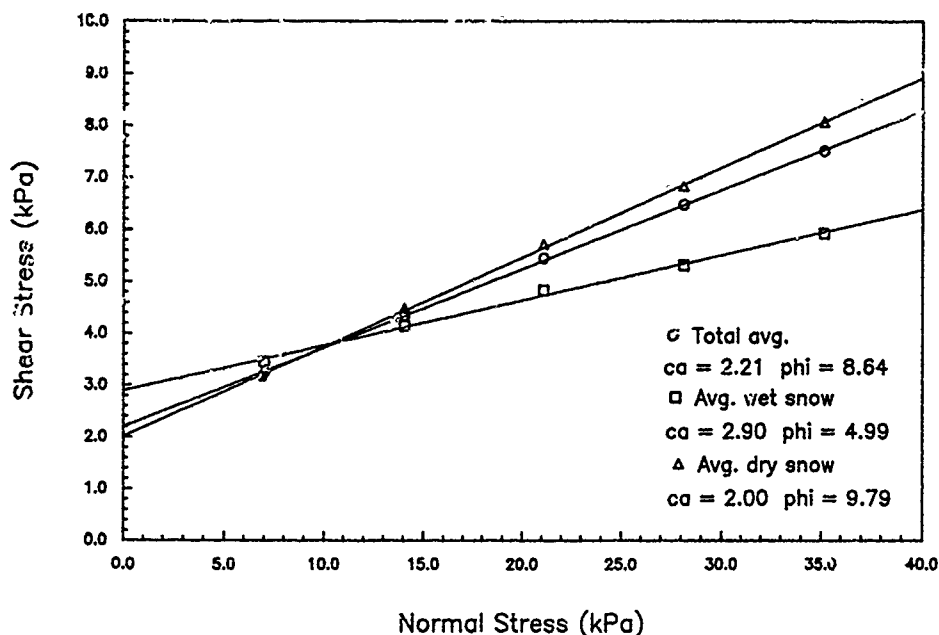
Figure 10 Effects of Free Water Content

It can be seen that $\emptyset$ decreases considerably for wet snow due to the decrease in friction afforded by the free water present. Conversely the cohesion is increased due to the increase in particle bonding set up by the water. The differences between wet and dry snows are apparent from this graph.

SUMMARY

Research in the development of a portable, easily operated snow strength measuring device is important to making the mobility models useful to troops in the field. Studies conducted with the bevameter at ISR has been useful in determining how future research will be conducted throughout the next year or more. This work will involve testing devices alongside the bevameter to insure that the results are comparable to the large system. The development of this system will enable any operator to measure the snow conditions on site as accurately and rapidly as possible.

Relationships between the basic properties of snow and the strength parameters used in mobility models do exist and can be developed further by use of the bevameter. Preliminary studies have resulted in simple relationships between average snow pack density and the shear strength parameters. Future work will involve reducing existing plate sinkage data to develop the correlation between the compressive strength parameters and density.

Free water content in the pack has a definite affect on the strength of the snow. To date, only visual observations of the free water present have been made. The results of these observations have resulted in relative differences between wet and dry snows. Future work in this area will include measurement of the free water content using an alcohol calorimeter.

REFERENCES

Alger, R.G., 1988, "Effect of Snow Characteristics on Shear Strength," Preliminary Project Report to USACRREL, Institute of Snow Research, Houghton, MI, May 1988.

Alger, R.G., and M.D. Osborne, 1987, "Snow Characterization Field Data Collection Results," Project Report to USACRREL, Institute of Snow Research, Houghton, MI, June 1987.

Bekker, M.G., 1969, Introduction to Terrain-Vehicle Systems, The University of Michigan Press, Ann Arbor MI.

Harrison, W.L., 1979, "Proceedings of the International Society for Terrain-Vehicle Systems Workshop on Snow Traction Mechanics," CRREL Special Report 81-16, USACRREL Hanover N.H.

Karafaith, L.L., and E.A. Nowatzki, 1978, Soil Mechanics for Off-Road Vehicle Engineering, TRANS TECH Publishing, Clausthal, Germany.

Wong, J.Y., 1983, Evaluation of Soil Strength Measurements, Publications Sales and Research Office, National Research Council of Canada, Ottawa, Ontario.

Yong, R.N., E.A. Fattah, N. Skiadas, 1984, Vehicle Traction Mechanics, Elsevier Science Publishing Company Inc., New York, N.Y.

A Microstructurally Based Constitutive Law for Snow

Robert L. Brown[I] and Puneet Muhajan[II]

ABSTRACT

The properties of snow are described in terms of the microstructure of the material. Restrictions imposed by the second law of thermodynamics and the principle of material frame in difference are used to describe the constitutive law in as general a way as possible. The constitutive theory is then completed by developing governing evolution equations which show how the microstructure changes during loading. The microstructure is described in terms of grain size, bond radius, neck length, coordination number, and intergranular slip distance. Sample calculations for simple stress states are provided.

INTRODUCTION

The mechanical properties of snow has been under investigation for some time. Since snow seasonally covers a large portion of the earth's land area, thereby affecting transportation, communications, and nation's productivity, this is not surprising. The earlier studies during the 1950's and 1960's were concerned primarily with properties such as elastic moduli, viscosity, strength, etc., and little in the way of rigorous constitutive modelling was accomplished. In particular not much was done on large deformation properties of snow.

Salm (1971) and Brown and Lang (1974) were among the first to characterize the properties of snow under large strain conditions. These studies and others that followed (Brown, 1976; Salm 1975) utilized a continuum approach and did not attempt to use a microstructural approach to describe the material properties in terms of microstructural properties. The first successful attempts at using a microstructural description are probably those of St. Lawrence et al. (1974) and Kry (1975).

While the continuum approach offers what is probably the easier way to describe the constitutive behavior of snow, interpretation of properties in terms of microstructural processes provides for a better understanding of the dominant deformation processes taking place. Ultimately it may lead to more exact modelling of constitutive behavior. At the same time, rigorously formulated continuum constituti. theories utilizing restrictions of the second law of thermodynamics and material frame indifference insure the resulting formulation is correct in many required ways.

I Professor, C/AE Dept., Montana State University, Bozeman, MT 59717
II Ph.D. Student, ME Department, Montana State University, Bozeman, MT 59717

What is attempted here is a formulation which is described in terms of microstructural processes and is based on a continuum mechanics formalism. The results which are discussed here are of a preliminary nature, as work is still in progress. What is demonstrated is that microstructurally based continuum formulations for snow do have potential for improving on current theories. This has, to a certain extent, already been demonstrated by the author (Brown, 1980, 1981; Hansen and Brown, 1988). The two earlier papers were concerned with volumetric deformation processes, while the latter study was of a more general nature.

In what follows the constitutive theory is presented. Basically the material is represented as an assembly of ice grains connected by necked regions. These necked regions are assumed to account for most of the deformation, since these are structurally the weak points in the material. The theory is presented as a three-dimensional theory, although only uniaxial stress states are considered as an example. The work presented here is of a preliminary nature and reports on current results. However, it does show how the properties of snow are determined by properties of ice and the geometry of the ice matrix. Snow is a very complicated material, and any constitutive theory utilizing microstructural processes will necessarily be quite complex. However, with computer capabilities now available and with the future computational speeds of new generation computers, it makes no sense to not develop more sophisticated formulations.

THERMOMECHANICAL BASIS

The behavior of a material must be consistent with restrictions imposed by the second law and the principle of material frame indifference. If ϕ is the Helmholtz free energy, η the entropy, θ the absolute temperature, T the second Piola-Kirchoff stress tensor, and E the Lagrangian strain tensor, the second law may be written as:

$$\rho_0 \dot{\phi} - \rho_0 \eta \dot{\theta} + tr(T \dot{E}) - (1/\theta)F^{-1}q \cdot \nabla\theta \leq 0 \qquad (1)$$

F is the deformation gradient and ρ_0 is the initial snow density. This law places restrictions on the directions in which processes can evolve. Later we will use it in the development of the constitutive law. The principle of material frame indifference is the statement that the properties of a material are intrinsic, i.e. the manner in which it responds to a process (loading or deformation) depends on the material itself (Billington and Tate, 1981). If Q is a rotation of coordinates from one coordinate system x to another x^*, i.e.

$$x^* = Qx \qquad (2)$$

then the constitutive law, if it has the representation

$$T = F(E), \qquad (3)$$

must transform as

$$T^* = F(E^*) = QF(E)Q^T \qquad (4)$$

where E^* is the strain defined relative to the x^* coordinate system. Eqs. 1

and 4 need to be satisfied by the constitutive law.

We begin our formulation by assuming ψ to be dependent upon the stress T, the temperature θ, and an internal state vector ξ. This state vector,

$$\xi = (\xi_1, \xi_2 \ldots \xi_n) \tag{5}$$

is a set of scalar valued variables which describe the internal state of the material. Later we chose these ξ_i to represent variables such as bond diameter, neck length, intergranular slip distance, etc. Now make a change of dependent variables by introducing the complimentary energy ψ, which has the value $T:E - \phi = \psi$.

Differentiating ψ respect to time,

$$\dot{\psi} = (\partial\psi/\partial T):\dot{T} + (\partial\psi/\partial\theta)\dot{\theta} + (\partial\psi/\partial\xi)\cdot\dot{\xi} \tag{6}$$

and substituting into the second law of thermodynamics allows us to arrive at the following results if the second law is to be satisfied:

$$E = \rho_0 \; \partial\psi/\partial T \tag{7}$$

$$\eta = -\rho_0 \; \partial\psi/\partial\theta \tag{8}$$

Using Equation (7), a differential change in the strain can be written as:

$$dE = \rho_0 \; (\partial^2\psi/\partial T\partial T):dT + \rho_0 \; (\partial^2\psi/\partial\xi\partial T)d\xi = d^e E + d^P E \tag{9}$$

$d^e E$ is the elastic change in the strain, while $d^P E$ is the plastic change in the strain. The compliance tensor M is defined to be

$$M = \rho_0(\partial^2\psi/\partial T\partial T) = M(\xi,\theta) \tag{10}$$

and is a fourth order tensor consisting of various elastic coefficients. The plastic change can be broken into two parts

$$d^P E = dM:T + dE^P \tag{11}$$

Where the first term represents a strain increment due to changes in the compliance tensor, and dE^P is the change in the plastic strain (permanent set). If the material compliance doe snot change significantly, then $d^P E$ and dE^P are equal. E^P is the strain which remains when the stress is released, i.e. E^P is just $E(0, \theta, \xi)$.

Now define the vector f to be the thermodynamic conjugate to the state vector ξ,

$$f = \rho_0 \; \partial\psi/\partial\xi \tag{12}$$

Then, one can show that (Hansen and Brown, 1988) the following Maxwell relation holds:

$$\partial f/\partial T = \partial E/\partial\xi \tag{13}$$

Substituting this into Eq. 9 and integrating gives, after some algebra

$$\rho_o \psi = 1/2 \; T: M:T + E^p:T + \rho_o \; \psi_o \tag{14}$$

where ψ_o is a stress independent term. The first term on the right hand side is the elastic strain energy and is the usual quadratic form for this type of strain energy. The form of E^p needs to be determined. This is best approached by finding a specific form for f. One can readily determine that

$$f = \rho_o \; \partial \psi_o / \partial \xi + 1/2 \; T:(dM/d\xi):T + T:dE^p/d\xi \tag{15}$$

ψ_o and E^p are both stress independent terms. Therefore the above equation shows that f has a quadratic dependence on T if M is a function of ξ, as it surely must be, and that f must also be linear in T as required by the last term. Given Eq. 12, ψ must have a similar dependence on T.

Using the above relations, and requiring ψ to be a scalar valued invariant function of T, an appropriate form for ψ is

$$\psi = \psi_o + (1/2)T:M:T + tr \; (H \; T) \tag{16}$$

where tr ( ) is the trace of the tensor inside the parentheses. H is a second order symmetric tensor which changes as the microstructure changes during inelastic deformation, i.e. it is a function of ξ and θ.

The strain, from Eq. 7 becomes

$$E = \rho_o \; M:T + H \tag{17}$$

and we see that H is closely related to the plastic strain.

The elastic strain energy part of ψ can be reduced to the following form

$$1/2 \; T:M:T = (1+v)/2E \; tr(T^2) - v/2E \; (trT)^2 \tag{18}$$

if the material is isotropic. v and E are Poisson's ratio and Young's modulus and are functions of ξ. Let C_1 and C_2 be the coefficients of $tr(T)^2$ and $(trT)^2$ expressed directly in terms of elastic properties.

$$C_1 = 1+v/2E, \; C_2 = - \; v/2E \tag{19}$$

They can be expanded as a Taylor series in ξ:

$$C_1 = C_{10} + \Sigma \; [C_{11i} \; (\xi_i - \xi_i) + C_{13i} \; (\xi_i - \xi_i)^3] \tag{20}$$

$$C_2 = C_{20} + \Sigma[C_{21i} \; (\xi_i - \xi_{io}) + C_{23i} \; (\xi_i - \xi_{io})^3] \tag{21}$$

where ξ_{io} are the initial values of each state variable. In the above an odd dependence on ξ_i was assumed. A similar form for H is assumed:

$$H_{ij} = H_{ijo} + \Sigma \; [H_{ij1k} \; (\xi_k - \xi_{ko}) + H_{ij3k} \; (\xi_k - \xi_{ko})^3] \tag{22}$$

338

The coefficients in the above equations can be determined from experiments, although many will be assumed to be negligible based on physical reasoning and symmetry arguments.

Finally, evolution equations which govern the rate of change of the state variables ξ must be found. These are of the form

$$\dot{\xi} = \dot{\xi}(T, \theta, \xi) \tag{23}$$

In order to determine these, the details of the microstructure of the material must be considered.

MICROSTRUCTURAL DESCRIPTION

The vector $\xi = (\xi_1, \xi_2m \ldots \xi_n)$ consists of a set of n scalar valued variables which describe the microstructure of the material. For the purpose of this study, these variables are assumed to be

1 = neck length vector
r = neck (bond) radius
λ = intergranular slip distance vector
n_3 = bonds/grain

These variables should be considered as mean values averaged over small volume elements. The material is represented as a collection of grains joined by necks of a definite length and radius. When two ice grains are brought into contact, a bond forms due to cohesion processes. This neck normally grows due to sintering effects and evolves into a necked region connecting the two grains. Consequently all snow that has been on the

(a) stress components and   (b) neck displacement
     unit vectors.   components
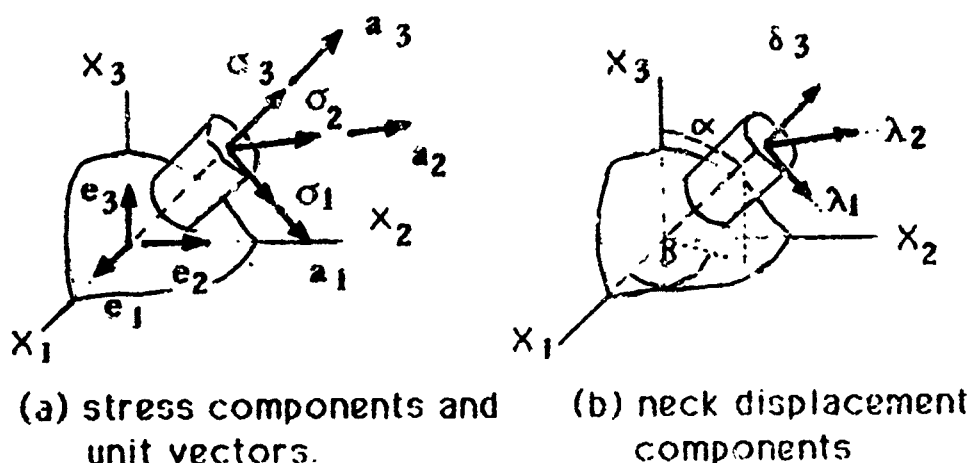
Figure 1. Schematic of typical ice grain and neck.

ground for a finite time has this type of structure. However, the ability to measure bond radius and neck length in snow is still a difficult task and has to date not been adequately solved, even with modern image analysis techniques. As the theory of quantitative stereology and the capabilities of image analysis systems continue to improve, these problems will be resolved.

The fundamental geometry of an ice grain and a neck as modelled in this paper is presented in Figure 1. We assume most of the deformation takes place in the necks which are considerably more flexible than the grains.

The ice grain has a radius R, while a typical neck is located at the spherical coordinates α, β and has a radius r and length l. Contrary to the impression given in the figure, the neck length is typically much smaller than the grain radius. The stresses acting on the neck have the local coordinate components σ_{13}, σ_{23}, and σ_{33}. Using an appropriate constitutive relation for ice (Szyszkowski and Glockner, 1987) the rate of deformation tensor d can be found for the necked region. The full details of this constitutive law for ice cannot be given here due to space limitations. A more general constitutive law (Brown, 1987) is currently under development, but the formulation of Szyszkowski and Glockner (1987) has been shown to represent the properties of ice for small and intermediate strains. The rate of deformation is given by the relation

$$d = d^e + d^p + d^r \tag{24}$$

where
$$d^e = (1/E_0)[(1+v)\dot{\sigma} - \mu tr(\dot{\sigma})1] \tag{25}$$

$$d^p = (1/v_2)[\sigma/(1-w)]^n[1 + \alpha(\epsilon^p/\epsilon_0^{-1})] \tag{26}$$

$$d^r = (1/v_1)((\sigma^{11})^n \tag{27}$$

d^e, d^p, d^r are respectively instantaneous elastic, plastic, and delayed recoverable (viscoelastic) parts of d. σ is the stress tensor in the neck, of which σ_{33}, σ_{13} and σ_{23} are the only nonzero components. E and v are elastic properties of ice, w is a crack damage factor, and σ^{11} are stress variables in the neck. Consult Szyszkowski and Glockner (1987) for a more detailed discussion. w is a crack damage factor which characterizes the internal damage resulting from microcracking.

d can then be used to determine the deformation of the neck, i.e. change in length, shearing deformations, and change in radius r. The motion of one end of the neck relative to other end is given by λ_1, λ_2, and δ, where λ_1, and λ_2 give the shearing motions and δ is the change in length of the neck. See Figure 1(a) for an illustration of these three quantities.

The rate of change of the neck length, $\dot{\delta}$, and the two intergranular slip rates, $\dot{\lambda}_1$ and $\dot{\lambda}_2$, are related to d in the following manner:

$$\dot{\delta} = ld_{33}$$

$$\dot{\lambda}_i = 2 d_{i3}l , i = 1,2 \tag{28}$$

In arriving at these relations, it was assumed that rotational effects

in the neck during deformation is negligible. Normally this is a good approximation if the strains in the neck are not large. It should be mentioned here that λ_1 and λ_2 represent the displacement of one end of a neck relative to the other end in a direction perpendicular to the neck axis. Here we consider displacements due to viscoplastic deformation. Slip due to neck fracture and glide are not considered here. Studies are currently underway to include this in the formulation.

These have the vector forms for their rates of change

$$\dot{\lambda} = \dot{\lambda}_1 \, a_1 + \dot{\lambda}_2 a_2 \tag{29}$$

$$\dot{\delta} = \dot{\delta} a_3$$

the vectors a_i are local orthogonal unit vectors illustrated in Figure 1. $\dot{\lambda}$ and $\dot{\delta}$ can be uniquely determined from the tensor d, the rate of deformation tensor for the neck.

At this point it is necessary to relate the neck stress σ to the globally applied stress T, which is the snow stress. Once this is done, the formulation is essentially complete. To this end, we define a probability function $P(\alpha, \beta, n_3)$ which gives the probability that the point on the surface of a grain lies on a point where a neck is attached to the grain. This function must be properly normalized, i.e.

$$\int_0^\Pi \int_0^{2\Pi} P(\alpha, \beta, n_3)\sin\beta d\alpha d\beta = n_3 \, \Pi(r/R)^2 \tag{30}$$

P is obviously linear in n_3. For the purposes of this study we will assume an isotropic distribution of necks around the grains, so that P becomes a constant with respect to α and β. However, it is worth noting that anistropy can readily be modeled by making P variable in α and β. Indeed, as deformations become large, P would normally acquire some anistropic properties. In the case where P is constant, it must have the value $n_3(r/2R)^2$. If T is the stress tensor applied to the snow, the stress vector $\sigma^{(n)}$ applied to the neck can be shown to be (Hansen and Brown, 1986):

$$\sigma^{(n)} = \sigma^i \, a_i = [a/p(\alpha,\beta, n_3)]n \, T \tag{31}$$

$$= A \, n \, T$$

n is the unit vector parallel to the direction of the neck axis.
A represents the augmentation factor which provides for the increase in the neck stresses over what stresses are distributed over the snow. a is the density ratio, ρ_i/ρ_s, of the ice density over the snow density. The vectors a_1, a_2, and a_3 shown in Figure 1 have the values

$$a_1 = \cos\alpha\sin\beta e_1 + \sin\alpha\cos\beta e_2 - \sin\alpha\beta e_3$$

$$a_2 = -\sin\alpha e_1 + \cos\alpha e_2 \tag{32}$$

$$a_3 = \cos\alpha\sin\beta e_1 + \sin\alpha\sin\beta e_2 + \cos\beta e_3$$

where the vectors e_i are the unit cartesion base vectors for the x_i coordinates.

Under a three dimensional state of stress, T, applied to the snow, the strain rate E for the snow can be calculated using the above equations. First $\sigma^{(n)}$ on a neck situated at the position (α, β) can be calculated by using Eq. 31. From this, the rate of deformation tensor d for the neck can be found using the constitutive equation for ice, Eqs. 24-25. Then the rate of change of the microstructural variables λ and 1 $(1 - \delta)$ can be found with Eqs. 28-29. This gives the rates λ and δ in the global cartesian coordinate system, x_i, and then integrating over the grain surface results with averaged values of the projections of λ and 1 in the global coordinate directions. Integration over an octant $0 \leq \alpha \leq \Pi/2$, $0 \leq \beta \leq \Pi/2$ can be done if one assumes sufficient symmetry of the probability function $P(\alpha, b)$. These averaged values, δ and λ are

$$\delta = 8((2R/r)^2/n_3) \int_0^{\Pi/2} \int_0^{\Pi/2} P(\alpha,\beta)\delta(\alpha,\beta)\sin\beta d\alpha d\beta \qquad (33)$$

$$\lambda = ((2R/r)^2/n_3) \int_0^{\Pi/2} \int_0^{\Pi/2} P(\alpha,\beta) \lambda(\alpha,\beta)\sin\beta d\alpha d\beta \qquad (34)$$

where λ and δ are transformed to the global coordinate components. Once this is done the evolution equations, Eqs. 25, are essentially determined. With these determined, the rates of change of the compliance tensor (here characterized by C_1 and C_2) and the tensor H can be determined from Eqs. 19-21, and then Eq. 9 can be used to calculate the strain rate E,

The above full program has not yet been completed, but results have been obtained for simple uniaxial states of stress. These are illustrated in the following section.

EVALUATION FOR UNIAXIAL STRESS STATES

We consider here the strain response to a uniaxially applied load. We consider medium density snow ($\rho_0 = 355$ kg/m^3). For this snow, surface section analysis has determined the following initial microstructural variables

```
R = 0.484  mm
r = 0.23   mm
1 = 0.19   mm
n3 = 2.53
a = 2.58
```

These values have been taken from a study (Hansen and Brown, 1986) utilizing an image analysis system to evaluate the initial microstructural geometry of the necks. The material coefficients for the constitutive equation for the ice (Eqs. 24-27) are provided by Szyszkowski and Glockner (1986) and will not be repeated here. Applying the previous equations to the case of a uniaxial stress state

$$dE_{11} = 2\rho_o(C_1 + C_2)dT_{11} + 2\rho_o(\partial C_1/\partial \xi + \partial C_2/\partial \xi)d\xi + dH_{11} \qquad (35)$$

provides for an increment in the axial strain during a time increment when the stress T_{11} is varied or the microstructural variables ξ_i are varied.

For the case of uniaxial loading, we can simplify the above formulation somewhat by calculating the total intergranular slip λ rather than the two components λ_1, λ_2 in the α and β directions indicated in Figure 1. Likewise, rather than dealing with the three vector components of the neck length vector 1, we can deal strictly with the scalar value, 1, of the neck length. Under more general loading conditions where deformations in all their coordinates are of concern, this is not a valid simplification. The terms $\partial C_1/\partial \xi$ and $\partial C_2/\partial \xi$ then acquire the forms

$$\partial C_1/\partial \lambda = C_{11\lambda}3C_{13\lambda}(\lambda-\lambda_o)^2, \quad \partial C_1/\partial l = C_{111} + 3C_{131}(1 - l_o)^2 \qquad (36)$$

$$\partial C_2/\partial \lambda = C_{21\lambda} + 3C_{23\lambda}(\lambda-\lambda_o)^2, \quad \partial C_2/\delta l = C_{311} + 3C_{331}(1-l_o)^2 \qquad (37)$$

$$\partial H_{11}/\partial \lambda = H_{11\lambda} + 3H_{13\lambda}(\lambda - \lambda_o)^2 \qquad (38)$$

$$\partial H_{11}/\partial l = H_{11} + 3H_{131}(1 - l_o)^2 \qquad (39)$$

Utilizing experimentally determined values of the coefficients in the above equations, the rates of change of H_{11}, C_{11}, and C_2 can be obtained as the microstructure changes, since H_{11}, C_1, and C_2 can be determined directly in terms of Eqs. 36-39 and the rates of change of λ and 1. λ and 1 can be found from Eq. 28. This then is all applied to Eq. 35 and integrated numerically with respect to time.
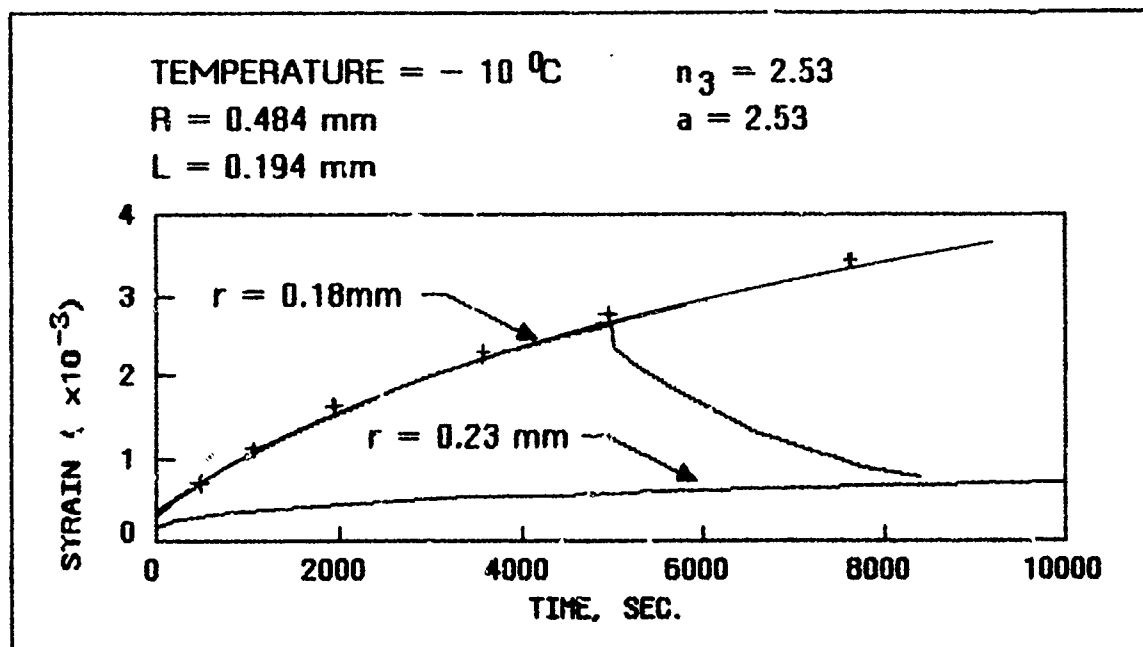
Figure 2. Typical creep/recovery curves for snow loaded in tension.

Figure 2 illustrates creep curves for medium density snow subjected to a tensile stress of 0.01 MPa for a prescribed period of time and then unloaded. As can be seen the material exhibits all of the usual characteristics of snow. Also contained in that figure is the creep curve for an actual experiment carried out on medium density snow. Unfortunately the data was collected in 1974, and the relevant microstructural variables were not recorded. Consequently it is not known if this data is relevant to the case used here.

DISCUSSIONS AND CONCLUSIONS

The properties of snow are determined in part by the properties of the matrix material ice. Consequently accurate modelling of the ice properties is needed. However, the snow properties are also strongly influenced by the geometry of the material microstructure. Correctly modelling this is the more difficult of the two processes. Work is currently in progress to obtain a more complete representation of the deformation processes in terms of what happens at the granular level.

This type of constitutive equation, while quite involved, can be used to more accurately analyze problems involving large multiaxial deformations of snow. Such examples include vehicle mobility over snow covered terrain, building footing settlement into snow cover, and impact problems. With ever improving computational capability, the use of microstructurally based stress strain equations is now becoming a reality.

ACKNOWLEDGEMENTS

REFERENCES

Billington, E.W. and Tate, A., 1981, The Physics of Deformation and Flow, McGraw Hill, New York.

Brown, R.L. and Lang, T.E., On the Fracture characteristics of snow, Proceedings of the International Conference on Snow Mechanics, Grindewald, Switzerland, 1974.

Brown, R.L., A Thermodynamic Theory for Simple Materials Representable by Multiple Integral Expansions, International Journal of Engineering Science, Vol. 14, No. 11, 1976.

Brown, R.L., A Volumetric Constitutive Law for Low Density Snow, Journal of Applied Physics, Vol. 51, No. 1, Jan. 1980.

Brown, R.L., A Volumetric Constitutive Equation for Snow, Journal of Glaciology, Vol. 26, No. 24, 1980.

Brown, R.L., A Constitutive Equation for Sea Ice Based on Microstructure and Irreversible Thermodynamics. 6th OMAE Conference Proceedings, Houston, TX 1986.

Hansen, A.C. and Brown, R.L., A New Constitutive Theory for Snow Based on a Microstructural Approach, Mechanics of Materials. (in press), 1988.

Kry, P.R., The Relationship Between the Visco-elastic and Structural Properties of Fine-grained snow, Journal of Glaciology, Vol. 14, No. 72, 1975.

St. Lawrence, W.F. and Bradley, C.C., The Deformation of Snow in Terms of a Structural Mechanism. Proceedings of the International Symposium on Snow Mechanics, Grindewald, Switzerland, 1974.

Salm, B., On the Rheological Behavior of Snow Under High Stresses, Contributions of Institute of Low Temperature Science, Hokkaido University, Series A, Vol. 23, 1971.

Salm, B. A Constitutive Equation for Creeping Snow, IAHS Publication 114, 1975.

Szyszkowski, W., and Glockner, P.G., Modelling the Mechanical Properties of Ice, Proceedings of the 6th OMAE Conference, Houston, TX, 1987.

Viscosity of Slush

S. Kobayashi[I] and K. Izumi[II]

ABSTRACT

Measurements of the viscosity of slush (fluid water-snow mixture) were carried out by two methods: use of a cylindrical viscometer and measurement of flow along an inclined flat surface. From the former method the values of viscosity were determined for shear rates up to 1.0 s^{-1}. The viscosity of slush under high values of shear rate (e.g., from 25 to 75 s^{-1}), was determined using the latter method. Slush showed a nonlinear relationship between viscosity and the shear rate.

INTRODUCTION

It is most important to know the values of viscosity in snow/water mixture flows. The hydraulic conveying of snow by pump-pipeline or channel system has been used recently in Japan. Many forms of slush exist in nature such as slush avalanches and frazil ice in rivers and seas. A full-depth avalanche occurs when sufficient meltwater reaches the ground and produces a slush layer near the snow-ground interface (Horton, 1938; McClung, 1987; McClung and Clark, 1987).

Measurements of the viscosity of slush (snow/water mixture) were carried out by two methods in a 0°C cold room: a) use of cylindrical viscometer; and b) measurement of flow along an inclined flat surface. The former method was applied to measure the viscosity under a low shear rate between 0.5 and 1.0 s^{-1}. With the latter method the values of viscosity were determined under high shear rates between 25 and 75 s^{-1}.

The results obtained from the two methods showed that the viscosity of slush decreased with increasing shear rate. A fluid with this type of behavior is known as a "non-Newtonian."

METHODS

Cylindrical Viscometer

A cylindrical viscometer was used to determine fluid viscosities from measurements of torque and angular velocities (Fig. 1A). Of the numerous

---

(A)

(B)
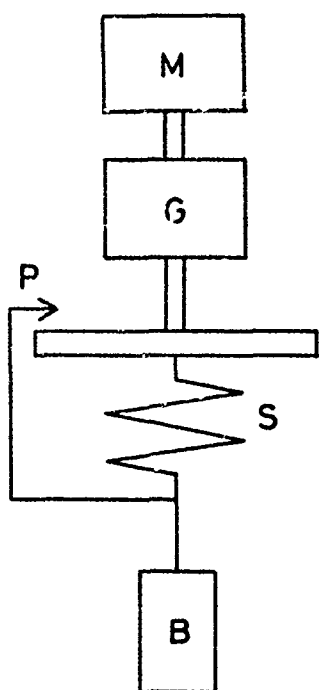
Figure 1(A). Diagram of
cylindrical viscometer.
M: synchronized motor;
G: speed exchanger;
S: Spring; P: spring
indicator; B: rotor.
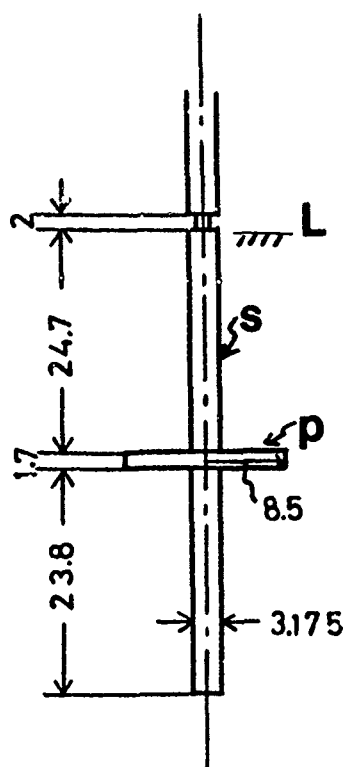
Figure 1(B). Dimensions
of rotor (in mm).
P: plate; S: spindle;
L: slush surface.

types of rotor, the rotor shown in Figure 1B was used in the present study.
The rotor was immersed in slush up to line L.

The shear stress was obtained from the torque measurements. The torque T
is

$$T = A \cdot r \cdot S ,\tag{1}$$

where A is the surface area of the immersed rotor, r is the radius of rotor
and S is shear stress.

The torque may also be expressed approximately as

$$T = k \cdot \theta ,\tag{2}$$

where k is a spring constant and θ the torsion angle of the spring. From
equations 1 and 2 the shear stress is

$$S = \frac{k \cdot \theta}{A \cdot r} = K_1 \cdot \theta .\tag{3}$$

347

where K_1 is the shear stress constant:

$$K_1 = \frac{k}{2\pi R^2 h + 2\pi R_0^2 h_0 + \frac{4}{3}\pi R^2} .$$ (4)

In equation 4, R is the radius and h the thickness of the plate (Fig. 1B), and R_0 and h_0 are radius and length of the spindle, respectively. $K_1 = 0.298$ with the dimensions of Figure 1B.

The shear rate D is given by

$$D = - r \frac{d\omega}{dr} ,$$ (5)

where ω is the angular velocity of the rotor. According to the Couette equation (Bird et al., 1960), Eq. 5 is written as

$$D = \frac{2 \cdot \omega \cdot \kappa^2 \cdot R'^4}{(1-\kappa^2) \cdot \kappa^2 \cdot R'^4} - \frac{2\omega}{(1-\kappa^2)}$$ (6)

in which $r = \kappa R'$, where R' is the radius of the outer cylinder and κ is a magnification of less than unity. Alternatively, the angular velocity is

$$\omega = \frac{2\pi \cdot N}{60} ,$$ (7)

where N is the number of revolutions of the rotor (rpm).

Equations 6 and 7 give

$$D = K_2 \cdot N$$ (8)

with

$$K_2 = \frac{0.2094}{(1-\kappa^2)} .$$ (9)

K_2 is the shear rate constant determined experimentally for a standard liquid of known viscosity. $K_2 = 0.244$ for the case under study. According to Newton's law of viscosity,

$$\mu = \frac{S}{D} = \frac{K_1}{K_2} \cdot \frac{\theta}{N} ,$$ (10)

where μ is the viscosity.

In our experiments the slush was made by varying the amount of snow from 10 to 100 g in 0°C water, with the total volume of the slush maintained at 500 mL. The measurements of viscosity using this method succeeded with up to 1.0 s^{-1} of shear rate. At a higher shear rate a slip occurred at the boundary between the rotor and the slush. For this reason we used a different method for high shear rates.

Figure 2 is an example of the relation between the torsion angle of spring and added amount of snow.
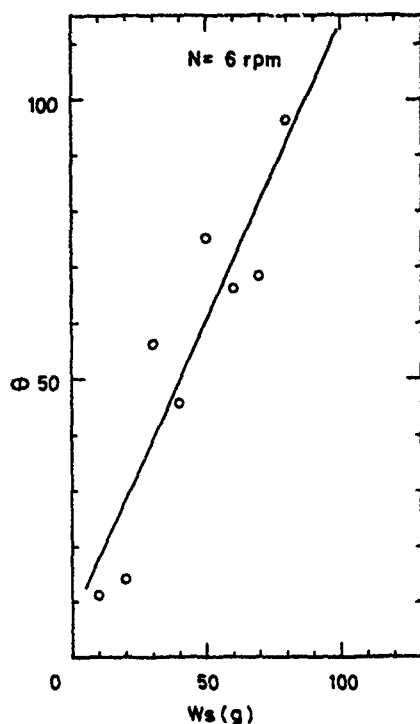
Figure 2. Torsion angle of spring θ (°) as a function of added amount of snow W_s (g) under a speed of the rotor N=6 rpm.

(A)
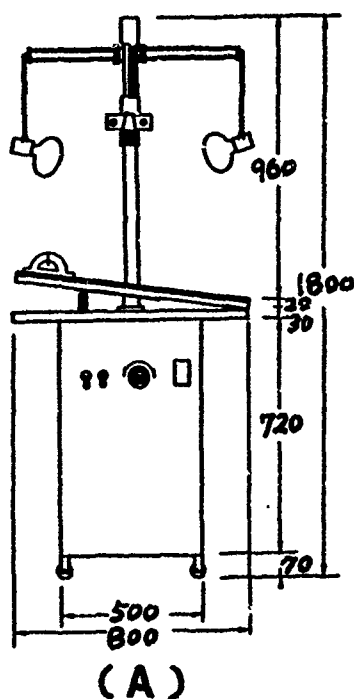
Figure 3(A). Table with variable inclination (Suzuki and Fujita, 1983).

(B)
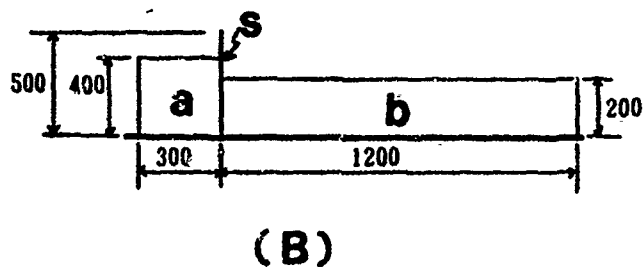
Figure 3(B). Open transparent channel (mm). a: slush reservoir; b: slush run-off section; s: shutter.

Flow of Moving Slush

We used the flow of slush along an inclined flat surface for measurements of the viscosity of slush under high shear rates. Figure 3A shows the measurement table that can be inclined (Suzuki and Fujita, 1983), and 3B an open channel (width 150 mm) that can be placed on the table. The channel, made of transparent material, consists of two parts divided by a shutter (S): (a) a slush reservoir, and (b) a runoff section.
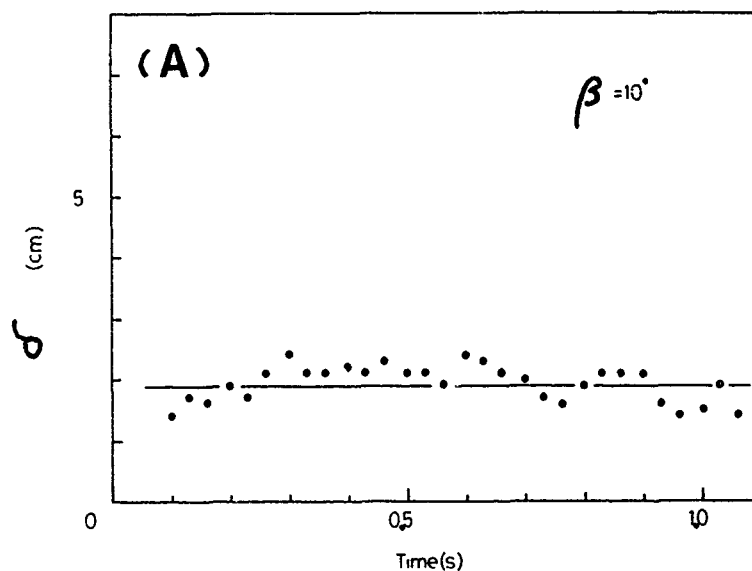
Figure 4(A). Time variation of thickness (δ).
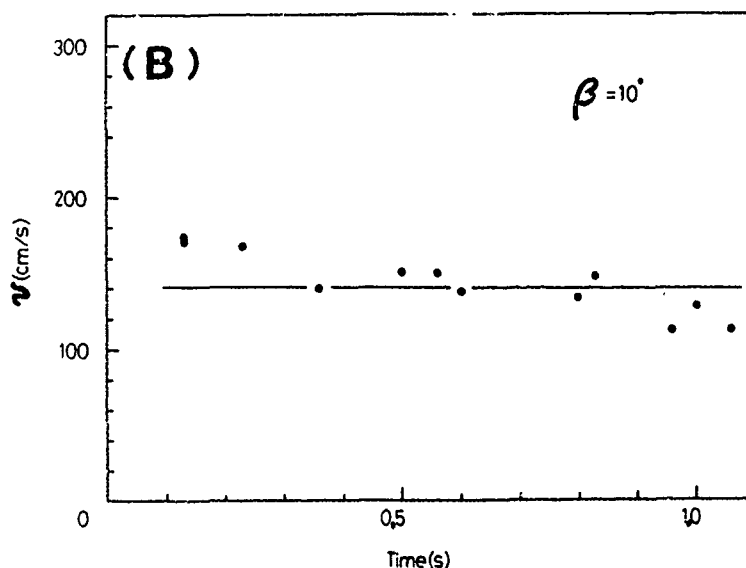
Figure 4(B). Velocity (v) of moving slush in the case of an inclination angle of 10°.

From a consideration of shell momentum balance (Bird et al., 1960), the maximum velocity assumed to be the velocity at the slush flow surface is:

$$v(max) = \frac{\rho \cdot g \cdot \delta^2 \cdot \cos\beta}{2\mu} \quad , \tag{11}$$

where ρ: density of slush, g: gravitational acceleration, δ: thickness of the slush, and β: angle of inclination.

We have measured the maximum velocity and the thickness of slush flow under three inclinations: $\beta = 3$, 5, and 10 degrees. The slush was made by mixing 5 kg of water and 1 kg of snow. To measure the thickness and surface velocity of the slush, we used a video camera and read the pictures every 1/30 second. Figure 4A shows the thickenss and Figure 4B the surface velocity of slush flow of an experiment under the inclination of 10 degrees.

Two important results were obtained from our experiments: a) the viscosity of slush decreases with increasing ratio of weight of water/snow, and b) the fluid behavior is "non-Newtonian." Figure 5 shows the relation between the viscosity and the weight ratio of water/snow for two different shear rates obtained with the viscometer experiments. The viscosity of slush under a high shear rate has lower values than that under a low shear rate. The decrease of viscosity was smaller under a high shear rate than under a low shear rate. The viscosity as a function of shear rate is shown in Figure 6. The viscosity decreased rapidly with increasing the shear rate. The viscosity might be observed to reach that of water for 0°C (1.787 cp) if an experimental setup for very high shear rates were possible.
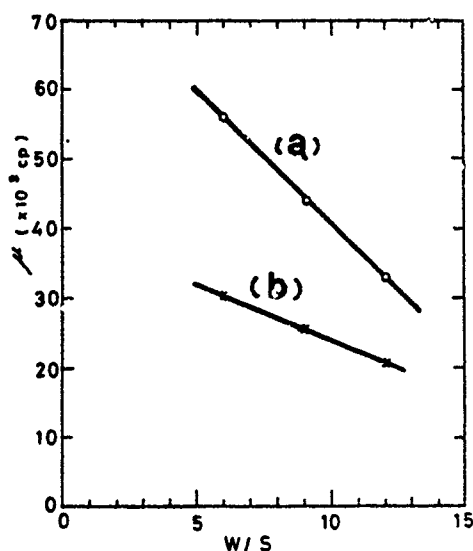
Figure 5. Relation between the viscosity (μ) and the weight ratio of water/snow (W/S). Line (a): shear rate 0.36 s^{-1}. Line (b): shear rate 0.73 s^{-1}.
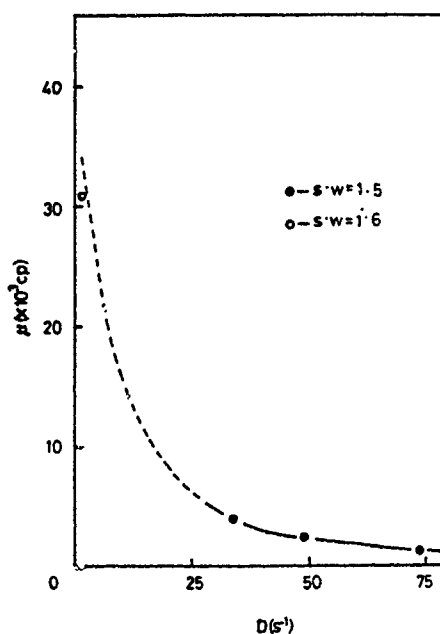
Figure 6. Viscosity of slush μ as a function of shear rate D. o: viscometer experiment. •: falling slush flow experiment.

DISCUSSION AND CONCLUSION

According to Newton's law of viscosity, the curve of shear stress versus shear rate for a given fluid should be a straight line through the origin, and the slope of this line would be the viscosity of the fluid at the given temperature and pressure. A mixture of water and snow has a constant temperature of 0°C under atmospheric pressure. Fluids with this behavior are known as Newtonian fluids. Materials that cannot be described by the conditions above are referred to as non-Newtonian fluids.

Our experiments have shown that slush behaves as a non-Newtonian fluid. The behavior is termed pseudoplastic when the viscosity decreases with increasing shear rate, such as with solutions of carboxymethylcellulose, paper pulp, and cement rock in water. For pseudoplastic fluids, a power law applies (Bird et al., 1960):

$$S = \mu \cdot D^n \quad , \tag{12}$$

where n is a non-Newtonian index of viscosity $1 > n > 0$. Assuming an apparent viscosity, η_a, substitution of Eq. 10 into Eq. 8, then gives

$$\eta_a = \frac{S}{D} = \frac{\mu \cdot D^n}{D} = \mu \, D^{n-1} \quad . \tag{13}$$

Therefore, if $n < 1$, the $n - 1 < 0$, and η_a decreases with increasing D. Accordingly, the values of viscosity obtained here should be regarded as the apparent values.

Dent and Lang (1983) have used a biviscous modified Bingham model to simulate the mechanics of flowing snow. Well-known materials of the Bingham type include paints, greases, concrete, and toothpaste. The model takes the form of a two-viscosity system in which a large viscosity is employed in the low stress regions of the flow and a smaller viscosity is used in the high stress regions. This model agrees with our conclusions.

ACKNOWLEDGEMENTS

REFERENCES

Bird, R.B., W.E. Stewart and E.N. Lighfood, 1960, Transport Phenomenon. John Wiley & Sons, Inc., New York, London, Sydney.

Dent, J.D. and T.E. Lang, 1983, "A Biviscous Modified Bingham Model of Snow Avalanche Motion," Annals of Glaciology, Vol. 4, 42-46.

Horton, R.E., 1938, "Phenomena of the Contact Zone between Ground Surface and a Layer of Melting Snow," Int. Union Geod. Geophys., [Edinburgh - Rep. and Tech. Notes of the Commission of Snow and Ice], Int. Assoc. Sci. Hydrol. Publ. 23, 545-561.

McClung, D.M., 1987, "Mechanics of Snow Slab Failure from a Geotechnical Perspective," IAHS Publication No. 162, 475-508.

McClung, D.M. and G.K.C. Clarke, 1987, "The Effect of Free Water on Snow Gliding," Journal of Geophysical Research, Vol. 92 (B7), 6301-6309, June 1987.

Suzuki, K. and Y. Fujita, 1983, "Experimental Apparatus of the Landslide," Annual Report of Research Institute for Hazards in Snowy Areas, Niigata University, No. 5, 127-132, December 1983.

Thermal Performance of Cooling Air Jacket Walls for Underground Cold Storage[1]

Chen Qigao and Lu Shii[11]

ABSTRACT

This paper discusses the thermal performance of the cooling air jacket wall for an underground cold storage facility. It addresses the problems of developing underground cold storage facilities in the world, especially in China where about 200 underground cold storage facilities have been constructed within the tropical and the temporate zones where the annual mean underground temperature is always positive. The refrigerated rock walls for underground cold storage are damaged by the cycles of freezing and thawing, which can be prevented by installing thermal insulation on the surrounding rock walls. The cooling supplied to the space of the underground cold storage facilities can make the relative humidity of the air considerably lower, which is the reason for weight loss for wet goods in stores, such as meat, vegetables, fruit and so on. The cooling air jacket wall layer inside the insulation layer can solve the abovementioned problem. This paper describes the thermal performance of the cooling air jacket walls that can improve the storage conditions and also save energy and money.

INTRODUCTION

In the last 20 years, underground cold storage facilities have been constructed everywhere in the world. In places where the annual mean underground temperature is negative, the walls of an underground cold storage facility can be bare without any insulation. But in other places, such as in the center and south of China, within the tropical and temperate zones where the mean annual underground temperature is always positive, the refrigerated rock walls of an underground cold storage facility may be damaged by repeated freezing and thawing, which is enhanced by the moisture phase change and moisture transfer.

The process of underground cold storage development in China can be roughly divided into three periods, i.e., the beginning, the developing and the developed.

In the beginning period, there was no experience. The plan of an underground cold storage facility was designed as several short parallel or radiant storage tunnels to be connected by a pass tunnel. As shown in Figure 1, which is the original typical plan of underground cold storage facilities, these were not well designed for energy conservation in operation.
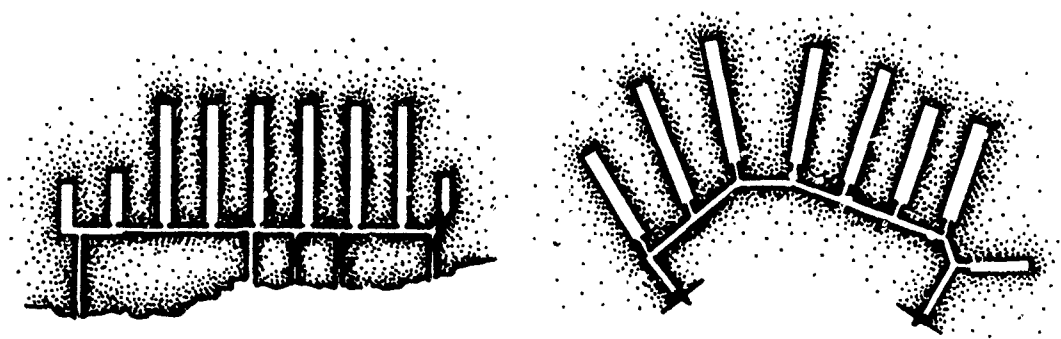
Figure 1. The typical original plan.
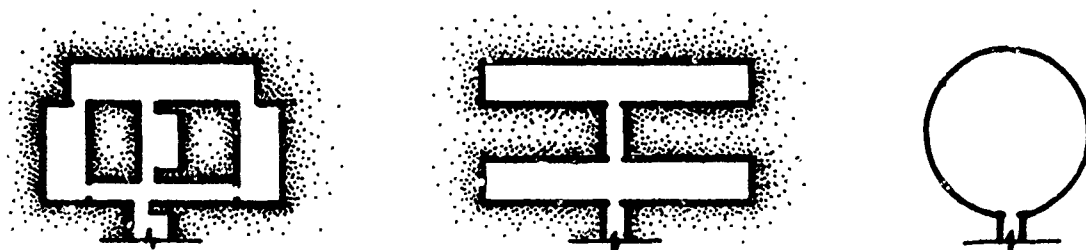
Figure 2. The typical plan during the developing period.

In the developing period, the "five words" of design experience for underground cold storage were summed up; that is to say, for the thermal performance of an underground cold storage facility to be optimal, it must be larger (dimension), deeper (buried), grouped (centralized), uniform (temperature), and higher (air humidity). These five words guided the design of the underground cold storage facilities during this developing period. The typical plan during this time is shown in Figure 2. The thermal performance of these is much better than those with the original plan. In these, energy loss in operation and the weight loss from the wet goods in store are both decreased.

In the developed period, insulation has been installed on the surrounding walls. Many crevices had appeared in surrounding rock, because of damage from repeated freeze and thaw. As shown in Figure 3, the insulation has made
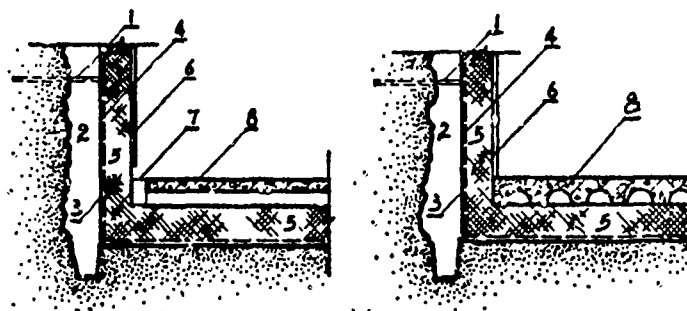
Figure 3. The insulation on the walls.
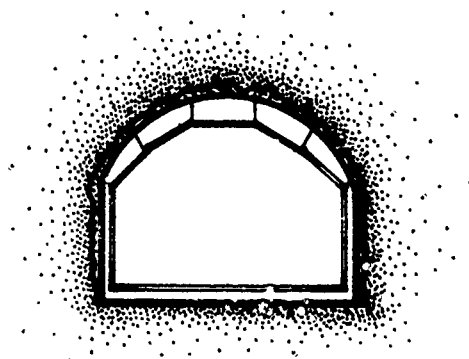
Figure 4. A cooling air jacket wall.

the rock wall temperature positive everywhere. And all the volume of a small underground cold storage with a capacity of about one thousand tons can be centralized into a larger cavern. If the engineering geological condition is appropriate, the volume can be even larger; this can lessen the amount of insulation surface and the heat transfer area.

The underground cold storage rooms are much drier after insulation is installed. Moisture coming from the surrounding rock is greatly decreased and the condensation on the lower temperature pipes comes only from the goods in store. So the weight loss from the wet goods is very great, and the thermal performance is worsened. This problem can be solved by the adoption of cooling air jacket walls. An example of the cooling air jacket wall is shown in Figure 4.

This paper describes the behavior of the cooling air jacket walls, which can improve the thermal performance of the storage and humidity conditions. It can be seen that the improvement of the thermal performance by the cooling air jacket walls will bring savings of energy and money.

DRYING FACTORS IN COLD STORAGE

The drying factors in underground or aboveground cold storage facilities are as follows: the air humidity ϕ_r, the absolute vapor pressure e_p, the temperature difference $(t_s - t_r)$ of the surrounding surface temperature t_s minus the air temperature t_r; and the temperature difference $(t_r - t_p)$ of the air temperature t_r minus the pipe temperature t_p. The drying process in a cold storage room is discussed as follows:

Drying by Thermal Radiation

As the surrounding surface temperature t_s is higher than the air temperature t_r, the quanta of infrared rays from the surface can be caught by sub-microparticles of moisture on the wet goods in store, which cause the wet goods in store to dry. And as these microparticles are vaporized in the space near the goods, the air temperature will be lowered, which can intensify drying of the goods.

356

The Guhmann number, Gu, can be used to describe the space vaporization phenomenon, as

$$Gu = (T_r - T_m)/T_r \tag{1}$$

where T_r and T_m are, respectively, the absolute dry bulb and wet bulb temperatures.

The Guhmann number Gu' with the surface radiation is

$$Gu' = (T_s/T_r)(T_r - /T_m)/T_r \tag{2}$$

where T_r, T_s and T_m are the absolute air temperature, the absolute surface temperature and the absolute wet bulb temperature, respectively.

The specific moisture flow caused by the vaporization due to the Guhmann's phenomenon is

$$m_{Gu} = \alpha(T_r/L)Gu' \tag{3}$$

or

$$m_{Gu} = (\alpha/L)(T_s/T_r)(T_r - T_M) \tag{4}$$

where α is the heat transfer coefficient and L is the latent heat of vaporization.

It can be seen that the vaporization moisture due to the Guhmann phenomenon can be diminished under the condition of the dried bulb temperature t_r and the wet bulb temperature t_m being equal to each other, which is to say that the air in the store space is saturated; i.e., it has a relative humidity of 100%.

Drying by Moisture Transfer

The specific moisture flow q_m by convection coming from the wet goods in store is

$$q_m = \alpha_m(e_s - e_r)/P \tag{5}$$

where e_s is the vapor pressure on the surface of wet goods in store, e_r is the vapor pressure in air, E_r is the saturated vapor pressure under the air temperature, P is the atmospheric pressure and $e_r = \phi_r E_r$. So, the last expression can be written as

$$q_m = \alpha_m(e_m - \phi_r E_r)/P. \tag{6}$$

The condition $q_m = 0$ is for the store goods without weight loss. This condition holds if

$$e_m - \phi_r E_r = 0 \tag{7}$$

or

$$\phi_r \sim (e_m / E_r) .\qquad(8)$$

Since the goods in store are kept fresh the vapor pressure on the surface of
the goods can be taken as the saturated vapor under the air temperature.
Thus, $\phi_r = 100\%$, which is the same result as the condition for drying by
thermal radiation.

Therefore, we can say that, as the air humidity is 100% in the storage
space, there is no Guhmann drying weight loss and there is no moisture con-
vection weight loss.

Drying By Freezing Pipes

Cooling is supplied by the parallel pipes of the air cooling machinery.
All parallel pipes are set by the walls or below the arch. The former are
called wall pipes, and the latter are called top pipes. All parallel pipes
of air cooling machinery are placed together in a box.

The pipes are placed where the temperature is the lowest in the store
volume. So, all moisture coming from the wet goods or other sources must
freeze on the pipe surface.

The specific moisture flow of frozen on the pipes is

$$q_{mp} = \alpha_{mp} (e_r - e_p)/P\qquad(9)$$

where α_{mp} is the moisture transfer coefficient on pipes by natural convection
for the pipes and forced convection for air cooling machinery, and e_p is the
absolute humidity on the pipe surface. The expression

$$e_p = E_p\qquad(10)$$

can hold for the freezing frost surface; P is the atmospheric pressure.

It can be seen that frost on the pipes with the lowest temperature is
considerable, which is in proportion to the vapor pressure difference (e_r-
e_p). Therefore, the method for decreasing the frost on the pipes makes the
difference (e_r-e_p) as small as possible.

As mentioned above, the reason for the weight loss for wet goods in
store within an underground cold storage facility is due to the temperature
nonuniformly in the store space. The moisture from the place with higher
temperature transfers into and freezes on the place with lower temperature.
Thus, diminishing the weight loss can be accomplished by making the tempera-
ture uniform in the space within the underground cold storage.

THE THERMAL PERFORMANCE ON HEAT TRANSFER

The Heat Balance in Underground Storage

The heat from the surrounding envelopes transfers into the space of the
underground cold storage facility and then is absorbed by the cooling pipes.

This abovementioned process can be expressed as

$$\alpha_{qs}F_s(t_s-t_r) = \alpha_{qp}F_p(t_r-t_p) \tag{11}$$

where α_{qs} and q_{qp}, F_s and F_p, t_s and t_p are the heat transfer coefficient, the area, and the temperature for the surfaces of envelopes and pipes, respectively.

From the last expression to solve for t_r, we have

$$t_r = (\alpha_{qs}F_s t_s + \alpha_{qp}F_p t_p)/(\alpha_{qs}F_s + \sigma_{qp}F_p) \tag{12}$$

where t_r is the weighted mean of t_s and t_p. So, in general, the inequality

$$t_p < t_r < t_s . \tag{13}$$

The Thermal Performance Criterion

The last equation for t_r can be written as

$$t_r = (t_p + Gi_q t_s)/(1 + Gi_q) \tag{14}$$

and

$$Gi_q = \alpha_{qs}F_s/\alpha_{qp}F_p \tag{15}$$

where Gi_q is called the thermal performance criterion.

It can be seen that the smaller is Gi_q, the better is the condition improvement. As t_r approaches t_p, the weight loss from the wet goods in store changes to zero. And the last equation can be written as

$$t_r-t_p = Gi_q(t_s-t_p)/(1 + Gi_q) \tag{16}$$

where the temperature difference $(t_r - t_p)$ is a function of the temperature difference $(t_s - t_p)$.

THERMAL PERFORMANCE DURING MOISTURE TRANSFER

The Moisture Balance Equation

The moisture transfers from the surrounding surfaces and the surfaces of the wet goods in store and to the surfaces of the pipes and freezes into frost. The balance equation is

$$q_{ms}F_s + q_{mg}F_g = q_{mp}F_p \tag{17}$$

and

$$q_{ms} = \alpha_{ms}(e_s-e_r)/P \tag{18}$$

$$q_{mg} = \alpha_{mg}(e_g-e_r)/P \tag{19}$$

359

$$q_{mp} = \alpha_{mp}(e_r - e_p)/P \tag{20}$$

where α_{ms}, α_{mg} and α_{mp} are the moisture transfer coefficients for the surrounding surface, the goods' surface and the pipes' surface, respectively; q_{ms}, q_{mg} and q_{mp} are their specific flows, respectively; F_s, F_g and F_p are their areas, respectively; e_s, e_g and e_p are the vapor pressures on them, respectively, and e_r is the vapor pressure in the stored space.

When the weight loss of the goods in store remains at zero, i.e.,

$$q_{mg} = 0 \qquad \text{or} \qquad e_q - e_r = 0 \tag{21}$$

we can get the moisture balance equation as

$$F_s \alpha_{ms}(e_s - e_r)/P = F_p \alpha_{mp}(e_r - e_p)/P \tag{22}$$

From the last equation we can get the following expressions:

$$e_r - e_p = (e_s - F_p)Gi_m/(1 + Gi_m) \tag{23}$$

$$e_r - e_p = Gi_m(e_s - e_r) \tag{24}$$

$$Gi_m = \alpha_{ms}F_s/\alpha_{mp}F_p \tag{25}$$

where Gi_m is similar to Gi_q, which is also called the moisture performance criterion. But it is still called thermal performance criterion because

$$Gi_q = Gi_m \tag{26}$$

which can be proven by the formulas as

$$\alpha_{ms} = Le\ \alpha_{qs} \tag{27}$$

and

$$\alpha_{mp} = Le\ \alpha_{qp} \tag{28}$$

where Le is Lewis's ratio.

Evidently, in this case, it must be

$$e_p = E_p \tag{29}$$

and

$$E_r = E_p \tag{30}$$

The Meaning of Thermal Performance Criteria

As mentioned above, the thermal performance evaluation of an underground cold storage facility can be expressed as the thermal performance criterion Gi_q or Gi_m. And there are two formulas which can describe the thermal-moisture state as

$$t_r - t_p = (t_s - t_p)Gi_q/(1 + Gi_q) \tag{31}$$

and

$$t_r - T_p = Gi_q(t_s - t_r) \; ; \tag{32}$$

$$e_r - E_p = (e_s - F_p)Gi_m/(1+G_m) \tag{33}$$

and

$$e_r - e_p = Gi_m(e_s - e_r) \; . \tag{34}$$

The Criteria for Some Modes of Cooling Supply

The parallel pipes' cooling is accomplished by convection in cold storage. But the thermal performance of that mode is not good. In this case $\alpha_{qs} = \alpha_{qp}$, $F_s = 4F_p$, and then $Gi_q = \alpha_{qs}F_s/\alpha_{qp}F_p = 4$. Assume $t_r = -18°C$, $t_s = -15°C$, then $t_r - t_p = Gi_q(t_s - t_r) = 4[-15-(-18)] = 12°C$ and $t_p = t_r - 12 = -30°C$.

The Air Cooling Machinery By Forced Convection

In this case, $\alpha_{qs} = 10\alpha_{qp}$ and $F_s = 10F_p$, then $Gi_q = 1$. Still assuming $t_r = 18°C$, $t_s = 15°C$, then $t_r - t_p = Gi_q(t_s - t_r) = 3 \cdot 2$, and $t_p = t_r - 3 = -21°C$.

The Half Cooling Air Jacket Wall

The cooling air goes along an air jacket under the arch and goes back along an air jacket beneath the floor. For this case it is natural convection in the stored space, i.e., $\alpha_{qs} = \alpha_{qp}$ and $F_s = F_w$, $F_p = F_f + F_c$ then $Gi_q = 1$. But the thermal performance of this is better than the last case because of t_r nearing t_p and t_s nearing t_r.

The Full Cooling Air Jacket Wall

In this case, $F_s = 0$. If F_s is all the area of the hotter surrounding surface, then the $Gi_q = 0$. So $t_s - t_p = Gi_q(t_s - t_r) = 0$; i.e., $t_r = t_p$ and $e_r - e_p = Gi_m(e_s - e_r) = 0$, $e_r = e_p$. It is shown that the weight loss in this case is completely diminished.

The effects of the abovementioned cases had been tested in situ.

SOME MODES ON COOLING AIR JACKET WALLS

There are several modes for the operation of cooling air jacket walls. The wall pipes or ceiling pipes can be reformed by constructing a steel plate to form a cooling air jacket as shown in Figure 5.

The cooling wind machinery can be reformed by cycling air flow through the jacket, so that the upper half has the cooling wind starting and the lower half has the cooling wind returning, which is draughted by a fan in combined operation, as shown in Figure 6.

The combined operation method can save electrical energy, due to the enhanced effectiveness of the fan. So, two tunnels with air cooling jacket walls can be combined in operation as shown in Figure 7.
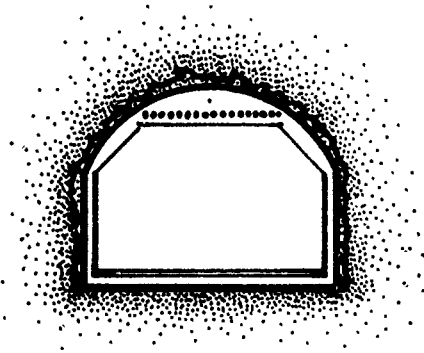
Figure 5. A cooling air
jacket wall on cold pipes.
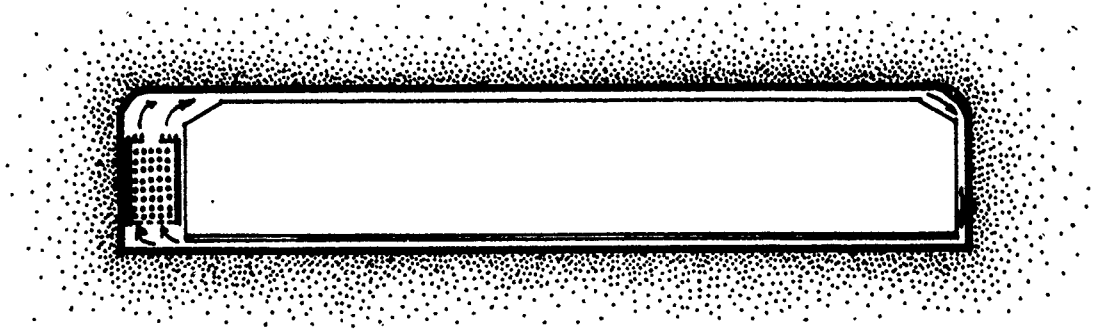
Figure 6. A cooling air jacket wall with cooling wind machinery.
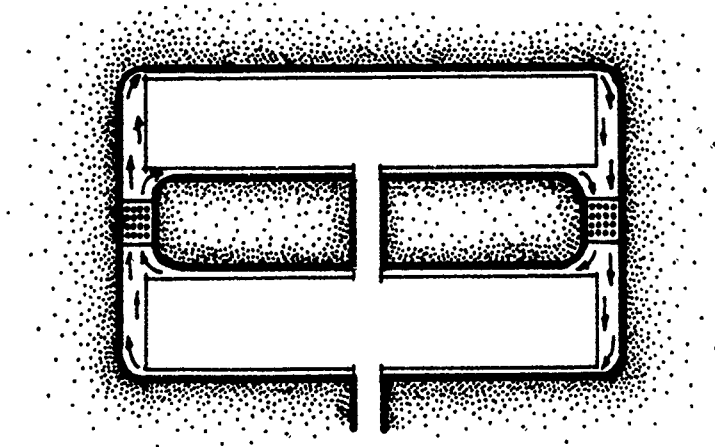
Figure 7. The conjugated operation on
two cooling air jackets.

CONCLUSIONS

As mentioned above, the conclusions are as follows:

An underground cold storage facility with cooling air jacket walls can keep the air temperature uniform and the relative humidity high, which are the best conditions for the storage of wet goods.

The cycling cooling air flow in the jackets is of very low humidity, which causes the adjacent insulation to remain dry, saving energy loss from the surroundings.

The cooling air jacket wall is a good surrounding construction for an underground or an aboveground cold storage facility for storing fresh, wet goods, because weight loss and the latent heat loss are greatly reduced.

ACKNOWLEDGEMENTS

REFERENCES

Chen, Q.G., 1980, "Heat Transfer Theory of Refrigerated Walls of Subsurface Cold Storage," _Subsurface Space_, Vol. 1, 358-367, Pergamon Press, Oxford.

Chen, Q.G. et al., 1980, "The State of Low Cost Subsurface Storage in China, "_Subsurface Space_, Vol. 3, 1159-1160, Pergamon Press, Oxford.

Lu, S.X., 1986, "Insulation Practice for Subsurface Cold Storage," _Advances in Gectectural Design_, Minnesota university, June.

Chen, Q.G., 1986, "Research on Thermal Performance of a Sweet Orange Cellar," _Advances in Geotectural Design_, Minnesota University, June.

Lu, S.X., 1986, "The Storied Cold Storage in Large Cavern," _Large Rock Caverns_, Proc. of International Symposium, Helsinki, Finland, Pergamon Press, London.

Chen, Q.G., 1980, "The Theory of Thermal Physics for an Underground Cold Storage Design," _Refrigeration Journal_, Volume 3.

Chen, Q.G., 1978, "The Optimum Thermal Condition for Cold Storage and Underground Cold Storage," _Refrigeration Technique_, Volume 3.

Chen, Q.G., 1980, "Heat Transfer Theory on Underground Cold Storage," _Building Physics_, Vol. 1.

Snow Density for Structural Snow Load in Moderate Climate

Andrzej Sobolewski[1] and Jerzy A. Zuranski[2]

ABSTRACT

Snow density is one of the variables connected with snow load esti-
mation. The paper deals with the dependence of the ground snow
density on the snow depth /up to 1 m/. The dependence of the snow
density on winter time is also shown. Two approaches to the snow
density estimation for snow load prediction are compared. Required
number of measurements for correct snow density estimation is also
discussed.

INTRODUCTION

Probably most meteorological stations in many countries collect data
on snow in terms of snow depth only. For structural calculations these data
must be converted into snow loads using appropriate relationship between the
snow depth and its density.

Two snow densities must be distinguished: /1/ local density of each
layer of the snow cover, which depends on the succesive snow-falls, weather
changes and time, all influencing snow metamorphosis, and /2/ bulk mean
density, averaged over total depth of snow. Only the second density is of
interest for snow load evaluation.

Snow density depends not only on the above mentioned factors but also
on the underlying material: soil or roof and their thermal influences.
Density of snow on a roof differs from the density of snow on the ground.
Unfortunately, most available data are related to snow on the ground. This
kind of snow density is discussed here.

DATA ON SNOW DENSITY

All meteorological stations in Poland belong to the Institute for
Meteorology and Water Control, which adopted the following procedure of
snow measurement: /1/ snow depth is measured every day /when snow is
present/ at 6 GMT, /2/ increment of snow depth is measured immediately after
each snow-fall, /3/ snow density is evaluated every five days, starting from
the first day of every winter month, and also: /a/ after each snow-fall,
/b/ every day during the thaws.

All measurements have been unified for many years and made using the
same snow sampler. This sampler, the same as in use in the USSR, consists
of a steel tube with a saw-tooth cutter fixed to its lower end, and an arm

---

1/ Research and Design Centre for Industrial Building "BISTYP", Warsaw,
    Poland

2/ Institute for Building Technology, Warsaw, Poland

balance /reading directly in water - equivalent units/ to weight the tube
and its contents. The tube is 0.5 m long /in a mountainous area it may be
longer/; its inside diameter is 80 mm. The scale partition is 10 mm for snow
depth and 10 N/m^2 for snow load on the ground.

WINTER VARIATION OF SNOW DEPTH AND DENSITY

Poland is situated on the border of two moderate climates: maritime
and continental. Influence of these two climates on the snow depth and its
density as well as on the snow load on the ground is demonstrated in
Figures 1 and 2. Diagrams are based on the data from the same meteorological
station located in Lublin /51.2°N, 22.5°E/; the snow density was there
measured every day.

Winter variations of snow data presented in Figure 1 are typical for
maritime climate i.e. several periods of snow accumulation separated by the
thaw periods. In Figure 2 snow variations are typical for continental
climate i.e. permanent accumulation of snow up to the begining of March
when the snow runoff starts.

The dependence of mean value of the snow bulk density on time is
shown in Figure 3. Mean values of snow density for every day were calculated
on the basis of 25 years data, from the period 1948/49 to 1973/74 /except
1960/61 winter/; zero values were omitted.

For these data the mean, expected value of snow density may be
expressed by the formula

$$\varrho = 129 + 1.1 \ t, \ kg/m^3, \hspace{2cm} /1/$$

where t is the time, in days, since the 1 November.

In this formula, all factors influencing snow density, as snow-falls,
wind, air temperature and humidity changes, snow sublimation and evaporation,
are included in the statistical way. Standard deviations are marked in Fig.3
from both sides of the mean value. It can be seen that the coefficient of
variation may reach even 0.5.

SNOW DEPTH AND SNOW DENSITY

Newly fallen snow is light and at the begining of winter the mean
density of a thin snowpack is of the order of 150 kg/m^3. During the thaw
period the snowpack of the same depth may have much higher density, even up
to 700-800 kg/m^3.

This is shown in Fig.4, where all measured values of snow density
versus snow depth are plotted. It is seen that there is no dependence of
bulk snow density on snow depth. Only one characteristic feature is, that
the higher the snow depth the closer the snow density to its mean value.
This feature is seen also in other meteorological stations.

SNOW DENSITY FOR SNOW LOAD PREDICTION

If snow load is to be predicted exclusively on the basis of snow
depth measurements, a serious problem arises how to evaluate the appro-
priate value of snow density. To resolve this problem two approaches are
used.

In the first approach the mean value of all registered snow densities in a region are used. It is seen in Fig.4 that mean value of snow density corresponds to the highest depth of snowpack. As a predicted depth for a long return period is high enough, mean snow density seems to be appropriate for the snow depth conversion to snow load.

In the second approach /Grünzer, 1983/ the so-called "load factor" is adopted. It represents the ratio of annual maximum snow load on the ground S_{max} to the annual maximum snow depth d_{max} during the same winter. Usually they do not occur at the same time and a ratio

$$\gamma = S_{max}/d_{max}, \quad kN/m^3, \qquad \qquad /2/$$

represents a fictive snow unit weight used only for the snow depth to snow load conversion.

This relation may be easily found plotting S_{max} versus d_{max} as in Fig.5. Hence

$$\gamma = 2.56 + 0.077/d, \quad kN/m^3, \qquad \qquad /3/$$

where d is the annual maximum or predicted depth of snowpack, in meters.

The Joint Committee for Structural Safety /Joint Committee, 1976/ recommended the following formula for snow unit weight for continental Europe

$$\gamma = 3 - 2 \, e^{-1.5 \, d}, \quad kN/m^3, \qquad \qquad /4/$$

where d is the snow depth, in meters, as above.

This formula is compared in Fig.6 with Eq.3 and measured values from Lublin. As it is seen, Eq.4 does not fit the experimental data in this particular geographical region.

The results of the two presented approaches are compared using snow data from Lublin /Table 1/. Predicted values of snow load for several return periods snow that loads calculated for the "fictive" snow unit weight /Eq.3/ are closer to the values estimated from the direct load measurements than values calculated on the basis of mean snow density /Table 2/. The differences are within 6% for the first approach, and 14% for the second.

ACCURACY AND REQUIRED NUMBER OF MEASUREMENTS

As it is seen in the Table 2 maximal differences between the results obtained by the three methods are within 0.1 to 0.2 kN/m^2. Therefore an important question arises: what should be the measurement accuracy if these differences are to be considered as non significant.

Even in calm weather a snowpack formed after snow-fall is not always quite uniform. Snow-falls may be accompanied by wind which increases the non-uniformity of snow cover. Therefore every day snow measurements should be repeased several times. Usually, at meteorological stations they are repeated three times.

With a view of establishing the relationship between the number of

measurements and the accuracy of snow depth and load evaluation a series of measurements was made by the first author in Warsaw during the winter 1978/79. As a result of calculations made with the assumption that the probability distribution of the snow load on the ground during measurements was normal, and using t-distribution for the evaluation of small number samples, it was found that the accuracy of 0.1 kN/m^2 could be obtained by 6 measurements and for the accuracy of 0.05 kN/m^2 at least 20 measurements were required. From the practical point of view 20 every day measurements seems too be excessive. They would be not only too laborious but may also lead to a quick destruction of the snow cover at meteorological stations.

CONCLUSIONS

The use of fictive snow unit weight for the conversion of snow depth into snow load seems to be more justified than the use for this purpose of a mean value of snow density averaged over the teritory under consideration. Therefore, equations similar to Eq.3 or 4 should be established for relatively small geographical regions.

REFERENCES

Gränzer,M., 1983, Zur Festlegung der rechnerischen Schneelasten, Bauingenieur, vol.58, 1-5, January 1983.

Joint Committee for Structural Safety, 1976, Common Unified Rules for Different Types of Construction and Material, CEB-Bulletin d'Information No 116, Paris 1976.

Table 1. Snow data from Lublin meteorological station

Parameter		depth, m	load, kN/m^2
measured	mean	0.226	0.501
	standard deviation	0.098	0.275
Gumbel distribution	U	0.182	0.377
	α	13.087	4.664

Mean value of snow density $\bar{\varrho}$ = 223 kg/m^3

Table 2. Predicted values of snow depth and snow load, Lublin meteorological station

Return period yrs	s kN/m^2	d m	γ kN/m^3	γ^d kN/m^2	ϱ^d kN/m^2
5	0.699	0.297	2.301	0.683	0.663
20	1.014	0.409	2.372	0.970	0.913
50	1.214	0.480	2.400	1.152	1.071
100	1.363	0.534	2.416	1.290	1.192
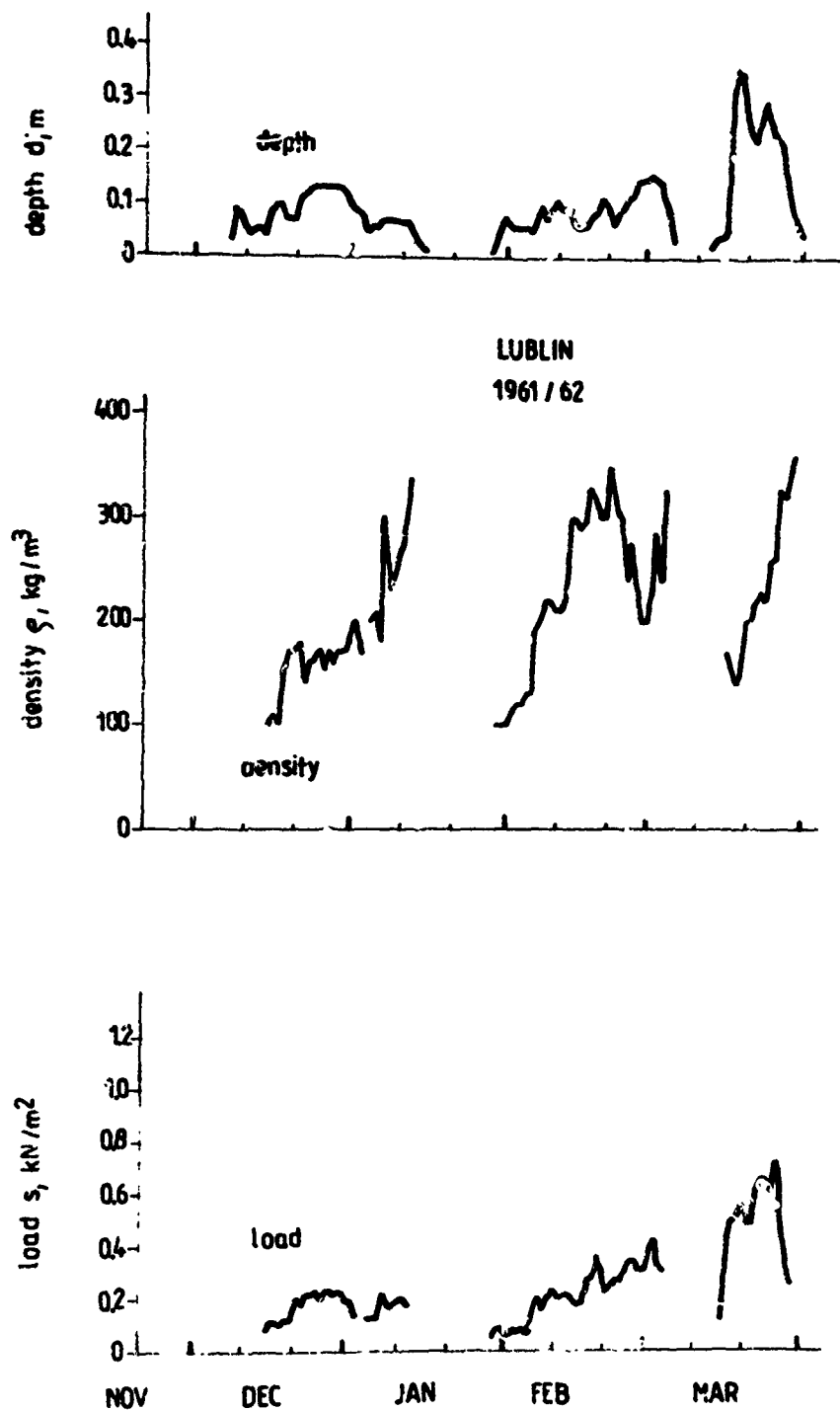
Figure 1 Snow depth, density and load time histories
during 1961/62 winter. Lublin meteorological
station
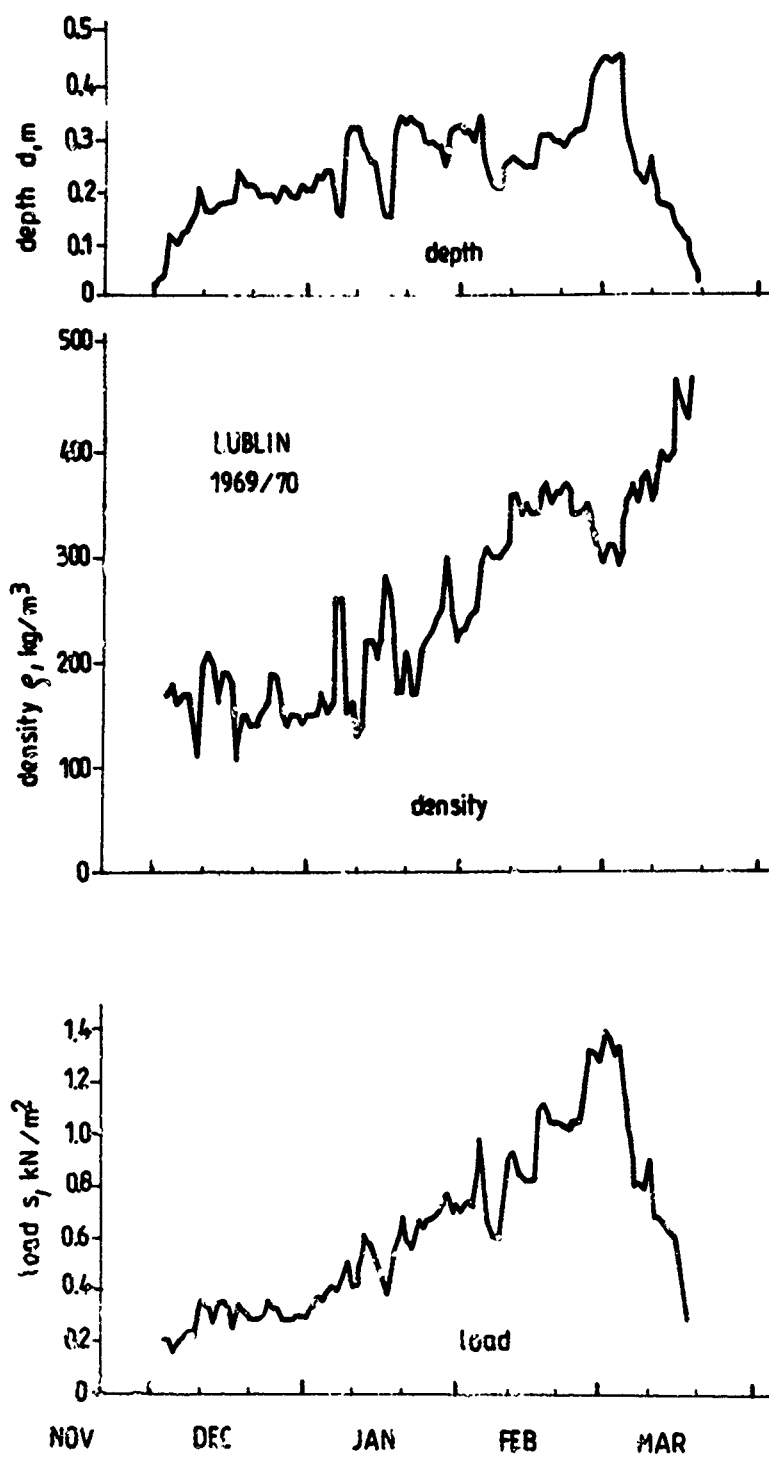
Figure 2 Snow depth, density and load time
histories during 1969/70 winter. Lublin
meteorological station
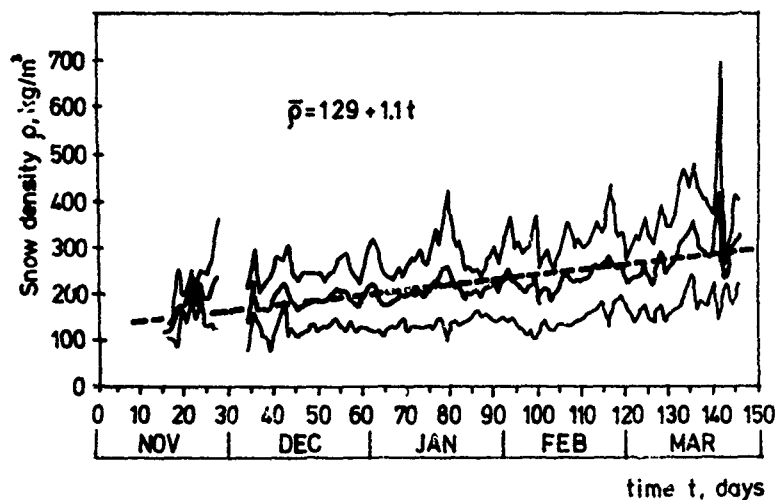
Figure 3 Dependence of the mean value of snow
density on time. Lublin meteorological
station
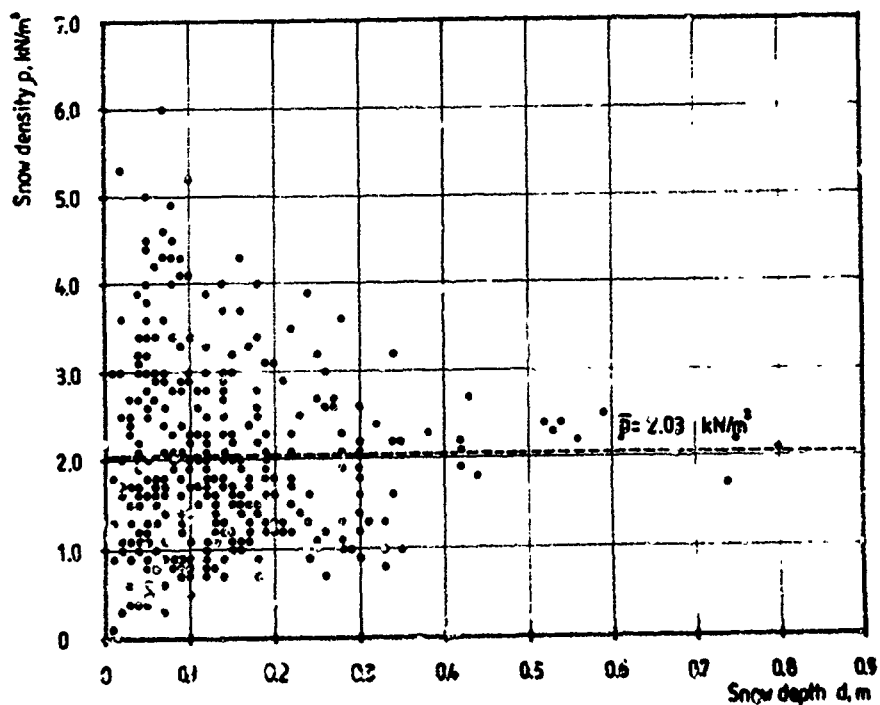
Figure 4 Bulk snow density versus snow depth.
Cracow meteorological station
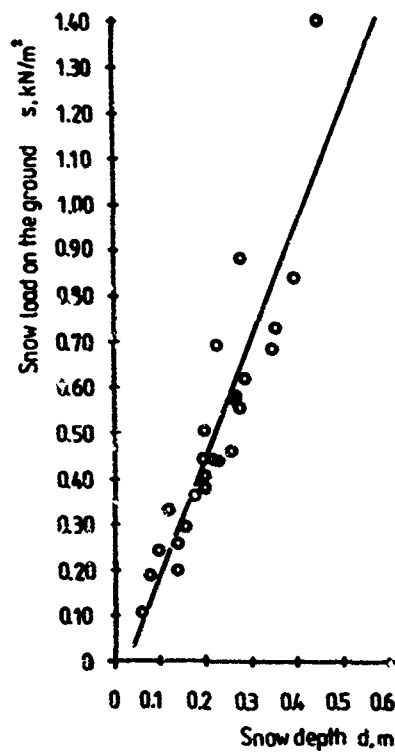
Figure 5 Annual maximum snow load on the ground versus
annual maximum snow depth. Lublin meteorological
station
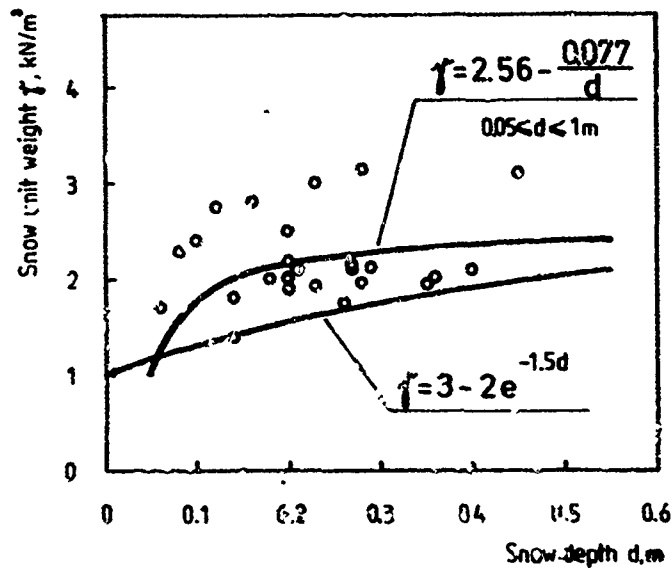
Figure 6 Snow unit weight versus snow measured or
predicted depth. Lublin meteorological station.
Equations 3 and 4 are plotted

Study of Ice Adhesion and Sintering

Wei Shen and Sung M. Lee

ABSTRACT

Most engineering problems relating to snow and cold
environments require good understanding of the dynamical
nature of snow. The morphological changes that accompany
sintering of spherical particles initially in point
contact have been studied by many investigators primarily
for metals. When the general theory of metal sintering is
applied to ice, investigators have come to different
conclusions as to which sintering mechanism is
predominant for ice. The verdict on these contradicting
but equally persuasive results is not yet in. Some recent
experiments have shown that the growth rate of an ice
bond formed at the interface between an ice particle and
glass is almost the same as that of ice sintering. Since
different hydrophilic substrate materials have different
surface energies, this type of adhesion experiment is
likely to yield additional information on the mechanisms
of ice sintering. In addition, the experimental data on
ice adhesion will be useful to many practical engineering
applications. This paper will present our current effort
in this direction.

INTRODUCTION

The morphological changes that accompany sintering of
spherical particles initially in point contact have been studied
by many investigators primarily for metals. Among the earliest
theories was that by Kuczynski (1949) in which he proposed four
mechanisms of sintering for metallic particles under pressureless
conditions. The relationships between the radius x of the
interface of a neck formed during sintering between two particles
of radius a and time t are given by

$$(x/a)^n = A(T)t/a^m \qquad (1)$$

where a is the radius of the metal sphere, x is the radius of the
neck and t is time. A(T) is a constant which depends on the

Wei Shen: Graduate student, Department of Physics, Michigan
        Technological University, Houghton, Michigan 49931
Sung M. Lee: Professor of Physics and Director, Keweenaw
        Research Center, Michigan Technological University

temperature, while m and n are numerical constants that depend on the working mechanism. Sintering theory of powder metallurgy yields the values of n and m as follows:

(1) viscous and plastic flow   n=2, m=1
(2) evaporation and condensation   n=3, m=2
(3) volume diffusion   n=5, m=3
(4) surface diffusion   n=7, m=5

These four mechanisms are illustrated in Figure 1.
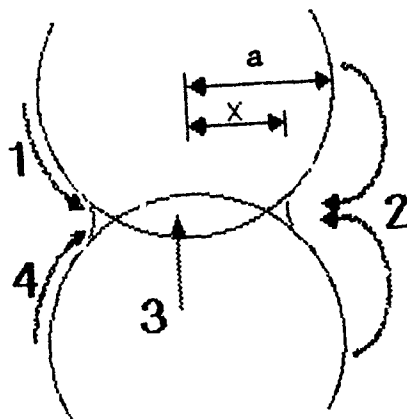
Figure 1. Four mechanisms of sintering process

Sintering of spherically shaped ice particles were similarly studied by various investigators by observing the growth rate of a neck between two spheres of ice. It was generally expected that these four mechanisms for powder metallic particles were also applicable to ice in many cases though the melting point of ice is much lower than that of metals.

Kingery (1960) studied surface diffusion of ice by measuring the growth rate of the neck between two polycrystalline ice spheres. He showed that for spheres in the size range of 0.1 mm to 3 mm radius and in the temperature range of -2°C to -25°C the values of n were between 6.1 and 7.1. It indicated that the mass transfer by surface diffusion was dominant especially at the beginning of sintering.

On the other hand, Kuroiwa (1961) showed that the volume diffusion is dominant between 0°C and -10°C and the surface diffusion becomes increasingly important at lower temperatures.

Hobbs and Mason (1964) found the results that for polycrystalline and single crystal ice, in the form of spheres of diameter 50 μm to 700 μm at temperature between -3° and -20°C, the evaporation-condensation is the principal mechanism. They pointed out that because of the high vapour pressure over the small radius of curvature surfaces, the sintering of ice spheres in air will take place by evaporation of material from the

374

surface of the spheres, diffusion through the air, and condensation into the concave region of the neck.

Although Maeno and Ebinuma (1983) extended this theory to six different mechanisms, they concluded that the vapor diff..sion is the dominant mechanism during pressureless sintering of ice. However, when large stresses are applied to snow, lattice diffusion from a dislocation source was expected to become more significant.

The studies described above were done on the sintering between two ice particles. The theory of sintering developed for metallic particles yields conflicting, but equally convincing, results which indicate one of the three mechanisms (evaporation-condensation; volume diffusion; surface diffusion) is the dominant process for ice.

More recently, experimental studies were made by Mizuno and Wakahama (1983) which provided direct observation of formation of ice bonds at plane interfaces of substrates. See Figure 2. They showed that the growth rate of bonds between ice particles and hydrophilic substrates, such as glass, was approximately the same as that of ice sintering. For instance, experiments performed below $-10^\circ C$ with particles of radius in the range of 100 μm to 500 μm yielded the values for n:

$$
\begin{array}{lll}
\text{ice} - \text{ice} & \quad & n \simeq 5.1 \\
\text{ice} - \text{glass} & \quad & n \simeq 4.9
\end{array}
$$
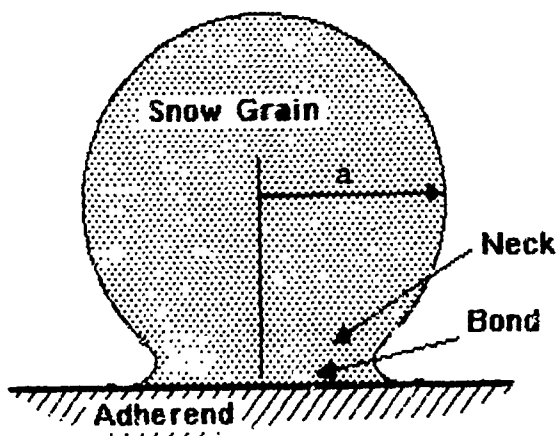
Figure 2. Formation of an ice bond on a plane surface

The experiment also demonstrated that no bond was formed at the interface between ice particles and the plate of hydrophobic material such as teflon. Since different substrate materials have different surface energies, the work by Mizuno and Wakahama suggests that the study of ice adhesion on hydrophilic materials is likely to offer additional information to the study of ice sintering.

ADHESION ENERGY

When two different surfaces are in contact or very close to each other, the molecules of each exert an attractive force on the molecules of the other. The interface acquires a surface tension of its own, or interface energy γ_{AB}. Suppose W_{AB} is the energy required to separate a unit area of the two materials after adhering and γ_A and γ_B are the surface energies of the two materials. The relation between them is

$$W_{AB} = \gamma_A + \gamma_B - \gamma_{AB}. \qquad (2)$$

When the adhesion energy is zero $\gamma_{AB}=0$, i.e., there is no interaction between the two phases, or the two materials are completely compatible, Eq. 2 becomes $W_{AB} = \gamma_A + \gamma_B$. Thus, the creation of the interface by joining the two free surfaces of the two materials does not gain any free energy. When the adhesion energy γ_{AB} is very small, $0 < \gamma_{AB} < \min(\gamma_A, \gamma_B)$, the two materials are still compatible and $W_{AB} > |\gamma_A - \gamma_B|$. On the other hand, if the adhesion energy γ_{AB} is very large, i.e., the two materials are not compatible $W_{AB} < |\gamma_A - \gamma_B|$. The fact that the two materials stick together requires that the interfacial energy be less than the total surface energies of A and B: $W_{AB} > 0$. In the case of ice sintering, the grain boundary energy, i.e., interfacial energy, should be less than the total surfce energies of two ice particles, or less than the total surface energies of ice particles and an adherend.

A system is in the most stable state or in a thermodynamical equilibrium if and only if its energy is at minimum. For ice particles in contact to form a system which is in equilibrium its energy should be a minimum. Once an ice particle is brought into contact with the adherend surface, a bond between the ice and the adherend will begin to grow in order to lower the system energy. This is because at the surface of materials the molecules are usually at a less well balanced state than the interior which gives a higher energy state at the surface. The major energy change during sintering is the decrease in surface energy which is initially high in a fine particle state. This can be considered to be where the "driving force" comes from for the sintering process.

The magnitude of surface energies of materials are very difficult to measure, but the relative surface energies of different materials can be determined more easily by measuring the contact angle.

If a liquid drop rests on a solid substrate in a gaseous atmosphere, γ_{sv}, γ_{sl} and γ_{lv} can be related to the equilibrium contact angle θ made at the intersection of the solid-vapour, solid-liquid and liquid-vapour surfaces, respectively. For the case in which the liquid does not completely wet the solid surface, i.e., $0^\circ < \theta < 180^\circ$, the condition of equilibrium at the intersection of the three interfaces is $\gamma_{sv} = \gamma_{sl} + \gamma_{lv}\cos\theta$,or

$$K = \cos \theta = (\gamma_{sv} - \gamma_{sl})/\gamma_{lv}, \qquad (3)$$

where $-1<K<1$. See Fig.3.

For the two materials A and B in Fig. 4, as an illustration, $\theta_A < \theta_B$ and therefore, from Eq. 3, $K_A > K_B$. This means that the surface energy of material A is higher than that of material B and the bond of ice is easier to form on material A.
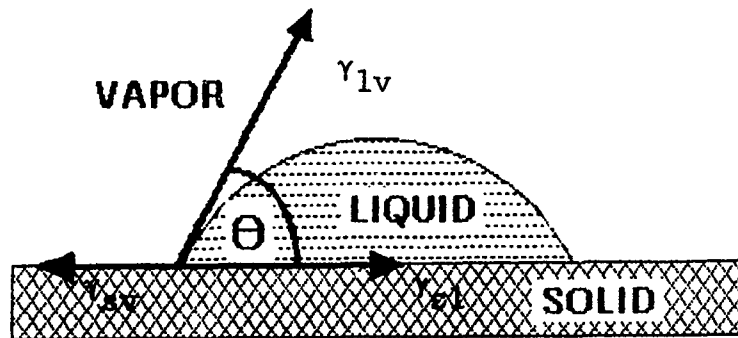
Figure 3. Surface energy diagram

EXPERIMENT

In our experiment, the sintering of ice particles was investigated by observing adhesion of ice to different materials such as teflon, aluminum and concrete, each of which had a different surface energy as compared to the ice surface. A statistical calculation was used to analyze the images of ice particles which had many bonds instead of just a few. The experimental procedure and the results are described below.

The experiments were carried out in a cold room with a temperature range of -6° to -8°. The ice particles were prepared by spraying droplets of distilled water into liquid nitrogen in a metal tray. The collected ice particles, which have uniform diameters of approximately 500 μm, were annealed for more than one week. The ice particles were placed in a container which had the bottom plate constructed of a specified material for a required period of time (approx. 30, 120, 240, and 960 minutes). Two sets of experiments were carried out: one with a five-pound

(a)   (b)
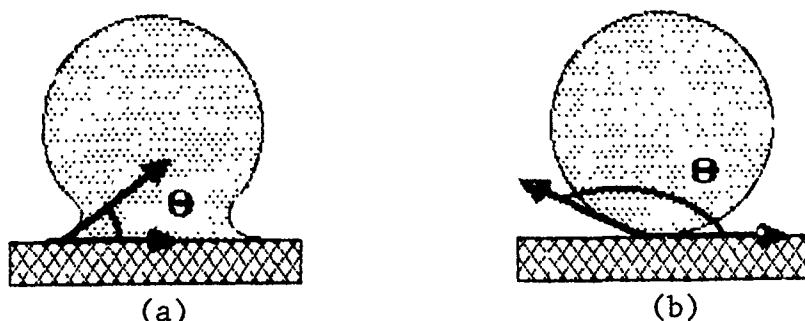
Figure 4. Two different modes of adhesion

377

load on it and the other without any load. Then the bottom of the material was heated until we could separate the ice bonds from the adherend before the ice bonds melted.

The sample was then placed in a small container lined with teflon and filled with dimethylthalate, which has the melting point of -4°C. The surface which had adhered to the adherend was placed in contact with the teflon at the bottom of the container. The sample was then frozen in dry ice at -20°C and extracted from the container. In doing this, the bottom surface would now expose the ice bonds which had formed during the test and were now frozen to prevent the danger of neck and bond dimensions changing with time. Carbon powder was then rubbed on the surface of the sample to stain the pores. A picture of the surface was then taken using a 55 mm micro lens.

Next, the sample was placed in a microtome and a 10 μm slice removed. The newly exposed surface was again stained and photographed. This was repeated until the necks were completely removed. Then "Thunder Scan" program was used to save these photographs as images in a computer. In order to analyze the images the "Ice Program" was used in a selected area and the mean sizes of the bonds were obtained as a result. The basic idea of this program is that the computer sums up the total area of the bonds and counts the number of bonds in the selected area. Then it divides the total area by the total number of bonds and thus the mean size of the bond is determined.

The data obtained in this manner can be plotted in a graph which relates the size of the bonds divided by the ice particle size to the time, i.e., x/a vs. t. The slope of the curve in a log-log graph yields the value for n in Eq. 1. The results of our experiment on ice adhesion on different adherends are summarized below:

n	teflon	aluminum	concrete
without load	8.91	2.40	7.50
with load	8.89	--	5.80

Table 1. Values of n for different substrate materials

DISCUSSION

The theory of sintering indicates that the growth rate of ice bonds not only depends on the kinetic transfer mechanism, but also on the surface energy of sintering adherent. As it was discussed earlier, the relative surface energy of one kind of material can be determined by measuring and comparing the contact angles with other materials. Figures 5, 6, and 7 show a drop of water on the surface of teflon, aluminum and concrete, respectively. The contact angles are 90° for teflon, 65°for

Figure 5. A drop of water on a teflon coated plane surface

Figure 6. A drop of water on an aluminum surface
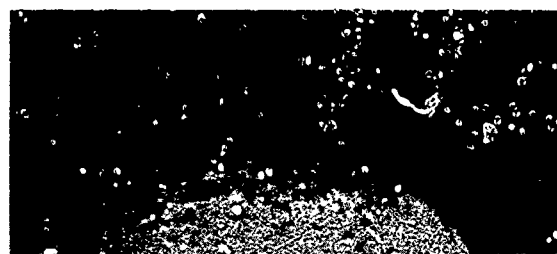
Figure 7. A drop of water on a concrete surface

aluminum, and 73° for concrete. Thus, the relative surface energies can be compared as

$$\gamma_{aluminum} > \gamma_{concrete} > \gamma_{teflon}.$$

Since from our experiment

$$n_{aluminum} < n_{concrete} < n_{teflon},$$

it can be concluded that the smaller the surface energy, the larger the value of n.

Mizuno and Wakahama (1983) have shown that the growth rate of ice bonds formed at the interface between an ice particle and the plate of glass was equal to or slightly larger than that of ice sintering. The value of n for the former was obtained to be 4.9 and for the latter 5.1. The contact angle between a drop of water and a plate of glass is known to be in the range of 66° to 68°, which is slightly larger than that for aluminum plate. Therefore among the three substrate materials used in our experiment, only aluminum offers the most simple and direct means of interpreting the results in light of the sintering equation, Eq. 1.

Comparison of contact angles indicates that the surface energy of aluminum is slightly larger than that of glass and, therefore, that of ice. Theoretically, the growth rate of an ice bond on aluminum should then be slightly larger than that of ice on glass and, therefore, that of ice sintering, i.e., the value of n for aluminum will be smaller than that for ice on glass and, therefore, that of ice sintering. The value of n that we obtained from our experiment of ice adhering on aluminum was 2.4 as shown in Table 1. Although n=2.4 is closer to 2.0 than 3.0 and, thereby, tends to suggest plastic flow as a dominant sintering mechanism for ice from Eq. 1, it is more plausible to interprete the value of n to be close to 3.0 and view evaporation-condensation as the dominant mechanism.

There are several factors that would support this interpretation. Ice, adhering on aluminum under no pressure loading and in a cold room environment, in which the air was not ice vapour saturated, is not likely to undergo plastic flow as the dominant mechanism. The mean free path of water molecules in the vapor phase is about 10^{-5} cm and for ice particles of about 100μm in radius the concave neck radius exceeds the value of 10^{-4} cm. In this condition, water molecules can easily be transferred from the surfaces of the particle to the neck by diffusion through the pavour phase rather than other ways. In addition, the rate at which the latent heat of sublimation at the particle surface needs to be considered. In metals, this effect would be expected to be very small since the latent heat can be conducted away quickly through the metal spheres with high thermal conductivity. Ice, on the other hand, has a low thermal conductivity and a high latent heat, so the heat will escape largely by convection through the environment.

In fact, these last two factors make the direct application of the metal sintering theory to ice incorrect. With these factors included, Hobbs and Mason (1964) developed a modified equation of ice sintering by evaporation-condensation. Diffusion coefficients measured by Mason and also by Riehl and Dengel (1962) supports the theory of evaporation-condensation.

The value of m in Eq. 1 would have given a more definitive answer as to which sintering mechanism is predominant for ice. This can be done by examining the effect of sphere radius on time required to reach a specific geometry x/a, i.e., from a log-log graph of radius vs. time for a given value of x/a. Unfortunately, our experiment so far has not yielded sufficient data to obtain this information. This will constitute an important aspect of our continuing study.

CONCLUSION

An experimental study of ice adhesion on substrates made from materials of different surface energies tends to indicate that the predominant mechanism of ice sintering is that of evaporation-condensation. This result supports the conclusion reached by several other investigators. Although the study reported here contributes to the discussion on the sintering theory of ice, it does not lend sufficient substance to the as yet unsettled question of which sintering mechanism is the dominant one for ice, primarily due to the fact that only a limited amount of experiment has been done so far. Further study is in progress.

REFERENCES

Hobbs, P.V., and Mason, B.J., 1964, "The Sintering and Adhesion of Ice", Philosophical Magazine, Vol. 9(98), 181-197, 1964.

Kingery, W.D., 1960, "Regelation, Surface Diffusion, and Ice Sintering, Journal of Applied Physics, Vol. 31(5), 833-838, 1960.

Kuczynski, G.C., 1949, "Self-Diffusion in Sintering of Metallic Particles", Transactions of the American Institute of Mining and Metallurgical Engineers, Vol. 185, 169-178, 1949.

Kuroiwa, D., 1961, "A Study of Ice Sintering", Tellus XIII, Vol. 2, 252-259, 1961.

Maeno, N., and Ebinuma, T., 1983, "Pressure Sintering of Ice and Its Implication to the Densification of Snow at Polar Glaciers and Ice Sheets", Journal of Physical Chemistry, Vol. 87, 4103, 1983.

Mizuno, Y., and Wakahama, G., 1983, "Experimental Studies on Snow Accretion at Subzero Temperatures", Annals of Glaciology, Vol. 4, 192-197, 1983.

Riehl, N., and Dengel, O., 1962, Reported in Colloquium on the Physics of Ice Crystals, Erlenbach-Zurich, 1962.

ACKNOWLEDGEMENT

7
CODES AND STANDARDS
Michael O'Rourke, Chairman
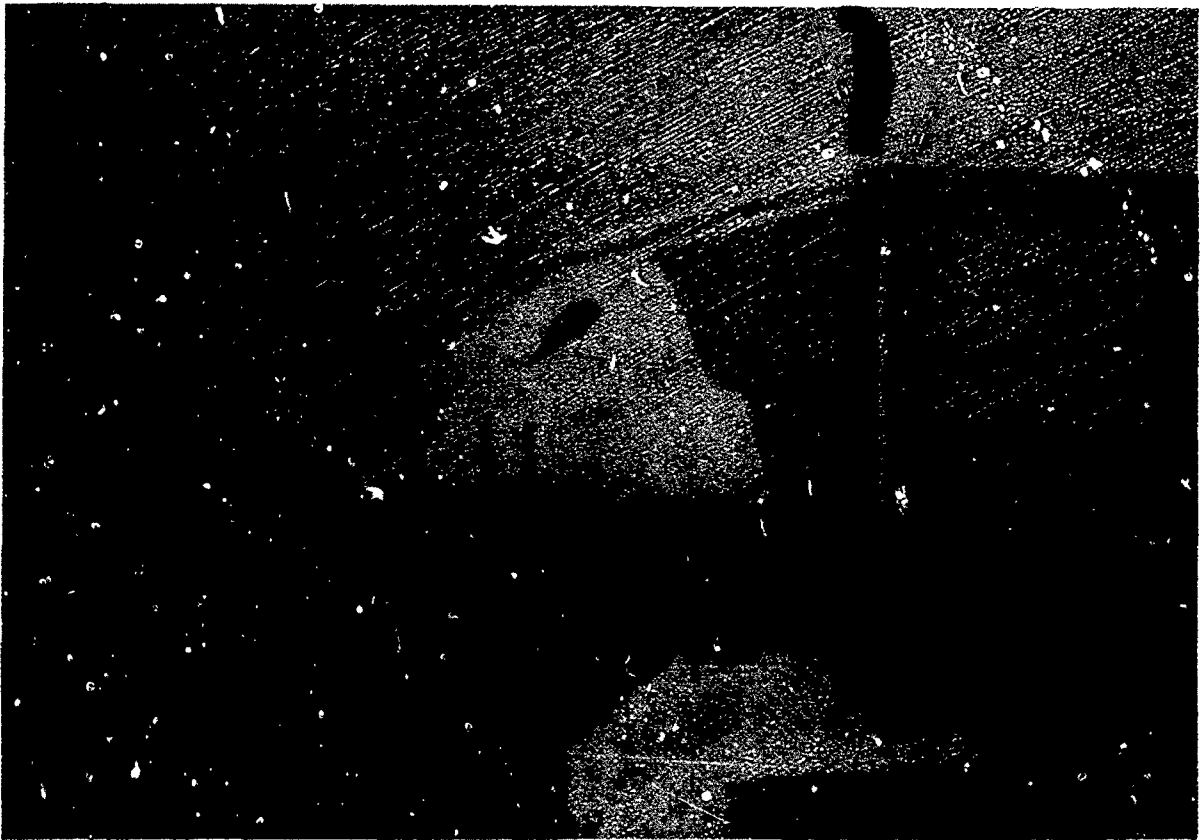
Drift loads are an important design consideration. The peak load intensity in this drift was nine times the uniform value on the roof above. (Photograph by Wayne Tobiasson.)

New Developments in Code Specifications and Standards for Snow Load

Kristoffer Apeland[1]

ABSTRACT

Revisional work has been started on the ISO Standard 4355, "Bases
for design of structures - Determination of snow loads on roofs".
In this connection, the paper discusses the problems connected
with the introduction of research and new findings into code speci-
fications, and in particular into International Standards.

The basis for the development of an ISO Standard, especially in the
field of codes of practice, is briefly discussed.

A new format of the snow load distribution function is presented,
in which parameters representing exposure, thermal effects, roof
surface material effects, roof geometry, etc, are defined.

In addition to the general format, the paper concentrates on four
major topics, i.e.:

- The effect of exposure on the snow load
- Snow load on heated roofs, in particular glass roofs
- Snow load on arches
- Snow load on multilevel roofs

In all of the abovementioned fields new findings may lead to impor-
tant changes in the standard.

In particular national requirements have been put forward to the
international working group about presenting useful specifications
for snow load on glass roofs. A model for such specification is
presented in the paper.

A brief discussion is given about principles for making the stan-
dard more applicable in connection with computer aided design.

I. Professor, dr. techn., Oslo School of Architecture, Oslo, Norway

1.0   INTRODUCTION

The first International Standard on snow loads on roofs, ISO 4355 "Bases for design of structures - Determination of snow loads on roofs" was prepared a decennium ago by a working group under the ISO Technical Committee 98, Subcommittee 3. The document became an ISO Standard on August 15, 1981. ISO 4355 has formed the basis for a number of National Codes of Practice for snow loads on roofs.

In view of the fact that some objections had been raised about the snow loads prescribed in ISO 4355 for arches and for multilevel roofs, ISO TC 98/SC 3 decided to take up revisional work on the standard. During this revisional work it has turned out that new findings in the field may lead to greater changes than was foreseen when the revisional work was started.

Some of these changes are discussed below.

2.0   BASIS FOR DEVELOPMENT OF ISO STANDARDS

An ISO International Standard is a document with prescriptions of variant limitations of a product,object, method etc., for which there is an international concensus among the ISO member bodies.

Due to practice in a number of countries, standardization has also been applied in connection with building regulations, codes of practice, etc..

An International Standard will in general be developed and proposed by one of ISO's Technical Committees.

In the field of Actions or Loads the ISO/TC 98 "Bases for Design og Structures", with the Secretariat in Poland, is the responsible committee.

The Technical Committee TC 98 has produced a governing ISO Standard ISO 2394 "General principles on reliability for structures", the first edition of which was adopted in 1973, and a revised version has been adopted in 1985.

The ISO 2394 has been developed on the basis of work of JCSS, "Joint Committee on Structural Safety", which has members from a number of international organizations.

The ISO/TC 98 has several subcommittees, of which SC 3 "Loads, Forces and other Actions" is responsible for the snow loads, and SC 3 has appointed a Working Group to take care of the revision of the snow load standard.

ISO has a general rule that only prescriptions which are found in National Standards may be introduced into an International Standard. This rule presents a number of problems, in particular in the field of safety

of structures, in which there has been extensive developments in recent years, however, where only some of these developments have been introduced into the National standards.

One example from the Snow Load Standard may illustrate the problem. In recent years the application of glass roofs has had an enormous development in many of the European an the North American countries. This has lead to a pressure on the working group on snow loads, to come up with a prescription on how to deal with this problem in design. In particular, this pressure has been put forward in Norway, where the general snow loads are high, and where glass roof areas have had an exponential increase over the last few years.

Fortunately, the ANSI A 58.1-1982 has introduced a thermal coefficient into their snow load format. Thus, there already is a National prescription in this field, and the international working group may introduce a prescription in the field without meeting with formal objections. Thus, this has been done in the proposal.

The author feels that, although there may be a sound basis for the restrictions about introducing new developments into the ISO Standards, there should be a dispensation rule for fields, in which the research and development results are the only reason for the requirement of revision of an ISO Standard, although these have not been introduced into National Standards.

3.0   SNOW LOAD ON ROOFS (s)

3.1   General function describing intensity and distribution of the snow load on roofs

Formally, the snow load on roofs may be defined as a function of several independent parameters. Thus

$$s = F \{s_0, C_e, C_t, C_m, \mu_m, \mu_\beta, \mu_d, \mu_s\} \qquad (3.1)$$

where:

s - the snow load on the roof
s_0 - the characteristic snow load on the ground
C_e - an exposure reduction coefficient, defining the basic load on a flat roof of a cold building, as a fraction of the characteristic snow load on the ground, and as a function of the exposure of the roof
C_t - a thermal reduction coefficient, defining the reduction of the snow load on the roof as a function of the heat flux through the roof
C_m - a surface material smoothness coefficient

μ_β - a slope reduction coefficient, defining the reduction of the snow load on the roof by sliding off snow due to the slope of the roof, β
μ_m - a surface material smoothness modification coefficient on the slope reduction coefficient μ_β, depending on the surface material smoothness coefficient C_m and the slope β

μ_d - a drift load coefficient, defining amount and distribution of additional load on a leeward side or part of a roof, depending on the exposure of the roof and geometrical configurations of the roof or the roof complex

μ_s - a slide load coefficient, defining amount and distribution of slide load on a lower part of a roof, or a lower level roof

Since sufficient data of long term direct measurements of the snow load on roofs are not yet available, the determination of the snow load on roofs must be obtained by approximations of the more complex function defined by equation (3.1).

3.2 Approximate formats for the determination of the snow load on roofs

An assumption that the snow load on the roof will be proportional to the characteristic snow load on the ground, has lead to the widely used format:

$$s = s_0\mu \; \{ \; C_e, \; C_t, \; C_m, \; \mu_m, \; \mu_\beta, \; \mu_d, \; \mu_s \; \}= s_0\mu \tag{3.2}$$

Since the function μ of equation (3.2) is depending on a number of parameters, the format (3.2) requires extensive spesifications and illustrations for various kinds of roof complexes, roof exposure, roof temperature, roof material, etc..

The proposal for the International Standard defines the snow load on the roof as the sum of a basic load, s_b, a possible drift load part, s_d, and a possible slide load part, s_s. Thus, for the most unfavorable condition (lower roof on leeward side):

$$s = s_b + s_d + s_s \tag{3.3}$$

Effects of the various parameters are simplified by the introduction of product functions. Thus,

$$s_b = s_0 C_e C_t \mu_m \mu_\beta \tag{3.4.a}$$

$$s_d = s_0(1-C_e)C_t\mu_m(\mu_\beta\mu_d) \tag{3.4.b}$$

$$s_s = s_0 C_t\mu_m(\mu_\beta\mu_s) \tag{3.4.c}$$

The exposure coefficient, C_e, is defined in paragraph 4.1.
The thermal coefficient, C_t, is defined in paragraph 4.2. The surface material smoothness coefficient C_m and the surface material smoothness modification coefficient μ_m are defined in paragraph 4.3. The shape coefficients μ_β, μ_d, μ_s are defined in paragraph 4.4.

3.3 Partial loading due to melting, sliding and snow removal

The designer should always consider whether more severe imbalances may be expected from snow removal, sliding, melting etc., and decide whether the snow load should be applied with zero value at specific parts of the roof.

In particular, such considerations are important for arch structures, which are sensitive to the form of the load distribution.

4.0 SNOW LOAD COEFFICIENTS

4.1 Wind exposure coefficient, C_e

The wind exposure coefficient, C_e, is a reduction coefficient, defining the basic load on a flat roof of a cold building, as a fraction of the characteristic snow load on the ground, and as a function of the exposure of the roof.

Methods for the determination of C_e as a function of climatological and topographical data will be given in an annex to the standard.

An approximate definition for C_e is given as a function of the mean winter wind speed v only, in the following way:

$$
\begin{aligned}
C_e &= 1.0 & \text{for } \quad v < 2 \text{ m/sec} \\
C_e &= 1.2-0.1 \text{ v} & \text{for } \quad 2 \leq v \leq 8 \text{ m/sec} \\
C_e &= 0.4 & \text{for } \quad 8 \text{ m/sec} < v
\end{aligned}
\tag{4.1}
$$

For regions where there is not sufficient data available about the mean winter wind speed v, it is recommended to set v = 4 m/sec, which yields $C_e = 0.8$

The approximate formulae (4.1) are deduced for climatic regions having average winter temperature $\overline{T} \leq - 5^{\circ}C$.

For regions having average winter temperature $\overline{T} > - 4^{\circ}C$ it is recommended to control the structure for a condition of zero drift, i.e. $C_e = 1.0$.

4.2 Thermal coefficient, C_t

The thermal coefficient, C_t, is introduced to account for effects of thermal conditions in the roof, in particular for glass covered roofs, and for the thermal conditions in the space under the roof.

Values of C_t are given in the table 1.

A method of determining snow melting reduction by thermal flux theory is presented in an annex of the proposed standard.

Table 1   Thermal coefficients

Roof type	Thermal condition of roof and space under the roof	U-value of roof $W/m^2/K$	Temperature of space under roof T_{min} 1) ^oC	C_t 2)
Roofs with non-trans-parent cover-ing	Roofs over cold buildings	-	-	1.00
	Roofs over heated build-ings, ventilated (cold) roofing surface	< 0.4 $\geq$ 0.4	$\geq$ 20	1.00 0.95
	Roofs over heated build-ings, not ventilated (warm) roofing surface and where melted snow water and rain water will be drained away	< 0.25 0.25-0.4 > 0.4	$\geq$ 20	1.00 0.95 0.90
Glass covered roofs	Roofs over partially climatic conditioned space	1.5-2.5 2.5-4.0 > 4.0	0-20	0.9-0.0225 T_{min} 0.8-0.0200 T_{min} 0.7-0.0175 T_{min}
(Trans-parent roofs)	Roofs over fully clima-tic conditioned space	1.5-2.5 2.5-4.0 > 4.0	$\geq$ 20	0.45 0.40 0.35

1) T_{min} is defined as the lowest temperature over the winter season in the space under the roof

2)   The C_t-values are determined for climatic regions having a minimum average monthly winter temperature $\overline{T}$ monthly $\geq$ - 7^oC. For colder climatic regions, i.e $\overline{T}$ monthly < - 7^oC the C_t values should be increased by a factor 1.1, however, $C_t \leq$ 1.00

4.3   Surface material smoothness coefficient, C_m, and modification coefficient, μ_m

The amount of snow which slides off the roof will to some extent depend on the surface material of the roofing.

The surface material coefficient, C_m, defines a reduction coefficient for surface materials with less surface roughness than roofing paper, as a fraction of the snow load on a corresponding roof covered with roofing paper.

Provided statistical data have been established by measurements the material smoothness modification coefficient μ_m may be introduced in the form:

$$\mu_m = 1 - (1 - C_m) \sin (1.5 \beta) \qquad (4.2)$$

for $1.0 \leq C_m \leq 0.8$

Unless significant statistical data have been determined by measurements the proposal for the International Standard recommends to set $C_m = 1.0$, and $\mu_m = 1.0$

4.4 Shape Coefficients μ_β, μ_d, μ_s

4.4.1 General principles

The shape coefficients define distribution of the snow load over a cross-section of the building complex, primarily depending on the geometrical properties of the roof complex.

For buildings of rectangular plan form, the distribution of the snow load in the direction parallel to the eaves is assumed to be uniform, corresponding to an assumed wind direction normal to the eaves.

In the International Standard the shape coefficients are defined on the condition that there are no obstructions that may prevent snow from sliding off the roof at the eaves.

For roofs having snow fences or other obstructions, reduction as a function of slope can not be assumed.

In the existing ISO 4355 and in the National Codes the variation of the shape coefficients as a function of the roof slope β is discontinuous.

With the purpose of presenting a continuous variation and in order to make the standard more adaptable to computeraided design, a proposition of defining the variation by fairly simple trigonometric functions has been proposed.

In Figure 1 it is shown that the proposed continuous variation for pitched roofs serves a double purpose. For small and large β-values it is a question of curve fitting, whereas the continuous variation yields a better representation of the snow load for β-values between 20-35 degrees.

4.4.2 Slope reduction coefficient, μ_β

The reduction of the snow load on the roof due to the slope, β, of the roof, is defined by the shape coefficient μ_β, which is given by the function:

$$\mu_\beta = \cos (1.5 \beta) \text{ for } 0 \leq \beta \leq 60^0$$

$$\mu_\beta = 0 \qquad\qquad \text{for } \beta > 60^0 \qquad\qquad\qquad (4.3)$$

For roofs with snow fences and/or obstructions preventing the snow from sliding off, $\mu_\beta = 1.0$

4.4.3 Drift load coefficient, μ_d

The geometrical influence of the shape on the drift load accumulating on the leeward side of a pitched roof is defined by the shape coefficient μ_d, which for a roof with roof angle β is defined by the function:

$$\mu_d = 4 \sin^3 (3\beta) \quad \text{for } 0 \leq \beta \leq 60^0$$

$$\mu_d = 0 \qquad\qquad \text{for } \beta > 60^0 \qquad\qquad\qquad (4.4)$$

For a lower level roof in a multilevel roof complex, the magnitude of the drift load and the distribution will depend on several geometrical parameters of the roof complex, as well as on the amount of snow that may drift onto the roof. An approximate drift load model is presented in the proposal, in which the drift load distribution is assumed to be linear.

For arch roofs a continuous distribution of the drift load is proposed.

For climatic regions having average winter temperature $\bar{T} > -4^0C$, a design situation without drift should be considered.

4.4.4 Slide load coefficient, μ_S

Slide load on a lower part of a roof, or on a lower roof of a multi-level roof complex, will depend on the amount of snow that may slide down, and on the geometrical configuration of the roof complex.

The distribution of the slide load and the spreading out of the load will, in addition to the geometrical shape of the roof complex, depend on the compound of the sliding snow and on the friction on the upper roof, from which the snow is sliding.

The slide load magnitude and distribution is incorporated in the shape coefficient μ_S.

An approximate slide load model is presented in the proposal, in which slide load distribution is assumed to be linear.

The impact loading effect on multilevel roofs due to slide should be considered by the designer.

4.4.5 Snow load distribution on selected types of roofs

In the proposal for the standard, snow load distributions are illu-strated for a number of types of roofs, as shown in Figure 2-9.

Several of the presented values, in particular on multilevel roofs and arches, are still open for discussion.

5.0   PLAN OF FURTHER WORK

After the meeting of the Working Group in Santa Barbara, July 1988, another meeting is scheduled to be held in London, UK in October 1988.

After the London meeting it is the plan of the group to forward the document to ISO TC 98/SC 3 for further processing in the ISO system. Hopefully, the revised ISO 4355 may become an ISO Standard in a couple of years.

6.0   REFERENCES

International Standard ISO 4355 "Bases for design of structures - Determination of snow loads on roofs", First edition - 1981-08-15.

ISO 4355 Working draft June 1988, Unpublished.

International Standard ISO 2394 "General principles on reliability for structures" Revised edition 1985.

American National Standards Institute: "ANSI A 58.1-1982".
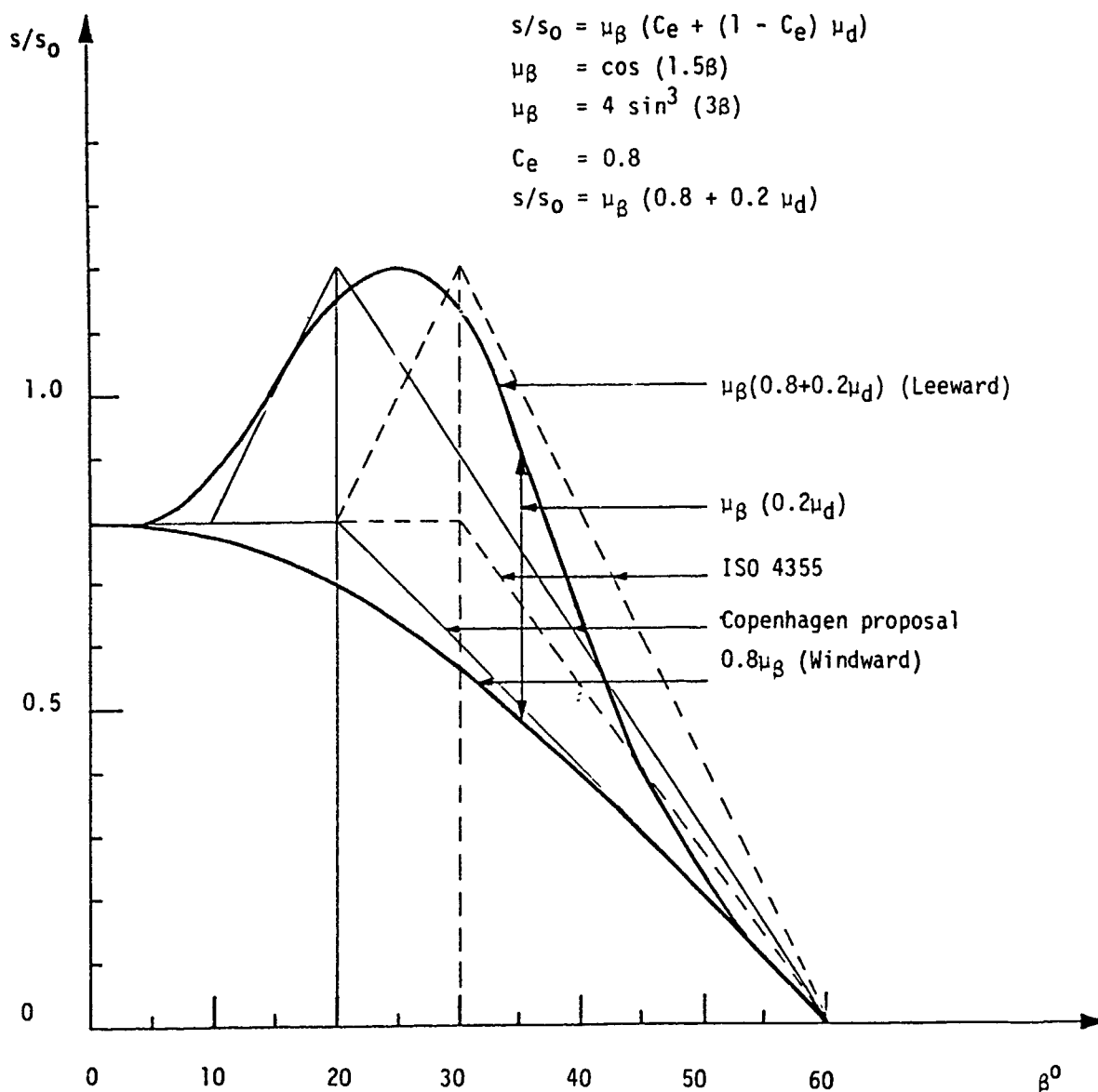
Figure 1   Variation of snow load on pitched roofs as a function
of roof slope

Simple pitched roofs (positive roof slope) [1]

wind direction

Windward side : $s = s_b$
Leeward side : $s = s_b + s_d$

$s_b = s_0 C_e C_t \mu_m \mu_\beta$

$s_d = s_0(1-C_e)C_t \mu_m (\mu_\beta \mu_d)$

s_0 – see Clause 4

C_e – "   " 5.1

C_t – "   " 5.2

μ_m – "   " 5.3

s_b

μ_β

$\mu_\beta = \cos(1.5\beta)$

$\mu_\beta = 0$ for $\beta > 60^o$

s_d

$(\mu_\beta \mu_d)$

$(\mu_\beta \mu_d) = \cos(1.5\beta)4\sin^3(3\beta)$

$(\mu_\beta \mu_d) = 0$ for $\beta > 60^o$
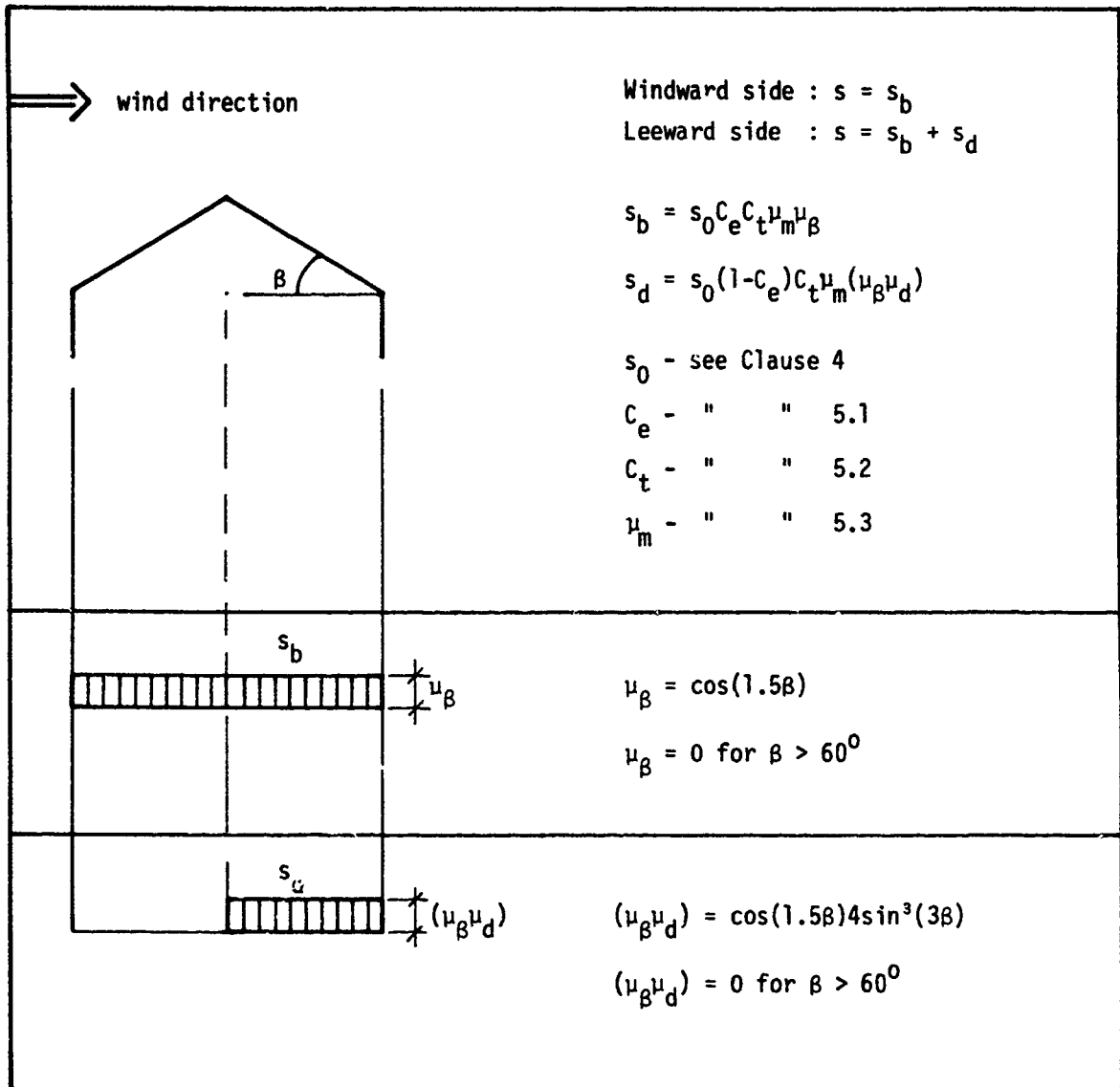
[1]

For asymmetrical simple pitched roofs, each side of the roof shall be treated as one half of corresponding symmetrical roofs.

Figure 2 Distribution of snow load on pitched roofs

Simple flat and monopitch roofs

wind direction

Windward slope : $s = s_b$

Leeward slope : $s = s_b + s_d$

$s_b = s_0 C_e C_t \mu_m \mu_\beta$

$s_d = s_0(1-C_e)C_t \mu_m [0.5(\mu_\beta \mu_d)]$

s_0 - see Clause 4

C_e - " " 5.1

C_t - " " 5.2

μ_m - " " 5.3

s_b

μ_β

$\mu_\beta = \cos(1.5\beta)$

$\mu_\beta = 0$ for $\beta > 60^\circ$

s_d

$[0.5\mu_\beta\mu_d]$

$[0.5\mu_\beta\mu_d] = \cos(1.5\beta)2\sin^3(3\beta)$

$[0.5\mu_\beta\mu_d] = 0$ for $\beta > 60^\circ$
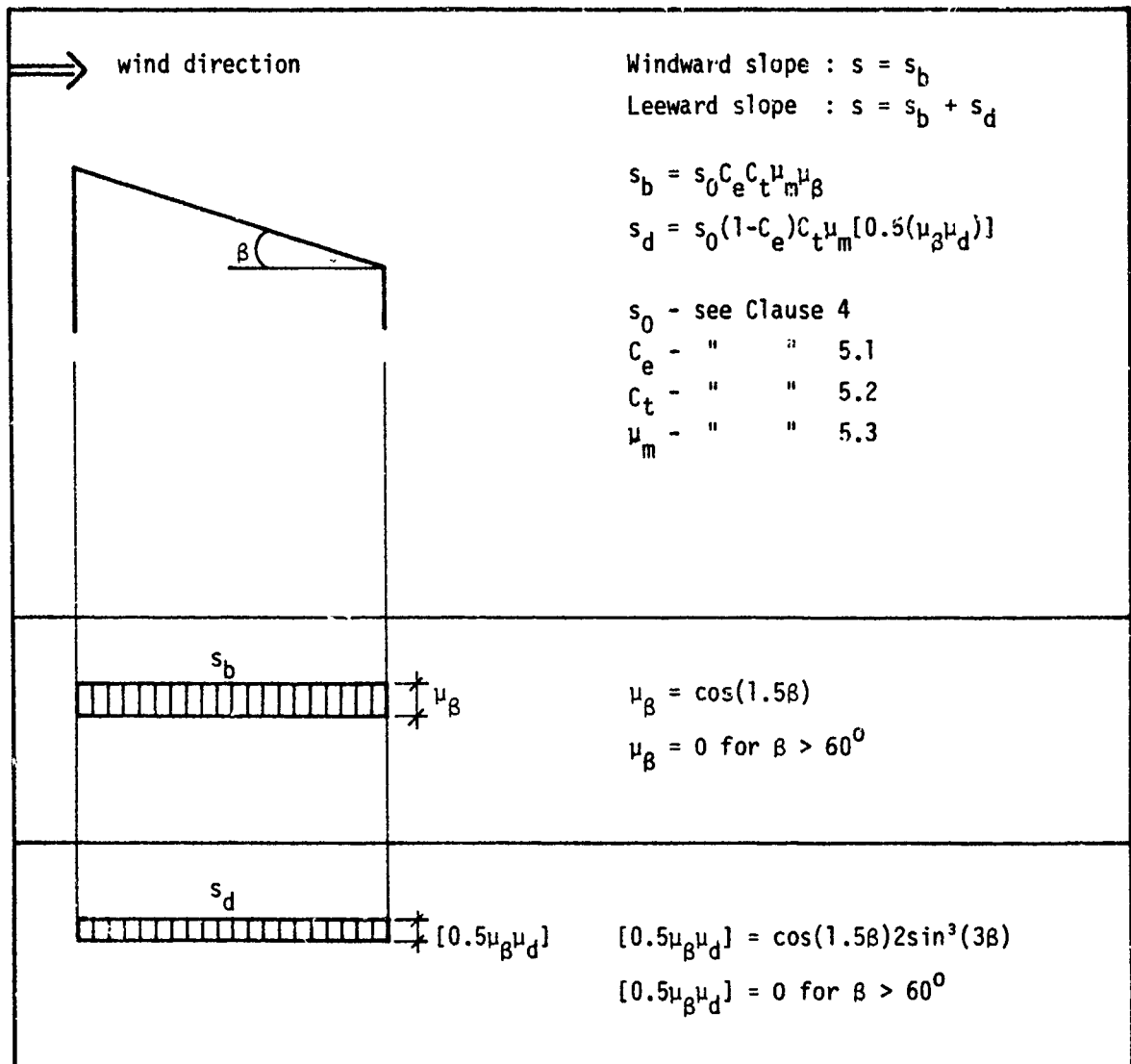
Figure 3   Distribution of snow load on flat and monopitch roofs

Simple or multiple pitched roofs, and hanging roofs
(inner bay negative roof slope) [1]

wind direction

Windward side   : $s = s_b$

Leeward side   : $s = s_b + s_d$

Slide distributed: $s = s_b + s_d + s_s$

$s_b = s_0 C_e C_t \mu_m \mu_\beta$

$s_d = s_0 (1-C_e) C_t \mu_m (\mu_\beta \mu_d)$

$s_s = s_0 C_t \mu_m (\mu_\beta \mu_s)$

$\beta = \dfrac{\beta_1 + \beta_2}{2}$

s_0 - see Clause 4

C_e - "   "   5.1

C_t - "   "   5.2

μ_m - "   "   5.3

s_b

$\mu_\beta = \cos(1.5\beta)$

$\mu_\beta = 0$ for $\beta > 60^0$

s_d

$(\mu_\beta \mu_d) = \cos(1.5\beta) 4 \sin^3(3\beta)$

$(\mu_\beta \mu_d) = 0$ for $\beta > 60^0$

$\mu_\beta \mu_s = \mu_s$, $\mu_\beta = 1$ since snow can not slide away from roof

$\mu_s = [1-\cos(1.5\beta)][2C_e + 4(1-C_e)\sin^3(3\beta)]$

s_s

$\mu_s = 2C_e$ for $\beta > 60^0$

$(\mu_\beta \mu_s)$
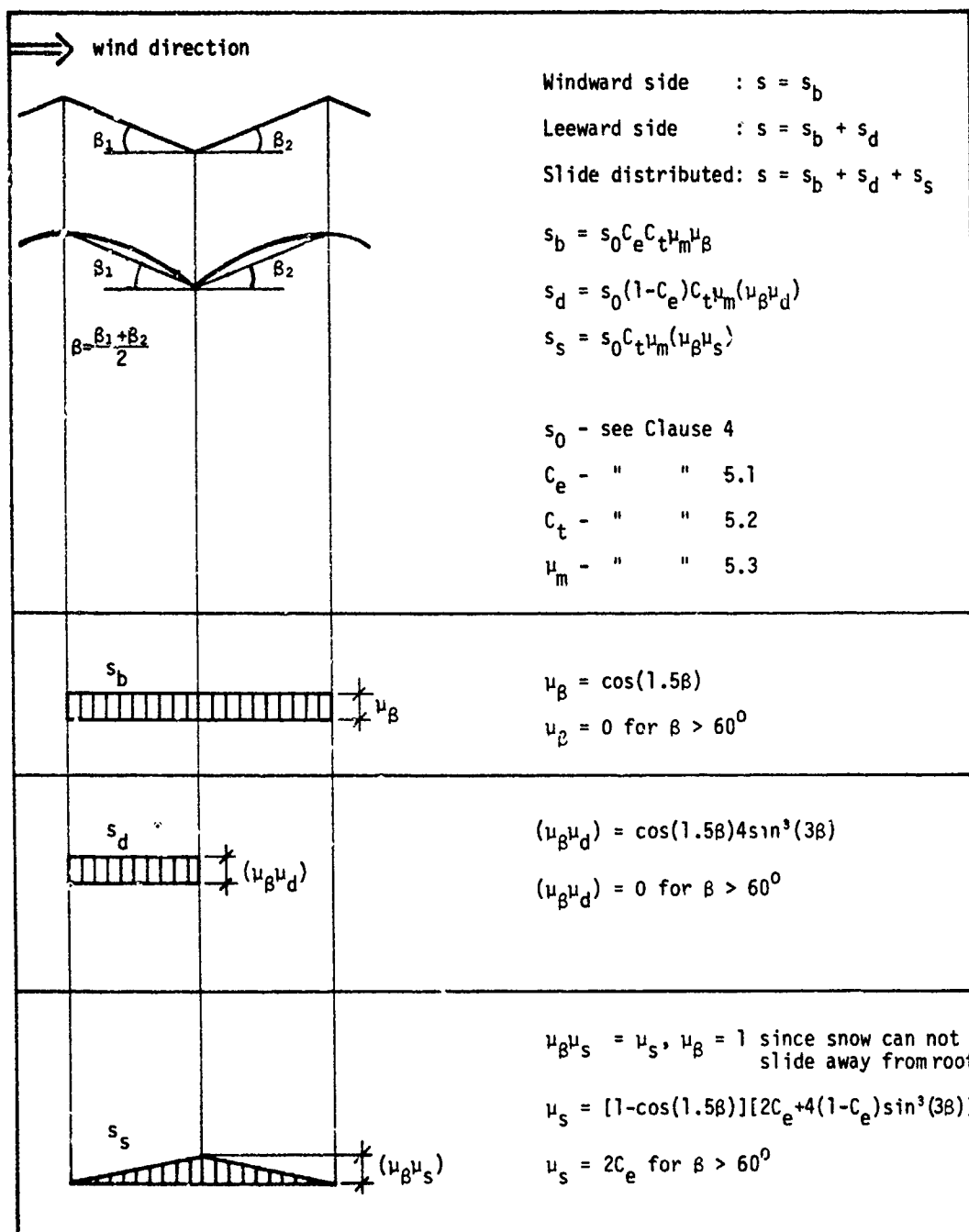
[1]

For hanging roofs of circular or oval plan form the μ-values for the basic and sliding load may be considered as load values along a diameter, whereas the drift load may be assumed to refer to one specific direction.

Figure 4   Distribution of snow load on multiple pitched roofs and hanging roofs

Two-span or multispan roofs

wind direction

Windward side   : $s = s_b$
Leeward side   : $s = s_b + s_d$
Slide distributed : $s = s_b + s_d + s_s$

$s_b = s_0 C_e C_t \mu_m \mu_\beta$

$s_d = s_0 (1 - C_e) C_t \mu_m (\mu_\beta \mu_d)$

$s_s = s_0 C_t \mu_m (\mu_\beta \mu_s)$

s_0 - see Clause 4
C_e -   "   "   5.1
C_t -   "   "   5.2
μ_m -   "   "   5.3

s_b

μ_β

$\mu_\beta = \cos(1.5\beta)$

$\mu_\beta = 0$ for $\beta > 60^0$

s_d

$(0,5\mu_\beta\mu_d)$

$(0.5\mu_\beta\mu_d) = \cos(1.5\beta)2\sin^3(3\beta)$

$\mu_\beta = 0$ for $\beta > 60^0$

s_s

$(\mu_\beta\mu_s)$

$\mu_\beta\mu_s = \mu_s$, $\mu_\beta = 1$ since snow can not slide away from roof

$\mu_s = [1 - \cos(1.5\beta)][2C_e + 2(1 - C_e)\sin^3(3\beta)]$

$\mu_s = 2C_e$ for $\beta > 60^0$
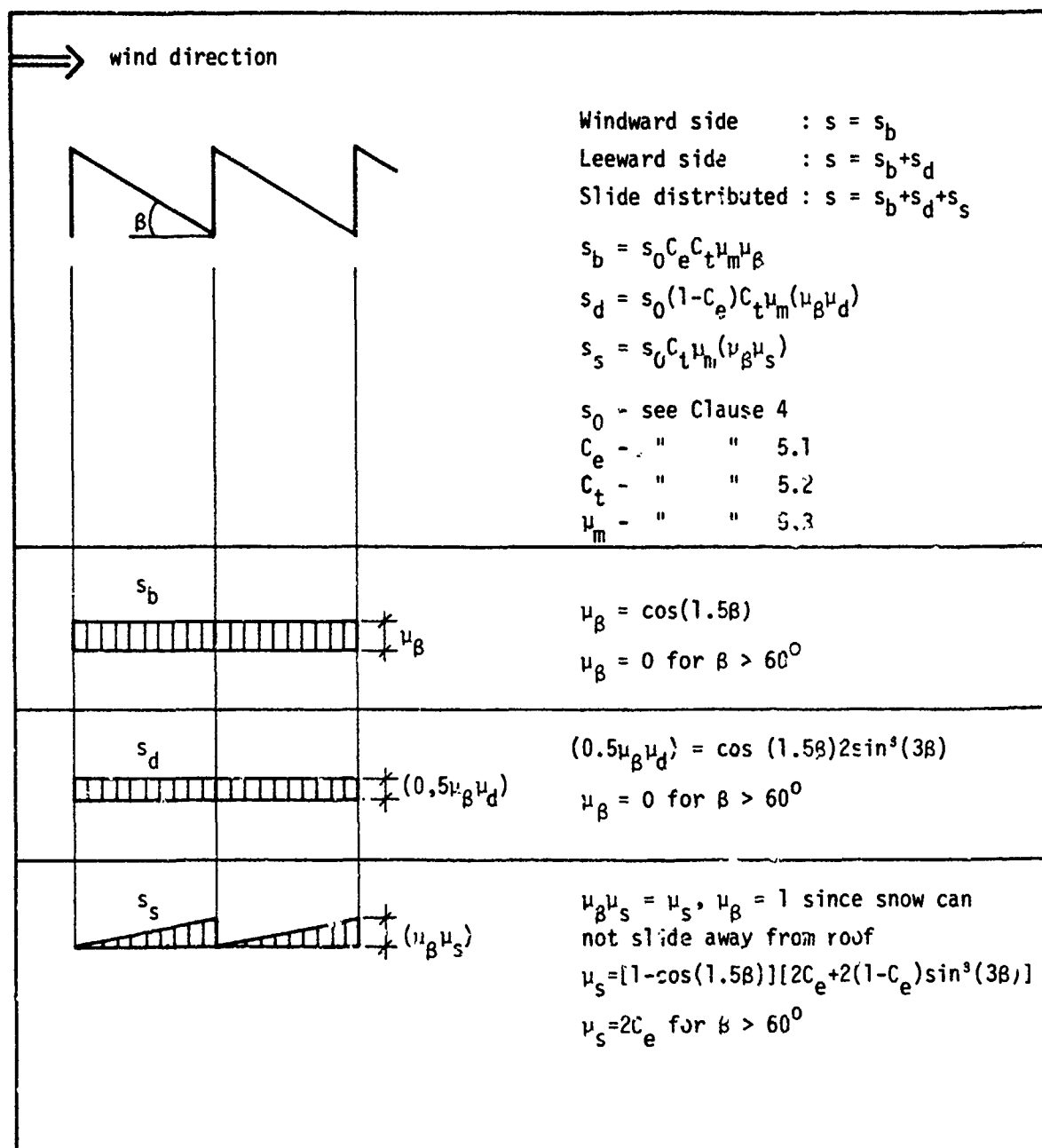
Figure 5   Distribution of snow load on two-span or multispan roofs

wind direction

Windward side : $s = s_b$

Leeward side : $s = s_b + s_d$

$$s_b = s_0 C_e C_t \mu_m \mu_\beta$$

$$s_d = s_0 (1-C_e) C_t \mu_m (\mu_\beta \mu_d)$$

s_0 - see Clause 4

C_e - " " 5.1

C_t - " " 5.2

μ_m - " " 5.3

s_b

μ_β

$$\mu_\beta = \cos(1.5\beta)$$

$$\mu_\beta = 0 \text{ for } \beta > 60^0$$

s_d $(\mu_\beta \mu_d)$

$$(\mu_\beta \mu_d) = \cos(1.5\beta) 4 \sin^3(3\beta)$$

$$(\mu_\beta \mu_d) = 0 \text{ for } \beta > 60^0$$

Alternative load case

$s = s_d$

$(\mu_\beta \mu_d) = 1.0$

$\mu_\beta \mu_d$ $(\mu_\beta \mu_d) = 0 \text{ for } \beta > 60^0$

1) For domes of circular or oval plan form the basic load may be considered as load values along a diameter, whereas the drift load may be assumed to refer to one specific direction.

Figure 6 Distribution of snow load on simple curved roofs, pointed arches and domes

399

Multilevel roofs
(Shape coefficients for lower roof with slope)

wind direction

"Windward side" : $s = s_b$
Leeward side : $s = s_b + s_d$
Slide : $s = c_s$

Upper roof

$s_b = s_0 C_e C_t \mu_m \mu_\beta$

$s_d = s_0 C_e C_t \mu_m (\mu_\beta \mu_d)$

$s_s = s_0 C_t \mu_m (\mu_\beta \mu_s)$

s_0 - see Clause 4

C_e - " " 5.1

C_t - " " 5.2

μ_m - " " 5.3

s_b [1]

$\mu_\beta = \cos(1.5\beta_L)$

$\mu_\beta = 0$ for $\beta_L > 60°$

$(\mu_\beta \mu_d)$ s_d

$\mu_\beta = \cos(1.5\beta_L)$

$\mu_d = \frac{\rho g}{s_0} 0.42[(1+0.12 s_0)\sqrt[4]{l_1}-1]$ [2]

$\mu_d \le \frac{\rho g}{s_0} h \cdot \mu_\beta$, and $\mu_d \le (1-C_e)\frac{l_1}{2h}$

where l_1, h are in metres
s_0 is in kN/m^2
ρg is in kN/m^3

$l_d = 4h \cdot \frac{\mu_\beta s_0}{\rho g}$ [3] , $l_d < 15$ m

$(\mu_\beta \mu_s)$ s_s [4]

$\mu_\beta = \cos(1.5\beta_L)$

$\mu_s = \frac{1.8 h_u}{l_s tg\beta_u}$

$l_s = h_u \sqrt{\frac{2h}{k h_u}} \cos\beta_u (\sqrt{1+k} -1)$ [5]

where
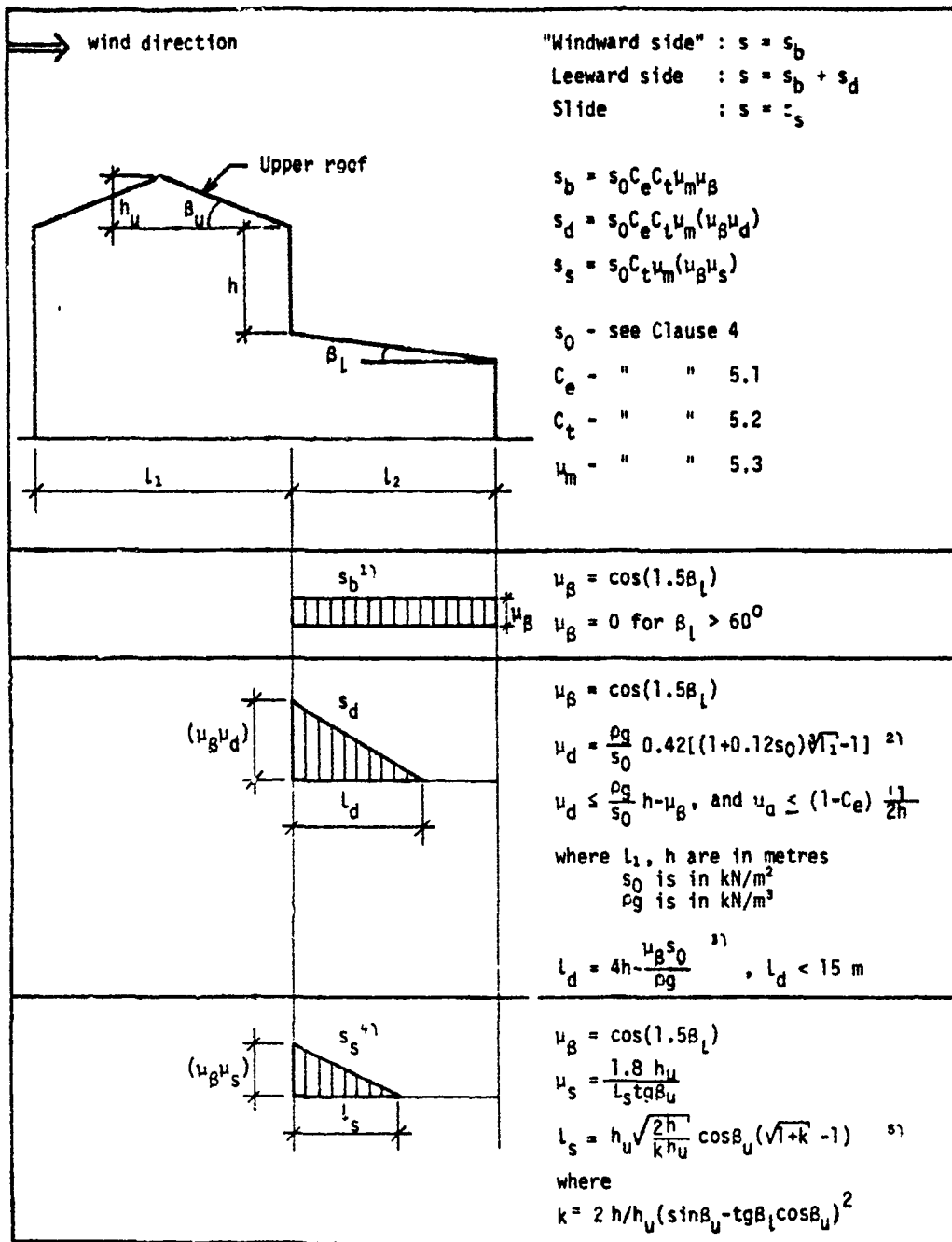
$k = 2 h/h_u (\sin\beta_u - tg\beta_L \cos\beta_u)^2$

[1] For lower roofs with slopes normal to the cross section of the figure the basic load must be determined according to 5.4.5.1-5.

[2] More comprehensive formulas for μ_d are described in annex C

[3] If $l_d > l_2$, μ_d is determined by setting $l_d = l_2$

[4] Impact effects should be considered

[5] If $l_s > l_2$, μ_s is determined by setting $l_s = l_2$

Figure 7   Distribution of snow load on multilevel roofs

Sliding load (and drift load)accumulated on
ground or on lower level roof, acting
against the upper arch or pitched roof [1]

$$s = s_0\mu_s$$

$$\mu_s = 2.0$$

$$l_s = \frac{4\ s_0}{(\rho g)}$$

where
s_0 is in kN/m^2
(ρg) is in kN/m^3
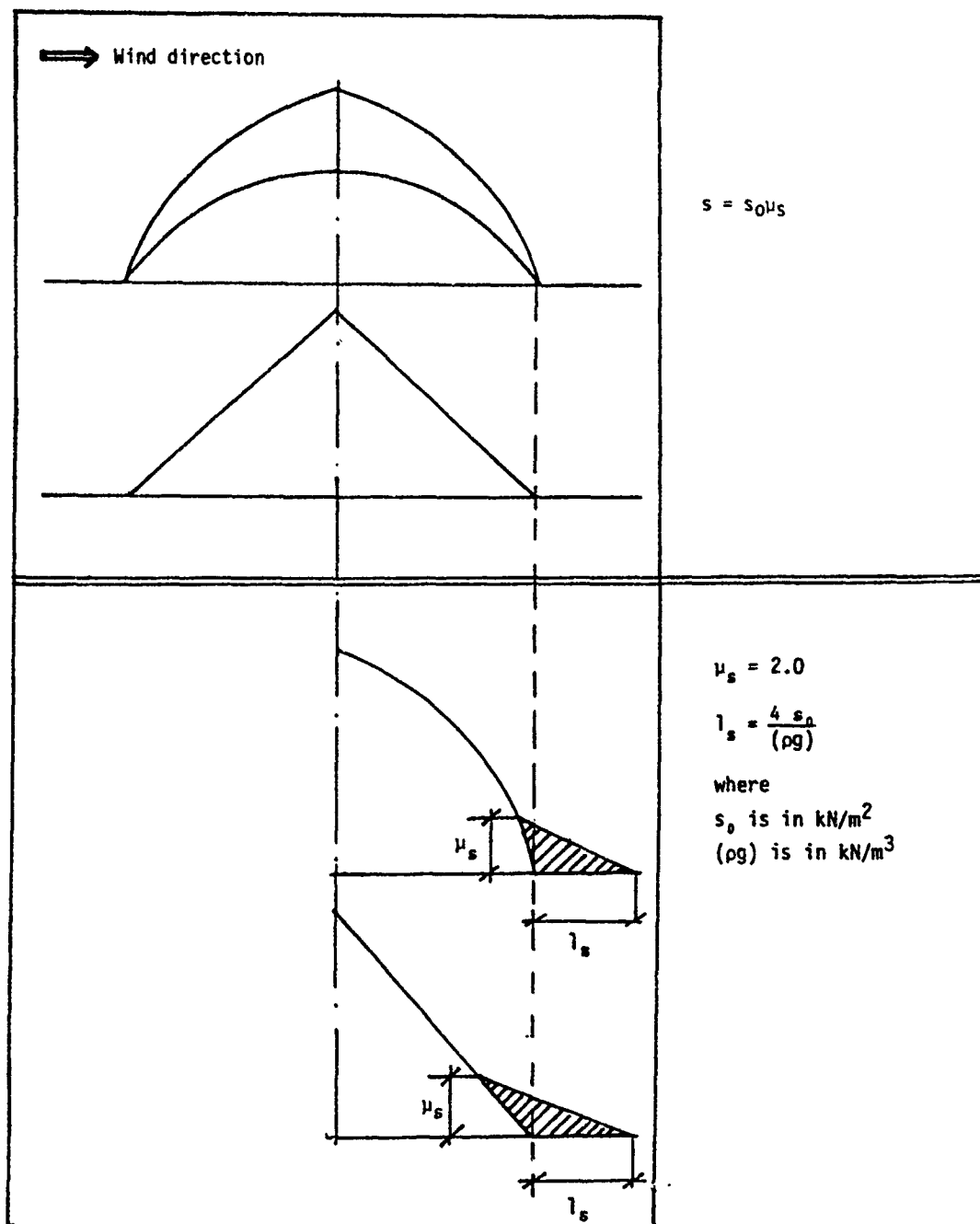
[1] A lower level roof should be checked for the sliding load as an alternative
load case as compared with the load cases of 5.4.5.6. Impact effects should
be considered.

Figure 8   Distribution of sliding load and drift load accumulated
on ground or on lower level roof, acting against an arch
or pitched roof

401

Roofs with local projections and obstructions

Wind direction

Windward side: $s = s_b$

Leeward side: $s = s_b + s_d$

$s_b = s_0 C_e C_t \mu_m \mu_\beta$

$s_d = s_0 C_t \mu_m (\mu_\beta \mu_d)$

s_0 – see Clause 4
C_e – " " 5.1
C_t – " " 5.2
μ_m – " " 5.3

μ_β

$\mu_\beta = \cos(1.5\beta)$

l_d

$(\mu_\beta \mu_d)$

$$(\mu_\beta \mu_d) = \frac{(\rho g)}{s_0 C_t \mu_m}\left(h - \frac{s_b}{(\rho g)}\right)$$

$$l_d = 4\left(h - \frac{s_b}{(\rho g)}\right)$$

$$5\text{ m} < l_d < 15\text{ m}$$

where
h is in metres
s_0 is in kN/m^2
(ρg) is in kN/m^3
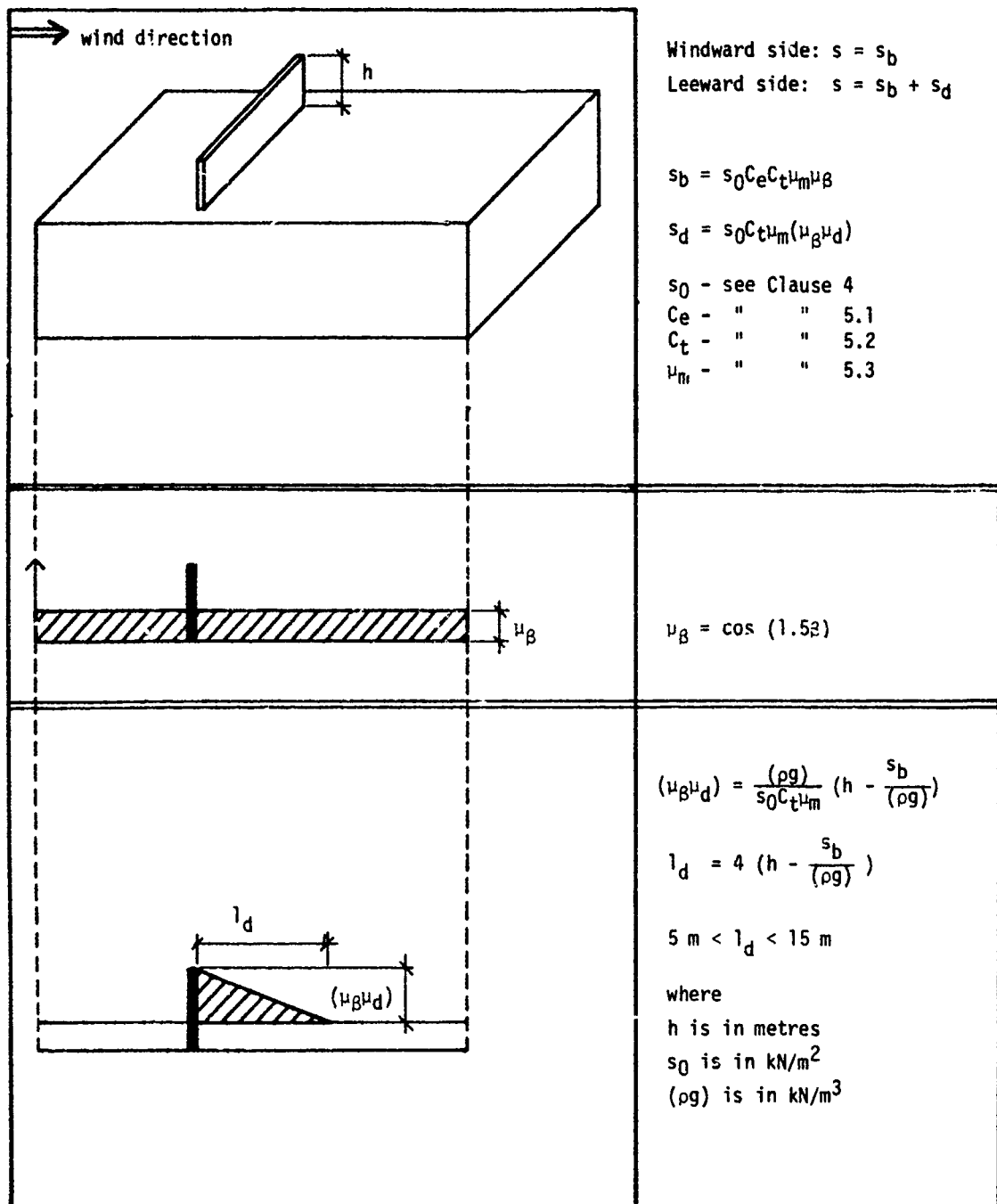
Figure 9   Distribution of snow drift for roofs having local projections and/or obstructions

Developing the Eurocode

Christopher J. Judge[1]

ABSTRACT

At the present time work is proceeding within Europe on the drafting of a code of practice for snow loads. This code is one part of a Eurocode on Actions on Structures which is intended for use with a number of design Eurocodes also being drafted. These Eurocodes are for use within Member States of the European Economic Community.

This paper describes the background against which the code is being drafted. It identifies some of the problems which are being encountered and indicates some of the proposals to overcome them. In particular the paper concentrates on the problems of producing a common basis for determining the snow load on the ground and providing a treatment of snow load shape coefficients which is capable of coping with the varying climates within the Member States.

INTRODUCTION

For a number of years the Commission of the European Communities has been developing codes of practice for use in the design of structures. These codes have become known as the Eurocodes and they cover the principal building materials, see Table 1.

Table 1 Eurocodes for use in Structural Design

Number	Title
1	Common Unified Rules for Different Types of Construction \and Material
2	Common Unified Rules for Concrete Structures
3	Common Unified Rules for Steel Structures
4	Common Unified Rules for Composite Steel and Concrete \Structures
5	Common Unified Rules for Timber Structures
6	Common Unified Rules for Masonry Structures
7	Common Unified Rules for Geotechnics, Design
8	Common Unified Rules for Structures in Seismic Zones

The impetus for this work is the removal of barriers to trade within the Member States of the European Economic Community (EEC), the intention being that a design to any of these codes should be acceptable in any of the Member

I.Head of Loading Section, Building Research Establishment, United Kingdom

States.

The Eurocodes were originally intended to be used with national loading codes and with national appendices giving the partial factors. However, in 1985 it was decided that use of the Eurocodes would be facilitated if there was a Eurocode for loads on structures. Drafting of this code was agreed, it being known as the Eurocode for Actions on Structures (as yet no number has been assigned to it). As it was intended to cover all the loads for the design of buildings and bridges, some 22 potential parts for the code were identified. To meet the agreed target of removing barriers to trade within the Member States of the EEC by 1992 it was agreed to concentrate the drafting initially on the parts required for the design of building structures. These parts are listed in Table 2.

Table 2   Priority Parts of the Eurocode on Actions on Structures

Part No.	Title
1	General Rules
2	Densities of construction materials and stored materials
3	Permanent Actions due to Gravity
6	Imposed Loads on Floors and Roofs
7(i)	Snow Loads
8(i)	Wind Loads (Static)

This paper describes the progress to date in drafting the part on snow loads, identifying where problems are being met in the drafting. The next draft is expected to be available for a meeting in September 1988.

EXISTING NATIONAL CODES WITHIN MEMBER STATES OF THE EEC

Most of the Member States of the EEC have code clauses covering snow loads, see Table 3.

The task of drafting the part of the Eurocode on Actions on Structures dealing with the snow loads thus becomes one of attempting to produce a code which initially gives approximately the same values for a particular region as is given by the national code covering that region. It also needs to be capable of being developed as new data for the various Member States becomes available.

In addition to taking into account the national codes it was also necessary to recognise the International Standard on snow loads. This code, ISO 4355 "Bases for design of structures – Determination of snow loads on roofs", was published in 1981 by the International Organisation for Standardization (ISO). However, it is not a self-contained operational document as it does not contain information on ground level snow loads. Further, although specified for various roof configurations, the snow load shape coefficients were only to be used in the absence of better national data. (ISO 4355 is currently under revision by ISO Technical Committee TC98.)

The first step in drafting the Eurocode was a study of the content of the various national codes. These are summarised in the following

sub-sections.

Table 3 Snow Loading Codes from Member States of the EEC

Country	Code	Title
Belgium	NBN B 51-001 1977	Steel structures (Clause 1.1.4)
Denmark	DS 410 1982	Code of practice for loads for the design of structures (Section 16.3)
Eire	as UK	
France	Fascicule No 61 Titre IV - Section 7 (N84) 1985	Snow loads on structures
Germany	DIN 1055 Part 5 1975	Design loads for buildings; Live loads; Snow load and ice load
Greece	German Standard used?	
Italy	CNR 10012/85 1985	Rules for the evaluation of forces on structures (Section 6)
Luxembourg	choice between Belgian, French or German codes	
Netherlands	NEN 6702 1985	Technical principles for building structures TGB 1986 - Loads (Section 7.7.2)
Portugal	Decreto lei 235/83 31 May 1983	Safety and loading regulations for the structures of buildings and bridges (Section VI)
Spain	Norma MV 101 1962	Actions on buildings (Chapter 4)
United Kingdom	BS6399 Part 3 1988	Code of practice for imposed roof loads

Belgium

Belgium is treated as a single region with a basic snow load of 0.4 kN/m^2. For altitudes over 200 metres this load is increased linearly to 0.7 kN/m^2 at an altitude of 900 metres. For roof slopes greater than 50 degrees it is not necessary to consider snow loads. There is no

additional treatment required for drifting of snow on roofs.

Denmark

Denmark is treated as a single zone with a basic snow load of
0.75 kN/m^2. For roof slopes greater than 30 degrees this value decreases
linearly to zero for a slope of 60 degrees (no reduction is permitted on
sloping roofs with projecting parts that prevent the snow from sliding down).
Half the uniform load is to be treated as a fixed action while the other half
is to be treated as a free action. For drifting of snow a weight density of
3.0 kN/m^3 is to be assumed with a depth equal to half that of the 'pocket',
subject to a maximum of 1 m (there are no diagrams illustrating where
drifting can occur). An additional limitation is that the load in the drift
should not exceed that equivalent to the area on the roof from which the
drifted snow will come, loaded with a uniformly distributed load of
0.75 kN/m^2. There is no correction for altitude.

France

This code is based on the ISO standard with the exception that it goes a
stage further and identifies a number of different loading situations related
to the severity of the wind. France is divided into four types of region
with a specified snow load intensity for each for altitudes less than 200
metres. For altitudes between 200 metres and 2000 metres three linear
equations are given for calculating the appropriate snow load; the equations
correspond to altitudes between 200 metres and 500 metres, between 500 metres
and 1000 metres, and between 1000 metres and 2000 metres. The snow load on
the roof is given by the product of the snow load intensity and a shape
coefficient. Unlike the ISO standard separate equations are given for roofs
with devices to inhibit snow sliding from the roof. Additionally, as already
referred to, several snow patterns are given for each roof depending on the
loading situation. The ground level snow loads correspond to a 50-year
recurrence interval.

Germany

Four different zones within Germany are identified with the snow loads
related to altitude for each. The snow load is given as the uniform load on
a flat roof and is assumed to be constant up to an altitude of 200 metres;
for altitudes in excess of 1000 metres the appropriate load is to be
specified by the local Building Authority in conjunction with the German
Meteorological Service. Reduction coefficients for roof pitch are given in
tabular form. Although reference is made to drifting of snow on roofs no
snow load shape coefficients are given. The snow loads correspond to the 95%
fractile of the statistical distribution of annual maxima values over a
30-year observation period. When considering drifted snow a weight density
of 5.0 kN/m^3 is recommended.

Italy

For localities having an altitude of not more than 2000 metres, three
zones are identified. Within each zone the ground level snow load intensity
is calculated from an equation which takes into account the altitude. Two
equations are given for each zone depending upon whether the altitude is
greater or less than 750 metres. The calculated loads have a recurrence
interval of 50 years. The load on the roof is calculated from the product of

this load, a shape coefficient and a factor to take into account the desired return period and the duration of the snow on the ground. The shape coefficients are similar to those given in the ISO Standard.

Netherlands

The country is treated as a single zone with a ground level snow load intensity of 0.7 kN/m^2; there is no altitude correction. The load on the roof is calculated from the product of the ground level snow load intensity and a shape coefficient. The shape coefficients are similar to those in the ISO Standard.

Portugal

In Portugal it is only necessary to consider snow loads at locations having altitudes in excess of 200 metres in specified districts. The appropriate ground level snow load is calculated from a linear equation involving the altitude of the site. The roof load is calculated from the product of the ground level snow load intensity and a shape coefficient. The shape coefficients are similar to those in the ISO Standard.

Spain

Spain is treated as a single zone with the snow load on horizontal surfaces specified in a table according to the altitude. For pitched roofs the snow load is taken as the product of the tabulated load and the cosine of the roof slope. For areas on a roof where snow accumulation may occur, this has to be allowed for using an appropriate snow weight from three specified. There are no diagrams showing where snow accumulation may occur. To allow for assymmetric loads a maximum discrepancy between loads on distinct parts of a roof of 30 kg/m^2 is quoted.

United Kingdom

The UK has a new code of practice on imposed roof loads which contains a comprehensive treatment of the snow loads. It is based on the ISO Standard. Ground level snow load intensity is obtained from isopleths on a map of the UK. An altitude correction is necessary for site locations higher than 100 metres. The load intensities are quoted as being values with a mean recurrence interval of 50 years. The roof snow load is obtained from the product of the ground level snow load intensity and a shape coefficient, with provision for an adjustment of recurrence interval if appropriate. The shape coefficients are based on the ISO Standard but the limiting conditions have been adjusted to take account of maximum conditions known to have occurred in the UK. In a similar manner to the French code, separate load cases are required to be considered corresponding to different wind conditions.

PROPOSED FRAMEWORK FOR THE PART OF THE EUROCODE ON SNOW LOADS

Format

Several of the national standards have been produced taking account of the International Standard. Further, ten of the twelve Member States of the EEC had approved it during voting within ISO. It was therefore a logical choice to base the format for the first draft on that adopted in the International Standard. By this it is meant that the snow load on the roof

should be derived by multiplying the snow load on the ground (s_0) by a snow load shape coefficient (μ_i). (It is known that ISO 4355 is under revision and this work will be taken into account as that code passes through its various draft stages.)

To be an operational document the Eurocode must contain sufficient data to allow the determination of both s_0 and μ_i. Both the initial deposition and any subsequent movement of snow on a roof are affected by the presence of wind. However, there are little data on the combined action of wind and snow to allow a direct statistical treatment. In design this is normally overcome by considering one or more critical design situations. These are usually snow deposited when no wind is blowing and snow deposited when the wind speed is sufficient to cause drifting, but without quantifying the precise wind speed. In areas where snow accumulates from several falls of snow these two design situations are usually combined in a single load case but in maritime type climates it may be more appropriate to consider them as separate load cases.

Scope

The scope of the code will be limited to the calculation of snow loads on roofs which occur from natural conditions. It will be applicable for use in all Member States of the EEC but will exclude regions where snow is present all the year and sites at altitudes higher than 2000 metres above mean sea level.

It is not intended that it will give guidance on impact snow loads resulting from snow sliding off a higher roof (dynamic snow loads) as there are little data available. This load will be a function of the amount of snow which slides off the roof as a single entity, the velocity at which it leaves the roof and the amount by which it falls. If likely to be critical it is assumed that it will be avoided by the use of some form of artificial restraint, eg snow fences.

The loading which could result from accumulation of melt water if snow and ice blocks the gutters, and any local accumulation of melt water which could result from melting of snow on some parts of the roofs and not on others due to differences in internal temperature and insulation will not be covered by the Eurocode. It is recognised that these loads can be considerable but it is thought to be better for the roof to be designed such that accumulation of melt water does not occur.

The code will not give any information on the change in wind load due to the presence of snow. However, the combination of design values for snow loads and wind loads (determined assuming no snow) usually results in a conservative design.

Loads for cleaning and maintenance of roofs will not be given in the code, neither will the minimum imposed loads necessary to cover other environmental effects such as ice, rainfall and temperature. These will be contained in Part 6 of the Eurocode on Actions on Structures.

Definitions and Symbols

Those adopted for the Eurocode will be similar to those given in

ISO 4355. However, additional subscripts will probably be included to help avoid confusion with symbols likely to be used for other parts of the Eurocode, eg the part on wind loads.

Method of assessment of snow load on roof

The snow load on the roof at a particular location will be dependent upon several parameters, including the amount of snow which has fallen, the wind speed and direction at that point (which is dependent upon the shape of the roof and the general wind speed and direction), the shape and size of the part of the roof up-wind of the point (and to a lesser extent the shape and size of the roof down-wind), the heat loss through the roof, the air temperature at the roof and the amount of sunlight.

There are insufficient data to allow the snow load to be determined statistically and therefore a procedure has been developed which allows the principal parameters to be taken into account. This procedure involves using the snow load on the ground, which it is assumed would have been present in the absence of the building structure under no wind conditions, and a number of snow load shape coefficients. The snow load shape coefficient is the assumed ratio of the snow load on the roof to the undrifted snow load on the ground. There are different snow load shape coefficients for different wind conditions. By using a few idealised shapes to model the snow load pattern on the roof, eg uniformly distributed load, variably distributed load, it is possible to obtain estimates of the likely critical snow loads on the roof at any point, and therefore the likely critical snow loads on any tributary area. (Here a variably distributed load is defined as a load which has a variable distribution in at least one direction. When dealing with snow loads the variation is usually a linear decrease away from the face of the obstruction causing the drift.) Several values for the snow load on the roof at a point may have to be calculated for different critical conditions.

Some of the differences between the national snow load clauses within the CEC countries can be attributed to the different types of climate within different parts of Europe. It is therefore proposed that Europe should be subdivided into four regions. These are:

REGION A - where snow seldom falls;

REGION B - where snow normally falls only once or twice a year so that
the maximum snow load on the ground results from a single
fall of snow;

REGION C - where snow normally falls more than once a year so that the
maximum snow load on the ground results from accumulation
from several falls;

REGION D - where snow is present all the year.

The method for calculating the snow load on the ground may be different in some of the regions. Further, the limiting values for the shape coefficients may be different in some of the regions.

Characteristic value of snow load on the ground

The snow load on the ground is that assumed to occur in perfectly calm conditions. It is usually determined from records of snow load or snow depth measured in a well sheltered area: ISO 4355 recommends in a deciduous

forest! If snow depths are measured an appropriate value for the density of the snow is required. Values currently used include 219 kg/m³ (Germany), 150 kg/m³ (France and UK) and 120 kg/m³ (Spain).

Several countries have determined characteristic values for the snow load on the ground based on a statistical analysis of meteorological data. Germany has a characteristic value based on an annual probability of occurrence of 0.05; France, Italy and UK have characteristic values based on an annual probability of occurrence of 0.02 (however, Italy factors this by 1.5 for designs with expected lives of 50 years or greater). The characteristic value for the snow load on the ground has been defined initially for the Eurocode as the value with an annual probability of being exceeded of 0.02. The variation of this snow load with geographical location will be given in map form.

In most National Codes the same value for the snow load on the ground at a specific location is specified for all altitudes up to a certain height (usually 100 or 200 metres). For the Eurocode it is proposed that the snow load on the ground should be given as a constant for any location for all altitudes up to 200 m.
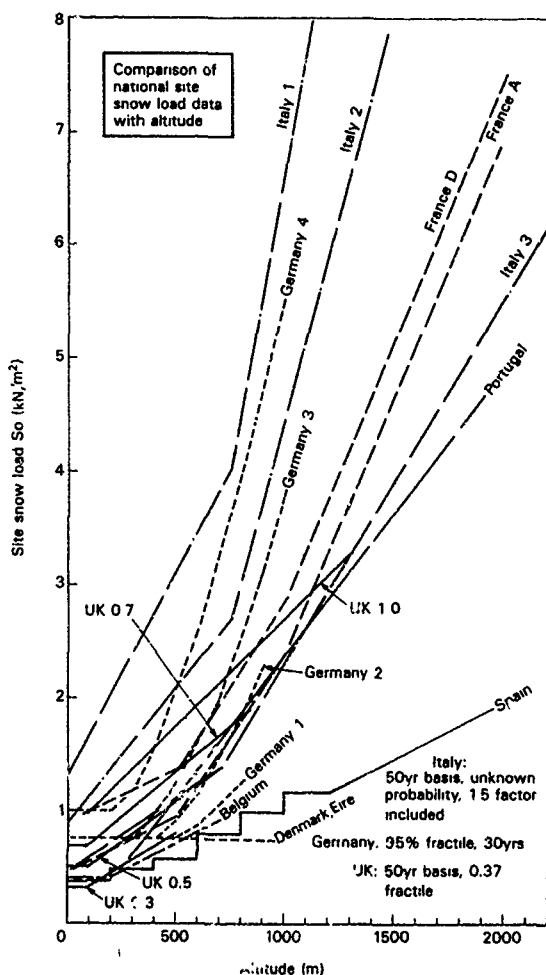
Figure 1 Comparison of national site snow load data with altitude

410

Corrections to the basic value for the effects of altitude are usually given in mathematical form. A visual comparison of the variation of site snow load data with altitude, Figure 1, shows that there is apparently little agreement on how the snow load on the ground varies with altitude. However, there are some similarities and it would appear possible and also highly desirable to replace the random curves with a Eurocode family of curves. This would allow a specific line to be used with the known altitude of the site to obtain the appropriate characteristic value for the snow load on the ground. By taking care in the preparation of the map of Europe it should be possible to ensure that similar ground level snow loads are obtained as are currently calculated by using the existing National Codes.

Initially the calculation of the snow load on the ground will probably be based on existing practice. In the future, calculation methods for determining the snow load on the ground in the specific regions A - D are likely to be agreed. In region A, without snow fall in several years, the characteristic value will probably have to be determined from the parent distribution of snow load or depth and not the extreme value distribution. In region B there is similarly unlikely to be sufficient extreme value data to justify the use of an extreme value analysis. In region C there is likely to be sufficient data to allow the use of an extreme value analysis to obtain the characteristic value. This data is likely to be annual or seasonal maxima values. In region D it is assumed that snow will be present all the year and, while a conventional extreme value analysis should be adequate, it would be advisable to consult specialised local knowledge. This region is not considered to be covered by this code.

Snow load shape coefficient

Several different snow load shape coefficients must be considered for every design. These relate to different climatic conditions before, during and after the snow fall. The different snow deposition patterns are:

(1) With no snow on the ground initially, snow falling in the absence of wind will result in a uniform layer being deposited over all roof surfaces. The mean load intensity of this uniform layer will rarely equal that on the ground as it will be reduced by heat loss from within the structure.

(2) Following condition (1), if the wind starts to blow, snow could be redistributed on the roof or even blown off it. Any resulting redistributed snow pattern will be dependent on the strength and direction of the wind.

(3) With no snow on the ground initially, snow falling in windy conditions is likely to be deposited in patterns similar to condition (2).

(4) Following conditions (2) or (3) it is conceivable that the wind direction could change significantly, possibly resulting in further redistribution. This condition is rarely critical.

(5) With snow already covering the ground (and roof) snow may fall. This may be under zero wind conditions, in which case a uniform layer of snow will be deposited on the snow already present. Alternatively it may fall under windy conditions, resulting in the falling snow

411

being redistributed. Some redistribution of the original snow could also occur.

All the above conditions do not have to be considered separately. Condition (1) will apply in all regions. Conditions (2), (3) and (4) are only likely to be critical in areas where the maximum load results from a single fall of snow (regions A and B). Condition (5) will be critical for areas where snow accumulates from multiple falls of snow.

The reason for separating the single fall of snow areas from the multiple fall of snow areas is that the snow load shape coefficient is likely to be less in the multiple fall areas, as different wind speeds, including zero wind, and different wind directions accompanying the falling snow will tend to give a more uniform distribution. The exceptions to this are areas where local topography channels the wind in a particular direction.

It is proposed that values of snow load shape coefficients should be given for only three groupings of the above conditions. To avoid confusion they have been renamed.

Condition X relating to a snowfall in the absence of wind.

Condition Y relating to snow and wind interactions in areas where only single falls of snow are likely.

Condition Z relating to snow and wind interactions in areas where snow is likely to accumulate from several falls of snow.

Condition X and Y must be checked independently for all roofs in regions A and B while condition Z must be checked for all roofs in region C. In areas where local topography channels the wind in one particular direction, this could lead to an underestimate of the local snow loads in region C.

In the clauses from which the snow load shape coefficients are calculated, the limiting values applying to the single fall of snow regions is likely to be based on the new UK code. It is recognised that these are exceptional values, although they are based on known cases in the UK, and they may need to be modified for some areas in regions A and B if the climate is less windy than in the UK. The limiting values for the multiple fall of snow regions are likely to be based on ISO 4355.

CONCLUSION

This paper has shown that, although there are significant differences between the existing code clauses on snow for the Member States of the EEC, it should be possible to produce a harmonised snow code. In this code it is likely that Europe will be divided into a number of regions, each region associated with a different type of climate. Within each region the snow load on the ground is likely to vary. Initially this variability is likely to be based on existing meteorological data but it is hoped to determine a specific means of collecting and analysing meteorological data so that in the future a common basis will be used for determining ground snow load in each region. The determination of the snow load shape coefficients is likely to be similar for each region but the limiting values may be different. Further the number of load cases to be considered may be different for each region.

Changes Coming in Snow Load Design Criteria

Wayne Tobiasson[1]

ABSTRACT

Sponsorship of ANSI Standard A58.1-1982, "Minimum Design Loads for Buildings and Other Structures" has recently been transferred to the American Society of Civil Engineers. ASCE expects to publish a new version of the A58 Standard in 1989.

For the past two years the A58 snow loads subcommittee has been active in updating the snow load design criteria in that Standard. Some revisions have been made to the ground snow load maps in Minnesota and the Dakotas. Sliding snow provisions have been changed and drift load calculations have been expanded to include an appreciation for the length of the upwind roof.

INTRODUCTION

I chair the American Society of Civil Engineers (ASCE) subcommittee tasked with updating the snow load design criteria in American National Standards Institute (ANSI) Standard A58.1-1982 "Minimum Design Loads for Buildings and Other Structures." Ronald Sack, Michael O'Rourke, Robert Redfield, Arthur Held, Louis Steyaert, Donald Taylor, William Schriever, Dale Perry, Lynn Leslie and Robert Albrecht also serve on that subcommittee.

The objective of this paper is to overview the changes in snow load design criteria that will be incorporated into the new version of that Standard to be published by ASCE in 1989.

Because the A58 Standard is in U.S. customary units, this paper presents information in those units. Convert to SI units as follows:

Multiply	by	To convert to
feet	0.3048	meters
psf	47.88	Pa
pcf	16.02	kg/m^3

Changes have been made in four areas:

* Ground load maps
* Balanced and unbalanced snow loads
* Sliding snow loads
* Drift snow loads

---

[1]. Research Civil Engineer, U.S. Army CRREL, Hanover, New Hampshire, USA

Since the ANSI A58 document was published in 1982, several designers have expressed concern about the high mapped values in portions of the north central states. In response to those concerns, the Cold Regions Research and Engineering Laboratory (CRREL) comprehensively reexamined the meteorological data base in that area. As a result of that reexamination, mapped values of the 50-year mean recurrence interval ground snow load have been reduced somewhat in portions of Minnesota and the Dakotas. Figure 1a shows that portion of the 1982 map and Figure 1b shows the changes made in that area.
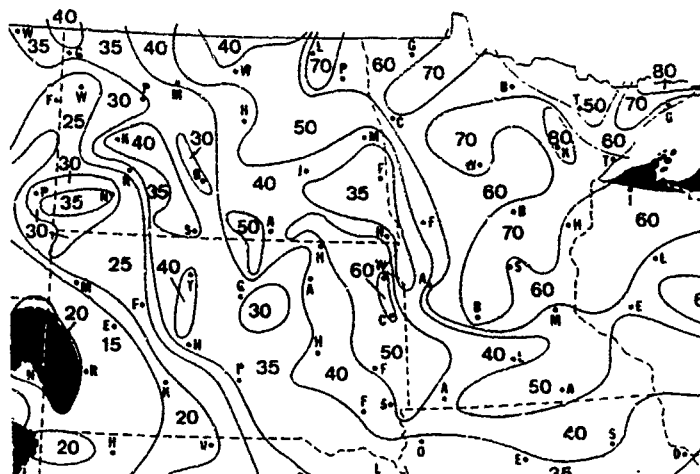
a. A portion of the map in the A58-1982 Standard.
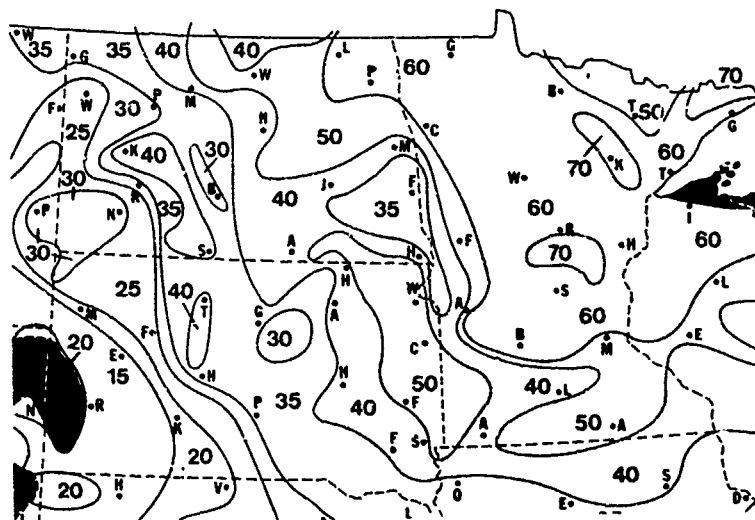
b. Changes to the A58-1982 map.

Figure 1. Ground snow load values, which have changed in Minnesota and the Dakotas.

The meteorological information on which the snow load maps in the A58 document are based is current through the winter of 1979-80. Work is underway at CRREL to update that data base through the winter of 1987-88. That update will not be completed in time to be included in the 1988 version of the National Standard but it will be published before the next update. To allow use of the new information or other updated studies, a phrase is being added to indicate that if statistical studies which contain more recent meteorological information are available, they should be used.

BALANCED AND UNBALANCED LOADS

Several questions have been raised since 1982 about combining balanced and unbalanced snow loads. Since balanced and unbalanced loads are alternative loads, a statement has been added to indicate that they should be considered separately.

SLIDING SNOW LOADS

As a result of recent research on sliding snow, the values of C_s have been reduced for unobstructed slippery surfaces. For warm roofs (i.e. those with C_t equal to or less than 1.0) the value of C_s will decrease linearly from 1.0 to 0.0 as the slope increases from 0 to 70 degrees. In the past, C_s for such roofs remained at 1.0 from 0 to 15 degrees and then began to decrease. For cold roofs (i.e. those with C_t greater than 1.0) C_s will decrease from 1.0 at 15° instead of remaining at 1.0 up to 30°. Figure 2a shows the 1982 slope factors and Figure 2b shows the new factors.
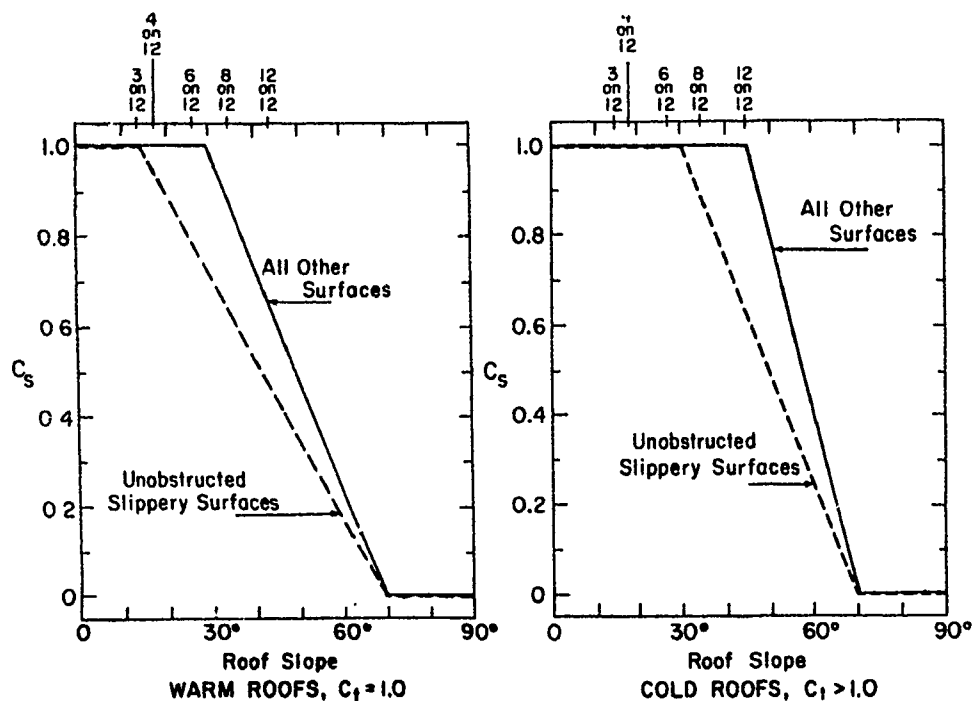
a. Slope factors in A58-1982.

Figure 2. Slope factors for slippery surfaces.
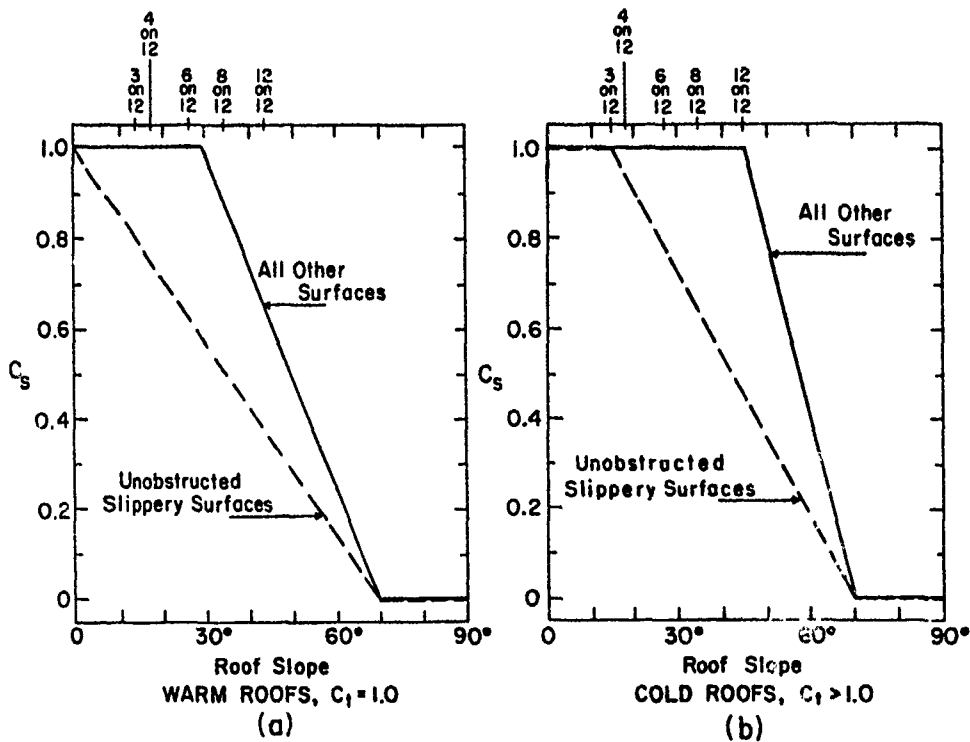
Interpolation is inappropriate

b. Slope factors, as changed.

Figure 2 (cont'd). Slope factors for slippery surfaces.

Statements have been added to indicate that (1) the unobstructed slippery surface values should only be used if there is sufficient space available below the eaves to accept the sliding snow; (2) interpolation between the "unobstructed slippery surfaces" and "all other surfaces" curves is inappropriate for situations where some but not all the requirements of an "unobstructed slippery surface" are met and; (3) load from snow that slides onto a lower roof should be added to the balanced snow load on that roof.

No changes have been made to the relationship between C_s and slope for "all other surfaces" (Figs. 2a and 2b).

DRIFT SNOW LOADS

Several changes have been made to drift loads as a result of recent research and feedback from the design profession.

In the past, drifts were not considered if the ground snow load was 10 psf or less. Several southern designers have argued convincingly that drifts should also be considered where the ground snow load is 10 psf. That recommendation has been adopted.

416
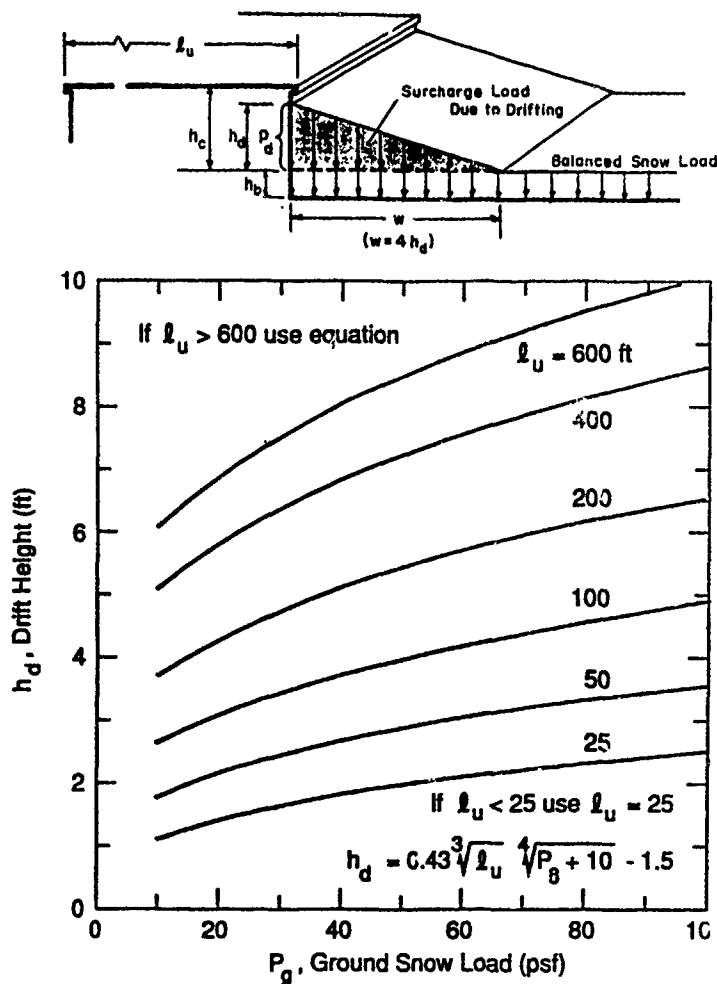
Figure 3. Drift surcharge height (h_d), which
will be a function of the ground snow load
(P_g) and the length of the upwind roof (i_u).

Drift loads have been related to the length of the roof upwind of the
drift. Because the resulting relationship is complex, it will be presented
graphically as well as mathematically as shown in Figure 3.

The relationship between drift density and ground snow load has been
improved to avoid the three-step function of the past (Fig. 4). The maxi-
mum density of drift snow will be limited to 35 pcf.

In the past, the width of the drift varied from 3 to 4 times the maxi-
mum height of the drift. That will change to a constant width of four
times the maximum drift height.

The height of drifts around the perimeter of a building with a parapet
will be limited to half the height of drifts in the lee of obstructions.

417
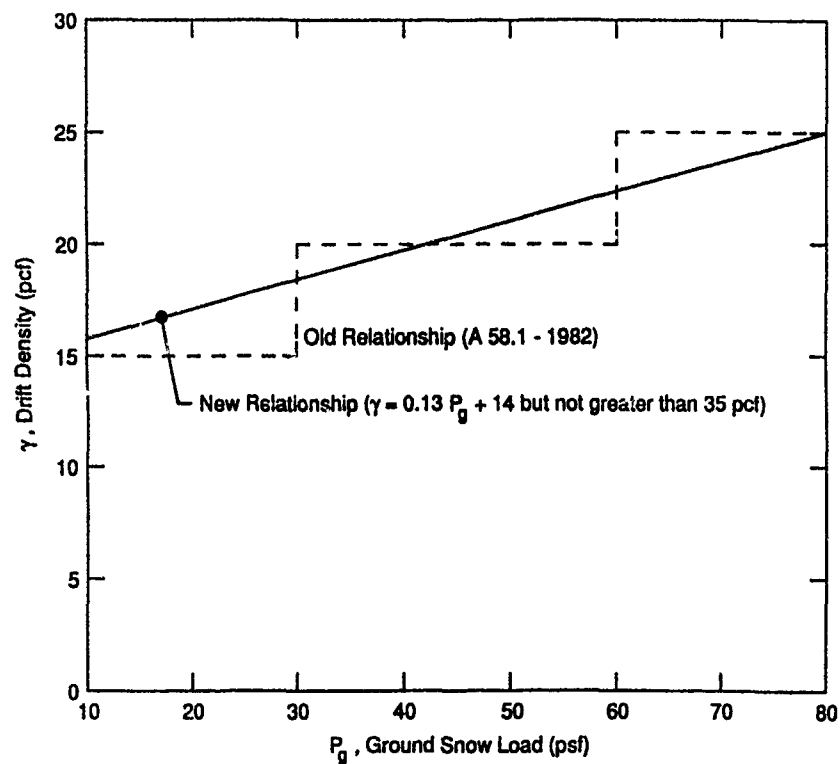
Figure 4. New drift density relationship, which is linear.

REFERENCES

References will be added to the Standard to support the above changes.

Snow Loads on Roofs in East European Standards
and Codes of Practice

Jerzy A. Zuranski[1]

ABSTRACT

The paper deals with the snow loads codes of practice in East Euro-
pean countries of the Council for Mutual Economic Aid /CMEA/. Early
assumptions for standardization of snow loads in this region are
shortly presented as a historical background. Unification of snow
load values in some CMEA countries after the second World War is
also shown.
Present state of snow load standards is discussed with special
attention paid to the limit state design philosophy used in codes,
methods of establishing ground snow load characteristic and design
values as a reference values as well as shape factors and other
factors in standards of USSR, Poland, Czechoslovakia, German Demo-
cratic Republic, Hungary, Rumania and Bulgaria.
The consequences of the adaptation of ISO Standard for snow loads
are also discussed.

INTRODUCTION

The development of standards and codes of practice results in the
trends to unifying them over some territories. These trends are especially
distinct within the economic or political regional organizations. It is
explicity seen in Europe where two main organizations border: the European
Economic Community /EEC/ and the Council for Mutual Economic Aid /CMEA/.
This paper outlines the present state of codes of practice and standards for
snow loads in the countries belonging to the CMEA. Although most of them are
situated in central Europe /Fig.1/ they belong to the East European organiza-
tion and hence the paper deals with the East European codes of practice.

HISTORICAL BACKGROUND

A hundred years ago, in 1886, a civil engineering professor at the Lvov
Technical University, Maksymilian Thullie, wrote in his book on statics
/Thullie 1886/:

> "In our countryside snow layer on roofs is usually not higher than
> 0.6 m /.../. Taking this value and assuming that snow is approxi-
> mately 8 times lighter than water is, we receive /.../ a round
> value of snow load 80 kg/m^2".

This definition certainly reflects the widespread opinion on snow load
in this part of Europe at the end of XIX century.

The alternate national status of this countryside during the past
explains, to some extent, the territorial range of this opinion.

1/ Institute for Building Technology, Warsaw, Poland

A hundred years ago this countryside belonged to the Austro-Hungarian Kingdom /being a part of old territory of Poland before 1772/. After the World War I it belonged to Poland, after the World War II it belongs to USSR /Fig.1/.
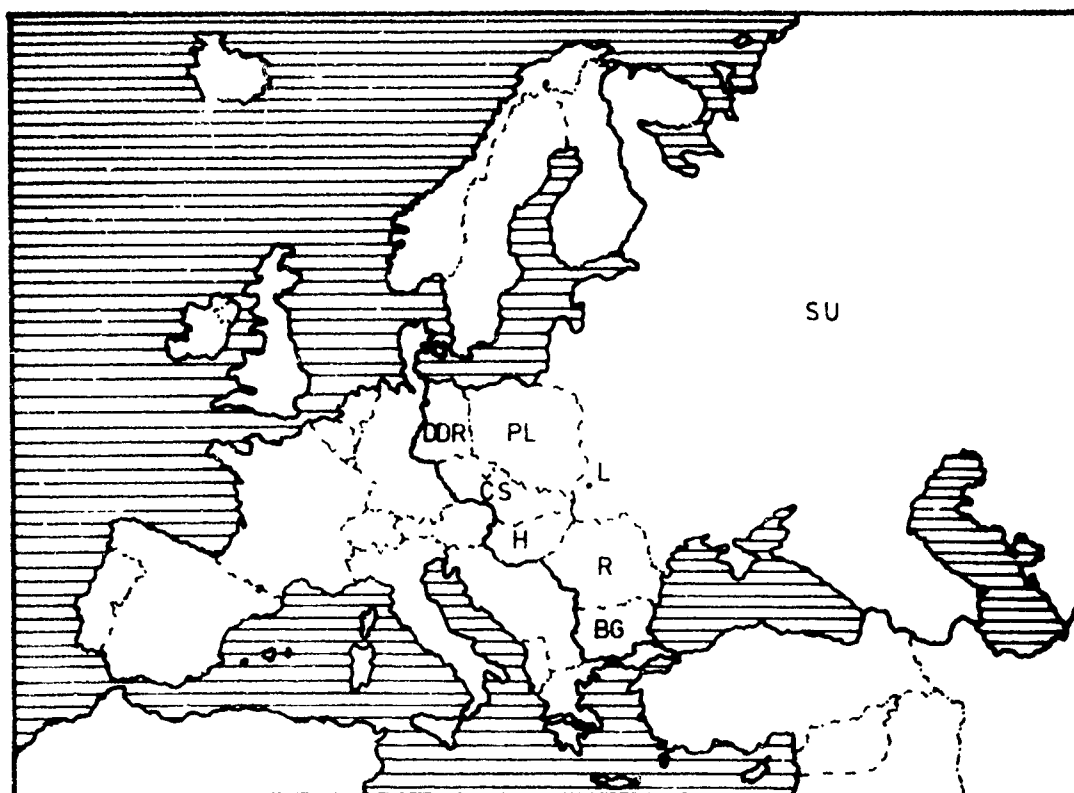
Figure 1. CMEA European countries: BG - Bulgaria, CS - Czechoslovakia, DDR - German Democratic Republic, H - Hungary, PL - Poland, R - Rumania, SU - Soviet Union. Also: L - Lvov

The snow load value resulting from this definition as 0.6 x /1000 : 8/ = = 75 kg/m² /0.75 kN/m²/ is still in force in actual snow load standards in Austria /JNORM B4013, 1983/ and in Federal Republic of Germany /DIN 1055, T.5, 1976/ for lowest parts of their territories. It is also used in German Democratic Republic /TGL 32274/05, 1976/ in the case of lightweight roof structures. In West Germany this value has now a statistical definition as a 95% fractile of annual maximum snow depth probability distribution multiplied by the mean snow density 215 kg/m³.

The round value 0.8 kN/m² is given in actual Hungarian standard /MSZ 15021/1-86, 1986/. In all mentioned standards they are roof snow loads, as a hundred years ago /for flat and slightly sloped roofs/.

The 0.8 kN/m² snow load was also used in structural calculations in Poland. Initially, according to the first official rule from 1923, it was used only in Eastern parts of the country and next, since 1938, all over the territory. After the World War II this value of snow load suffered several changes. These changes may serve as an interesting example of the arbitrary reduction of snow load.

All changes are presented in Table 1 for the I zone of snow load which has been usually covering more than a half of the territory of Poland.

Table 1. Snow loads and their return periods in Polish Standards since 1923, zone I

Standard or rule year	roof load kN/m^2	ground load if $\mu = 0.8$ kN/m^2	mean return periods, yrs, of:	
			characteristic value	design value for $\gamma_f = 1.4$
1923	0.60	0.75	6.2	20.7
1938	0.80	1.00	16.9	85
1946	0.70	0.875	10.2	42
1952	0.60	0.75	6.2	20.7
1964	0.50	0.625	3.7	10.2
1980	0.56	0.70	5	15.6

As in all standards before 1980 the shape factor for flat and nearly flat roofs was 1.0. It was assumed therefore that the snow loads values given in old regulations represented roof snow loads. Hence the ground – to – roof factor value 0.8 was adopted here in order to calculate ground snow loads and their return periods. Safety factor was assumed as now, i.e. $\gamma_f = 1.4$, although in old regulations it was much more higher.

It is seen that since 1946 to 1964 roof snow load was reduced from 0.8 kN/m^2 to 0.5 kN/m^2. The intention of the first reduction in 1946 was probably an attempt to minimize the costs of reconstruction of the economy after the WW II. The last reduction in 1964 was introduced as a consequence of the CMEA recommendations.

This trend, which led to very short return period, considered now as dangerous one, was stopped in 1980 /Kuś et al. 1980/.

EARLY CMEA RECOMMENDATIONS

In 1962, the first CMEA recommendations for loads on building structures were accepted. Although officially non-required they were progressively introduced to the national standards, except Hungarian one. Those recommendations followed strictly the Soviet code of practice. Therefore it would be interesting to know the first Soviet load regulation. Unfortunately, the writer had no possibility to find older Soviet standard for snow load than from 1940 /OST 90058-40, 1940/.

In this standard snow load was presented as a product of the unit weight of snow cover and a factor depending on the shape of a roof. This snow load model is still in use in actual standards.

The unit weight of snow cover i.e. ground snow load sequence was as follows: 0.5, 0.7, 1.0, 1.5 and 2.0 kN/m^2.

This sequence, completed later by the value 2.5 kN/m^2, is still in almost all CMEA standards, except Hungarian /there is only one value/ and Polish ones. It has been also introduced into the ISO standard for snow loads /ISO 4355, 1981/.

The shape factors were given for a few simple and general schemes of snow load distribution on roofs. The CMEA 1962 recommendations however, as the later Soviet standards, were much more rich with snow loads schemes. These schemes, more or less modified, were also introduced to almost all national standards. Some of them were presented in the CIB Commission W21 report /Schriver, Otstavnov, 1967/.

PRESENT APPROACH

Present approach to the snow load in most of CMEA countries is based on the limit state design method. This method is described in the ISO standard on the general principles on reliability for structures /ISO 2394, 1986/ as well as in the CMEA standard /ST SEV 384-76, 1976/. According to ISO standard the limit states are divided into the following two categories:

a/ the ultimate limit states which generally correspond to the maximum load carrying capacity /safety related/;

b/ the serviceability limit states which correspond to the criteria governing function related normal use.

The calculation model expressing each limit state under consideration contains a specified set of basic variables, loads included. For different purposes different values may be assigned to each load.

The main load value is the characteristic value.

Characteristic values are normally defined in the terms of probability. According to the ISO 2394-1986 a characteristic value of a variable action should be defined as a 98% fractile of its annual maxima probability distribution, i.e. it should have the 50 years return period.

In the actual standards snow load characteristic value is presented by the formula

$$S_k = S_{gk} \cdot \mu, \quad kN/m^2 \qquad \text{/1/}$$

where: S_{gk} – characteristic value of the ground snow load, kN/m^2,

μ – roof-to-ground snow loads ratio /shape factor/.

In several codes an additional factor is introduced which takes into account the self-weight of the light-weight metal structures. Hence

$$S_k = S_{gk} \cdot \mu \cdot k, \quad kN/m^2 \qquad \text{/2/}$$

where: k – factor depending on the unit weight of a roof structure.

Design value of an action is obtained by multiplication of the characteristic value with partial safety factor γ_f

$$S_d = S_k \cdot \gamma_f, \quad kN/m^2 \qquad\qquad /3/$$

The partial safety factor γ_f takes account of

- the possibility of unfavourable deviations of the actions from their characteristic values,
- uncertainty in the loading model.

Usually the partial safety factor is defined as a ratio of two fractiles of the probability distribution of a load or it is arbitrary established.

ACTUAL NATIONAL STANDARDS

Ground snow load

Ground snow load was defined from the direct measurements of winter maximal values of the ground load or indirectly as a product of the statistically defined depth of snow cover and its density. The last method was used in Hungary /Karman 1974/ and Bulgaria /Moralijski 1987/, also partially for a complementary analysis of data in Czechoslovakia /Boháč 1976/ and in Poland /Kuś et al. 1980/. In the remaining countries ground snow load data were probably used.

Two main methods of statistical data evaluation were used.

In the Soviet Union, the German Democratic Republic and Bulgaria the characteristic values of snow load or depth were defined as mean values of winter extreme values from the periods of measurements not shorter than 10 years. If the Gumbel probability distribution are to be used for probabilistic evaluation of the snow data then the mean value of winter extremes has a return period 2.3 years. So in these countries snow load return period is approximately 2 years.

Gumbel probability distribution was used in Poland and in Hungary, and also for most data evaluation in Czechoslovakia.

In Poland, ground snow load characteristic values have the 5 years return period. In Rumania 10 years return period is assumed /STAS 10101/21-78, 1978/.

In Czechoslovakia design and characteristic values were obtained as follows /Boháč 1976/: design values were calculated to have 100 years return period. The characteristic values were obtained dividing the design values by the total safety factor 1.7 /as 1.4 x 1.2 ≅ 1.7/. Therefore the characteristic values have no longer than approximately 10 years return periods.

In Hungary the yearly /winter/ maximum snow depth values were transformed into the 50 years maximum values using Gumbel distribution. Next the 95% fractiles of the 50 years extreme values distribution were calculated. Thus the design values of snow loads have approximately 1000 years return period.

Snow density - 160 kg/m^3 is quoted in the Hungarian standard and 245 kg/m^3 in the Polish standard.

Despite of the great differences between the return periods assumed in each standard the ground snow load values in almost all CMEA countries are the same. The Soviet sequence of ground snow load from the 1940 standard and early CMEA recommendations has been adopted in all countries except Poland where

only one zone has a CMEA value /Fig.2/. It is often pointed out that the two bordering zones, along the Polish - Soviet border, have quite different snow load, 0.9 and 1.1 kN/m^2 in Poland against 0.5 kN/m^2 in Soviet Union. It is easier to unify the method of data evaluation than to reduce twice the snow load values of long tradition and to shorten their return periods /despite of the reduction in zone I/.

There are five snow load zones in Soviet Union, Bulgaria, Czechoslovakia and Rumania, four in Poland and one zone in Hungary and DDR but with snow load increasing with elevation.

It should be noted that in Soviet Union and Czechoslovakia there are also so called long-term snow loads treated as quasi-permanent loads. They concern only III to V snow zones and constitute a part of the characteristic values.

Dependence of the ground snow load on the elevation

In mountain regions snow load depends on the elevation. It is taken into account in all standards but on the different ways.

In Soviet Union mountain regions are included to the snow zones with higher snow loads or it is recommended to make a special individual analysis of the predicted snow load.

In Czechoslovakia snow load zones were subordinated to the elevation expressed by the contour lines.

In German Democratic Republic the CMEA snow load sequence is also subordinated to the contour lines and the stepwise curve of the snow load versus elevation may be drawn up.

In Hungary, Poland and Rumania the linear dependencies of the snow load on the elevation are given in standards.

A formula from old Polish rule is as follows:

$$S_g = 0.8 + 0.0012 \ /H - 400/, \quad kN/m^2, \tag{/4/}$$

while the actual formula for zone IV is

$$S_g = 0.9 + 0.003 \ /H - 300/, \quad kN/m^2, \tag{/5/}$$

where: H - height above sea level, m.

This last formula is restricted only to the heights 300 m $\leqslant$ H $\leqslant$ 1000 m. Above 1000 m a special analysis is recommended.

In Hungary snow load dependence on the elevation is presented by the formula

$$S_g = 0.8 + 0.01 \ /H - 300/, \quad kN/m^2. \tag{/6/}$$

and in Rumania as

$$S_g = 0.7 + 0.0015 \ /H - 600/, \quad kN/m^2. \tag{/7/}$$

All above quoted formulae are shown in Fig.3.
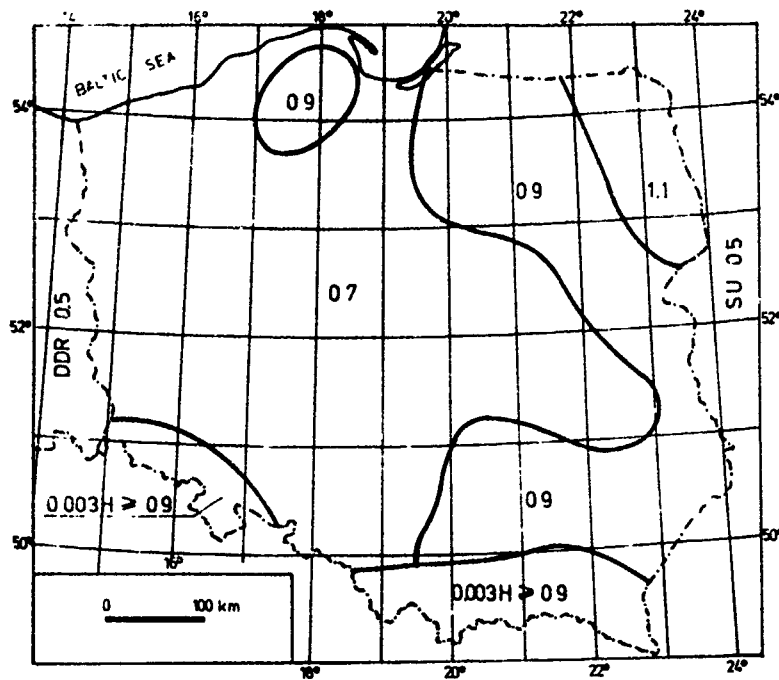
Figure 2. Snow load zones in Poland. Load values in kN/m^2
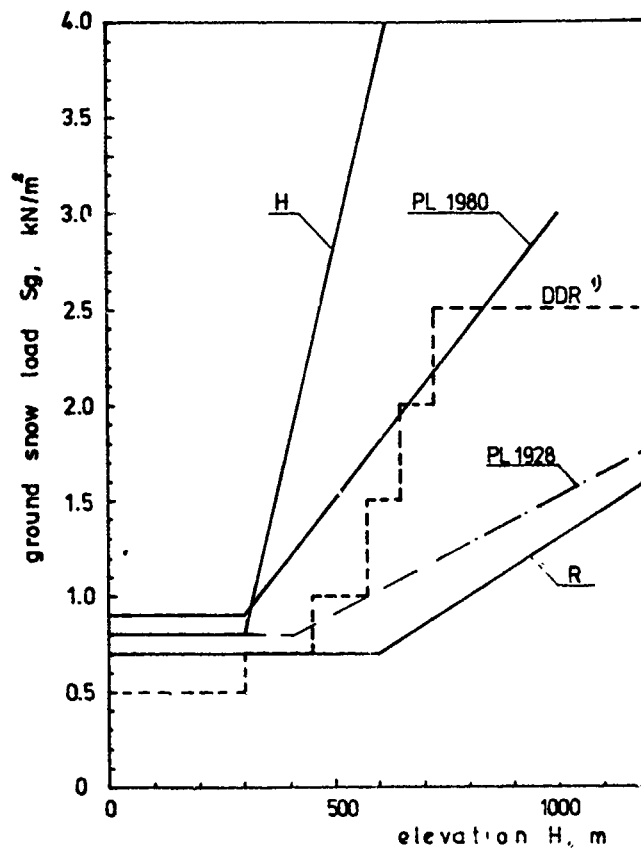
Figure 3. Dependence of the ground snow load on the
elevation. Symbols as in Fig.1. Note 1:
Harz mountains not shown here

Shape factors

In the Soviet code of practice from 1974 /SNiP II-6-74/ there were 11 schemes of snow loads distribution on roofs, almost all schemes in two variants. These schemes have been introduced to the remaining CMEA standards except Hungarian and Polish.

In the Hungarian standard there are only few schemes specially prepared. In Polish standard all schemes were taken from the ISO Draft Standard. Introducing of the ISO shape factors with the basic value μ = 0.8 into the Polish standard was accompanying with the increase of the ground snow load values. Otherwise roof snow loads would have the return periods shorter then 3 years.

The main Soviet shape factors and snow loading schemes are presented in the CIB report no 9 /Schriever, Otstavnov, 1967/. They are: simple flat and monopitch roofs, simple pitched /twopitch/ roofs, curved and arche roofs, multiple pitched roofs, simple pitched roofs with skylights, saw-tooth roofs, multispan roofs, multilevel roofs, roofs with attics and local obstructions and hanging roofs /SNiP 2.01.07-85, 1985/.

Safety factors

In all standards one value of safety factor γ_f = 1.4 has been accepted. For light-weight metal structures however, an additional safety factor k in the formula /2/ has been introduced. It depends on the self-weight of a roof structure. The values of this factor are not unified.

In Czechoslovakia k = 1.2 for the roof structures with a self-weight below 0.5 kN/m^2 and k = 1,0 for the unit weight 1.0 kN/m^2 and more is adopted. The same values is given in Polish standard for light roof structures over non--heated spaces.

In other standards this factor depends on the ratio of snow load to the unit weight of a roof or inversly.

In Hungary, if the unit weight g of a structure is less than 40% of snow load then it should be k = 1.25; if g = S then k = 1.0.

In German Democratic Republic k = 1.5 for S/g $\geqslant$ 3 and k = 1.0 for $^-/g \leqslant 0.5$.

In all standards the intermediate values are to be calculated from linear interpolation.

In Rumanian standard this additional safety factor is presented by the formula

$$k = 0.85 + 0.45 \frac{S}{g} \qquad /8/$$

with the restriction $1 \leqslant k \leqslant 1.2$.

In the Soviet code of practice, for g/S $<$ 0.8, the partial safety factor γ_f should be 1.6 instead of 1.4.

Other factors

In the Soviet code of practice there is a possibility to reduce the snow load on several kinds of roof shape, including simple pitched roofs with

slope less than 12%. If the mean wind speed during three winter months is higher than 2 m/s snow load should be reduced using the coefficient

$$k_v = 1.2 - 0.1 \ V \qquad \qquad /9/$$

where: V - mean wind speed, m/s.

CONCLUSIONS

1. Although CMEA recommendations for loads are not officially required in its part concerning snow loads a significant unification of snow load standards within the CMEA countries has been achieved for the past 25 years. It concerns the sequence of ground snow load values, shape factors and partial safety factor. Only standards from two countries, Hungary and Poland, differ significantly from the remaining CMEA standards.

2. Despite of the unification of the ground snow load values there are differences between their return periods ranging from approximately 2 years in Soviet Union to approximately 1000 years in Hungary. The same structure designed to bear the same snow load would have quite different safety margin in the two countries. Unification of load values without the unification of basic assumptions may sometimes be illusoric.

3. The first ISO standard for snow loads was established in 1981, so the national standards prepared before did not take it into account. The revisions of three standards, Soviet, Hungarian and Czechoslovak were done after 1981 but the ISO standard was not adopted there, too. It was adopted in Polish standard only.

4. If the ISO shape factors are to be introduced into the East European standards, in which they have been not introduced before, a significant reduction of snow load for flat and slightly roofs may occur. So the changes of shape factors should accompany the changes of ground snow load values and/or zones borders.

REFERENCES

1. Boháč, A., 1975, "Revíse mapy sněhových oblastí v ČSN 730035 "zatíženi konstrukcí pozemnich staveb" /Revision of the map of snow regions in the Czechoslovak Standard ČSN 730035 "Loading of Building Structures", in Czech/, Stavebnicky Časopis, vol. 23, 840-862, Nov. 1975.

2. ČSN 730035, 1986, "Zatíženi konstrukcí pozemnich staveb" /Czechoslovak Standard 730035 Loading of Building Structures/, 1986.

3. DIN 1055 Teil 5, 1976, "Lastannahmen für Bauten. Verkehrslasten. Schneelast und Eislast" /Design loads for buildings; live loads; snow load/, Deutcher Normenausschuss, Berlin 1975.

4. ISO 4355-1981, 1981, Bases for design of structures. Determination of snow loads on roofs, 1981.

5. ISO 2394-1986, 1986 /first edition 1974/, General principles on reliability for structures, 1986.

6. Kármán, T.G., 1974, "Snow Loads in Hungary", CIB 6th Congress, Congress Book, Vol. II, 112-120, Budapest 1974.

7. Kuś, S., Sobolewski, A., Żurański, J.A., 1980, "Obciążenie śniegiem w Polsce wg dawnych przepisów i w ujęciu PN-80/B-02010" /Snow load in Poland according to old regulations and PN-80/B-02010, in Polish/, Inżynieria i Budownictwo, 243-246, July 1980.

8. Moralijski, E., 1987, "Provision of climatic service for building design in Bulgaria". Building Climatology, Proceedings of the 2nd International Symposium /CIB/, Part 3, 148-152, Moscow, USSR, May 12-15, 1987.

9. MSZ 15021/1-86, 1986, Építmények teherhordó szerkezeteinek erőtari tervezése. Magasépítési szerkezetek terhei /Design of load bearing structures of buildings. Design loads for buildings - in Hungarian/, Budapest 1986.

10. ÖNORM B 4013, 1983, "Belastungsannahmen in Bauwesen. Schnee-und Eislasten" /Design loads in buildings; snow and ice loads/, Österreichisches Normungsinstitut, Wien, 1983.

11. OST 90058-40, 1940, "Snegovaja nagruzka" /Snow load, in Russian/, Moscow 1940.

12. PN-80/B-02010, 1980, "Obciążenia w obliczeniach statycznych. Obciążenie śniegiem" /Loads in static calculations. Snow load, in Polish/, PKN,MiJ, Warszawa 1980.

13. Schriever, W.R., Otstavnov, V.A., 1967, "Snow loads: preparation of standards for snow loads on roofs in various countries with particular reference to the U.S.S.R. and Canada", CIB Report no 9, 13-33, CIB Commission W23, 1967.

14. SNiP II-6-74, 1976, "Stroitelnyje normy i pravila, normy projektirovanija, nagruzki i vozdejstvia" /Building standards and codes, design standards, loads and actions, in Russian/, Gosstroy, Moscow 1976.

15. SNiP 2.01.07-85, 1986, "Nagruzki i vozdejstvia" /Loads and actions, in Russian/, Gosstroy, Moscow 1986.

16. STAS 10101/21-78, 1978, "Acţiuni in construcţii. Încărcări date de zăpadă" /Actions on structures. Loads due to the snow, in Rumanian/, Institutul Roman de Standardizare, Bucuresti 1978.

17. ST SEV 384-76, 1976, "Stroitelnyje konstrukcii i osnovanija. Osnovnyje položenija rasčeta" /Building structures and fondations. Basic design assumptions, in Russian/, CMEA, Moscow 1976.

18. SNiP 1407-78, 1978, "Stroitelnyje konstrukcii i osnovanija. Nagruzki i vozdejstvia" /Building structures and fondations. Loads and actions, in Russian/, Gosstroy, Moscow 1978.

19. TGL 32274/05, 1976, Lastannahmen für Bauwerke. Schneelasten /Design loads for buildings. Snow loads/, DDR, 1976.

20. Thullie, M., 1886, "Podręcznik statyki budowli dla inżynierów, architektów i słuchaczów szkół politechnicznych" /Handbook of statics of buildings for engineers, architects and students of technical schools, in Polish/, Lvov 1886.

8
DESIGN CONSIDERATIONS
Ian Mackinlay, Chairman
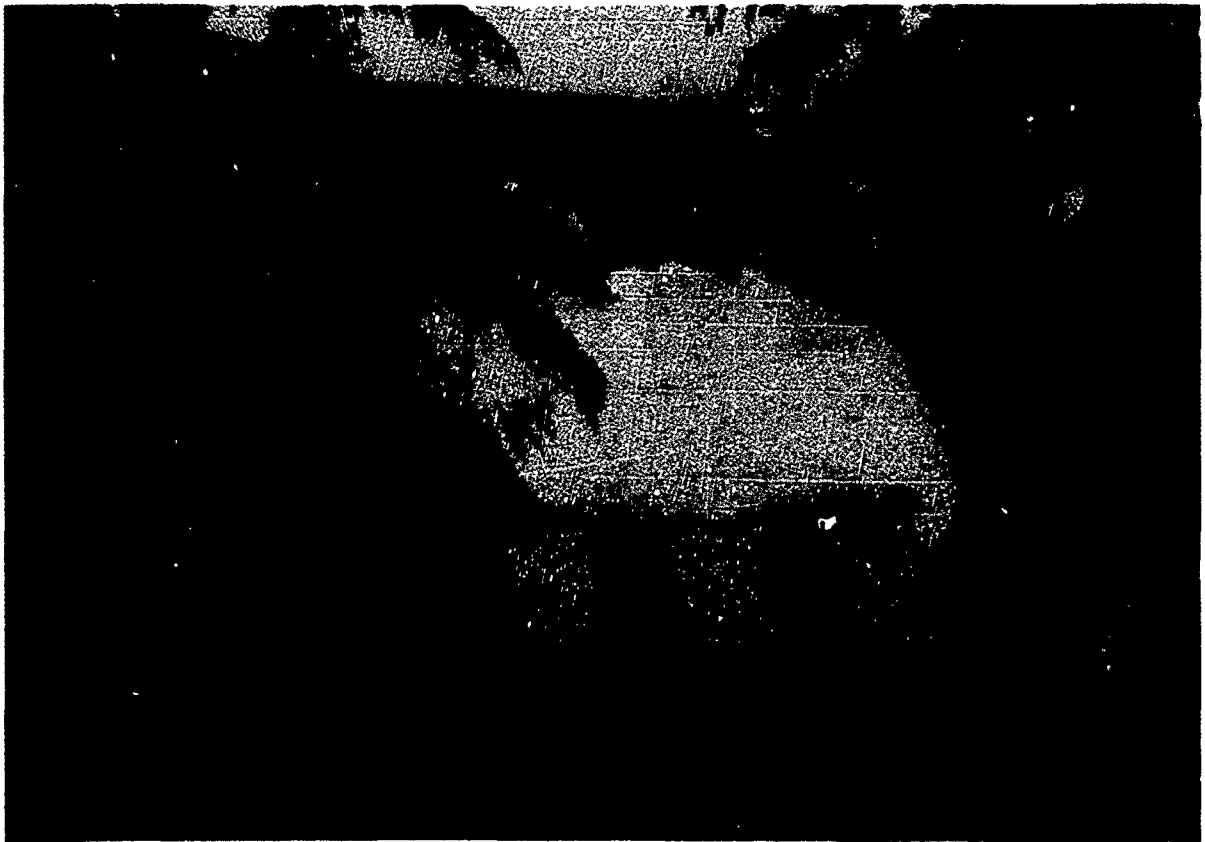
These skylights have prevented sliding of snow from a steeply sloped metal roof. (Photograph provided by Jonathan Paine.)

A Structural System Designed to Resist Creep and Glide Forces

Robert G. Albrecht[I]

ABSTRACT

At the request of an Architect and a property owner, a structural
system was designed for a house to be located at an elevation of
1600 meters on the western slope of the Cascade Mountains in the
state of Washington. The house was to be sited on a lot which had
a declevity of close to 45 degrees. The maximum snow depth at the
site could be four meters. The steepness of the site, the potential
for very deep dense snow, and the Architect's design combined to
produce conditions for very large creep and glide forces, as well
as hydrostatic forces against the uphill wall of the house. The
creep and glide forces were calculated from the literature
available at the time. A structural system to resist these forces
was incorporated into the house design. This structural system
involved stabilizing the uphill wall of the house with horizontal
trusses in the plane of the floors. These trusses carried the
lateral snow forces to the end walls which had diagonal bracing
connected to the slope with rock bolts. The house has been through
nineteen Cascade winters (including a record snowpack during the
winter of 1975) without damage due to snow creep and glide.

INTRODUCTION

There are numerous examples of buildings sited on or near the base of
steep slopes which have been damaged by lateral snow pressures. The
following is a case history of the design and evaluation over time of a
building sited on a nearly 45 degree slope in deep snow country. The form
of the building as established by the Architect, the elevation of the site,
the direction of the prevailing storm winds, and the nature of the tree
cover suggested that deep deposition of snow could take place against the
uphill wall of the building. This paper contains a description and
schematic details of the structural system used to resist the lateral snow
pressures on the building and an evaluation of the performance of this
system in resisting the forces for nineteen winters. A photograph of the
completed house with about 1.5 meters of snow on the ground is shown in
Figure 1.

I.   Associate Professor, Department of Architecture, University of
     Washington, Seattle, Washington.

Figure 1

432

ARCHITECTURAL PROPOSAL AND SITE DESCRIPTION

An elevation view of the proposed architectural design for a vacation house for Mr. and Mrs. Mundy is shown schematically in Figure 2. (The deck was deleted from the final design.) This house was to be built at 1600 meters in the Crystal Mountain Ski Area on the western slope of the Cascade Mountains in Washington State. The site, located on a nearly 45 degree hillside above the ski area, had an expansive view of the surrounding mountains. The site was covered with 1.2 to 1.8 meters of earth over 27 to 46 cm. of weathered rock and andesite bedrock. There was no weather data for the site but the maximum snow depth observed by nearby residents over a ten year period (including several very heavy snow winters) was approximately 4 meters.

Since the Architect realized he was unfamiliar with the snow loading at the site, he asked me to size some of the roof beams for this vacation house. While examining the drawings and designing the roof beams, I realized that there were a number of potential problems with the design unrelated to the roof beams. Site conditions including deep snow and steep terrain needed to be considered in the structural design. The Architect agreed that I should study the problems and make some recommendations.

SNOW COUNTRY DESIGN PROBLEMS

The most obvious architectural features of this house which could cause structural difficulties due to its location on a steep slope in a heavy snow zone were as follows:
1) The roof was to be covered with split shakes and was to be a "warm roof." Ice dams would develop which could cause other associated problems.
2) The roof snowpack would unload and demolish the deck during the periodic thaws which are common in this part of the Cascade Mountains. There was an added danger that this snow could strike the deck with such force as to tip the house from its foundations. The additional structural elements required to prevent this mode of failure would be very expensive.
3) The earth pressure and lateral snow pressures against the uphill wall would cause severe structural problems for a house of this geometry.

After investigation of the site, these were the most important factors I felt should be considered in the structural design of this house to resist the downslope forces due to earth and snow.
1) A house on this site would be exposed to very strong southwest winds, the snow-bearing winds of the northwest. These winds would deposit deep snow on the steep slope above the house.
2) Snow pressure against a structure built on a 45 degree slope would be very high.
3) Trees at the site were bent indicating earth and snow creep down the steep hillside.
4) Lateral earth pressure against a below-grade basement wall would be high on this 45 degree slope since the site was covered with 1.2 to 1.8 meters of earth.

NORTH ELEV.

Figure 2

5) The house could be destabilized by these downslope forces unless the internal structure was specifically designed to resist these forces.

I recommended the following alternatives:
1) The perimeter of the house could be changed to a shape more favorable to the conditions. The house walls could be lengthened in the down-slope direction in order to increase the stability and shortened across the slope to reduce the snow pressure against the uphill wall.
2) The house could be built according to the Architect's original plan if it was strengthened internally.

The Architect objected to changing the form of the house because having a wide angle view out of the front wall of the house was an important feature of his design. Therefore, the owner agreed to alternative number 2 which included a bracing system used to stabilize the house against the downslope forces due to earth pressure and snow creep and glide forces.

SNOW CREEP INFORMATION

In order to design the structural system some rational way of evaluating design loads from the snow on the uphill side of the building was needed. For this I turned to my old mountaineering and skiing friend, Dr. Edward LaChapelle for advice. At that time Ed was teaching and doing research at the University of Washington in the Department of Atmospheric Science. He gave me a copy of Avalanche Control in the Starting Zone (U.S. Forest Service, 1962). Formulas and data intended for the design of avalanche starting zone barriers were obtained from this publication and used to calculate the forces for which the bracing system was designed.

CALCULATION OF SNOW AND EARTH LATERAL FORCES

The lateral forces against the uphill wall were due to earth pressure against the basement wall, plus snow creep and glide forces and snow hydrostatic pressure on the wall between the first and second floors. The lateral pressure on the basement wall due to earth was computed using values typical of the Coulomb-Rankine formula.

Two terms are used to describe the tendency of the snowpack to move down the slope: "snow creep" and "glide". Snow creep is the downslope motion of individual snow particles of layers within the snowpack. Glide takes place at the interface between the ground and snow; the entire snowpack moves downslope. The forces shown in Figure 3 were used for the design of the structural system of the Mundy house. The values for snow creep and glide are probably on the high side because the actual angle of the slope is somewhat less than the 45 degrees used in the calculations. On the other hand, snow hydrostatic pressure should have been included in the calculations even though snow creep and glide constitute the greatest force for a structure on such an extreme slope.
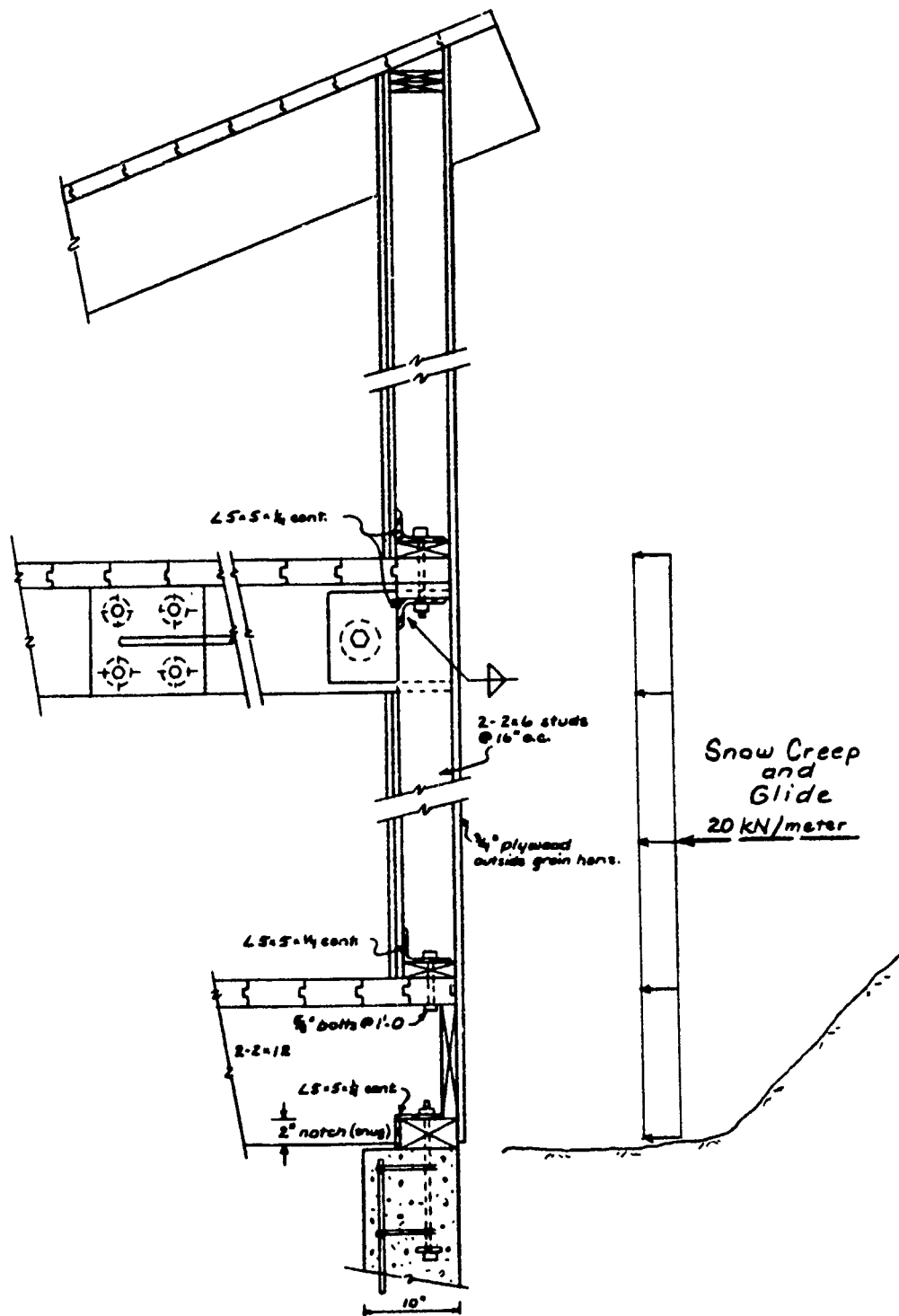
Figure 3

STRUCTURAL SYSTEM

The part of the structural system of the house which was designed primarily to resist the downslope forces due to earth and snow pressures, consisted of the following:

1) As shown in Figure 4, the uphill wall exposed to these forces consisted of vertical spanning wood members (studs) between the first and second floors. The calculated forces in these members due to snow were so large that special collectors (steel angles) were required to pick up their horizontal end reactions and carry them to the horizontal diaphragm trusses. A conventional reinforced concrete basement wall was used to resist earth pressure. The basement wall was supported laterally at the bottom by the basement slab and at the top by the first floor diaphragm (truss).

2) Conventional plywood horizontal diaphragms based upon unit shears as allowed by the Uniform Building Code (International Conference of Building Ofiicials, 1967) were not nearly strong enough to carry the forces which they would receive to the end walls. As illustrated in Figure 5, trusses in the plane of the first and second floor diaphragms were used. The diagonal web members of the trusses were steel rods with turnbuckles. The turnbuckles were used to tighten the diagonal rods once they were in place. For the sake of appearance, the Architect chose to make a visual feature of these diagonal rods; and, in fact, made them double diagonals, as shown in Figure 5.

3) The end walls, as shown in Figure 2, were braced against the forces which they received from the first and second floor diaphragms by a diagonal steel strap in the plane of the wall studs, notched into the inside face of the studs. The diagonal straps were embedded in the reinforced concrete basement end walls with bolts through holes in the plate. (Figure 2.)

4) The reinforced concrete end walls were secured to the bedrock of the mountainside with rock anchors. The anchor bolts used an expanding wedge device and were grouted into the holes after the anchor device was activated. (Figure 2.)

EVALUATION

This building, constructed in the autumn of 1969, has sustained the forces from snows of nineteen winters. The snow depth for the majority of the winters was approximately 2.5 meters. However, during the winter of 1975, the snow depth reached 4 meters. The water content of this near-record snowpack, typical of Cascade Mountain snowpacks, was very high. After nineteen years, there is no evidence of damage or permanent deflection due to downslope snow pressures.

It would be interesting to know the actual values of the downslope forces due to snow which the structural system of this building resists during periods of heavy snow. Unfortunately, no measurements of these forces have been made. Since the building has been kept partially heated during the winter months, the downslope pressures are probably not as great as they would have been if the building had been unheated. The uphill wall was not insulated in order to allow the adjacent snowpack to melt.

SECTION

Figure 4

MAIN FLOOR
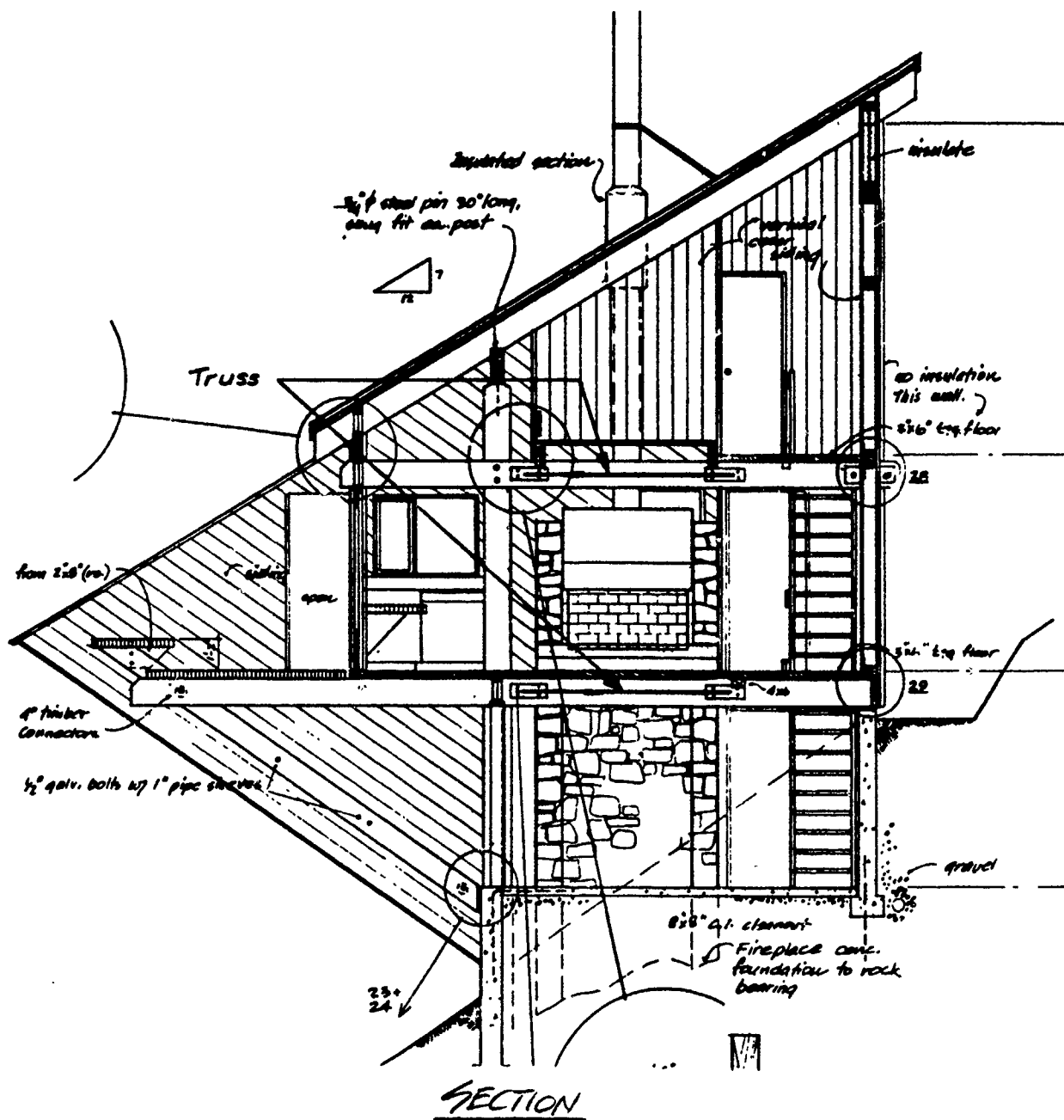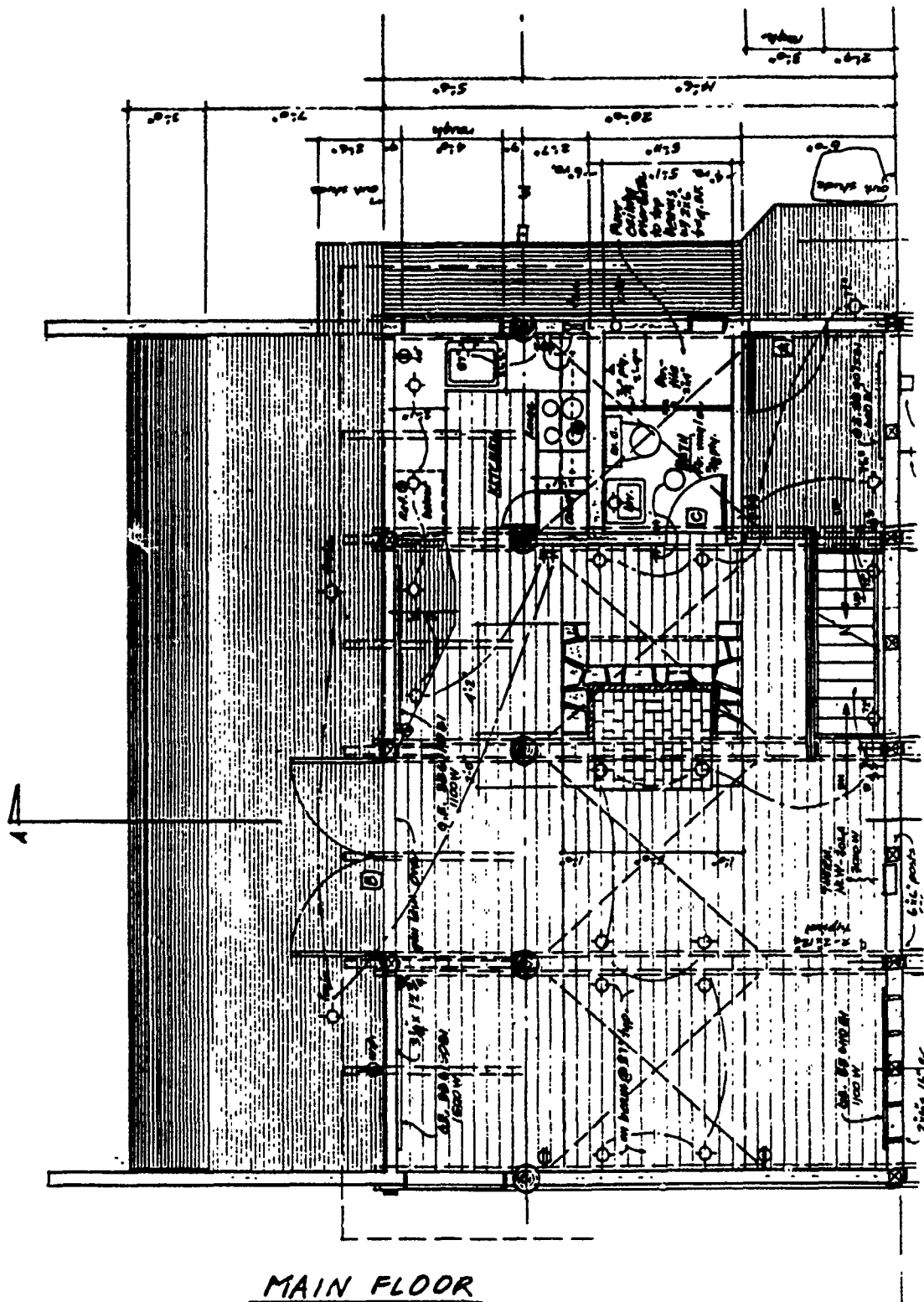
Figure 5

For the purposes of continued evaluation of the performance of this structure, I am looking forward to future winters when the snow depth may exceed the depth already resisted by the structure so that additional observations might be made.

RETROSPECT

In the preparation of an unpublished report made for the U.S. National Park Service, measurements were taken of lateral displacements of the tops of columns in the National Park Inn at Paradise on Mt. Rainier, Washington. Paradise is at an elevation of 1,693 meters on the south side of Mt. Rainier and is subject to very deep and dense snow. The column top displacements were due to lateral snow pressures. These displacements were up to 13 cm. at the top of first story columns and up to 10 cm. at the tops of second story columns. These displacements took place prior to 1976 and some likely occurred during the heavy snow winter of 1975. Although the snow depths on the uphill side of the Paradise Inn were deeper (up to 9 meters total) than at Crystal Mountain where the Mundy house is located, the average slope of the hill above the Paradise Inn is only 11.5 degrees in the first 122 meters horizontal and 14.5 degrees in 610 meters horizontal. These slope angles are much less than those above the Mundy house which are close to 45 degrees. The slope above the Mundy house is, however, at the present time more heavily wooded than the slope above the Paradise Inn. Only future heavy snows will prove whether the structure used in the Mundy house is adequate to resist the long term lateral snow forces at this site.

REFERENCES

Brown, C. and Evans, R. J., "Effect of Glide and Creep on Rigid Obstacles". Proceedings of the Grindlewald Symposium, April 1974, IAMS-AISH Publication No. 114. 1975.

International Conference of Building Officials, The Uniform Building Code, International Conference of Building Officials, Whittier, California, 1967, p. 110.

U.S. Forest Service, Sept. 1962, "Avalanche Control in the Starting Zone," Station Paper No. 71, Fort Collins, Colorado.

Architectural Design in Regions of Snow and Cold

Ian Mackinlay[1]

ABSTRACT

The design of structures in regions of snow and cold require special knowledge of such an environment and the development of design techniques which are appropriate to it. These techniques may be quite different from those suitable to other locations. The forces which impact on snow country buildings result from the climate, exposure, snow depth at the site, and the form of the structure. Flat roof design is often appropriate and may reduce the problems frequently encountered in sloping roof design where the snow slipping from the roof is often blocked by ice dams. These obstructions can produce serious leakage and can cause dangerous avalanches from roofs. Ice dams can be reduced by proper roof design in several ways which are discussed. Building codes should also be strengthened to provide the architect or engineer wishing to work in the snow country, with a sound basis for design. Never the less, there is no substitute for experience in snow country design.

INTRODUCTION

The basic principles of architectural design in the regions of sub-freezing weather are not well understood by most architects and some engineers. Snow is a wily material with very complex properties. Snow and ice together can do major damage to structures in a single winter season. Not only can buildings be crushed, but snow cascading off roof surfaces can cause injury, property destruction, and death. Snow, when it first falls, is downy soft and deceptively fragile. It's crystalline structure with inter-locking barbs can make it adhere to very steep surfaces (see Figure A). Depending on the always-changing conditions of sun, wind, humidity, temperature and surface material, the newly-fallen snow can remain on roofs for long periods or cascade gently off as dust. The longer the snow remains on a steep roof, the more potentially dangerous it becomes. Ice builds up, weight increases, internal instabilities within the snow pack develop, and new snow or rain adds to the mass. The forces acting on the building can exceed the design load. When the snow mass does slip, it can carry away parts of the structure or crush what it falls on. Current codes in use in the United States do not define well snow load problems. Often, the judgment as to what to do is left in the hands of the "building official", who may not understand the problems of snow and cold any better than does the designer. This paper will outline some of the basic approaches to cold country design and suggest amendments to the current codes so that designers can be better informed and the public better protected from the hazards of snow and cold.

1. Architect/Chairman, MWM,Mackinlay/Winnacker/McNeil & Assoc.,Inc., Oakland, CA

CODES AND STANDARDS

In the United States, several building codes apply. In the West, the Uniform Building Code (UBC) has been adopted by most jurisdictions. The UBC is, at best, a minimum standard and public safety in regions of snow and cold relies very heavily on the judgment of the building official who is named by the UBC as the determiner of snow loads. The building official may adjust the ground snow load when a registered architect or engineer submits data substantiating the adjustment. The recently-issued 1988 UBC has a more extensive section in its appendix to guide the snow country designer but it is still not a complete document. The architect and engineer should look at other standards and make-up their minds as to what is a reasonable ground snow load and how it should be applied to the structures under design, rather than operating in blind reliance on the opinion of the building official or on the letter of the text in the applicable code.

ANSI

The American National Standards Institute, Inc. (ANSI) issued in 1982 "Minimum Design Loads for Buildings and Other Structures" which contains an excellent chapter on "snow loads". This document, together with the National Building Code of Canada, forms a comprehensive basis for snow and cold design in North America. Both ANSI and the Canadian Code are currently being refined. If the UBC and other American codes would follow the lead they supply more closely, it would benefit the design profession. But, even these standards must be applied with judgment.

GROUND SNOW LOAD

Fundamental to all the building codes and standards mentioned in this article is the ground snow load which exists at the construction site. Maps of typical ground snow loads exist for most of North America. Some regions have not been mapped; some have such extreme local variations as to preclude mapping at a convenient scale; some areas have such extreme topography or weather variation as to make mapping difficult. The snow country designer should be especially cautious in such areas. Where ground snow loads are mapped, there is a two percent annual probability of the indicated load being exceeded, based on a fifty-year mean recurrence interval, thus even in these areas, sometimes heavy snow loads can be experienced. However, in most locations, it is possible to form a reasonable estimate of the ground snow load. The amount of this load that applies to structures is a complex problem which requires the consideration of many (often conflicting) factors.

SLIPPERY ROOFS

ANSI 1982 does continue the long-standing practice of permitting a reduction in roof snow loads for steepness. This reduction is greater for "slippery" roof surfaces and for "warm" versus "cold" roofs. These practices must be considered carefully by the snow country designer. Obstructions, such as plumbing vents and dormers may hold snow on roofs of very steep pitch roofs. Normally, metal roofs are considered "slippery" but standing ribs in metal roofs tend to freeze into a snow blanket. In some cases, the ribs can support the entire weight of the snow pack so that the flat portions of the metal

which lie in the plane of the roof are not in contact with the snow. That is to say that building heat has melted the contact face and the snow has bridged between the ribs. At times this can form what amounts to a cold roof with freezing air circulating under the snow. This condition can lead to a snow blanket of considerable depth on what might be thought as a slippery roof. When the snow does detach from the ribs, it falls in a climax avalanche which is much more dangerous than the slower migration of snow supported on such less slippery roofing materials as wood shakes or asphalt composition shingles. It is true that, in general, metal roofs shed snow more often than most other roofing materials but they sometimes hold snow and, if conditions are right, they may hold it to a point that equals or even exceeds the ground snow load (see Figure B). The snow country designer should not be quick to conclude that the material he has selected is "slippery" and normally slippery roofs must have safe areas into which the snow that builds-up on them can be deposited safely when it slides. Particular attention must be given to snow and ice sliding from a higher roof surface to a lower which already is loaded with a snow blanket. The impact load may be enough to cause the lower roof to fail. In general, designs where higher roofs cascade onto lower roofs should be avoided.

WARM ROOFS

It seems logical that warm roofs would slip snow sooner and more often than do cold roofs but, as in so many design elements in the snow country, this too is to some degree counter-intuitive. If only the temperature of the roof is considered, it is quite true that warm surfaces both melt and slip the snow more quickly than cold roofs but sloping warm roofs tend to form ice dams at their lower (eave) edges. These dams are very effective snow arrestors which block slippage and greatly increase snow density (ice). On the other hand, cold roofs experience less melting especially on the north-facing roofs (in North America) and the snow blanket can be considerably reduced by wind stripping on the windward side. In most cases, the snow country designer should make special provisions for concentrated ice load on the roof edges of warm roofs especially on the north face or in shaded locations. The snow retaining effect of ice dams must be considered in reduction of snow load for slope as permitt·d by many current codes.

It should be recognized that the term "warm roof" is relative to the thickness of the insulation and snow cover. As will be discussed below, the critical factor is where the melting point occurs. If it is below the roof surface, ice damming will be minimized and the roof will act very much as a "cold" roof (see Figures 1 and 2).

COLD ROOFS

A "cold" roof might be described as an umbrella over a warm roof. It picks-up the snow, rain and sun and shelters the structure below. It is a serious error for the snow country designer to think that a cold roof will solve all ice damming problems - it will not. Under some conditions, it can actually intensify ice damming but where the air temperature is normally below freez-ng, cold roofs can reduce ice dams and keep the snow pack on the roof lighter and less icy than will be found on a warm roof. The important ingredient in cold roof design is good cold air circulation. The underside of the upper

(umbrella) roof is sheltered from the sun and exposed to cold air (see Figure 10). This inhibits melting of the snow it supports if the circulated air under the umbrella is below freezing. Any heat leaks into the space between the upper and lower roofs may raise the air above freezing and cause melting, so great care must be taken to seal the lower (warm) roof from the circulating air. Air circulation between the upper and lower roof surfaces is caused by wind pressure and heat convection, preferably the former. If the air heats too much, the utility of the cold roof is compromised. It is wise to provide as much unobstructed space as possible between the inner and outer roofs. The ridge vent should be designed so that it cannot normally be blocked by snow. As wind pressure against the building is the best way to circulate the cold air, eave and ridge vents should encourage circulation. The lower roof must be completely sealed so as to prevent air leakage from interior heated spaces. Also, the inner roof must be completely waterproof (just as one would wear a raincoat under an umbrella). The storm wind can being in snow dust (very fine powdered snow crystals) which coat the spaces between the roofs and melt when the air temperature rises or under the influence of building heat. If the lower roof is not waterproof, this snow melt will leak into the building. If insulation material is used as the upper face of the inner roof, it must be waterproof and completely sealed. Fiberglass or similar water absorbent materials should never be used unless they are covered and sealed completely.

A serious fire code problem exists for the conventional cold roof on wood frame buildings (this might consist of, say, 1/2 inch plywood above and below with 2 x 6's used as spacers running vertically). These roofs are unblocked by the necessity of air circulation but they constitute a flue which can cause very rapid flame spread. Any fire at the lower face of the eave will be sucked up by flue action into the cold roof and vent at the ridge. There have been serious snow country fires due to combustible cold roofs and, in most cases, the space between upper and lower roofs should be sprinklered or con-structed of incombustible materials. When contemplating using a cold roof, the designer should ask if the environmental conditions are correct for this technique, if the extra costs are justified, and if there is some other method (such as a cold attic) of achieving the same result at less expense and risk. Building codes should be amended to provide standards for cold roof construc-tion.

FLAT ROOFS

In the Lower 48 states, ANSI 1982 assumes that flat (minimum pitched) roofs will carry seven-tenths of the ground snow load, increased or decreased by exposure, thermal conditions and importance. This seems overly simplistic as it does not consider roof size. A small flat roof in a location where the wind blows during periods of snow fall will be wind stripped to much less than ground snow load (see Figure C). The area of the roof, the size of the roof edge parapets, and the magnitude of the storm wind influence the amount of snow that will accumulate. But under most exposed conditions, snow loads on flat roofs will be substantially less than the ground snow load. As the area of the roof increases, the snow load on the lee side of the roof (away from the prevailing wind) will increase to full ground snow load or even may exceed it due to cornice formation on the downwind side (see Figure 11). This will create an uneven load across the roof with the snow being stripped on the windward side and piling up on the leeward side. Large flat roofed structures should be designed for this uneven loading.

Roof obstructions are as important in flat as in sloping roofs. Roof mounted air handlers for example, can cause local snow drifting which can result in concentrated loads far beyond ground snow loads.

Adjoining flat roofs of irregular height can cause concentrated loads, the configuration of which vary depending on wind direction. A relatively small flat roof below and downwind of a large flat roof might accumulate two to three times its snow load. There is a tendency for snow to accumulate in courtyards which are encircled by flat roofs. The wind strips the snow off the roofs and deposits it in the courtyard and this can result in accumulations of double (or more) ground snow load. Such design should be avoided in the snow country.

FLAT ROOF DRAINAGE

If the structure below the flat roof is maintained above freezing continuously, interior drainage is usually more satisfactory than sheet drainage off the roof edge. Ice dams can form at roof edges even with minimum sloped roofs. Building heat will keep internal drains ice free and water from snow melt will run to the drains under the snow blanket. A slope of two percent to drain in the roof surface provides for water movement. Multiple drains and overflow scuppers should be provided. If these scuppers are on the exterior edges of the roof (as contrasted to interior overflow drains), a quick visual check is provided to drain function. If the scupper is dripping or shows ice, the drain should be checked. Flat roofs must be frequently maintained to assure that roof drains are not blocked by leaves.

The melt water which enters the building is at, or very close to, the freezing point. This will cause condensation on the piping if the building air is at all moist. Provision must be made in the design to pick up this condensation moisture and carry it away safely. If these drains are insulated, they may be obstructed with ice and condensation may occur where the insulation is terminated inside the building. Similar condensation will occur on all cold liquid pipes entering a warm moist building.

Even buildings which are sometimes permitted to go below freezing can be drained by heated internal drains, but the temperature inside the structure may stay cold long after the exterior temperature causes roof snow to melt. The layer of ice over the frozen roof under the snow blanket may inhibit the flow of melt water to drain. This causes in effect an ice dam which can considerably increase the snow load. Flat roofs designed over buildings which are permitted to freeze from time to time must be designed for greater loads than roofs over buildings which are continuously heated. Where roof insulation is relatively thick compared to the snow blanket, the freezing point may occur below the roof surface which will also lead to roof icing and may prevent melt water from flowing along the roof surface to drain. This may be effectively prevented by placing some of the insulation above the roof membrane and a drainage blanket over the membrane so that the melting point will always occur above it.

SLOPING ROOFS

It is traditional to regard a sloping roof as a more natural snow country design than a flat roof. A Swiss chalet is characterized as time tested snow country design, and so it is, but the principles which underlay the design style are not well understood. Typically, the traditional chalet has the farm animals below, giving their body heat to the humans on the floors above. Above the habitation is a thick layer of straw which insulates the cold attic above from the warmth below. The chalet walls are sheltered by a great sloping roof, usually of heavy rough slate, with broad eaves which protects all below. This roof slopes away to the sides and the entry is isolated from potential snow and ice cascade. The chalet walls are heavy solid wood which provide insulation and are held tightly together by the weight of the roof, preventing air infiltration. The ratio between the structure height and snow load is high and any ice dams that do form on the eaves only add to the load and press the structure more firmly together. Ice dams along the eaves result from atmospheric melting and solar radiation, not from the building heat below. Such a roof holds the snow, except during periods of prolonged thaw, but it is subject to wind stripping. In most locations the snow load on a chalet roof will be considerably less than the ground snow load.

As has been stated, a properly drained flat roof structure over a heated building does not usually form ice dams, but any sloping roof building in the snow country will form ice dams to some degree at the eaves. The magnitude of these dams are increased if a warm roof design is employed. The melt water, which on a flat roof would move to an interior drain, which remains ice free due to building heat, moves down the roof slope to the roof edge, where it is subject to refreezing (see Figures 1 through 8). In regions where there is a freeze-thaw cycle each day (very common in the American and Canadian far west), the roof edge freezes solid each night and this block of ice melts very slowly during the day as two-thirds of it is buried in insulating snow. All the while, melt water from building heat is migrating under the insulating snow blanket to the roof edge. This water builds up behind the ice dam at the eave and flows over its top. As soon as the air temperature falls below freezing (and it may have been freezing all day), a new dam forms on top of the old one . This process also leads to the formation of icicles which can grow to frightening size (see Figure D). The author has observed solid ice dams in the Sierras six feet above the roof edge which contained a retained lake of melt water in liquid state almost as deep. Under these conditions, icicles can form that reach to the ground from the eaves of a three-story building. The hydrostatic pressure of the lake behind the dam is sufficient to drive water through the smallest crack in the roof membrane. The combination of the ice and the water behind the dam produces loads on the eaves that may exceed ground snow by a factor of three.

It is apparent from this discussion, that sloping roof design in the snow country requires great care be taken. In many cases, higher standards are required for sloping roofs than flat roofs. The vast majority of sloped roof buildings in North America are plagued by ice dams. It is remarkable how little is understood about their formation, habits and control. Until very recently, they have virtually been ignored by the drafters of the building codes, even though they are the leading cause of snow country defects. More laboratory and field investigation is required to gain a comprehensive understanding of this nemesis.

WARM VS COLD EAVES

It is a basic principle of sloping roof design that a warm roof should be carried all the way to roof edge, in the same way that a cold roof (the umbrella) is carried to (or beyond) the roof edge. Ice dams are greatly enlarged by cold eaves, especially if roof insulation is thin or defectively installed and building heat produces considerable melting at the sloping roof surface. It is desirable to leak some building heat at the eaves in a warm roof design, as well as carry the building warmth to the outer roof edge. This will not eliminate ice dams, but it will reduce them. These warm eaves may be coated with a slippery material (flat seam stainless steel, for example). The combination of warmth plus smooth surface will reduce ice dam formation at the eave considerably.

In the same way, warm areas of the roof should not be designed up slope of cold areas. Ice dams will form at the warm/cold juncture. This can be of particular concern where skylights penetrate a cold roof or where heated spaces are above unheated porches. Unexpected problems may develop where some parts of a building are unheated while others are occupied.

SLOPING ROOF OBSTRUCTIONS

All vents and pipes should be excluded from sloping roof surfaces. This rule becomes more absolute as the down slope edge of the roof is approached, and it applies to both warm and cold roofs. Unless the snow blanket is very thin, vents will be covered by the snow and rapidly become ice encased. Even if they are carried above the anticipated snow blanket, they will still cause localized ice dams which intensify snow loads and can lead to leaks. There is no type of snow splitter that can cover a mid-roof vent pipe which will permit it to work properly in the deep snow country. All mechanical and plumbing vents should be located at the ridge or on the side walls, away from the slope of the roof.

Dormers are traditionally seen in snow country roof design but are often the cause of snow retention, ice dam formation and leakage. The junction between the dormer roof and the main roof is a natural snow trap, even in slippery warm roofs. It is not uncommon to see vast amounts of snow festooned around a metal roof dormer after the main body of the roof has shed its snow. In general, if dormers must be incorporated in the design, make them as steep and smooth as possible and do not locate them close together.

Chimneys are a major source of sloping roof failure in the snow country. If possible, locate chimneys in side walls away from sloping roofs so that no part of the chimney housing is in the slope plane of the roof. An ideal place for a chimney is at the ridge and the savings of locating it there may justify running the flue a considerable distance inside the structure. If the design dictates that the chimney housing must be located in the plane of the roof slope, it must be treated like a dormer. Ideally the chimney housing should be a snow splitter, so formed as to cause minimum snow blockage. At a minimum, assume the full ground snow on the roof from chimney to ridge, at a ninety degree fan from chimney to ridge bearing on the chimney housing. To design for less, runs the risk of sudden detachment of the chimney from the building. Even a strong, steeply cricketed chimney will produce large ice

dams. The chimney housing and the adjoining roof must be coated with an impermeable membrane well above the height of any anticipated ice dam.

SNOW ARRESTERS

In order to prevent snow and ice from cascading from steeply sloping roofs, it is possible to install snow arresters to hold the snow blanket on the roof. The forces on such devices are very great. They must be designed for at least the full ground snow load back up the slope of the roof to the ridge or to the next snow arrester. This may require considerably more structural support than a comparable flat roof design would require. Thin amounts of snow may slide under the arrester and large ice dams (with impressive static water heads behind them) may develop. When using snow arresters, a roof should never be designed for less than full ground snow load, and in shaded locations on the north side of roofs, and on the downwind side, double or triple ground snow load should be considered. A snow arrester should be thought of as a permanent ice dam and all similar precautions taken. Snow arresters do not mitigate icicle formation but rather intensify it.

GUTTERS

In an ideal snow country setting, the snow that falls on the roof will slip off into a safe resting place on the ground in an orderly manner. Unfortunately, the designer sometimes must locate his or her building close to others or organize the sloping roofs in such a way as to bring the down sloping roofs over habitable spaces. In such cases it is very desirable to not only prevent snow from cascading from the roof with a snow arrester, but to prevent the dripping of melt water which leads to icicle formation and dangerous ground ice. It is possible to design gutters at the downslope edges of such roofs. These gutters must be located so that they can not be carried away by slipping snow. They must be heat traced to inhibit icicle formation and blockage by ice. Careful consideration must be given to the disposal of water caught in a snow country gutter. If it is lead off in an exterior downspout, these must be fully heat traced to a storm water drain that is below the frost line. Failure to provide complete heat tracing will result in ice blockage and destruction of the leaders. It is also possible to run the gutters beyond the roof edge and have the water fall to the ground or run down a chain. This will produce a great mass of ground ice which is not always easy to deal with in the landscape. The gutter can also be drained in hard piping inside the heated building in a manner similar to a flat roof design. Again, the heat trace must be carried deep enough into the heated enclosure so that no chance of freezing exists. Clearly, sloping roofs, snow arresters, and heated gutters represent an expensive alternative to flat roof design which can only be justified on aesthetic grounds.

UNEVEN ROOF LOADING

A very common sloped design in the snow country is the traditional saddleback (pitched) roof (see Figure 9). If this roof design is located so that its ridge runs east/west, the major faces of the roof will face north/south, which means (in North America) that much less solar radiation will reach the north side. As snow is a black body to the infrared component of sunlight, considerable melting and sublimation will occur on the south roof face. Also, if

448

the roof is warm and slippery, the snow pack is much more likely to slip on the south facing slope. If the prevailing wind also comes from the south, the added factor of wind stripping is added to the south facing snow reduction. Depending on climate and location, very little snow may accumulate on the south face of the roof. In contrast, the north face may receive far more than ground snow load. Some of the snow that is stripped from the south is deposited on the north face. There is little solar melting on the north and building heat causes melting at the underside of the snow blanket, which produces an ice dam at the lower edge of the roof. Daily freeze thaw adds to this dam until the snow pack approaches the height of the ridge. Despite the slope of the roof, there is little tendency for the snow and ice to slip on the north face and the limiting factor is the ridge height. As the snow blanket thickens, it also becomes more massive and a considerable amount of it can approach the full weight of water. Clearly the hydrostatic pressure at the roof surface can be very great.

Given the scenario outlined above, it would not be unusual for such a roof to have little snow load to the south and two times (or more) ground snow load to the north. Structural (and architectural) design in the snow country should take such factors into account. Building codes should be amended to reflect these effects.

HORIZONTAL FORCE FACTORS

Buildings in the snow country are more at risk from horizontal forces than those in many other climates. Consider the scenario outlined above, and add to it a large magnitude earthquake. The structure is already subject to un-balanced loading; if it is shocked by an earth tremor, the horizontal bracing in the building can be subjected to abnormal forces, especially at the found-ation level. The current UBC permits a reduction of up to seventy-five percent of the roof snow load be considered in seismic design with the approval of the building official. This reduction is unjustified in most cases. In some cases, more than the full ground snow load, acting in an un-balanced fashion on the roof, should be required for seismic design.

INSULATION AND VAPOR RETARDERS

All sides of heated buildings subject to sub-freezing temperatures for long periods, should be insulated and vapor protected. Walls, floors, and roofs all have their individual design problems, the details of which are beyond the scope of this article. Let it suffice to note a few important principles. If batt insulation is used, it must be tight fitted (see Figure E). Even small cracks on the sides of the batts permit a great amount of warm, moist air to circulate around the insulation and reach the exterior face of the structure, which can lessen or even eliminate the utility of the insulation. A competent vapor retarder must be installed on the inner (warm) side of heated buildings. If warm, moist air condenses on the inner face of exterior elements it can cause what appears to be leaks. This condensation water inside exterior building elements can cause rot and rapid degradation of the structure. The integrity of the insulation and vapor control system is of paramount importance to the snow country designer and they should be considered early in the design process.

CONCLUSION

The snow country designer must first determine the site conditions that prevail at the building location under consideration. Ground snow load, prevailing storm wind, freeze/thaw cycle, solar radiation, humidity, and seismic forces are among the factors that must be considered. A proper design must satisfy all of these as well as the functional and aesthetic requirements of conventional architecture. Secondly, the form of the building must be chosen to bring it into harmony with its environment. A designer who works in the snow country for the first time is well advised to retain the assistance of knowledgeable consultants. The snow is both beautiful and deadly. The designer's objective is to retain the former and avoid the latter.

TEMPERATURE GRADIENT
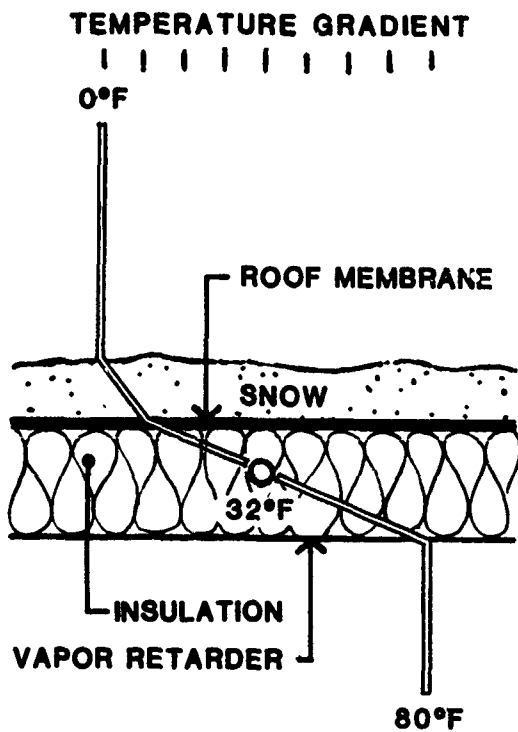
Where snow depth is thin relative to insulation, no melting will occur from building heat. Figure 1
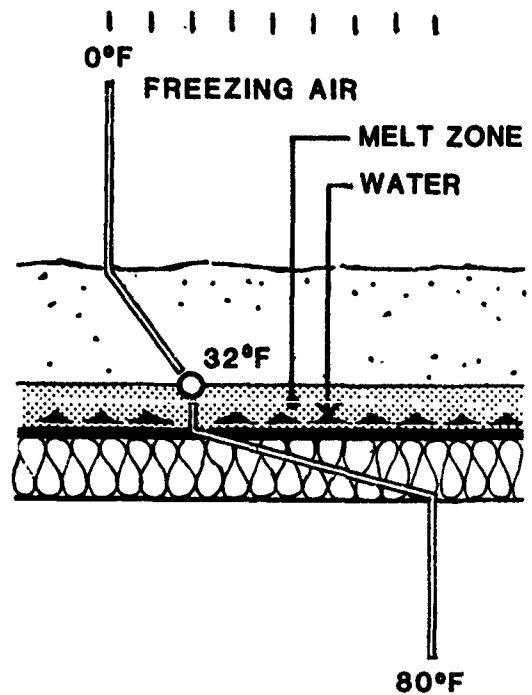
Where snow blanket is thick, a melt zone will exist above roof membrane. Figure 2
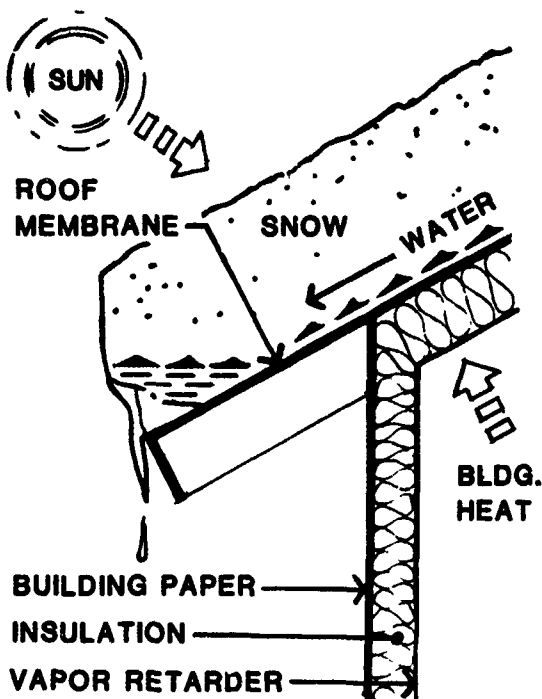
Melt water from building heat and solar radiation will run to eaves. Figure 3
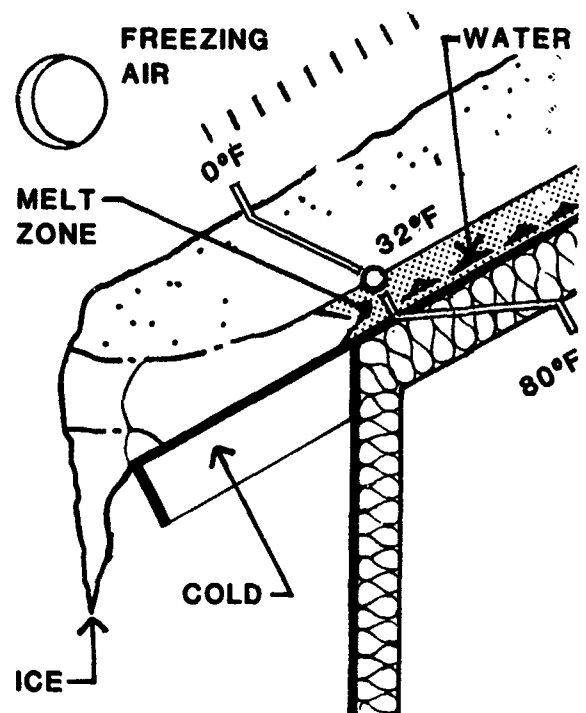
If snow blanket is thick, melt water will freeze solid at cold eaves. Figure 4

451
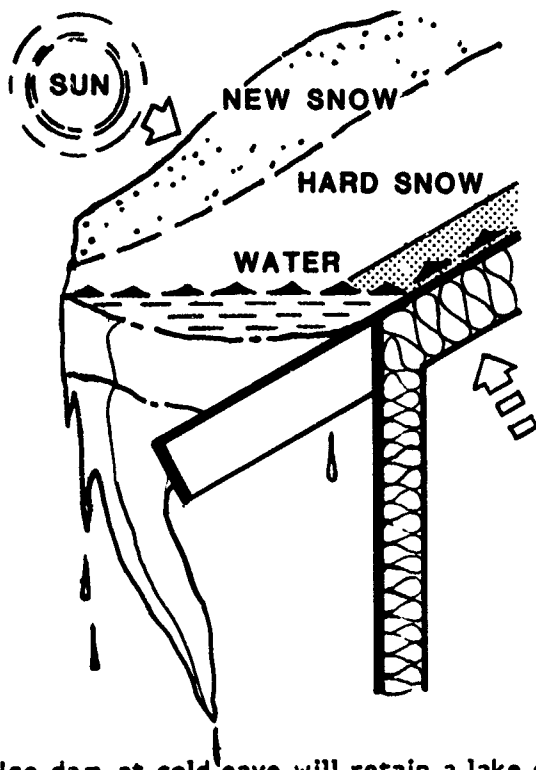
Ice dam at cold eave will retain a lake of melt water. **Figure 5**
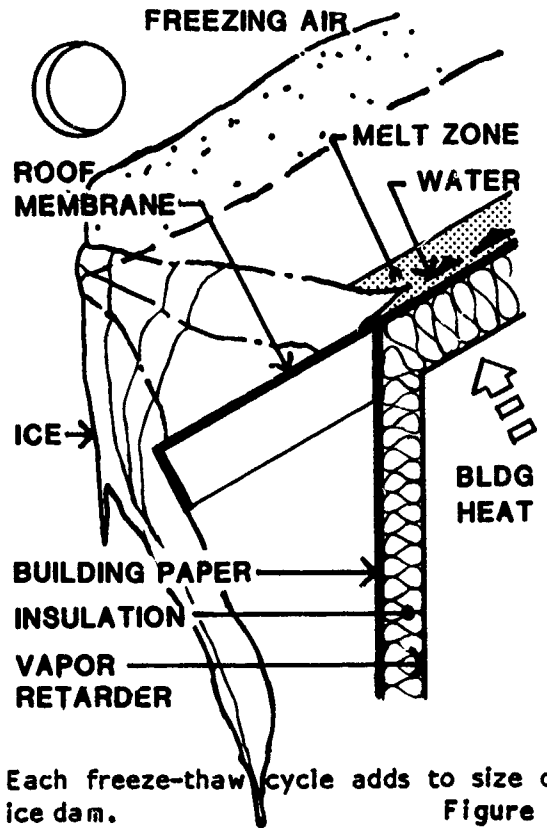
Each freeze-thaw cycle adds to size of ice dam. **Figure 6**
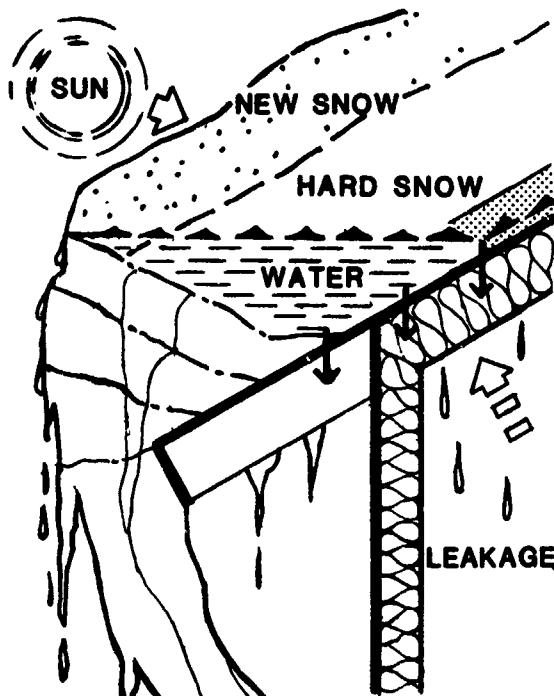
Surplus melt water runs over top of ice dam forming icicles. **Figure 7**
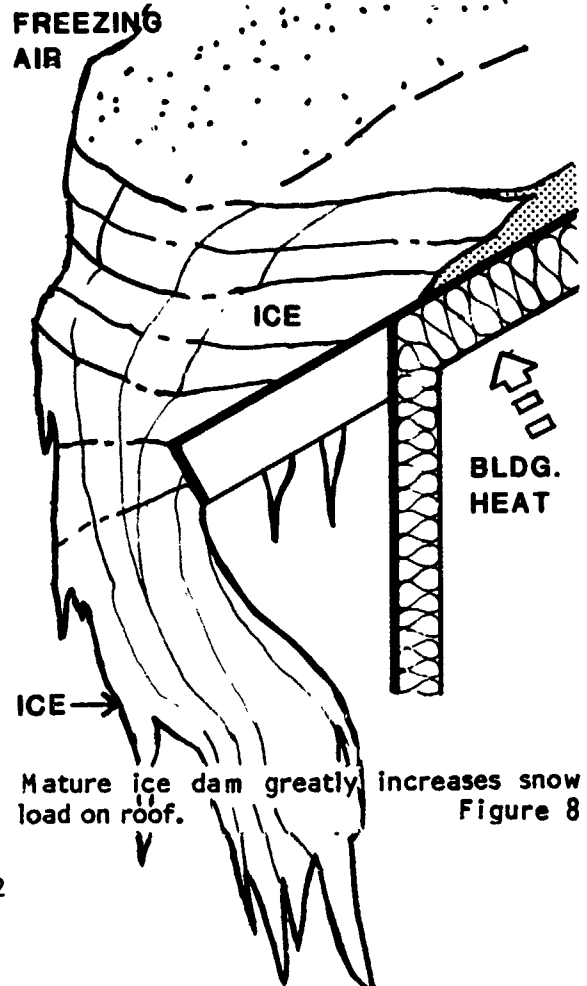
Mature ice dam greatly increases snow load on roof. **Figure 8**

SOUTHERN EXPOSURE

WIND PRESSURE

NEW SNOW

HARD SNOW

ICE

ICE

WATER
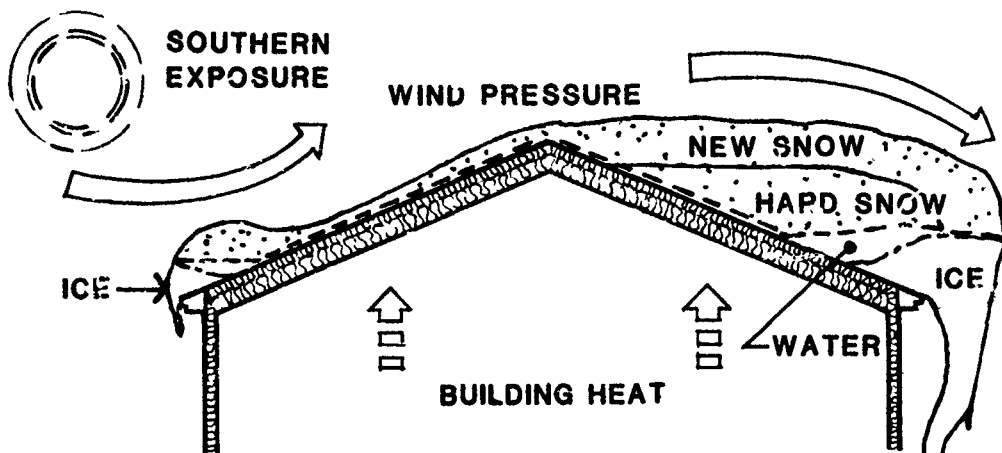
BUILDING HEAT

Snow is stripped to windward and deposited to leeward; ice dams can block snow from slipping and snow can build-up to ridge on warm roofs. Figure 9

WIND PRESSURE

SNOW

ICE

ICE

WIND PRESSURE

WATER
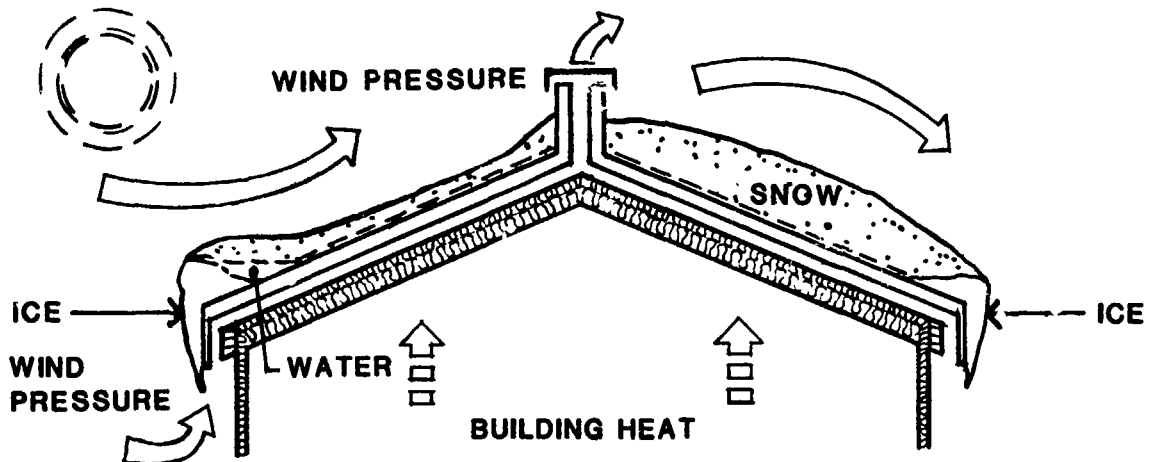
BUILDING HEAT

In cold roofs, upper roof acts as an umbrella over lower (warm) roof. Building heat does not reach upper roof. Snow is removed by wind stripping. Figure 10

WIND PRESSURE

ROOF DRAIN

WATER

SNOW

SCUPPER
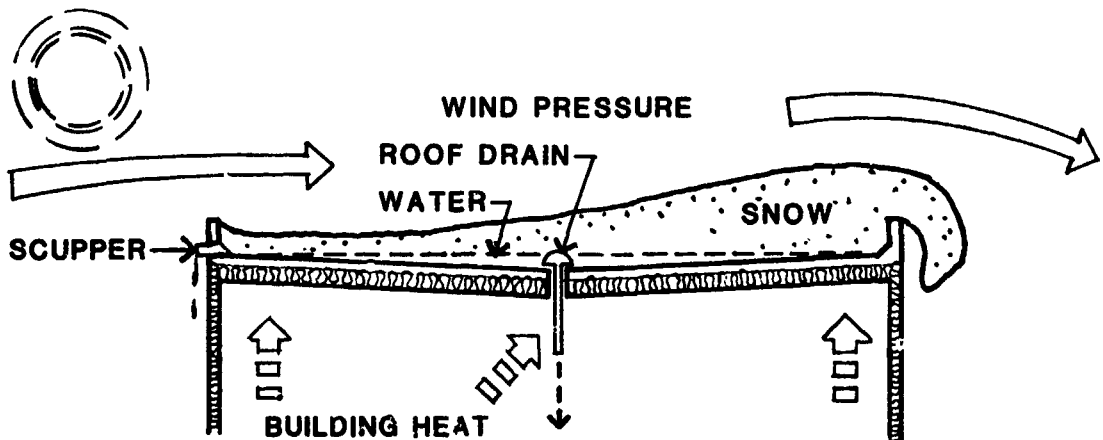
BUILDING HEAT

In flat roof design, snow is stripped off roof on windward side. On larger roofs, snow builds up cornice on leeward side. Where building is continuously heated, drainage should be internal. Drains are kept ice free by building heat. Figure 11
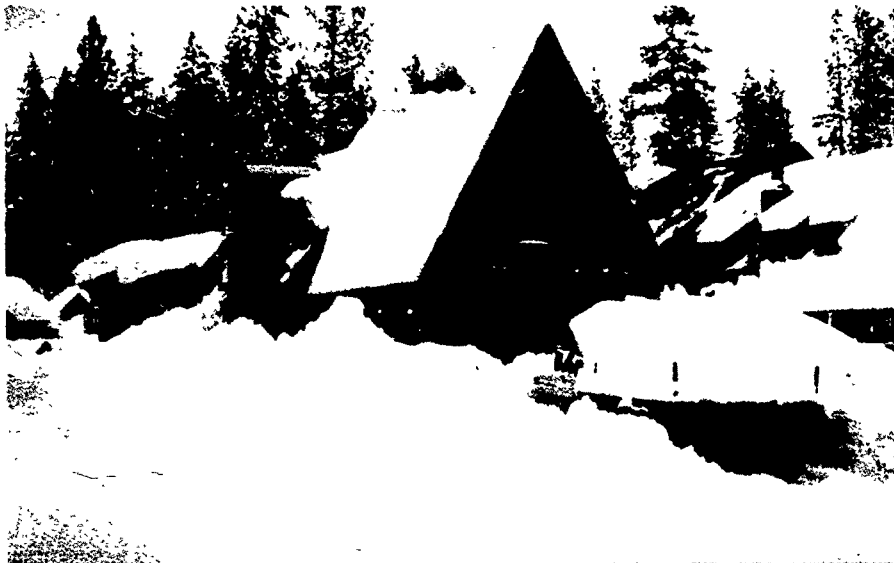
Steep metal roofs can retain considerable snow if conditions are right. Figure A

Snow can creep-off roof edges and apply loads far beyond ground snow load. Figure B

Flat roofs are stripped of snow by the wind and are often subject to less load than sloping roofs with ice dams. The Boreal Ridge Lodge at Donner Summit where ground snow loads can exceed 400 psf. Figure C

Ice dams can build-up at roof edges and work outward, putting pressure on roofs and threatening to break windows.   Figure D

Loose fitting insulation and improperly installed vapor retarder can allow building heat and moisture to reach roof surfaces causing snow melting and condensation on cold surfaces.   Figure E

Determination of Ground and Roof Snow Loads at a Particular Site

Douglas R. Powell*

The determination of maximum expected roof snow loads at the actual site of a building is vital to the proper economical and safety design of that building. This requires an accurate prediction of ground snow loads in the vicinity of the building, especially extreme values, and an understanding of how snow loads may be distributed on the roof. For many communities, and some mountain areas in the United States and Canada, generalized maps of ground snow loads are available. However, such maps are too often not useful for ascertaining ground and roof loads at a specific site. Such factors as topographic relief, the directional orientation of the site, exposure to prevailing winds, minor changes in elevation, variations in local vegetation, and the percentages of sunlight and shade can lead to significant differences in snow accumulation within short horizontal distances. After some 35 years of measuring snow water equivalents in the Sierra Nevada of California, Afghanistan, and Chile, primarily for stream flow forecasting, the author of this paper is acutely aware of these variations in snow depth and water equivalent within small areas. Following are some observations, gleaned from this experience and research, which might be useful to workers investigating snow conditions at a particular site.

A first basic step is to consult all available weather data relevant to the site. For general synoptic weather patterns this may include an area of thousands of square miles, but much smaller areas for details of precipitation, temperature, and wind. All too often, reliable data in meaningful proximity to the site is sparse, discontinuous, or lacking, with disturbing extrapolations from the nearest data stations necessary. However, a major effort should be made to investigate all possible records which might have relevance. The most reliable sources are records compiled by official weather services, but amateur and volunteer observers may often have detailed records closer to the site than official stations. It may take much time and diligence to uncover this private weather data, which require careful appraisal for accuracy and reliability, but such records can be very helpful in an analysis of weather patterns at a site not adjacent to an official weather station. In a study of basic weather patterns applicable to the site, attention to the following parameters is valuable: average annual precipitation, especially snowfall (the latter is often not available); extremes of precipitation; intensity and duration of snowstorms; the density of snow as it falls and as it accumulates throughout the season; seasonal distribution of rain and snowfall; the time of maximum snow depth and water equivalent; duration of maximum, or near-maximum, snow depths and water equivalents; rain events on snow; temperature data indicating the onset of melt seasons or thaws during the accumulation periods; and wind velocity and prevailing wind direction. For many sites, especially those in mountainous areas away from cities, the weather record will be sparse, short,

* Lecturer, Department of Geography, UC Berkeley

or non-existent, which emphasizes the necessity to search intensively for all applicable records, official or private.

Towns and cities may well have official daily snowfall and accumulation records, but for determination of snow loads in mountainous or rural areas, an especially valuable source of information is data acquired by snow surveying agencies for the purpose of forecasting stream flow. In western United States, there are over 2,000 stations called snow courses, at which measurements of snow depth and water equivalent are taken, usually on or near February 1, March 1, April 1, and May 1, earlier and later at some sites. Most of these snow courses are located in mountainous regions where little or no other snow data are available. In California, the chief snow surveying agency is the California State Department of Water Resources. In Oregon, Washington, and the Intermountain and Rocky Mountain states, the chief agency is the Federal Soil Conservation Service, with local offices in each state. In Canada, each province has an office for taking and coordinating snow surveys, as the Surface Water Section in the Ministry of Environment in British Columbia.

At most snow courses, the instrument used for determination of snow depth and water equivalent is the Federal Snow Sampler, composed of sections of hollow aluminum tubes, generally 30 inches (65 centimeters) in length. The sampler, with sufficient sections to reach from the top of the snowpack to the ground, is pushed through the snow to the ground acquiring a core of snow. The bottom section is fitted with a steel cutter tip to cut through dense snow and ice layers. The inside of the cutter tip is slightly smaller in diameter than the rest of the tube which prevents the snow core from sliding out through the bottom when the sampler is lifted out of the snowpack. The diameter of the cutter tip is 1.485 inches; one inch depth of water of this diameter weighs exactly one ounce; thus a scale calibrated in ounces is used to determine the water equivalent of the snow sample in inches. After the sampler is driven through the snowpack to the ground, the snow depth is recorded by reading the scale marked along the sampler's length; then the sampler is lifted out of the snow and weighed. By subtracting the weight of the empty sampler, the water content of the core is obtained. Usually, ten samples 50-100 feet apart in the United States, are taken at each snow course. These samples are averaged to obtain one value of snow depth and water equivalent for each snow course. Samples and scales calibrated in the metric system are available. Other variations of metal tube instruments are used, but the Federal Snow Sampler, sometimes called the Mount Rose Sampler, is by far the most common. With minor variations, it is the same instrument designed by James Church, a professor of classics at the University of Nevada, in the first decade of the twentieth century, and first employed on and near Mount Rose in the Sierra Nevada along the California-Nevada border.

Although the determination of snow water equivalent at these snow courses is used primarily for stream flow forecasting, this parameter is vital in the determination of ground and roof snow loads at any site. Thus, snow course data is extremely valuable in investigation of snow loads, and is often the best, or even the only, reliable and long-term data source in mountainous regions or other areas away from weather stations. Many of the snow courses have continuous data from the 1930's to the present, especially in California. Personal possession of a Federal Snow Sampler, with a sufficient number of sections to reach the ground or roof with the snow depths to be expected at the site, is a valuable asset to any serious worker in snow load investigations. Using the sampler effectively does not call for great technical skill or

457

extraordinary physical strength, but experience with all possible conditions, especially when adverse or unpleasant, is critical for consistency and reliability in data acquisition. Common problems encountered in sampling are: difficulty in penetrating ice layers along the ground or within a deep pack; collecting a full core in light/powder snow; sticking of snow inside the tubes in warm weather; and ponding of water at sites during active snowmelt. Ample field experience with the sampler under a wide gamut of weather and snow condition can prepare the investigator to recognize the limitations of the sampler and prevent inaccurate data collection. In general, one can assume that the data published by the snow survey agencies is reliable, as accurate as the equipment allows.

Verification experiments in the field indicate that in deep snowpacks, with high densities and high water equivalents of 40-50 inches or more, the Federal Sampler tends to overweigh (additional snow may be forced into the core) and so water equivalents measured by the sampler may be too high, perhaps as much as 70 percent above the actual water equivalent at the particular sample point. This is a subject calling for additional investigation, my own experience with the sampler casts doubt on overweighing of this magnitude, but investigators of snow load problems should be aware of this possible error in snow survey data dealing with high water equivalents.

Since the 1960's, another device for measuring snow water equivalent has been increasingly employed at snow survey courses and other locations where this information is desirable. This is the snow sensor, an automated device with a telemetered system for transmitting the data to a receiving office. The principal snow sensor used is called a Snow Pillow, a butyl rubber or steel envelope filled with an antifreeze solution. The snow above the surface of the envelope changes pressure on the antifreeze fluid proportional to the weight of the water equivalent in the snowpack. This snow water load is read by a pressure transducer and the magnitude of this force can be telemetered to a central master receiving station, such as Sacramento, California, Boise, Idaho, and Ogden, Utah. The technology of the transmission system is impressive. In California, the data is sent by radio to a Geostationary Operational Environmental Satellite (GOES) which is "parked" 22,300 miles above the equator at 135 degrees west longitude, then relayed to a receiver terminal in Sacramento for storage or on-call use. The Soil Conservation Service transmits radio signals skyward, which are reflected downward from ionized meteorite trails in the upper atmosphere between the data sites and the master stations at Boise and Ogden. Both transmitting systems generally use solar panels for a power source.

These systems make daily readings of water equivalent possible, and many sensors also transmit other data, as daily air temperatures. Snow depths are not recorded, so density readings are not available. The data is subject to error--pillows may leak and they may be slow in responding to quick changes in water equivalent, particularly during heavy storms or rapid snowmelt. Bridging of the snow and accumulation of melt water above the sensor may result in inaccurate data and the electronic equipment may malfunction. However, sensors are increasingly employed, there are perhaps 600 currently in existence in the Western United States. Many sensors are located on pre-existing snow courses, and dual sets of water equivalent data, by federal sampler and telemetered sensor, are available. The figures from the two sources are, as to be expected, often very similar. It should be kept in mind that the

sensor data are from one point, whereas the federal sampler data are an average of many points, usually 10.

There are other automated and telemetered devices for ascertaining water equivalent at a particular site. One type installed on the ground at a chosen location is a radioactive gauge, which operates on the principle of measuring the degree of attenuation by a snowpack of gamma ray radiation from a source to a counter. This can be calibrated in inches or centimeters of water. Another is a Nuclear Profiling Gauge, consisting of parallel tubes, about 26 inches apart, extending through the depth of a snowpack, containing a gamma radiation source and counter, and measuring water equivalent by the attenuation of the radiation between the tubes. These devices are expensive, not numerous, and used mostly for research in snow hydrology, but some date useful for snow load determination is available from them.

Another method of measuring gamma ray attenuation is being developed by the Office of Hydrology, United States Weather Service, in Minneapolis, Minnesota. This depends on measuring gamma radiation from an instrumented aircraft flying 500 feet above the ground over a designated strip of terrain, roughly 10 miles long, 1,000 feet wide, in gentle terrain; smaller areas are used in mountainous country. The designated strip is flown over without snow cover to acquire background gamma radiation readings, then at various times during the winter with snow cover to measure the water equivalent from the degree of attenuation of the gamma radiation by the snowpack. All of these methods of using gamma radiation have one serious limitation. If the water equivalent is about 40 inches or more, the radiation recorded by the counter drops down to amounts difficult to measure without major error. But these aerial surveys show much promise in gentle terrain with low to moderate snowpacks, and will produce data from much of midwestern and western United States in the next few years, including many areas where data is now sparse or non-existent. All of the automated, telemetered systems use occasional ground truth water equivalent measurements by snow tube samplers to verify their data.

This data from the snow courses and sensors can be most useful in investigation of snow loads. The data are reasonably accurate for water equivalent measurements at the site of the course or sensor. Records are often of many years duration, and are available without charge from the measuring agencies. They are worthy of intensive study. The records can produce more information than just water equivalent. From the manually measured snow courses, density figures are available, particularly throughout the snow accumulation season; average densities for each month or other time intervals can be calculated. The time of maximum accumulation of ground snow loads and the duration of these high loads can be known. Of utmost importance in snow survey and sensor records is finding the extreme maximum value of water equivalent accumulation at the site of the snow course. I, for one, am somewhat skeptical of the value of recurrence interval projections, and place more confidence in actual measurements, particularly in a record of many years. In a snow course with 10 sample points there will often be significant variation in the measurements from point to point that are masked in the course average, so observation of the detailed course notes can give the observer a feel for variation in short distances.

There is the inevitable and difficult problem of extrapolating the data from snow courses to the particular building site. In general, the closer the two are together, the better. This calls for

the most careful comparison of course site to the building site, and is always subject to imprecision and error. The location and detailed descriptions of course and sensor sites, giving elevation, exposure, orientation, surrounding topography, and vegetation are available from the measuring agency and can be very helpful. I recommend personal reconnaissance of the snow course locations, if possible. It is worth repeating that in many areas snow course and sensor data, from the nearest available location and maybe even in a different watershed, could be the best source of data for the particular building site.

Several snow course and sensor data points may be applicable to the specific building location. Of particular value is the existence of more than one course or sensor in the area near the building site that differ in elevation and/or exposure. This can be helpful in drawing ground snow load contours, using the measured sites as reference points, over an area large enough to include the building sites. Snow accumulation varies with elevation, especially on leeward slopes of mountain barriers of more than a few hundred feet, and with change in exposure, especially to prevailing storm winds. An effort to determine ground snow load contours from a location with measured water equivalent data to the building site is desirable. The reliability of these contours is enhanced in direct proportion to the number of data locations applicable to the building site. In comparisons between snow course and building sites, a thorough knowledge of and experience with the weather patterns and topography of the region are desirable.

Consulting with people with knowledge and experience of weather and snow conditions in the vicinity of the site under consideration may be useful and even vital to an analysis of snow loads. This is particularly true of wind velocity and prevailing wind direction, where printed records are often totally lacking. This brings up the thorny problem of assessing the reliability of the informant. It requires the utmost diligence in seeking out informants and the utmost care and skill in evaluating the accuracy of their information. I have found one test useful in eliminating unreliable observers. Ask the potential informant questions to which you know the answer and evaluate the accuracy of their answers. Very few weather observers, other than weather services or snow survey agencies, take water equivalent measurements, so estimates of densities are necessary in analysis of local, private snowfall and snow depth readings. Knowledge of weather patterns and temperatures during snowfall, and extrapolating density figures from the nearest applicable snow course, are valuable aids to density estimates.

A careful study of the immediate environment of the buildings, topography, compass orientation, wind direction of snowfall, amounts of sunlight and shade, is necessary and vital. Of particular importance is the alignment of the roofs in regard to prevailing storm wind direction. If perpendicular, or largely so, to prevailing storm winds, then unbalanced snow loads on lee roofs are likely. In wind analysis, the testimony of reliable local observers can be very helpful and may be the only source of usable information.

Although difficult to gather, and again, local informants can be helpful, data on the frequency of significant storms and the intensities of extreme events at the building sites are highly desirable. At many sites, shoveling snow off roofs is used to diminish snow loads. Knowledge of storm frequencies and intensities can be valuable in estimating feasibility and costs of shoveling. In mid-February, 1986, mid-elevation sites in the Sierra Nevada of California received 20-40 inches of snow water equivalent in ten days, often accompanied by high winds.

Shoveling of roofs was essentially impossible during this storm period. Massive buildups of roof snow loads not amendable to shoveling can occur during such storm events, especially on lee roofs perpendicular to the storm wind direction.

Another important environmental factor at a building site is seismic risk. The possibility of earthquakes of Richter Scale of 5.0 or higher (especially above 6.0) occurring at times or high of maximum roof snow loads, must be considered in any analysis of snow load conditions. General seismic risk maps are valuable. Earthquake risk is not as variable in short horizontal distances as snow accumulation. The dates of historic earthquakes along the east side of the Sierra Nevada show that many have occurred between March and May, the period of maximum snow accumulation in that region. This has led to speculation by geologists and seismologists, not conclusive proof as yet, that the weight of large ground snow loads could be a triggering factor in causing earthquakes. In any event, knowledge of the earthquake history of the building site area is important in proper snow load assessment.

In this paper I have outlined some major considerations and problems in determination of ground and roof snow loads at a particular building site, which may be some distance from sites of reliable weather records. Even with close proximity to weather stations, variations in snow accumulation, in short horizontal distances, make extrapolations of data difficult and very much subject to personal evaluation. Much attention is given to data from snow courses and snow sensors, as this data may often be the most relevant for investigation of snow loads at any one site. Records and testimony from persons with knowledge and experience of weather in the vicinity of the site can be useful and important additions to snow load investigations, if the persons are carefully screened for reliability and accuracy. There is no substitute for the investigator possessing a good general knowledge of weather patterns in the vicinity of the site.

Roof Design in Cold Regions

Wayne Tobiasson[1]

ABSTRACT

Roofs continue to be a problem in cold regions even though many excellent membrane and water-shedding systems are available. Dead flat roofs of any type are a design mistake. In cold regions, membrane roofs should have a slope of 1/4 in./ft and should drain internally. It is usually best to slope roofs by inclining the frame rather than using tapered insulation.

Most water-shedding roofs drain to cold eaves and are thus subject to ice dam problems. Such problems can be minimized by designing a "cold" ventilated roof, by insulating it well, by minimizing the overhang at the eaves, by increasing the roof slope and by providing an unobstructed slippery surface from which snow will slide. However, when using slippery-surfaced systems, it is essential to provide a place for the snow to slide where it will not endanger people or damage property.

INTRODUCTION

Roofs continue to be a problematic component of buildings in cold regions even though many excellent membrane and water-shedding systems are available. Some designs that work well elsewhere have limitations due to icings at eaves and sliding snow.

TYPES OF ROOFING

Tiles and shingles are examples of *water-shedding* systems that work well on relatively steep slopes where rainwater and snow meltwater can flow off them, and their configuration (e.g. their overlap) prevents wind from forcing water up behind them and into the building.

So-called "tar and gravel" roofs and the newer rubber and plastic "single plies" are watertight *membrane* systems totally sealed against water penetration. Membrane systems should have some slope to preclude the ponding of water on them. A "dead flat" membrane is a design mistake. A minimum slope of 1/4 in./ft works well in cold regions. It is usually best to create the slope by sloping the frame rather than using tapered insulation.

I. Research Civil Engineer, U.S. Army CRREL, Hanover, New Hampshire

Flaws at flashings, penetrations and seams are the primary cause of leaks for **membrane** roofs. Attention to these details is a critical design issue.

Standing-seam metal roofs have many membrane roof features. However, in cold regions where water can back up behind ice dams and slush can form on roofs, it is wise **not** to think of metal systems as membranes since they are usually not watertight in their valleys, at their eaves and ridges and at penetrations. Standing-seam metal roofing systems perform very well in many areas but they have some limitations in cold regions.

SYSTEM CONFIGURATION

Water-shedding and membrane systems can be used on either **framed** or **compact** roofs but it is common to have compact membrane systems and framed water-shedding systems.

A **compact** roof with membrane waterproofing is shown in Figure 1. The insulation is placed above the roof deck. There is little opportunity for air movement within a compact system because (1) it contains no air spaces, (2) the insulations used are usually of low permeability, and (3) wires and pipes are seldom routed within it. A compact roof topped with a waterproofing membrane is very resistant to air leakage. Because of this, such systems suffer few condensation problems in cold regions. This is particularly true of built-up systems that have their components adhered together in solid moppings of hot bitumen.

Many designers no longer use built-up membranes because of past problems. However, these membranes are now made of much improved materials that perform well in cold regions.

Some loose-laid single-ply systems are experiencing condensation problems in cold regions. I expect that these problems are caused by the loose nature of the systems and the many penetrations in their air-vapor retarders by mechanical fasteners. This looseness decreases their resistance to air leakage. Nonetheless, many single-ply systems work well in cold regions.
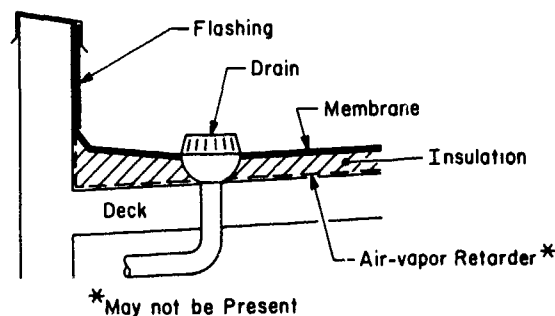
Figure 1. A typical **compact** roof.
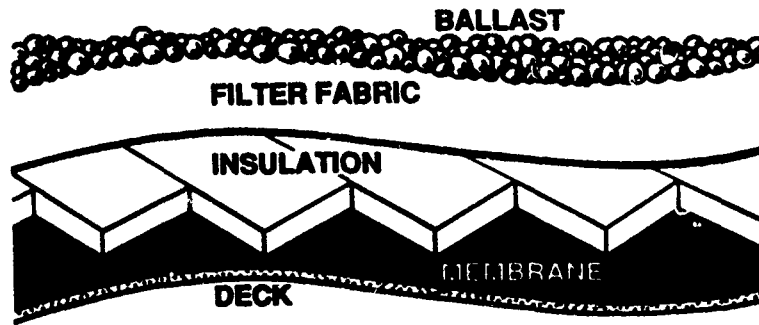
Figure 2. A protected membrane roof.
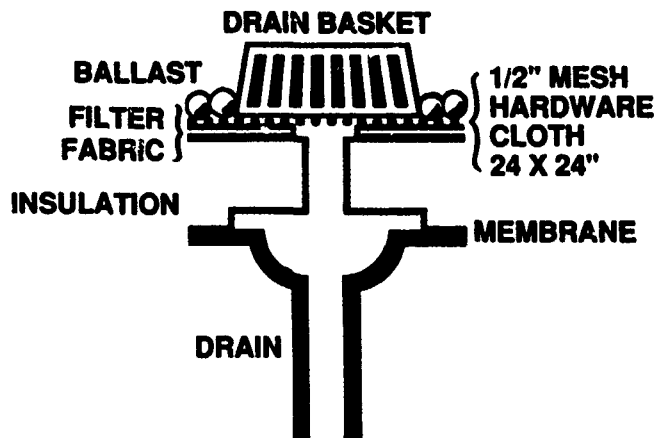
Figure 3. The drains of a protected membrane roof are insulated to prevent icings there.

Protected membrane roofs (Fig. 2) have an excellent track record in cold regions. Located below the insulation, the membrane is protected from the sun, mechanical abuse and traffic. It remains at a relatively constant temperature day and night, summer and winter. In winter the membrane is warmer than the surface of the roof; thus any meltwater at the base of the snow is warmed as it moves down to the membrane and then to the drains. This greatly reduces the potential of ice forming at the drains, provided that they are also insulated (Fig. 3). The filter fabric above the insulation "rafts" the system together and reduces the ballast needed over most of the roof to 10-12 psf no matter how much insulation is used. The filter fabric also keeps dirt out of the system, which facilitates drainage.

A **framed** roof is shown in Figure 4. It is insulated below the deck between framing members. Often relatively inexpensive batts of permeable fibrous glass or rock wool insulation are used. It is common for elec-

trical wires to be placed among the batts and for fixtures to be recessed up into the roof. Many air leakage paths are present in such roofs.

Airtightness and vapor control are important in cold regions, because warm, moist indoor air tends to move upward into the roof in cold weather where it can cause condensation problems. In cold regions most roofs need air-vapor retarders. The secret of condensation control is air-vapor retarder **continuity,** to minimize the leakage of moist indoor air past gaps and flaws in the "as built" retarder. Continuity is very hard to achieve in **framed** roofs. As an acknowledgment of this difficulty, most framed roofs in cold regions contain a ventilated air space above the insulation as shown in Figure 4. Such enclosed rafter spaces, open at each end, can usually provide enough ventilation to take away any moisture that passes a reasonable air-vapor retarder in roofs with a slope of 3:12 or more, provided the air passage is not much over 20 ft
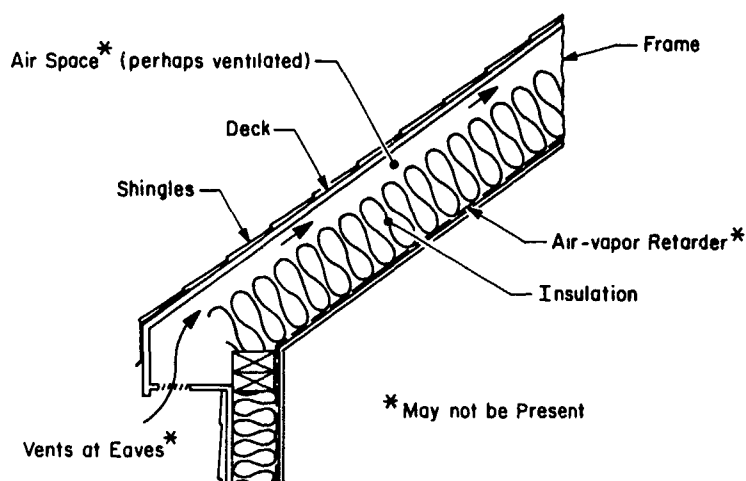
Figure 4. A typical **framed** roof.
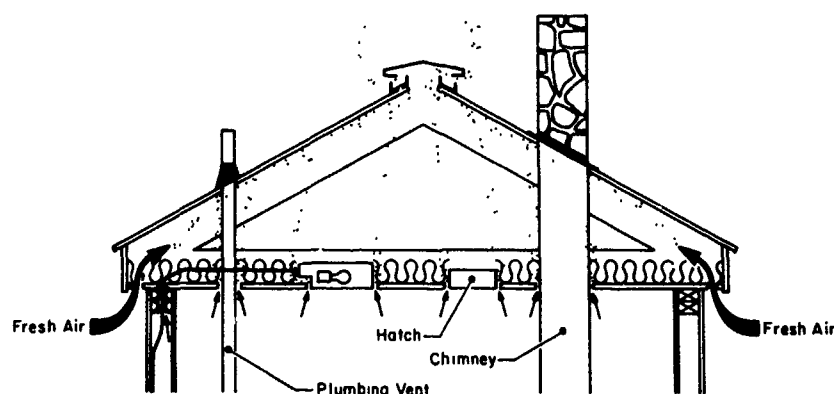
Figure 5. Air leakage paths into an attic.

465

long. At lower slopes it is usually appropriate to interconnect all in-
dividual air spaces by installing purlins on the rafters before the deck
is laid.

In very cold regions *framed* roofing systems with a slope of less
than 1:12 usually should be avoided, since they are difficult to seal
against air leakage and they are hard to ventilate.

When an attic is present below a sloped roof, it is relatively easy
to ventilate away any moisture that moves up through the ceiling. Con-
tinuous vents at the eaves and ridge are usually quite effective, pro-
vided that leakage of moist indoor air into the attic is controlled.
Typical air leakage paths are shown in Figure 5. Seals against air leak-
age are needed at these locations.

DRAINAGE

Membrane roofing systems should drain internally (Fig. 1). The use
of over-the-eaves drainage or drainage through scuppers is problematic
since icings form at these cold places (Fig. 6 and 7), allowing water to
pond on the roof until the dam melts in warmer weather. However, scup-
pers elevated a few inches above the membrane can be used for secondary
(i.e. emergency) drainage in the event that the primary drains become
blocked (Fig. 8).

Figure 6. Scuppers should not be used for primary drain-
age in cold regions.
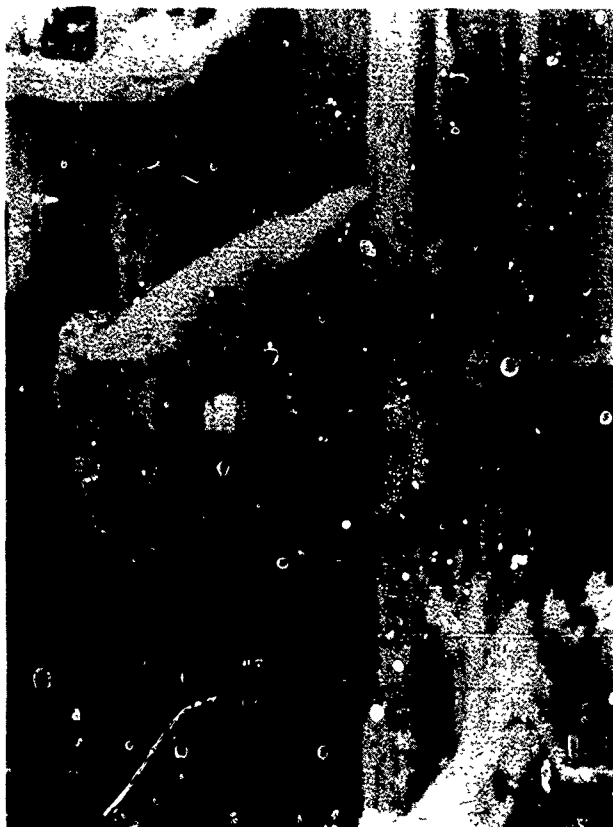
Figure 7. Icings from roof meltwater.

Most **water-shedding** systems drain at their eaves, and thus they are subject to ice dam problems. Several features can be incorporated into roofs to minimize icings at eaves. First and foremost, the roof can be ventilated to cool the u. erside of its top surface. Periods during which meltwater is created by building heat are reduced when a **cold** ventilated roofing system is used. (Building heat, not the sun, is usually the primary cause of ice dams, since the sun also warms the eaves.)

The amount of ventilation provided to prevent condensation problems is usually enough to minimize icings at eaves in reasonably well-insulated buildings.

Icings can also be reduced by increasing the amount of thermal insulation in the roof, by increasing the slope of the roof, by making the surface slippery so that snow slides off, by not installing gutters and by reducing the overhang at the eaves. However, overhangs should not be less than 6 in. on roofs without gutters for fear of wetting the walls below or having icings form on them (Fig. 9).

Since some icings are still likely, it is appropriate to convert the lower portion of the roof from a water-shedding system (that will

467

Figure 8. Elevated scuppers can be used for secondary (emergency) drainage.
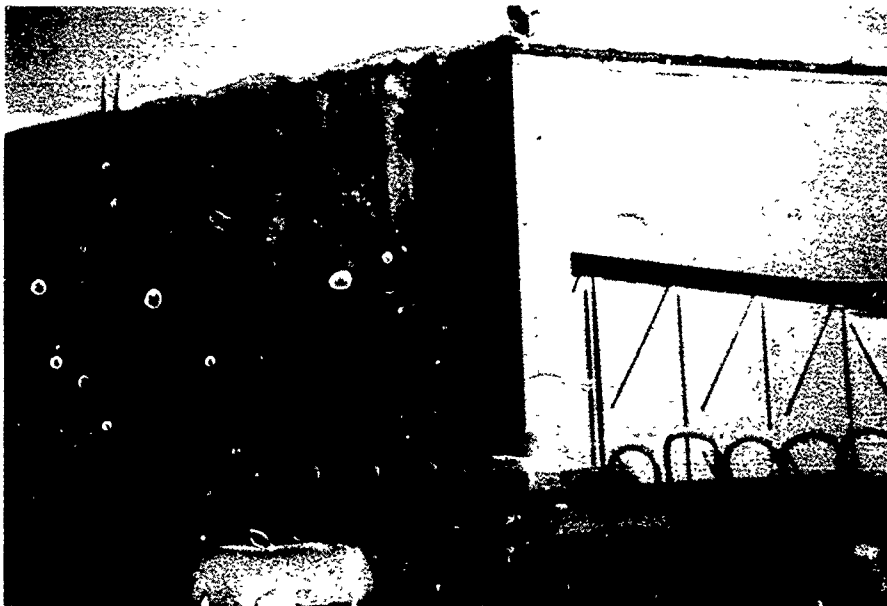
Figure 9. Icings can form on walls if the eaves do not overhang far enough.

Figure 10. Electrical heating cables were needed on this roof to prevent the formation of large ice dams.

leak if water ponds on it) to a membrane system that can resist ponded water. A good way to accomplish this is to place a 2-1/2- to 4-ft-wide strip of modified bituminous sheet material (i.e. a rubberized asphaltic sheet) on the deck under the water-shedding system in valleys and along eaves.

In most cases, a properly designed roof will not require electrical heating cables zigzagged along the eaves. However, if large icings form on a roof, such cables (Fig. 10) can be used to melt holes through that ice to prevent water from ponding on the roof and leaking into the building. Hammers, hatchets and salts used at the eaves usually do more harm than good.

Low Winds

Baffle

High Winds and Snow
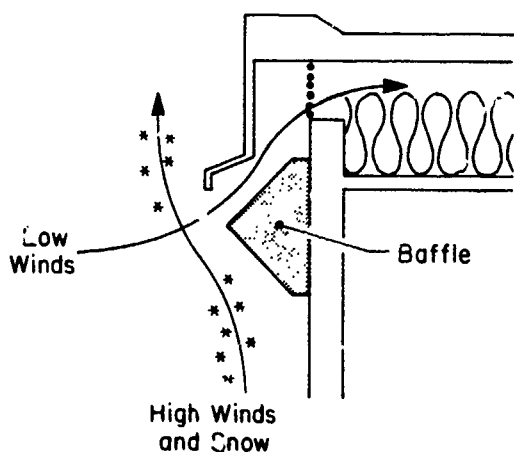
Figure 11. Baffle used in Sweden to prevent vents from ingesting snow during high winds.

Wind Baffle
Drain Hole

*Some Ridge Vents Contain a
Fibrous Glass Filter in this
Space to Prevent Snow Infil-
tration
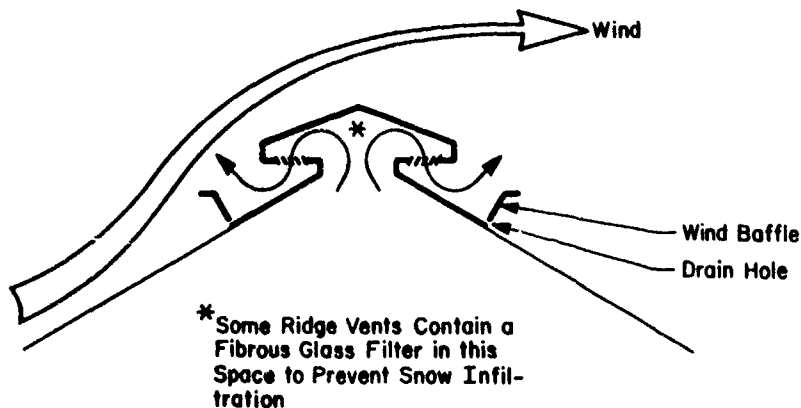
Figure 12. Ridge vents
should be baffled to
prevent ingestion of
driving rain and blow-
ing snow.

SNOW INGESTION

During high winds the openings needed for ventilation of **cold** roofs
may ingest snow. Both intakes and exhausts can be affected. Baffles that
deflect strong winds from intakes (Fig. 11) are usually preferred over
filters in the opening since filters can become blocked with dust and
pollen. Ridge vents should be baffled to prevent ingestion of driving
rain and blowing snow (Fig. 12).

SLIDING SNOW AND ICE

Property has been damaged (Fig. 13) and people have been killed by
ice and snow falling from sloped roofs. Snow guards may be needed to
hold snow on such roofs. Several types of snow guards are available;
most are rather robust since snow and ice can exert great forces on them
(Fig. 14).

Figure 13. Army van damaged by ice from a roof.

470

Figure 14. A typical robust snow guard used in Europe.

To compensate for thermal movements in standing-seam metal roofing systems, the metal roof panels are fastened to the building frame only at one end (usually the eaves). They are secured to the rest of the roof frame with sliding clips that allow the metal roofing to expand and contract freely. Unfortunately some snow guards are being attached through the metal to the purlins, thereby defeating the sliding-clip feature and causing leaks. Since effective snow guards are not yet available for most standing-seam metal roofing systems, other roofing systems should be considered for situations where sliding snow will create problems.

SUMMARY

Sliding snow and blockage of drainage by slush and ice are problems that must be confronted when designing roofs that slope to cold eaves in cold regions. The most reliable way to minimize icings is to ventilate above the insulation with outside air to create a *cold* roof. However, since some icings are still apt to form on occasion, it is also prudent to install a waterproofing membrane along the eaves.

The sliding of snow off a roof can be beneficial since it reduces snow loads. However, sliding snow can endanger people and damage property. Thus it may be necessary to install obstacles (snow guards) on the roof to prevent sliding.

In cold regions, standing seam metal roofing systems should be thought of as water-shedding not membrane systems. They are usually not

471

watertight in their valleys and along their eaves where slush and ice can cause ponding.

Low-slope membrane roofing systems should not drain to cold eaves or scuppers since ice that forms there will cause ponding on the roof. Internal drains and a slope of 1/4 in./ft are key ingredients to successful low-slope membrane roofing systems in cold regions. While many of the newer bituminous built-up and single-ply membranes perform well in cold regions, additional assurance of trouble-free service can be achieved by configuring them as **protected** membranes.

Field Experience in Control and Prevention of Leaking from Ice Dams in Northern New England

Henri de Marne

ABSTRACT

Although ice dams are a common winter problem to most roofs in cold regions with substantial snowfall, they are not unknown in the greater geographical area of the United States where they may manifest themselves sporadically.

Ice dams not only can cause damage to certain roof coverings and shorten their life expectancy, but also can cause leakage inside the building's eaves, walls and ceilings with deleterious effects.

Various methods of leakage prevention have been devised and are reviewed in this paper, but the emphasis is on the design of residential roofs that should prevent ice dam formation under most conditions or limit it to a minor occurrence without the potential for structural damage it otherwise presents.

Both designs of new roofs and repair or retrofitting of existing roofs are discussed.

INTRODUCTION

Ice dams are common to most roofs in cold regions with substantial snowfall; in fact, for many it is an accepted, though not welcome, winter occurrence. Grainge and Hendricks (1976) indicate that problems are created by ice dams over most of the United States. This paper focuses on ice dams on residential construction in northern New England.

The snow cover on a roof melts mostly from the effects of the building's heat loss during the winter. The resulting meltwater must be evacuated by one means or another. Whereas on flat roofs this is generally best accomplished, particularly in cold regions, by interior drains, most residential roofs are pitched and, therefore, meltwater will drain towards the eaves.

As meltwater reaches cold eaves or gutters, it freezes and an ice dam begins to build up on the eaves or the gutters fill with ice, or both.

The free passage of additional meltwater is thus blocked by this ice formation and the ice dam grows in size. Water ponds behind it where it is protected from freezing by the snow's insulating blanket and heat loss from the building.

I. Residential Construction Consultant, Waitsfield, Vermont, USA

Unless the roof covering is intended to be absolutely watertight, as in the case of membrane roofing, water will find its way into the building through the joints in the roof covering.

Membrane roofs themselves are often not immune to water penetration. Ice build-up at the eaves can exert such pressure as to delaminate the membrane from imbedded edge metal; water penetrates into the insulation and wood below and rot is not far behind.

COMMON CONTROL MEASURES

Over time several methods have been devised and used to lessen or eliminate leaks caused by ice dams.

Snow removal

Partial or total snow removal from the roof either by snow rake or shovel or by providing a surface that allows the snow to slide off the roof has long been advocated.

In my experience, only timely total snow removal is successful in eliminating ice dam formation. Partial snow removal by snow rake often causes an ice dam at the higher snow cover line with the risk of water penetration in a less desirable place (Fig. 1).

This may also be the case where wide metal snow belts were installed at the eaves of the building. As atmospheric and other physical forces release the ice and snow cover over these belts, a new ice dam may form at the vulnerable edge of the shingle line.

Figure 1. Secondary ice dam that has formed at the snow line on a roof where snow was removed along the eaves.

Figure 2. Secondary ice dams on both sides of electric heating cables.

Electric cables

Although electric cables have been used for years to create slanted passages or tunnels through which ponded water can run off, their use can create huge icicles which, when joined to the ice dams that form on each side of the Vs, can also trap water and lead to leakage (Fig. 2). Their effectiveness, therefore, is limited by the amount of snow accumulated on the roof and the duration of below freezing temperatures.

Moreover, they can short out and lead to other dangers.

Metal roofs

Unobstructed, smooth metal roofs, given a certain pitch and provided they remain slick, can shed snow accumulation with reasonable regularity. However, valleys, plumbing stacks, chimneys and other obstacles, such as the heads of fasteners, rust, creosote deposits, and oxidation, even if very slight, may impede the timely discharge of snow. The texture and the amount of the snow also plays an important part as do atmospheric conditions and the amount of heat loss from the building.

For instance, with corrugated or ribbed roofs and with standing seam roofs, even a medium snowfall bridging over these projections from the roof covering may not want to slide directly downward but rather with a twisting motion. This, in fact, locks it against these projections and it does not slide off.

And since it is very rare to find a roof that has been on for a while and remained slick, the sticky deposits and the pitting caused by oxidation, dust, chemical pollution, acid rain, creosote deposits from wood burning, and oil deposits from a poorly adjusted furnace offer enormous resistance to the

Figure 3. Old metal roofs may not shed snow.

Figure 4. Obstacles such as those created by converging roof planes prevent metal roofs from shedding snow.

Figure 5. Ice dams do form on metal roofs (courtesy of "New England Builder").

timely discharge of the snow load. Figures 3 and 4 illustrate the resistance to sliding encountered by snow under some of the conditions described above.

Ice dams do form on metal roofs (Fig. 5).

In my years of experience in Vermont I have found none of the above methods of controlling leakage caused by ice dams to be completely effective except for timely and total snow removal by whatever means: a procedure that may turn out to be expensive over a winter of frequent snowfalls and not too practical when the roof is steep and appropriate help is difficult to come by or too busy to do the task before problems develop.

Moreover, metal roofs are not without their problems. They are difficult to flash at plumbing vents, chimneys, skylights, valleys, etc.

Clips on standing seam roofs and nails on corrugated or V-crimp roof sheets are often subject to popping from expansion of the metal under a hot sun, and require periodic inspection and maintenance.

BETTER METHODS OF CONTROL

There are several ways to prevent leakage at vulnerable points of the roof such as the eaves, valleys, skylights, chimneys, etc. Some do not eliminate ice dams but seal the roof against water penetration while others prevent ice damming.

477

Underlying membrane

Some roofers use a wide strip of bituminous material applied onto the sheathing at all vulnerable points before nailing the roof covering on.

A preferred method, in my opinion, is to use one of the new self-adhering rubberized asphalt/polyethylene membranes that are applied directly to clean sheathing and through which the final roof covering is nailed. These membranes are self-sealing.

This method is well suited to repairs or re-roofing of existing houses where it is not practical physically or financially to increase levels of insulation and ventilation at the vulnerable points. Its disadvantage is that it does not relieve the stresses caused by ice on the roof covering itself. However, in areas where ice dams are not a common winter phenomenon, this may not be a serious drawback.

Self-adhering rubberized asphalts/polyethylene membranes should also be considered in roofs designed to minimize or eliminate ice damming, such as cold roofs, whenever skylights and chimneys may induce melting of snow from internal sources.

Cold roofs

Based on years of experience and observation, it would appear that cold roofs are the best means of controlling ice formation at the eaves.

Cold roofs consist of high levels of insulation in order to reduce the amount of heat loss into the attic and high levels of effective ventilation above the insulation but below the roof deck in order to keep the underside of the roof sheathing as close to the ambient outside temperature as possible. On its way up the roof slope and out the ridge vent the cold and dry outside air also absorbs attic moisture.

There are several ways of obtaining a cold roof.

On existing houses with sloping roofs and full attic, continuous soffit vents should be installed as far away from the house walls as possible to avoid penetration of light snow under windy conditions. A continuous ridge vent should also be installed but it must be the type with a non-perishable baffle that deflects wind, snow and rain over it rather than allowing them to penetrate. Non-baffled ridge vents have admitted large quantities of water and snow under windy conditions.

Often existing houses either have no insulation over the walls' top plates or the entire joist/rafter bays above the plates are filled with insulation blocking air circulation. Both conditions should be corrected.

Where insulation is lacking over the wall plates, it can be added, but care must be exercised not to block ventilation. Specially-designed cardboard baffles can be installed to guarantee an air passage between the cold side of the insulation and the roof sheathing. Such baffles also prevent infiltration of ventilating air into the end of the fibrous insulation.

478

In trussed roof construction, the top of the truss directly above the exterior walls should be several inches above the top of the insulation in the attic. This "raised truss" approach allows that problematic corner to be properly insulated without constricting roof ventilation.

In standard rafter construction, an elevated rafter seat can easily be obtained by nailing a 2x4 or 2x6 flat on top of the attic's floor joists at their end. The rafters are set on this new member instead of being set on top of the wall plate next to the floor joists. This design also permits the use of a full thickness of insulation over the exterior wall plates (Fig. 6).

Existing houses with cathedral ceilings needing more insulation offer significant challenges. If the ceiling contains properly installed insulation with an air space above for ventilation, the logical way to provide additional insulation is to add rigid insulation underneath the existing ceiling and cover it with a new ceiling finish.

If the existing roof is unventilated, insulation can also be added underneath, as discussed above, but more is needed to keep the roof cold. Because no ventilation is provided, this is considered to be a high-risk procedure. Ice damming is likely.

For unventilated cathedral ceilings a better, but more expensive alternative is to remove the roof covering, install rigid insulation over the existing deck, then provide ventilation, a new deck and new roofing above.
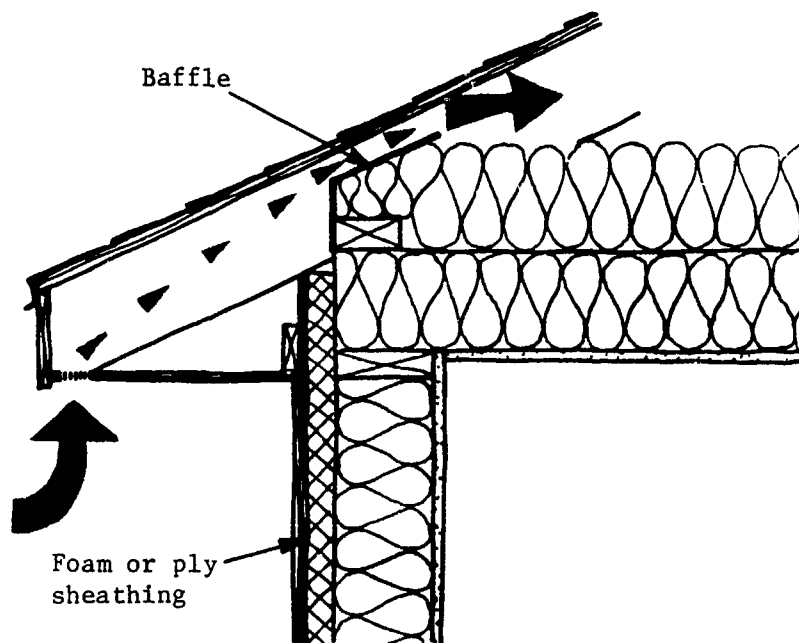
Figure 6. The raised rafter seat and specially-designed cardboard baffle allow for ventilation above the well-insulated corner (courtesy of "New England Builder").
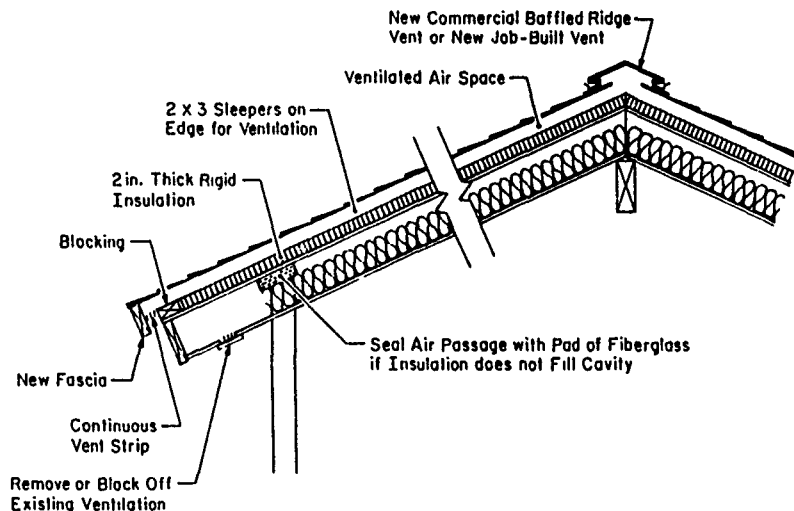
Figure 7. Retrofit of a ventilated cathedral ceiling by sealing off the ventilated space, then insulating and ventilating above.

This alternative can also be used where the existing cathedral ceiling is ventilated provided that the existing ventilation paths are sealed (Fig. 7). If they are not sealed, the expensive insulation placed above will be largely short circuited.

It is also very important to seal all possible airways from the heated parts of the building to prevent moist warm air from convecting out of the living space into the unheated part of the roof. Insulation should be moved aside from all plumbing vents, electric wires, recessed lights, bathroom ventilators, etc. and the joints sealed with duct tape, foaming urethane caulking, acoustical sealant, polyethylene boots, or any other suitable means. After this is done, the insulation should be repositioned.

Openings around chimneys, pulldown stairways, and scuttle hole hatch panels should also be sealed or weatherstripped with suitable materials to prevent warm, moist air from migrating from the living quarters to the attic.

If additional insulation is needed, and it often is, care must be exercised to take into consideration the problems that may arise from covering heat producing appliances with insulation. Attic accesses should also be insulated.

In new construction, it is much easier to provide the amount of insulation and ventilation needed to minimize ice dams. Nonetheless, self-adhering underlying bituminous membranes should be installed where ice dams may form.

In all cases, extreme care must be used to seal all penetrations in the air-vapor retarder to prevent convection of warm, moist air into the insulated space. It is also advisable to reduce or even eliminate all

480

unnecessary perforations by avoiding the use of recessed light fixtures or installing them in a dropped ceiling and by placing bathroom exhaust fans in walls and venting them downward through the basement or crawl space band joist.

Design considerations

Designers of residential dwellings to be built in heavy snowfall regions have a responsibility to avoid designs and details that are conducive to the retention of snow on metal roofs where the intention is to shed it (valleys, dormers, chimneys and plumbing stacks in the lower portions of the roof, skylights, etc.).

They also have a responsibility to avoid designs and details that would make it difficult--or even impossible--to provide the necessary ventilation to all areas of the sheathing unless they can incorporate effective, compact insulation either in board or foam form that is more resistant to heat transfer than fibrous insulation.

CONCLUSIONS

Most of the United States is subject to ice damming; the colder the climate and the greater the amount of snow, the more of a problem ice damming may become.

Effective strategies to prevent ice dams run the gamut from total and timely snow removal, metal roofs with steep pitches designed for snow shedding, and underlying membranes at the eaves, to cold roof designs in which levels of insulation and ventilation are commensurate with the local climate.

Penetration of roof coverings by water ponded behind ice dams can be eliminated by the installation of rubberized asphalts/polyethylene self-adhering sheets onto the sheathing at the eaves, valleys, chimneys and skylights.

Cathedral ceilings may present special challenges.

Adoption of special construction techniques makes possible higher levels of insulation at wall plates without restricting ventilation.

Great care should be exercised to seal all possible convective paths to prevent warm, moist, interior air in the heated spaces from migrating into the attic.

Special consideration should be given to eliminating, or minimizing, design features restricting ventilation of attics or the shedding of snow from the roof.

In cold regions, most roofs that slope to cold eaves should be well insulated and ventilated. It is often best to design the roof to retain snow loads. However, if the roof is designed to shed snow by sliding, features that restrict sliding should be avoided.

481

REFERENCES

Grange, H.L. and L.T. Hendricks (1976) "Roof Snow Behavior and Ice-Dam Prevention in Residential Housing." Agricultural Extension Service, Univ. of Minnesota Bulletin 399.

Building Design for Heavy Snow Areas

Jonathan C. Paine[1]

ABSTRACT

This paper deals with some of the problems encountered when designing roofs for buildings in heavy snow areas. The problems that can be encountered at valleys of intersecting roofs, roof obstructions, and of snow shedding are discussed and some design solutions are presented. Recommendations are given for the design of snow stops, lateral loads due to snow shedding, and trajectories of avalanching snow.

INTRODUCTION

In the mountainous areas of British Columbia and the United States, total winter snowfalls of six meters or more are common. In these areas, roof snow loads often exceed 5 Kpa by the late winter or early spring.

Designing buildings for these heavy snow areas requires unique skills of the designer that are not required in other climates. Many buildings constructed in heavy snow areas are actually designed to suit either coastal or lighter snow climates. Although these buildings are strengthened for the loads, leaking and snow shedding problems are much more prevalent than overstressing of the structural members.

This paper will deal with some of the concepts used in designing buildings for heavy snows. The subjects considered will be architectural design, snow load analyses and structural design.

ARCHITECTURAL DESIGN OF THE BUILDING

In Europe flat and shallow pitched roofs have been accepted for centuries. These buildings avoid many snow-related problems by their shape and also by their siting. The large roof overhangs avoid snow and water buildup against the buildings, and leave a clear pathway all around. The shallow roof pitches avoid snow shedding and all the related problems. In the event that the roof snow does avalanche, the siting of the buildings with space between, allows for snow dump and for snow storage areas.

[1]   Jonathan C. Paine; Structural Engineer and Consultant on buildings in snow country; principal of Snow Country Consultants Ltd., Whistler, B. C., Canada.

In North American resorts land is often expensive due to both the servicing costs and market demand. Because of this, the building designers are under pressure to maximize the use of the land while still maintaining a "mountain resort" feel. To create this feeling most buildings have roofs of moderate to steep pitches and are closely spaced.

The design team's task is to design these buildings in such a way as to avoid snow-related problems and still meet the owners' expectations.

Avoiding problems:

Many problems caused by snow can be avoided or their effects reduced to a tolerable level by organizing the building elements. Some of the most common building related problems encountered due to heavy snowfalls occur in these three areas:

1) Valleys of intersecting roofs:
Heavy accumulations of snow in valleys caused by both drifting and slumping of the snow pack tend to form glaciers which creep down the valleys. This movement is at an angle to the ribs of metal roofing and is across the run of shingle or tile type roofing. Metal roofing can be bent and damaged; shingles and tiles can be twisted. This damage often leads to leaks and general deterioration of the roof over time. Melt water building up behind these glaciers or ice dams is a common occurance, and often leads to leaks. In the spring snow can often be seen hanging up in the valleys of the roof. With the warmer temperatures the snow can release suddenly, creating deadly projectiles. Snow wedging between two dormers creates large lateral forces which can twist and distort the structure.

2) Chimneys and obstructions:
Snow buildup behind chimneys can cause leaks and damage. A chimney can retain a wedge of snow behind it which can creep and crush the chimney or avalanche and shear off both metal and masonry chimneys. This not only causes property damage and leaks but could also lead to fires.

3) Snow shed areas:
Snow shedding towards areas that are used for access to and from buildings is a much more serious problem than leaks and damage of roofing. A small avalanche of snow from a second storey roof is enough to crush a car, cause injury or death to people and animals. Lawsuits for this often overlooked problem can be in the hundreds of thousands of dollars.

Solutions:

The challenge is to maintain the desired architectural style or feel while organizing the building is such a way as to avoid the problems. As with any problem there are many solutions. Not all solutions work in each situation. Here are some of the steps we have used to help alleviate the problem areas.

1) Valleys of roofs:

a) Redesign to avoid the valleys, or reduce the numbers of valleys and intersecting roofs. The use of shed dormers instead of gable dormers avoids many of the roof problems (although they may create a shedding problem).

b) Standing seam metal roofs are more susceptable to bending and damage than stiffer ribbed roofs. The use of heavier gage roofing with more frequent fastening in the areas in and around valleys helps avoid damage.

c) Using wider exposed flashing, i.e. keeping the roof back 45 to 60 cm. away from the valley leaves a smoother valley. This has a better chance of keeping clear of snow and meltwater and therefore the amount of ice build up is reduced. The valley flashing should run well up under the main roofing to give good protection in an ice dam situation.

d) Adequate venting of roofs is essential to reduce condensation, heat loss, ice damming, etc. Dormer and valley areas block the path of air movement by their shape. In these areas the use of a "cold roof" and a waterproof membrane are essential. The cold roof will lower the chances of ice damming by allowing better ventilation; the membrane will prevent any leaks if an ice dam does occur. Ridge venting helps considerably (cold roofs are often eliminated for short-term cost savings).

e) Heat tracing of the valleys tends to be a temporary solution. Under heavy snow it can be pulled off and rendered useless. This solution is hard to depend on and should only be used as a last resort. Roofs should not have to depend on an energy supply to work properly.

2) Chimneys and Obstructions:

a) Avoid placing chimneys in the path of moving snow. The bottom edge of sloping roofs or near valleys are bad locations. Near the ridge of the roof is best.

b) All obstructions should be protected with "crickets" or snow diverters. These must be high enough to deflect the snow around the object and be framed as part of the structure. Diverters can be subjected to tremendous shear forces.

3) Snow shed areas:

a) Avoid having entries, decks, parking etc. on the eaves ends of the roof.

b) Direct the snow to shed in areas designated for snow, such as landscaped areas.

c) Ensure that pedestrian areas are clear of the trajectory of shedding snow.

d) Avoid shedding snow at hillsides that slope back to the building. There are many cases of buildings being knocked off their foundations because of the impact of snow rebounding against the building. Calculating the lateral forces from rebounding snow and designing to resist these forces is very difficult.

Steep slopes may also be prone to snow sliding or avalanching, putting the building at risk.

e) The use of snow stops works well for retaining snow on shallow roof pitches. The steeper the slope, the closer the spacing must be. On steep slopes the snow may shear over the top of the snow stop and should not be relied on to prevent an avalanche. Snow stops must be designed for the snow load and fastened directly into the framing, not attached to the roofing.

Example:

An example of a building which was reorganized to address some of the anticipated problems is shown in figures 1 & 2. Figure 1 is the original building design. The diagram indicates problems with congestion between the dormers and at the chimney, as well as severe access problems due to snow shedding.

Figure 2 shows the reorganized version which was presented to the architect who then redesigned, incorporating the revised shape. Although the snow shed problems were not completely solved, the snow was directed to a location where it can be managed. It is anticipated that the snow accumulation may have to be removed occasionally at the same time as road clearing.

SNOW LOAD ANALYSES AND STRUCTURAL DESIGN

Before designing roofs of buildings the designer must realize the implications of the roof shape. In general, flat roofs are simple to design, easy to build and maintain. Simple sloping roofs are also simple to design, build, and maintain. Complex roofs are costly to design, expensive to build, and the snow build-up is somewhat unpredictable.

The load cases which must be considered by the engineer include:
1) an even blanket of snow
2) an uneven deposition - drifts, solar effects etc.
3) redistribution from shedding and shifting.

The National Building Code of Canada includes a commentary on snow loads which considers all of these load cases in detail.

FRONT ELEVATION
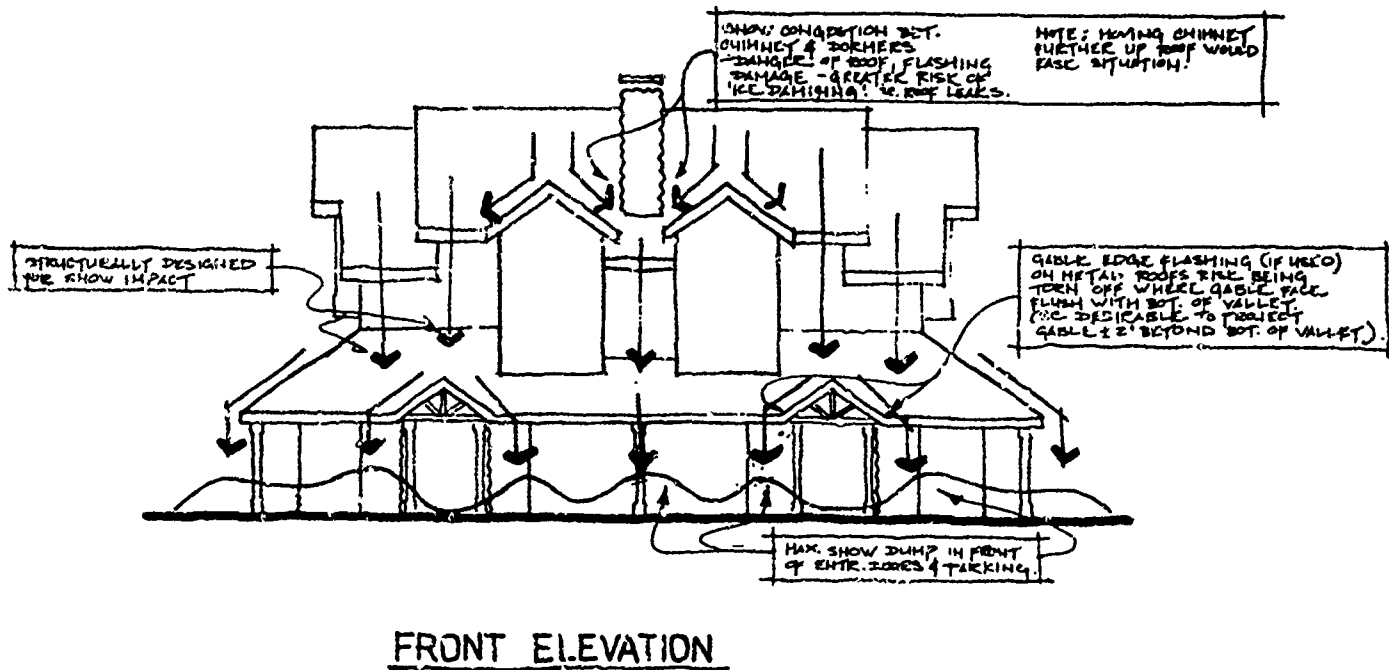
Figure 1.   Original design indicating problem areas.

FRONT ELEVATION MODIFIED
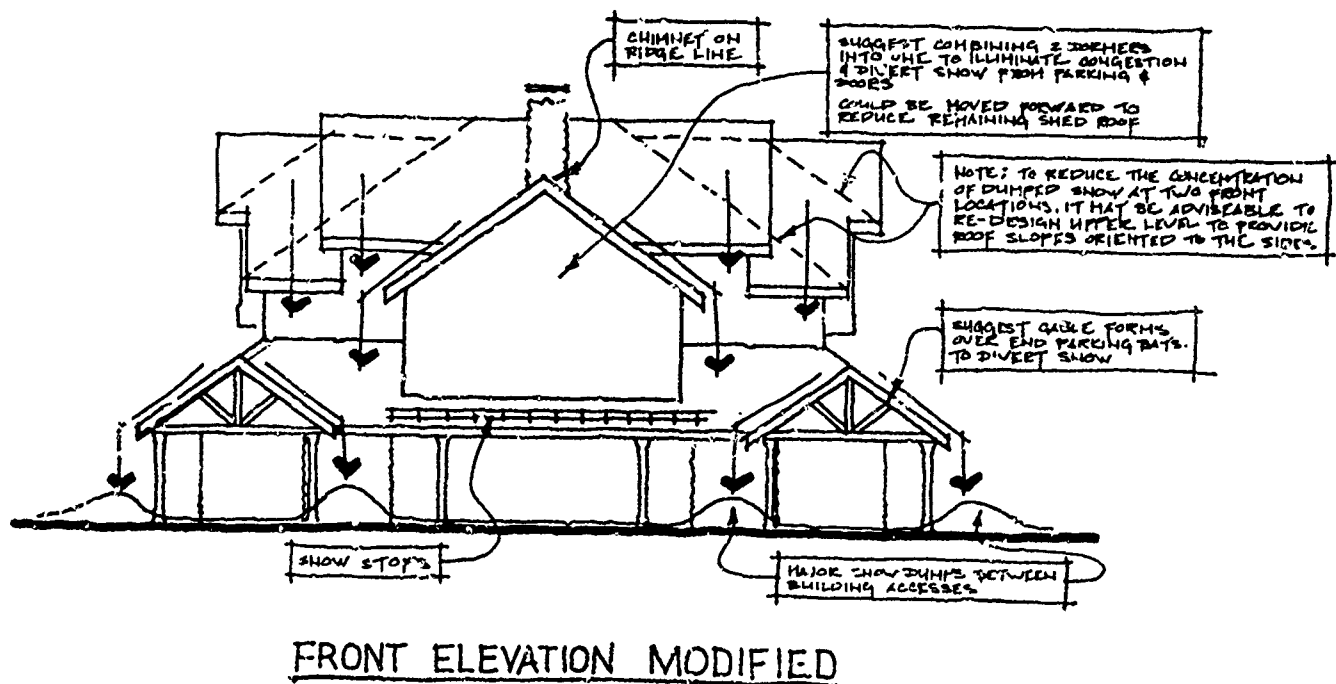
Figure 2.   Redesigned version.

In a previous paper given at the International Snow Science Workshop, we discussed the movement of snow on roofs. The following section is a condensed excerpt from that paper:

At the Conference Center in Whistler a snowpack about 1.5 meters deep with an average density of 0.40 started creeping down the slope. The roof was a 4 in 12 pitch with cedar shingle roofing. Due to the hidden gutter detail, the large laminated wood facia beams were subjected to shearing forces. The adjacent underground parking structure was closed and temporarily shored to prevent collapse in the event that a sudden avalanche occurred. Three hours after the beams were first heard cracking, the roof avalanched but with no serious damage.

With proper forethought, snow shedding can be designed to be problem free. Indeed, if roofs are designed to shed snow safely into planned areas, the results can be exciting to watch.
Here we will look at the roof snow in three conditions; 1. static condition; 2. dynamics during movement; 3. trajectories and impact after it leaves the roof.

1) Static Condition:

Snow on a sloping roof is affected by a combination of forces:
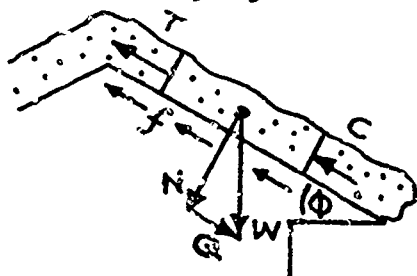
W=weight

N=normal force
 =W cos ∅

Q=sliding or shear force
 =W sin ∅

Figure 3. Forces affecting the snowpack.

The forces that resist shedding are:
T = tension from a block of snow which is anchored to the roof
C = compression from snow frozen to an overhang, from a snow retainer etc.
f = friction between the snow mass and the roof surface
V = shear resistance along the sides of the snow mass (anchored block of snow, side wall etc.)

If the sum of T + C + f + V is more than Q, avalanching does not occur. (a plastic flow or creeping may occur resulting in snow cantilevering beyond the eaves).
The magnitude of the sliding and resisting forces are affected by several factors:

SLOPE: It appears that slopes between 20 and 45 degrees are the most dangerous. Less slope and avalanching is unlikely; more slope and less snow accumulates.

ROUGHNESS: As the coefficient of friction between the roof and the snow increases, the force Q required to cause sliding increases. The coefficient of friction must account for roofing profile, fasteners, flashing, all of which increase the effective coeficient.

Our observations show that on metal roofs sliding is generally unlikely until the roof slope is 14 degrees or more. This corresponds to a coefficient of friction u=.25 which is higher than expected between painted metal and snow. The higher value must be due to the roofs irregularities as well as the effect of some of the other forces.

TEMPERATURE: Cold snow freezes and bonds to the roof and also has a higher coeficient of friction. Wet snow is lubricated and more likely to slide at lower slopes.

OBSTRUCTIONS: Obstructions of any kind can hold large masses of snow on a roof. The shearing forces on obstructions can be calculated as per the following example (assume friction u=0 since the snow may be wet and lubricated).
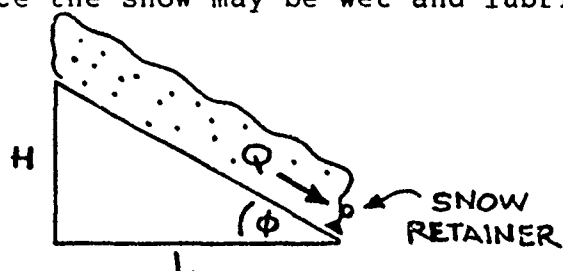
u = coefficient of friction
Q = shear force
W = weight of snow on roof

$$Q = W (\sin \phi - u \cos \phi) \quad \text{EQ.1}$$

Figure 4. Force on obstructions.

Note though that an obstruction such as a chimney or vent can hold back a triangle of snow behind it so that the snow load W becomes harder to estimate. As the roof slope increases the tendancy is to retain a smaller wedge of snow behind the obstruction. Average roof slopes appear to hold a wedge about 45 degrees each side. Valleys and dormers have a similar effect.

The National Building Code of Canada allows a reduction of the snow load for slopes over 30 degrees unless the snow is restricted from sliding. Figure 5 shows the roof plan and loads for a typical sloping roof.

2) Dynamics during sliding

The acceleration (a) of the snow mass down the slope is resisted by friction (u) at the roof surface (g = acceleration of gravity).

$$a = g (\sin \phi - u \cos \phi) \quad \text{EQ.2}$$

It should be noted that there is a difference between static and dynamic friction although both are hard to estimate. Loss of energy due to air friction and due to internal forces within the snow mass have been ignored.
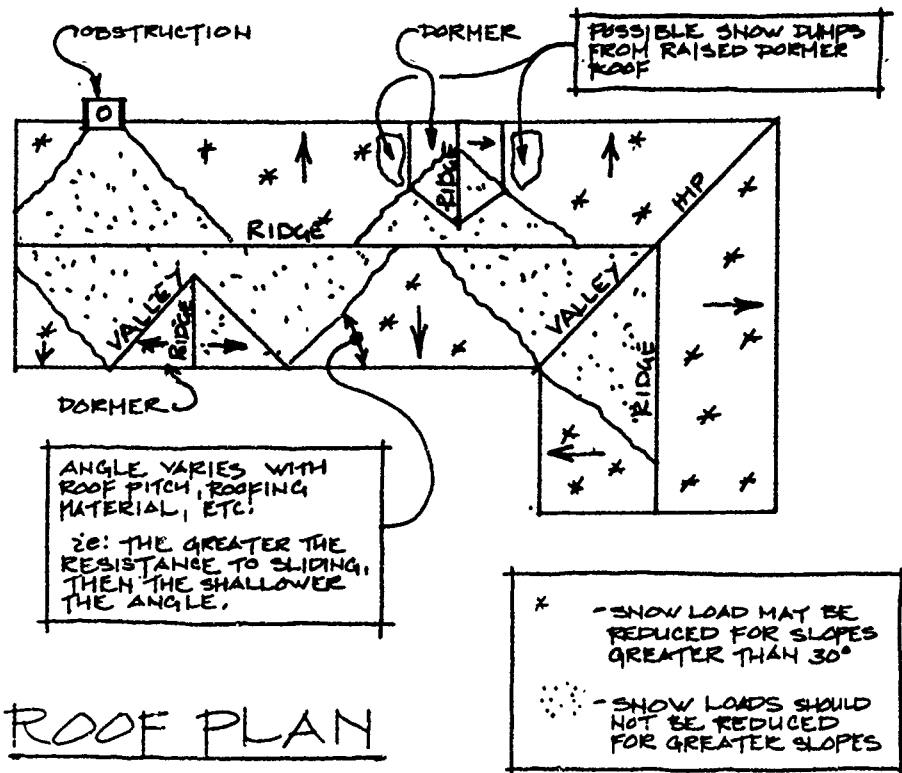
Figure 5. Roof plan indicating areas of reduced snow load.

The lateral forces on the building due to the horizontal acceleration of the snow (a_h) are often higher than wind or earthquake loads.

Horizontal acceleration: $a_h = g\,(\sin\phi\,\cos\phi - u\,\cos^2\phi)$ EQ.3

Lateral force: $F_h = W\,(\sin\phi\,\cos\phi - u\,\cos^2\phi)$ EQ.4
       where W = weight of roof snow

Example:

snow load = 5 KPa
      W = 180 KN
if u = 0 F_h = 72 KN
if u = 0.25 F_h = 36 KN
Note how small changes in the coeficient of friction have a significant effect on the lateral load. Also as the snow mass leaves the roof, the lateral load diminishes.
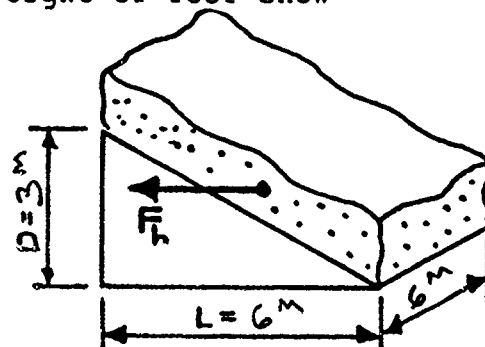
3) Trajectories and impact:

The trajectory of the snow sliding off a roof depends on the velocity as it leaves the roof. In general the first snow to leave the roof will have a lower velocity than the last snow. In order to define a danger zone, the trajectory should be calculated from the ridge of the roof.

490

We assume here that there is no loss due to air friction and that the snow acceleration on the roof is linear. These assumptions may give a slightly conservative answer but seem appropriate for low buildings.
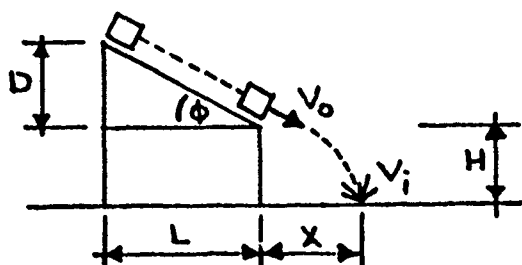
t = drop time
g = acceleration of gravity
V_0 = original velocity at roof edge
V_i = impact velocity

Figure 6

The velocity (V_0) at the edge of the roof is:

$$V_0 = (2 g D (1 - (u/\tan \phi)))^{\frac{1}{2}} \qquad \text{EQ.5}$$

The drop time (t) is:

$$t = ((V_0^2 \sin^2 \phi + 2gH)^{\frac{1}{2}} - V_0 \sin \phi) /g \qquad \text{EQ.6}$$

The danger zone (x):

$$x = t (V_0 \cos \phi) \qquad \text{EQ.7}$$

$$x = [V_0^2 \sin \phi \cos \phi / g][(1 + (2gh/V_0^2 \sin^2\phi))^{\frac{1}{2}} - 1] \qquad \text{EQ.8}$$

The impact velocity (V_i) and angle of impact can be calculated, and from this an estimate of the impact forces:
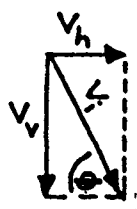
θ = angle of impact
V_h = horizontal velocity = $V_0 \cos \phi$
V_v = vertical velocity = $V_0 \sin \phi + gt$

$$V_i = (V_h^2 + V_v^2)^{\frac{1}{2}} \qquad \text{EQ.9}$$

EXAMPLE: For a roof with a rise (D) of 3.0 M and a run (R) of 6.0 M, coefficient of friction u=0.25, and a drop H=3.7 M

V_0 = 5.5 M/sec.
t = .65 sec.
x = 3.2 M
V_i = 10.0 M/sec.

CONCLUSION

Designing roofs of buildings for heavy snow loads can be a simple or as complex as the roof shape. The designer must be aware of how the snow will react in different circumstances and take it into account when configuring a roof.

If snow is a major design consideration from the start most problems can be avoided.

References

D.M. Grey and B.H. Male, eds 1981. "Handbook of Snow, Principles, Process & Use". Pergamon Press, NY.

Taylor, D.A. 1985. "Sliding Snow on Sloping Roofs". Canadian Building Digest, National Research Council of Canada.

L. Bruch and J. Paine 1986. "Avalanches of Snow from Roofs of Buildings". Snow Science Workshop, Lake Tahoe, California.

9
PERSPECTIVES—PAST,
PRESENT, FUTURE
Ronald Sack, Chairman

Keeping things in perspective.

Perspective: Past, Present, Future ...
Physical Modeling Techniques

Jack E. Cermak[1]

Physical modeling of snow movement by wind and gravity (aerodynamic and gravitational forces) using small-scale models in a wind tunnel has attracted the attention of engineers and scientists with ever increasing interest since early studies in the period of 1930-1950. During this period characteristics of natural winds were not modeled and similitude principles were not applied. In spite of these deficiencies, useful qualitative information on snowdrifting was obtained by investigators such as Finney (1934), Nøkkentved (1940), Kimura and Yoshisaka (1942) and others identified by Mellor (1965, 1970). The 0.6 m x 0.6 m x 1.8 m "wind tunnel" used by Finney (1934) was typical for this era in which flaked mica, fine sawdust, powdered gypsum and other materials were used to simulate snow.

Significant advancements in physical modeling of natural winds and snow movement were made in the two decades 1950-1970. Scaling criteria were developed through dimensional analysis by Kelly, Keitz and Strom (1960). Furthermore, Strom, Kelly, Keitz and Weiss (1962) designed, constructed and used a 2.1 m x 1.1 m x 13.7 m wind tunnel for snow-drifting studies in which snow was simulated with powdered borax. In this same period a meteorological boundary-layer wind tunnel was constructed and validated through comparison of wind-tunnel and micrometeorological boundary-layer mean flow and turbulence data as reported by Cermak and Arya (1970). Development of the meteorological boundary-layer wind tunnel achieved the first requirement for physical modeling of snow movement by wind (simulation of natural winds); however, the proper choice and appropriate relaxation of nondimensional scaling criteria for simulated snow which will assure quantitative data free from uncertainties were and are still questionable. Water channels also were used by Theakston (1963) for qualitative modeling of snow drifting. Although water channels are still used for some qualitative studies, wind tunnels have become the preferred flow facility for both quantitative and qualitative studies.

Since 1970 three important developments have stimulated the use of physical modeling in both snow-engineering research and practice. One is the establishment of numerous boundary-layer wind tunnel laboratories in

---

1. University Distinguished Professor, Fluid Mechanics and Wind Engineering, Department of Civil Engineering, Colorado State University, Fort Collins, Colorado 80523 and President, Cermak Peterka Petersen, Inc., 1415 Blue Spruce Drive, Fort Collins, Colorado 80524.

tne United States, Canada, Japan, Australia and other countries. As evidenced by papers presented at this workshop, both open and closed wind-tunnel facilities, are providing sources of data on snow loads, drifting and deposition control for use in architectural and engineering planning and design. Similitude studies such as those of Iversen (1982) have enhanced test formulation and interpretation in the use of these facilities. However, further studies are needed to fully utilize the wind-tunnel capabilities particularly in respect to scaling of rate processes. A second advancement is development of simulated snow with adhesive properties. This development, through use of activated clay by Anno (1984), presents a technique whereby deposition of "sticky" snow on steep surfaces can be modeled. The third development is use of cold-room laboratories to study sliding of snow and ice as described by Sack, Arnholtz and Haldeman (1987).

The future use of physical modeling for snow-engineering applications is expected, based on current trends, to increase both in acquisition of data for design and as input for development of numerical models. Continuous research and development are required to attain the degree of reliability and scope of applications such as have been realized in wind engineering for wind loads on buildings and structures. Areas needing further attention are the following:

A. Wind modeling. For flow over buildings, fences, trees, etc. systematic wind-tunnel studies are needed to determine a minimum Reynolds number for which the local flow becomes Reynolds number independent.

B. Snow transport and deposition modeling. Qualitative agreement between full-scale and modeled drift patterns is found to be insensitive to violation of wind and particle similarity criteria. However, as emphasized in the paper of Isyumov, Mikitiuk and Cookson (1988) presented at this workshop, systematic research is required to reduce uncertainties in quantitative relationships for (a) falling snow in the presence of wind and (b) snow movement at and near surfaces of snow deposits. In particular, studies are needed to establish the following: appropriate form (forms) for the Froude number, conditions for which the particle-to-fluid density ratio is not important, appropriate scaling for adhesive and cohesive properties of snow and, most importantly, correct scaling for rate processes. Coordinated full-scale field and small-scale laboratory studies should be organized to validate similitude between model and prototype systems. This is particularly necessary for scaling of the rate processes. Small-scale studies in the natural environment such as reported by Tabler (1980) can be useful in reaching a better understanding of "near-surface" transport phenomena.

C. Snow-ice loading and sliding. Further development of cold-room modeling techniques can provide valuable knowledge of both fundamental and practical value. Addition of radiation cycling and rain simulation to existing cold-room facilities would provide a significant advancement. Serious consideration should

be given to development of a sufficiently large cold room to contain a wind tunnel. Test panels covered with snow could then be subjected to essentially all natural combinations and cycling of environmental conditions.

D. <u>Meteorological data analysis</u>. Realistic application of wind-tunnel test data requires knowledge of the relationship between meteorological variables during snow storms at a specific site. The minimum information that should be developed from data available from the National Climatic Data Center, Asheville, North Carolina and similar data centers in countries other than the United States is joint probabilities for wind speed and direction during snowstorms at a number of locations of heavy annual snowfall. In order to facilitate determination of heat transfer rates to and from snow covered surfaces, joint probabilities for wind speed and air temperature at various locations should be determined.

E. <u>Coupling of physical and numerical modeling</u>. Physical and numerical modeling, as illustrated in the paper of Gamble and Irwin (1988) at this workshop, can be used in conjunction to develop quantitative information which cannot be produced by either physical or numerical modeling alone. Furthermore, physical modeling closely coordinated with numerical modeling can provide a means for refinement of numerical codes and reliability of predictions resulting from their use. This type of research constitutes the theme of studies underway at the new Fluid Mechanics Laboratory at NASA Ames which can provide valuable guidance for similar efforts related to snow and wind engineering.

F. <u>Provisions for physical modeling in building standards and codes</u>. Physical modeling is currently in common use to provide snow deposition and loading data for roofs of complex geometry or of large area and the effects of adjacent buildings and/or topography. Modeling techniques have been developed sufficiently to make these predictions, when properly related to local climatological statistics, the best predictions available. In view of this, a statement in the snow-load provisions of standards that snow-load determination by wind-tunnel tests is acceptable -- a statement similar to that for wind-load determination by wind-tunnel tests in ANSI 58.1 (1982) -- would serve the engineering profession well. The ASCE Manual and Report on Engineering Practice "Wind-tunnel Model Studies of Wind Transport of Snow and Sand" now in preparation by the ASCE Sub-Committee on the Wind Transport of Snow and Sand (Aerodynamics Committee, Aerospace Division, ASCE), chaired by Dr. Isyumov, will provide a basis for such a statement.

REFERENCES

ANSI, 1982, "Minimum Design Loads for Buildings and Other Structures," ANSI A58.1-1982, American National Standards Institute, New York. N.Y., 1982.

Anno, Y., 1984, "Requirements for Modeling of a Snowdrift," Cold Regions Science and Technology, Vol. 8, 1984.

Cermak, J. E., and S. P. S. Arya, 1970, "Problems of Atmospheric Shear Flows and Their Laboratory Simulation," Boundary-Layer Meteorology, Vol. 1, No. 1, 40-60, 1970.

Finney, E. A., 1934, "Snow Control on the Highways" Michigan Engineering Experiment Station, Michigan State College, Bulletin No. 57.

Gamble, S., and P. Irwin, 1988, "Use of the Finite Area Element Technique for Predicting Snow Loading on the Roof of the Toronto Skydome," Proceedings of the Engineering Foundation Conference, A Multidisciplinary Approach to Snow Engineering, Santa Barbara, California, 10-15 July 1988.

Isyumov, N., M. Mikitiuk, and P. Cookson, 1988, "Wind Tunnel Modeling of Snow Drifting with Application to Snow Fences," Proceedings of the Engineering Foundation Conference, A Multidisciplinary Approach to Snow Engineering, Santa Barbara, California, 10-15 July 1988.

Iversen, J. D., 1982, "Small-scale Modeling of Snow-drift Phenomena," Proc. Int. Workshop on Wind Tunnel Modeling Criteria in Civil Engineering Applications, Gaithersburg, Maryland, 522-545, Cambridge University Press.

Kelly, G. R., E. L. Keitz, and G. H. Strom, 1960, "Scale Model Studies on Snow Drifting," New York University, College of Engineering Research Division, Progress Report No. 549.01, 56 p.

Kimura, K., and T. Yoshisaka, 1942, "Scale Model Experiments on Snowdrifts Around Buildings," Seppyo, Vol. 4, 96-99 (in Japanese).

Mellor, M., 1965, "Cold Regions Science and Engineering, Part III, Section A3c, Blowing Snow," U.S. Army Materiel Command, Cold Regions Research and Engineering Laboratory, Hanover, New Hampshire.

Mellor, M., 1970, "A Brief Review of Snowdrifting Research" in Snow Removal and Ice Control Research, Special Report 115, U. S. Army Cold Regions Research and Engineering Laboratory and the Highway Research Board, National Research Council, Washington, D.C., 196-209, April, 1970.

Nøkkentved, C., 1940, "Drift Formulation of Snow Fences," Stads-og Havneingeniøren, Vol. 31, No. 9, 1940.

Sack, R. L., DeAnn Arnholtz, and J. S. Haldeman, 1987, "Sloped Roof Snow Loads Using Simulation," ASCE Journal of Structural Engineering, Vol. 113, No. 8, 1820-1833, August, 1987.

Strom, G. H., G. R. Kelly, E. L. Keitz, and R. F. Weiss, 1962, "Scale Model Studies on Snow Drifting," USA SIPRE, Research Report 73.

Tabler, R. D., 1980, "Self-similarity of Wind Profiles in Blowing Snow Allows Outdoor Modeling," Journal of Glaciology, Vol. 26, No. 94, 421-434, 1980.

Perspective on Analytical Methods

Peter A. Irwin

The snow accumulations on and around a building at any instant in time are the result of a number of physical processes: the previous history of snowfall rate; the influence of wind on where the falling snow lands; the drifting of snow after it has fallen; sliding; and melting. When determining design snow loads, it is also necessary to consider the surcharge of load caused by rain that may have been absorbed by the snow. As a result, the prediction of snow accumulations by analytical methods, scale model methods or combinations of these approaches is, in most cases, a complex task. This has led those with the compelling responsibility of formulating snow load provisions for building codes to rely primarily on available field records of snow depths or loads on particular buildings. Although the available field data has tended to be fragmentary in nature (because of the large effort involved in obtaining comprehensive records), this approach has been mostly successful and has the advantage of being conceptually simple. One simply observes the end product of all the processes at work and makes predictions on a semi-statistical basis. However, roof collapses from snow load are still one of the more common forms of structural failure so there is clearly a need for improved prediction methods.

In the session at this conference on analytical methods, we have seen a variety of approaches to predicting snow loads or snow sliding phenomena.

The first paper by Baumgartner, Sack and Scheldorf described analytical/computational studies of snow on a double-layered roof. A finite volume computational model was developed of the roof including heat transfer effects and air flows in the space between the two layers. The computer studies were tied in with experiments in a cold room. This paper falls into the category of examining in detail a selected number of the processes affecting the snow accumulation. This approach would appear to be useful in comparing different roof designs.

The next paper, by Gamble and Irwin, described a combined computational and wind tunnel method for predicting snow loads on an unusually large, novel shaped roof, that of the new Toronto Skydome. This approach used a wind tunnel model to determine the wind velocity patterns over the roof as a function of wind direction and then all other processes affecting the snow distribution, including drifting, were handled by computer. The method used detailed historical records of snowfall, wind, rainfall and temperature and produced time history simulations of snow load patterns on the roof. The time histories of snow load patterns could then be treated rather like field data and design load cases selected.

The paper by Lepage and Schuyler on sliding snow and lift-off of snow by wind on tall buildings addresses an important issue which has been the subject of litigation in recent years. Again, a time history type of computer simulation was developed using detailed meteorological records and again some input for

---

Rowan Williams Davies & Irwin Inc., 650 Woodlawn Road West, Guelph, Ontario, Canada, N1K 1B8

the computer simulation came from scale model tests, in this case both in a water flume and in a wind tunnel. The model results from the water flume provided information on the effects of wind on the falling snow and the wind tunnel data provided information on the local wind pressures affecting the lifting off of snow.

The paper of Mikitiuk, Isyumov and Helliwell examined the variability of snow loads on flat roofs primarily through computation approaches; again, the time history method proved useful. It was shown how important the climatic variables are in deciding whether a roof's greatest snow loads are due to a single snowfall or due to cumulative effects of successive snow storms.

Mihashi, Takahashi and Izumi presented interesting analytical fits to field data obtained on roofs. They expressed the ratio of roof load to ground load as a function of daily mean wind speed.

O'Rourke's paper presented a new analytical model of the drifts that form at step changes in roof elevation. The model was derived from 35 field cases and includes within a simple analytical expression the effects of step height, roof size and Characteristic Blizzard Intensity. The Characteristic Blizzard Intensity simplifies the effects of the meteorological variables affecting the snow accumulations by representing them all in a single parameter. It consists of a snowfall depth (maximum three-day value) multiplied by the excess of wind speed over the drifting threshold integrated over three days. This approach is in a sufficiently simple form to be suitable for building code use. One can see interesting possibilities for further refinements of this type of formula by comparing it with more detailed results from computer simulation methods of drifting on roofs such as Gamble and Irwin's and Mikitiuk, Isyumov and Helliwell's.

The papers of this session provide a representative snapshot of current efforts to develop analytical methods for snow accumulation prediction. The current trend appears to be towards making greater use of computer power and meteorological data but using scale models of full-scale mock-ups to fill in information where the computational methods are weakest, such as predicting wind flow patterns and detailed sliding behaviour. At the same time, use is being made of field data to improve and develop simple code-type formulae and to refine the full computer simulation methods. It appears likely that in the future we can expect to see greater use of the detailed computer model approach to explore in a systematic way the effects of parameters such as roof size, roof height, step height, building shape and exposure to wind.

The power and flexibility of computer methods is at present being limited by lack of detailed data on the behaviour of real snow. For example, the relationship between snow drifting flux and wind speed needs to be better defined in terms of the age of the snow and the history of air temperature and solar radiation the snow has been exposed to. The effects of surface slope and wind turbulence on the flux relation need further research. Further work is needed on the melting process and on the ability of snow to retain meltwater and to absorb rainwater. Finally, there is a need for very well documented,

detailed field recordings of actual snow accumulations on buildings so that computer models can be properly validated.

Perspective on Mechanical Properties of Snow

Robert L. Brown[1]

INTRODUCTION

There were only a few papers presented at this workshop which made considerable use of the mechanical properties of snow in addressing engineering problems associated with snow. One reason for this is that the properties of snow are not yet well enough known for use with a high degree of confidence. Snow, as a natural geological material, is found in a wide range of densities, stages of metamorphism, free water content, etc., and it's properties have been determined only for a few cases. This is unfortunate, since computational methods are currently available to solve a number of problems. In what follows, I discuss some properties, which, if adequately known, could be used to analyze some important engineering problems.

These are broken into three categories: quasi-static properties, dynamic properties, and airborne snow properties. The purpose for this is that snow mechanical properties are substantially different under these three different regimes. All three regimes have relevance to a large number of engineering problems. Further separation could have been made into wet snow vs. dry snow, low density vs. high density snow, etc., but for the purposes of this perspective, I feel the classification used here will suffice. Finally a last section describing some important miscellaneous properties is briefly presented.

DISCUSSION OF IMPORTANT PROPERTIES

Quasi-static Properties:

These properties apply to a number of important problems. The steady state response of snow to relatively low level loads or stresses can be characterized by time dependent stress-strain equations. If known, these stress-strain equations can be used to determine creep loads on roofs, railings, and other structural elements. With the use of available finite element methods, many of the questions regarding improved designs of railings, eves, etc., can be answered. Other areas where the properties of snow can be of use include foundation settlement of buildings constructed on firn, vehicle mobility on snow covered terrain, and snow loads on avalanche defense structures. These topics were not discussed in the conference, but they are important engineering problems.

Dynamic Properties

Very little which was relevant to the dynamic properties of snow was discussed at the workshop. However, there are a number of engineering problems which require such knowledge. By dynamic properties I imply the behavior of the material when subjected to very high rates of loading such that inertial effects become important. Such topics as avalanche impact on structures, response to explosives used for initiating avalanches, performance of snow moving and snow handling equipment, performance of military ballistics in snow, etc., are examples for which the dynamic properties are important. For instance, ski areas frequently construct lifts across areas with frequent avalanche potential, and these lift towers must be protected by constructing either defense

---

1 Professor of Mechanics, C/AE Department, Montana State University, Bozeman, MT 59717

structures or reinforcing the tower itself. There is a general feeling among ski area operators that these structures are over designed. Much the same can be said about snow handling equipment in the sense that much more efficient designs for snow plows and snow blowers are possible. Up to now, most designs have been on an ad hoc basis in which improvements are made on a trial and error basis with little rigorous engineering analysis. As the properties of snow become better understood, advances in design based on engineering analysis should be possible.

Airborne Snow:

This topic was one which received considerable attention at the workshop, since airborne snow leads directly to snow loads on roofs. However, there is a whole array of important engineering problems related to blowing and drifting snow. Foremost among these are drifting snow as it effects transportation systems. As evidenced by the papers presented at the workshop, blowing and drifting snow has been and is still being studied by both wind tunnel modeling and actual field studies. Much knowledge has resulted from these approaches. In contrast, relatively little has been accomplished by means of analytical modeling. Part of the reason is the lack of knowledge about snow particle/air flow interaction, so that accurate constitutive equations describing the snow entrained turbulent air flow have not been available. Another reason is the difficult problem of adequately describing turbulent air flow around obstacles with complicated boundaries. This is a difficult mathematical and computational problem. Recently, however, progress has been made at resolving these difficulties, and future advances will certainly come.

Associated with this problem is snow scour and saltation. To date much is still unknown about the mechanics of these processes, and current constitutive equations relating scour and saltation rates to wind environment are not fully developed. Until such relations can be developed, analytical methods of studying blowing and drifting snow will not provide fully satisfactory results.

Other Properties

The thermo-mechanical properties which effect the transfer of heat and mass through snow into structures in cold environments is a serious problem. On one hand snow can serve as an insulating material since it is not a good conductor of heat. However, it can also be a source of water vapor transport which under the right conditions can be a problem. Another area needing study is snow melt runoff and drainage as it applies to roofs and other structures. A more thorough understanding of these snow properties would provide needed information for engineers and architects.

CONCLUDING REMARKS

The brief discussion presented here alludes to some of the mechanical properties of snow which are relevant to engineering. Much is still unknown about these various properties. As the knowledge base on snow properties expands, analytical and computations methods to study engineering problems will become more common place. As a result this expanded knowledge base should be of use to the design engineer and the architect for more efficient and reliable designs.

Perspective: Design Considerations

Ian Mackinlay, FAIA[1]

PERSPECTIVE: <u>DESIGN CONSIDERATIONS</u>

Design considerations permeated this conference and were by no means restricted to any single section of the program. These were as diverse as snow creep on steep hillsides and snow removal by turning it to "jam." Although the underlying thrust of the conference was technical, almost every paper had something in it for those of us interested in **design**. This gave strong support to the soundness of the multidisciplinary approach of this conference. I wish more architects could have attended.

There seemed to be general agreement that the traditional concept of considering snow loads as "live loads" is foolhardy. A theme which ran through many papers concerned the drifting of snow on buildings and sites. It seemed clear to all participants that snow drifting has a major effect on the design of structures, but the exact nature of the forces produced by drifting requires additional investigation. There did seem to be a consensus that once snow drifts were established on roofs they might persist for long periods, thus, effectively adding to the structure's "dead load" or what is often called "environmental load."

It became clear from the papers presented, that even geometrically simple flat roofed structures can have complex snow drift patterns on their roofs. Relatively small flat roofed structures (say 100 feet on a side), with clean unobstructed roofs, will wind strip to a fraction of the ground snow load, but large flat roofed buildings will drift snow downwind and form cornices overhanging trailing walls. This can lead to localized roof loading that can approach or even exceed the ground snow load.

Of special interest to snow country designers were the discussions of drifting on multi-level roofs. Even a small difference in the height of adjoining flat roofs can produce abnormally higher snow loads on the lower roof. This varies somewhat depending upon whether the lower roof faces into the wind or is in the lee of the higher roof. In either case, more snow will be deposited and greater loading must be anticipated. It was brought out that some roof shapes can concentrate the snow more than others and that the geometry of roofs is an important design element, although one which defies broad generalization. In most cases, snow concentrates on the lee sides of roofs, in shadows, around obstructions, such as dormers and mechanical equipment, and in valleys, especially on the downwind side away from the sun. Complex roofs require modeling and computer aided analysis.

A fascinating aspect of this conference was the extensive discussion of snow drift modeling. Many techniques have been employed and many materials used to simulate snow. My reaction, as an

---

[1]Chairman, Architect, MWM/Mackinlay/Winnacker/McNeil & Associates, Inc., Oakland, CA

architect, is that none of these have been entirely successful in predicting snow accumulation on buildings. It is very hard to find a material which has the complex character of snow when it drifts. We saw examples of some large and exotic buildings, such as the Toronto Sky Dome, which have been studied using a combination of scale model tests and computer simulations. Some of these tests have been done with silica sand in water flumes, while others have been done with various materials at various scales in wind tunnels. The more closely the modeling can be related to similar situations in full-scale snow country application, the more comfortable the designer should be with the predictions. Snow drift control, using wind deflectors and blower fences, is a subject that the architect who works with snow-bearing air needs to understand, and modeling offers a partial guide to effective design solutions.

Snow fence technology offers a realistic source of information to the snow country designer. The photographs of the "Wyoming" fence were remarkably applicable to building design. The wall of a warehouse (or ski lodge) is something like a snow fence. The extraordinary amounts of drifted snow deposited around a four meter snow fence should attract the attention of every site planner who works where the snow blows.

Several papers were addressed to what is, after snow drifting, the leading design problem in regions of snow and cold, the **ice dams** that form on the downslope edge of roofs covered with snow. That this is a truly international problem was clearly demonstrated at this conference. Ice dams are formed by snow melt water which runs under the snow blanket, protected by it from freezing by its insulating properties, and refreezes at the cold eaves. These dams can form on any exterior drained sloping roof in the snow country and can, under some conditions, reach two meters or more in height. The dams retain lakes of melt water, producing strong hydrostatic pressures at the roof surface that can force water through tiny cracks in the roofing material which ordinary rain water would never penetrate. Such leaks plague millions of structures throughout the regions where snow falls worldwide.

As unpleasant as is ice dam related leakage, far more serious is the additional structural load these dams can impart to the roofs where they form. Typically, in structural analysis, sloping roof surfaces are calculated as the flat roof snow load (which is some fraction of ground snow load) multiplied by a reduction factor for slope. This is a dangerous over simplification. Ice dams can block slippage of snow from even steep roofs for long periods of time and, coupled with drafting and melting at the roof surface, produce snow loads which can considerably exceed ground snow loads. When weather conditions change, these heavily loaded steep roofs can discharge, crushing anything in their path. Current building codes do not give this phenomenon the attention it deserves.

Several papers suggested solutions to the ice dam problem. Leakage can be controlled by use of self-sealing impermeable underlayments. The size of ice dams can be reduced by heated eaves or cold roofs. Minimum sloped roofs can be internally drained. Snow arresters can control the slippage of snow and ice into occupied spaces or onto lower roofs where impact loads could crush structural elements. Icicle formation, which often accompanies ice damming, can be reduced by the proper use of heat traced gutters. Sloping roofs can be tilted toward the sun which in moderate latitudes is a great help in lessening the snow blanket on the roof (such roofs should not be shaded by trees or other buildings). Warm roofs should not be located "upstream" of cold

roofs. Perhaps of primary importance, as most ice dams are caused by escaping building heat, proper insulation and vapor retarders must be installed.

The development of reliable ground snow loads was discussed in several papers. Most existing building codes (the Uniform Building Code, for example) treat snow loads as live loads - "Where snow loads occur, the snow loads shall be determined by the building official." Until recently, building officials have had little guidance in making this judgment call. Now, in both the United States and Canada, it is possible to get reliable ground snow data for many locations, and techniques exist for ground snow predictions in most of the areas subject to deep snow. New techniques are being developed for more accurate measurement in remote locations.

From a designer's viewpoint, snow engineering still is in a transitional state. Much has been learned about the characteristics of snow that influence building design, but there is much more to be learned. This conference was a great help to my understanding of the subject, for it focused my attention on the complexity of the problems that exist in the lands of snow and cold. These design concepts need to be better understood by the profession at large.

Codes and Standards: Perspective

Michael O'Rourke[1]

INTRODUCTION

Four papers were presented in the session dealing with Codes and Standards. The papers addressed present and/or proposed provisions for snow loading on buildings in the International Standards Organization (ISO), a proposed Eurocode, the 1988 ASCE/ANSI standard and Codes of Practice in Eastern Europe.

GROUND LOADS AND SHAPE COEFFICIENTS

The basic approach taken in all of the referenced codes is similar. That is, the roof snow load is determined by multiplying a ground snow load with a specified Mean Recurrence Interval (MRI) by a shape coefficient.

In some cases the ground snow load is given as a specific function of elevation for regions with significant variations in ground elevation. Table 1 presents a brief summary of information about the ground load used in each of the referenced codes.

The shape coefficients or ground-to-roof conversion factors address drift situations as well as flat and gable roof situations. In some codes, the drift load for a multilevel roof is an increasing function of the length of the upper level roof while in others it is simply a multiple of the ground load. The shape coefficient for nominally flat roofs is often a function of the exposure of the roof to wind (i.e. exposed, sheltered, etc.) and occasionally also a function of the thermal characteristics of the roof (i.e. well insulated, poorly insulated, etc.), and the self weight of the roof (in some Eastern European Standards). Table 2 presents a brief summary of information on shape coefficients.

DISCUSSIONS

The discussion during the Session itself as well as during the Codes and Standards portion of the Perspective Session focused on four topics: the importance factor, ground load variation with elevation, roof size effects on flat roof shape coefficients, and physical modeling.

Importance Factor:

Dan Taylor questioned the need for the importance factor, I, in the ASCE/ANSI provisions. It was pointed out that the sole purpose of the importance factor is to modify the ground snow load MRI. That is, the design of relatively unimportant structures is to be based upon a 25-year MRI ground load while the design basis for important or critical structures is a 100-year MRI. The vast majority of structures, however, are still based on a 50-year MRI ground snow load in ASCE/ANSI.

I. Assoc. Prof. Civil Engr., Rensselaer Polytechnic Institute, Troy, N.Y.

Ground Load Variation with Elevation:

Mike Newark noted that the 1990 version of the National Building Code of Canada does explicitly incorporate elevation in the determination of ground loads. This is certainly logical and hence desirable. However it is not necessarily an easy feature to incorporate into codes and standards.

Roof Size Effects on Flat Roof Shape Coefficients:

Ian Mackinley observed that if a well-insulated nominally flat roof is very large, the situation approaches that of the ground. Jim Harris noted that the shape coefficient for an "average size" roof is about 0.7 and that it would approach 1.0 as the roof becomes larger. It appears that this feature has yet to be incorporated into codes and standards.

Physical Models:

The use of wind tunnels and/or water flumes for developing snow drift loads has potential. At present, it appears that such physical modeling techniques yield useful information on equilibrium shapes. However, it appears that further calibration work is needed before these techniques can be used to predict loads and non-equilibrium shapes. The ASCE Task Committee on Modeling Drifting Sand and Snow chaired by Nick Isyumov is looking into this issue.

Table 1 Ground Loads

Code or Standard	Ground Load MRI	Specific Consideration of Elevation
ISO	50 Years* (preferably)	*
Eurocode	50 Years	Yes
ASCE/ANSI	50 Years	No
Eastern Europe	Varies**	Yes (in most)

* Ground snow load to be available in national standards.

** 2 years to 1000 years depending on country.

Table 2   Shape Coefficients

Code or Standard	Multilevel Roof Drift Function of Roof Length	Wind Exposure Considered	Thermal Charac. Considered
ISO	Yes	Yes	Yes
Eurocode	Yes *	Yes	Yes
ASCE/ANSI	Yes	Yes	Yes
Eastern Europe	Varies **	Varies **	Unknown

*   Likely to be based upon ISO.

** Yes in U.S.S.R; unknown in others.

Case Histories of Snow Loads on Roofs

Donald Taylor[1]

ABSTRACT

Case histories of snow loads are discussed; specifically what they are and what the reasons are for recording them. Reference is made in this short review, to those papers given at this conference which are based, in part, on case histories. A distinction is made between case histories and surveys. It is argued that case histories should be documented because they can be used for the development of expertise, codes and standards, and modelling of snow drifting.

INTRODUCTION

A case history is a detailed description, usually of heavy snow or ice loads on a roof but occasionally of an unusual distribution of snow or of an accumulation on a roof shape for which no snow load information is given in design standards. Regular observations on roofs are termed *surveys* rather than *case histories*. The latter tend to be "one of a kind."

A good case history includes careful snow depth and density measurements of roof and ground snow, the geometry of the roof and building, and surrounding buildings, trees, hills etc. Photographs are very helpful. Wind direction, speed, and duration from instrumentation set up at the site or, more often, from the nearest weather stations, should be included. Records of snowfall, rainfall and temperatures are also helpful.

WHY CASE HISTORIES?

Case histories aid in:

- the development of expertise. They provide the background and understanding that are part of expertise in snow loading. Such expertise is drawn upon by designers and code writers everywhere to aid in the safe design of (unusual) buildings in snow regions.

- the development of standards and codes. Cases of unusual snow or ice loads (or distributions) which turn up from time to time often result in warning flags or specific clauses in standards.

- the development of procedures for modelling snow deposition and drifting in water flumes and wind tunnels, and the development of computer models.

I   Senior Research Officer, Institute for Research in Construction, National Research Council of Canada, Building M-20, Montreal Road, Ottawa, Ontario, K1A 0R6

INTERNATIONAL EXPERIENCE

Case histories have been collected for many years. In Canada, for example, when the first surveys of snow loads on buildings were started in 1956, case history studies were also begun. People across the country volunteered to measure depths and occasionally densities of unusually deep or interesting accumulations of snow and ice on roofs and to make sketches of the buildings and local surroundings. The combination of survey and case history data had an early and major impact on the National Building Code. New case histories continue to have an influence.

Taylor's paper at this conference, while primarily describing results of a survey in deep snow regions, presented design advice for such areas. The advice was distilled from case histories obtained by people not involved in the survey. In their presentation, Srivastava and Dickey described a case study, for comparison with a wind tunnel model, in which placement of a wall and other landscaping features reduced the drifting of snow at an entrance. Williams and Irwin also presented a case study of deflector fins used to reduce snow accumulation at a roof step and showed good comparisons with a model study.

Collections of case histories in the U.S. have influenced their model codes. Recent analyses of case histories, many of them recorded after structural collapses, are having an impact on the new ASCE/ANSI A-58.1 Standard soon to be released. The research presented here by O'Rourke and Galanakis, an analysis of 35 case histories, will clearly have an impact on future standards.

The new British Standard BS 6399:Part 3:1988 for imposed roof loads on buildings was aided by case studies of the failures that occurred during the winter of 1982 and of 27 other cases of structural failures since 1969. BS 6399, in reflecting the ISO 4355 standard on the determination of snow loads on roofs, in a sense, is also a product of the case histories collected in many countries and brought together in the ISO Standard; so are other standards derived from it. The ISO standard is an important unifier.

Case histories of snow loads on roofs and of snow on collapsed buildings are also collected in Poland. Papers by Sobolewski, Zuranski and Wilbik discuss the results of such cases recorded during the heavy snow winters of 1969-70 and 1978-79. Design and construction errors seemed to be the most important contributors to collapse.

Case histories from heavy snow which caused failures in Japan during the winters of 1962-63 and 1980-81 were discussed at this conference by Mihashi, Takahashi and Izumi and by Suzuya and Uematsu. Sakurai, Joh, and Shibata described careful measurements of wind and snow on a large dome which will be very helpful for studies on the modelling of snow drifting. Further, these and other case histories have contributed to a revision of Japan's snow load code.

In contrast to these case histories, the paper by Hoibo presents the findings of a regular survey conducted over a 20 year period in Norway.

CONCLUSIONS

The collection of case histories is clearly an important part of the study of snow loads on roofs. Regular surveys are the most important but case histories often expose situations not covered by standards that should be. It is crucial, however, that standards committees and designers not overreact to isolated events described by case histories. Each case must be evaluated carefully and evidence for similar ones sought before action is taken.

Perspective: Ground Loads and Mapping

Wayne Tobiasson[1]

INTRODUCTION

The papers in this session and the discussion they evoked focused on three topics:

- Data Problems
- Methods of Analysis
- Mapping Srategies

DATA PROBLEMS

The humans that collect and reduce meteorological data, like all of us, make mistakes. Because of this, readings must be cross checked whenever possible and questionable information rejected. For example, an increase in the depth of snow on the ground during a period of no precipitation is probably a mistake.

The instruments and methods used to measure snowfall are also imperfect. Winds can greatly affect the catch of snow gauges. Snow depths can vary enough within a small area so that a few measurements may not properly represent the average. End-of-month measurements are usually not the maximum values that occurred that month.

In most places, only the depth of snow on the ground is measured. Assumptions have to be made to convert snow depths to snow loads. Where both depths and loads are measured, it is apparent that the maximum depth and the maximum load do not always occur concurrently.

A portion of any rain that falls on a snowpack is retained in the snow and is included in ground snow load measurements. However, the amount retained varies with, among other things, the depth and temperature of the snow and the time that has lapsed since the rain fell.

METHODS OF ANALYSIS

It is common to base snow loads on an extreme value, statistical analysis of maximum annual ground snow depths or loads. It is generally agreed that these annual maxima are not normally distributed. However, there is disagreement as to what skewed distribution provides the best fit. Various tests are

---

1. Research Civil Engineer, U.S. Army CRREL, Hanover, New Hampshire, USA

512

available to compare the fit of candidate distributions. These tests are beginning to be used in the selection process.

The mean recurrence interval selected for design varies widely among nations from a low of 2 years to a high of 50 years. In some places, special structures are designed for mean recurrence intervals of 100 years or more.

Since snow loads vary with elevation, load factors that are normalized for elevation are being developed in some areas. The duration of snow cover may also be considered.

The question of dependence of snow and rain loads is still being debated. The trend is to consider rain and snow separately so that in the process of generating roof design loads, unrealistic combinations, such as "drifted" rain, are avoided.

The extreme variability of snow conditions often makes it necessary to divide a nation into several zones and then analyze each zone separately.

The development of ground snow loads from measurements of the <u>depth</u> of snow on the ground is being handled in many different ways. Where the record of concurrent depth and load measurements is limited, techniques are being developed which also consider older depth-only measurements.

MAPPING STRATEGIES

Maps are more commonly used than tabulations. It may be necessary to smooth site-specific statistical data before it is mapped. Maps may be in the form of isolines or zones of ground snow load or of values normalized with respect to elevation. Separate maps may be needed for snow and for rain.

The trend is toward detailed regional mapping, but even then, extreme local variations preclude mapping in some mountainous areas.

Increased international cooperation is expected to result in better maps for all concerned.